Spatiotemporal disaggregation of GB scenarios depicting increased wind capacity and electrified heat demand in dwellings

Ed Sharp

9th September 2015

UCL
Energy Institute
Energy and the Built Environment

Supervisors

Dr. Mark Barrett, Dr. Paul Dodds, Dr. Catalina Spataru

Examiners

Professor Gareth Harrison

Professor Tim Cockerill

I, Ed Sharp, confirm that the work presented in this thesis is my own. Where information has been derived from other sources, I confirm that this has been indicated in the thesis.

Abstract

National Grid's future energy scenarios depict increased wind capacity and use of domestic heat pumps under four different pathways at a national annual resolution. The factors which will drive the resultant electricity generation and demand vary over significantly smaller resolutions in both space and time. This study presents a method which disaggregates these scenarios temporally to an hourly resolution and spatially to a 0.5^{o} x 0.5^{o} grid, which covers the GB land mass and offshore waters.

The gridded framework facilitates the development of a wind generation simulation model, SpWind, and a hybrid energy demand simulation model, SpDEAM, that are both driven by climate reanalysis data, which provides spatiotemporally homogeneous and accurate hindcasted weather data over the 25 year period of the scenarios. A range of methods are identified and applied to disaggregate non spatial data and redistribute non gridded spatial data to the grid, which depict scenarios, and drivers of wind generation and energy demand.

Evaluations of the reanalysis wind speed data, SpWind and SpDEAM demonstrate a reasonable degree of accuracy; the data, in combination with a gridded approach, is appropriate for simulating turbine output and electricity demand, though some uncertainty and error remains. Wind capacity and heat pumps are assigned to the grid, ensuring that each are exposed to realistic weather conditions.

The implications of the scenarios on residual demand variability, geographical diversity and extreme events are explored in detail revealing the relative impact of different factors driving demand and supply.

The disaggregated modelling described by the thesis is shown to augment aggregated scenario analysis and provide several important insights on the impacts of future changes to the GB energy system.

Publications

Sharp, E. Life, Death and Gridded Population Datasets. Royal Geographical Society Annual Conference, Edinburgh, Scotland. 2012.

Sharp, E. Interdisciplinary experiences: a postgraduate geographer's perspective. Journal of Geography in Higher Education. 2014.

Sharp, E. Spataru, C. Barrett, M. and Dodds, P. Incorporating building specific heat loss and associated energy demand into electricity demand models for Great Britain. Building Simulation and Optimisation UCL, London, UK, 2014.

Sharp, E. Dodds, P. Barrett, M. and Spataru, C. Evaluating the accuracy of CFSR reanalysis hourly wind speed forecasts for the UK, using in situ measurements and geographical information. Renewable Energy, 77, 527-538. 2015.

Zeyringer, M. Daly, H. Fais, B. Strachan, N. Sharp, E. A temporally and spatially explicit framework for analysing long term decarbonisation strategies, a case study for wind energy in the UK. 14th IAEE European Energy Conference, Rome, Italy. 2014.

Sharp, E. Spatial and temporal disaggregation of GB energy scenarios depicting increasing wind capacity and electrified heating to 2035. EST, Karlsruhe, Germany. 2015.

Sharp, E. Spatiotemporal Disaggregation of GB Scenarios Depicting Increased Wind Capacity and Electrified Heat Demand in Dwellings. 38th IAEE International Conference, Antalya, Turkey, 2015.

Some analysis performed in this thesis has also been published online in blog form at

www.esenergyvis.wordpress.com and www.bartlett.ucl.ac.uk/energy/latest/blogs

Acknowledgements

I would like to thank my superviors, Mark Barrett, Paul Dodds and Catalina Spataru for their advice and encouragement. Also all of my friends and colleagues at the institute who have offered support, advice and knowledge.

Thanks, of course, to my wonderful girlfriend for her unnering support and excellent proof reading skills.

I would like to acknowledge EPSRC support for the London-Loughborough Centre for Doctoral Research in Energy Demand, grant number EP/H009612/1.

Contents

List of Tables

List of Figures

List of Equations

List of Acronyms

AONB	Area of Outstanding Natural Beauty
ASHRAE	American Society of Heating, Refrigerating and Air Conditioning Engineers
BM	Balancing Mechanism: Part of the Balancing Mechanism Reporting System
BMRS	Balancing Mechanism Reporting System
BREDEM	Building Research Establishment Domestic Energy Model
BSRIA	Building Services Research and Information Association
BWEA	British Wind Energy Association
CDEM	Community Domestic Energy Model
CFSR	Climate Forecast System Reanalysis
CFSR v1	CFSR version 1 - covering 1980 - 2010
CFSR v2	CFSR version 2 - covering 2010 - 2015
CHM	Cambridge Housing Model
COP	Coefficient of Performance
CORINE	Coordination of Information on the Environment
DCLG	Department of Communities and Local Government
DEAM	Dynamic Energy Agents-based Model
DECADE	Domestic Equipment and Carbon Dioxide Emissions
DECarb	Domestic Energy and Carbon
DECC	Department for Energy and Climate Change
DECM	Domestic Energy and Carbon Model
DEM	Digital Elevation Model
DNO	Distribution Network Operator
ECMWF	European Centre for Medium-Range Weather Forecasts
ECUK	Energy Consumption in the United Kingdom
EEA	European Environment Agency
EHCS	English House Condition Survey
EHS	English Housing Survey
EST	Energy Savings Trust
ETSU	Energy Technology Support Unit
GCM	Global Circulation Model
GG	Gone Green (National Grid scenario)
GIS	Geographical Information System
GMAO	Global Modelling and Assimilation Office

GPW	Gridded Population of the World
GRUMP	Global Rural Urban Mapping Project
GSFC	Goddard Space Flight Centre
HYDE	History Database of the Global Environment
LCL	Low Carbon Life (National Grid scenario)
LLSOA	Lower Layer Super Output Area
LNG	Liquefied Natural Gas
MIDAS	Met Office Integrated Data Archive System
MLSOA	Medium Layer Super Output Area
MOD	Ministry of Defence
NAO	North Atlantic Oscillation
NASA	National Aeronautics and Space Administration
NCEP	National Centre for Environmental Prediction
NG	National Grid
NIE	Northern Ireland Energy
NP	No Progression (National Grid scenario)
OFGEM	Office of Gas and Electricity Markets
ONS'	Office for National Statistics
REPD	Renewable Energy Planning Database
RHI	Renewable Heat Incentive
RO	Renewable Obligation
ROC's	Renewables Obligation Certificates
SAC	Special Areas of Conservation
SAP	Standard Assessment Procedure
SEDBUK	Seasonal Efficiency of Domestic Boilers in the UK
SKM	Sinclair Knight Merz
SP	Slow Progression (National Grid scenario)
SpDEAM	Spatiotemporal DEAM
SPF	Seasonal Performance Factors
SpWind	Spatiotemporal Wind model
SRTM	Shuttle Radar Topography Mission
SRTM DEM	Shuttle Radar Topography Mission Digital Elevation Model
SSSI	Sites of Special Scientific Interest
UKDCM	UK Domestic Carbon Model
UKFES	National Grid's UK Future Energy Scenarios
UKMO	UK Met Office
UN	United Nations
US DOE	United States Department of Energy
WAsP	Wind Atlas Analysis and Application Program
WPD	Western Power Distribution

1. Introduction

1.1. Context

The UK was the first country to legislate greenhouse gas (GHG) targets in the form of the Climate Change Act (2008), which introduced legally binding targets to reduce emissions by at least 80% below the 1990 baseline by 2050. According to the latest full release of DECC statistics, energy supply is responsible for 33% of UK GHG emissions, transport 21%, residential 16%, business 14% and the remaining energy demand sectors 17% (agriculture, waste management, industrial processes and public) [DECC, 2013].

Overall the UK achieved a 28% reduction in GHG emissions between 1990 and 2013. In the same period, the energy supply sector reduced emissions by 32%. Some of the reduction in emissions has been driven by an increase in renewables. However, the decline of coal as a fuel, accompanied by an increase in the use of gas, which has a lower carbon content, has also contributed [DECC, 2013].

As well as direct emissions as a result of burning fossil fuels, there are numerous environmental problems with their extraction and transportation. Historically the available resources have been concentrated in a small number of places, many of which are geopolitically at odds with consumers. The UK is a net importer of fossil fuels and import dependence is set to increase over the next decade [Skea et al., 2011].

Renewable energy sources offer potential for further emissions reductions, and the availability of the resource in and around the UK means that the other problems with fossil fuels can be avoided. Medium-term European Union (EU) energy policy requires 20% of primary energy to be supplied by renewables and a 20% reduction in greenhouse gas emissions from 1990 levels by 2020 (an agreement colloquially known as EU 202020) [European Commission, 2015]. The UK's target is to supply 15% of its energy demand from renewable resources by 2020, which represents a substantial increase on the 4% contribution of renewables in 2012 [DECC, 2013c]. 2030 targets have now been accepted, which have increased the primary energy level to 27%, alongside a 40% reduction in greenhouse gases and a 30% increase in energy efficiency; this is seen by some as a weaker target, which is not binding. Currently, renewable electricity is the largest contributor to these targets. This is due in part to the Renewable Obligation (RO) which dictates that suppliers must meet an increasing proportion of electricity sales from renewable sources, compliance is proven through submitting RO Certificates (ROC's).

Wind capacity is the largest contributor to renewable electricity in Great Britain (GB[1]); however, other renewable energy sources are available and could play a significant role in meeting demand.

[1] Great Britain (GB) and United Kingdom (UK) are widely used as geographical references in this thesis. Their use is deliberate and distinguishes between England, Scotland and Wales and associated Islands (GB) and GB plus Northern Ireland (UK). GB is more widely used as Northern Ireland is excluded from later modelling.

Recent years have seen a significant increase in wind capacity from a low historical level (Figure 1.1). The integration of wind power into an electricity system is complicated by the inherent variability of wind, which is driven by the variation of wind speed over temporal resolutions ranging from seconds to decades, and spatial resolutions ranging from hundreds of kilometres to metres. Variable electricity supply at low levels of penetration has been reasonably easily integrated into the GB system with limited need for extra matching mechanisms[2]. Larger capacities may result in the need to significantly increase the size of these mechanisms as a result of higher magnitude variability.

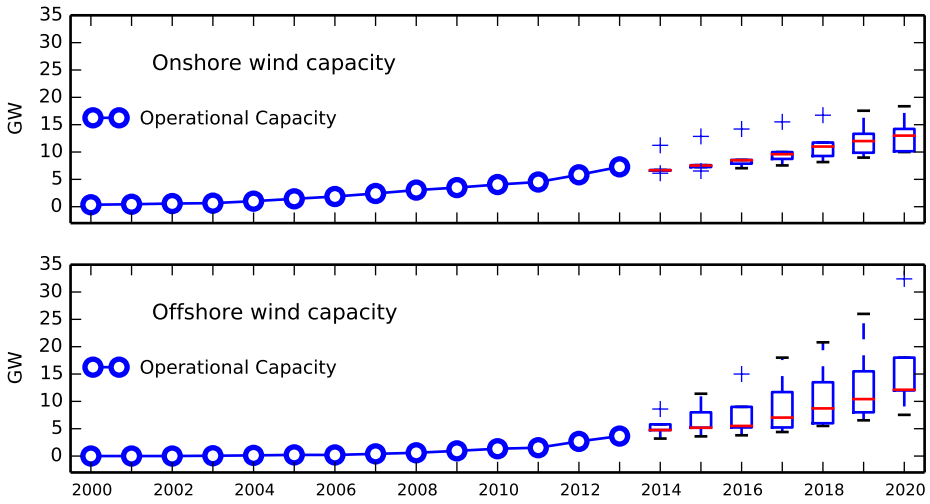

Figure 1.1.: Installed and projected wind capacity, derived from data on installed capacity from DECC [2014a] and forecasts from DECC [2011], National Grid [2011], Renewables advisory Board and Douglas Westwood [Scottish-Enterprise., 2009]. The boxplots represent the forecasts, the central line is the median and the edges of the box are the 75th and 25th percentile. The whiskers are the most extreme points which are limited at 1.5 x the limit of the boxes, the gap between the dash and the whiskers is due to the fixed length of the dash and the pluses are outliers outside of 1.5 x the interquartile range.

As well as showing historical capacity, Figure 1.1 summarises a number of medium term forecasts on wind capacity. The spread of values, steadily increasing in magnitude, demonstrates that beyond the next several years there is a great deal of uncertainty about the extent to which wind will contribute to the UK energy mix. The onshore forecasts appear low compared to the installed capacity; this is because some of the forecasts were made before this capacity was installed, further illustrating the difficulty in predicting future capacities. According to these scenarios, the largest predicted combined capacity by 2020 may be more than 50 GW and the smallest less than 20 GW. The location of future capacity is also unknown, which further increases the uncertainty of potential wind generation due to the spatial variability of wind speeds, particularly if far from shore locations are used where wind conditions may be different from those experienced by historical capacity.

Alongside changes to the way in which energy is supplied, energy efficiency measures are key to achieving UK emissions targets [Ekins et al., 2013]. These measures are of particular importance in light of the fact that energy demand and associated emissions have increased since the 1990 baseline used for emissions targets (though emissions have fallen since a 2005 peak).

[2]Matching mechanisms is a term used throughout this thesis for those elements of the energy system that are necessary for incorporating variable wind generation, see Chapter 8 for a detailed description.

If the electricity supply system is decarbonised, through increased renewable capacity, then it is possible for electricity to replace the burning of fossil fuels in other sectors, further reducing emissions. Unlike the energy sector, residential emissions have increased since 1990. The main source of emissions in the residential sector is burning natural gas for heating and cooking [DECC, 2013]. Efficiency improvements in new buildings are encouraged through building regulations. Demand policies designed to encourage uptake of efficiency measures in existing dwellings include the Green Deal, where loans, linked to energy bills, are used to pay for home energy efficiency improvements [UKGOV, 2015], and the Renewable Heat Incentive (RHI), which provides payments for heat generated from renewable technologies including biomass boilers, solar thermal and heat pumps. However, the Green Deal has been introduced and discontinued within the time that it has taken to complete the research described in this thesis, demonstrating the uncertainty surrounding suitable measures to increase efficiency.

Electrical heat pumps can be used to reduce the use of gas for heating. There are, however, a number of issues with the widespread introduction of this technology. The magnitude and pattern of electricity demand may change and the location of this demand may be different to current demands, which raises the possibility of the need for grid strengthening or other local matching mechanisms. Heat pump demand is dependent on temperature which strengthens the link between electricity demand and weather. When combined with wind or solar generation this may change the nature of the variability and alter the matching mechanisms necessary to ensure that demand is met. As with wind capacity, the extent to which heat pumps will be installed in domestic buildings is unknown (there is uncertainty in non domestic buildings, but these are not the focus of this study). There is also a great deal of uncertainty over other drivers of demand; for example population is very likely to continue to increase but the location of this increase is unknown. Furthermore, humans will influence demand in different ways as their behaviour is uncertain. Finally, energy demand within buildings is likely to change not only from shifts such as electrification of heat and transport but also from efficiency measures such as insulation, low energy devices and smart meters.

1.2. Modelling and weather data

Scenarios are a well-established solution for representing the uncertainty surrounding changes to both energy supply and demand. The nature of scenarios, which are designed to represent a version of reality and are necessarily simplified, mean that projections are provided at a national annual resolution. Wind speed and therefore generation is variable at fine spatial and temporal resolutions. The diversity of wind speeds experienced by future wind capacity is very likely to increase as a result of the increasing focus on offshore generation in contrast to historical capacity which has been predominantly placed onshore. Wind generation is therefore variable over both space and time and this variability is dependent not only on the magnitude of absolute capacity, but the location of this capacity. This means that it is difficult to understand the implications of these scenarios without some additional modelling and analysis.

Historically low wind capacity means that there is a lack of data on which to base future depictions of wind generation. There are countries with high wind penetrations such as Denmark and Germany on which to base analysis, but electricity systems in these countries operate in different

ways and weather conditions vary making comparison difficult. There has been significant work investigating the variability of the wind resource in GB and the UK through simulation of wind generation. The state of the art simulations of GB wind fleets have used the MERRA (Modern Era Retrospective Analysis for Research and Applications) reanalysis to provide wind speed data at a disaggregated resolution. There is an alternative in the form of NCEP CFSR (National Centre for Climate Prediction Climate Forecast System Reanalysis), but the accuracy of this dataset and its suitability for wind generation simulations has not yet been established.

Previous studies which have simulated wind generation have focussed on the variability of the wind resource and its impacts on wind integration. As a result they have tended to simulate static wind capacities rather than changing capacity under different scenarios. This means that some of the variation in generation that will result from varying capacities in different locations has not been represented, especially as the static capacities are based on installed or historical capacities, which have been predominantly onshore. Methods exist for identifying suitable areas for wind farm development as a result of the significant body of work on estimating the wind resource, but they have not been employed by variability studies.

Some of the studies examining wind speed variability in GB have included demand in their analysis and explored the implication of wind generation on residual demand. Those studies have used historical demand data, sometimes statistically altered to represent demand growth for example. It is difficult to incorporate demand from new sources such as heat pumps into this data and temporally disaggregated data is not available at a spatially disaggregated resolution. Therefore the temporal profile of demand in this case may not represent that which is likely in the future. There are other new possible electricity demands such as electric vehicles which will also change the current profile of demand.

As with wind capacity the historical and current number of operational heat pumps is low compared to some of the projections. Because of this, there is little data available on demand at the scope of GB or over the spatial and temporal resolutions at which the factors which drive heat demand occur (e.g. temperature, building characteristics and population), meaning that it is necessary to model demand for heat. Methods exist which could be applied over the same spatial and temporal resolution as modelling of wind generation, but they have not been utilised in the past. This thesis aims to explore how these existing methods, alongside those from variability studies and resource estimates can be combined so that scenarios can be disaggregated over both space and time allowing an exploration of the hourly variability of the GB electricity system as a whole.

1.3. Hypothesis

Following this brief description of the identified research topic, the hypothesis of this thesis is that national annual resolution scenario modelling can be complemented through spatiotemporally disaggregated modelling which captures the inherent variability of wind generation and weather driven electricity demand; furthermore, disaggregation of scenarios can be achieved using existing methods and data.

1.4. Thesis structure

Chapter 2 contains the introductory literature review, including a summary of wind resource estimates that cover GB, methods for simulating wind turbine output at a disaggregated spatiotemporal resolution, studies which utilise these methods, a review of how these studies represent electricity demand, and a review of how these methods could be improved. This review provides an introduction to the issues explored within this thesis, demonstrating the research gap and providing initial methodological justification. Subsequent chapters build on this review with more in depth reviews of relevant methods, data and results. Research aims and questions are stated.

Chapter 3 evaluates the accuracy of the weather dataset, identified in Chapter 1 as a potentially suitable driver for modelling, NCEP CFSR. This evaluation is performed using all available in situ onshore and offshore wind speed measurements and utilises a number of spatial datasets to demonstrate the skill of the dataset at estimating wind speed over the complex terrain of GB. The analysis shows that estimating skill matches or outperforms the alternative wind speed data options at this scope and scale, as a result the dataset is used to drive both the supply and demand models in ensuing chapters. The analysis also demonstrates that CFSR data should not be used to simulate turbines above 600 m elevation.

Chapter 4 describes the development of a model designed to estimate potential wind generation through simulation. The model uses methods established in the literature and is driven by CFSR wind speed data. The model is extensively evaluated against both spatially and temporally disaggregated, measured data. The results of this evaluation demonstrate the accuracy of the model, describing a linear scaling factor which takes into account error introduced by factors not included in the model. Alternative methods for simulation and scaling are explored and discounted.

Chapter 5 presents the development of SpDEAM, an electricity demand model for GB, based on the existing DEAM. Methods for the spatial disaggregation of DEAM to the same resolution as CFSR and therefore the wind simulation model, are described. SpDEAM focusses on the domestic sector so that changes to the way that electricity is used in the home can be incorporated into subsequent analysis. All demand for electricity is modelled, however, so that total demand can be compared against electricity generated from wind. The chapter presents the calibration of SpDEAM outputs to measured data over a 10 year period. This calibration demonstrates that there is demand for electricity that is not accounted for in SpDEAM, therefore methods to build this demand into the model are presented. Following calibration SpDEAM is evaluated against a further four years of data under scenario conditions. The end result demonstrates that the model output is accurate over a long period of time at a temporally disaggregated resolution. Spatially disaggregated evaluation is performed but it is difficult to analyse outputs owing to the lack of measured data; this also makes spatiotemporally disaggregated evaluation impossible.

Chapter 6 presents the scenarios used in subsequent analysis. These scenarios are based on National Grid's Future Energy Scenarios, with supplementary projections used where necessary. Methods for the creation of spatial scenarios, in particular of wind capacity, are presented and the resultant resource estimates analysed.

Chapter 7 presents results from the scenario modelling discussing generation and demand separately. Outputs from both the wind model and SpDEAM are compared against NG data and the reasons for divergence discussed. Analysis of wind generation examines capacity factors, GB

wind speed conditions over space and time, load duration, and the geographical diversity of wind generation under each scenario. Analysis of demand examines annual total electricity demand, domestic demand and non domestic total electricity demand, electrified heat demand in domestic dwellings, peak electricity demand, and the potential change to electricity demand profiles under each of the scenarios.

Chapter 8 presents further results from the scenario modelling, considering the combined implications of changes to demand and supply. The chapter includes an analysis of mean hourly residual demand for each of the scenario years, changes in hourly residual demand, excess wind generation (in terms of peaks and accumulation), the frequency of variability of wind generation, electricity demand and residual demand (including visualisation and discussion of seasonal and annual changes in variability), extreme wind generation, electricity demand and residual demand events, and the correlation between electricity demand and wind generation.

Chapter 9 concludes the thesis by detailing how it has addressed the research aims and questions. A discussion of the motivation for the thesis, the methods used and the main findings are presented under the headings; evaluation of CFSR data, wind generation simulation, electricity demand simulation, and residual demand. The final conclusion describes the contribution of the research, summarises the main findings in bullet points, describes the strengths and limitations of the employed approach and a number of avenues for future work.

2. Literature Review

2.1. Studies examining the potential of wind generation in GB

2.1.1. Geographical estimates of the wind resource

The first step towards integrating wind power into low carbon energy systems is to quantify and characterise the resource and identify viable locations for wind farm placement. Wind farms in these locations must produce enough electricity to justify the high capital expenditure necessary to complete planning, construction and commissioning. Fundamentally, wind turbines need wind speeds between a certain range to produce electricity, most commonly 2-25 m/s, but ideally between 12 m/s and 15 m/s to produce the largest amount of electricity, for the longest time possible. Therefore, initial attempts to estimate the potential of wind power focussed on quantifying spatial variation in wind speed at an aggregated temporal resolution. This resulted in several widely used wind speed maps, most notably for GB from Troen and Petersen [1989b] and Burch [1992].

Using these datasets describing the spatial variation in wind speed, suitable locations for generating electricity from wind turbines can be selected. Suitable sites are most often identified as those with an annual mean wind speed above a certain threshold, but can also be selected using wind power densities e.g. 400 Watts/m^2 at 30 m elevation [Grubb and Meyer, 1993] (wind speed at different heights is discussed in Section 2.1.3). Capacity can be estimated assuming a number of turbines, or capacity, per unit area. The electrical resource is then derived using technical assumptions on conversion and system efficiencies (e.g. Grubb and Meyer [1993] use a capacity factor of 22.5% (capacity factors are described in Section 2.1.2)), or by assuming a mean power production per square kilometre (e.g. World Energy Council [WEC, 1994] use 0.33 MW/km^2). Table 2.1 summarises the outcomes of wind resource estimates that cover GB. The table demonstrates that studies performing this type of estimate either quantify the resource as an amount of electricity that can be produced in one year, or as an amount of capacity that can be installed in the suitable locations, or both. The geographical scope and resolution of these studies varies, although few of those using these methods perform analyses below country level. Most studies quantify onshore and offshore resource separately. Allocating offshore resource can be difficult, in the case of the UK the seabed up to 12 nautical miles offshore is managed by the Crown Estate and should therefore be automatically allocated. EEA [2009] go further and attribute exclusive offshore economic zones to nations.

Technical Potential Several projects have estimated the technical wind resource potential, assuming that all locations that experience a mean annual wind speed above a certain threshold are utilised. The large range of estimates, described in Table 2.1, produced by Gross and Chapman [2001], Grubb and Meyer [1993] and EEA [2009] (317 TWh, 2600 TWh, 4500 TWh respectively

Study	Scope	Resource estimation (each year)	Capacity estimate
WEC (1994)	Western Europe	1300 TWh	635 GW
EEA (2009)	Onshore UK (no restrictions)	4500 TWh	
	Offshore UK, Economic Exclusive Zone (no restrictions)	4800 TWh	
Grubb and Meyer (1993)	Onshore UK no restrictions	2600 TWh	
	Onshore UK first order	760 TWh	
	Onshore UK second order	20 - 150 TWh	
	Offshore UK second order	200 TWh	
Gross and Chapman (2001)	Onshore economic potential UK	58 TWh	22.1 GW
	Onshore technical potential UK	317 TWh	120.6 GW
	Offshore economic potential UK	100 TWh	42.3 GW
	Offshore technical potential UK	3500 TWh	1479.8 GW
Gross (2004) supplementing analysis from DTI (1998)	Onshore technical potential UK	317 TWh	
	Onshore practicable potential UK	8 TWh	
	Offshore technical potential UK	3000 TWh	
	Offshore practicable potential UK	100 TWh	
Hoogwijk et al. (2004)	Western Europe	4000 TWh	
ETSU (1994)	Onshore GB	310 TWh	
	Onshore Scotland	190 TWh	
	Onshore England and Wales	120 TWh	
	Offshore UK	380 TWh	
Brocklehurst (1996) (Base case)	Onshore Scotland	11 TWh	3.4 GW
	Onshore England	2.5 TWh	0.9 GW
	Onshore Wales	1 TWh	0.4 GW
	Onshore GB	14.5 TWh	4.7 GW
Garrad Hassan (2001)	Onshore Scotland	45 TWh	11.5 GW
	Offshore Scotland	82 TWh	25 GW
Boehme et al. (2006)	Onshore Scotland Scenarios		0 - 6 GW
	Offshore Scotland Scenarios		0 - 3 GW

Table 2.1.: Wind resource estimation from studies covering GB, in order of citation in the text.

onshore) demonstrates that these can vary significantly despite no restriction being placed on development. There is less variation in offshore resource estimates from Gross [2004], Gross and Chapman [2001] and EEA [2009] (3000 TWh, 3500 TWh, 4800 TWh) perhaps because of the more abundant high quality wind sites. Other restrictions such as sea depth and grid connections are used to identify the available offshore resource. Much of the variation within these studies can be attributed to the selection of criteria which are used to identify suitable sites, for example WEC [1994] identify classes of mean wind speed used by previous studies (5.1 - 5.6 m/s, 5.6 - 6.0 m/s and 6.0 - 8.8 m/s). The criteria used are not always stated in these studies. The effect of using different criteria for the density of turbines is clearly demonstrated in the different estimates of offshore technical potential 2 years apart by the same author [Gross and Chapman, 2001, Gross, 2004].

Constrained potential There are studies which perform a more sophisticated wind resource estimate for GB through the use of a number of geographical restraints on development, as well as identifying areas with high wind speeds. These restrictions can broadly be categorised as environmental, technical, economic and social (Archer and Jacobson [2013] classify wind power potential under the headings of theoretical potential, technical potential, practical and economic). Restrictions are often divided into those which are absolute and those which rely on a set of criteria, which may be based on cost and are part of a set of scenarios. The effect of restrictions can be demonstrated by comparing those studies which estimate the same geographical scope (although different methods and criteria may be used). For example the Hoogwijk et al. [2004] estimate of

technical potential is far greater than the WEC [1994] estimate, which is constrained by the extent of the grid (4000 TWh and 1300 TWh respectively).

Absolute constraints EEA [2009] provide an estimate of the wind resource that is constrained by absolute environmental restrictions, using EU classifications of protected areas (Natura 2000 and a Common database on Designated Areas). Unfortunately, the report does not provide geographically disaggregated revised estimates of the wind resource (despite describing the technical potential of the UK). However analysis within EEA's report demonstrates that available land decreases by 13.7%. Grubb and Meyer [1993] carry out what they term a first order potential estimate removing "undisputable constraints" (p. 187), such as cities and mountain areas, resulting in a 70% reduction in UK onshore potential.

Economic constraints Economic constraints on development are applied in a number of ways. For example WEC [1994] impose a distance to grid restriction of less than 50 km, locations outside of these areas are assumed to be too expensive to develop. Gross and Chapman [2001] introduce an economic constraint per unit of power (3 p/KWh onshore and 2.8 p/KWh offshore), which results in an 80% reduction of the onshore resource and a 93% reduction offshore. There is much discussion in the literature on the economics of wind supply. This aspect is not covered in detail in this thesis, primarily as it is not the focus of the research, but also because the view is taken that the indirect benefits of increased wind capacity, including decreased emissions, provide a long term economic gain far greater in magnitude than the combined costs of integrating wind into the GB energy system.

GB specific constraints Although many restrictions on development apply irrespective of location, classifications, criteria and policy may change according to the region which will incorporate the wind capacity. There has been work on developing restrictions that are specific to GB. The Energy Technology Support Unit [ETSU, 1994] estimated the available onshore wind resource in the UK using annual mean wind speed data and land use limitations. Land areas were excluded from the analysis based on "physical and institutional constraints" (p. 45) at a resolution of 1 km. No further information is given on the constraints used, however, the study demonstrates that these factors were being considered before the widespread use of the technology (Figure 2.1 shows that before 1994 less than 10 wind farms had been built, all of which consisted of small turbines). The values in Table 2.1 show that ETSU's estimate is greater than found by Gross and Chapman [2001] who use a simpler, but evidently more stringent, set of constraints. This demonstrates again that the selection of criteria to apply to constraints is a decisive factor in resource estimate outcome. Grubb and Meyer [1993] perform a similar analysis, referred to as second order potential, showing as much as a 99% reduction on the technical potential and 97% reduction on the first order potential, the restrictions are referred to as being based on surveys and field experience, with reference to social factors such as visual impact, but no specific criteria are provided. This highlights the subjective nature of the constraints, particularly for large scale studies at this time. Gross [2004] uses "a variety of technical and non-technical constraints" (p. 1906) and shows a similar reduction onshore and offshore of approximately 97%.

ETSU's work was continued using a similar method, described in Brocklehurst [1996]. This study gives more details on environmental restrictions and other physical constraints based on turbine

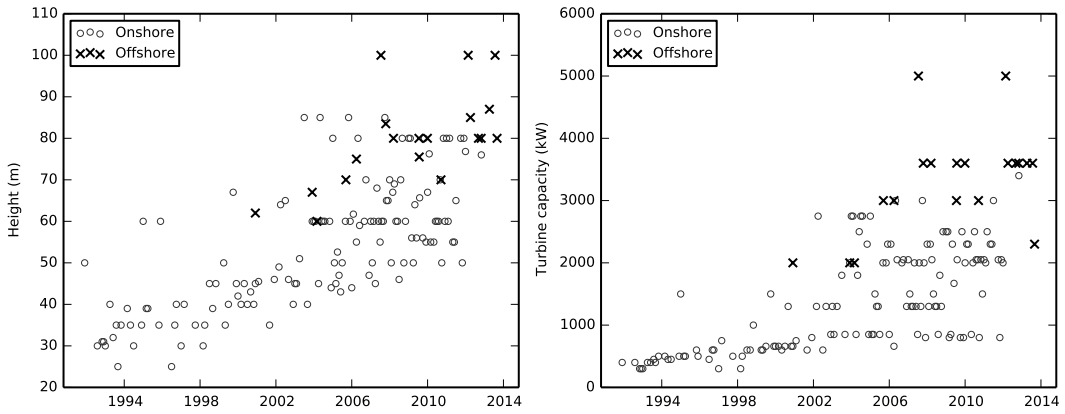

Figure 2.1.: Evolution of turbine height (left) and single turbine capacity (right) at GB wind farms 1991- 2012. Each point represents a wind farm. Data sources: Hughes [2012], Staffell and Green [2014], Renewable Energy Planning Database (REPD) [DECC, 2014a] and site specific data from operator websites.

spacing and farm size. The base case, described in Table 2.1, demonstrates that this severely limits the available resource in comparison to ETSU [1994]. Both ETSU [1994] and Brocklehurst [1996] use annual mean wind speed as a limiting factor on suitable sites (5 m/s and 7 m/s respectively). The same conference proceedings show that more work was being done on using Geographical Information Systems (GIS) for wind farm site selection [Kidner, 1996]. No resource estimate is presented but rather a method for combining restrictions and finding suitable land using a GIS, the authors are the first to cite a source for absolute restrictions on wind farm development [Friends of the Earth, 1995]. Other criteria applied are referred to as "common sense".

Baban and Parry [2001] made the most significant progress on the development of restriction criteria for GB, which were created through the use of a questionnaire answered by a range of stakeholders. They found that wind speed and minimum distance from settlements were the prime locational factors; others included topography, land use, population and site access. Cost was incorporated as a distance from the electricity grid. These criteria were applied to a single 40 km^2 square, therefore no national resource estimate was made. As in ETSU [1994], a threshold of 5 m/s mean annual wind speed was used to select this site. Baban and Parry [2001] were able to produce an analysis of the suitability of land area from weighted overlay, where restrictions were given relative importance, as a result of improved data availability, computational power of modern GIS and a small study area.

The criteria and method established by Baban and Parry were developed further by Garrad Hassan [2001] with the addition of a wide range of up to date environmental restrictions, low flying areas, and social restrictions (through a socially acceptable capacity per unit area). Despite these restrictions, their resource estimate is larger than that found by Brocklehurst [1996], as a result of applying different criteria to restrictions. The same method has also been applied by Boehme et al. [2006] to 1 km^2 grid squares covering Scotland, ranking them in terms of suitability for wind farm development, creating the most robust analysis of available wind resource that covers a significant part of GB. Boehme et al. [2006] apply a mask which excludes areas which cannot be developed, then choose sites dependent on the annual energy output. Detailed information is provided on the data used for restrictions. As Table 2.1 demonstrates, the Boehme et al. [2006]

study represents a departure from studies that estimate capacity and annual loads as they model scenarios of capacity, which include other renewable energy sources and look in further detail at hourly dynamics of wind generation.

2.1.1.1. Summary

It is clear from this review that identifying suitable locations for wind capacity based on wind speed alone leads to overestimates of the potential of the resource. Different combinations of restrictions on development and the use of varying criteria affect the estimation of the available resource in different ways. There has been significant work done on developing criteria, specific to GB, that helps to eliminate areas which may have high wind speeds, but would not be suitable for development. Alongside developments in software and computational power this has increased the sophistication of the method and criteria. These methods and criteria have only been applied to Scotland. Although work exists over smaller scopes (e.g. Gormally et al. [2012]), there has not been an extensive analysis of GB as a whole, or an up to date resource estimate including in depth restriction analysis or identification of suitable wind farm locations. Restrictions on GB development are analysed in more detail in later analysis (Section 6.2.2).

2.1.2. Variability/Intermittency

As described above, the study by Boehme et al. [2006] represents the next step in the analysis of the wind resource for GB, from those studies which have produced annual estimates of the wind resource, by including analysis of temporally as well as spatially disaggregated dynamics of supply. This is important because wind speed is influenced by factors that change over small spatial resolutions, such as terrain, elevation and buildings, as well as air density and other weather influences [Gipe, 2004]. These changes can result in local measured differences of up to an order of magnitude [Kaltschmitt et al., 2007]. The same factors influence changes in wind speed over all temporal resolutions from seconds (e.g. gusts due to building driven wind tunnels) to decades (e.g. changes in weather and climate). Wind generation, driven by these variable wind speeds, is therefore uncontrollable, other than through curtailment, and can fluctuate. Fluctuation is referred to as either variability or intermittency. The varied terrain in GB means that there is considerable spatial diversity in this intermittency. While these terms are used interchangeably in the literature, here the term variability will be used, to distinguish from traditional sources of electricity, which can also be considered intermittent, as thermal plant can be out of action for about 170 hours a year due to unforeseen circumstances [Milborrow, 2007]. Research on the impacts of intermittency existed before large amounts of variable capacity was introduced to GB's electricity grid, as illustrated by Grubb [1991], who recognises that variable resources such as wind are difficult to use in small scale applications but can be integrated into larger power systems where, for example, geographical diversity can smooth the overall output of wind supply and there will be natural reserve from rapidly dispatchable generation such as hydro power or gas turbines. Grubb's paper summarises the key questions that must be answered on the integration of variable renewables (p. 670):

- What penalties do variations and limited predictability impose on the operation of the rest of the system?

- How much backup capacity is required to maintain a reliable system, and how does this affect the economics?
- How much benefit might be obtained from greater geographical and source diversity, and how might this compare with the additional transmission requirements?
- How would incorporating renewables affect the optimal plant mix and system operation in the longer term, and to what extent might the special characteristics of many renewables constrain their feasible long-term contribution?

Research still strives to answer these questions today in the context of a system where significant amounts of variable wind supply have been integrated, but where the level and mix of future variable renewable supply is uncertain. Gross et al. [2006] carried out an extensive review of the costs and impacts of variability, specific to GB electricity network, and provide a number of definitions of issues that cover the questions introduced by Grubb. Coker [2011] summarises these issues as capacity credit, balancing cost, curtailment, supply duration, supply shape and cycling cost. The following paragraphs discuss those issues relevant to this study using Gross et al. [2006] and Coker [2011] as a guide.

Capacity credit This describes the amount of existing generation that can be replaced by variable generation, which can be reported as an amount of plant that can be replaced in e.g. GW or a cost per kWh. Important factors in capacity credit are plant margin (the amount of plant required to back up wind supply) and loss of load probability (the likelihood of demand not being met by supply). Voorspools and D'haeseleer [2006] describe methods for calculating capacity credit in depth. Gross et al. [2006] review studies investigating capacity credit, finding that wind energy does achieve a positive capacity credit, but this reduces as penetration increases. Coker [2011] points out, however, that several studies have found that wind generation can be very low at times of peak demand [Oswald et al., 2008, Pöyry, 2009a]. Dale et al. [2004] assume that the wind output experienced at times of high demand will follow a typical distribution, finding that low penetrations of wind will not affect plant margin too much, resulting in a capacity credit of 35%. However, at higher penetrations (26 GW is modelled), this reduces to 20%. Grubb [1991] noted that, at the time, there was debate over the correlation between wind and energy demand in the UK as "winds increase thermal loss from buildings but high demand can also coincide with periods of very cold clear calms" (p. 676), recognising, however, that results of correlations were ambiguous, citing Cook et al. [1988].

Maximum penetration Gross et al. [2006] review previous studies showing that the majority of studies do not investigate penetrations greater than 20%, although greater penetrations are discussed elsewhere (for example Milborrow [2007] examines the implications and costs of 100% wind supply). Figure 1.1 shows that 20% may be a conservative estimate of penetration as the maximum combined projected capacity may be as much as 50 GW or 83% of peak demand (assuming 60 GW peak, later analysis discusses changes to peak demand) and the peak contribution of wind to electricity demand to date is 24%. Gross et al. [2006] note that, based on evidence from the reviewed literature, high capacities should not compromise supply, but may increase cost.

Curtailment Curtailment is the restriction of supply when it is not required, also referred to as spill [Gross et al., 2006]. This is very likely to occur with wind due to the unpredictability of wind

speeds. As penetrations increase, the economic penalty associated with curtailment increases, as the current operation of the electricity system guarantees a price for wind power. This means that larger capacities increase the overall cost of introducing wind to the system. Inoperation of turbines due to high wind speeds when they are shut down for safety reasons is not considered to be curtailment here as these periods are likely to be outside of the range of power producing wind speeds as described below. Cannon et al. [2015] state that on average less than 0.1% of GB capacity was curtailed in 2012.

Capacity factor The capacity factor is the amount of electricity produced by a generator as a percentage of the theoretical maximum (the term "load factor" is sometimes used). Capacity factor is most often calculated as an annual value. Not only does this change at finer temporal resolutions, but calculations often assume a static capacity over a year. Development in GB over recent years means that capacity may change significantly month to month. The capacity factor of a wind turbine or number of wind turbines is primarily influenced by wind speed. However, there are a number of other factors which drive lower capacity factors including maintenance shut down periods, failure and curtailment. Capacity factors have been assumed to be in the range of 30-35% for several decades but recent research has shown that they may be as low as 21% and is 26.1% on average in the UK [Boccard, 2009]. Historic capacity factors are based predominantly on onshore wind farms due to the lack of offshore development, so for this reason care must be taken when using these capacity factors to investigate future capacities where offshore is likely to dominate. Boccard notes that several of the studies estimating wind energy potential at large scale, summarised in Section 2.1.1, use realistic capacity factors (Grubb and Meyer [1993] 22.5%, WEC [1994] 25.1% and Hoogwijk et al. [2004] 26.5%). Capacity factors will vary between turbines, farms and fleets and the variation between these has implications for the analysis of output.

The variability of wind clearly introduces complexity into the operation of the electricity system and therefore may make it more difficult to ensure security of supply. In order to begin to understand the implications of this complexity, how future wind capacities might effect it and what measures can be taken to counter these effects, there has been research which attempts to estimate generation from future deployments at a spatially and temporally disaggregated resolution.

2.1.3. Methods for estimating generation from wind turbines through simulation

Historically, wind capacity in the UK has been small, particularly when compared to feasible future penetrations (Figure 1.1). Data from operational wind farms in the UK are only available over a short time period, which may not include low frequency climate events such as extended periods of high or low wind speeds. It is also unlikely that the wind speeds experienced by existing capacity are as diverse as those that will be experienced by future wind farm fleets, particularly with the addition of offshore capacity, due to greater geographical dispersion and the difference between offshore and onshore wind conditions. Consequently, it is difficult to extrapolate current generation trends to future deployments, especially as there is little data available on generation at a disaggregated level. This is the case for most other countries, Denmark, however, offers a contrast. Wind power in Denmark is more mature with higher levels of integration, coupled with a policy of free high resolution data, this means that insights into future operation can be gained

from measured data [see, for example, Østergaard, 2008]. More data are becoming available at a disaggregated resolution, both spatially and temporally for a number of other countries. An alternative approach to using measured data to analyse wind generation is to estimate generation using wind speed data from either weather station observations or from weather or climate models. This method provides a temporally disaggregated time series and therefore facilitates analysis of the variability of wind and the issues described above.

Electricity generation from a turbine can be estimated from these wind speed data using a power curve, which are available online from manufacturers. The curves in Figure 2.2 describe wind turbines that are representative of those installed in GB, both onshore and offshore. These curves show the amount of energy that a turbine should produce at a given wind speed (to the nearest m/s). The cut in speed, at which point a turbine begins to produce electricity, is between 2 - 5 m/s. The curve then shows a power law range with an exponent between 2 and 3 [Kiss et al., 2009], curves then plateau between 11 - 15 m/s. The power law range and the maximum power output are determined by the size of the turbine, larger turbines produce more power. Early turbines installed in GB were small, around 30 - 50 m hub height and producing 300 - 400 kW at the peak. The most recent onshore turbines are over 3000 kW and up to 80 m, this size is limited by planning and social acceptability. Offshore turbines can be up to 5000 kW and *over* 80 m tall (Figure 2.1). The cutout wind speed, where wind turbines cease to produce power due to excessive wind speed and resultant forces on the structure, is 25 m/s for almost all turbines at present. Almost all of the studies simulating output from GB capacity use a representative turbine curve. This curve is usually representative of the turbines that are installed in GB, but can be very small, e.g Green and Vasilakos [2010] use a 1.75 MW turbine, which may result in conservative estimates of output. Very large turbine curves are sometimes used, e.g. SKM [2008] use 7.5 MW turbines, which may result in overestimates of output. Some of the error introduced by using unrealistic turbine curves can be alleviated through scaling to a desired capacity, for a wind farm or area.

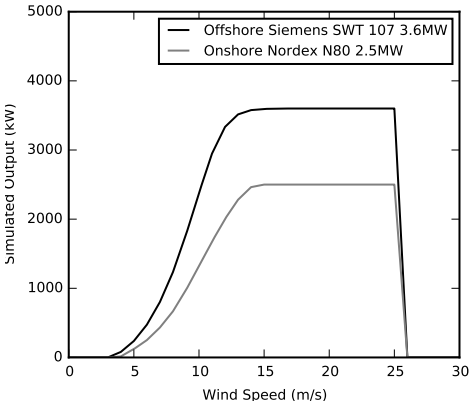

Figure 2.2.: Turbine curves used for estimating electricity generation from wind speed.

Turbine curves are produced as a result of testing, and are therefore a realistic representation of turbine output in isolation when new. Turbines do not, however, operate in isolation and are therefore subject to the influence of their surroundings. A key influence is other turbines, as when a turbine is operating it reduces the wind speed downwind. Therefore closely sited turbines can lead to drops in the amount of energy produced of up to 60%, due to losses in the power of the

wind [Schallenberg-Rodriguez, 2013]. Wind speed is also dependent on local conditions such as topography and weather characteristics such as vertical wind profiles and layer mixing, which drive the rate at which energy is replaced within the wind. Faults and maintenance will affect the output of turbines and curtailment may stop output at times. As turbines age they become less efficient at harnessing wind, an issue explored in detail by Staffell and Green [2014].

Modelling of these drivers is difficult, as there is often not sufficient data, therefore methods have been created to allow for these effects. Methods include numerical models and heuristic models e.g. artificial neural networks and genetic algorithms [Schallenberg-Rodriguez, 2013]. There are methods which attempt to take these effects into account through the use of an adapted turbine power curve, which are a variation of the approach developed by Norgaard and Holttinen [2004], described and evaluated in Section 4.1.3. Alternatively these drivers can be counteracted through the use of a correction factor. A commonly used method is to correct wind speed data to match a desired annual capacity factor which represents nationally averaged historical output; for example Sinden [2007] uses a value of 30%. The problem with this method is that recent data and research, described above, has indicated that this may be an overestimation of the capacity factor, and it is likely that the capacity factor will be different in the future when capacity increases in both absolute terms and geographical diversity. It is also possible to apply a correction factor which breaks down factors affecting output; for example Boehme et al. [2006] account for down time through using the statistic that European wind turbines are available 98% of the time, and Boehme and Wallace [2008] use wake reduction (linear in proportion to turbine density), 2% downtime and 2% electrical loss. An alternative approach is to correlate simulated generation against measured data to develop a correction factor that incorporates all of the factors not included in the method. This method is applied in UK based research by Hawkins et al. [2011] and Staffell and Green [2014] and is explored further in Chapter 4. Increased data availability at finer spatial and temporal resolutions means that this method should improve the accuracy of wind turbine simulation in the future.

2.1.4. Simulation using weather station data

2.1.4.1. Onshore simulation

Some studies estimate the spatiotemporal variation of wind generation across large onshore areas by interpolating historical measurements from synoptic weather stations. Electricity generation from a turbine can then be estimated from these data using the power curve approach described above. The use of historical data, also referred to as hindcasting, assumes that that conditions experienced in the past will match those experienced in the future. This is a necessary assumption due to the difficulty with forecasting wind speeds, which may be possible over the short term (e.g. 24 hours) but is difficult in the long term due to, for example, climate change and at spatiotemporal resolutions in the long term due to variability. In the UK there are several studies which have used this data to investigate the impacts of variability. These studies can be broadly categorised as those assuming weather stations represent wind conditions across GB and those assuming weather station data represents a region.

Studies assuming weather stations represent wind conditions across GB Sinden [2007] carried out the most comprehensive study on the variability of the GB wind resource, using 66

simulation sites and data over 30 years. The study uses the synoptic MIDAS data[1] [UKMO, 2012] and assumes that the wind harnessed by farms, in what is referred to as a diversified network (e.g. p. 115), is represented by a subset of these stations. Using simulated generation data Sinden looks looks in more detail at the potential smoothing effect of geographical diversity of wind turbine placement introduced by Grubb [1991] and explores temporal changes in capacity factors at a range of resolutions. The use of geographical variation in wind speed and potential power output as a method for smoothing the integration of variable generation into an energy system is explored in detail by Østergaard [2008] who shows that the smaller the system (in terms of plant number, variations in energy sources and geographical extent), the greater the need for reserve capacity or flexibility within the system. Archer and Jacobson [2007] find that there is no saturation to the benefits of increasing the number of geographically diverse wind sites, albeit in a North American example.

Pöyry [2009a] use a smaller number of stations (28) to represent the conditions over UK, looking at the impacts of intermittency on GB and Irish electricity markets. Like Sinden, Pöyry correct electricity generation using a capacity factor. They use an aggregated power curve "derived from a standard power curve that has been adjusted to take into account the output associated with a group of turbines over a given area" [Pöyry, 2009b, p. 8]. Coelingh [1999] looks at the effects of geographical diversity of wind across Ireland using 10 years of data from five stations. The study is interesting as different wind heights (40, 60 and 80 m) are used alongside a range of turbine curves, rather than a single representative curve used in other studies.

Studies assuming weather station data represents a region An alternative use of station data is to assume that the wind speed time series from a point represents the surrounding region. This method allows simple scaling of output as a region can be assigned a capacity or range of capacities. The consultancy firm Sinclair Knight Merz [SKM, 2008] model 19 regions of GB assigning wind capacity under three scenarios to 2020. SKM state that data are "numerically processed" (p. 24) to take into account hub height, turbine characteristics, and losses from wake and availability. This approach allows them to look at the implications of the growth of wind capacity on the electricity grid.

Green and Vasilakos [2010] simulate output from 30 regions onshore and offshore using MIDAS data from 1993 - 2005, they spatially allocate national capacity based on existing and under construction wind farms and scale this capacity up to 11 GW onshore (using projections from National Grid). They select appropriate weather stations on the basis of proximity to wind farms and synthesise data to fill gaps through interpolation and regression. This work is extended by Green et al. [2011], who investigate whether using excess wind generation to produce hydrogen through electrolysis is an effective measure for coping with variability.

Oswald et al. [2008] simulate the output of 25 GW capacity using a single weather station to represent eight regions, they create scaling factors after comparing output to ROC's. The paper recognises that this is a small number of regions especially given the number modelled by Sinden [2007], justifying this approach by saying that there is little to be gained from increasing number of locations, however, it is likely that wind conditions would vary considerably in areas this large. They find that a diversified system is volatile, despite smoothing, demonstrating a variation of

[1] MIDAS is the UK Met Office (UKMO) Integrated Data Archive System

between 5.5 GW and 56 GW of other required plant on the system to meet demand over a month. This volatility is not found by all studies, for example the analysis of Østergaard [2008] and Archer and Jacobson [2007] finds contrasting results. Coker et al. [2013] use MIDAS data for simulation of generation for an area around the Bristol channel. They fill gaps in the time series with mean values from surrounding time periods and reject time series with longer gaps.

Issues with weather station data The UK network of synoptic weather stations is spatially diverse and onshore appears to be spatially comprehensive (Figure 2.3). Outside of the UK, spatial gaps between weather stations are much larger with uneven coverage [Archer and Jacobson, 2005]. Station networks are generally biased towards populated areas where wind farms cannot be built, and towards low lying areas that experience lower wind speeds [Dobesch et al., 2007]. Moreover, the land uses at many weather stations are unsuitable for the location of turbines, for example urban areas or wetlands (restrictions on wind farm development in GB are examined in detail in Chapter 6). It is also possible that the locations which are suitable for wind farm development are not used due to other reasons, such as planning restrictions or low wind speeds. There is no existing research that explores the impact of synoptic station location with respect to either wind turbine simulation or evaluation of other wind datasets other than to retrieve location specific roughness lengths for wind height correction methods through land use maps. Boehme and Wallace [2008] note that met station data may be accurate to a few percent but irregular maintenance may result in this accuracy degrading, for example if trees grow around the site.

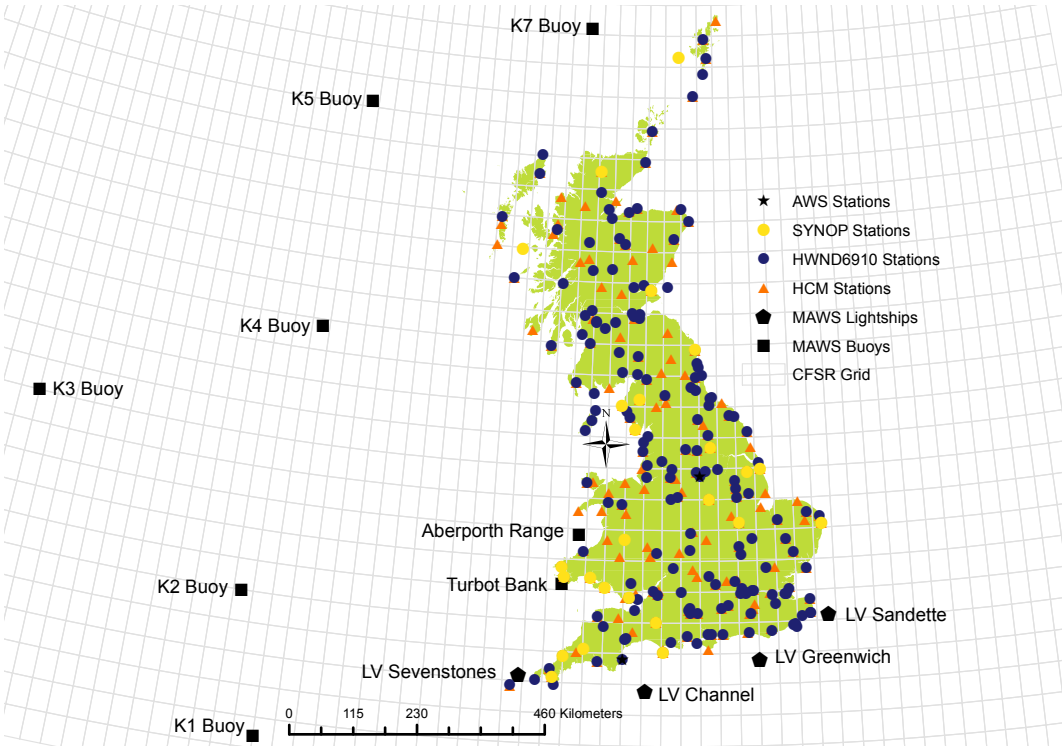

Figure 2.3.: Locations of synoptic weather stations onshore and offshore of GB. The map shows the message types that are individually reported to MIDAS. Each grid square represents the area covered by a single reanalysis hourly weather value (e.g. wind speed) from NCEP CFSR.

MIDAS onshore wind speed observations are taken at a height of 10 m. Figure 2.1 demonstrates that wind turbine hubs are far above this. It is therefore necessary to estimate wind speeds above

10 m (wind speed is provided at 10 m by most other datasets). There are several conventional statistical methods for wind height correction, the influence of the coefficients used in these methods is examined in the context of GB in Kubik et al. [2013b], the methods are reviewed in Section 4.1.3. These methods have the potential for introducing error, which is not recognised by all studies. Hub height wind speed has been challenged as a standard, Clack et al. [2014a] found in comparison the rotor equivalent speed [see Wagner et al., 2009, for a description], which takes into account vertical wind shear across the turbine blades, produces a lower estimate of wind power production. This study is conducted in the United States and the largest differences are found at high elevations, which are not found in GB.

MIDAS wind speed observations are provided as hourly mean values at the most temporally disaggregated level. This represents a compromise compared to using measured turbine output, as these mean values have been shown to vary between +/- 30% to 40% when compared to minutely values, resulting in some variability being smoothed [Kaltschmitt et al., 2007]. MIDAS, in common with all weather observation datasets, has gaps and duplications. Data are also provided at multiple temporal resolutions, with repeated time steps and apparently erroneous values. These discrepancies must be filtered in order to obtain a continuous dataset.

These data quality issues have the potential to adversely affect the results of wind generation simulations. For example in Sinden [2007], sites were selected based on the completeness of the time series, however, because MIDAS data is discontinuous, average wind output per hour is calculated using only those sites with valid data. Therefore power output is determined to a certain extent by data availability rather than wind speed. Sinden also only used this data to simulate a single turbine per weather station, whereas in reality there may be many turbines harnessing the wind conditions at one site and none at another. Therefore, although MIDAS data provides a good approximation of the average UK hourly wind conditions over a time period that should capture climate extremes, the data is not necessarily representative of the conditions which will be experienced by operational or future turbine fleets.

There are critics of the use of wind speed data and manufacturer turbine curves. For example Strbac and Ilex Consulting [2002] found that simulated wind generation overestimated generation and underestimated variability, therefore they performed analysis on measured generation data. They created different scenarios of renewables using 14 regions of GB, allocating capacity using regional renewable assessments as a guide. Their small subset of generation data (a 200 MW sample for 1 year) is not representative of the conditions experienced by the 24 GW of wind that is simulated (this is noted in their paper). They used "time slipping" which overlays wind output time series and shifts them by half an hour, creating a pseudo weather system moving across GB (p. 24). The spatially disaggregated nature of their analysis is harnessed in a network flow model used to assess whether scenarios may exceed the limitations of the system.

Alternative uses of MIDAS wind speed data There are studies which use supplementary data alongside MIDAS data. Boehme et al. [2006] use the 'Wind Atlas Analysis and Application Program' (WAsP) developed by Risø National Laboratory in Denmark. The program extrapolates wind measurement horizontally and vertically, which means that wind speeds can be estimated at a finer spatial resolution and at a desired height. This method has the advantage of taking into account orography, surface roughness and obstacles. Boehme et al. [2006] used this method to create a wind speed time series for 1 km^2 grid squares covering Scotland, appropriate grid squares

were selected using their geographically constrained resource estimate described above. They simulated electricity generation using a single turbine curve. In a companion publication Boehme and Wallace [2008] describe the atmospheric and topographic data in more detail, these are covered in more detail in Chapter 4 and Chapter 6.

Brayshaw et al. [2011b] recognise the lack of operational data and the potential problems of using MIDAS data alone for wind power forecasting. They investigate the use of weather circulation patterns, using North Atlantic Oscillation (NAO) indexing as a supplementary data source. They characterise individual months of MIDAS data at two GB locations according to the NAO. Wind power output is then calculated over the extent of the turbine using Equation 2.1 (which is essentially the same rotor equivalent speed method explored by Clack et al. [2014a]) then divided by the swept area of the turbine to convert energy density to energy for different parts of the wind turbine curve. The effect of the NAO on turbine output is then investigated. The results show that wind generation is affected by the NAO, demonstrating the need for long time series that encapsulate variations in climate that may occur with a frequency of several years. This study demonstrates that the method can be applied to problems other than variability.

Other notable uses of the data and methods include Früh [2013] who looks for evidence of climate change in MIDAS data from Scotland finding step changes in wind generation, driven by annual changes in wind speeds and a slight reduction in the wind resource, but no conclusive evidence of the impact of climate change on wind speed and therefore generation. This finding is echoed by Pryor and Barthelmie [2010] who find no detectable change which would jeopardise the exploitation of wind energy in northern Europe. These studies raise an important point, which is that use of historic wind speeds may not represent the climate of the future.

The method applied by Brayshaw et al. [2011b] has the advantage of taking into account air density. Equation 2.1 shows that the energy in the wind is the cube of the wind speed, therefore small changes in wind climate can result in large changes in the wind energy [Pryor and Barthelmie, 2010]. Also that air density affects the energy density of wind and therefore turbine power output. Air density is inversely proportional to air temperature [Pryor and Barthelmie, 2010], this means that winter wind should be more productive in the UK when demand is greater.

Equation 2.1 Wind Power. E = energy density (W/m^2), p = air density (kg/m^2), U = wind speed (m/s).

$$E = \frac{1}{2}pU^3$$

2.1.4.2. Offshore simulation

There are very few stations that record UK offshore wind speed (Figure 2.3). As a result, some of the studies described above do not attempt to model offshore output. Others use additional methods to create wind speed time series. One method used assumes that the wind speed experienced at onshore coastal stations also represents offshore conditions. For example, 11 of the 30 regions modelled by Green and Vasilakos [2010] are offshore. The regions used by Oswald et al. [2008] also extend offshore, however, the use of onshore data alongside a small offshore turbine curve (2 MW) means that it is likely that power estimates using this method will be conservative. Although, as with all studies, if the output of smaller turbines is scaled up this error may be small, as most turbines have similar shape curves.

Boehme et al. [2006] use data from the Met Office Waters Wave Model to simulate wind generation. This dataset provides eight simulations of wind speed and direction each day at 10 m above sea level, at a spatial resolution of one-ninth of a degree of latitude by one-sixth of a degree of longitude. They use WAsP to create wind speed time series from this data at a resolution of 100 km by 150 km (this is a significantly coarser spatial resolution than the same study is able to use onshore). As with the onshore simulation a reference wind turbine is used to estimate electricity generation (5 MW). They placed offshore capacity in areas further than 5 km from shore, where sean depth does not exceed 40 m are there are no environmental protections in place. SKM [2008] provide more information on offshore locational factors used in their analysis, which include; wind speed, depth, distance to shore, proximity of connection points, environmental restriction, shipping and Ministry of Defence (MOD) areas with restricted access. This leads to the allocation of capacity in 9 broad geographical offshore areas. Four nearby met station time series are used for each site and scaled using statistical methods derived from the world wind atlas.

2.1.5. Simulation using reanalysis data

As a result of the disadvantages of station data, some researchers have looked for alternative data sources to drive simulations of wind generation. One option is climate reanalysis, which provide a global time series for a range of climate variables, on a gridded basis, at a number of different altitudes. All of the latest generation of climate reanalyses utilise a core of conventional data, including wind speed, temperature, moisture and air pressure, as well as other data including precipitation. Data sources change, due to new technologies being introduced; current platforms include, but are not limited to, radiosonde, satellite, buoys, aircraft and ship reports [Dee et al., 2014]. Data are run through a Global Circulation Model (GCM) in hindsight.

Reanalysis models are produced by a number of organisations including NCEP , ECMWF (European Centre for Medium-Range Weather Forecasts) and NASA (National Aeronautics and Space Administration) through the GSFC (Goddard Space Flight Centre) (also referred to as the GMAO (Global Modelling and Assimilation Office)). Table 2.2 shows the available climate reanalysis products from these organisations and several other significant datasets. The convention is to produce an analysis of the GCM every 6 hours. Two climate reanalysis products are available that provide forecasts from these 6-hourly analyses at an hourly resolution (the same as station data); NASA - MERRA [Rienecker et al., 2011a] and NCEP - CFSR [Saha et al., 2010]. These are what Decker et al. [2012] refers to as "second generation reanalyses", which build on previous versions by incorporating new data sources and improve the spatial resolution (see Table 2.2 for comparison). Modelling has also improved over the iterations; recent versions have built upon atmosphere only models to use coupled models (ocean-atmosphere-sea ice). CFSR and MERRA are based on the same set of observations and use similar models to extrapolate these data over space and time to the same temporal scope. CFSR is provided at a marginally finer spatial resolution (0.5^o x 0.5^o vs. 0.5^o v 0.66^0). Despite this, Decker et al. [2012] found that, globally, MERRA provides more accurate hourly wind speed data than CFSR in a comparison using flux tower observations [NCAR, 2013].

The hourly resolution of MERRA and CFSR mean that these datasets are more likely to capture extremes such as storm peaks than other reanalyses that provide data at 6 hourly intervals [Jørgensen et al., 2005]. Variability at a smaller temporal resolution (e.g. wind gusts) will not be captured by any dataset that provides hourly values; this requires either downscaling (which

is described in detail on page 43) or use of other data, for example from MIDAS (such as daily maximum gust speed, analysis of which has been carried out by Hewston and Dorling [2011]). Reanalysis GCM's operate at a temporal resolution of around 20 minutes, but results are always aggregated over longer periods.

Access to the data is not as straight forward as MIDAS data and requires a little more knowledge and programming skill. Over the course of this study ease of access has improved, at least in the case of CFSR, data can now be downloaded through a web interface rather than an FTP, although the file format still negates widespread use, as it is only conventional in meteorology. Reanalyses have been used for aggregated estimates of the wind resource, such as those described above, here only those looking at the variability of wind speed are of interest and are therefore described below.

Dataset	Spatial Resolution (degrees)	Finest Temporal Resolution	Tempoal Scope	Reference(s)
NCEP - NCAR (R1)	2.5	6 hours	1948 - present	Kalnay et al. (1996), Kistler et al. (2001)
NCEP - NCAR (R2)	2.5	6 hours	1979 - present	Kanamitsu et al. (2002
NCEP - CFSR	0.5	1 hour	1979 - present	Saha et al. (2010)
NCEP - FNL	1	6 hours	1999 - present	
ECMWF - ERA15	2.5	6 hours	1979 - 1993	Gibson (1997)
ECMWF - ERAinterim	~ 0.7	6 hours	1979 - present	Simmons et al. (2007)
ECMWF - ERA40	1.125	6 hours	1958 - 2000	Uppala et al. (2005)
GSFC - MERRA	0.5 x 0.66	1 hour	1979 - present	Bosilovich (2008), Rienecker et al. (2011)
NOAA - ESRL 20CR	2	6 hours	1871 - 2010	Compo et al. (2006), (2011)
JMA - JRA25	1.25	6 hours	1979 - present	Onogi et al. (2007)

Table 2.2.: Summary of the range of climate reanalysis datasets

2.1.5.1. Onshore

All of the studies that have used reanalysis data to simulate wind turbine generation in GB have used MERRA data, with the exception of Hawkins et al. [2011]. The largest centre for this type for this type of research in the UK is Reading University, other universities using reanalysis data in wind generation simulations include Imperial College London, Strathclyde University and the University of Edinburgh . Reading provide an extraction tool for MERRA which circumvents some of the difficulty in the use of CFSR. This tool was used by Ofgem [2012c], which is cited by Staffell and Green [2014] as the first practical application of reanalysis data to the simulation of wind turbines. Ofgem's (Office of Gas and Electricity Markets) capacity assessment uses MERRA to simulate historical capacities at UK wind farms. It is not explicitly stated but it is likely that the nearest grid point value is used, a generic turbine curve is used for simulation. Comparison against monthly ROC data shows that this method overestimates winter onshore capacity factors (average 36% compared to 30%), this is despite wind speeds being reduced by 1.2 m/s after finding overestimation in comparison to 7 MIDAS stations. The overestimate of simulated power is attributed to turbine availability, turbine curve selection, capacity level changes over time, quality of ROC data and wind speeds. No mention is made of correction of wind speed to hub height at any point in the report.

Several papers have been published by researchers at Reading using MERRA data. Kubik et al. [2013a] bi-linearly interpolated one year's worth of data MERRA data to the location of 8 met stations in Northern Ireland to the nearest 0.1°. After height correction to 60 m, a single 2.5 MW turbine curve was used to simulate output for both the MERRA and met mast data. The

output was scaled to national capacity (289.5 MW). Results show that the simulation from the reanalysis data is more closely correlated to measured generation data (half hourly) and the Root Means Square Error (RMSE) is lower. Analysis raises concerns over low readings from mast data, attributed to anemometer sticking and high readings from both datasets, this is attributed to the lack of allowance for turbine availability.

The study published by Cannon et al. [2015], also produced by Reading based researchers, represents the most recent development in the harnessing of reanalysis data for wind simulation and has been published at the very end of this project. MERRA data is bi-linearly interpolated to the location of wind farms operating in 2012. Hub height correction is performed in per farm basis but a single archetype curve representing a 2.3 MW turbine is used to simulate the capacity at each site (a static annual capacity is used with no changes modelled during 2012). As well as a manufacturer curve, two adjusted curves are examined, the first made using advice from National Grid, reduces the maximum output to take account of wake losses, turbine availability and ageing (this advice is not publicly available). Interestingly the curve is adjusted so that turbines come back online at 21 m/s after cutting out at 25 m/s, this method is not used elsewhere. The second curve is referred to as an "Ofgem curve" which is that used the latest Ofgem electricity capacity assessment, an example of a curve produced using the multi turbine curve approach. Comparing the output to measured generation they find a correlation coefficient of 0.96 for both curves (no statistical difference in output), this suggests that MERRA data is accurate and their method makes good use of it. They also go further and look at how MERRA predicts changes in power output over different time scales, finding that correlation improves as the data is aggregated (3 hours R = 0.77, 6 hours R = 0.86, 12 hours R =0.93), overall they find that MERRA underestimates short lasting events and overestimates long lasting events, the most extreme events are reproduced well. The outputs of the simulation are also used to investigate extreme wind generation events.

There is research being conducted by researchers at other universities. Staffell and Green [2014] perform the most spatially disaggregated analysis of GB wind turbine output to date, in an analysis of the reduction in wind turbine performance as they age. They use MERRA data and interpolate to the location of a wind farm. The use of a location specific approach means that, in contrast to other studies, the hub height and turbine curve matched the wind farm being simulated. A multi turbine curve approach as described by Norgaard and Holttinen [2004] is used, it is still necessary to apply a correction factor to reduce the error in comparison to ROC and Elexon data. Results are very good, as described in detail in Chapter 3.

Alternative uses of reanalysis wind speed data Reanalysis data allows the extension of methods to greater geographical scopes. Examples of this include Czisch and Ernst [2001], who look at a wind supply system across Europe and North Africa. This is facilitated through the use of ERA 15. The 6 hourly product is used to simulate output using 1.5 MW turbines at 80 m. They build on the analysis of correlation between theoretical wind farms at different locations by analysing the correlation of the change of wind power over different time spans, finding that, over larger distances (up to 600 km), long term fluctuation (12h) can be reduced as well as short term (5 minute). As with met station data, there are studies that are investigating the use of reanalysis datasets for evidence of climate change and the impact that this will have on wind generation in the UK [e.g. Cradden et al., 2014].

Interpolation and downscaling The studies described above have interpolated wind speed data to a point or smaller grid square using statistical techniques which utilise a number of grid point values from MERRA. The most widely used method is bilinear interpolation which uses the four closest grid point values and assumes that wind speed is more likely to be similar to the closest point. This method does not take into account any physical factors which influence changes in wind speed such as topography.

An alternative, more sophisticated, method for estimating wind speed at a finer spatial resolution than provided by raw reanalysis data is to use mesoscale modelling, which is also referred to as dynamical downscaling. Atmospheric mesoscale modelling is operated over the scope of a few hundred kilometres at the spatial resolution of a few kilometres Landberg et al. [2003]. Mesoscale models generally operate by reanalysing a large scale climatology using a dynamic statistical approach [Landberg et al., 2003], which provides a gridded dataset at a finer spatial resolution than the input reanalysis data. These benefit in terms of wind speed from the use of land use mapping and orography data, therefore taking into accoutre physical factors. Another benefit of the approach is the preservation of the homogeneous nature of the base reanalysis dataset. To achieve very fine resolutions (less than 1 km) require a huge amount of computing power, but these have the potential for representing atmospheric and terrain conditions that influence wind winds at the smallest scale. Both statistical interpolation and mesoscale modelling have provided very accurate results, as described in Chapter 3. The drawback of downscaling, particularly mesoscale modelling, is that it is extremely computationally intensive and therefore not always practicable.

Hawkins et al. [2011] use mesoscale modelling, with the NCEP FNL model providing boundary data to the Weather Research and Forecasting (WRF) model [Skamarock et al., 2005], to create a ten year time series at the spatial resolution of 0.1°. No details are given for onshore simulation as the focus is offshore, but they achieve a very high R^2 (0.94) after applying a linear correction factor to take account of drivers that have not been modelled.

2.1.5.2. Offshore

There are only two studies to date which simulate offshore wind capacity using reanalysis data. Ofgem [2012c] use the same method as onshore and find that winter capacity factors are again overestimated (41% compared to 36%). Hawkins et al. [2011] use the same method as described above, wind capacity is placed in round 2 sites using a 3 MW turbine for simulation and round 3 sites using a 5 MW turbine (see Chapter 6 for a discussion of offshore wind farm development zones). They describe high correlation with in situ measurements. A scaling factor to reduce error was not necessary offshore, but breakdowns and maintenance (referred to as technical availability) was found to have an effect.

There are a number of studies which compare reanalysis data, raw, interpolated and downscaled, onshore and offshore, to in situ wind speed measurements, these are discussed in detail in Chapter 3.

2.1.6. Review of wind turbine simulation

An established method for simulating wind generation from historical wind data has been described. Adaptations of the method to take into account some of the factors that cause loss from wind

turbines have been identified. Two sources of wind speed data have been described and the users of this data in UK research summarised. The most widely used data source for this type of simulation has been weather station data in the form of MIDAS. The studies using MIDAS data to investigate impacts of variability do so either by assuming that a subset of the stations represent the wind conditions over GB, or by selecting a station to represent a region. There are a number of issues with station data, including station location, data quality and availability, that mean neither of these methods is ideal. All of these studies find it difficult to model offshore output, due to the lack of offshore measured wind speed data.

Reanalysis models can be used to estimate wind speed over long time periods at any onshore or offshore UK location, as they produce data for the entire planet for up to 30 years. Therefore simulations of wind generation can be performed across a large spatial area without the drawbacks of irregular and discontinuous data that are encountered when using synoptic weather station data. The use of reanalysis for wind turbine simulation in GB has, however, been limited. The first of the studies reviewed above was published in 2012. MERRA has been used for almost all of this research, which has paid significant attention to the accuracy of the data to establish its validity. The outcomes of these evaluations are promising, high levels of accuracy are demonstrated. There is no use of CFSR in GB specific studies, despite the slightly enhanced spatial resolution compared to MERRA. This may be because wind speed is provided at multiple heights in MERRA, aiding interpolation to hub height, which is where wind turbine curves measure the relationship between power and wind speed. There is some use of CFSR in studies of other European countries. A number of studies compare wind speed data from different reanalyses, these are summarised in Chapter 3.

The studies using a reanalysis either interpolate or downscale the data. Kubik et al. [2013a] argue that dynamical downscaling is possibly too computationally intensive to be practical, and show that it is possible that MERRA data may be useful in its raw form. Here the same question will be asked in the context of CFSR without the use of interpolation or downscaling, adopting an approach similar to the regional studies using MIDAS data. The use of a regional approach with CFSR data reduces the spatial resolution to approximately 30 - 50 km^2 and increases the number of regions to over 200 onshore, in comparison to the largest existing study with MIDAS data using 30 including offshore. This will allow the exploration of multiple scenarios of wind capacity, something that *none* of the studies reviewed above consider. Provided that CFSR can be shown to represent the conditions within these regions, or grid squares, adequately this approach will allow an analysis of spatial scenarios of capacity more easily than if the wind speed must be interpolated to the site of each wind farm under different scenarios. This approach also means that suitable sites for wind farm development can be identified as an area within a grid square, rather than a specific site, which may be an unrealistic level of precision.

Reanalyses have been recognised as the "best approximation of the state of the atmosphere based on both data and dynamic models" [Decker et al., 2012, p. 1917]. However, several problems remain. First, the wind speed is homogeneous across the whole of a grid square, which onshore may incorporate variable terrain that can alter wind speed. It is well recognised that gridded weather data can result in extreme values being misrepresented [Ensor and Robeson, 2008]. Data, as with MIDAS, are provided at 10 m above the surface (offshore buoy data at 6 m) and therefore reflect the state of the climate near the Earth's surface and are subject to the influences surrounding the station including (e.g. topography), which may not be evident at turbine height. These issues,

alongside the planned regional approach, mean that it is necessary to evaluate the weather data from reanalyses as comprehensively as possible. Comprehensive evaluation is possible through the use of in-situ measurement of both weather data and generation data. GB is well covered in that respect with weather data from MIDAS and generation data available in the form of hourly generation by fuel type from Elexon [2014b] and monthly aggregated generation from wind farms that are part of the Renewables Obligation Certificate (ROC) scheme. The evaluation of reanalysis data with respect to in situ measurements is covered in Chapter 3 and the simulation of wind output using this data, including evaluation against measured data, is covered in Chapter 4.

2.2. Wind supply and electricity demand

The review to this point has shown that there has been extensive research on the spatial variation of wind in GB, that has been complemented by temporal and spatiotemporal analysis of the wind resource. To understand the value of electricity produced by wind turbines it is also necessary to examine these spatiotemporal dynamics alongside electricity demand. Some of the studies reviewed above have done this. All of the studies reviewed above that have considered demand in the analysis of an electricity system featuring wind have done so by using measured demand.

2.2.1. Methods used by wind variability studies

2.2.1.1. Raw national values

A number of these studies have used measured demand without altering the data. This has been done by studies that are not considering future capacities, but rather the characteristics of the wind resource. For example SKM [2008] carry out significant analysis of supply vs. demand at an hourly national resolution, they assume that there is no growth in electricity demand, the peak remains at 63.3 GW and the annual total at 375 TWh. The most likely source of demand data is the half hourly data from National Grid, although this is not explicitly stated. SKM carry out an analysis of network flows based on divisions created around critical network boundaries. As described above, renewable generation is estimated at a geographically disaggregated resolution. The method for spatially disaggregating demand data is not described. A result of the lack of growth in electricity demand is that their analysis of the need for grid reinforcement is likely to lead to conservative estimates and the lack of detailed spatial disaggregation of demand means that it could well be performed in the wrong place. Pöyry [2009a] use hourly demand data for the same period as the wind modelling (2000 - 2007) from National Grid and EirGrid.

Spatial Subset A lack of comprehensive data in the past has lead to some studies not being able to use data that covers the whole of GB or UK. Sinden [2007] uses hourly electricity demand data for an 8 year overlap period with the wind speed measurements and simulated wind power output described above. The data only represents England and Wales, whereas the supply data covers the UK. The study does, however, deal in detail with the relationship between demand and supply. Coker et al. [2013] use demand data for a single grid supply point from National Grid, which provides accurate data for a small area. This would be an interesting method to explore if the data were publicly available over a larger geographical scope, their study is limited to a single

year. Zachary et al. [2011] use England and Wales data to represent peak demand, stating that it makes up 90% of demand at peak times.

Temporal subset Some studies focussing on extremes have used a temporal subset of data which is chosen, for example, to represent periods of high demand and low wind. Oswald et al. [2008] model January wind output. Their selection of demand periods is interesting as they explore the idea that peak demand occurs at times of low temperature and high winds. They find that the load factor of modelled wind varies during these periods, but can be 0%, though this only occurs once. They link these periods to low pressure weather systems over GB and show that these extend across Europe, demonstrating that this situation may result in a load on alternative electricity sources over a large geographical extent. Zachary et al. [2011] look further into the weather patterns that drive periods of peak demand, finding that extreme demand events are "typically associated with the advection of cold air into Britain from the north or east" (p. 1). Their analysis covers peak demands over 9 years.

2.2.1.2. Statistically altered national values

There has been some recognition that demand will grow in the future in studies which use historical data. This is predominantly dealt with through simple growth factors. Boehme et al. [2006] use total system demand from Scottish Power and Scottish and Southern Energy for a period covering 2001 - 2004. Where the two datasets do not overlap, demand is estimated using demand curves at different levels of temporal aggregation from other years, which are then mapped onto the desired period. The resultant time series is scaled to 2020 assuming an annual growth factor of 1%, no changes are made to the temporal patterns of demand. This method results in a prediction of peak electricity demand of 72.9 GW and average electricity demand of 41 TWh (p. 40). In contrast to the single forecast of demand, the study uses scenarios of supply with 750 MW, 1.5 GW, 3 GW and 6 GW of capacity assigned to different technologies based on price. Area scenarios are also examined, dividing Scotland into 10 zones. This highlights the power of their approach in terms of the ability to spatially disaggregate. Little information is given on the spatial disaggregation of demand scenarios, only a note stating that "appropriate" time series were chosen (p. 44). Green and Vasilakos [2010] use measured demand data, scaled to 2020 using Supergen Futurenet scenarios. They note that there is no allowance for the impact of climate change on demand.

Hawkins et al. [2011] use half hourly data from National Grid, normalising to an "Average Cold Spell" and scaling so that peak demand reaches 60 GW. The results are compared to the hourly load factors of the simulated output described above. Only winters (November - March) are investigated, as this is when electricity demand is at its highest. The relationship between peak demand and load factor is examined, alongside loss of load probability, loss of load expectation and capacity credit using the Effective Load Carrying Capability (ELCC) approach (see [Dent et al., 2010] for an explanation of this method) including the modelling of other generation types. Their handling of capacity growth is interesting as it uses the crown estate auctions and weights load factors based on capacity in each location and the results of the previously described modelling. This is one of the better spatially explicit capacity projections of the UK and the only one that covers offshore. However, given the very fine resolution of the weather data, it would have been possible to take further steps, especially considering the considerable effort made to create mesoscale wind data.

Their eventual findings suggest a capacity credit of 10%. This is the only study simulating turbine output using reanalysis data that compares supply and demand.

Temporal subset Strbac and Ilex Consulting [2002] depict different scenarios of demand based on growth rate, but only apply these to demand profiles for a single day. They use this data to analyse the costs of integrating increased wind at a range of temporal resolutions, all at the national level, despite modelling spatially disaggregated supply, because demand is national. They look at a number of short term issues including response, reserve and curtailment.

2.2.1.3. Summary

The use of historical demand data in analyses of the characteristics of the wind resource with respect to electricity demand is appropriate. Studies using this data to investigate the impact of future wind capacities have, however, only used simple adjustments to measured electricity demand data. This means that the only change to electricity demand has been growth. There is no recognition of the fact that the temporal pattern of demand will change if any of a number of technologies are integrated into buildings and transport. There is also no explicit consideration of population changes. There has also been no consideration of the effect of the spatial weighting of these changes. Despite this, the approaches described above offer a potentially very strong basis for modelling demand alongside supply as they have made significant steps in the spatiotemporal modelling of weather in the context of one part of the electricity system, which is also a major driver of demand.

All of the studies reviewed with respect to electricity demand are very careful in the way that they deal with weather on the supply side. By using measured demand they rely on the fact that the weather conditions represented by this weather very closely matches that experienced in reality over both space and time. Yet, that may not be the case, as described above, neither station data or a reanalysis can be a perfect representation of the weather system. If demand is modelled using the same weather data as supply then this issue can be alleviated to some extent, as changes in weather will be mirrored in both sides of the equation. There are a number of methods already utilised in the literature which can be used to harness the power of a climate reanalysis at the same spatiotemporal scope and scale as the proposed wind modelling.

2.3. Modelling GB electricity demand

In order to depict electricity demand into the future it is necessary to incorporate demand from all sectors. It is the intention, however, to focus efforts on changes to the domestic sector, in particular heat demand. Heat demand from buildings is affected by weather, therefore electrified heat demand has potentially interesting impacts on residual demand after wind supply has been taken into account. This new electricity demand has arguably the largest potential to change the temporal patterns of the national demand profile. The investigation of electrified heat therefore offers a perfect vehicle for the exploration of the use of climate reanalysis for driving demand modelling, and ideal companion to the wind modelling. There are a number of possible changes to the system such as demand side management and electrified transport which also have significant

impacts on when electricity will be demanded, however these changes to demand in non domestic buildings, industry etc. are outside the scope of this thesis.

The focus of this review is therefore methods and models that can be used to depict future changes to electricity demand in domestic dwellings, with an awareness that methods must also be developed to incorporate national demand for electricity from other sectors.

2.3.1. Models

There are a number of approaches to modelling the consumption of energy in buildings. Many studies have attempted to classify these approaches. These classifications are well reviewed by Fumo [2014], so will not be described in detail here, instead a common approach, used by Swan and Ugursal [2009] is adopted, which defines models as top down or bottom up. There are also models which use both methods, these are often referred to as hybrid models, a term which can be used for any model that combines multiple approaches. Figure 2.4 describes model classifications from the reviews using top down and bottom up descriptions.

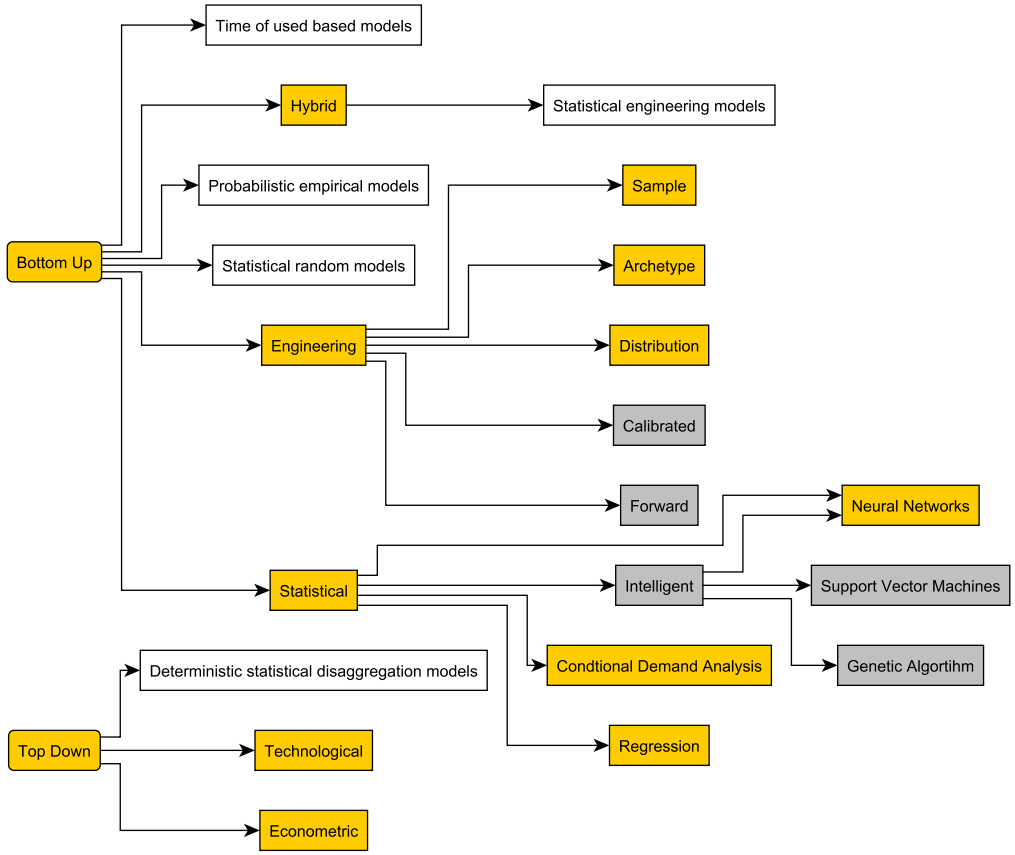

Figure 2.4.: Methods for modelling energy consumption, yellow boxes are classifications from Swan and Ugursal [2009] and Fumo [2014], grey boxes from Fumo [2014] only and clear boxes from Grandjean et al. [2012].

There are a number of comprehensive reviews of energy demand models and methods. These are referenced where relevant, for further details on specific models; Swan and Ugursal [2009], Fumo

[2014] and Pedersen [2007] concentrate on building energy demand. ASHRAE [2013] comprehensively review modelling methods. US DOE [2014] maintain a comprehensive list of tools that can simulate various aspects of energy demand from the smallest element to the whole building. Zhao and Magoulès [2012] review models which predict energy consumption including those which include artificial intelligence. Pedersen [2007] cover some of the input data for building energy model including weather files. Fumo [2014] and Foucquier et al. [2013] provide a comprehensive review with a focus on US studies. Grandjean et al. [2012] give in depth analysis of fewer studies under their own classification scheme (Figure 2.4) including flow diagrams. Kavgic et al. [2010] review bottom up building physics based models used in GB research. Suganthi and Samuel [2012] offer a comprehensive review covering economic models and Swan and Ugursal [2009] focus on models of regional or national demand as a sum of the constituents.

2.3.1.1. Top down

According to Swan and Ugursal [2009], top down models regress the consumption of a stock of buildings as a function of top level variables, e.g. macroeconomic indicators. Energy demand for the entire sector can be attributed to sub sectors, but they suggest that the top down approach is not concerned by end uses. They define two types of top down models; econometric which primarily model energy use in relation to economic variables (e.g. income, GDP and fuel price) and technological, based on other variables, for example technological progress and structural change [Kavgic et al., 2010]. Both methods require historical data on energy use and drivers of demand.

Tornberg and Thuvander [2005] produced an example of a spatially explicit top down energy model using the building register of Göteborg containing details on over 68,000 buildings. They distribute energy data from an energy supplier to buildings, based on usage and age, spatial analysis and visualisation is used to identify areas of high demand. An example of a top down model of the UK housing stock is the annual delivered energy price and temperature model developed by Summerfield et al. [2010], which is based on average heating season temperature and inflation adjusted energy price; it is a regression model. They use this model to investigate the consequences of changes in temperature and energy price on demand for energy in dwellings. The method is widely used in scenario planning where only aggregated values are required.

Advantages of top down models Grandjean et al. [2012] state the advantage of this type of model as simplicity and ease of comparison with published consumption statistics. Top down models have the advantage of the need for only simple input data and relying on historical data means that general patterns are incorporated, as Swan and Ugursal [2009] point out, paradigm shifts such as electrification are rare. This is particularly the case with econometric models as the focus is on macroeconomic variables [Kavgic et al., 2010]. Kavgic et al. [2010] state the advantages of this type of model as the ability to model the interactions between the economy and energy demand using aggregated economic data, the ability to avoid detailed technology descriptions and the ability to model the impact of different policies.

Disadvantages of top down models Kavgic et al. [2010] state the disadvantages of this method as the dependence on past energy economy interactions to project future trends, the lack of techno-

logical detail which makes technology specific scenarios such as electrified heat difficult to model, and the assumption of efficient markets. In the context of this study the major disadvantage of this type of model is the inability to model technical breaks or new end uses, due to the dependence on historical data. This means that it is unlikely that using this method alone will be suitable for modelling electrified heat and it will be necessary to explore complementary methods.

2.3.1.2. Bottom up

Grandjean et al. [2012] define bottom up models as those which compute demand for representative households, then extrapolate the results to the desired geographical scale. Kavgic et al. [2010] describe them as "built from data on a hierarchy of disaggregated components, that are then combined according to some estimate of their individual impact on energy use" (p. 1684). Swan and Ugursal [2009] considers the bottom up approach to be one where energy demand from a sub set of buildings is extrapolated to regional or national levels. They define sub methods as either statistical, where historical information and regression analysis attributes energy consumption to end use, or engineering, where power ratings and system uses and thermodynamics are used. Fumo [2014] looks further at bottom up approaches and classifies sub sectors exploring intelligent statistical methods in the form of genetic algorithms, neural networks and support vector machines. Fumo also adds forward, which uses known relationships to predict output, known data is used to define a mathematical description of the system, these are taken from ASHRAE [2013]. Figure 2.4 shows the merged classifications from Swan and Ugursal [2009] and Fumo [2014]. Those methods marked as intelligent in the figure include the use of artificial intelligence in modelling, it is not the intention to use any of these methods in this study, therefore they have not been reviewed, see Zhao and Magoulès [2012], Foucquier et al. [2013] and Fumo [2014] for more detail.

Statistical bottom up Statistical bottom up methods rely predominantly on billing data, which is not available for this study but can use other measured data, Swan and Ugursal [2009] summarise methods and studies.

Engineering bottom up Zhao and Magoulès [2012] define bottom up engineering models as those which "use physical principles to calculate thermal dynamics and energy behaviour on the whole building level or for sub-level components" (p. 3587). Swan and Ugursal [2009] identify three types of engineering method.

1. Distributions: appliance ratings and distributions are used to calculate energy consumption. These can also include population distributions or potentially building stock distributions.
2. Archetypes: housing stock is broadly characterised by vintage, size, house type etc. Energy demands are classified using these archetypes and they are scaled up to the desired scope. Archetypes can be developed based on a number of criteria. Examples of this type of model in the UK are predominantly based on Building Research Establishment Domestic Energy Model (BREDEM), some are also based on the Standard Assessment Procedure (SAP). These models are often referred to as building physics models and are summarised in more detail in Section 2.3.1.3.

3. Sample: Empirical data for representative buildings are scaled up. No sample studies of GB are cited by Swan and Ugursal [2009], however, samples may contain archetypes and can then be built up.

Advantages of bottom up models Swan and Ugursal [2009] cite the strength of this type of model as the depth of information incorporated; including dwelling characteristics, equipment information, occupant behaviours and climate information, leading to the ability to model technological options. This offers a clear solution to modelling heat demand and electrification of heat. Grandjean et al. [2012] state the advantage as the ability to model high level demand and therefore represent evolutions without the need for historical data. Zhao and Magoulès [2012] state that statistical bottom up models are easy to develop, but may be inaccurate and inflexible. Kavgic et al. [2010] state the advantages of statistical bottom up models as the inclusion of macroeconomic and socio-economic effects, the ability to determine typical end-use energy consumption, ease of development and the lack of requirement for detailed data. They state the advantages of bottom up engineering models as the ability to describe current and prospective technologies in detail, the use of measurable data, the ability to target policy, the ability to quantify the impact of different combinations of technologies and estimate the cost of technological measures.

Disadvantages of bottom up models Bottom up models, at least the engineering based models, may be difficult to perform in practice due to high complexity and the need for large amounts of input data. Grandjean et al. [2012], Zhao and Magoulès [2012] and Kavgic et al. [2010] state the disadvantages of bottom up statistical models as the limited capacity to assess the impact of energy conservation measures, reliance on large historical samples and lack of flexibility. They state the disadvantages of bottom up engineering models as the neglect of the relationships between energy use and macroeconomic activity, the poor description of market interactions, the need for large amounts of data and the need for external assumptions to determine human behaviour.

2.3.1.3. BREDEM and SAP based models

As stated above, the basis for the majority of bottom up models of domestic energy demand in the UK is BREDEM. BREDEM [Dickson et al., 1996, Anderson et al., 2002] is a bottom up, physics based model which uses empirical data, heat balance equations and empirical relationships to derive annual or monthly energy demands. The combination of these elements depends on the version. Four end use types are modelled; space heating, hot water, cooking, lights and appliances. The model is modular, which means that elements can be easily adapted. Electricity demand from lights and appliances is calculated based on relationships between occupancy and floor area; this element is changed most often. Algorithms developed by the Domestic Equipment and Carbon Dioxide Emissions (DECADE) team at the University of Oxford are regularly used.

SAP is an implementation of BREDEM, developed in the 1980's, intended to be simple but realistic, it is a compliance tool and is designed to rate the performance of a building rather than predict consumption. SAP has been criticised for inaccurate representation of energy flows within low energy housing [Reason and Clarke, 2008] and gaps have been found between real and estimated dwelling performance from SAP [Hong et al., 2006]. There are problems associated with calculating energy use from water heating, cooking, lighting and appliances [Lowe, 2007].

The main differences between models that have been based on BREDEM and SAP are the number of archetypes and the analysis performed on the outcome. Although the models "generally have the ability to estimate the baseline energy consumption of the existing housing stock and predict the future energy demand, energy saving and CO_2 emission reduction for a variety of scenarios." [Cheng and Steemers, 2011, p. 1187]. All of the studies use the English House Condition Survey (EHCS) or the English Housing Survey (EHS) which is a combination of EHCS data and data from the Survey of English Housing. These surveys contain information on a number of characteristics of a subset of dwellings in England (approx. 17,000), similar surveys of other UK countries exist, but they are used less in these studies. These datasets provide the ideal basis for the creation of archetype or sample based bottom up engineering models. The multiple variables recorded including type (e.g. detached), age etc. allow a large number of combinations of the variables and therefore archetypes.

The models are reviewed in detail by the review papers cited above, in particular Kavgic et al. [2010]. Therefore, they are only briefly summarised here, specific details on method, variables and datasets in demand modelling are covered in Chapter 5. Shorrock and Dunster [1997] use 1000 categories in BREHOMES to model annual energy demand, these are defined by age group, built form, tenure type and ownership of central heating. Jones et al. [2007] use OS data to calculate floor area and other geometric features, then augment this with historical data and drive by surveys to include other aspects such as building type, age and window area in the Energy and Environment Prediction model (EEP). These details are run through SAP with estimations of other features. They analyse some spatial aspects of energy demand in buildings such as clustering and average demand per ward. This is one of the few explicitly spatial methods, but could not be carried out on a national scale without significant automation. This spatially explicit method allows them to link with other spatial data and include analysis of health implications, highlighting the advantage of a more spatial approach.

Yao and Steemers [2005] consider household composition, occupancy patterns, energy consumption and ownership of different appliances in detached, semi detached, mid terraced and flats and generate random daily aggregate energy consumption profiles for different scenarios. Good agreement with national statistics is shown, results are within 3.4% of annual gas demand and 1.0% of annual electricity demand. National statistics on energy demand in domestic buildings are often outputs of analysis performed using the Cambridge Housing Model (CHM) (see below), as a result of the limited availability of empirical data. This means that many models are evaluated against modelled data. Yao and Steemers [2005] evaluate their outputs at a spatially disaggregated resolution using DECC's sub national statistics. They evaluate against Local Authority level data, scaling demand using dwelling numbers from the 2001 census. They find a high correlation (0.943 for gas and 0.974 for electricity) and low mean absolute errors (15.1% and 9.5%), albeit with annual values. The work of Yao and Steemers [2005] is built upon in the Domestic Energy and Carbon Model (DECM) by Cheng and Steemers [2011] who augment SAP with BREDEM algorithms and deal explicitly with temporally disaggregated demand. This is the only one of the bottom up studies reviewed here which considers demand at a temporal resolution finer than a month. SAP and BREDEM assume 9 hours of heating a day on weekdays and 16 hours a day on weekends, this allows comparison of energy demand between dwellings but does not reflect the usage patterns in real houses. Cheng and Steemers [2011] use occupancy hours based on employment status.

Johnston et al. [2005] produce what they term a selectively disaggregated model, based on BREDEM.

They use just two dwelling types, dividing by age rather than the archetypes seen in other studies, they justify this on the basis of data availability and that dwelling type has a lesser effect on energy demand than building fabric and system efficiencies. This is a valid point but does not recognise that these characteristics are built into archetypes in other studies. The age defines the building size, occupancy levels, fabric, internal temperature, space and water heating efficiencies and appliance consumption. These are then used to explore the carbon dioxide emissions of the building stock under different scenarios to 2050. The study uses national annual values with no spatial or temporal disaggregation performed.

Oxford University's 40% house project uses the UK Domestic Carbon Model (UKDCM). The model is described in ECI [2005] and their results are analysed in Boardman [2007]. In contrast to Johnston et al. [2005], they use very large number of archetypes (approximately 20,000). Their stock model projections are more sophisticated than other studies, as demolition of old stock is taken into account, as well as new construction, changing house size, altering building characteristics and changing demographics. They use EHCS data, but supplement this with other national surveys.

Natarajan and Levermore [2007] model increased population and efficiency measures and decreasing household size to depict dwelling numbers in their Domestic Energy and Carbon (DECarb) model. Monthly average gridded climate data provided at 50 km grid are averaged to 300 km to give four UK regions, this is used to model energy demand for 64 unique combinations of dwellings in 6 age bands. Results are shown to be within 5% of national statistics.

Firth et al. [2010] model 47 archetype dwellings in 9 age bands in the the Community Domestic Energy Model (CDEM), at a national, city and neighbourhood resolution to predict the CO_2 emissions of future housing stock, concentrating on uncertainty in the model and performing a sensitivity analysis.

Cambridge Housing Model The Cambridge Housing Model, based on SAP and BREDEM building physics, calculates emissions and energy demands from the English housing stock using EHCS and EHS data to determine the characteristics of the stock [Cambridge Architectural Research, 2014]. Data from this model is used widely in UK energy demand research, as it provides a large amount of data for DECC, which is disseminated in the DUKES database. The downfall of the model, with respect to this study, is the low spatial and temporal resolution of the data. In particular weather data, which is provided as monthly mean values by region. Because of this scaling, demand cannot follow regional variation well. The coarse temporal resolution means that this variation may not make a difference. However, clearly this model is not appropriate for exploring demand variation at fine spatial and temporal resolution.

Summary The above review has shown has shown that there are a significant number of models simulating the energy demand of the UK housing stock. All of the methods summarised above are based on the same underlying model. This is a bottom up engineering model so is subject to the advantages and disadvantages described above. More specific advantages include the well established nature of the modelling, the transparency (as the basic model at least is publicly available), the model has been based on measured data, it has been improved over time and it is well documented. Specific disadvantages include the fact that many of the energy demands are

based on simple relationships and that it is very generalised. Crucially in the context of this study the model is not temporally disaggregated. There has been some effort from, for example, Cheng and Steemers [2011], to include better time of use profiles, however other studies focus on annual or monthly demand. Because the aim of this study is to analyse the temporally disaggregated demand profile with respect to wind these models are therefore not suitable in their current form. Another issue is the way in which the models handle weather, this is currently highly aggregated, with few regions and often temporally averaged values, this is clearly an aspect which can be improved through the inclusion of climate reanalysis data.

Spatial aggregation and disaggregation The archetype bottom up energy demand modelling method is most often aggregated to a national resolution using national statistics. Yao and Steemers [2005] have aggregated to Local Authority level using 2001 census data. Outside of the UK Tornberg and Thuvander [2005] have used the method the other way to disaggregate in the top down model. Heiple and Sailor [2008] have used a building stock database and attach metered and modelled consumption profiles for a subset of these buildings. Sorenson and Meibom [1999] consider demand on an area basis, using population density distribution data redistributed to a 0.5^{o} grid and United Nations (UN) population projections and assumptions on energy demand per capita to give a very simple version of a spatially explicit energy demand model. Sailor and Lu [2004] also disaggregate through population densities, demonstrating that there are other spatial datasets and potentially other parts of the census which can be used for extrapolating the bottom up models and disaggregating top down models. These data and methods for aggregation and disaggregation are explored further in Chapter 5.

Temporal disaggregation None of the models reviewed above are spatially explicit temporally disaggregated models. There is reference to the creation to the creation of a load curve for the residential sector in Grandjean et al. [2012], which recognises the need to model demand a temporally disaggregated resolution, as two buildings with the same annual or daily demand and similar characteristics (e.g. household size, dwelling type, appliances etc.) may have very different load curves due to human behaviour. The classifications described in Figure 2.4 show that this recognition leads to Grandjean et al. [2012] regarding models in a different way, describing deterministic statistical disaggregation models as those which disaggregate measured load curves to identify end uses and statistical random models as those which generate curves in a random procedure. Probabilistic empirical models define probabilistic procedures based on real collected data and time of use models construct diversity from time of use surveys. Finally the statistical engineering model adds diversity to measured data through statistical coefficients.

DEAM Models do exist which incorporate both top down and bottom methods and have the ability to temporally disaggregate. These hybrid models offer the potential benefit of being able to use the best elements of both approaches. One of these models is the Dynamic Energy Agents Model (DEAM). DEAM was developed by Barrett and Spataru [2014] to represent energy demand and supply from both consumers (in the domestic, non domestic and transport sectors) and suppliers, as agents, both in the present energy system and under future scenarios. These agents demand energy for different end uses (lighting, heating, hot water etc.) and meet these end uses using energy converters (boilers, solar panels, etc.). Where needs are not met by on site generation,

public energy suppliers deliver energy (electricity, gas, heat, etc.) to consumers to satisfy the remaining demand.

DEAM is designed to depict energy demand and supply at a half hourly temporal resolution and can operate at a range of spatial scales within the GB energy system. The model has been used previously to calculate the energy flows for agents connected to a local electricity substation, to investigate the possible future loads using a representative set of data from the Distribution Network Operator (DNO), Western Power Distribution (WPD)[Barrett and Spataru, 2012]. The model has also been applied to analysis of grid supply point demand in collaboration with National Grid.

DEAM uses two distinct methods for calculating end use demands, the first method is calculated top down and encompasses those demands which *are not* influenced by building fabric, defined here as non space heat demands. This method relies on input data which predict future energy demand, therefore will rely on statistical regression modelling being performed elsewhere. The second method encompasses space heating and cooling demand which *are* influenced by building characteristics, these demands are calculated bottom up, using similar methods to BREDEM. DEAM is described in the context of the modelling in Chapter 5.

2.4. Research outline

As described above, a gridded approach is taken so that a wind model and demand model can be built on the same spatiotemporal resolution, scope and referencing system. Both of these will be driven by CFSR. The validity of this approach will be evaluated through testing of the wind speed data[2] also through testing the outputs of both the supply and demand model. The models are then used to disaggregate scenarios of electricity demand from National Grid, exploring the spatiotemporal variation in wind supply and electricity demand including increases in population, changes in buildings and increased electrification of heat.

2.4.1. Research aims

The need to learn more about potential changes to to the GB energy system and research gaps identified in the literature review prompted the following research aims;

1. Establish the validity of a climate reanalysis, NCEP CFSR, as a meteorological driver of energy models in GB.
2. Establish methods for the estimation of potential wind generation in GB driven by CFSR, which can estimate output from a range of scenarios without the need for significant changes to the model.
3. Determine where wind capacity can be developed across GB so that realistic locations and wind conditions can be used in analysis of the implications of variability.

[2] weather data for input into the demand model, including temperature and solar radiation, are less variable over resolutions smaller than a CFSR grid square so it is assumed that these are more accurate and represent the conditions in the grid square. This may not be the case, particularly in cities where temperatures may vary they should represent the average that is experienced by the stock.

4. Develop methods to spatially disaggregate an existing demand model (DEAM) to the same resolution as the wind model so that the demand model can be driven by the same weather conditions as the wind generation model.
5. Use the same meteorological data as inputs for the wind supply and electricity demand models; this removes the assumption that the weather data matches reality and allow depiction of years where there is no measured demand data.
6. Adapt published national scenarios of increased wind capacity and electrified heat demand to the same scope and resolution of the developed models.
7. Integrate scenario modelling and the adapted demand model to so that all electricity demand can be simulated.
8. Use these methods to examine the disaggregated dynamics of wind supply and electricity demand under published scenarios.

2.4.2. Research questions

Following the gaps identified in the literature review, the research questions are:

1. Is reanalysis wind speed data suitable for simulating turbine output?
2. Can DEAM be adapted to accurately model electricity demand at the same spatiotemporal resolution as CFSR?
3. Is a gridded approach appropriate for the disaggregation of national scenarios of increased wind capacity and electrified heat?
4. What are the combined implications of electrifying heat and introducing more wind capacity?

3. Evaluating the accuracy of NCEP CFSR wind speed data

As noted in Chapter 2, the scope and resolution of the CFSR reanalysis model, combined with its ease of use compared to observed data, which requires quality checking and contains gaps, makes it a viable alternative to both in situ and downscaled data for estimating the generation potential of wind capacities, provided that the wind speed data is of reasonable accuracy. While CFSR wind speeds have been compared with observations at a number of locations, the potential benefits of this data source have not been examined for the UK. Also existing studies have not used an extensive network of stations.

This chapter therefore evaluates how well the wind speed data from the NCEP CFSR climate reanalysis represents the complex conditions over GB. Only wind data is analysed, due to the greater spatial variability compared to other weather variables used in the modelling (temperature and solar radiation). This evaluation also serves as a quality check on the data, which is not simple to obtain and use. Content in this chapter has been published in Sharp et al. [2015].

Studies that have evaluated reanalysis wind speed data are summarised. The gridded referencing system used in all future modelling and the adaptation of raw CFSR data to this grid is described. CFSR wind speed data are compared to hourly in situ measurements from 264 onshore and 12 offshore stations. This is the most comprehensive evaluation of the NCEP CFSR reanalysis model hourly wind speed hindcasts to date, and the first for the UK.

UK onshore weather stations locations represent a range of topographic conditions and land uses and experience different wind conditions. This means that a single average value for a grid cell that may contain a large variety of these conditions may not represent some weather stations within the cell well. This chapter explores the impact of these spatial factors on the skill of the CFSR model for the first time.

The evaluation demonstrates that the accuracy of CFSR estimation of wind speed is as accurate as any other reanalysis for GB. CFSR data are not as accurate as data that has been spatially downscaled onshore, however are comparable for offshore locations. Overall CFSR is shown to represent wind speed effectively across a range of complex terrains including where terrain varies within an area represented by a single CFSR wind speed value. Wind speed at the highest elevation locations are not well estimated, however these are shown to be unsuitable for wind turbine location. Overall, CFSR is found to be a viable dataset for simulating wind turbine output in GB. The consequences of the accuracy of the simulations using the data on a GB scale are explored further in Chapter 4.

3.1. Review of the evaluation of reanalyses

Reanalyses are evaluated both by the creators of the datasets and those users that need to have an idea of the accuracy of the data. The global accuracy of CFSR is assessed by its originators; Saha et al. [2010] find that it is considerably more accurate than previous the NCEP reanalysis, through analysis of the 5 day forecasts. They admit that it is difficult to comprehensively assess accuracy at this scale, accepting that it is necessary to evaluate the dataset for specific purposes. There have also been external global reviews of CFSR, Ebisuzaki and Zhang [2011] compared CFSR to an ensemble of alternative reanalyses. Through analysis of a recent year they found that CFSR captures daily variability better than previous NCEP reanalyses and compares favourably with operational reanalyses. However, their research suggests that inter annual variability is captured less successfully, as CFSR data regularly provide outliers with a unique warming trend observed in the tropics. This presents a possible disadvantage of the dataset. As described above it is key to capture this variability when estimating generation from wind capacity. However, Ebisuzaki and Zhang [2011] do note that long term variability is difficult to accurately capture, due to small variations and difficulties associated with observation platform changes. The difficulty of integrating platform changes has also been noted by Wang et al. [2010] who observed dramatic changes associated with precipitation, cloud cover and solar radiation. The same study also noted that CFSR represents a significant improvement in the depiction of surface air temperature (2m above surface) over R1 and R2, although ERA 40 is shown to provide the most accurate data.

Several studies have assessed the skill of different reanalysis and mesoscale models at estimating the wind speed in different countries, those considering onshore areas are summarised in Table 3.1 and those considering offshore areas are summarised in Table 3.2. Notably, none of the studies examining onshore areas have considered the importance of topography and land use. Studies which evaluate the accuracy of wind generation estimates covering GB using reanalysis or reanalysis driven simulations are also summarised in the tables. Where the spatial resolution of the study is referred to as site, wind speed data has been interpolated to the in situ location, otherwise the resolution refers to the grid square, with the nearest grid point value used for comparison. There are a number of studies which evaluate the accuracy of mesoscale modelling output using reanalysis data for boundary conditions outside of the UK. Since this type of dataset and the geographical scope are not the focus of this study, only those studies which consider those results alongside raw reanalysis data are included in the review, with the exception of Carvalho et al. [2014b] and Carvalho et al. [2014c] who conduct a comparative analysis of WRF outputs driven by different reanalyses and analyses.

A limited number of metrics are used to evaluate the correlation between both wind speed and simulated output time series in these studies. RMSE and a correlation coefficient (either Pearson's R or R^2) are the most commonly used; bias is also used, predominantly in offshore studies. The results found by Decker et al. [2012] are not included in the table as a ranking system is used in the place of statistics; this means that the findings cannot be compared to the rest of the studies. Correlation metrics for simulated data cannot be directly compared to those for wind speed values as simulation is subject to a number of uncertainties that affect correlation, including error introduced through height correction, scaling factors and the simulation method itself.

Evaluation of reanalyses against in situ wind speed measurements is discussed in this chapter, simulation of wind turbine output is discussed in Chapter 4.

		Author	Spatial: Scope	Spatial: Resolution (degrees)	Temporal: Scope	Temporal: Resolution	Data	Reference	Correlated to	Correlation: Pr	Correlation: R^2	RMSE	Bias (m/s)
Onshore	Wind Speed	Liléo and Petrik [31]	Sweden	0.5	Length of mast data (1-30 years)	Hourly	NCEP - CFSR	Saha et al. [19]	25 meteorological and telecommunication masts	0.79 - 0.87 (mean 0.83)			
				0.6			NASA - MERRA	Rienecker et al. [18]		0.75 - 0.89 (mean 0.84)			
				2.5		6 hours	NCEP - NCAR	Kanamitsu et al. [52]		0.64 - 0.83 (mean 0.73)			
		Hawkins et al. [27]	UK	3 km	10 years	Hourly	NCEP - FNL + WRF	Skamarock et al. [42]	220 MIDAS stations		0.96	0.44 m/s	0.02
		Kiss et al. [41]	Hungary	0.75	2.5 years	6 hours	ECMWF ERA-interim	Simmons et al. [43]	2 grid points to 2 towers	0.73 - 0.77			
		Staffell and Green [24]	UK	Site	20 years	Hourly	Downscaled MERRA		157 MIDAS stations				5.5 +/- 1.6
		Shravan Kumar and Anandan [34]	India	2.5	1 year	6 hours	NCEP - NCAR		NARL Doppler Sodar	0.56 - 0.78			
		Bao and Zhang [30]	Tibet	Site	4 months	6 hours	NCEP - CFSR		Radiosondes at 11 stations	U = 0.93, V = 0.86			~ 1
							NCEP - NCAR			U = 0.9, V = 0.83			
							ERA - interim			U = 0.93, V = 0.89			
							ERA 40	Uppala et al. [40]		U = 0.93, V = 0.88			
		Lledó et al. [32]	Europe	2.5	Unknown	Daily	NCEP - NCAR		37 "Tall Towers"		0.64		
				0.5			NCEP - CFSR				0.74		
				0.75			ERA - interim				0.73		
				0.6			NASA - MERRA				0.66		
		Carvalho et al [29]	Portugal	0.083	1 year	Hourly	NCAR(R2) + WRF		13 stations	0.69		2.49	0.49
							ERA - interim + WRF			0.79		2.1	0.34
							CFSR + WRF			0.78		2.19	0.47
							MERRA + WRF			0.76		2.26	0.49
							NCEP - FNL + WRF			0.77		2.17	0.31
							NCEP - GFS + WRF			0.78		2.13	0.3
		Liléo et al. [33]	Norway, Denmark, Sweden	0.75	1 - 8 years	6 Hours	ERA - interim		18 stations and 24 masts at turbine sites	median 0.8			
				0.5		Hourly	CFSR			median 0.8			
				0.6		Hourly	MERRA			median 0.85			
				0.1		Hourly	ERA interim + WRF			median 0.83			
				0.1		Hourly	FNL + WRF			median 0.83			
Simulated		Kubik et al. [23]	Northern Ireland	0.1	1 year	Hourly	MERRA		Measured generation data	0.91		12%	
				Site			MIDAS	UKMO [15]		0.88		14%	
		Staffell and Green [24]	UK	Site	10 years	Monthly	Downscaled MERRA		Renewable Obligation Certificates		0.84		

Table 3.1.: Summary of studies evaluating the accuracy of reanalysis data, onshore. Blanks indicate that the metric is not used.

3.1.1. Measured against in-situ wind speed data

3.1.1.1. Onshore

Table 3.1 demonstrates that raw reanalysis wind speed data is reasonably close to onshore in-situ measurements with Pearson's R between 0.56 and 0.87. Bao and Zhang [2013] describe larger correlation coefficients; this may be a result of considering the U and V components of wind separately. However, the difference may also be due to topography, as the research was carried out on the Tibetan plateau, or because of the in situ measurements as radiosondes are used (multiple pressure levels are examined but only those closest to the ground (100 hPa) are described in the table). Liléo and Petrik [2010] have demonstrated that the finer spatial resolution models, CFSR and MERRA, provide more accurate data than the coarser resolution NCEP - NCAR model for Sweden, although the different temporal resolutions mean that the results are not directly comparable. Bao and Zhang harmonise their analysis to 6 hours for all datasets and find that the finer spatial resolution datasets perform marginally better. Lledó et al. [2013] find that CFSR and ERA – interim perform better than the lower resolution NCAR, but MERRA only performs marginally better. Liléo et al. [2013] are the only authors evaluating multiple datasets to find that the correlation between CFSR and hourly synoptic weather station measurements is worse than MERRA, as Decker et al. [2012] found when comparing them against flux tower observations. Even in extremely mountainous terrain in India, good correlations between the NCEP – NCAR reanalysis models and in situ measurements have been observed [Shravan Kumar and Anandan, 2009].

Evaluation of the output of mesoscale models has been performed onshore by several authors. Hawkins et al. [2011] show that using NCEP FNL to provide boundary conditions for WRF produces a very good correlation with UK in situ measurements ($R^2 = 0.96$) and a low RMSE (0.44 m/s), when compared against a long time series of data from a large number of onshore stations. Liléo et al. [2013] demonstrate similarly accurate results from mesoscale data; however these are only marginally more accurate than those found when using raw CFSR or ERA – interim data in the same locations and are worse than raw MERRA data. Carvalho et al. [2014c] show that the correlation coefficients for mesoscale models are similar in magnitude to those found for raw reanalysis data. Interestingly the range of metrics used show that using an older, coarser resolution reanalysis dataset (ERA-interim and the FNL and GFS analyses) results in the most accurate of the mesoscale models. Using CFSR data as an input produces marginally superior results compared to using MERRA.

Cannon et al. [2015] bilinearly interpolate MERRA data to MIDAS station sites finding a correlation of 0.73. They find a correlation with the mean wind speed over all sites of 0.94, stating that this will mean that it should be good at reproducing regionally aggregated generation. They also go further and look at how MERRA predicts changes in wind speed, important because changes in generation from wind must be met in other ways and knowing the magnitude and frequency of these events means they can be planned for and secured supply is more likely. They find that MERRA under predicts short term (3 hours) variability at individual MIDAS locations but becomes more accurate over longer time spans (24 hours), extreme events are under predicted and the largest errors occur at high elevations, like raw wind speed the spatial mean is very high R = 0.96. They also look at spatial variability by calculating the difference between location pairs for both MERRA and MIDAS then plotting the correlation between the two corresponding difference

time series against distance between the sites, demonstrating that aggregation improves results. This is extended to show over what temporal scales this is captured, this shows, unsurprisingly, that temporal aggregation smooths fluctuations and MERRA more closely matches MIDAS. They state that above 300 km and 6 hours the changes are matched closely by MERRA, but below this care must be taken. This is the most in depth comparison of a reanalysis and in situ measurements performed for GB.

With respect to the use of this data for the estimation of wind generation, Kubik et al. [2013a] bilinearly interpolate MERRA data to MIDAS station sites in Northern Ireland to the nearest 0.1°. They then simulate total installed capacity using both in situ and reanalysis data, at a given capacity factor, assuming that this capacity is evenly distributed across these sites, and using the simulation method described above. While the comparison with measured generation data demonstrates that both datasets result in a good correlation, interpolated reanalysis data is marginally more accurate (Table 3.1). Interestingly the analysis performed by Staffell and Green [2014] shows that downscaled data achieves a similar correlation, although R^2 is used rather than R and the evaluation data is considerably more temporally aggregated.

3.1.1.2. Offshore

Offshore wind speed, especially in areas that are not close to land, is not subject to many of the spatial factors that influence changes in wind speed onshore; as a result is likely to be more homogeneous over larger areas. This means that it is potentially easier to produce accurate offshore wind data using a reanalysis. The results described in Winterfeldt et al. [2010] support this assertion as they find a low RMSE for offshore wind despite using a reanalysis provided at a coarse spatial resolution (~200 km^2) and having to apply temporal downscaling (6 hours - 1 hour).

Carvalho et al. [2014b] find that raw reanalysis data provided at all spatial resolutions finer than NCAR achieve a similar and superior correlation, and the finer temporal resolution datasets perform well, despite the greater complexity of wind speed at the 1 hour resolution. This pattern is echoed in the other metrics used (RMSE and Bias), where CFSR provides the best results.

Stopa and Cheung [2014] find that CFSR performs well over a very large geographical scope and long time series; however the buoys providing in situ measurement are very sparse. The RMSE of CFSR is slightly lower than found in the Iberian Peninsula in most locations [Carvalho et al., 2014b]. Chawla et al. [2013] find a similar result to Stopa and Cheung [2014] in a subset of the same locations; R^2 values of CFSR in these locations are similar to the results found by Carvalho et al. [2014a], demonstrating the consistency of performance of CFSR across the Atlantic and Pacific oceans.

Table 3.2 demonstrates that spatial downscaling reduces error; this is best illustrated in the comparison of results from Carvalho et al. [2014b] and Carvalho et al. [2014a], where the same locations are used for mesoscale and raw reanalysis data respectively. There is a reduction in RMSE and Bias in almost every case for the mesoscale data. Unfortunately comparison of correlation between these papers is difficult owing to the use of different coefficients. However comparing the results from Carvalho et al. [2014a] and Stopa and Cheung [2014] shows that mesoscale modelling does not significantly improve the correlation between CFSR derived data and offshore in situ measurements. The results described by Menendez et al. [2011]and Hawkins et al. [2011], are similar to

other mesoscale models and the raw reanalysis data from Stopa and Cheung [2014] and Chawla et al. [2013]. This review of the literature suggests that mesoscale modelling does not necessarily represent an improvement on raw reanalysis data and that CFSR performs at least as well as MERRA both onshore and offshore.

When the downscaled data created by Hawkins et al. [2011] were used for simulation, a very high correlation was found to both onshore and offshore turbine output; however, as with Staffell and Green [2014], this was aggregated to monthly load factors where detail is lost.

Offshore	Wind Speed	Sim	Author	Spatial		Temporal		Data	Reference	Correlated to	Correlation		RMSE	Bias (m/s)
				Scope	Resolution (degrees)	Scope	Resolution				Pr	R^2		
			Hawkins et al. [27]	UK	3 km	10 years	Hourly	NCEP - FNL + WRF		Buoys, lightships, platforms		0.89	1.33 m/s	-0.02
			Menendez et al. [39]	Spain	15 km	20 years	Daily	ECMWF ERA-interim + WRF		Buoys	0.7 - 0.9			0 - 1
			Winterfeldt et al. [35]	North Sea	2.5	< 10 years	1 Hour	NCEP - NCAR		Buoys, lightships, platforms			2.7 m/s	
			Staffell and Green [24]	UK	Site	20 years	Hourly	Downscaled MERRA		Buoys, lightships, platforms				5.5 +/- 1.6
			Carvalho et al. [28]	Iberian Peninsula	0.083	10 Months	Hourly	NCAR(R2) + WRF		5 Buoys	0.76		2.43	0.34
								ERA - Interim + WRF			0.88		1.85	0.48
								CFSR + WRF			0.87		1.94	0.6
								MERRA + WRF			0.86		2.01	0.59
								NCEP - FNL + WRF			0.87		1.89	0.53
								NCEP - GFS + WRF			0.88		1.89	0.56
			Carvalho et al. [38]	Iberian Peninsula	2.5	1 year	6 hours	NCEP - NCAR (R2)		5 Buoys		0.64	3.43	0.87
					0.75		6 hours	ERA - interim				0.78	2.45	0.58
					0.5		Hourly	CFSR				0.87	1.85	0.16
					0.6		Hourly	MERRA				0.87	1.93	0.52
					1		6 hours	NCEP - FNL				0.85	2.3	0.98
					0.5		6 hours	NCEP - GFS				0.87	1.89	0.22
			Stopa and Cheung [36]	Peru	0.5	1979-2009	Hourly	CFSR		1 Buoy	0.81		1.37	6.14%
				Hawaii						4 Buoys	0.86		1.37	-3.90%
				Gulf of Mexico						5 Buoys	0.87		1.52	0.42%
				NW Atlantic						5 Buoys	0.89		1.73	4.23%
				Alaska						5 Buoys	0.91		1.7	3.90%
				NE Pacific						5 Buoys	0.91		1.5	2.38%
			Chawla et al. [37]	Atlantic/Gulf of Mexico	0.5	1979 - 2009	Hourly	CFSR		12 Buoys		0.84	1.74	-0.03
				Pacific/Hawaii						10 Buoys		0.87	1.49	-0.21
			Hawkins et al. [27]	UK	0.1	10 Years	Monthly	NCEP - FNL + WRF		Renewable Obligation Certificates		0.94	1.33	0.05

Table 3.2.: Summary of studies evaluating the accuracy of reanalysis data, offshore.

3.2. Data and Methods

The scope and resolution of the CFSR reanalysis model, combined with its ease of use compared to observed data, that requires quality checking and contains gaps, makes it a viable alternative to both in situ, interpolated and downscaled data for estimating the generation potential of wind capacities, provided that the wind speed data is of reasonable accuracy. While CFSR wind speeds have been compared with observations at a small number of locations in Sweden, the potential benefits of this data source have not been examined for the UK. The following section describes the evaluation of the dataset using hourly in situ measurements from 264 onshore and 12 offshore stations.

UK onshore weather stations locations represent a range of topographic conditions and land uses and experience different wind conditions. This means that a single average value for a grid cell that may contain a large variety of these conditions may not represent some weather stations within the cell well. Therefore, this chapter also investigates spatial factors that affect onshore correlation, including land use, proximity to coast, mean wind speed and elevation.

3.2.1. Creation of the model grid

CFSR reanalysis data are provided as grid point data, representing the weather at the centroid of a Gaussian grid defined by NCEP, designated T382, the resolution is approximately 38 km x 38 km. This study takes the grid point to represent wind speed for the whole of the grid square. Gaussian grids are predominantly used by climate scientists to model weather variables on a sphere. Longitudes are evenly spaced, but latitudes are not. The latitude spacing is defined by the 'Gaussian quadrature'.

There are a number of advantages to using a grid as the spatial reference for modelling performed in this thesis. The greatest of these is the ability to directly compare datasets or integrate data into a model without the need for adapting complex boundaries. This is true even if data is provided referenced to census geographies and needs to be redistributed to the grid, as these often do not align. The use of a grid also allows comparison of data over time as boundaries are constant. This is in contrast to census geographies, which are continually revised, as are administrative boundaries and political borders. In the case of the UK this can be seen in the change from enumeration districts, used from 1971-1991, to output areas, used from 2001.

The scalability of a grid based system is also an advantage over census geographies, as they rarely translate across political borders. A grid can be continuous across the whole globe if necessary and the extraction of a subset of data is much simpler than with more complex boundaries. Using a grid simplifies models, as they can be created on the basis of an array, meaning that a geographical model can be run without the need to link to a GIS. The reduced load needed to handle the spatial element of the model and consistent simple spatial referencing means that handling time within the modelling becomes much simpler. The use of a grid also simplifies the disaggregation of data that are provided at coarser spatial resolutions, described in Section 5.2.2.3.

There are disadvantages to using a grid for geographical modelling. Many of the datasets used here need to be redistributed to the common grid. It is possible to do this within models, however the intention is to make the model as geographically light as possible to allow speedy iteration.

Therefore it is necessary to perform much of this adaptation outside of the model. Some of the data used here are provided at a fine spatial resolution, which would yield more geographical detail in analysis of modelling outputs, if modelling were performed at that resolution. The relative resolution of data and outputs are discussed in Section 5.2.2.3.

Many of the advantages of a grid would be negated by using the Gaussian grid defined by NCEP due to its bespoke nature. Therefore a new grid was chosen, the data from CFSR has been interpolated to a 0.5° x 0.5° decimal grid. Fortunately, the need for a standard geographical referencing system is recognised by NCEP, therefore the wgrib2 software provides a method for conversion to this grid (wgrib2 is the latest version of the grib program which manipulates and decodes grib files, the file type for CFSR weather data). Several methods are available, bilinear interpolation has been used here. This is the simplest method which uses the four nearest pixel values to the desired value to obtain a spatial average.

The CFSR grid covers the entire globe, this results in a very large dataset, much of which is not of interest to this study, and the use of which would increase the computational power and time needed for modelling and analysis. Therefore a subset of data was extracted at the same time as the interpolation. The extent of the grid was set so that all potential future deployments of wind turbines in GB and offshore could be modelled, therefore the British sovereign waters were chosen as the limit of the grid, with a small number of contingent grid squares around the periphery. The resultant geographical scope and resolution is shown in Figure 3.1. The grid contains 2720 grid squares, each with an associated weather value. The grid is 80 squares wide and 34 high, the Latitudes boundaries are 48° N and 65° N and Longitudes boundaries 30° West and 10° East. This defines the model grid which is used in all ensuing analysis. Onshore modelling is limited to the GB land mass as this marks the extent of the electricity grid over which supply and demand are balanced, this means that there are 209 grid squares that contain land. Currently a large amount of the offshore grid is not economically viable for development, due to depth restrictions and high maintenance costs, that would arise if wind farms were developed far from shore (restrictions on development both onshore and offshore are analysed in detail in Chapter 6). These areas have been included in the model grid so that reduced development and maintenance costs can be modelled later, as well as creating a grid that simplifies the modelling process. The grid squares define the minimum spatial resolution in all future analysis. This means that in some cases evaluation etc. could be performed at a less aggregated resolution, potentially altering results. However the benefits of consistency of data integration and analysis and reduced computational load outweigh the potential benefits of increased disaggregation.

Several more steps were required to facilitate the integration of CFSR data into both the wind model described in Chapter 4 and the demand model described in Chapter 5. Wind data is provided as U and V components, U is the zonal velocity and represents the horizontal wind towards east, V is the meridional velocity and represents the horizontal wind towards north. This is useful for studies that require direction, for example single wind farm simulations that are interested in the wind direction for wake effects. Here only scalar winds are of interest, therefore the data was converted using wgrib2. Wgrib2 was also used to convert the data from meteorological grib files to csvs (comma delimited files that facilitate use in different software), finally, the data was converted to numpy arrays to facilitate fast integration into the model (numpy is a python module which defines the manipulation, storage and analysis of array based data).

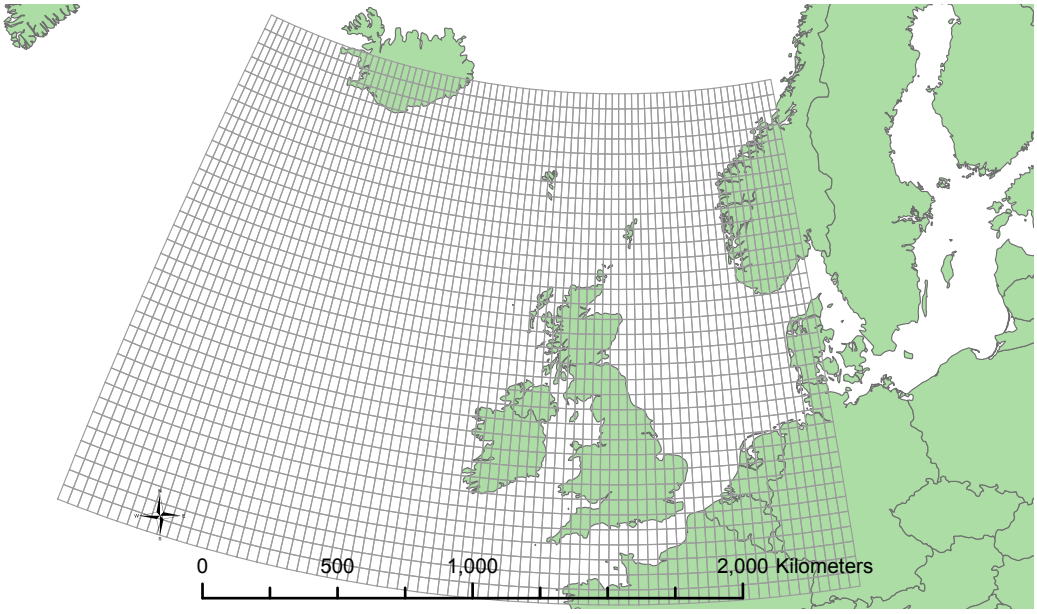

Figure 3.1.: Map showing extent of modelling area.

Temporal boundaries CFSR data is available from 1979 to near present. Only data from the beginning of 1980 to the end of 2010 is utilised in this thesis. The length of the times series means that the wind speed data should encompass decade level differences, which can vary considerable, for example in Northern Europe Troen and Petersen [1989a] have shown that there has been a difference of 30% in terms of high and low mean annual wind energy. Data should also cover variations over longer time periods, where mean power from wind can have a standard deviation of 10% from one 20 year period to the next [Petersen et al., 1998b]. There is an argument for longer time series to be used as "climatic variables exhibit cyclic variation over very long time periods" of 50 years or more [Chatfield, 2003, p12]. However analysis by the UKMO has shown that there is no long term trend in wind speed over Europe and inter-annual differences are therefore the most important when estimating the energy potential of the wind resource (Met Office presentation, UCL Energy Institute). The finest temporal resolution of CFSR data (1 hour) is used, this results in some smoothing of wind variability, as described in Section 2.1.5, however, without the use of downscaling, this is the best resolution available.

3.2.2. In situ wind speed measurements

Hourly wind speed measurements were obtained from the Mean Hourly Wind, UK Hourly Weather and Global Marine Observations databases of the British Atmospheric Data Centre (BADC). The BADC maintains and distributes atmospheric data produced by Natural Environment Research Council (NERC) projects to UK researchers. Owing to the size of the dataset, it was necessary to automate quality checking. First, the data was filtered to exclude those sites and time series outside of the spatial and temporal boundaries. Then the points that had not been quality checked by the UKMO were removed from the remaining time series. The identical repeat values from points at which two different values are provided for the same time period were also removed. Values above 35 m/s were removed as outliers; most of these values were considerably higher (up to several hundred m/s) and isolated. Since 25 m/s is currently the upper threshold for power

generation, wind speeds above this threshold are largely irrelevant for simulation where a single curve approach is used (Figure 2.2). However, as higher values may illustrate correlation trends, 35 m/s was selected as the cut-off for this evaluation of CFSR. Following processing, the time series for most locations are discontinuous. Long data gaps were assumed to be an indicator of poor quality data collection and time series containing gaps of one week or more were therefore removed from the analysis. The offshore wind speed data for buoys were not altered from 6 m above sea level, because of the potential errors in the method necessary to bring them in line with the CFSR dataset (10 m). Although Winterfeldt et al. [2010] do correct offshore wind speed for height, several authors have demonstrated that the bias is very small – less than 0.5 m/s [Mears et al., 2001, Bourassa et al., 2003, Chelton and Freilich, 2005, Ruti et al., 2008]. Finally, the cleaned data was matched spatially to the appropriate CFSR grid square and temporally using timestamps.

The filtering resulted in 355 onshore time series, compromising data from the AWS, SYNOP, HCM and HWND6910 messages originating from stations that contribute to the MIDAS database. Some stations provide time series for multiple messages. Only a single instance has been used for each location. Therefore there are 264 unique onshore MIDAS station locations used in this analysis. There are 209 CFSR grid squares covering the GB land mass, of which, 98 have two or more stations within them, 45 have only one station and 71 have no stations. Offshore, 12 suitable time series have been extracted. Onshore and offshore stations are shown in Figure 2.3, which includes the relative distribution of message types. These MIDAS stations provide almost 36 million onshore and more than 1 million offshore hourly data points to compare against CFSR reanalysis data. Figure 3.2 shows that the majority of stations provide high quality data for over 95% of the time. There are, however, a small number of stations where there are more data points missing due to lack of observations or removal following the methods described above.

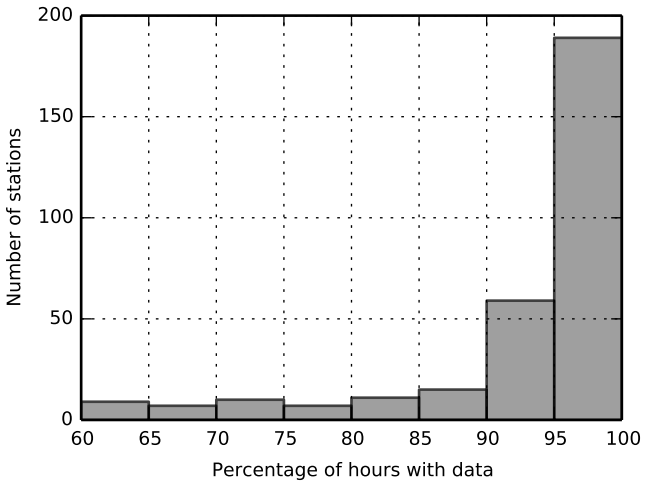

Figure 3.2.: Completeness of MIDAS wind speed time series used to compare against CFSR.

3.2.3. Onshore spatial factors influencing wind speed

In order to investigate the influences of onshore factors on wind speed, the MIDAS station points were characterised in terms of height above sea level at the station base using the Shuttle Radar

Topography Mission Digital Elevation Model (SRTM DEM) [USGS, 2006b] and according to land use using the Coordination of Information on the Environment (CORINE) land cover map [EEA, 2000]. Analysis of this land use data has revealed that the projection is not correctly defined, which leads to a slight mis-location of the MIDAS stations (<10 m). Therefore subsequent analysis uses an aggregated land use classification, which is provided within the CORINE dataset, to assign a land use to each MIDAS location as accurately as possible. This land use is used to analyse whether surface characteristics such as roughness are accounted for by CFSR. Using a buffer analysis, onshore stations within 5 km of a simplified shoreline were classified as coastal, with all other sites defined as non-coastal. Therefore, 46% of the stations are defined as coastal and 54% as non-coastal.

3.2.4. Statistical and spatial analysis methods

Due to the large amount of spatially disaggregated data it was necessary to use statistical methods to summarise the relationship between the matched time series over the study area. The analysis below shows the use of density plots to represent correlation, and, subsequently, to evaluate percentage error. Pearson's correlation coefficient (Pr) is used to measure the strength of the relationship, following the precedent set by previous studies. In order to measure the magnitude of average error across the data and according to the methods identified in the literature review, root mean squared error is used (Equation 3.1). This is expressed in m/s to allow analysis of its effect on turbine power curves. Finally, to determine the direction of this error (-ve, +ve), the bias of the CFSR data is measured (Equation 3.2). Correlation coefficients are derived using the python module, scipy [Jones et al., 2001a].

Equation 3.1 Root Mean Squared Error between MIDAS and CFSR

$$RMSE = \sqrt{\frac{\sum_{t=1}^{n}(CFSR_t - MIDAS_t)^2}{n}}$$

Equation 3.2 Bias between MIDAS and CFSR

$$Bias = Mean\,(CFSR_t - MIDAS_t)$$

3.3. Results and Discussion

Figure 3.3 demonstrates how the correlation between CFSR and the in situ wind data varies across the MIDAS stations. The large number of onshore sites necessitates aggregation to a histogram, whereas the relatively few offshore sites allow individual points to be plotted. The majority of onshore sites have a similar range of correlations as offshore; however, there are a number of sites that are less well correlated. This results show that mean onshore Pr = 0.81 and mean offshore Pr = 0.85. These results are in line with the published studies described in Table 3.1 and Table 3.2. In comparison to onshore raw reanalysis dataset the correlation is very similar to that found by Liléo and Petrik [2010] and Liléo et al. [2013] and an improvement on the coarser datasets examined in Kiss et al. [2009] and Shravan Kumar and Anandan [2009]. The correlation is not as good as

that found by Bao and Zhang [2013], although, as described above, their analysis is conducted in a different way. Onshore, the mean correlation is slightly better than mesoscale analysis in Portugal [Carvalho et al., 2014c] and slightly worse than in Scandinavia [Liléo et al., 2013]. The best correlated sites approach the correlation found in the UK downscaled study [Hawkins et al., 2011], although the majority have much lower correlation coefficients. Offshore, the correlation is in line with the analysis of raw reanalysis in Stopa and Cheung [2014] and Chawla et al. [2013], although slightly lower than some locations. Mesoscale modelling using CFSR and other reanalysis data show only slightly improved correlation coefficients than found here [Menendez et al., 2011, Carvalho et al., 2014b, Hawkins et al., 2011]. These results demonstrate that downscaling may not be necessary, particularly offshore, where wind speed is not influenced by the land mass, although mesoscale modelling of wind over the UK has achieved better correlation than found here.

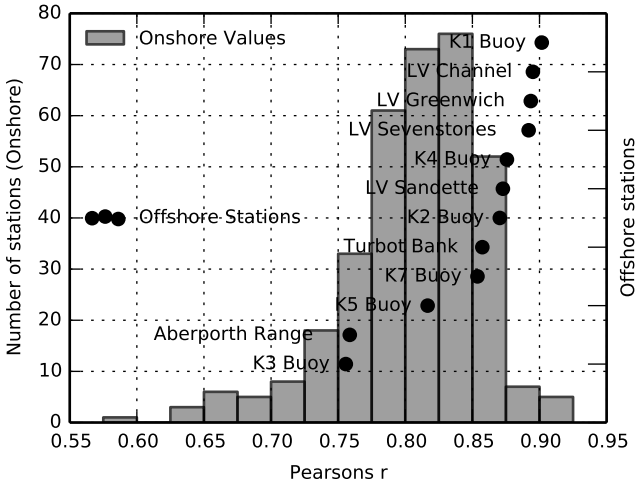

Figure 3.3.: Distribution of Pearson's correlation between MIDAS and CFSR time series. Offshore sites are named to allow comparison to Figure 2.3.

Figure 3.4(a) shows the relationship between CFSR and MIDAS at a single site with a Pr similar to the onshore mean (0.81). The plot shows that there are a large number of values that correlate well. There is, however, noise at all wind speeds, particularly below 10 m/s. Figure 3.4(b) shows the site with the highest correlation coefficient (0.91). This site experiences less error at low wind speeds than Figure 3.4(a), and has a higher density of values around the ideal correlation. The line of missing values between 17 and 17.5 m/s is consistent across all sites and is a result of the conversion of MIDAS data, which are provided to the nearest knot, to harmonise with CFSR which is provided in m/s. Figure 3.4(c) and (d) demonstrate that poor correlation may be due to wind speed being either under or over estimated by CFSR. Both sites exhibit problems with MIDAS error at the lowest wind speeds. A significant proportion of the data points are in the same bin, showing that wind speed is consistent and low or that there may be some measuring error.

Figure 3.5 shows that RMSE is similar onshore and offshore. As with Pr there are more outliers onshore, but in this case only with larger errors. Unfortunately, none of the studies evaluating raw onshore reanalyses use RMSE as a metric. The onshore error found here (mean 2.35 m/s) is much larger than the 0.4 m/s found by Hawkins et al. [2011] but in line with that found by Carvalho et al. [2014c], it may be that the mesoscale modelling works better for the UK, or that results are affected by using a longer time series as Hawkins et al. did. The mean RMSE in this study

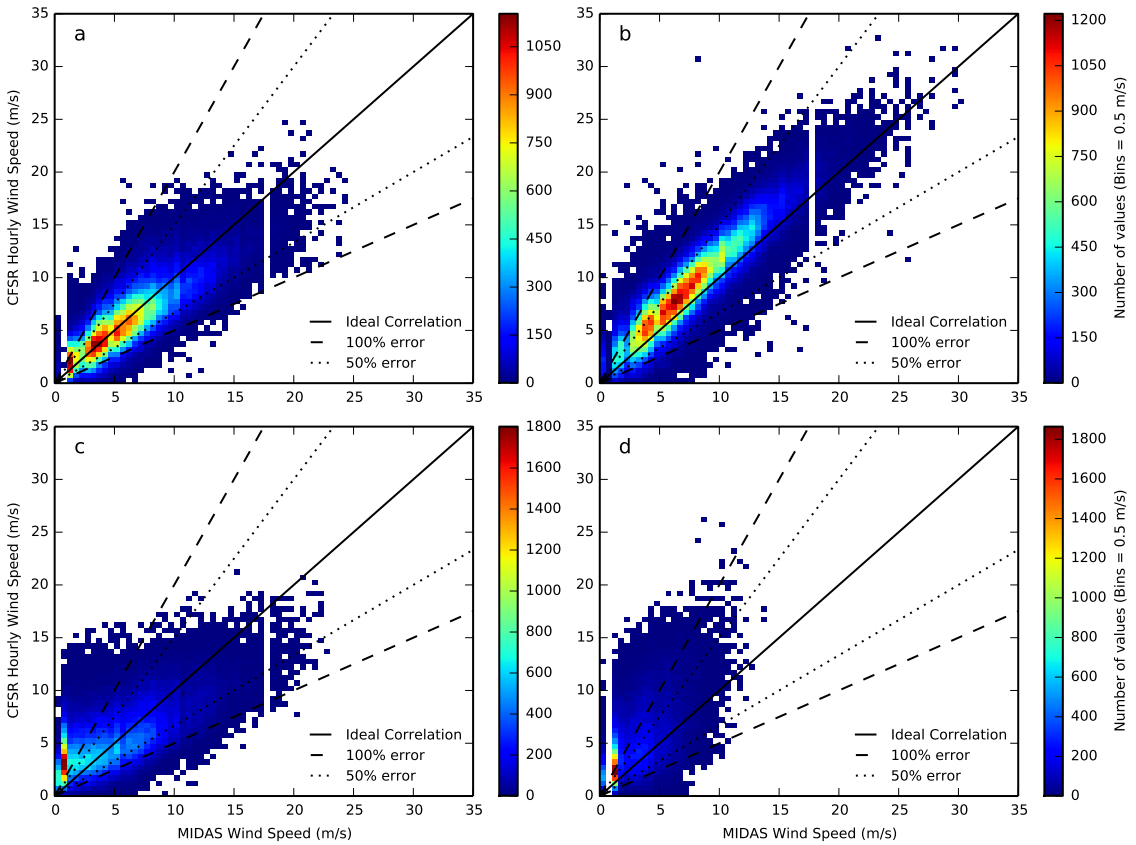

Figure 3.4.: Correlation between MIDAS and CFSR time series: a - illustrative typical correlation, b – The MIDAS site to which CFSR most closely correlates, and examples of sites where MIDAS and CFSR correlate poorly, due to either high (c) or low (d) wind speeds.

is higher for offshore sites, as found in Hawkins et al. [2011], although the difference is smaller (2.44 m/s compared to 1.33 m/s). The mean offshore error is smaller than the 2.77 m/s found by Winterfeldt et al. [2010], although this was found using an older, coarser resolution, dataset. The offshore RMSE found by studies in other areas of the world varies; the value found here is higher than found using raw CFSR reanalysis data in the Iberian Peninsula [Carvalho et al., 2014a], the oceans surrounding North America [Stopa and Cheung, 2014, Chawla et al., 2013], and most of the mesoscale models [Carvalho et al., 2014b]. However CFSR performs better than NCAR and ERA interim data from Carvalho et al. [2014a], and similarly to mesoscale model data driven by NCAR [Carvalho et al., 2014b].

In order to ascertain the extent to which these results are influenced by wind speed, particularly the RMSE values, Figure 3.6 compares both Pr and RMSE to the mean wind speed of the MIDAS time series. Pr appears to be independent of wind speed and the correlation between mean wind speed and RMSE is also unclear. Figure 3.6 does, however, highlight that the sites with the highest RMSE (>9 m/s) are those with a mean wind speed that is greater than experienced by most of the sites across GB (8 of 276). There are not enough offshore sites to discern a relationship between wind speed and either Pr or RMSE.

Bias may be a more useful measure than Pr or RMSE for ascertaining how the two datasets interact over time, as it gives an indication of which dataset is producing higher or lower wind

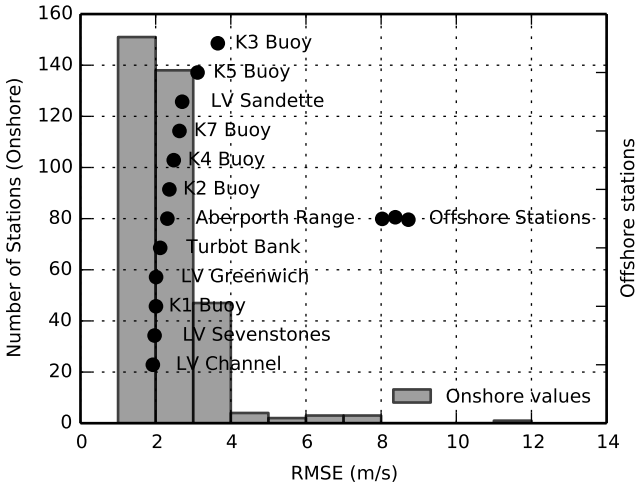

Figure 3.5.: RMSE of MIDAS and CFSR time series.

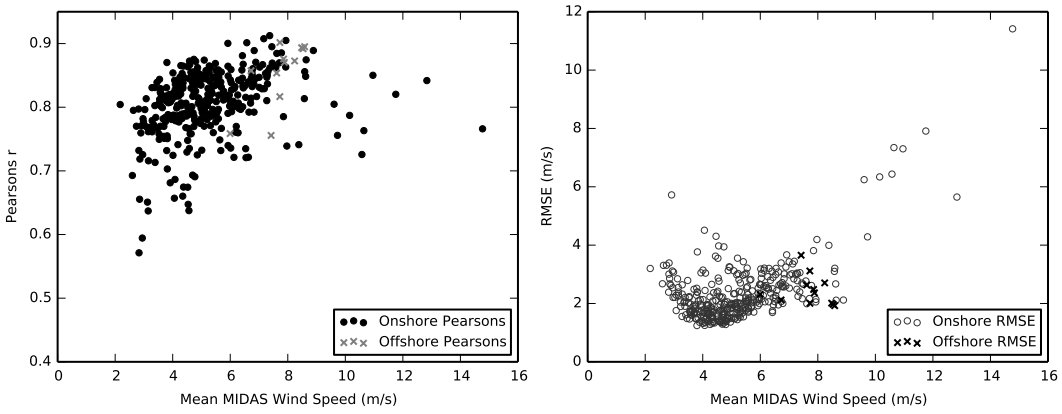

Figure 3.6.: Pearson's R (left) and RMSE (right) of MIDAS and CFSR time series in relation to the mean wind speed of the MIDAS time series.

speeds. Figure 3.7 shows how the bias is evenly distributed in the positive and negative directions for both onshore and offshore sites. Offshore sites show less extreme biases, which could be due to the homogeneity of the wind resource in terms of mean wind speed or could reflect that the offshore wind speeds are not as high as at the windiest onshore sites. The figure shows that the largest magnitude RMSE is created where CFSR underestimates the wind speed. These are the same eight sites identified in the analysis of Figure 3.6, reasserting that CFSR does not represent the sites that experience the highest mean wind speeds well. The mean bias is greater offshore (0.56 m/s) than onshore (0.35 m/s). Onshore, the bias is lower than the interpolated raw reanalysis data used by Staffell and Green [2014] and the mesoscale data driven by CFSR in Carvalho et al. [2014c], but not the better performing reanalysis models. The bias is larger than that found by Hawkins et al. [2011] both onshore and offshore. Offshore, the bias is similar to that seen in the mesoscale modelling in Carvalho et al. [2014b]; interestingly Carvalho et al. [2014a] find a much lower bias with raw CFSR data, but other reanalysis data exhibit a similar or higher bias to that found here.

The comparison of results to those in published studies has shown that CFSR is as accurate as

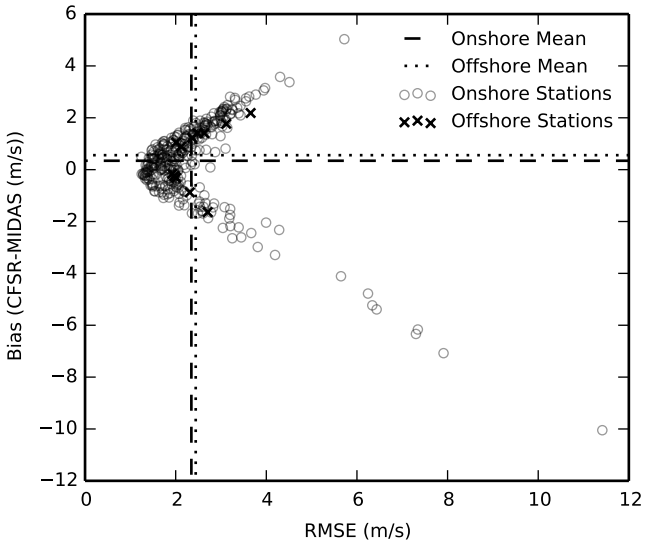

Figure 3.7.: Bias of CFSR vs. MIDAS as a function of RMSE.

any other raw reanalysis dataset for the UK, challenging the finding by Decker et al. [2012] that MERRA hourly wind speeds are more accurate than CFSR. In some respects raw CFSR data is also very close to the results obtained when using interpolated and downscaled data, although accuracy appears to vary dependent on location. Offshore CFSR data can even be closer to in situ measurements as wind speeds are homogeneous and the topographic data utilised by mesoscale modelling offer little benefit due to the lack of terrain. Downscaling does improve the correlation between similar reanalyses and in situ measurements onshore in the UK, but elsewhere results are variable and very often worse. As highlighted by Kubik et al. [2013a], mesoscale modelling is computationally intensive and long term datasets are therefore difficult to produce; the review of evaluations suggest that this effort does not always return a more accurate dataset.

3.3.1. Spatial factors affecting CFSR accuracy

Analysis has shown that the largest RMSE and bias between the MIDAS and CFSR time series is driven by high mean wind speeds. If this were the only factor driving correlation, it would be expected that, as mean wind speed increased, so would bias and RMSE, and that Pr would decrease. However, as Figure 3.6 shows, this is not the case. This suggests that there may be other influencing factors. Figure 3.8, Figure 3.9, Figure 3.10, Figure 3.11 and Figure 3.12 show the results of the investigation of spatial factors that affect correlation, comparing potential drivers of divergence between MIDAS and CFSR to Pr and RMSE (bias has not been plotted as RMSE can be considered to be a proxy for the magnitude of bias following Figure 3.7).

3.3.1.1. Elevation and mean wind speed

Figure 3.8 shows that the sites identified in Figure 3.6 as having high wind speeds and larger errors are those at a high altitude (above 600 m elevation), where wind speeds increase above a threshold that CFSR finds hard to represent. This could be problematic for the use of CFSR as a wind turbine

simulation tool, as these sites potentially provide the ideal wind resource for power generation. However, the low number of meteorological stations reflects the isolated nature of these sites; they are all on the peaks of GB's highest hills (e.g. Cairngorm Mountain and Great Dun Fell) and are therefore extremely unlikely to have wind turbines near them, not only due to inaccessibility but also as these are within zones with restricted planning rules such as national parks (Figure 3.9), see Section 6.2.2 for further analysis. This reinforces the assertion that many MIDAS sites are in areas unsuitable for wind turbine simulation. Removal of these stations from the analysis does not have a significant effect on Pr as the correlations between MIDAS and CFSR at these points are close to the mean. However it does slightly alter the RMSE; the mean reduces from 2.35 m/s to 2.20 m/s and the bias reduces from 0.34 m/s to 0.32 m/s. The impact of removal is very small as there are so few stations at this elevation. As GB is not very mountainous and the high elevation sites are not viable as turbine locations these can effectively be ignored when considering the suitability of CFSR as a wind speed dataset for simulation. This may not be the case in other countries and the data be tested against wind speed measurements at high elevations where turbines can be erected. Gridded data from a reanalysis is always above a geoid (a simplified surface representation), this is because a gridded model assumes that the surface within a grid square is uniform, in reality in the most mountainous terrain this could vary by several thousand meters (e.g. the base of Everest to the summit), although this is an extreme example and the variation in GB will be no more than the tallest mountain (Ben Nevis, 1344 m). This may be the reason that these sites are not well represented as they are furthest from the mean height of a grid square. Also the coarse spatial resolution relative to topography means that they cannot represent the fact that wind speed often increases at the top of topographical features, this is called speed up. This happens when wind flow hits the foot of a hill, initially decelerates and then accelerates to the top of the feature where the maximum wind speed is experienced. The wake of the hill will experience lower speeds as the flow decelerates.

Since this analysis was performed Cannon et al. [2015] published their study, which investigates the accuracy of MERRA over GB. They also found that higher elevations are not well resolved. They state that this is low due to artificially low wind speeds on unresolved peaks citing Howard and Clark [2007]. They find by removing stations over 300 m that the correlation coefficient improves by 0.03. This lower elevation may be due to a different method for representing Earth's Geiod in MERRA compared to CFSR.

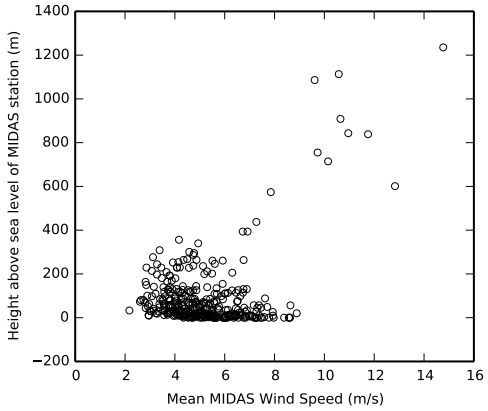

Figure 3.8.: Relationship between mean wind speed and height of MIDAS station.

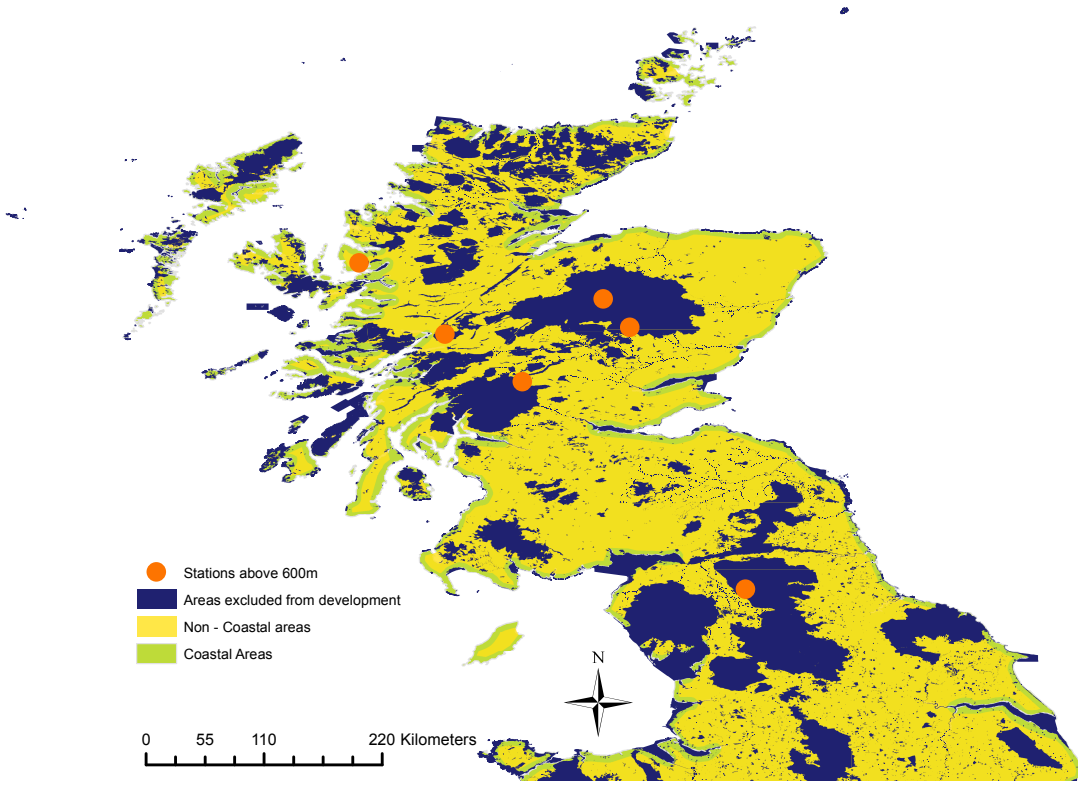

Figure 3.9.: Map of MIDAS stations above 600m with restricted development zones and the coastal zone.

3.3.1.2. Land Use

Wind speed close to the surface can change locally on account of the presence of buildings or a change in the surface roughness that causes turbulence. Figure 3.10 examines whether land use at a station location drives a divergence from CFSR wind speeds. The figure shows that within each land use band there is a range of Pr and RMSE. Those land uses with the poorest correlation also contain correlations higher than the mean and vice versa. This means that it is not possible to identify any specific land use that is not well represented by CFSR. It is possible that an analysis of individual grid squares with multiple stations may show more. However, although there are many such grid squares over GB, most of these only contain two stations and it is difficult to discern patterns from so little data. Sites on arable land are the best represented by CFSR with the smallest range of RMSE at the lowest magnitude. This may be because arable land can be homogeneous over large areas and represent the majority of a grid square, or that this land use is close to the mean conditions over much of GB. Interestingly, sites located on urban fabric show low error, despite the complex nature of this type of land use; this suggests that wind conditions could vary significantly from those across a grid square. With the exception of London, British urban conurbations are not large enough to cover a whole grid square; therefore, CSFR data must represent other land uses at the same time as urban fabric. This suggests that CSFR is very successful at representing wind speeds over a range of land uses and surface roughnesses.

Those land uses with extreme RMSE values represent the sites with the highest altitude. These are located on scrub land and open spaces with one site found in wetland or water. Given that

these land uses also contain low RMSE values, it is likely that the land use is not a driving factor of CFSR error at these locations.

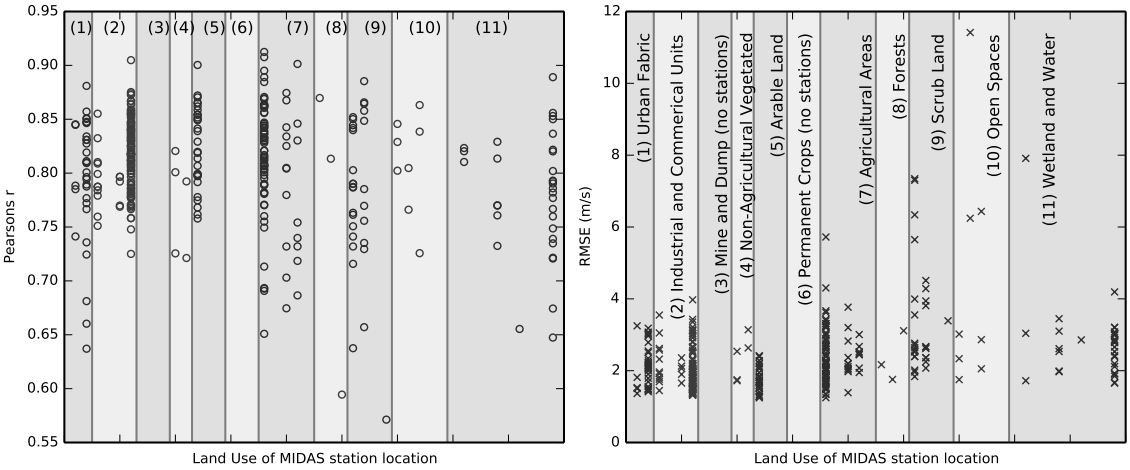

Figure 3.10.: Relationship between land use at MIDAS station location and correlation between MIDAS and CFSR time series. The land use classification shown from CORINE is aggregated as described in Section 3.2.3. This results in separate columns of data within the land use bands which represent less aggregated land use classifications.

3.3.1.3. Proximity to Coast

Coastal areas generally experience higher wind speeds than inland areas [Hau and von Renouard, 2006]. Provided that these areas are not subject to development restrictions, this makes them advantageous for wind turbines. CFSR data representing these areas not only covers the coastal land but also sea and inland areas. This means one value must represent a large variety of surface conditions, which may result in poor correlation with sites in a particular location. Coastal areas have also been identified as being a modelling challenge, due to topography, changes in roughness and variable thermal gradients [Beaucage et al., 2007, Carvalho et al., 2014b]. Figure 3.11 shows how correlation varies between coastal and non-coastal sites to test how CFSR deals with this challenge. It does not appear that there is any significant difference between those sites that are near the coast and those that are inland when looking at Pr. However, Figure 3.12 shows that RMSE is slightly higher for coastal sites; this pattern is reflected in the mean wind speed plot, suggesting that the larger error is caused by different wind conditions. However the RMSE and mean wind speeds are lower than for those sites which are at high elevations and poorly represented by CFSR. Coastal areas are likely to experience speed up if the wind is onshore as there will always be some increase in elevation from sea level. Therefore wind speed will depend on wind direction, more detailed analysis of sites on the coast should take this into account

3.4. Conclusions

This analysis has described the comparison of CFSR wind speed to the maximum number of on- and offshore in situ measurements using a number of metrics. Through characterising onshore stations with respect to elevation, land use, mean wind speed and proximity to coast CFSR wind

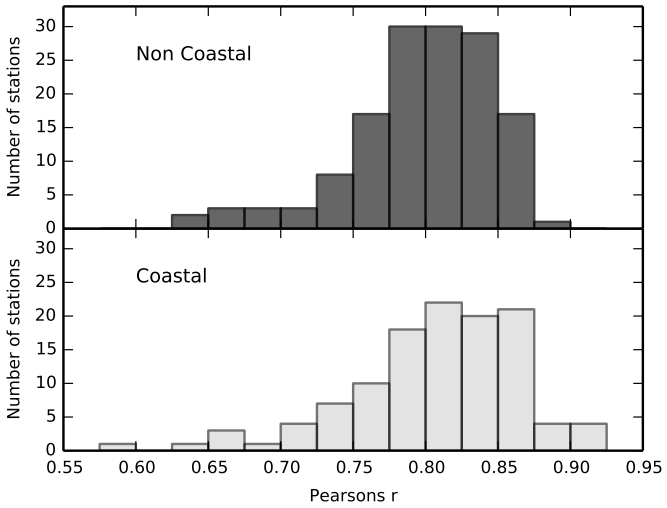

Figure 3.11.: Distribution of Pearson's correlation between MIDAS and CFSR with onshore sites classified as coastal and non-coastal.

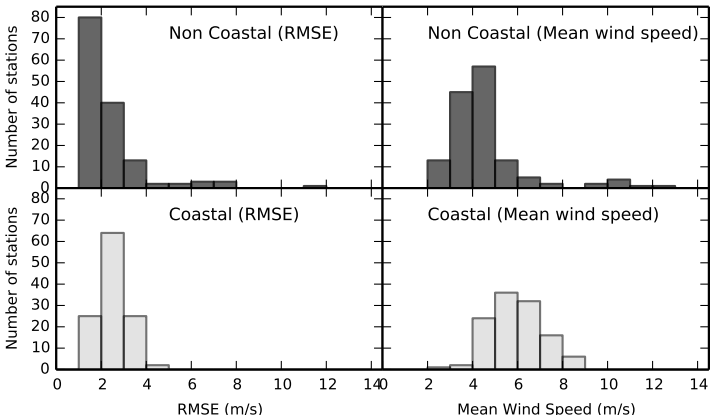

Figure 3.12.: Coastal sites have a slightly increased RMSE, this is predominantly down to the distribution of wind speed.

speeds were found to be less accurate at high elevation locations where mean wind speeds are higher than in the rest of GB. Yet CFSR is as accurate as any other raw reanalysis dataset that has been evaluated. CFSR data is comparable to downscaled data for onshore and offshore locations, although UK conditions may be better represented by mesoscale modelling. Comparative analysis of the methods for the UK would be beneficial. CFSR represents the impact of surface roughness variations on wind speed effectively across a range of complex terrain. In view of the high estimating skill and the advantages of spatial homogeneity and of spatiotemporal scope and scale, it is clear that CFSR may not only provide an alternative to in situ measurements for the UK but also compete with downscaled data which is much more difficult to produce.

4. Estimating potential wind generation through simulation

This chapter describes the wind model and the evaluation of the data and methods behind it. The selection of archetypal wind turbine curves and hub heights for future simulation is justified through analysis of installed capacity. Using these manufacturer wind turbine curves the wind model is shown to perform well according to correlation coefficients ($R^2 = 0.94$ against monthly measured data and 0.66 with hourly data). However, wind turbine output is consistently underestimated by the model. This is counter-intuitive if the physical factors not included in the model are considered. Therefore it is likely the wind speed height correction leads to conservative estimate of wind speed. Following methods used in the literature a linear correction factor is calculated. This reduces the magnitude of simulation error in comparison with both monthly and hourly measured data. Finally, an alternative method, designed to incorporate the effects of wind farms on turbine output, is applied and rejected on the basis of having negligible impact on output.

4.1. Simulation methods

4.1.1. Turbine curve selection

All of the studies simulating wind capacities reviewed in previous chapters, with the exception of Staffell and Green [2014] and Hawkins et al. [2011], have used a single, archetypal, turbine curve with or without statistical adjustments to represent losses and cut out etc., to represent the entire fleet. These curves vary in size, for example Sinden [2007] use a 2.5 MW curve, Green and Vasilakos [2010] 1.75 MW and Giebel [2000] 1 MW. This means that it is necessary to perform some analysis to decide which turbine curve to use for analysis performed here. Fortunately, there is data available which allows a turbine curve selection based on actual installed capacity, provided as part of the supplementary data in Staffell and Green [2014], which is based on information from Hughes [2012] and DECC [2014a]. The onshore data only describes wind farms with ROCs, however as Figure 4.1 shows, this covers the majority of GB capacity. Figure 4.2 summarises the turbine rated capacity using these data showing that, onshore, the mean turbine size is close to the median of 1.5 MW. There are, however, a number of turbines that are both larger and smaller than the mean, the modal bin is significantly larger (2 - 2.6 MW). Previous analysis, described in Figure 2.1 shows that the majority of the smaller turbines have been built during the earlier years of wind power development in GB (1990 - 2000) (note that the data in this figure describes the average turbine at each wind farm), these smaller turbines are still built today, alongside considerably larger ones. A similar pattern is seen with height, although the smaller capacity turbines have become taller, to take advantage of the increase in wind speed with height above ground. As the turbines in the

modal bin are larger they represent a greater percentage of capacity. Therefore a turbine from this band has been chosen for the archetypal onshore simulation curve. Turbines this size have very similar curves, the Nordex N80, 2.5 MW turbine has been selected as it is one of the most commonly used (Figure 2.2). The use of this turbine in scenarios depicting future online capacity should allow for replacement of smaller turbines with larger ones at the high wind speed sites that have already been developed.

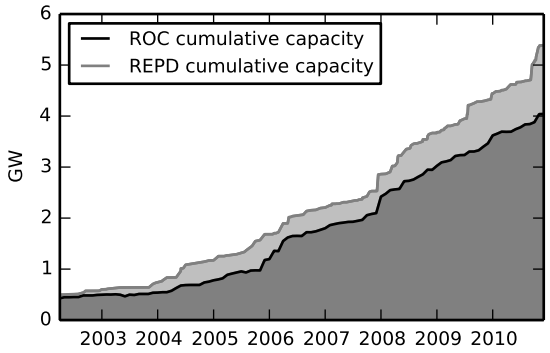

Figure 4.1.: Cumulative capacity recorded by ROCs.

Offshore turbines are more homogeneous in terms of capacity than onshore turbines, as a result of the shorter number of years that they have been in operation (Figure 4.2 and Figure 2.1). This makes the selection of an archetypal offshore curve easier as nearly 70% of the turbines are the same size (3.6 MW). Therefore the Siemens 3.6 MW curve, as described in Figure 2.2, has been selected. The increasing number of larger offshore turbines may mean that different curves should be used in simulations of future capacities alongside adapted wind heights, this is discussed further in Chapter 6.

It is possible to use the same data to find turbine curves that are specific to wind farms and alter wind speed to specific hub heights. This has been performed by Staffell and Green [2014], and good results have been demonstrated. However, these results still require a scale factor to bring it into line with evaluation data (from ROC's) and the use of multiple curves considerably complicates the simulation. Also, when scenarios of future capacities are simulated, it will be necessary to make assumptions on the size of wind turbines, as it is impossible to know what kind of turbines will be used. Therefore selecting turbine size by wind farm represents an unnecessary level of detail, provided that results are of a similar accuracy to that shown by Staffell and Green [2014].

Using these selected archetypal wind turbine curves, subsequent simulations calculate how many of these turbines are required to fill the capacity stated for each grid square and simulate the amount of power generated using the curve. At this stage, the simulations do not take into account wind turbines not being available during the evaluation process, due to the difficulty in knowing when maintenance and curtailment are happening. This may mean that generation is overestimated. Manufacturer curves provide generation values provided at each wind speed to the nearest m/s, CFSR reanalysis data is provided at a much higher precision. Therefore the selected curves have been linearly interpolated between wind speeds to provide information to the nearest 0.1 m/s, CFSR wind speed values have been rounded to the same level of precison.

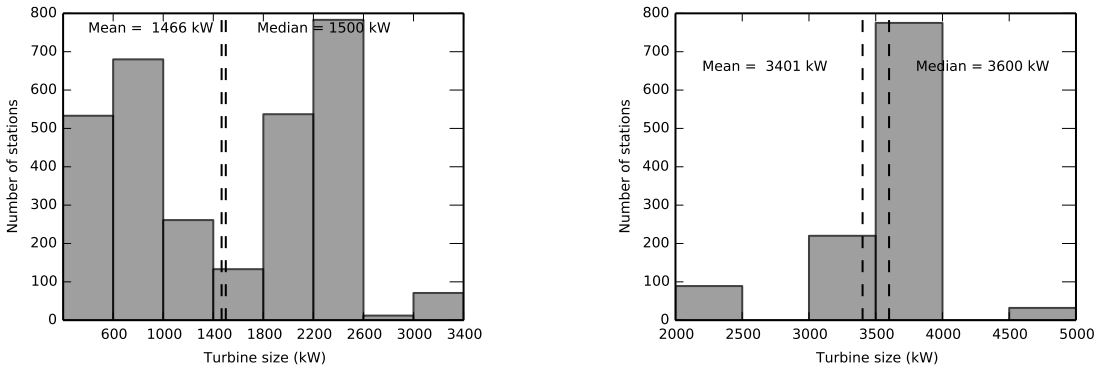

(a) Onshore ROC sites.

(b) Offshore sites.

Figure 4.2.: Capacities of installed turbines in GB.

4.1.1.1. Multiple turbine power curves

Following Section 2.1.3, it is clear that there are problems associated with applying a manufacturer wind turbine curve to a number of turbines. A method is described in Norgaard and Holttinen [2004] that adapts a single manufacturer turbine curve to represent many turbines over a large area, where only a single wind speed time series is available, and the more complex methods described in Section 2.1.3 are not possible. The method first takes the wind speed time series and alters it to better represent wind speed over a larger area. This is done using a block average with respect to the mean wind speed. Norgaard and Holttinen provide a chart that gives normalised standard deviations for a range of area sizes and wind turbulence intensities (a proxy for the effects of wind disturbance, caused by, for example, other turbines), an appropriate value is selected, based on the scope of the simulation. This is then used to alter the block averaged mean wind speed to produce an adapted standard deviation value.

The standard deviation value is used to create a normal distribution curve, this normal distribution curve is then used to create a probability density function around 0 m/s showing the probability of a power output being produced at an offset wind speed from the stated value. Figure 4.3 shows an example of the probability density function where the area is the largest provided (300 km^2) and a turbulence intensity of 10% is assumed (a metric which characterises the turbulence in the wind). This maximum area size is considerably less than the land mass of GB (~229,000 km^2), demonstrating that this method may not be suitable unless applied to smaller areas. The normal distribution is applied to the single turbine curve using the formula described in Equation 4.1. The effect of this equation on manufacturer curves is shown in Figure 4.4, which demonstrates the common effects of this method; smoothing of the curve at the cut in and out wind speed, and also the point at which the generation plateaus. The adapted curve is then used to simulate turbine output over the scope using the averaged wind speeds.

This method is widely applied, examples relevant to this study (UK based) include Staffell and Green [2014], who produce aggregate power curves for single wind farms, no reference to smoothing wind speeds is given, which is an example of the method being adapted to suit the needs of the user and the data available. The results of this approach are shown to be good when combined with reanalysis data and interpolation (R^2 with ROC 0.972). Staffell and Green [2014] cite Pöyry

Equation 4.1 Norgaard and Holttinen [2004] equation for the creation of aggregated power curves. Pm_j is the power created at a given wind speed for multiple turbines, Ps_j is the j^{th} element of the single turbine curve, Ps_i is the probability of that power being produced at a different wind speed according to Figure 4.3.

$$Pm_j = \sum_i Ps_{j+i} Ps_i$$

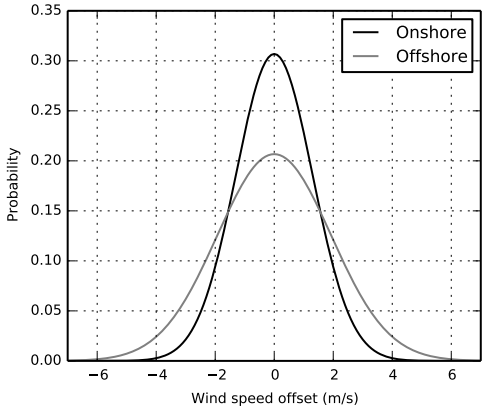

Figure 4.3.: Probability density function for the offset of manufacturer turbine curve wind speeds in a wind fleet distributed over 300 km^2 assuming a turbulence intensity of 10%.

[2009a] and Ofgem [2012a] as other users of the method. Pöyry [2009a] state that they use an aggregated power curve as a "group of wind turbines have a smoother output" and "will not all cut out together"; however no information is provided on the method for producing aggregated curves. Cannon et al. [2015] used both an adjusted and unadjusted manufacturer turbine curve, finding no statistical difference in the output in terms of correlation coefficient. Their paper does appear to show a small improvement in error, however this is not quantified and it is difficult to ascertain the extent of this improvement from the plots that they provide. They use the adjusted curve for analysis subsequent to the comparison.

As the aggregate power method apparently provides a simple alternative to single curves which may improve accuracy its use is explored in the evaluation of the wind model below. There are other variations on the manufacturer curve method including those which look further at the effect of atmospheric conditions.

4.1.2. Turbine hub height

The selected turbine curves (Figure 4.4) give information on the conversion of wind speed to power at the height of the turbine hub. The use of the hub height simplifies the effect of wind on a turbine. Wind speed increases with height and power is the cube of speed, therefore the top of a turbine experiences more power than bottom, and the average power will be above hub height. Studies estimating the generation of installed capacities have typically assumed that hub heights are around 80 m [see Kubik et al., 2011]. As described in Chapter 2, very few of theses studies include offshore simulation, therefore this height represents predominantly onshore turbines. The hub height of the archetypal curves described above varies between 60 m - 80 m onshore and is

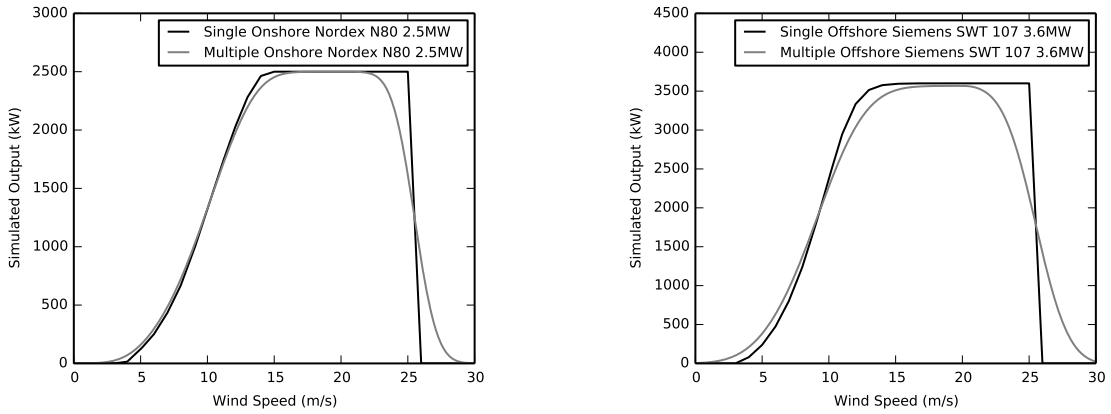

(a) Onshore.

(b) Offshore.

Figure 4.4.: Manufacturer wind turbine curves adapted to represent the conditions within a wind farm using the method from Norgaard and Holttinen [2004]. The curves are the same as shown in Figure 4.4.

usually 80 m offshore, but the same turbine can be operated at different heights. To ensure that the wind speed height used for simulations represents installed capacity and is not skewed by the selection of these curves, an analysis of installed turbine hub height was performed using the same data as for turbine size.

Figure 4.5a summarises this data, which represents the onshore wind turbines with ROCs, showing that the mean turbine height is 54 m and the median is 60 m. Staffell and Green [2014] state that the average onshore turbine hub height is 62 m. Figure 4.1 shows that ROC sites represent a significant proportion of the installed capacity in GB, therefore 60 m has been selected as a suitable height for onshore turbines in subsequent simulations. This represents a compromise between the value found here and that found by Staffell and Green [2014]. Studies using 80 m to represent installed capacity may be overestimating wind energy potential. Figure 4.5b summarises the hub height of operational wind farms offshore of GB, according to the REPD. The plot shows that the mean and median heights are very similar (82 m and 80 m respectively), with few turbines that are not between 80 and 90 m high. Therefore 80 m has been selected as an appropriate height for installed offshore turbines. Those turbines with a hub height above 90 m represent wind farms containing 5 MW turbines, these are currently in the minority in GB, but there are plans to increase their usage, as the size reduces the cost of installation per MW, that is a restrictive factor in offshore wind development. This change in capacity may have to be taken into account when simulating projected capacities (see Chapter 6). It is probably the case that this is less of an issue onshore where opposition to wind turbines can limit size. The selection of 60 m for onshore and 80 m for offshore turbines means that the wind speed height correction can be performed for all the weather data at the same time, reducing the computational load that would be necessary for "on the fly calculations" of site specific turbine heights. Using an archetypal turbine hub height, despite being an established method in the literature, represents a simplification of the real world. It may, therefore, result in inaccurate representation of generation. This is another reason for evaluating model outputs as well as inputs.

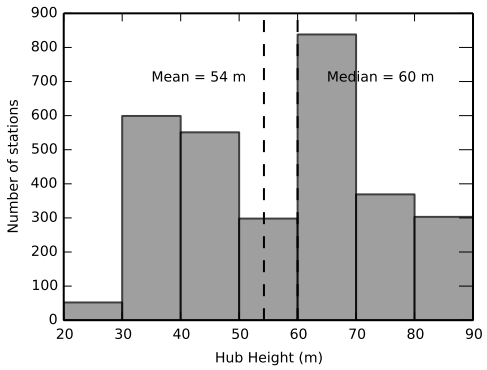

(a) Onshore sites. Data source: Staffell and Green [2014].

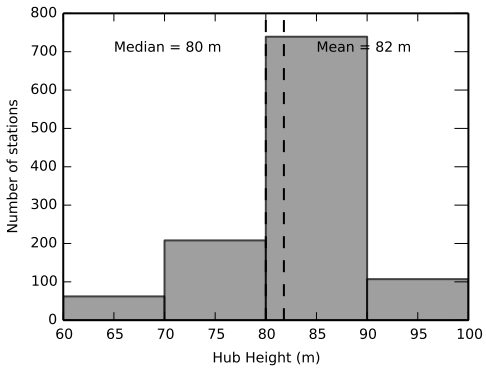

(b) Offshore ROC sites. Data sources: REPD, Hughes [2012] and site specific data from operator websites.

Figure 4.5.: Turbine hub height at GB wind farms.

4.1.3. Wind height correction methods

As shown in Section 2.1.3, measurements of near surface wind speeds are provided at 10 m elevation, either above the surface in the case of stations, or a geoid in the case of reanalyses (although MERRA provides wind speed data at 2 m, 10 m and 50 m above a surface displacement height). Section 3.3.1.1 discusses the implications of this on the representation of wind speed. Turbine hub height has increased over time to elevations far above the standard 10 m measurements of wind speed (Figure 2.1 and Figure 4.6). Horizontal wind speed increases with height, as friction exists at the surface due to roughness, and insolation from the sun thickens the boundary layer. Atmospheric stability also effects the rate of change, this is driven by heating and cooling of Earth's surface and the resultant mixing of air above the surface (states are referred to as stable, neutrally stable or unstable) [Schallenberg-Rodriguez, 2013]. The rate of increase of the speed as height increases is referred to as the wind gradient or wind shear. Wind speed values must therefore be altered to better represent conditions at hub height. There are two commonly used methods.

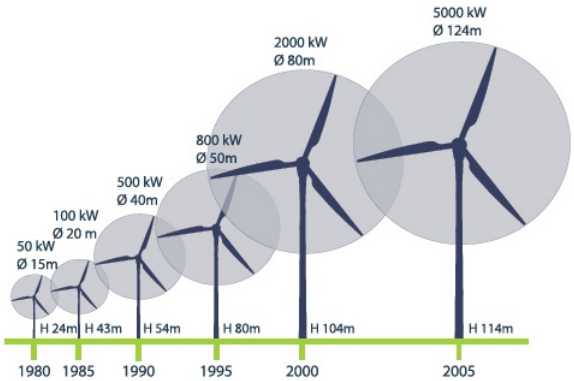

Figure 4.6.: Evolution of wind turbine size 1980-2010, source: Renewable-UK [2014] (formerly the British Wind Energy Association (BWEA)).

The first method assumes that the wind profile follows a power law and is sometimes referred to as the Hellman equation (Equation 4.2). Using this equation, wind speed is altered to a new height

using the the Hellman exponent which combines the increase in wind speed due the stability of atmospheric conditions and the surface roughness into a single constant. This characteristic exponent is in the range 0.1 - 0.6. Many studies use a value of 1/7 (~ 0.142) onshore, to represent neutral stability conditions, which results in reasonable conversion over large areas [Peterson and Hennessey Jr, 1978], or 1/9 (0.1') offshore [Hsu et al., 1994]. These values can, however, lead to conservative estimates of wind speed [Gipe, 2004], particularly at higher altitudes [Kubik et al., 2013b, Schallenberg-Rodriguez, 2013]. This could accentuate the poor representation of wind speeds at high elevations by CFSR described in the previous chapter. However, in the case of GB these locations are unlikely to be developed. Schallenberg-Rodriguez [2013] note that the single exponent should only be appropriate for smooth terrain with a low roughness, but may be accurate enough to use for wind conditions up to 100 m elevation for rural terrain, where the atmosphere is stable. This method is used by studies simulating large scale wind capacities in the UK [Pöyry, 2009a, Sinden, 2007, SKM, 2008].

Equation 4.2 Power Law (Hellman equation) equation for altering wind speed height to turbine hub height, $u(z_i)$ are the wind speeds at heights z_i, H is the Hellman exponent.

$$u(z_2) = u(z_1)\left(\frac{z_2}{z_1}\right)^H$$

The second method assumes a logarithmic profile law (Equation 4.3). Lookup tables provide a value for the roughness length as a function of the terrain [e.g. Manwell et al., 2010]. The lowest end of the roughness scale is calm open ocean and may have a constant of 0.0001, at the opposite end of the scale, sites with tall buildings may reach a constant of 3. This method is used by Coelingh [1999], Giebel [2000] and Kiss et al. [2009] amongst others. The logarithmic profile law is a simplification of the log-linear law (Equation 4.4), based on the assumption of neutral atmospheric stability. This log linear law is is less widely used as it introduces complexity by adding an atmospheric stability function, which requires information that is not often available.

Equation 4.3 Log Law for altering wind speed height to turbine hub height, $s(z)$ is the wind speed at the desired height z, z_0 is the roughness length (a measure of the surface roughness), u_* is the friction velocity and k is the Von Karman constant (Schallenberg-Rodriguez [2013] state that this is typically 0.4)

$$s(z) = \left(\frac{u_*}{k}\right) ln\left(\frac{z}{z_0}\right)$$

Equation 4.4 Log Linear Law for altering wind speed height to turbine hub height. $s(z)$is the wind speed at the desired height z,z_0 is the roughness length (a measure of the surface roughness), $u_*$is the friction velocity and k is the Von Karman constant. L is the Monin-Obukhov stability length (m) and A_m is the atmospheric stability function.

$$s(z) = \left(\frac{u_*}{k}\right)\left[ln\left(\frac{z}{z_0}\right) - \mathrm{A}_m\left(\frac{z}{L}\right)\right]$$

Kubik et al. [2013b] consider the use of the profile log law against the power law. In a review of the literature, they note that Elkinton et al. [2006] show that the profile log law and the power law perform equivalently with different methods working better depending on the site. Through their own analysis (which uses data from a single wind farm and a MIDAS station that is 10km

from the farm) they find that the use of a single Hellman exponent gives good results for a whole year, but can result in significant errors for hourly values. Importantly, they note that any error is exacerbated when converted to power, citing Kubik et al. [2011]. They also show that the exponent varies over time irrespective of surface roughness, demonstrating the impact of solar warming during the hotter months. The fact that the exponent varies temporally, due to the incorporation of atmospheric stability, illustrates the fact that this method only ever produces approximate wind speed values and therefore any model using wind speed altered in this way should be evaluated if possible against seasonally disaggregated data.

There has been research into the effects of topography on wind height correction methods. Gipe [2004] has shown that the two methods agree in coastal areas but less so inland. Also Elkinton et al. [2006] found that neither the log law or the power law provide good a estimation over complex terrain. Complex terrain is a broad term and is often used in the literature as a threshold beyond which methods do not work (see Section 3.1.1). As this is often a global perspective it seems reasonable to take the definition from Landberg et al. [2003] of mountainous terrain with steep slopes and sharp ridges and assume that these comments refer to conditions that are more extreme than found in GB. Therefore the term varied terrain is used here, distinct from the use of complex terrain in the literature.

Clearly, the use of single coefficients characterising land over large geographical scopes with variable topography is a simplification. It is likely that this will exacerbate the misrepresentation of higher altitude sites described in Chapter 3. The effects of speed up can only be taken into account if corrections are made at individual turbine/farm sites, where detailed topographical data is available. This could be extended to a set or fleet of wind farms through the use of for example a Digital Elevation Model (DEM), but doing this over large geographical scopes would be extremely computationally intensive and wind direction information would be needed. It may also be the case that reanalysis data is too spatially coarse to make this worthwhile, as it does not necessarily represent conditions at the base of a hill but rather a simplified, smoothed, topography. A large amount of analysis would be necessary to include this information, this explains why it has not been done previously and is the reason that it is not performed here. Wind direction can also be used in modelling of wake loss etc.

Where multiple wind time series are available there are other methods in the literature to correct the wind speed. For example, Kiss et al. [2009] find that a linear transformation between nacelle height wind speeds (65 m) and ERA-40 data, works very well. This is, however, performed at a single site and requires individual examination of the datasets. Calculating the Hellman exponent is simple if wind speeds at two heights are known, as the power law equation can be rearranged. An example of this can be found in Staffell and Green [2014], who utilise the multiple wind heights provided by MERRA by linearising Equation 4.2 and performing least squares regression on interpolated wind speed data.

There are also methods for determining the value of the Hellman exponent using the parameters of the log law. These may improve the accuracy of the outcome, but require information on surface roughness, which is most often gathered by visual inspection. Data does exist on land use from the CORINE database which is used elsewhere in this study. Landberg et al. [2003] mention its potential use but do not give specific examples. This method is suitable for site specific studies. However the use of reanalysis wind speed data means that the surface conditions represented by the wind speed are an average of a whole grid square and there is no established method for the

calculation of an average surface roughness.

There is ongoing work looking into improving methods for adapting wind height. There is no satisfactory answer and therefore the simplicity of the power law represents the most attractive option. The uncertainty of assuming even conditions over space and time means that it is very important to evaluate the outcome of wind height correction. It is often the case that the error caused by wind height adaptation can be corrected for in scale factors that also allow for other sources of error, these are described in more detail in Section 4.4.3. The extensive use of the method in the literature, combined with the lack of viable alternative and the ability to correct error through later evaluation of model output, means that the power law has been used here.

4.2. Evaluating the accuracy of wind turbine simulations using CFSR, with respect to measured generation

4.2.1. Comparing simulated output from wind speed data to measured data

The propagation of error is not linear due to the method of conversion from wind speed to power and the need to correct the wind height. Therefore some studies using reanalysis data for wind turbine simulation have evaluated the output of simulations as well as the input wind speed data. As noted in Section 2.1.6, there are several datasets that provide data on historical wind generation in GB. The most widely used of these is Ofgem's Renewables and CHP register which contains the monthly outputs of those wind farms that are enrolled in the UK Government's Renewables Obligation scheme.

The Renewables Obligation has been running from 2002 and continues to the present day. It is a mechanism to obligate suppliers to source an increasing proportion of electricity from renewable sources [Ofgem, 2014]. The supplier must present a certain number of ROCs, which are issued to accredited renewable generating stations for the eligible renewable electricity they generate. If suppliers do not have sufficient ROCs then they must pay for the equivalent value. This money is used to pay for the administration of the scheme with the remainder redistributed proportionally to suppliers. The reporting that is required to keep track of generation means that a consistent dataset is available for those simulating wind turbines to evaluate both datasets and methods.

A second less widely used dataset is provided by Elexon [2014b], who are responsible for the GB electricity system balancing mechanism, the data are disseminated from information provided by National Grid. These data are provided at five minute or half hourly intervals which is significantly less temporally aggregated than the ROC data. However the data covers a much shorter time period (November 2008 - present day) and only contains information on generation from a small sub section of GB wind farms that are aggregated; the wind farms are described further in Section 4.3.2. It is also possible to extract data for individual wind farms through final physical notification messages, this is rarely performed and to date only Staffell and Green [2014] have published research based on this data.

4.2.1.1. Onshore only

There are currently four studies which have simulated a fleet of turbines onshore of the UK and evaluated the output against measured data. Two of these only show the correlation for onshore sites [Kubik et al., 2013a, Staffell and Green, 2014], Hawkins et al. [2011] and Cannon et al. [2015] correlate both onshore and offshore sites. Correlation coefficients and error measurements are summarised in Table 3.1 and Table 3.2. These studies use the same metrics of correlation and error described in the previous chapter.

Staffell and Green [2014] correlate monthly wind speeds from their interpolated MERRA data to ROC data, both aggregated to a national scale, showing an R^2 of 0.972 over all months. The use of wind speed rather than generation shows only that there is minimal error introduced by wind height correction and interpolation. It does not say anything about the effect of turbine simulation or associated complications such as maintenance etc. Also monthly aggregation means that variability at less aggregated temporal resolutions is lost. These results are achieved using site specific turbine curves and hub heights.

Staffell and Green [2014] also correlate the monthly wind speed at each ROC site to the monthly load factor. Several examples are given that show good correlation, with a median R^2 of 0.84. In the plots provided there is no clear difference between correlations at high and low wind speeds.

Staffell and Green [2014] correlate simulated output directly against measured data, finding that the mean R^2 over all sites and all months is 0.59, 98% of the simulated outputs were lower than the measured load factors. There are no results shown that aggregate the results nationally, despite doing this for wind speed. This is because the focus of their paper is the performance of individual wind farms rather than aggregated output and variability. Staffell and Green [2014] also correlate the sites that are part of the Elexon data to hourly measured generation, no summary statistics are provided, however graphical comparison shows that subsequent to a linear correction factor of 0.698, the time series correlate well, although there is noise at all wind speeds, as well as a range of errors.

Outside of GB there is data available from other sources, for example Kubik et al. [2013a] obtained half hourly wind generation data from Northern Ireland's system operator. They bi-linearly interpolate MERRA data to MIDAS station sites in Northern Ireland to the nearest 0.1^{o}. They then simulate total installed capacity using both in situ and reanalysis data, at a given capacity factor, assuming that this capacity is evenly distributed across these sites, using the simulation method described above. While the comparison with measured generation data demonstrates that both datasets result in a good correlation, interpolated reanalysis data is marginally more accurate (Table 3.1) (MIDAS Pr= 0.88, Interpolated MERRA = 0.91).

4.2.1.2. Onshore and Offshore

Hawkins et al. [2011] simulate monthly ROC load factors for 196 onshore and 8 offshore wind farms, between 2006 and 2010, and find that after applying a linear scaling factor of 0.69, R^2 = 0.94 (onshore), which is very good and in line with the correlation between in situ wind speed and their downscaled data. Offshore they found a large deviation in the winter of 2006 - 2007, that they attribute to "low technical availability in the early stages of some offshore wind farms"

[Hawkins et al., 2011, p. 2], no R^2 value is stated, although the correlation appears similar but perhaps slightly less good than onshore in the graphical representation.

Cannon et al. [2015] bi-linearly interpolated MERRA data to location of 2012 GB capacity (they use a static capacity and do not take into account changes over the year). They use a manufacturer turbine curve and an adjusted curve as described in Chapter 2. They find a correlation between simulated and measured generation of 0.96, with no correction factor.

4.2.1.3. Correction factors

The result of the ability to quantify the divergence between modelled and measured wind fleet output is that correction, or scaling factors, can be created, that converge modelled output with measured data. Thus far these correction factors have been linear scaling factors designed to reduce the bias between modelled output and measured data. The correlations described above are a result of model output that has been subject to a correction factor, other than Cannon et al. [2015]. These correlation factors are applied after simulation and therefore encapsulate all the sources of error.

Hawkins et al. [2011] scale onshore turbine output by 0.69 to bring in line with ROC data, offshore they do not find that this is necessary, but they use the factor in analysis to ensure that results are not systematically over estimated. Staffell and Green [2014] look in more detail at the drivers of the need to scale results and attribute this to real world factors (machine availability (4-7% downtime) [Harman et al., 2008, Arwade et al., 2011], operating efficiency (2% reduction) [Harman et al., 2008], wake effects (5 - 15% reduction)[Barthelmie et al., 2004, 2007, Phillips et al., 2010, Ali et al., 2012, Schallenberg-Rodriguez, 2013], turbine ageing [Hughes, 2012] and site conditions (2-5% reduction plus 1% per 3% increase in turbulence intensity) [Johnson et al., 2008]). Using values from the cited literature they believe that this equates to a "performance ratio" of 0.725 [Staffell and Green, 2014, p. 780]. Staffell and Green's own findings suggest that the current wind fleet output is 7.5% lower than an as new equivalent due to turbine ageing. By measuring differences between simulated "ideal" load factors and measured load factors using monthly ROCs they find a scale factor of 0.69 (the same as Hawkins et al. [2011]) is suitable and therefore attribute 6% of the difference to site conditions.

Kubik et al. [2013a] do not apply a correction factor post simulation, instead a capacity factor of 0.312 is applied pre simulation. This value is significantly lower than used by Hawkins et al. [2011] and Staffell and Green [2014] demonstrating that the combination of the real world factors vary geographically (Kubik et al. [2013a] simulate Northern Ireland only) and that modelling methodology may play a part (different turbine curves are used and interpolation/downscaling methods vary). Therefore, although Hawkins et al. [2011] and Staffell and Green [2014] find the same correction factor for very similar geographical scopes and resolutions, wind capacities and temporal resolutions, the fact that there are only two studies means that it is necessary to create a new correction factor if new data or methods are used.

The lack of correction factor needed in Cannon et al. [2015] demonstrates that they have developed effective simulation methods including interpolation, wind speed height correction an curve selection which appear to take losses into account. This is particularly impressive given that a static capacity is used to model hourly output for a whole year, during a period of development. However,

it is unfortunate that this analysis was not performed over a longer time period given that more than 5 years of data is available as wind conditions and installed turbines will vary.

4.3. Evaluating the accuracy of the CFSR driven wind model with respect to measured generation: Data and Methods

Establishing that CFSR wind speed data is at least as accurate as other reanalysis models means that it is potentially a good dataset for wind turbine simulation. As described in Section 4.2.1 there are a number of real world factors that introduce error when using modelled wind speed data to simulate wind fleets, therefore it is also necessary to evaluate the output of simulations. The review showed that the most widely used data for this purpose is from the ROC recording system. This is due to the fact that it covers a large proportion of the installed capacity and it is available in an easy to use format. For this reason this dataset is utilised in the following evaluation. However, the obvious disadvantage of this dataset is the temporal resolution, which at one month means that much of the variability in wind generation is lost. Fortunately, although the proportion of capacity represented is smaller, the Elexon data is provided at the ideal temporal resolution for this study (1 hour, the same as the minimum temporal resolution of the modelling), therefore this is also used.

4.3.1. Ofgem ROCs

Data on monthly generation at ROC sites was obtained from the supplementary material provided by Staffell and Green [2014]. This was used in place of raw data due to the fact that cleaning and checking had already been performed. Thanks go to these authors for the provision of this material. The dataset contains location, generation and farm capacity data, however, cross referencing was necessary to join together location and other data. The data does not include offshore sites, these are assessed using the Elexon data, the variation in generation at onshore sites was considered to be of higher importance, because, as shown in the analysis above, these sites experience more complex wind speed changes and there is a far greater number of them. Therefore, the offshore ROC data, which is used by Hawkins et al. [2011], is not used in this analysis. Values were extracted from the beginning of the dataset (2002) to the end of 2010, which is the longest time series available within the model boundaries. Generation commencement was taken as the month where the ROC data started. It is possible this will result in overestimated generation as the wind farm may not have begun generating at the beginning of a month. However it is likely that initial generation will not be at full capacity (see Section 4.2.1.2). This illustrates a pitfall of temporal aggregation.

The data were adapted for integration into the model by allocating point data to the model grid. This analysis uses the data that cover Northern Ireland to increase the capacity covered and eliminate the need to clean the ROC data. Figure 4.7 shows the location and capacity of the ROC sites at the beginning, middle and end of the evaluation period. The map demonstrates the large and steady increase in capacity over time. Comparison with Figure 4.8 shows that the ROC sites represent greater spatial diversity than the Elexon sites. There is a bias towards Scotland, however more of the UK is represented by the ROC sites than with Elexon sites. A longer time period is covered, which means that the data incorporates months where UK wind capacity was relatively

small compared to the end of the evaluation period. The cumulative capacity is summarised in Figure 4.1. This demonstrates that a large percentage of the installed capacity is represented, despite the fact that no offshore sites are used in this analysis (Figure 4.7). Comparison with Figure 4.9b demonstrates that ROC sites represent a more significant percentage of capacity than those that contribute to the Elexon data. Therefore, although the temporal resolution is coarser, the output is potentially more representative of GB capacity.

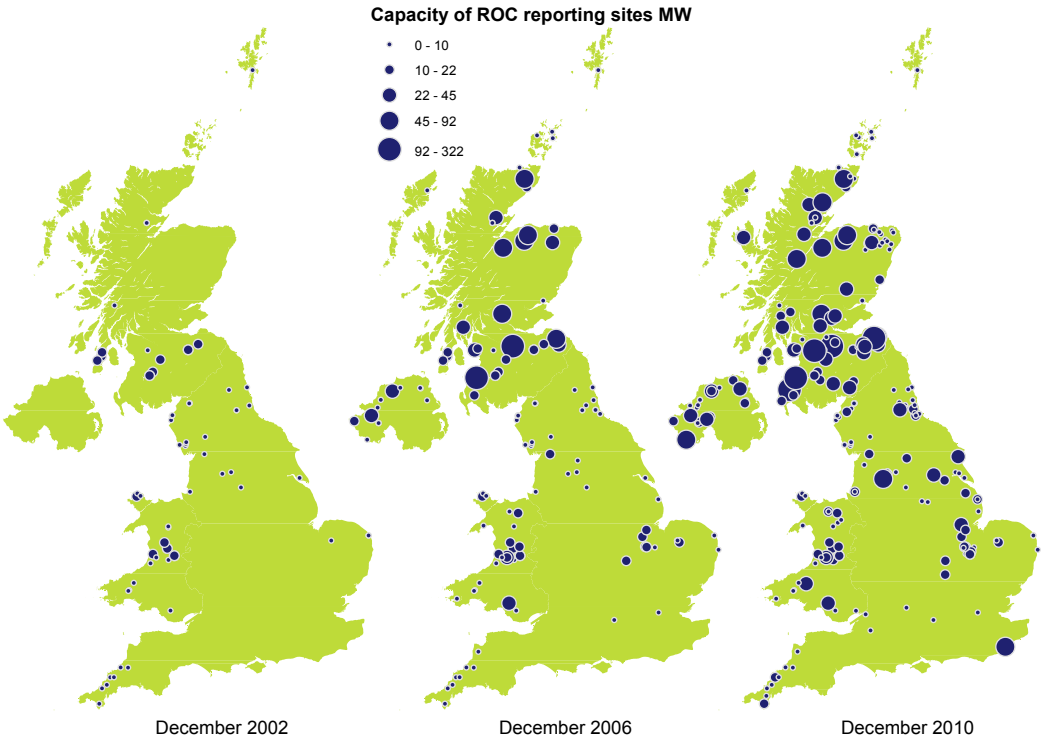

Figure 4.7.: Wind farms that are part of the Renewable Obligation Certificate scheme used in the evaluation of the wind model. Site and capacity data source Staffell and Green [2014], the years represent the beginning, middle and end of the data.

4.3.2. Elexon half hourly generation by fuel type

Data on generation from wind were obtained from Elexon [2014b]. Data are available half hourly and at five minute intervals from November 2008 to the present (minus a delay of one quarter). Hourly average values were derived from the half hourly data to the end of 2010 in alignment with the temporal boundaries of the model. As described above, these data only represent a portion of the operational wind capacity. Only the farms which record generation and provide information to National Grid's Balancing Mechanism Reporting System (BMRS) contribute. These sites were identified as those with associated Balancing Mechanism Units (BM) from Elexon [2014a]. The units within this database are not identified by fuel type, therefore the dataset required some cleaning to separate the wind farms from other generation types. A location and generation commencement date was assigned to each of these BM units using the latest revision of the REPD [DECC, 2014a]. Some additional cleaning was performed to remove not yet operational BM units and match the BM capacity to the REPD, where the unit may only represent a proportion of the

wind farms capacity, e.g. Gunfleet Sands and its extension have separate BM units. None of the sites that are part of the BMRS are noted as decommissioned in the REPD within the timespan of the Elexon data, therefore no end date is assigned for any of the capacity.

Using these data it was possible to create a spatially explicit longitudinal database of wind generation capacity. The location and capacity of the wind farms at the end of each of the years described in the Elexon data that contribute to the BMRS are shown in Figure 4.8, alongside the rest of the operational capacity. Clearly BMRS capacity does not fully represent the spatial diversity of the GB wind fleet over this period. Larger farms are well represented, which results in a consistent proportion of capacity being recorded by National Grid (Figure 4.9a). Also, most of the changes in capacity during the evaluation period are from sites recorded in the BMRS (Figure 4.9). The longitudinal capacity point dataset was allocated to the model grid to allow simulation of the changing capacity, a daily temporal resolution was used. This alleviates some potential issues associated with assuming a static capacity over longer time periods. Figure 4.10 shows a snapshot of the resulting dataset at the maximum capacity, accentuating the lack of spatial diversity and showing that no offshore Scottish farms are represented.

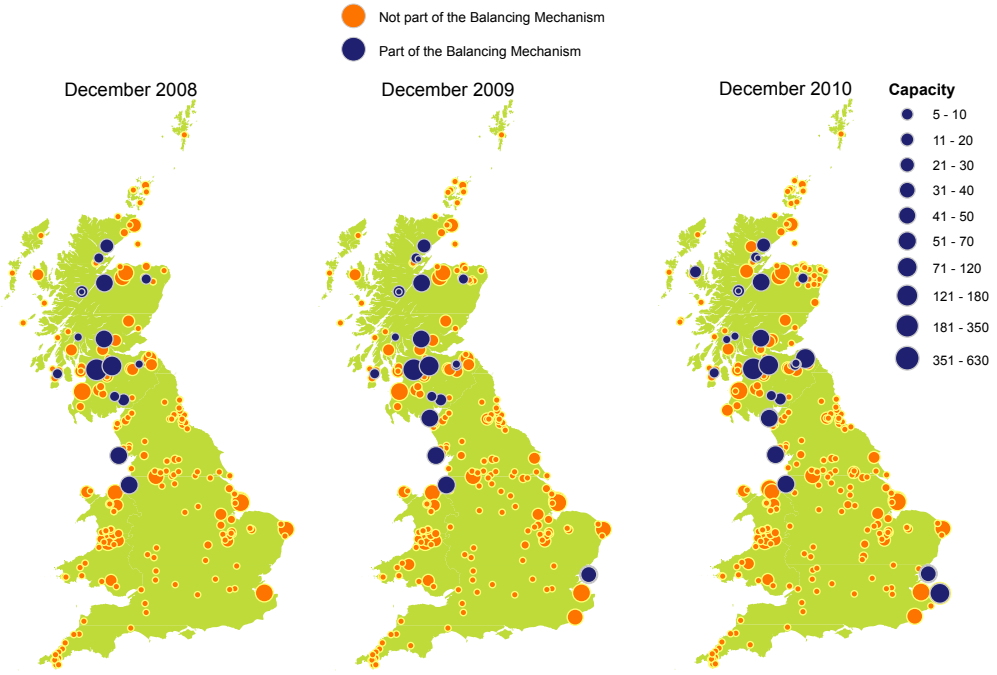

Figure 4.8.: Wind farms that are part of the Balancing Mechanism over the course of the Elexon half hourly measured data, the years represent the beginning, middle and end of the data.

Section 4.1.1 established a standard hub height and turbine curve for onshore and offshore simulations of installed capacity. As stated, the BMRS capacity only represents a fraction of the installed capacity. Therefore an analysis was done to ensure that the archetypal hub height and turbine size applied. Figure 4.11 shows an adapted version of Figure 2.1, highlighting the BMRS capacity. The figure demonstrates that the mean wind turbine size for onshore BMRS sites is larger than shown in Figure 4.2, but only slightly larger than the 2.5 MW onshore turbine curve selected as representative of onshore capacity shown in Figure 2.2. The offshore mean turbine size is the same as Figure 2.2, which is unsurprising due to the prevalence of this type of turbine offshore of GB as described in Section 4.1.1. Therefore the approach described in Section 4.1.1 was used.

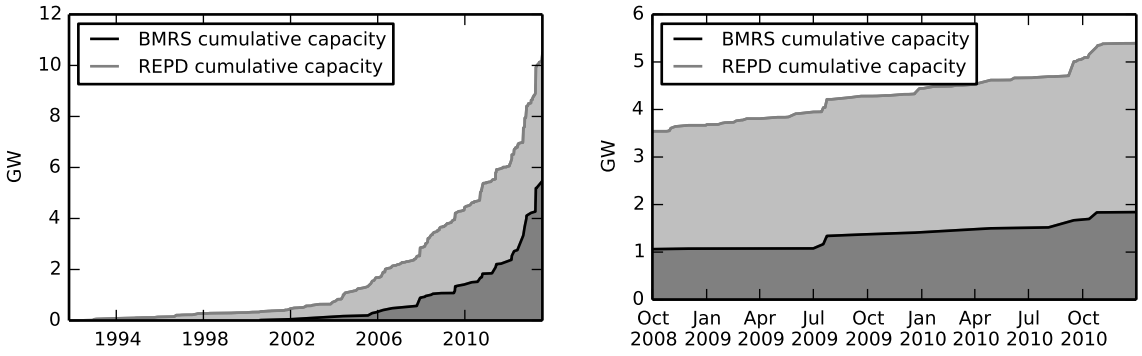

(a) Since the first wind generation.

(b) Over the evaluation period.

Figure 4.9.: Relative capacity of operational wind capacity and wind recorded on the BMRS.

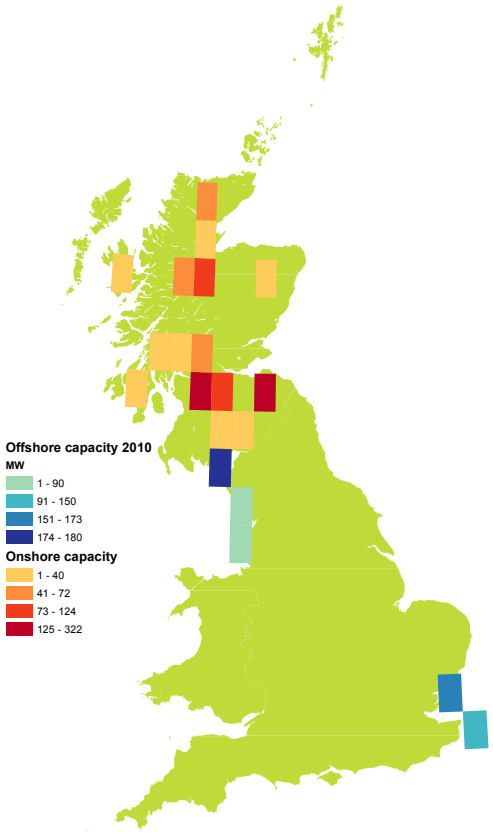

Figure 4.10.: Balancing Mechanism wind farms allocated to the model grid demonstrate the limited spatial diversity represented by the system.

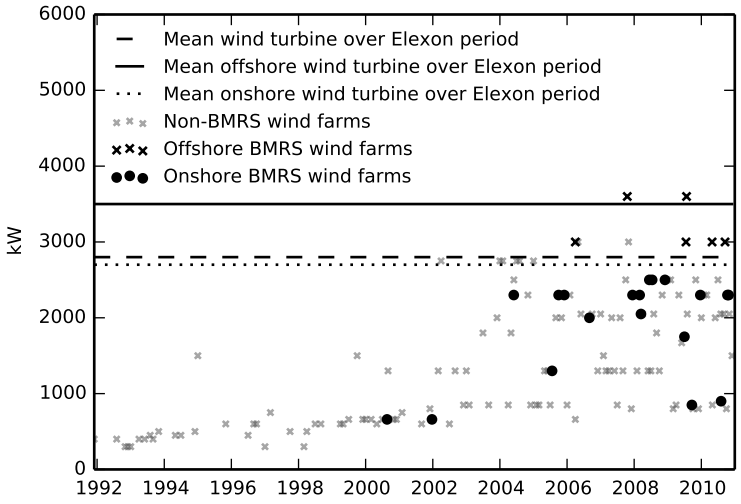

Figure 4.11.: Wind turbine sizes for all GB wind farms. Derived using data from DECC [2014a], Hughes [2012], Elexon [2014a], Staffell and Green [2014].

4.4. Evaluating the accuracy of the CFSR driven wind model with respect to measured generation: Results and discussion

4.4.1. Ofgem ROCs

Figure 4.12 shows the correlation between the aggregated simulated wind generation at ROC sites and the data on monthly ROC site output between 2002 and 2010. The correlation coefficient is directly comparable to Hawkins et al. [2011] as they aggregate all onshore farms. The comparison is favourable ($R^2 = 0.89$ compared to $R^2 = 0.94$), especially considering that their data is downscaled. Comparing to the results described by Staffell and Green [2014] is more difficult as their R^2 value of 0.59 is not for the fleet as a whole but rather the mean of the correlations between individual wind farm time series. Interestingly the results found here are similar to the correlation that Staffell and Green [2014] find between wind speed and load factors (nationally $R^2 = 0.97$, median of disaggregated $R^2 = 0.84$). Assuming that simulation introduces error, Staffell and Green's coefficients would be reduced and most likely be lower than those found here. The results described in Figure 4.12 have not been subject to a correction factor, but linear correction has no effect on correlation coefficients. It does, however, affect RMSE, this is already low at 0.16 GW (it is difficult to express as a percentage due to changes in capacity).

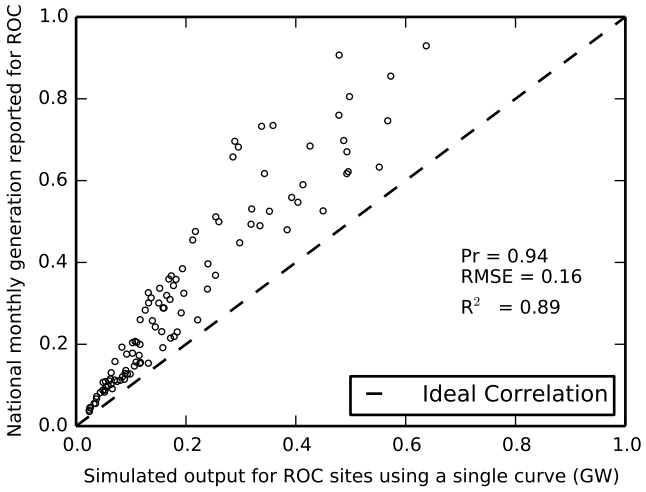

Figure 4.12.: Correlation between national wind generation recorded as part of the ROC scheme and simulated output at these sites. Monthly national values.

4.4.2. Elexon Balancing Mechanism

The method described in Equation 3.2 was used to calculate the bias between the aggregated simulated BMRS output and the Elexon data. Figure 4.13a shows that over the entire time series there is considerable noise in both the positive and negative directions. However, the mean bias is very low and slightly negative, showing that overall output is slightly underestimated. It appears that after September 2010 there is a greater underestimation of the output. Figure 4.13b shows

output for each year, the mean bias is similar each year and always negative, peak bias in 2008 is the lowest but there is a shorter time series available for comparison. Winter months in 2009 and 2010 exhibit noise at a greater magnitude, this is due to the greater range of higher magnitude wind speed during these months. Analysis was performed on the CFSR data to illustrate this point. The mean of all hourly onshore wind speeds in grid squares that contain GB land was calculated. Figure 4.14 demonstrates that there is clear difference in wind speed over GB between months or seasons. Summer months are characterised by a narrow range of mean wind speeds between 2 and 10 m/s with a resultant large number of hours spent at the wind speed in the middle of that range. Winter months experience higher wind speeds over a greater range of approximately 3 to 20 m/s. The larger range denotes greater variability in the windiness of GB in the winter. This pattern is potentially advantageous in terms of producing power from the wind as there is greater need for electricity in the winter months, particularly if more heat demand is converted from gas to electricity, provided that these high wind speeds are experienced at the right time (when power is needed, assuming that storage is limited) and in the right places (where turbines have been or will be placed). However, it also means that if CFSR wind speeds do not exactly match those experienced at wind turbine locations or the simulation method is imperfect, error will be accentuated. Variation in wind speed and temperature at different temporal resolutions is explored in (Section 8.4).

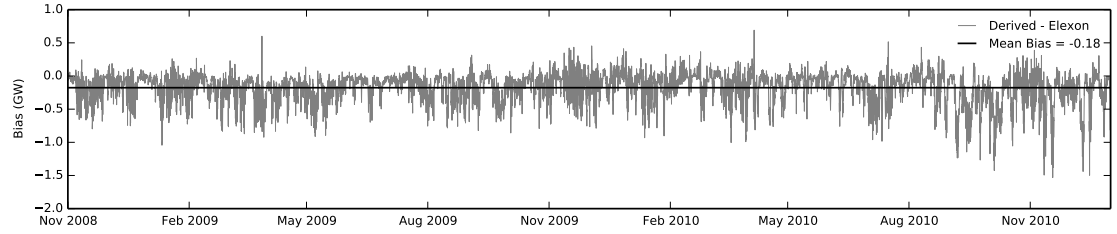

(a) Whole time series

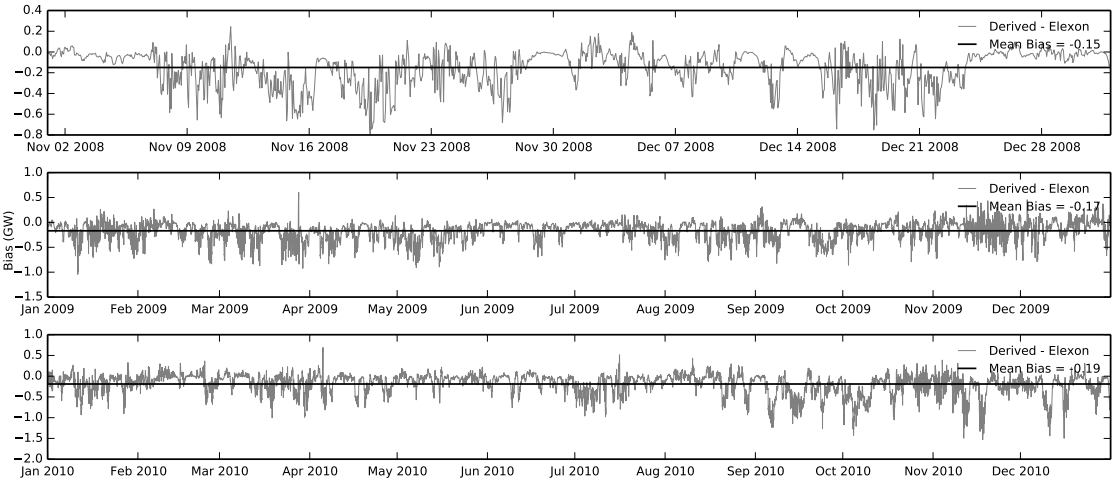

(b) Separated years

Figure 4.13.: Bias between simulated output and Elexon balancing mechanism data.

Figure 4.15, Figure 4.16 and Figure 4.17 show the correlation between the BMRS data and the simulated output for each hour of the simulation. Linear regression coefficients, Pr and RMSE have been calculated using the same method as described in Section 3.2.4. The whole time series

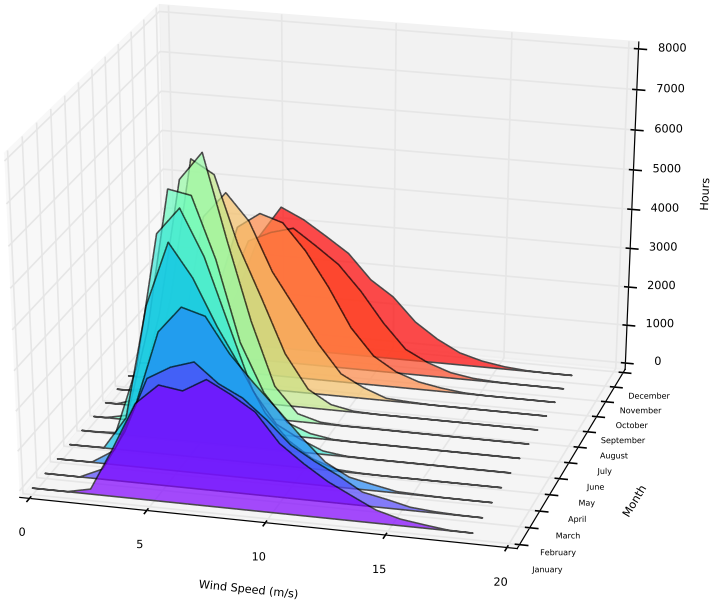

Figure 4.14.: Hourly GB mean wind speed during different months of the year.

shows that, despite a large amount of noise at all levels of output, the regression line is very close to ideal, R^2 is low (0.66) due to the noise, however so is the RMSE (0.28 GW)(Figure 4.15). Pr is lower than found by Kubik et al. [2013a] (0.81 compared to 0.91), however a far greater number of sites are used and the data is not interpolated to each individual site. Cannon et al. [2015] achieve a superior correlation with their data and method (0.96). They do not, however, state error statistics, but rather graphically represent the output, comparison to the figures shown here suggest that they also reduce noise.

Figure 4.15 shows a clear difference in the simulation of turbine between 2010 and the previous period. The statistics suggest that correlation is good for the whole of 2010 but output is consistently underestimated. Although still present, this pattern is less evident during 2008 and 2009, which is due to the increased capacity in 2010. In order to analyse the extent to which correlation is influenced by wind conditions, as well as establishing if solar warming during hotter months affects wind height correction as found by Kubik et al. [2013b] and described in Section 4.1.3, Figure 4.16 and Figure 4.17 divide the output from 2009 and 2010 respectively into months (this is not performed for 2008 due to lack of data for the whole year). The figures show that for both 2009 and 2010 the correlation coefficients are consistent over the year, including windy months e.g. April and relatively windless months e.g May. The worst fitting correlation lines are caused by greater underestimation of the output, but all months underestimate supply. The months during which poor correlation is evident are not consistent between years. Underestimation of output is an interesting finding, as all other studies that have simulated output have needed to apply a capacity or correction factor that reduces the simulated output. This suggests that there is error in the method, this is most likely to arise from the incorrect wind and height correction. Lack of interpolation to wind farm sites is also a possible source of error, but would more likely result in random error, rather than systematic underestimation. It should be noted that many factors

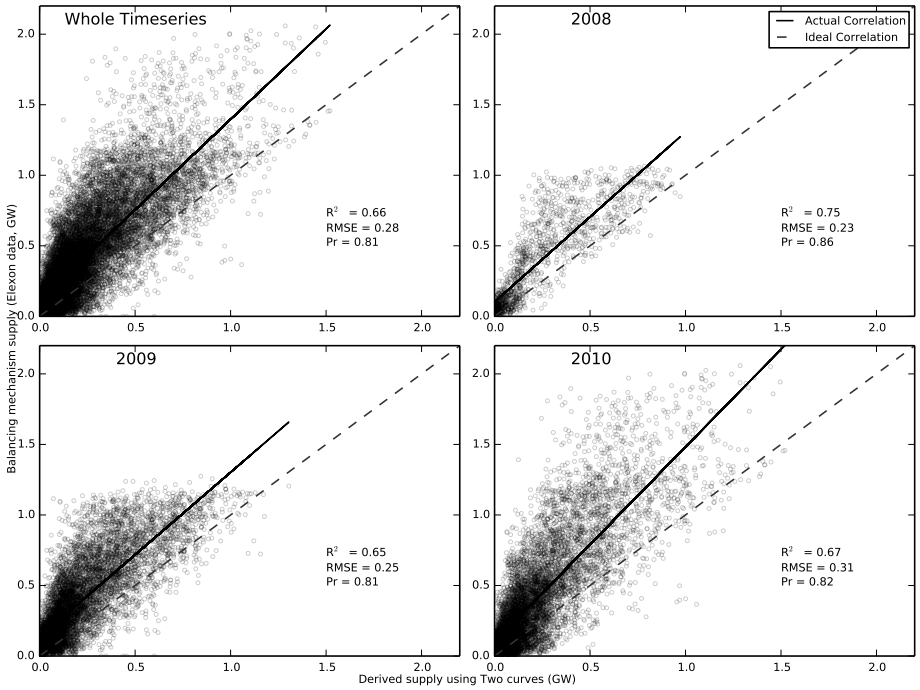

Figure 4.15.: Correlation between simulated output and Elexon balancing mechanism data.

affecting output are not included in the model, these are summarised in Table 4.1. Despite this underestimation, R^2 and Pr are uniform and very good for all months, suggesting that a linear correction factor may improve the regression line and reduce the RMSE. The more extreme bias seen at the end of 2010 in Figure 4.13b is not reflected by a reduced correlation during that period, this is probably because the extreme bias is seen during the hours producing the greatest amount of output and these are in the minority.

Factor
Wake Effects
Downtime
Lag in turbine operation
Energy Density over blades
Air density
Decline in performance with age
Wind speed changes $<$ 1 hour in frequency
Location specific turbine curves
Operating efficiency

Table 4.1.: Factors not taken into account by manufacturer turbine curve based wind model.

This analysis has shown that the method for wind height correction and turbine simulation work well in comparison to existing studies, which have used site specific wind speeds, height corrections and turbine characteristics, at least when aggregated to a national scale. There is room for improvement in terms of reducing error. As described above, potential methods for improving results include correction factors and multi turbine curve simulations.

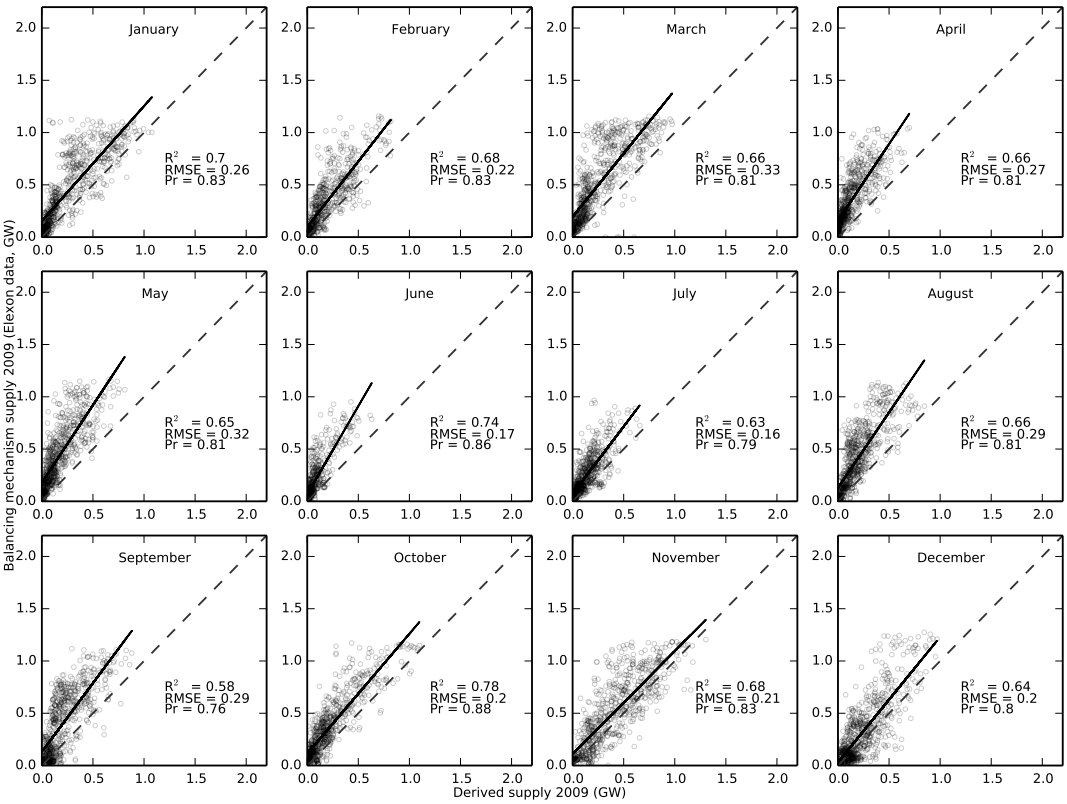

Figure 4.16.: Variation in correlation between simulated output and Elexon, monthly 2009.

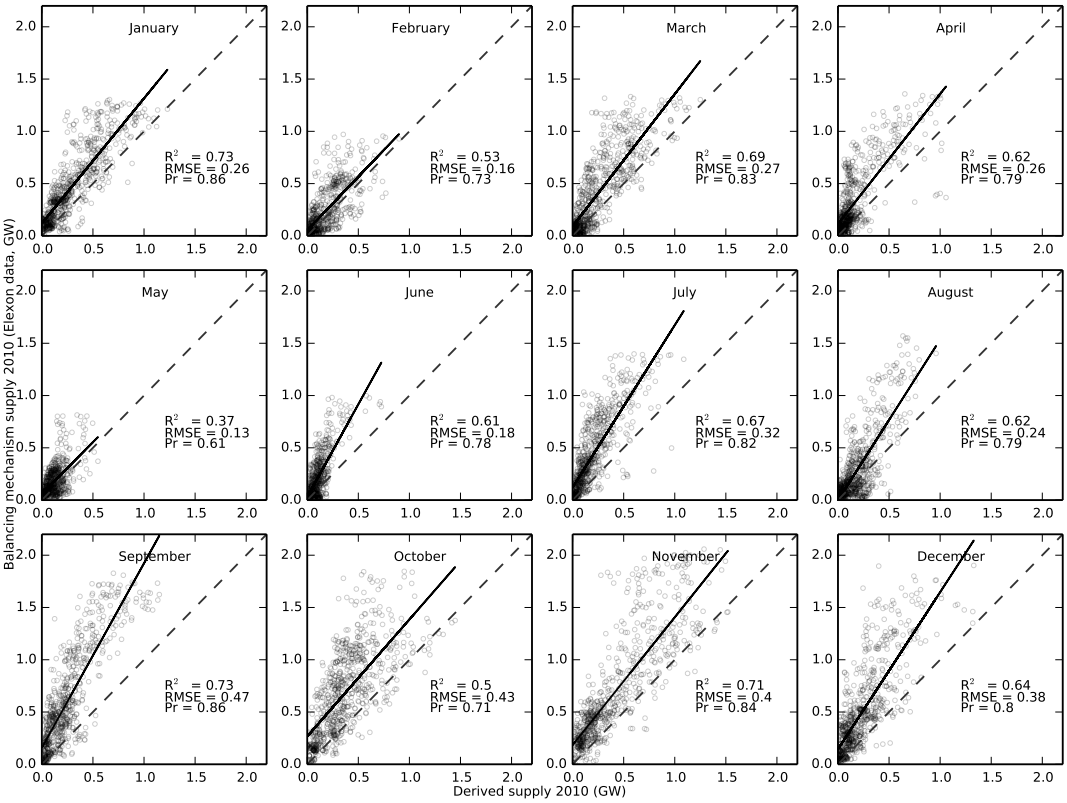

Figure 4.17.: Variation in correlation between simulated output and Elexon, monthly 2010.

4.4.3. Scaling results to improve accuracy

4.4.3.1. Hourly results

As established by previous studies, the error in simulated wind generation through the turbine curve method can be reduced through a linear correction factor of turbine output [Hawkins et al., 2011, Ofgem, 2012a, Staffell and Green, 2014]. In order to determine the optimum factor, the simulated time series was multiplied by a range of factors (the magnitude of which was determined from the plots above). The hourly values are altered first in this section as they depict the most detail in terms of simulation output and in some respects are the most important to correct. Figure 4.18 shows the results of these multiplications, in order to verify that the only metric of interest post correction is RMSE the plot shows Pr and R^2. These metrics remain constant. The lowest error (RMSE = 0.22 GW) is achieved with a correction factor of 1.54, which is a 22% improvement on uncorrected data. This, as expected from the analysis of the correlation plots, shows that it is necessary to increase the output from the simulation, rather than reduce it, which is what would be expected from other literature and the influence of real world factors including machine availability, operating efficiency, wake effects, turbine ageing and site conditions. Since previous analysis has shown that the underlying wind speed data does not exhibit systematic bias it is possible that there is error in the modelling process. Fortunately there is another source of evaluation data in the form of ROC data so this can be verified.

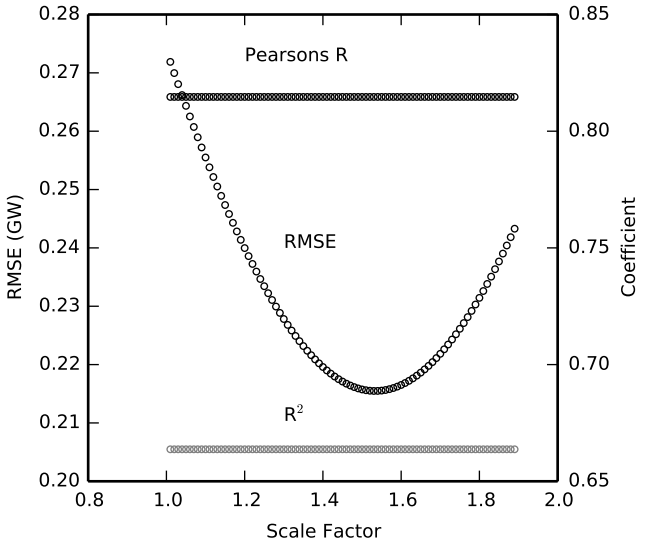

Figure 4.18.: Effect of scale factor on the correlation and error between simulated output and Elexon data.

Figure 4.19, Figure 4.20 and Figure 4.21 demonstrate the effect of the correction factor. Compared to Figure 4.15, Figure 4.19 shows that the underestimation of hourly generation is removed, although noise remains, it is more evenly distributed either side of the ideal correlation. The larger capacity in 2010 results in more noise as error is accentuated in absolute terms. There does appear to be some seasonal bias emphasised by the use of a single correction factor, the correlation is slightly skewed in January, February, October, November and December in both 2009 and 2010. This is a general trend however, as there is noise at all levels of generation. Applying a linear

correction factor means that there will be hours where output exceed maximum capacity. This is illustrated well by the 2008 and 2009 data in Figure 4.19, here there are a number of hours where simulated output exceeds the maximum output (approximately 1 GW in 2008 and 1.2 GW in 2009). This shows that it will be necessary to cap output if a correction factor is used.

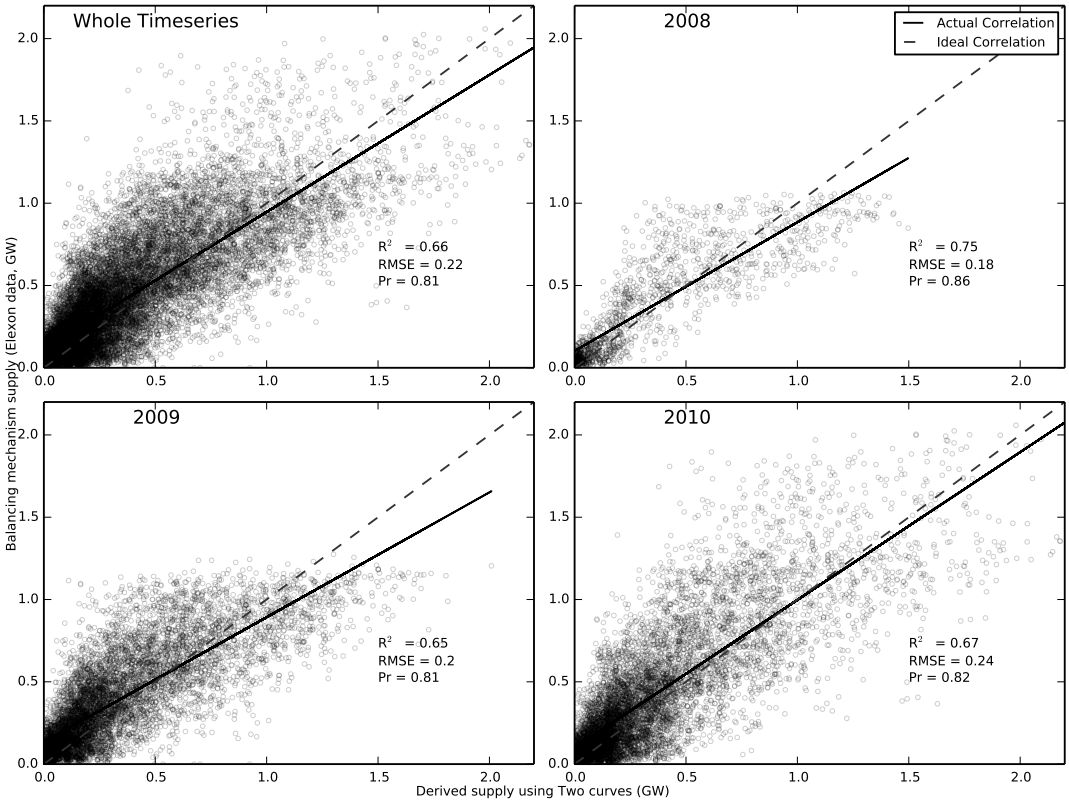

Figure 4.19.: Yearly correlation plot of hourly simulated data and Elexon following a single correction factor.

4.4.3.2. Monthly results

The effect of a range of correction factors on monthly simulated ROC capacity output was also investigated. Figure 4.22 shows that as the correction factor approaches 1.56 the error reduces to 0.08 GW, halving the RMSE. This correction factor is very close to that found in the comparison of the model output with Elexon. This shows that a correction factor is an effective and consistent tool in allowing for the error that is propagated throughout the modelling process. Provided that it is applied the output of the model at a national resolution can be trusted. This is particularly the case if the outputs are aggregated to a monthly temporal resolution.

The impact of this correction factor on the correlation between the two time series is shown in Figure 4.23. As with the previous analysis the points are now evenly distributed around the ideal correlation (compared to Figure 4.12). There is considerably less noise than seen in the hourly analysis, demonstrating the effect of temporal aggregation. The simulations of months with low output are particularly accurate. Figure 4.24a demonstrates that these low generation points are earlier in the time series, when the installed capacity was significantly smaller than installed in 2010. The plot shows that as a result the model follows measured supply closely. It appears

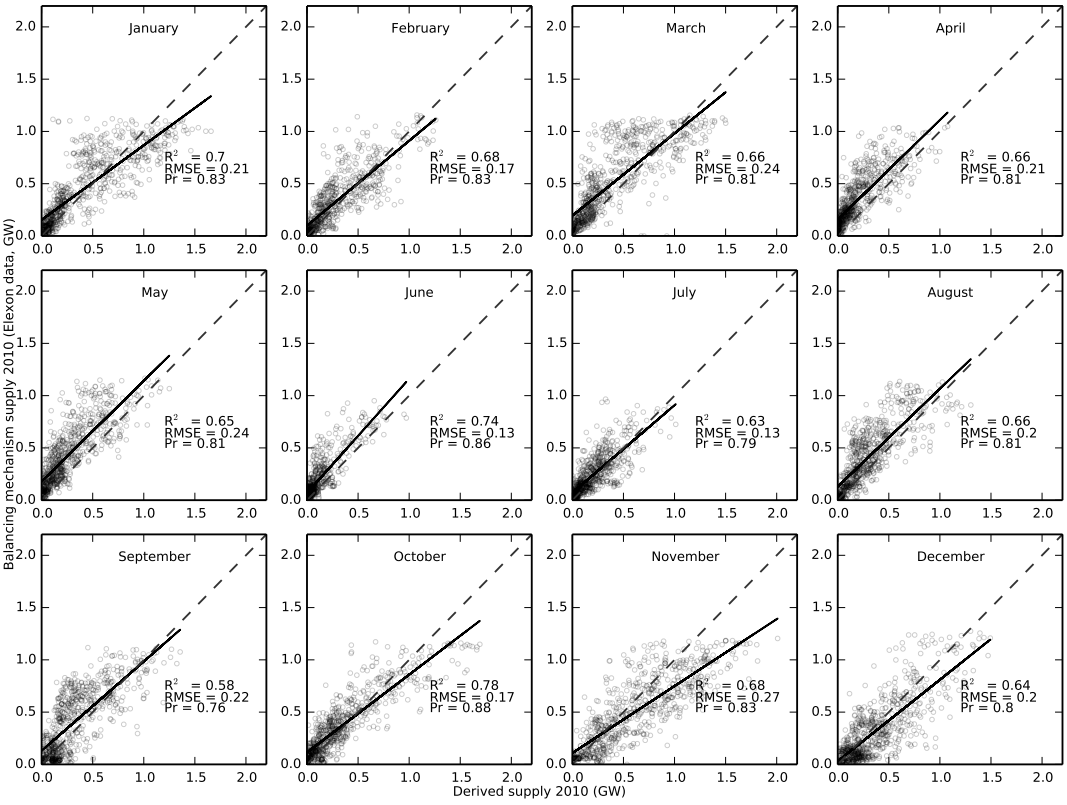

Figure 4.20.: Monthly correction plot of hourly simulated data and Elexon data following a single correction factor 2009.

that this continues through 2007 and 2008 when capacity is increased. After 2008 there is a greater level of variation, it is possible that this is due to the greater spatial diversity introduced by later capacities as shown in Figure 4.7 and the consequent increased variation in wind speed during any time period. The increased spatial diversity affects other factors which influence model accuracy, such as increasing the impact of not including maintenance breaks etc. The accuracy of the wind height correction is bound to be affected as greater spatial diversity increases the diversity of surface roughness and the likelihood of a range of atmospheric conditions around and above simulated turbines. This analysis shows the value of using both the ROC and Elexon data, although the hourly temporal resolution of the Elexon data provides greater level of detail in analysis, the longer length of the ROC time series reveals patterns the other dataset cannot.

Figure 4.24b shows monthly bias, demonstrating that the magnitude of error increases over time. This is driven by increased capacity and the spatial diversity of this capacity. However the percentage error remains consistent. The figure also shows that there is a seasonal pattern in the bias in the winter, the corrected time series is over estimating generation and in the summer it is under estimating generation. This may be a result of the effect of solar warming during hotter months on wind height correction observed by Kubik et al. [2013b]. It is possible that a more sophisticated, seasonal, correction factor will reduce error.

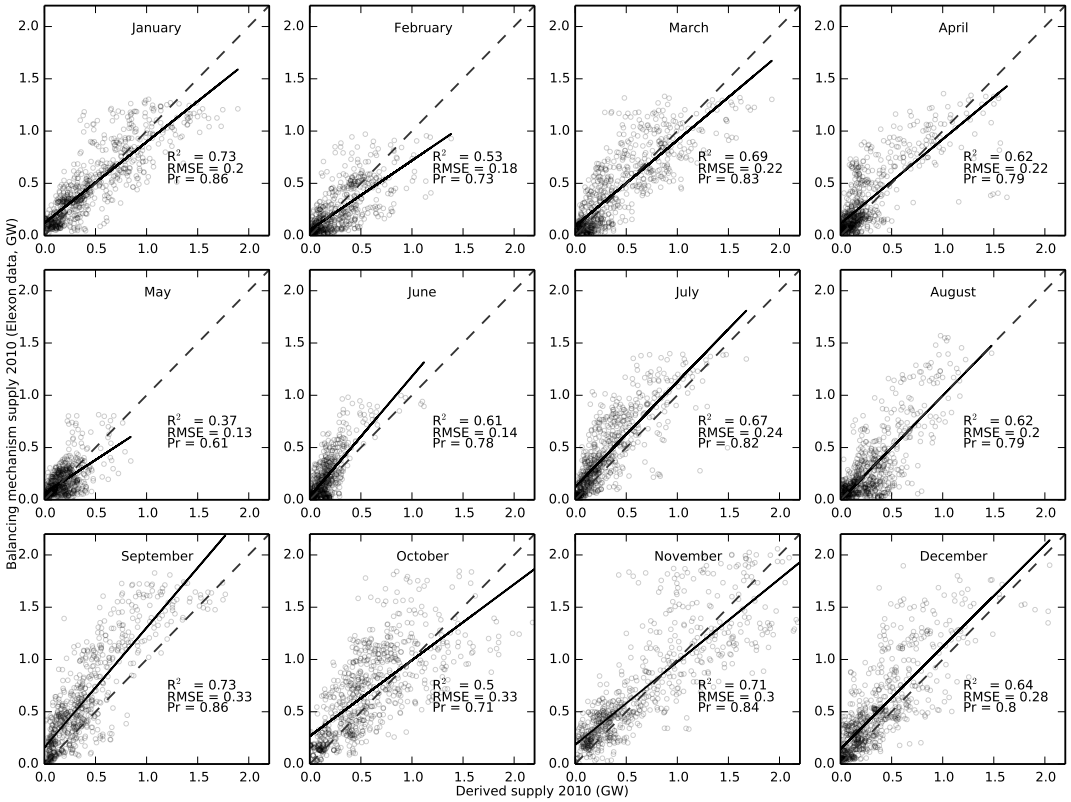

Figure 4.21.: Monthly correction plot of hourly simulated data and Elexon data following a single correction factor 2010.

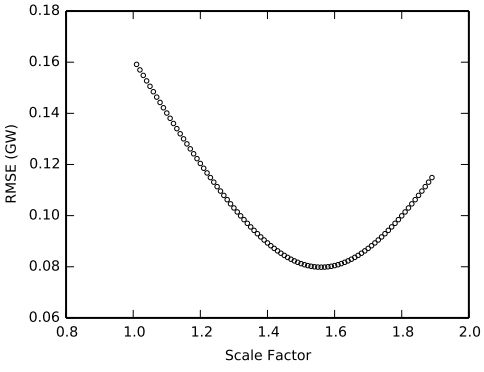

Figure 4.22.: Effect of a single scale factor to reduce the RMSE between measured and simulated output at ROC sites.

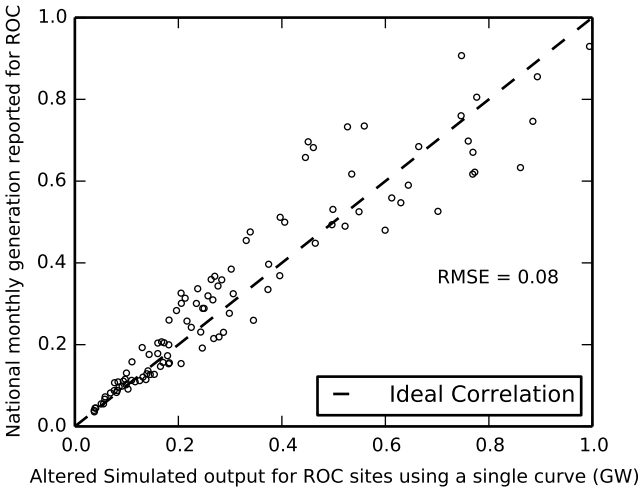

Figure 4.23.: Correlation between monthly measured and simulated generation at ROC sites using a single correction factor.

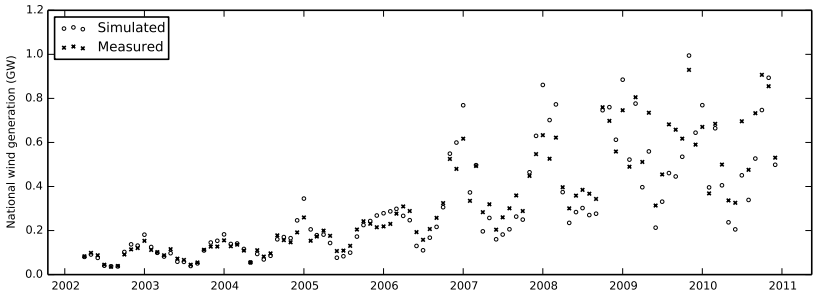

(a) Time series of corrected ROC values.

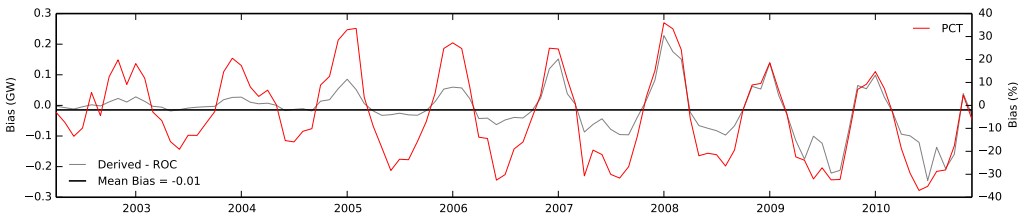

(b) Bias between simulated and measured ROC output after using a single correction factor.

Figure 4.24.: Difference between simulated output and ROC data over time.

4.4.3.3. Seasonal correction factor

To create a seasonal correction factor it is necessary to establish the appropriate boundaries for summer and winter. Figure 4.25 shows that bias in January, February, November and December is exclusively positive, excluding one outlier. Also, bias in March is predominantly positive and the values exhibit a narrow range. Therefore these months are assumed to need a different correction factor than the other months. The analysis shown in Figure 4.22 was repeated for the winter and summer months seperately. The results are described in Figure 4.26. The figure shows that there is indeed a difference between the two groups. The minimum RMSE in the 'summer' months is 0.044 GW when multiplied by 1.96, minimum RMSE in the 'winter' months 0.046 GW when multiplied by 1.39. These correction factors result in another 50% reduction in error.

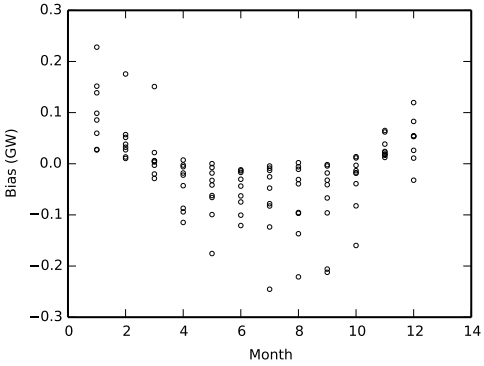

Figure 4.25.: Bias between measured and simulated ROC sites sorted monthly.

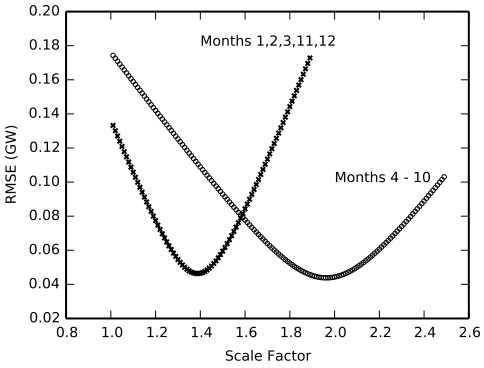

Figure 4.26.: Multiple scale factors to reduce the RMSE between measured and simulated output at ROC sites.

Correlation between simulated generation and ROC data following seasonal correction is shown in Figure 4.27 and Figure 4.28. The former of these figures demonstrates that some of the noise in the months with greater generation is eliminated. Mean RMSE over both seasons is reduced to 0.044 GW. The latter figure demonstrates that the seasonality of the bias is reduced, mean bias over the analysis period is reduced to 0.0001 GW.

To ensure that the divergence between simulated generation and measured ROC data was not originating from a particular wind farm or geographic area, a spatially disaggregated analysis was performed. The results described in Figure 4.29 demonstrate that, overall, the monthly error (of

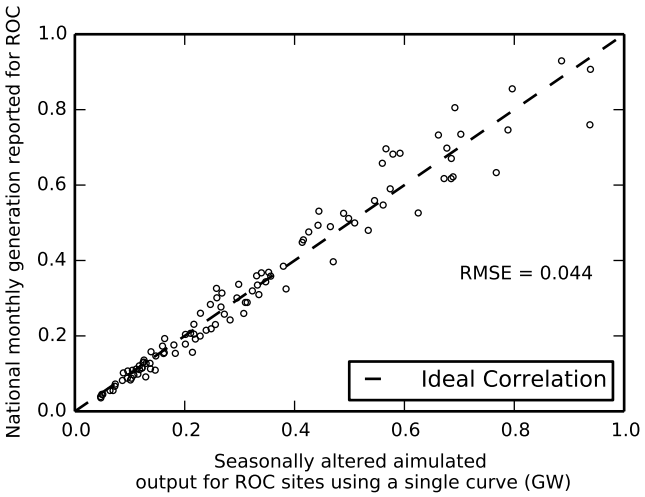

Figure 4.27.: Correlation between measured and simulated generation at ROC sites using multiple correction factors.

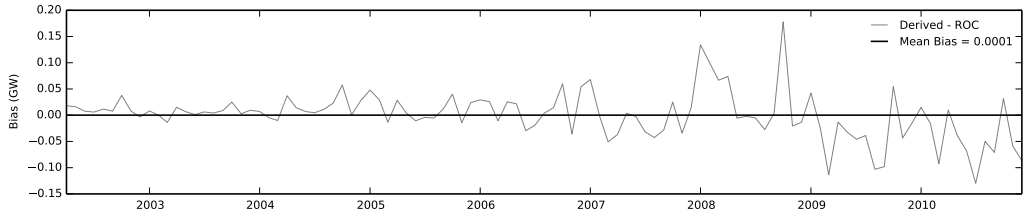

Figure 4.28.: Bias between simulated and measured ROC output after using multiple correction factors.

the corrected time series) is very low (mean 0%). There are some sites where the monthly output is not well estimated. The largest error is more than 60%, but there are also months with low error in the same location and there is no single location where there is consistent error, showing that the data and methods are spatially consistent. There are a number of factors that are not taken into account by the model which could be the source of this error. The plot was calculated as the simulated output minus the measured as a percentage of the capacity. Positive error represents the model overestimating generation and vice versa. Therefore it is possible that where there is a positive error there is something curtailing generation from the sites, such as maintenance or enforced curtailment due to for example transmission restrictions or market forcing from National Grid. Negative error demonstrates that the model is underestimating generation. This may be a result of capacity beginning production before the date given by the REPD.

Seasonal correction factor on hourly data Seasonal correction factors were applied to the hourly ouput and the results compared against the Elexon data. Figure 4.30 shows the results of this analysis. The figure demonstrates a similar pattern to the monthly analysis in that the factors are clearly seasonally divergent. The difference between seasons is however less pronounced. The reduction in error during 'summer' months is greater than 'winter' months. The minimum achievable winter RMSE using this method is 0.22 GW using a factor of 1.43, minimum summer RMSE = 0.21 GW using a factor of 1.72. This represents a very small improvement on the single factor.

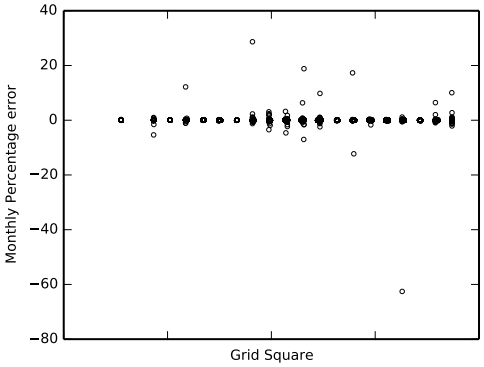

Figure 4.29.: Percentage error between output from an individual grid square, monthly.

These factors, unlike the single annual number, are different to those found in the analysis of the ROC data.

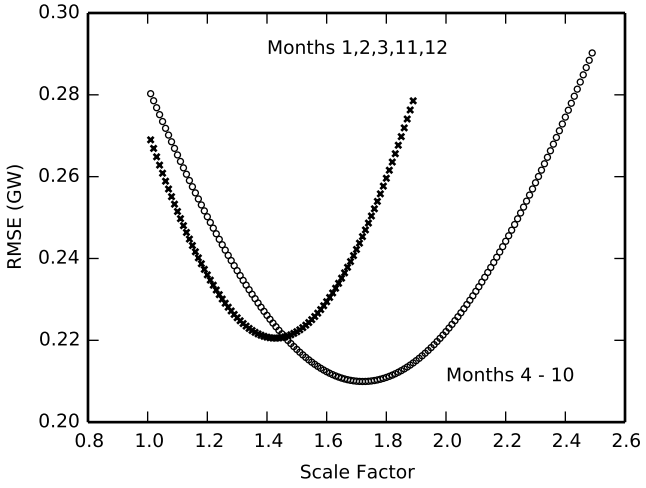

Figure 4.30.: Effect of seasonal correction factor from ROC analysis.

Final correction factor for future modelling The above analysis has shown that the use of a linear correction factor significantly improves the accuracy of simulated generation. Correlation of simulated generation to Elexon data suggests an optimum correction factor of 1.54, correlation to ROC data suggests 1.56. A seasonally dependent correction factor has been shown to improve the results further, particularly in comparison to monthly data. However, the use of a seasonal correction factor would result in discontinuous model output between seasons. Therefore future analysis will use a single number to correct wind model output (1.55), using the average of the analysis from the Elexon and ROC data. A cap will be placed on adapted output to ensure that it does not exceed maximum capacity. This method improves results and its use has been established in the literature, there are, however, problems with its use.

Despite being based on empirical analysis, there is limited physical basis for the factor. As described in Section 4.2.1.3, Staffell and Green [2014] attribute the need for a correction factor to the lack of account of machine availability, operating efficiency, wake effects, turbine ageing and

site conditions (see Section 4.2.1.3). Each of these factors is likely to result in simulation output being overestimated in contrast to the underestimation exhibited above. This suggests that there are other factors effecting the simulated output here. The most likely cause of the differences between the methods is the wind data that drives the model. Wind speeds in MERRA (as used by Staffell and Green [2014]) are unlikely to be systematically overestimated in comparison to CFSR (there is no suggestion of this in the analysis in Chapter 3 and they are based on the same data). Therefore the largest contributor to underestimation is likely to be the method used for wind height correction, as it has been recognised in the literature that whilst the values used in the power law equation are well established they are likely to result in conservative estimates of wind speed (see Section 4.1.3). Some difference is also likely to arise from the fact that wind data is interpolated to wind farm locations in Staffell and Green [2014], whereas CFSR grid point data is assumed to represent the whole grid square here, following analysis in Chapter 3 showing that this is a reasonable approach. Future work could improve the model by investigating how to include some of the factors summarised in Table 4.1 into the model, particularly with respect to improving wind height correction. Another option would be to consider a non - linear correction factor.

4.4.4. Testing the multi turbine curve approach

As noted above, Norgaard and Holttinen [2004] have developed a widely used approach for the statistical alteration of manufacturer turbine curves to account for some losses in generation associated with a wind farm, as opposed to a single turbine operating in isolation. In order to assess the potential of this method for improving the model output this method was used simulate generation from the BMRS sites.

It was assumed that the dimension of the area simulated was 300 km (the maximum shown in Norgaard and Holttinen's paper, which as previously discussed is significantly smaller than GB), and the turbulence intensity of the air was 10%. This results in a standard deviation of 0.25 according to data provided by Norgaard and Holttinen [2004]. The original method not only adapts the curve but also the wind speed data. This part of the method has not been used by any of the studies reviewed so far and there are other examples in the literature that also do not adapt the wind speed data. For example, Gibescu et al. [2009] do not block average the wind speed data. Given that one of the strengths of the approach used here is the quality and breadth of the high temporal resolution wind speed data it has not been altered in this example. Mean wind speeds are instead calculated from the MIDAS data used in the evaluation of CFSR (Offshore mean wind speed = 7.73 m/s, onshore mean wind speed = 5.21 m/s). The method requires that these values are multiplied by the standard deviation to create an adapted standard deviation (this results in values of offshore 1.93 m/s and onshore 1.30 m/s). From these values a probability density function was calculated which shows the likelihood of the curve being offset (this is based on a normal distribution). The resultant onshore and offshore probability density functions are shown in Figure 4.3. These were then used to generate aggregated turbine curves using the manufacturer curves shown in Figure 2.2 and the equation provided by Norgaard and Holttinen [2004] (Equation 4.1). The resultant curves are shown in Figure 4.31.

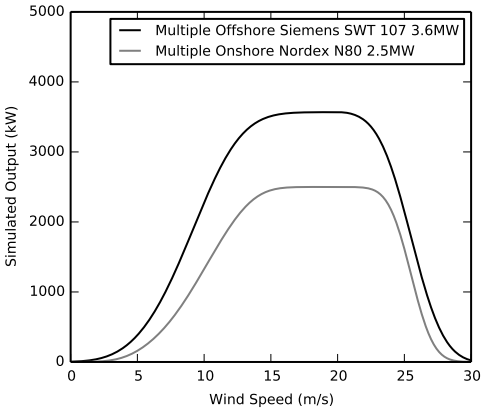

Figure 4.31.: Aggregate power curves produced using the method from Norgaard and Holttinen [2004].

Figure 4.32 compares the results of simulation generation using manufacturer curves and the aggregated power curves. The figure demonstrates that there is no statistical difference between the two approaches. Therefore, the simpler single curve approach will be used in subsequent simulations.

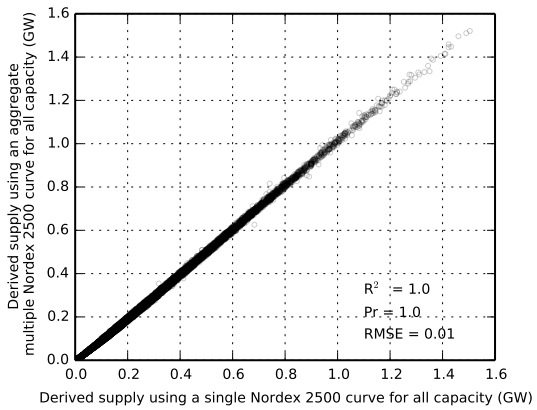

Figure 4.32.: Simulated output of single turbine curve vs. aggregated curve.

4.5. Summary

Data on installed capacity has been used to select appropriate turbine hub heights for wind speed height correction, onshore and offshore and appropriate manufacturer turbine curves, which represent onshore and offshore capacity. Their use means that an archetypal curve can be used in future simulations to approximately represent all wind farms. Though this is a well established approach in the literature, there is a study which uses location specific turbine curves and hub heights. This provides accurate results but is of more interest if the focus of research is installed capacity. The need to simulate future capacity means that there is uncertainty about the size of turbines, therefore it is unnecessary to model at this level of detail.

A method for statistically altering manufacturer turbine curves to incorporate losses has been described and investigated. The method is shown to make no difference to output and has therefore been disregarded.

Methods for wind height correction have been summarised. The power law has been used to alter 10 m CFSR wind speed to 60 m for onshore simulations and 80 m for offshore simulations. This method uses a Hellman exponent which assumes surface roughness and air stability to be consistent over land or sea. Subsequent analysis has shown that this is likely to be a cause of error in simulations, as generation is systematically underestimated. Some of this underestimation can be accounted for through the use of a correction factor.

Linear correction factors to account for errors in wind speed height correction and other factors not included in the method have been calculated through comparison of simulated output to all available measured generation data. This makes the model as robust as possible and means that this study is more comprehensive in this respect than any other simulating wind generation in GB. The correction factor is shown to significantly reduce the error in simulation and is very similar when calculated using two different datasets of measured generation. A seasonal correction factor is investigated and shown to improve monthly output, but is disregarded due to limited improvement of hourly output and resultant discontinuity.

Following the established methods for simulation and correction there is still, unfortunately, noise in the hourly output. This means that there will be some uncertainty in ensuing analysis. This can be countered to a certain extent by using the same weather to drive demand modelling, rather

than using measured demand, which assumes that there is no error in the weather data (and to a certain extent the simulation). It is also necessary to consider this noise when analysing future model results.

The previous chapter has shown that CFSR wind speed data represents GB wind conditions well, especially if some areas are removed from consideration fro turbine placement. This chapter has described the use of that data in wind turbine simulation. The estimation of wind generation from historic capacity has shown to be reasonably accurate and results have been in line with those described in the literature. Therefore the two chapters in combination have shown that CFSR wind speed data are suitable for simulating turbine output, although some uncertainty and error remains, answering research question 1.

5. Modelling Energy Demand

This chapter describes the development, calibration and evaluation of the electricity demand model Spatiotemporal DEAM (SpDEAM). SpDEAM has been built using the structure and algorithms of the existing Dynamic Energy Agents-based Model (DEAM); this model is described first. This is followed by a description of the methods and data required to develop SpDEAM. SpDEAM has been calibrated to national energy demand data for a ten year period (2000 - 2010). The results of this calibration are presented and discussed. SpDEAM is then evaluated against the same data sources from 2010 - 2014.

The extension of the model to cover future scenarios is discussed in Chapter 6. Some of the methods and results described in this chapter have been previously published in Sharp [2012] and Sharp et al. [2014].

5.1. The Dynamic Energy Agents-based Model (DEAM)

DEAM was developed by Barrett and Spataru [2012] to represent energy demand and supply from both consumers (in the domestic, non domestic and transport sectors) and suppliers, as agents, both in the present energy system and under future scenarios. DEAM, as described in Chapter 2, is a hybrid simulation model, which is designed to investigate the consequences of changes to the energy system at a disaggregated temporal resolution (half hourly). These changes can be input at an aggregated resolution through depictions of growth or decline in sectoral or end use demands from, for example, scenarios or historic data, which are investigated using the top down methods. The top down methods disaggregate demand values by end use and by time using activity profiles which describe the way in which energy is used over different time periods for each end use. The top down method encompasses those demands which *are not* influenced by building fabric, defined here as non space heat demand. With the exception of lighting, these demands are independent of weather. As discussed in the literature review, the advantage of the top down method is the simplicity, ease of comparison with published consumption statistics and the need for only simple data. This means that, in many ways, this type of method is ideal for the temporal disaggregation of scenario data.

The disadvantage of the top down method is that it cannot model what Swan and Ugursal [2009] refer to as paradigm shifts, such as improved heat loss in buildings or the introduction of a new technology such as heat pumps. DEAM therefore also includes bottom up building physics based methods, which have the ability to introduce new types of demand. The bottom up method is used here to simulate heat demand in dwellings, which *is* influenced by building characteristics and is weather dependent.

DEAM contains hybrid methods for calculating demand from transport and supply from renewables as well as bottom up methods for calculating energy demand from the non domestic sector, these

methods are not used here, so are not described. DEAM can incorporate any number of end uses and activity profiles, only those used in SpDEAM are described here.

DEAM has been used previously to calculate the energy flows for agents connected to a local electricity substation, by investigating the possible future loads using a representative set of data from the DNO, WPD [Barrett and Spataru, 2014]. DEAM has also been applied to analysis of grid supply point demand in collaboration with National Grid.

5.1.1. Non Space heat demand

To calculate non space heat end use demand, DEAM requires an annual energy demand value for each end use (for each fuel if possible), at the desired scale of the model, e.g. 2 x 10^6 Wh of electricity for lighting in a household. These data are gathered from published energy statistics or from another source, such as the previously mentioned DNO. The demands can be for any fuel or end use. The annual value is disaggregated temporally, first to the level of approximate average daily energy demand by dividing by number of days in the year, then to a half hourly value, using activity profiles, which are specific to the end use; in the case of the example, this would be domestic lighting (Equation 5.1).

Equation 5.1 Non space heat end use demand algorithm, *dailymeandemand* is the average daily demand for each end use, *Ap* is the normalised activity profile, which takes into account seasonal, weekly and hourly variability in demand (see Equation 5.2).

$$endusedemand = dailymeandemand * Ap$$

The activity profiles used in DEAM follow the method described in Equation 5.2, whereby values that describe the relative amount of energy that is used at different times of the year, week and day are multiplied by each other to provide a normalised value for each half hourly time step. This normalised value is used to divide the daily energy demand value. Using this method, the variation in energy use over different temporal resolutions is captured. Figure 5.5 demonstrates the resultant daily activity profiles for domestic heat demand during different seasons. Profiles differentiate energy use patterns in each sector as well as by end use. Where appropriate, profiles differentiate between end use behaviours.

Equation 5.2 Method for calculating the normalised value for energy demand.

sector month (Figure 5.1) * end use month (Figure 5.1) * sector day (Figure 5.2) * end use hour (domestic: Figure 5.3 or non domestic: Figure 5.4)

This method will capture regular variations in energy demand; annual changes are captured through the use of annual energy values and temporal activity profiles at different levels of aggregation capture variation over different time periods. It is clear, however, that weather driven variation will not be captured using this method. Therefore DEAM integrates physical drivers of energy demand which are responsible for some of the irregular variation. Within the top down section of the model, sunlight is used as a driver of lighting demand through the use of a darkness coefficient (Equation 5.3). This darkness coefficient is the first example of how the use of CFSR can improve the model, as homogeneous solar radiation data is available at the correct scope and resolution,

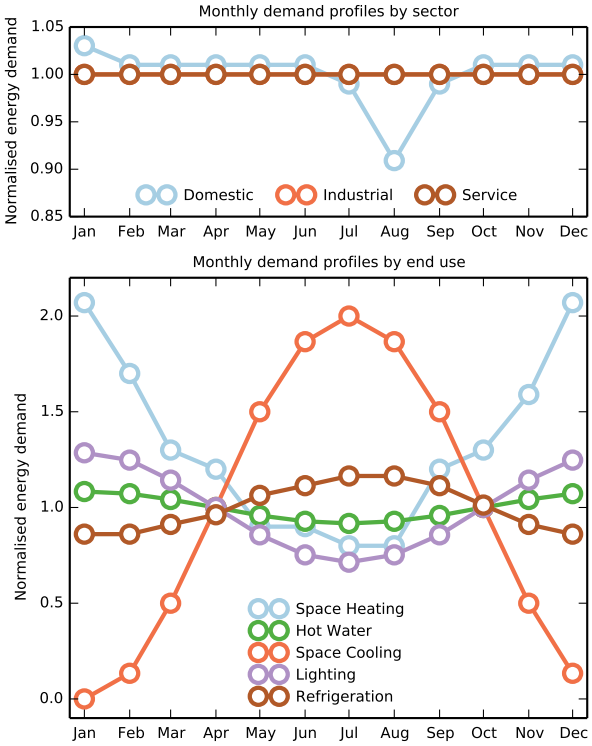

Figure 5.1.: Monthly activity profiles from DEAM, note that the industrial and service sector monthly profiles are the same.

which not only introduces varying daily cycles but also includes the effect of cloudiness. DEAM uses location specific weather data if available, otherwise synthesised weather data are used.

Other drivers may not be captured and it would therefore be expected that the model does not accurately capture variation in energy demand during periods such as Christmas and bank holidays (some summer holiday difference is taken into account in the monthly domestic profile (Figure 5.1)). These drivers of demand can be included through the use of more detailed activity profiles, which could be incorporated in future iterations of the model.

Equation 5.3 Darkness coefficient used in the calculation of lighting demand.

$$darkness = (1 - (solarradiation/1000))^4.$$

Load profiles are available in the literature, for example UKERC [2012] provide a comprehensive set of load curves which are disaggregated by sector and tariffs. DUKES provides energy use profiles disaggregated by sector and end use (DUKES Table 3.11) derived from demand data from 250 households from the Housing Electricity Use Survey 2010-2011 DECC [2011]. Profiles can also be derived from measured data, for example total gross system demand from Elexon [2014b] can be assumed to be equal to demand from all sectors (including station load, pumped storage and interconnector exports). These data include losses from transmission and, for example theft, where sales data is used, both of which may be significant. These losses are not calculated in DEAM, therefore it is probable that output from DEAM and SpDEAM will have to be corrected to include them. In order to extract and model individual end uses which are weather, population

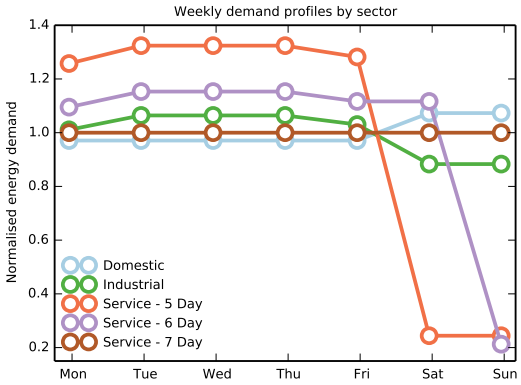

Figure 5.2.: Weekly activity profiles from DEAM.

or technology dependent, published profiles are not detailed enough. The profiles used in DEAM are informed by all of the described load curves, however they are bespoke, due to the need to model at a disaggregated resolution and the fact that some profiles represent aggregated demands (e.g. general profiles (Figure 5.4)), hence they are referred to as activity profiles, which are used to create load curves.

5.1.2. Space heat demand

The second method for calculating demand in DEAM is bottom up and encompasses space heating and cooling demand, which, unlike the demands calculated using the top down method, are influenced by building characteristics and weather (Equation 5.4). The model calculates the amount of energy required to heat a building, or stock of buildings, to a desired temperature, from the external temperature, using a heat loss coefficient normalised to the building floor area ($W/K/m^2$). Incidental gains are subtracted from the heat demand. These are calculated by assuming a number of watts contributed by each person and a portion of energy that is wasted as heat from other end uses e.g. excess heat from lighting or cooking (Equation 5.5 and Equation 5.6), as well as calculating solar gains. These gains require assumptions to be made on heat loss per person per hour for gains from people, glazed area per floor area for solar gains, the percentage of power that is wasted as heat for each end use, and the amount of this heat which is useful for heating a dwelling. Wasted heat from each end use requires inputs from the top down section of the model. The development of suitable values for these assumptions, from the literature and through modelling, is described in the calibration of SpDEAM (Section 5.3).

The method for calculating incidental gains and heat demand follows that which is utilised by the most widely used models of building energy demand in GB (BREDEM, SAP and CHM, which are described in Section 2.2). DEAM improves on this method by temporally disaggregating demand allowing the incorporation of physical drivers, which vary at this resolution. DEAM has an optional algorithm to include the effects of thermal mass in buildings, which is not currently included in SpDEAM.

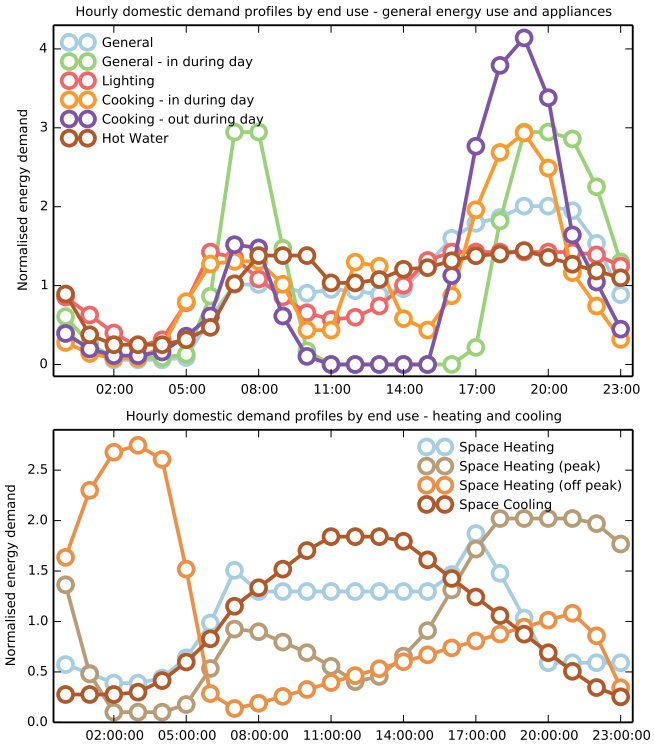

Figure 5.3.: Hourly domestic activity profiles from DEAM.

Equation 5.4 Space heat demand, W is the heat loss coefficient, T_{out} the external temperature and T_{in} the internal, Ap the activity profile and ef the efficiency of the heating technology.

$$Spaceheatdemand = (T_{out} - T_{in}) * W - gains * Ap * ef$$

5.2. Spatiotemporal DEAM (SpDEAM)

SpDEAM is an adapted version of DEAM. The overall aim of SpDEAM is to simulate all demand for electricity at the same temporal resolution as the wind model, so that residual demand can be calculated at a national spatial resolution and the impacts of increased wind capacity and demand changes can be explored. SpDEAM must be able to do this by disaggregating depictions of annual changes in demand from scenarios. Most of these changes take the form of increases and decreases of demands depicted by the temporal profiles described above. Therefore they can be disaggregated using the top down method. However, it is also an aim of SpDEAM to be able to introduce changes in temporal electricity demand from domestic heat pumps. This type of demand is not currently widespread in the GB energy system, therefore it cannot be introduced through statistical adjustments to historic demand, or top down modelling, as established in the literature review. For those reasons, the estimation of heat demand must be performed using bottom up methods,by simulating heat demand in dwellings and extrapolating the results to the desired geographical resolution. Therefore, in order to simulate demand at the same temporal resolution as the wind model SpDEAM has been designed to operate at the same spatial resolution as the wind model. This has the dual benefit of harnessing the data provided by CFSR and using weather data from the same source for both demand and supply modelling. This alleviates one of the problems of

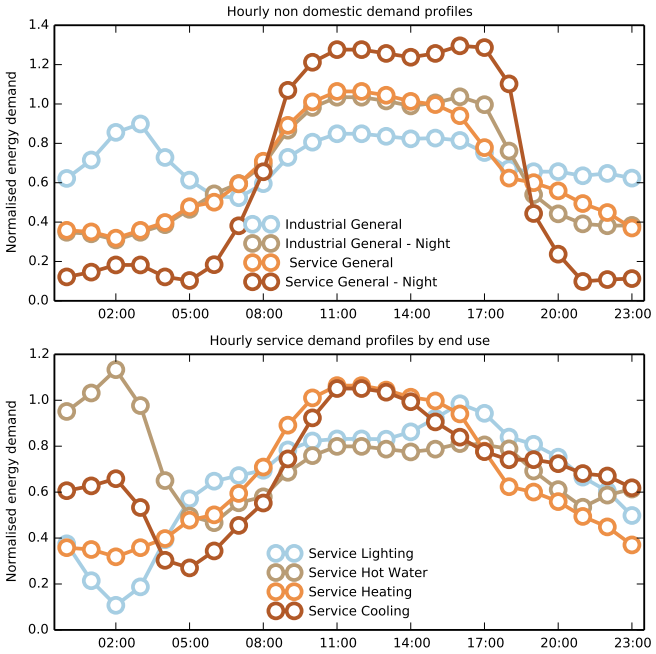

Figure 5.4.: Hourly non domestic activity profiles from DEAM.

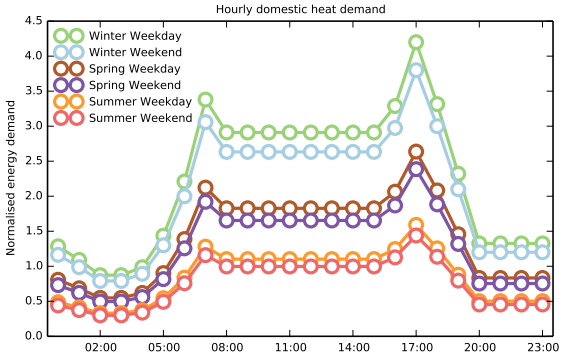

Figure 5.5.: Example hourly profiles for different seasons derived from DEAM, domestic heat demand.

comparing simulated wind generation against historical demand data, in that it is assumed that the weather data is correct. Here some of the inevitable variation between modelled weather data and reality is alleviated by differences mirroring each other on both sides of the equation. Although different variables are used in demand or supply simulation they are driven by the same GCM.

The overall work flow of SpDEAM is described in Figure 5.6. The diagram describes

- Which elements of DEAM have been altered.
- The division of top down and bottom up methods.
- Datasets used to spatially disaggregate top down demand
- Datasets used to extrapolate the bottom up demand
- Assumptions.

Equation 5.5 Calculating waste heat.

$$wasteheat = PctPowWasted * endusedemand * Usefulnessofheat$$

Equation 5.6 Calculating incidental gains.

$$Indidentalgains = wasteheat + (100W * people) + solargain$$

Each of the elements necessary to create SpDEAM are described in more detail in the following sub sections. The half hourly temporal resolution of DEAM is aggregated to one hour in SpDEAM to match the wind model and national demand data used for model calibration.

5.2.1. Non domestic demand and non space heat domestic demand

In SpDEAM, non domestic demand and domestic non space heat demand are calculated using the top down method. It is not the intention of this modelling exercise to investigate any changes to the non domestic sector, unlike the domestic sector where changes will be modelled in ensuing analysis. Therefore, if energy demand in the non domestic sector, particularly electricity demand, can be simulated using simple methods to a reasonable accuracy (which is investigated below), it is unnecessary to create bottom up methods. SpDEAM therefore only considers non domestic demand at an aggregated resolution (GB).

The top down methods from DEAM are used for both space heat demand and non space heat demand from the non domestic sector. National annual energy demand values are temporally disaggregated using the method described in Equation 5.1 and Equation 5.2. Industrial demand is classified as general and general night time using the associated profiles from Figure 5.1, Figure 5.2 and Figure 5.4. Service sector demand is calculated as 5, 6 and 7 day and end uses are calculated separately as described in the same figures. This simplified sub sectoral disaggregation is dictated by available data, this data is described in Section 5.3.

Domestic non space heat demand is calculated in the same way as non domestic demand, using the relevant curves shown in Figure 5.1, Figure 5.2 and Figure 5.3. Non - space heating demand in SpDEAM is divided into cooking, hot water, lighting and appliances. These represent an aggregated version of the demands modelled in DEAM. As stated above, DEAM and consequently SpDEAM can incorporate any number of end use and profiles; in this case aggregation was performed so that the model divisions aligned with published statistics, as described in Section 5.3. End uses and consequent energy demand can have very different profiles, for example, refrigerators have nearly flat diurnal profiles, whereas cooking typically has large early evening peak. Some end uses are incorporated into appliance demand e.g. refrigeration. This will result in some loss of detail, for example demand for electricity from refrigeration may not occur at the same time as charging a phone. However, the aggregated demands represent a smoother profile, which can be more easily represented in the model.

All of the modelled demands, other than lighting, can be analysed at a GB resolution as they are not subject to spatially disaggregated drivers, however as Figure 5.6 shows it is necessary to spatially disaggregate them so that the wasted heat from each domestic end use can be taken into

consideration in the heat demand equation. This also allows the influence of solar radiation on lighting demand to be applied. This spatial disaggregation is performed using gridded population data.

5.2.1.1. Gridded population data

As established in Section 3.2.1, there are a number of advantages to using a grid for spatial referencing over census, political or environmental based geographies. As well as addressing these issues, gridded data has a number of established advantages specific to population. Using gridded data represents a more effective way of revealing numerical change in population counts and changing spatial extents of populated areas over time [Martin, 2006] and gives a more realistic view of settlements, with better representation of density than with census geographies [Tate, 2000]. Despite the advantages of the format, there are few empirical gridded datasets; there are, however, a number of datasets that have been created using spatial redistribution methods (see Section 5.2.2.3 for a description of the methods).

All available gridded population datasets that cover the UK are summarised, including data citations, in Table 5.1. Several of these may be suitable for modelling purposes based on availability, resolution and temporal scope. The datasets include LandScan, the Gridded Population of the World (GPW), the Global Rural Urban Mapping Project (GRUMP), History Database of the Global Environment (HYDE) and a dataset created by Gallego [2010] (see the table for other dataset references). There is a small amount of literature which evaluates the accuracy of these datasets. Sabesan et al. [2007] compare LandScan and GPW using case study cities and one country. They use a range of spatially distributed difference and spatial dependence metrics, with a geospatial comparison based on exceedence thresholds. They find that the datasets do not agree well on the magnitude of high population values and show that LandScan has smaller and sharper population clusters than GPW. As a result of the paucity of available accuracy evaluations the potentially suitable datasets were evaluated against each other. A summary of that evaluation is provided here; data, methods and results are described in detail in Sharp [2012]. GB data was extracted from each dataset, harmonised to a single enumeration year (2000) and resolution (0.5 degrees), then mapped and summarised in terms of value frequency. The analysis showed that the LandScan dataset appears to provide excessively high levels of population, possibly due to corruption of floating point values. The LandScan dataset is not free, therefore it was not analysed further. The dataset from Gallego [2010] is based on a projection that prevents simple integration into a more common grid system, therefore this was also discounted. Of the remaining datasets, HYDE data appears to converge with the GRUMP/GPW data. However the associated metadata does not fully document the data sources used for temporal correction and some of those that are documented cannot be validated. This may make integration into applications requiring robust collection methods difficult. Therefore the choice of datasets for SpDEAM was between the remaining datasets GRUMP and GPW. GRUMP data is available over a range of ten recent years, and can also be aggregated to coarser scales. However due to the relatively small divergence between them and the need only for 0.5^0 resolution data, GPW is used here as it is provided at the desired scope and is among the most accurate and usable of the datasets.

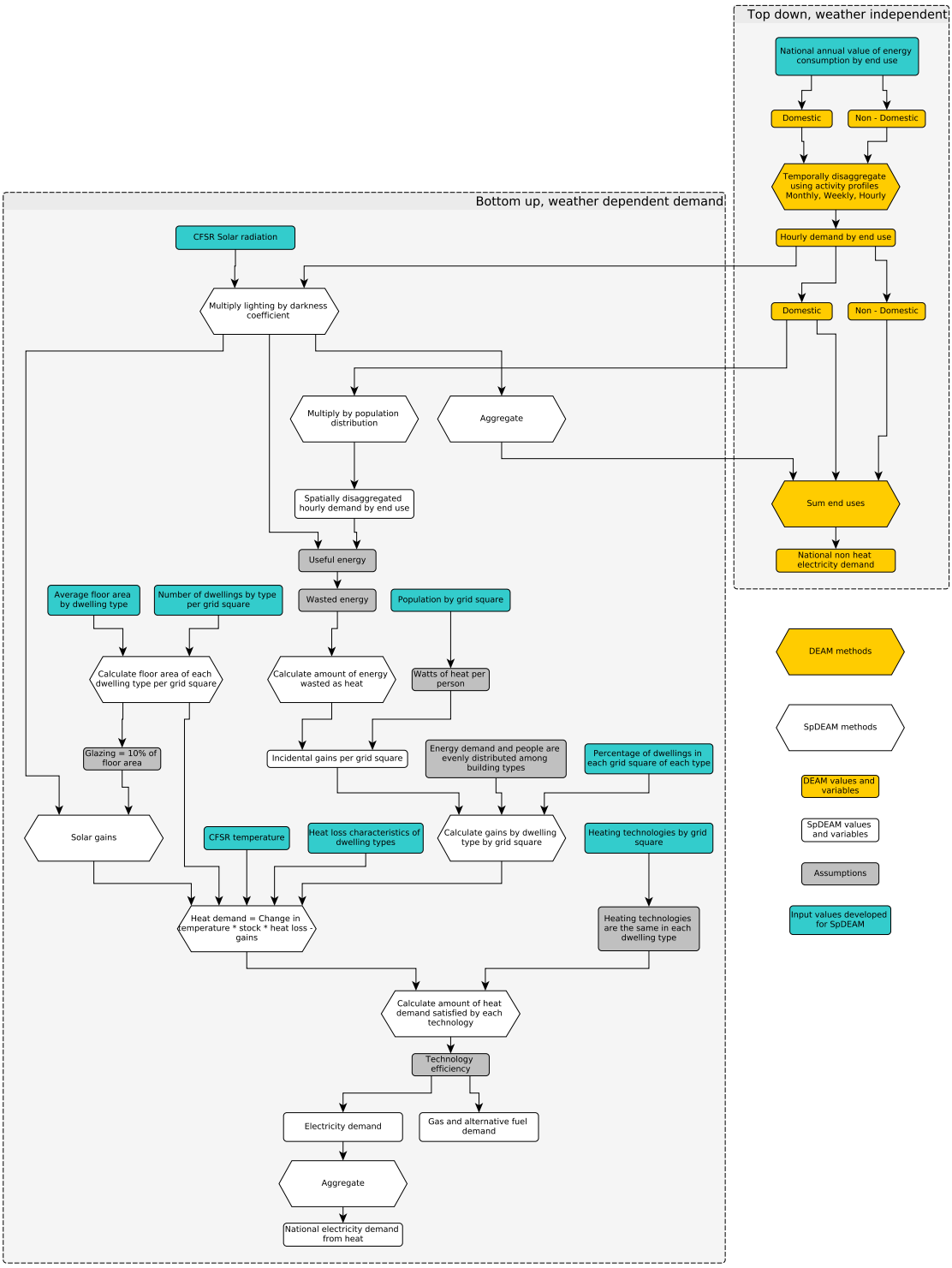

Figure 5.6.: SpDEAM work flow diagram, describing elements of the model which are new, those which are alterations of DEAM and those which use unaltered DEAM methods.

Name	Type	Resolution	Extent	Years Depicted	Format	Creators	Key references	Redistribution method
LandScan	Modelled	30″	Global	2010	Raster and .lyr	ORNL	(Dobson et al., 2000, Bhaduri et al., 2002, Bhaduri et al., 2007)	Smart Interpolation
GPW v1	Modelled	5′	Global	1994	.bil, .ascii, .grid	Tobler	(Tobler, 1979)	Pycnophylactic Interpolation
GPW v2	Modelled	2.5′	Global	1990, 1995	.bil, .ascii, .grid	CIESEN, IFPRI, WRI	(Deichmann et al., 2001)	Areal Weighting
GPW v3	Modelled	2.5′	Global	1990, 1995, 2000	.bil, .ascii, .grid	CIESEN, CIAT	(Balk et al., 2006)	Areal Weighting
GRUMP v1	Modelled	30″	Global	1990, 1995, 2000	.adf	CIESEN, IFPRI, World Bank, CIAT	(Balk et al., 2006)	Dasymetric Mapping
UNEP GPD	Modelled	60′	Global	1990	.dbf	UNEP	Unknown	Unknown
HYDE 3.1	Modelled/Projected	5′	Global	Every 10 years from 1700	.asc	NEA	(Klein Goldewijk et al., 2010, Klein Goldewijk et al., 2011)	Smart Interpolation combined with urban density datasets
FAO	Modelled	30″	Global	unknown	n/a	FAO	(Salvatore et al., 2005)	Dasymetric Mapping
Gallego	Modelled	100m^2	EU	2000/2001	.tif	EEA	(Gallego, 2010)	Dasymetric Mapping
SurfaceBuilder	Modelled	Variable (>100m^2)	UK	Dependent on inputs (2001-2009)	.ascii	Population 24/7 project	(Cockings et al., 2010)	Adaptive kernel estimation and Smart Interpolation
GPW 2015	Projected	2.5′	Global	2015	.bil, .ascii, .grid	CIESEN, CIAT, FAO	(Balk et al., 2005)	Areal Weighting and temporal extrapolation
CIESEN Downscale	Projected	15′	Global	1990, 2025	.ascii	CIESEN	(Gaffin et al., 2004)	Areal Weighting and Scenarios
Bengtsson	Projected	30′	Global	Every 5 years from 1900 to 2100	.ascii	JST	(Bengtsson et al., 2007)	Smart Interpolation and Scenarios

Table 5.1.: Gridded population datasets (resolution units: there are sixty seconds (″) in a minute (′) and sixty minutes in a degree (^{0}).

In the context of this study it is particularly important to note that a census represents population as a snapshot in time and place. Population based on this data is defined as residential, essentially depicting night time distribution, which can be misleading, for example if the data were used to disaggregate non domestic demand the output may not represent reality because people live in different locations to where they work. This is propagated into the gridded data used here. This means that any extension of the model to include, for example, greater detail on non domestic demand would need to incorporate ancillary data.

These gridded data are provided as numbers of people per grid square. In order to create a longitudinal dataset that can be adapted for future scenarios of population growth, this has been adapted to represent the percentage of the population of GB that live within each grid square. This distribution is assumed to be constant over all subsequent modelling, this allows the introduction of a total population value, which is redistributed using the gridded dataset to give the number of people per grid square during different years. No change is made to the spatial distribution of GB population in subsequent modelling. Future work could include changes, for example increased urbanisation.

The population distribution dataset is used in two ways in SpDEAM, the first is to redistribute the hourly demand from the top down part of the model. By assuming that each person uses the same amount of each end use, the total GB demand for each end use, calculated using Equation 5.1, is redistributed to grid squares using the percentage of GB population within each grid square (Equation 5.7). This redistributed data allows waste heat from each end use to be added to the incidental gains for the disaggregated space heat equation. The second use of the population dataset is also for incidental gains and allows spatially explicit heat gains from people to be introduced to Equation 5.6.

As well as assuming that each person uses the same amount of energy, this method assumes that people are evenly distributed amongst households. This is probably an oversimplification as households vary in size and different dwelling types contain different numbers of people, e.g. it is likely that a flat will contain less people than a detached house. At this resolution almost all of the grid squares will have a varied population and building stock, therefore these assumptions should not cause a large error. Potential improvements on these assumptions, which could be carried out in further work, include weighting population to floor area of dwellings and establishing the difference in energy use between people (there is information in the census on the location of different demographics). Census data could be used to introduce other spatial data that drives energy use, including income.

Equation 5.7 SpDEAM version of Equation 5.1 introducing spatial disaggregation using a population dataset.

$$endusedemand = dailymeandemand * Ap * Populationdistribution$$

5.2.2. Space heat demand

Following the DEAM method, SpDEAM calculates space heat demand as the amount of energy necessary to heat a dwelling to a desired temperature using the bottom up method described in

Equation 5.4. Currently there is no cooling demand in SpDEAM due to the lack of air conditioners in GB domestic buildings. CFSR is used to determine the external temperature in each grid square each hour. In order to extrapolate to the amount of heat required by grid square it is therefore necessary to develop a spatial dataset describing buildings for which heat loss characteristics can be set. It is also necessary to allocate this heat demand to different heat technologies. This is done at a grid square resolution to preserve the demand weighted to population, temperature and building characteristics.

5.2.2.1. Census buildings data

Data on the number of dwellings in each census geography has been gathered in the 1991, 2001 and 2011 censuses. The census provides data on the number of detached, semi-detached, terraced, purpose built flats, converted flats, flats in commercial buildings and caravans at the LLSOA level (see Section 5.2.2.3 for description of census geographies). Analysis has shown that the 1991 data contains errors, which are described in Figure A.5. Therefore only data from 2001 and 2011 are used here. This data was redistributed to the grid using the method described in Section 5.2.2.3, resulting in a dataset describing the number of each dwelling type per grid square. This allows the integration of dwelling specific heat loss coefficients into Equation 5.4. These heat loss coefficients, as described above, are available in $W/K/m^2$ (m^2 = floor area of dwelling). This means that it is necessary to estimate the total floor area per dwelling type in each grid square. In SpDEAM this is done by using data from the EHS [DCLG., 2013b] and the EHCS [DCLG., 2013a] which provides longitudinal data on floor area by dwelling type (Figure 5.7). The archetype dwellings do not perfectly align with the census definition, therefore some aggregation was performed. The housing survey data gives two values for terraced houses (mid and end), these were averaged to give a single terraced value, it was also assumed that flats in a commercial building have the same floor area as converted flats. Caravans were incorporated into detached demand, as there is no data on caravan heat loss coefficients. The number of each dwelling by grid square is multiplied by the appropriate average floor area, producing a floor area by dwelling type value by grid square, to incorporate into Equation 5.4. The values for floor area are clearly a generalisation of a complex variable. However, the data used to create the values is the best available for the study area. These values are also used by Cheng and Steemers [2011], although they model mid and end terrace separately.

As well as describing the number of each dwelling in each grid square, the census data was used to derive the proportion of dwellings within each grid square that are of each type (Section 5.2.2.3 contains examples). These data are used in SpDEAM to allocate the incidental gains calculated per grid square to each dwelling type. This allocation assumes that people are evenly distributed amongst dwelling types, which may not be the case, for example it would be expected that detached houses contain more people that flats. Incorporating these datasets into the heat demand equation results in Equation 5.8.

Solar gains are calculated by assuming that the glazed area of the building fabric that receives perpendicular solar radiation is equivalent to 15% of the floor area for each dwelling type. This is based on the zero carbon hub fabric efficiency worked example of modern buildings which suggests that the glazed area is approximately 20% [Zero-Carbon-Hub, 2012]. The 5% correction allows for the fact that glazing will be affected by the angle of the sun, as well as shading from buildings nearby and thermal solar transmittance of glass. This method is simplified due to the large number

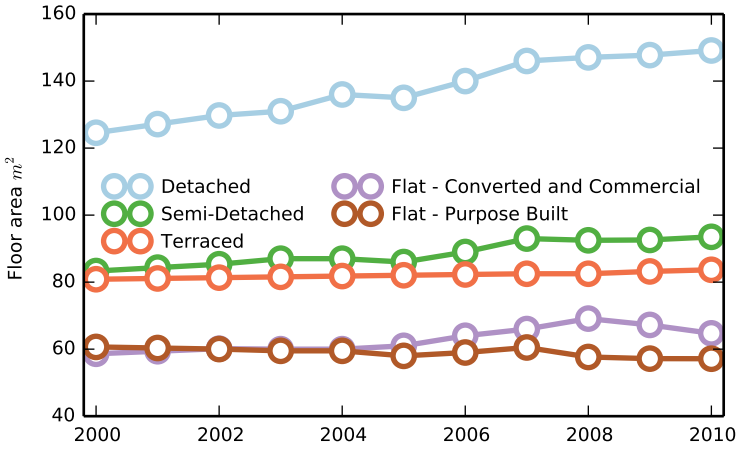

Figure 5.7.: Floor area by dwelling type, data adapted from DCLG. [2013b,a].

of buildings that are in each grid square and the differences in glazed area and orientation. The final remaining value in Equation 5.8 that has not become spatially explicit is the heating technology and associated efficiency.

Equation 5.8 SpDEAM version of Equation 5.4, StF is the floor area of each dwelling type, W is the heat loss coefficient, T_{out} the external temperature and T_{in} the internal, Ap the activity profile and ef the efficiency of the heating technology.

$$Spaceheatdemand = (T_{out} - T_{in}) * W * StF - gains * Ap * ef$$

5.2.2.2. Heating technologies

As in DEAM, SpDEAM satisfies heat demand with a range of technologies. In order to allocate heat demand to each technology on a grid square basis, spatial data on the use of those technologies was required. Data on central heating fuel types in dwellings are available from the 2001 and 2011 census for England and Wales but not for Scotland. Figure 5.8 summarises the data from the 2011 census. In order to align the model with published statistics, to enable evaluation and reduce some unnecessary complexity, the fuels with less associated demand have therefore been aggregated. Solid fuel, other fuel, two types and no central heating are grouped under alternative fuels.

These census data represent central heating rather than all types of heating. It is therefore likely that there are heating types that are not represented, for example oil based electric radiators. It is very difficult to counter this problem with the input data, especially at a disaggregated spatial resolution. Therefore it is possible that if model adjustments have to be made in future scenario modelling it will not be possible to incorporate greater detail. This highlights two issues with census data, firstly that questions are rarely perfectly suited to research purposes, secondly that the questions are open to interpretation and can be answered in different ways; for example, a respondent may have an oil based electric heater and select oil as the fuel type, despite the heater being powered by electricity. An indicator of the question being misinterpreted is the very small percentage of homes with no central heating shown in Figure 5.8 (2.1%), this proportion should

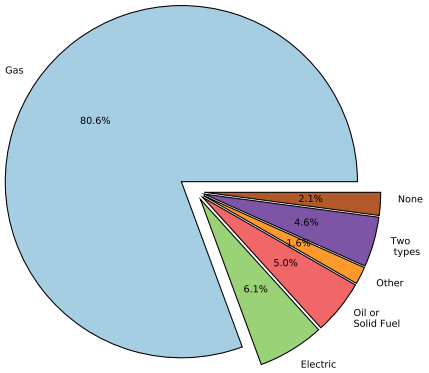

Figure 5.8.: Central heating fuel type, England and Wales average, derived from the 2011 census.

be higher (the EHS states that in 2001, 15% of homes had no central heating, falling to 10% in 2011 [DCLG., 2013b]), suggesting that respondents to the census may have misunderstood what constitutes central heating. Despite these problems, this dataset is an extremely good tool for spatially allocating domestic space heat fuel demand, therefore it was redistributed to the grid using the method described in Section 5.2.2.3.

Due to the lack of data for Scotland, it was necessary to make assumptions on the fuel usage and fill the remaining grid squares, the resultant values are shown in Figure 5.9. Those grid squares containing, or in close proximity to, the gas transmission network, were filled using mean values of heating technology use from the rest of GB as described in Figure 5.8. The remaining grid squares were filled using similar values to those shown in rural parts of GB, particularly west Wales, where most dwellings do not have access to the gas grid. Therefore the grid squares closest to the gas provided areas have an increased dependency on gas and the most remote areas (which have a small population and therefore will have a low demand) have no gas demand. These areas may have some gas demand due to unconventional supply such as Liquefied Natural Gas (LNG), this is considered to be an alternative fuel in SpDEAM. Further detail on the difference in heating technology distribution before and after adding the values for Scotland is given in Figure A.1 and Figure A.2. Comparison with Figure 5.10, which is derived from the DECC sub national statistics, indicates that zero gas demand areas are reasonably well identified. This map also reveals some interesting areas of zero gas demand in England which are surrounded by areas with a high gas demand. This suggests that there are areas in central England that are not on the gas grid.

The final values describing the percentage of heat demand that is satisfied by each technology are applied to Equation 5.4 for each dwelling type. This method assumes that all dwelling types are heated in the same way. This method could be improved through the use of the census to attribute heating types to dwelling types.

5.2.2.3. Methods for redistributing spatial data

As described above, several of the datasets used for disaggregation are based on census geographies and have been redistributed in order to align with the model grid. There are a number of methods available for spatial redistribution. Each of these methods is a variation on area weighting, where a grid is overlaid on the census polygons. Each cell of the grid is then assigned a value based

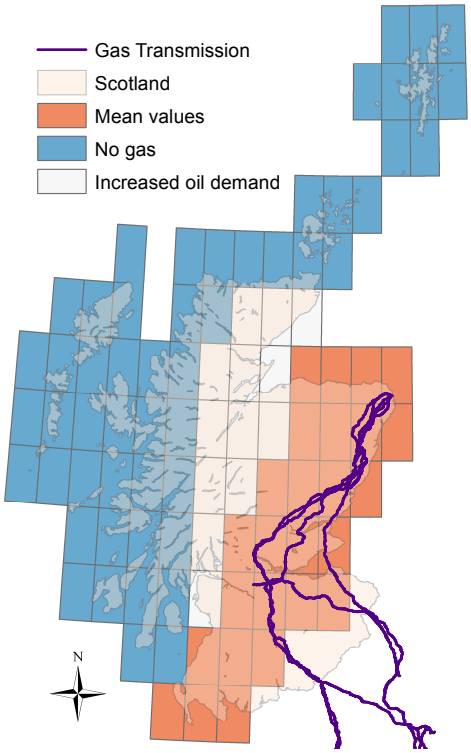

Figure 5.9.: Heating fuel type assumptions for Scotland.

on the proportion of the polygon that is beneath it [Goodchild and Lam, 1980, Goodchild et al., 1993]. The advantage of this method is that it is easy to implement, the disadvantage is that it presumes that people are distributed evenly within the polygon. However, since the polygons that lie along the boundaries of the grid will generally be small relative to the area of a grid squares, the error is likely to be low in percentage terms; therefore, this method is utilised for all non gridded data. This point is illustrated by Figure 5.11 and Figure 5.12. Figure 5.11 shows the LLSOA's for south west London and the surrounding suburbs that are contained in a single grid square. LLSOA's are boundaries designed to contain between 400 and 1200 households or 1,000 to 3,000 people and be consistent in terms of buildings and people where possible. Another census geography used in this study is the Medium Layer Super Output Area (MLSOA) which is the next level of aggregation, containing between 2,000 and 6,000 households and 5,000 to 13,000 people. The LLSOA's covering London (the top right hand corner of Figure 5.11) are very small, due to the density of the buildings and the resident population, whereas the areas outside of London (the bottom half of the grid square) are less densely populated, therefore, as an LLSOA represents approximately the same number of people, the polygons are larger. Figure 5.12 is an example of a grid square in one of the least densely populated areas of GB (central Scotland), this shows that there are grid squares where almost as much of the divided area is outside the grid square as inside it. Those grid squares with larger, less densely populated, census polygons along the boundaries are likely to be those with the largest error. This is because population may be concentrated at two ends of the polygon, which has resulted in the polygon being created to envelop both concentrations and therefore the correct number of people. The comparison of the two figures suggests that in grid squares containing densely populated polygons the result will be a low percentage error. Because even if there are large polygons at the edge of the grid square the

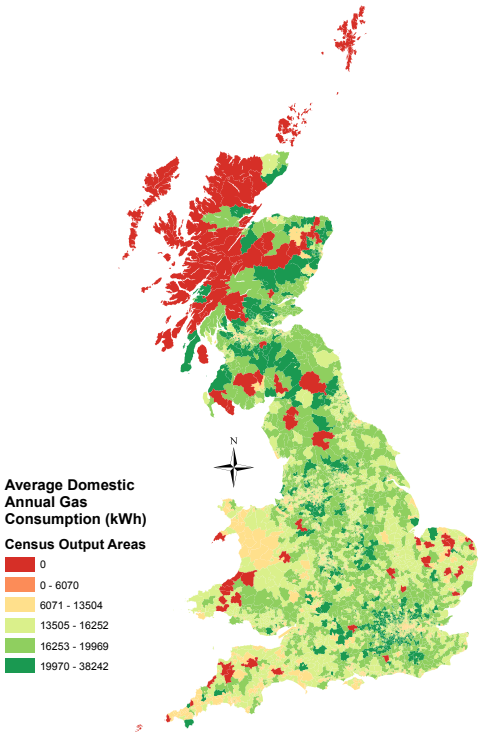

Figure 5.10.: Average gas consumption per household, 2010, data source: DECC [2012b].

proportion of population contained in these is low, whereas those grid squares containing sparsely populated areas may result in a larger percentage error.

Alternative redistribution methods which introduce complexity through a smoothing function (pycnophylactic interpolation [Tobler, 1979]), or ancillary data (dasymetric mapping and smart interpolation [Wright, 1936, Langford and Unwin, 1994, Mennis, 2003]) are described in more detail in Sharp [2012].

Figure 5.13 gives an example of a dataset before and after spatial redistribution. Census data on the number of dwellings that are detached in each LLSOA has been used to derive a percentage of total dwellings that are of this type in the LLSOA and the model grid. The figure demonstrates that the same areas are identified at either end of the scale e.g. cities such as London are identified as areas with a low proportion of detached housing and northern Scotland has the highest proportion of detached housing per grid square. There is, however, clearly a loss of detail, for example areas around London appear to have the same proportion of detached housing as the city according to the grid, while the census data shows that this is not the case. This difference between the census geographies and the model grid demonstrates that redistributed data can be used to locate differences in this type of variable but the location is generalised. This demonstrates that there is variation within the grid squares used for the model.

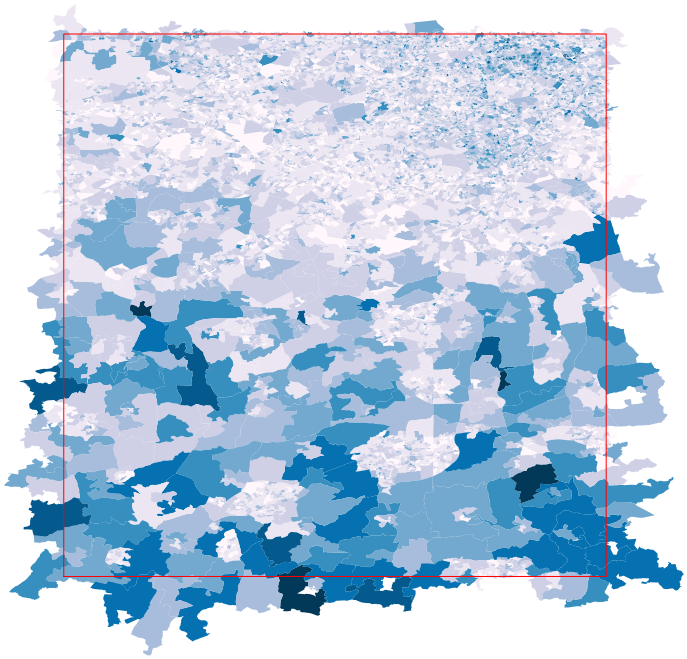

Figure 5.11.: A single 0.5^0 grid square (red line) over a densely populated area divided into LLSOA's.

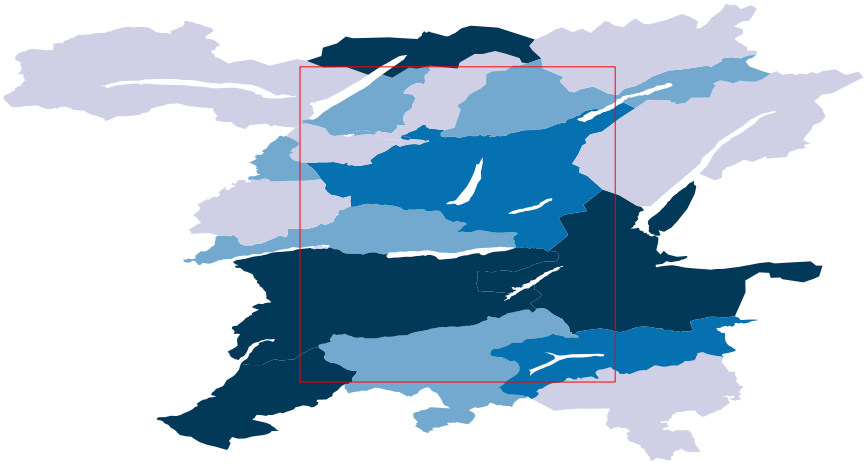

Figure 5.12.: A single 0.5^0 grid square over a sparsely populated area divided into LLSOA's (white polygons are bodies of water).

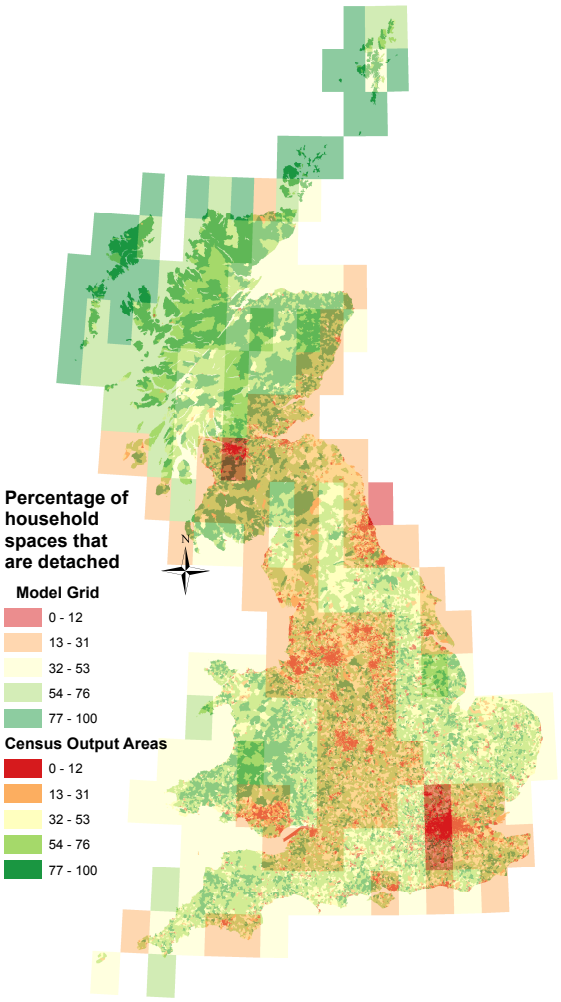

Figure 5.13.: An example of spatial redistribution of census area statistics to the model grid. Percentage of dwellings that are detached 2001. Figure A.4 shows separate maps of the data in the model grid and census geographies.

Figure 5.14 shows the results of the same redistribution done with raw data (number of houses rather than a derived percentage). The classification boundaries in the figure demonstrate the difference in scale between the original geographic units and the grid. The number of dwellings in a grid square is between 1,000 - 5,000 as many as in a census area. The figure also shows that values in coastal areas, where grid squares contain sea as well as land, can be distorted. Therefore care must be taken in the selection of variables and the way in which they are analysed.

This comparison is an effective way to show the resolution of the modelling. Given that there are over 200 squares containing GB land within the grid, it is valid to say that the model is approximately 200 times more spatially disaggregated than the majority of energy systems models which cover the whole country. However, given that some of the spatial data for GB that describes energy demand and supply drivers is available up to 5,000 times more spatially disaggregated it is clear that this approach may only be a step towards the level of disaggregation that is possible with greater computational resources, time and access to data.

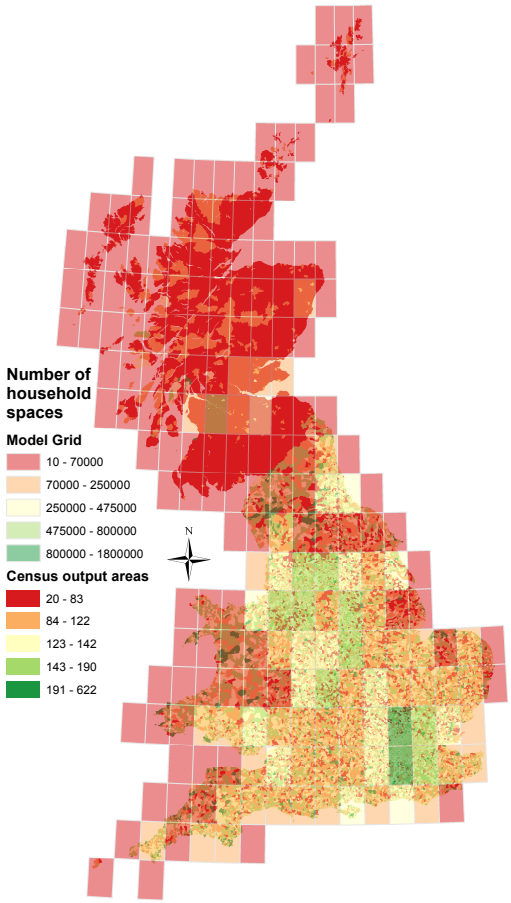

Figure 5.14.: Example of spatial redistribution of census area statistics to the model grid. Number of household spaces, 2010 census LLSOA data redistributed to the model grid.

5.3. Calibration of SpDEAM

The following section describes the calibration of the model against 10 years of measured data. The period 2000 - 2010 was selected because a wide range of data are available with minimal need for temporal interpolation. The weather over this period should encompass sufficient variability at different temporal resolutions; however, extremes that only occur at decade level intervals may not be present. Input data has been selected to represent reality as closely as possible over this period. This calibration is necessary to ensure that the input data and algorithms represent all electricity demand as closely as possible.

5.3.1. Input data and assumptions

Energy Demand National annual values for domestic energy demand by end use and fuel were obtained from DECC [2012c], these data are described in Figure 5.15 and Figure 5.16. The plots demonstrate that appliances constitute the majority of demand for electricity in domestic dwellings at a national scale and, disregarding space heating, hot water the most demand for gas. There is gas demand attributed to appliances by DUKES, which is used by gas powered washing machines etc.

(not cooking, which has its own value). The appliance demand in Figure 5.15 is a simplification, as illustrated by Figure 5.17, which shows that there are many demands other than lighting, cooking and water that have been enveloped into appliances. It is necessary to aggregate these demands in national scale modelling to avoid excessive computational loads and levels of precision that exceed knowledge of the processes.

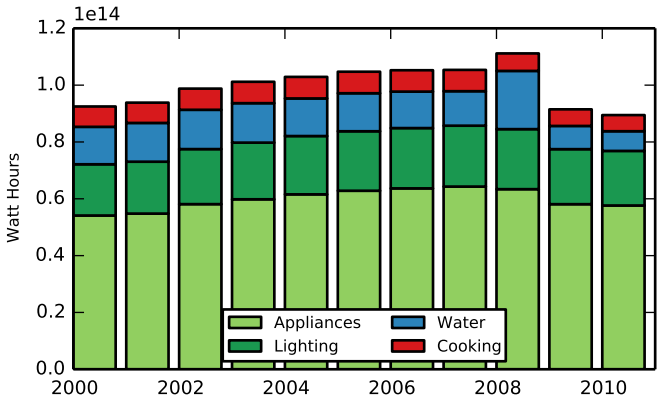

Figure 5.15.: Annual GB electricity demand by end use, absolute values derived from DECC [2012c].

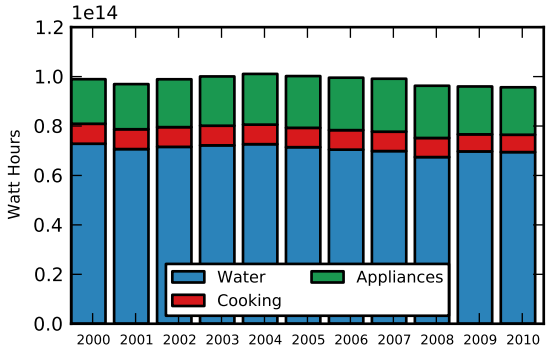

Figure 5.16.: Annual GB gas demand by end use, derived from DECC [2012c].

Annual values for non domestic demand for gas and electricity and the division of fuel demand by service end use were were obtained from Energy Consumption in the UK (ECUK) [Khan and Wilkes, 2014] (Figure 5.18). ECUK data in the non domestic sector is subdivided into industrial and service sectors. The service sector is divided into public administration, private commercial and agriculture, in SpDEAM these have been aggregated to service.

It was necessary to remove the electricity and gas demand associated with Northern Ireland from both DUKES and ECUK to obtain data for GB only. Northern Ireland Energy (NIE) provide electricity sales data from 1980 - 2010, which is sectorally disaggregated (agriculture, domestic and non-domestic) from 1991. Despite this data being referred to by DUKES and DECC sub national data documents and disseminated in documents from NIE, it is not available online. Therefore, it was necessary to gather data from indirect sources. Energy trends (table 5.5) provides data from 2002 - 2013 aggregated by sector and DECC sub national data (2008 - 2011) is divided by sector. From this data it was calculated that Northern Ireland uses approximately 2.5% (+/- 0.2%) of

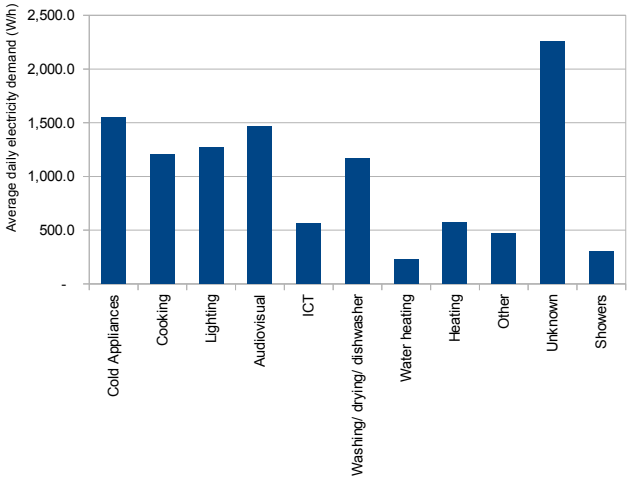

Figure 5.17.: Daily average household electricity use by end use, data source DECC [2012c], derived from the Household Electricity Use Survey (2010 -11).

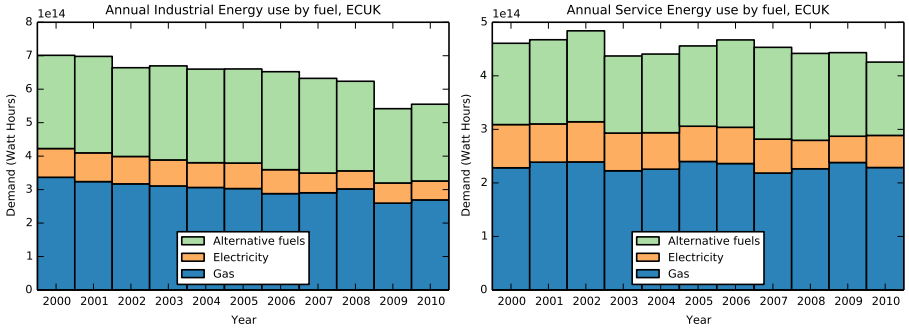

Figure 5.18.: GB annual electricity and gas demand by end use, non domestic.

UK domestic electricity and 4% (+/-0.6%) of non domestic electricity annually. This amount was removed from the national annual values. This proportion may fluctuate over longer periods of time, but such trends would be too small to materially change the model results.

Gas use is limited in Northern Ireland (gas is distributed to approximately 10 towns), natural gas has only been piped since 1996 and then only to Belfast until 2005. Currently about 170,000 houses and 12,000 businesses are supplied with gas [Devitt et al., 2011]. Unfortunately gas data are excluded from sub national statistics "due to difference in market structure". No other source for gas demand data was found. There is limited gas demand in the top down section of the model, and a very small amount would be used in Northern Ireland, therefore no correction was made to this data.

The DUKES data on energy consumption from end use is based on the Cambridge Housing Model v2.8 (cooking) and SAP (lighting and appliances), both of which are described in Section 2.3. DECC declare within DUKES table 3.05 that "the breakdown of energy by final use is based on modelling, and this is subject to uncertainty from housing data, behavioural data, climate data and building physics assumptions. The proportions used in the breakdown could vary by as much as 18%". The ECUK data is also not entirely empirical and is based on Purchases Inquiry, a sub survey of the ONS' Annual Business Inquiry and through analysis of DUKES data. The Purchases Inquiry surveys a sample of 6000 firms and then weights each sector to match totals with data

from DUKES [Khan and Wilkes, 2014]. The result of these values being modelled and scaled up means that inevitably any simulation from SpDEAM may not correlate perfectly with measured data.

Heat loss and population Heat loss characteristics by dwelling type data were gathered from DECC [2012c] (Figure 5.19). These coefficients are based on analysis of data from the EHCS and EHS by Cambridge Architectural Research, through the CHM. DUKES only provides values for 2008 to 2010. The coefficients are assumed to be static. These values are a generalisation of each dwelling type which may vary. Population data were gathered from the Office of National statistics Mid Year Estimates [ONS, 2014a] (Figure 5.20).

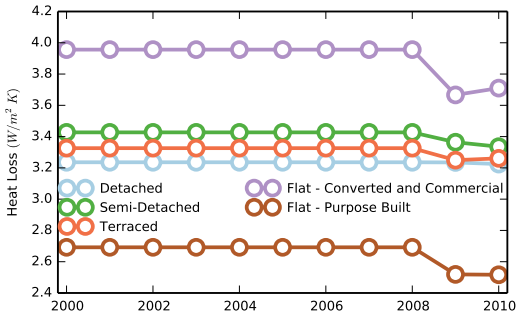

Figure 5.19.: Dwelling specific heat loss characteristics, data source DECC [2012c].

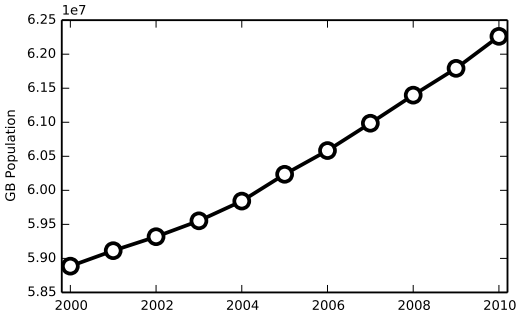

Figure 5.20.: GB Population 2000 - 2010, data source [ONS, 2014a].

Filling temporal gaps Many of the data used in the demand modelling evaluation and development do not cover all the desired years. Linear interpolation was used to fill gaps where necessary. This was performed at the same resolution at which the data is provided, these values are then considered to be constant over disaggregated temporal resolutions. This includes spatial datasets, no spatial movement is incorporated, rather the same growth rate is applied individually to grid squares e.g. to fill the gap between gridded data derived from the 2001 and 2011 census the difference between each grid cell was calculated and the change assumed to be even each year (1/10).

5.3.2. Summary of model data including parameters and assumptions

The input data described above is summarised in Table 5.2. Alongside this data it was also necessary to select model parameters and assumptions to use in the algorithms and to assign the national energy demand values to the activity profiles. In the first instance, values for model parameters reflecting reality have been chosen. Where values have been altered during the evaluation process this is noted. These values are assumptions based on imperfect data, many of them represent subjects which are currently being researched. In the future, better, more accurate, values could be used. The ensuing analysis means that the model is calibrated to measured data where possible, so to some extent any error introduced through these assumptions will be allowed for.

Input parameter or dataset	Method used to set parameter or create dataset
Temporal profiles	DEAM
Algorithms	DEAM
Weather data	CFSR
Population distribution	Gridded Population of the world, see Section 5.2.1.1
Population numbers	Data obtained from ONS [2014a]
Dwelling types and numbers	Redistributed census data from 2001 and 2010
Dwelling floor area	Data adapted from DCLG. [2013b,a]
Heat loss characteristics of dwellings	Data obtained from DECC [2012c]
Heating technology types	Redistributed census data from 2001 and 2010
Domestic annual energy consumption	Data derived from DUKES 2001 - 2010 [DECC, 2012c]
Non domestic annual energy consumption	Data derived from ECUK 2001-2010 [Khan and Wilkes, 2014]

Table 5.2.: SpDEAM input data and methods

- Internal temperature was set at 21°C, this is the same as used in SAP, whereas the CHM assumes 19°C for living areas based on Kane et al. [2011]. BREDEM uses 21°C in the living room and 18°C elsewhere. In a study of 427 English houses Shipworth et al. [2010] found that the average thermostat setting is 21.1°C with a standard deviation of 2.5°C.
- Boiler efficiency was set at 80%. This is in the middle of the Seasonal Efficiency of Domestic Boilers in the UK (SEDBUK) rating system, which lists the seasonal efficiency of boilers, based on trials of 20 boilers in 99 homes over three years. Boilers can be rated at over 90% efficient. The extent to which they under perform is unknown. There is also a large body of older less efficient boilers in use.
- There are separate domestic profiles for those people who are in during the day and those which are out, as shown in Figure 5.3. In order to assign demand from the national values to these profiles it was assumed that 70% of people are out during the day, 30% in during the day. This is based on the fact that a large number of people will be at work and school and a portion of those at home will be out for at least part of the day.
- Incidental gains from non space heat energy end uses are calculated using the percentage of wasted power and the amount of this that contributes to heat described in Table 5.3.
- The division of night and daytime non domestic demand was assumed to be 50% (Figure 5.4). There is no information publicly available on this division and the selection of this value represents a compromise.
- 50% of service demand is assumed to follow the 5 day profile described in Figure 5.2, 25% is assigned to the 6 day profile and 25% to the 7 day profile.

End Use	Useful wasted power %
Lighting	100
Hot Water	50
Cooking	50
Appliances	11

Table 5.3.: SpDEAM assumptions of power to heat for different end uses, all power is assumed to turn into heat.

5.3.3. Calibration data and methods

The model was initially run using the data, profiles and assumptions described above. The results were then correlated against the evaluation data summarised in Table 5.4 and described below. It was possible to correlate simulated domestic demand against sectorally disaggregated published data. There is no data available on non domestic demand, therefore this was evaluated against data on total demand after being combined with domestic demand. The difference between total SpDEAM demand and demand depicted by national data represents all un-modelled demand. The model was recalibrated to include these demands so that future applications of SpDEAM represent total hourly electricity demand. The recalibration was performed by altering the non domestic activity profiles. The domestic profiles are unaltered, which means that new electrified heat demand can be added in the scenario modelling. Using this method assumes that the domestic method does not contain error, which is discussed below. Correction factors were created by plotting the results of the model against the calibration data, the mean factor by which the profile at each time step would have to be altered by to converge the two sets of values was calculated. This mean factor was then applied to the activity profiles, in the case of electricity the hourly profiles were altered first, then the monthly, a recalibration and calculation of mean correction factors was performed in between each step. These profiles were chosen as they showed the clearest difference between periods e.g. SpDEAM total electricity at 12:00 correlated to the measured demand differently to SpDEAM output at 17:00. The same method was used for gas data, however it was only necessary to alter the monthly activity profiles. Correlation between SpDEAM and the gas and electricity data at each calibration step is described below and the total un-modelled demand is quantified.

Published data are available at a national spatial resolution at several different temporal resolutions. The only annual data available depicting GB energy demand have been used as model inputs. Nevertheless the data are used to verify that model outputs from the top down section of the model have not been altered. Outputs from the bottom up, weather dependent, section of the model are also compared to the annual data, which does not rely on the same data for inputs. It was assumed that the 2.5% of electricity demand attributed to Northern Ireland is consistent for all end uses and was therefore removed from the end use demands.

Quarterly gas demand data for GB, disaggregated to the domestic sector were obtained from DUKES (table 4.1). These data were used to verify domestic heat, hot water and cooking gas demand at a temporally disaggregated resolution. Unfortunately, no sectorally disaggregated data are available at a finer temporal resolution. Daily gas demand data for GB in the form of predicted seasonal normal demands (SND) (including warm and cold scenarios) were obtained from National Grid [2013] from 2001 to 2010. These data are derived from the Local Distribution Zone (LDZ) model, which predicts the entire gas demand including industrial and commercial customers. According to the audit of the methodology for calculating these loads by Frontier Economics [2006],

Variable	Dataset	Use in calibration
Annual domestic gas demand	DECC [2012c]	Verify top down method does not alter input data
Quarterly gas demand	DUKES table 4.1	Evaluate demand for gas from domestic heat, hot water and cooking
Annual domestic electricity demand	DECC [2012c]	Verify top down method does not alter input data
Annual domestic electricity demand for heat	DECC [2012c]	Evaluate bottom up methods
Annual domestic heat demand for other fuels	DECC [2012c]	Evaluate bottom up methods
Total daily gas demand	LDZ SND daily gas demand	Calibrate non domestic gas demand
Sub-national domestic electricity demand	DECC [2012b]	Evaluate spatial accuracy of SpDEAM
Sub national domestic gas demand	DECC [2012b]	Evaluate spatial accuracy of SpDEAM
Hourly total electricity demand	National Grid [2012]	Calibrate non domestic electricity demand

Table 5.4.: Data used for calibration of SpDEAM.

approximately 60% of this demand is domestic. However, analysis has shown that this percentage varies depending on the time of year (60% in the first and fourth quarters (+/- 8%), 50% in the second (+/- 5%) and 40% in the third (+/- 6%)). This data is therefore only used to evaluate total gas demand from all sectors. Data is collected from companies supplying more than 1,750 GWh to consumers, no information is given on scaling this to include smaller suppliers (data gathering methodology is described in DECC [2014a] p.79), however data is referred to as covering the UK. No correction is made to remove Northern Ireland demand. Demand from SpDEAM should therefore, be slightly lower than DUKES.

Half hourly electricity demand data were obtained from National Grid [2012] covering April 2001 to the end of 2010. These data are based on National Grid operational generation metering and do not include station load, pump storage pumping or interconnector exports. The data therefore includes all non-domestic and commercial demand covered by SpDEAM, plus losses, and is used to compare against the total aggregated electricity demand. The inclusion of losses, which are not modelled in SpDEAM, means that it is likely that SpDEAM will underestimate demand in comparison with these data.

Sub national data are available for both electricity and gas at annual temporal resolution. Sub national statistics on domestic gas and electricity consumption were obtained from DECC [2012b]. Both the gas and electricity datasets were redistributed to the grid from MLSOA geographies using the method described in Section 5.2.2.3, examples of the data before and after redistribution are given in Section A.1.3. Both gas and electricity datasets are predominantly based on measured data, there are, however statistical adjustments made to account for unmetered demand such as public lighting and theft. This is the case for all national statistics of energy demand as it is not possible to meter all demand. This means that when SpDEAM outputs are evaluated against this data any correction will ensure that the model includes these. The result of this is that there may

be an incorrect increase of individual demand elements. Sub national data may not be an ideal source for model inputs, due to issues with the data described below.

Sub national gas data, based on meter readings, are available from 2001 to the present day with a lead time of more than one year. The gas year in this data covers 1 October to 30 September rather than a calendar year as used by other datasets. Meter readings are classified as domestic or non domestic, based on a threshold of 73,200 kWh (this is the industry standard Annual Quantity). This results in many smaller non domestic customers being classified as domestic (approximately 2 million according to DECC). This classification system is appropriate for those interested in demand magnitude, but makes modelling sectoral changes to demand based on the data difficult. Gas consumption figures are weather corrected so that change in demand between years can be calculated irrespective of changes in temperature. These attributes, particularly the inaccurate sectoral classification, mean that it is difficult to compare SpDEAM outputs against this data. Therefore only *domestic* gas demand data is compared against SpDEAM for a single year. DECC recommends that 2005 is used as a base year for time series analysis (previous years use inconsistent methods of collection and analysis), therefore this year is used.

Sub national electricity data, also based on meter readings, are available from 2005 to the present day. Electricity consumption in GB is recorded by half hourly meters for large commercial and industrial customers. All other metered electricity consumption is recorded by non half hourly meters. Half hourly meters provide accurate annual figures, DECC estimate an annual consumption from two meter readings for non half hourly meters. Customers (on half hourly meters) are classified as domestic or non domestic based on the profile of their energy use. Total demand is also used for classification, if total electricity demand is over 100,000 kWh per year, and in some cases where the total is above 50,000 kWh, customers are defined as non domestic. Electricity data are not weather corrected and run over a calendar year. This means that the data should be comparable to model outputs, although there may be some disagreement due to different methods of sectoral division. Therefore *domestic* electricity demand data is compared against SpDEAM for 2005 - 2010.

5.3.4. Results

5.3.4.1. Domestic demand for gas

The domestic demand results presented in this section are created according to the method described above, this means that the method has not been altered as part of the model calibration. The results can therefore be considered an evaluation rather than a calibration, they have been included in the section to demonstrate why the correction factors have only been applied to the non domestic profiles. Figure 5.21 shows annual domestic gas demand against DUKES annual data. The plot shows that total gas demand, which includes demand modelled using both the top down and the bottom up method, does not exactly match the values provided in DUKES. However, the mean bias is very small (0.8%) and there are several years with almost no error. There are years with more significant bias, however none of these exceed 10%. The variable direction of the disagreement suggests that some of the variability incorporated into SpDEAM may not be included in the evaluation data, which is derived from the CHM and vice versa. Since the data used for evaluation has been modelled, a divergence of less than 10% for a complex variable is acceptable, especially as the data source states that error of up to 18% is possible (Section 5.3.1).

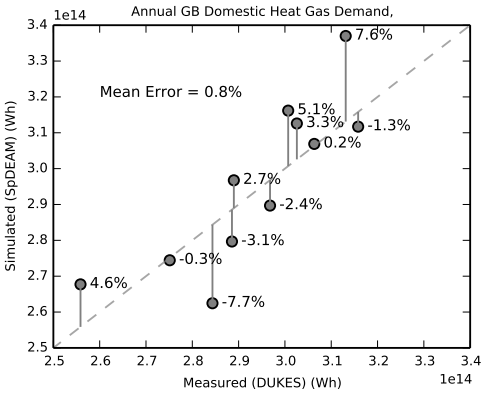

Figure 5.21.: Difference between SpDEAM and DUKES annual gas demand by end use.

Figure 5.22 shows that SpDEAM gas demand follows seasonal variability very well. There is no seasonal bias in terms of error, which may be expected as summer demand is likely to be uniformly low, whereas winter demand may vary.

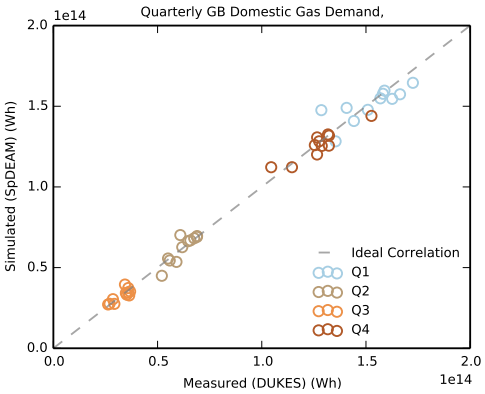

Figure 5.22.: Simulated vs. measured quarterly gas demand.

Figure 5.23 shows that SpDEAM matches the DECC sub national statistics closely across most of central and eastern England. SpDEAM output is lower than the DECC data across northern Scotland and the south coast of England and higher in Wales and a few parts of England. The difference in Northern Scotland could be attributed to the need to synthesise spatial data on heating technologies due to the lack of census data. The area considered to have low to no gas demand (Figure 5.9) is similar to that with the highest negative difference shown in Figure 5.23, suggesting that there is wider use of gas for heating in this part of GB than that represented in the synthesised data. The DECC statistics offer an alternative data source for heating type allocation, particularly with regards to gas, however they are subject to the problems described in subsection 5.3.3. Also, using gas demand data would only be a proxy for this heating technology as it includes cooking etc., whereas the census data specifically describes heating. Therefore no model changes were made based on the level of divergence between SpDEAM outputs and the sub national data. The black grid squares represent areas where there is no demand in the DECC dataset but there is demand from SpDEAM, this is because the population dataset includes some population where the DECC data does not. This demonstrates one of the problems with a model which aggregates some data, whereby the demand from small areas can be generalised over a larger area.

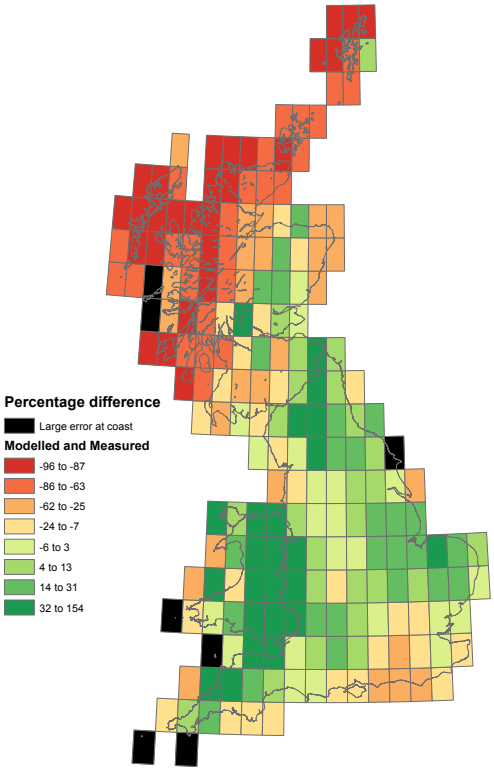

Figure 5.23.: Difference between model outputs and DECC sub national statistic, Gas 2005, data source: DECC [2012b].

5.3.4.2. Domestic demand for electricity

No error is introduced by the model for electricity demand from water and cooking. Figure 5.24 shows that demand from lighting and appliances is maintained, this is important as it is linked to weather and time using the darkness factor. Demand for electricity for heat (calculated bottom up) does not perfectly match the DUKES data (Figure 5.25). Little difference is shown from 2000 - 2007, after this error increases dramatically in both directions. Demand for electricity from heat in the DUKES data is very low (52% lower than 2007) and very high after that (52% higher than 2007), despite being very steady in the preceding years. This suggests that there is a change to modelling methodology. SpDEAM demand is coherent, therefore no changes are made to the model based on this difference. This illustrates the danger of using modelled data for evaluation or input. There is very little recognition in the literature of the fact that national statistics used for model input and evaluation are based on modelled data.

Figure 5.26 shows that the difference in electricity demand between DECC statistics and SpDEAM outputs has no national trend. Also there is little correlation in the spatial variation in divergence between gas and electricity, other than a low positive error in northern Scotland. Overall the percentage error is lower than with gas (Figure 5.23).

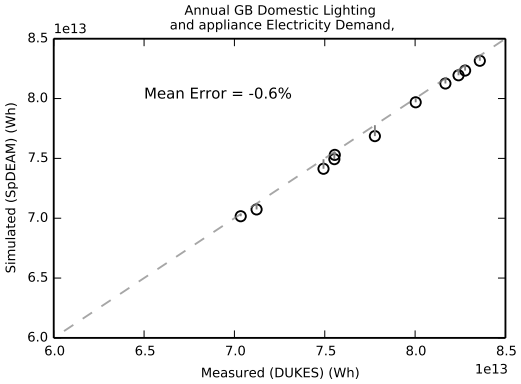

Figure 5.24.: Annual domestic electricity demand for lighting and appliances, SpDEAM and DUKES.

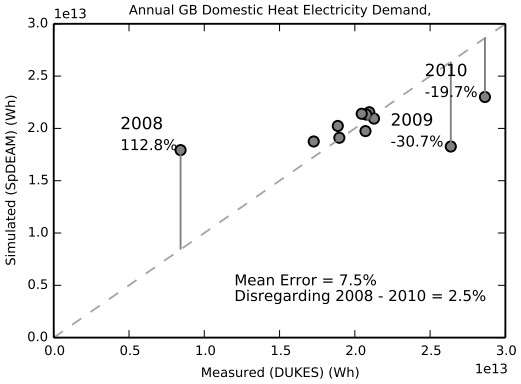

Figure 5.25.: Annual domestic electricity demand for heat, SpDEAM and DUKES.

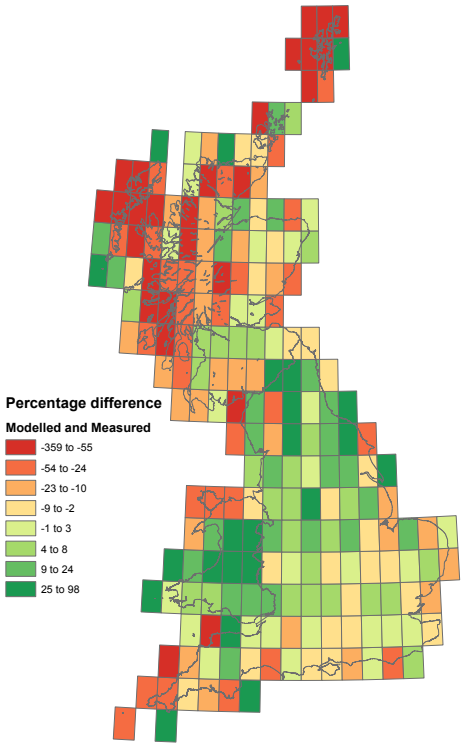

Figure 5.26.: DECC sub national and SpDEAM annual electricity demand 2010, data source: DECC [2012b].

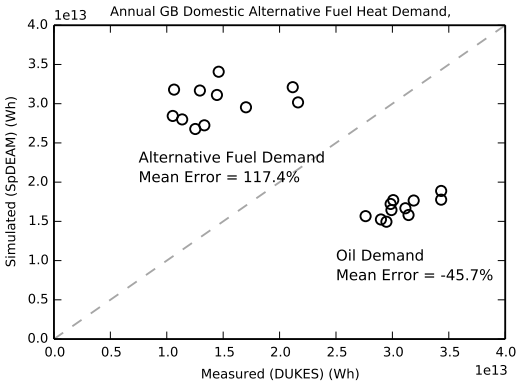

Figure 5.27.: Annual domestic space heat demand by fuel type, SpDEAM and DUKES.

Figure 5.27 shows that demand for oil from heat is lower in SpDEAM than DUKES and that demand for alternative fuel is higher in SpDEAM than DUKES. The divergence may be due to the way that heat demand is attributed to heating technologies and fuels described above. The lack of efficiency applied to this section of the model may also have an effect. There are, however many possible reasons, due to the complexity of the model. The lack of other data sources on demand for these other fuels means that making corrections to allow for the divergence is difficult. Care must be taken when analysing shifts in demand from these fuels to electricity in scenario modelling. In many cases a shift from non gas based heating to heat pumps is a more attractive economic option than shifting from gas based heating to heat pumps [Fawcett, 2011].

5.3.4.3. Total demand before calibration

Figure 5.28 shows SpDEAM total daily gas demand from all sectors compared with LDZ SND demand, demonstrating that SpDEAM underestimates daily gas demand for almost all days between 2001 and 2010. The bias is more than 100% of the SND value for many days, RMSE is 1140.07 GWh over the whole time series. Where SND demand is between 1.5 - 3.5 TWh the range of SpDEAM demands is relatively small (approx 0.5 TWh) in comparison to the higher SND demands (3.5 - 4.5 TW) where there is significantly more variation in the SpDEAM demand. These higher demands occur during the winter, where there is more variation in gas demand from the 'seasonal normal'. Despite the large bias shown by the plot there was a close correlation found between SpDEAM model results and the SND data ($R^2 = 0.71$, Pr = 0.84).

Figure 5.29 shows total hourly electricity demand from SpDEAM against National Grid data, demonstrating that SpDEAM underestimates total electricity demand for almost all hours. The bias significantly exceeds 100% of the National Grid value for many hours, RMSE is 15.6 GW over the whole time series. There is error exhibited at all demand magnitudes. The correlation coefficients demonstrate a lack of correlation between SpDEAM model outputs and National Grid data ($R^2 = 0.38$, Pr = 0.62).

The difference between the model outputs and published data represents demand not accounted for in the un-calibrated version of SpDEAM. Figure 5.30 quantifies this unaccounted for total gas and electricity demand for each of the calibration years. The plot shows that the difference in gas demand is between 285 TWh and 415 TWh. The difference is significantly lower in 2001, because

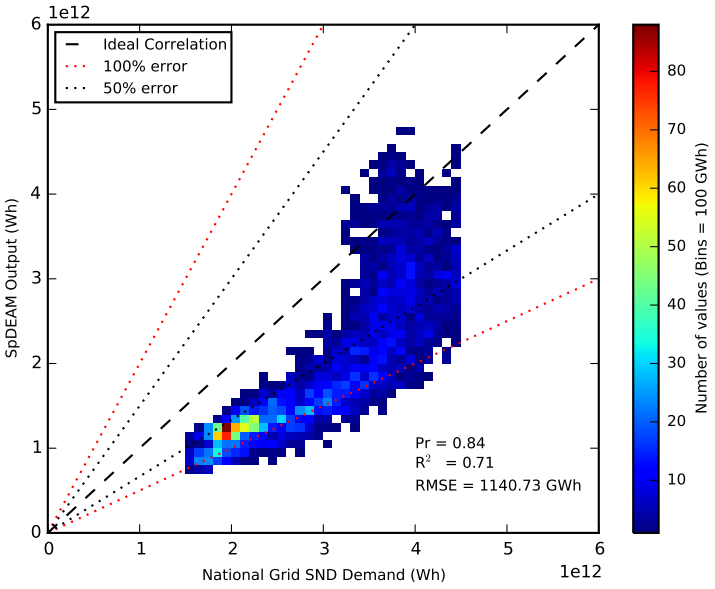

Figure 5.28.: Correlation between SpDEAM and LDZ daily gas, all time steps, before calibration.

the calibration data is not complete during this year. The percentage difference between SpDEAM and SND is quite large, between 34.8% and 38.4%.

Figure 5.30 shows that the electricity demand not accounted for by SpDEAM is between 64 TWh and 142 TWh each year. This difference is of a lower magnitude than the differences in gas, however the percentage differences are of a similar magnitude, between 29.7% and 44.4%. The difference in gas demand does not appear to have a trend over time, whereas the difference in electricity demand increases over time. Potential sources of un-modelled demand are discussed in section 5.5.

5.3.4.4. Calibration of gas demand

The un-modelled demand described above is not evenly distributed across time. The difference between SpDEAM output and measured demand data is larger in some years, months, days and hours than others. This is the reason why the model has been recalibrated by applying corrections to the activity profiles at different temporal resolutions. Figure 5.31 illustrates this point, the grey time series shows the correlation between daily SpDEAM total gas demand and SND demand grouped by year, month and day before calibration. When grouped by year and day there is little difference in RMSE or correlation between the time periods. However there are clearly months with greater RMSE and lower correlation than others.

The selection of temporal profiles to alter was dictated by the correlation between SpDEAM and measured data.

- The profiles with the largest variation in error were corrected first.
- A correction for each month was created by calculating the change necessary to converge each daily value with the SND data.
- The mean correction factor for that month was then calculated and applied to the non domestic profile.

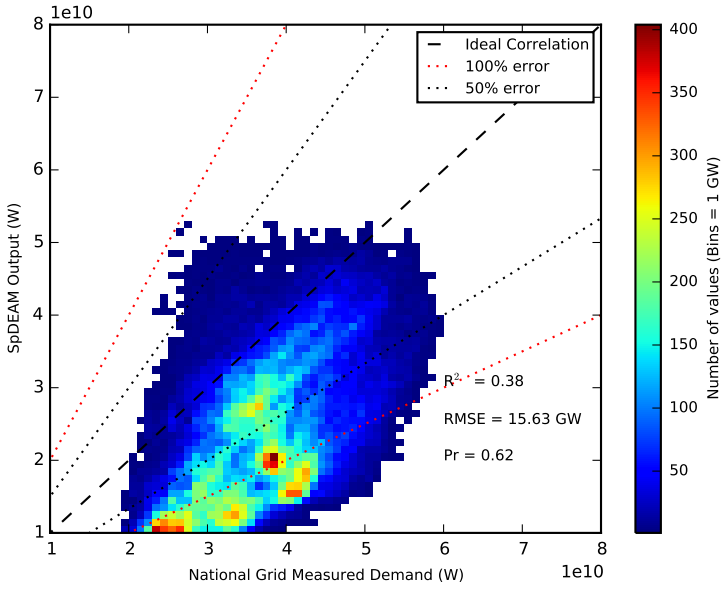

Figure 5.29.: Correlation between SpDEAM and National Grid electricity demand, all time steps, before calibration.

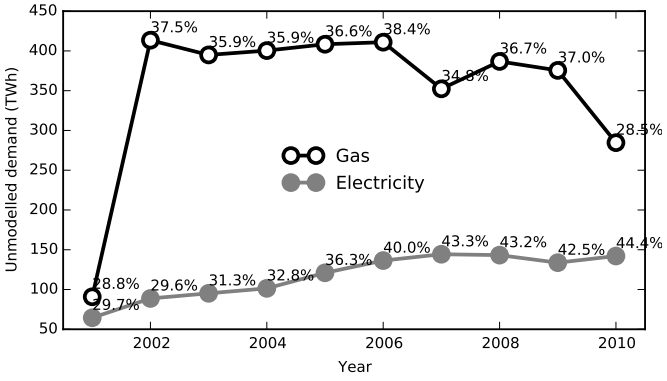

Figure 5.30.: Total gas and electricity demand not accounted for by SpDEAM in the calibration period.

In the case of gas, the monthly profiles were altered first. The results after correction are described by the black time series in Figure 5.31. The plot shows that overall RMSE was significantly reduced and the correlation increased after the model calibration. It was not possible to reduce error further due to the correction being applied on a monthly basis rather than hourly and the fact that the correction was only applied to the non domestic profiles. After this calibration, no significant temporal bias was noted at other temporal resolutions, so no further correction was applied. The results described by the black line, which is the final time series, are described in more detail by Figure 5.32, Figure 5.33, Figure 5.34 and Figure 5.35.

Figure 5.32 shows correlation between SpDEAM and SND daily gas for all available data after the calibration has been performed. The plot demonstrates that the calibration has resulted in a close correlation between SpDEAM and measured data (R^2= 0.81, Pr = 0.9). The RMSE is 397.41 GWh (0.397 TWh), total demand is between 1.5 - 4.5 TWh. Despite the overall underestimation of

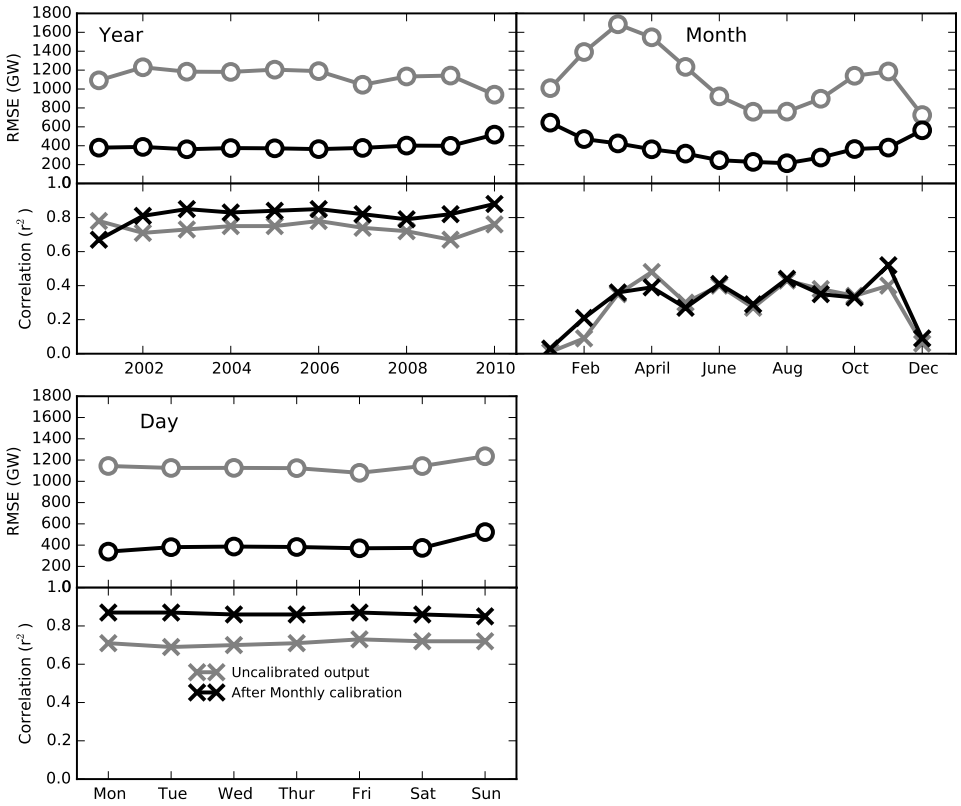

Figure 5.31.: Changing difference between total gas demand from SpDEAM and measured data over different time steps.

daily gas demand by SpDEAM, the plot shows that there are days where SpDEAM overestimates demand, particularly at lower magnitudes. There is noise at all demand magnitudes, almost all of this is within 50% error. The SND data describes a clear cut-off point at 4.5 TWh, a result of the National Grid forecasting methodology having a maximum demand. SpDEAM does not contain this cut off as it represents the range of demand across different meteorological conditions rather than a 'normal demand'.

Figure 5.33 demonstrates that there is no annual bias in SpDEAM outputs. Correlation coefficients are consistently high (R^2 between 0.79 and 0.88, Pr between 0.89 and 0.94 in years where there is complete data). The largest RMSE is shown in 2010, which is a result of cold weather conditions and high gas demand, which are reflected in SpDEAM, but not in the SND.

Figure 5.34 demonstrates that winter months have lower correlation coefficients and higher RMSE (R^2 between 0.03 and 0.36, RMSE between 640 GWh and 420 GWh) than summer months (R^2 between 0.27 and 0.52, RMSE between 215 GWh and 365 GWh). This is due to greater variation in SpDEAM gas demand than SND. Demand in the winter months is clearly harder to model than summer, when space heat demand is lower.

Figure 5.35 demonstrates that no daily correction factor is necessary because consistent, high, correlation coefficients are achieved after the correction of the monthly profiles. Weekend demand is slightly underestimated in SpDEAM compared to SND. This may be due to the weekend demand being less 'normal' than weekday, due to greater variability in activity, e.g. a person's weekday

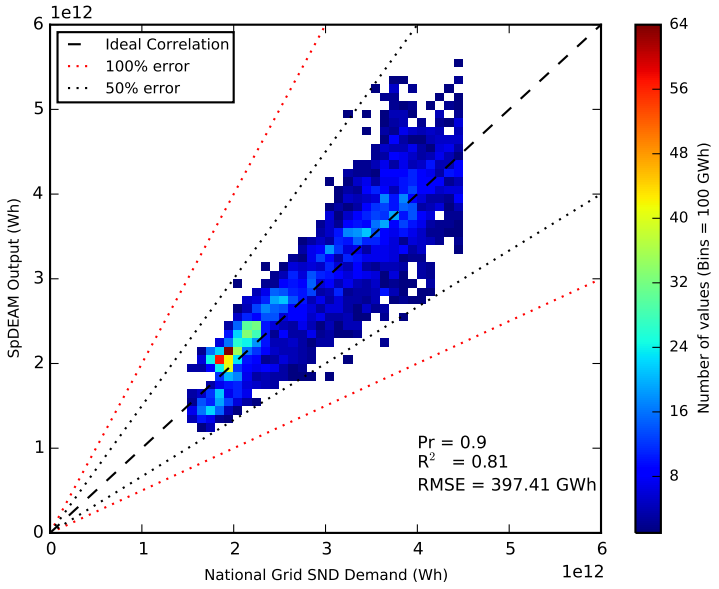

Figure 5.32.: Correlation between SpDEAM and LDZ daily gas, all time steps.

activity is dictated by work, whereas weekend activity is less rigid.

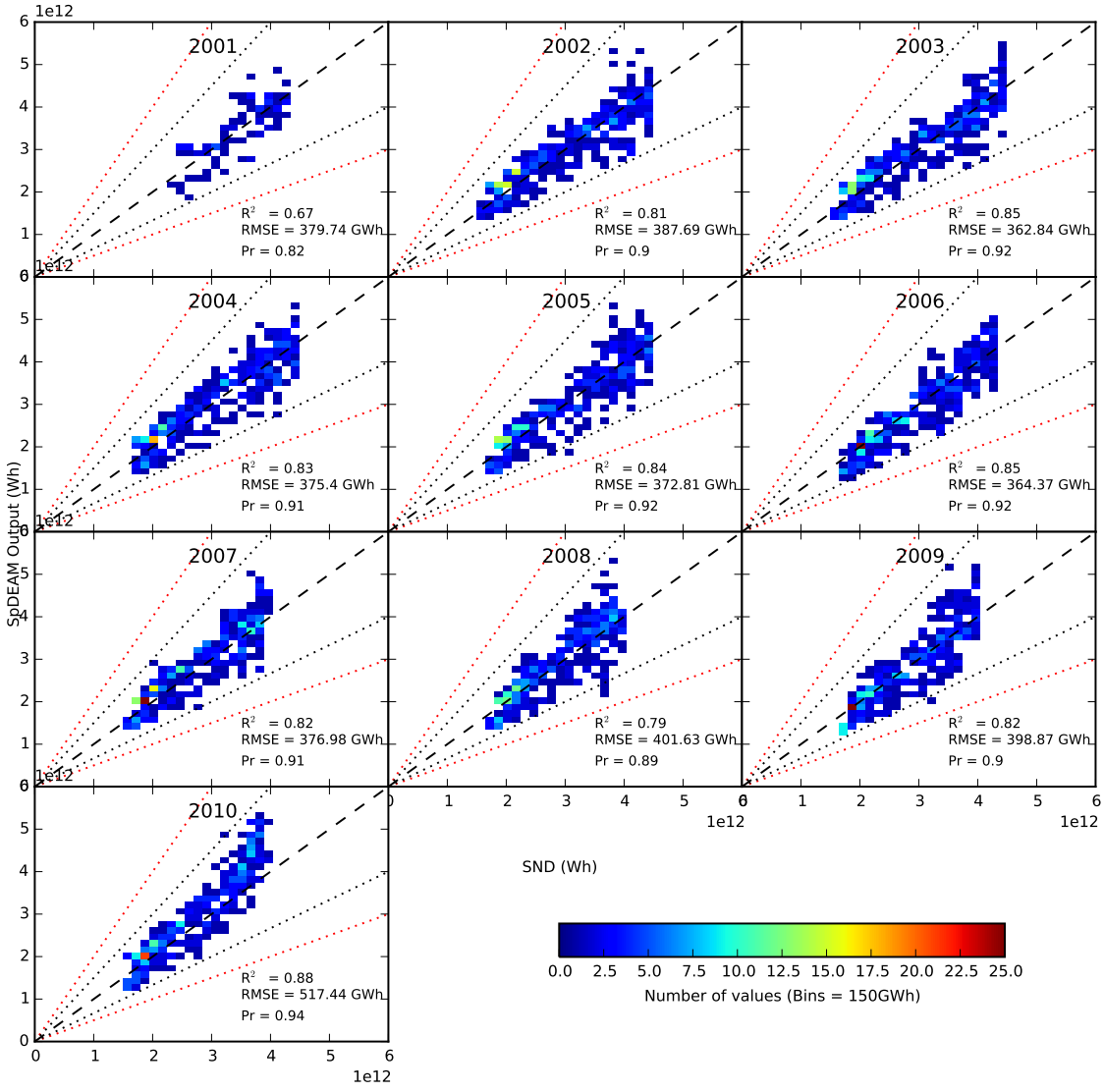

Figure 5.33.: Correlation between SpDEAM and LDZ daily gas, by year.

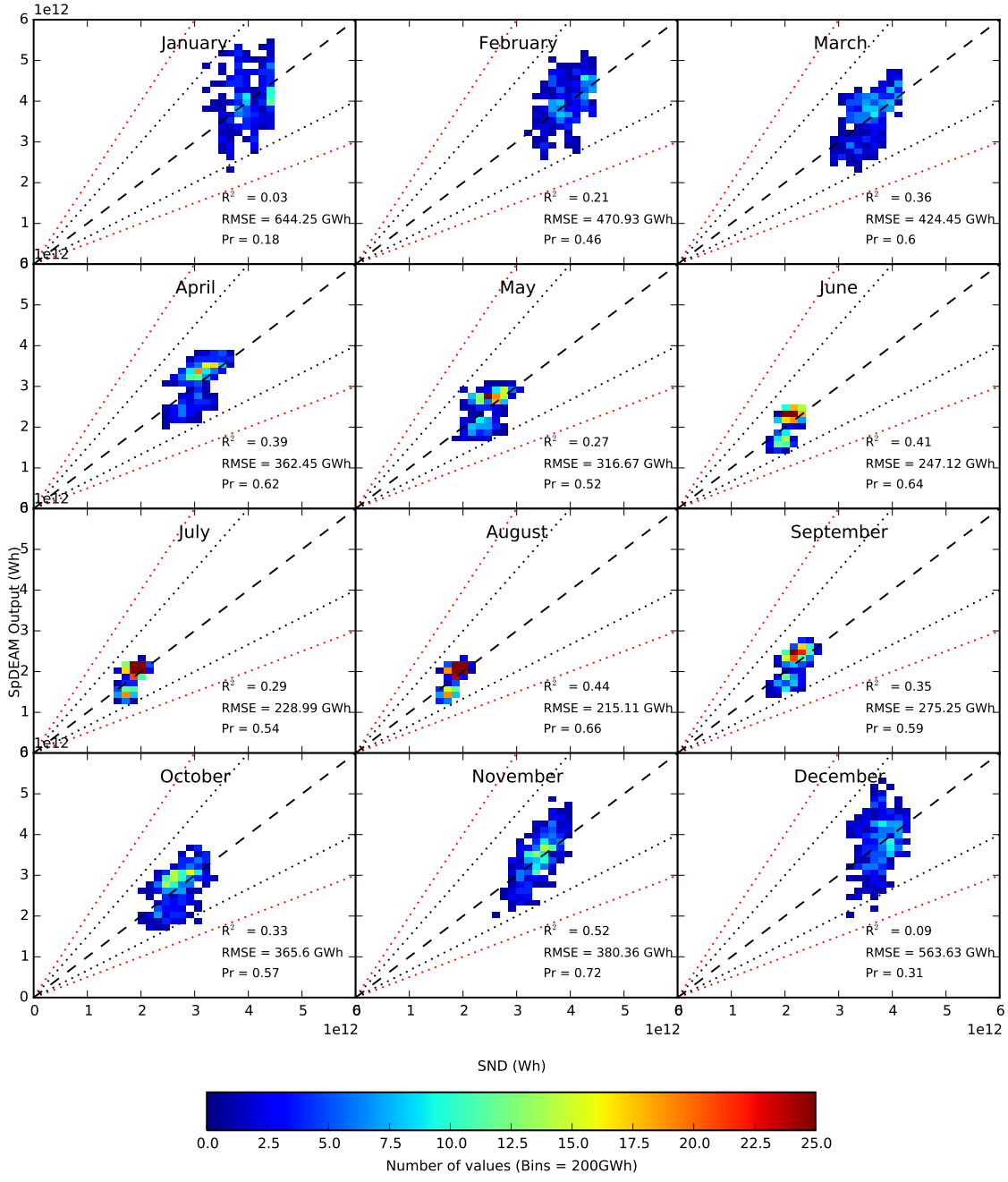

Figure 5.34.: Correlation between SpDEAM and LDZ daily gas, by month.

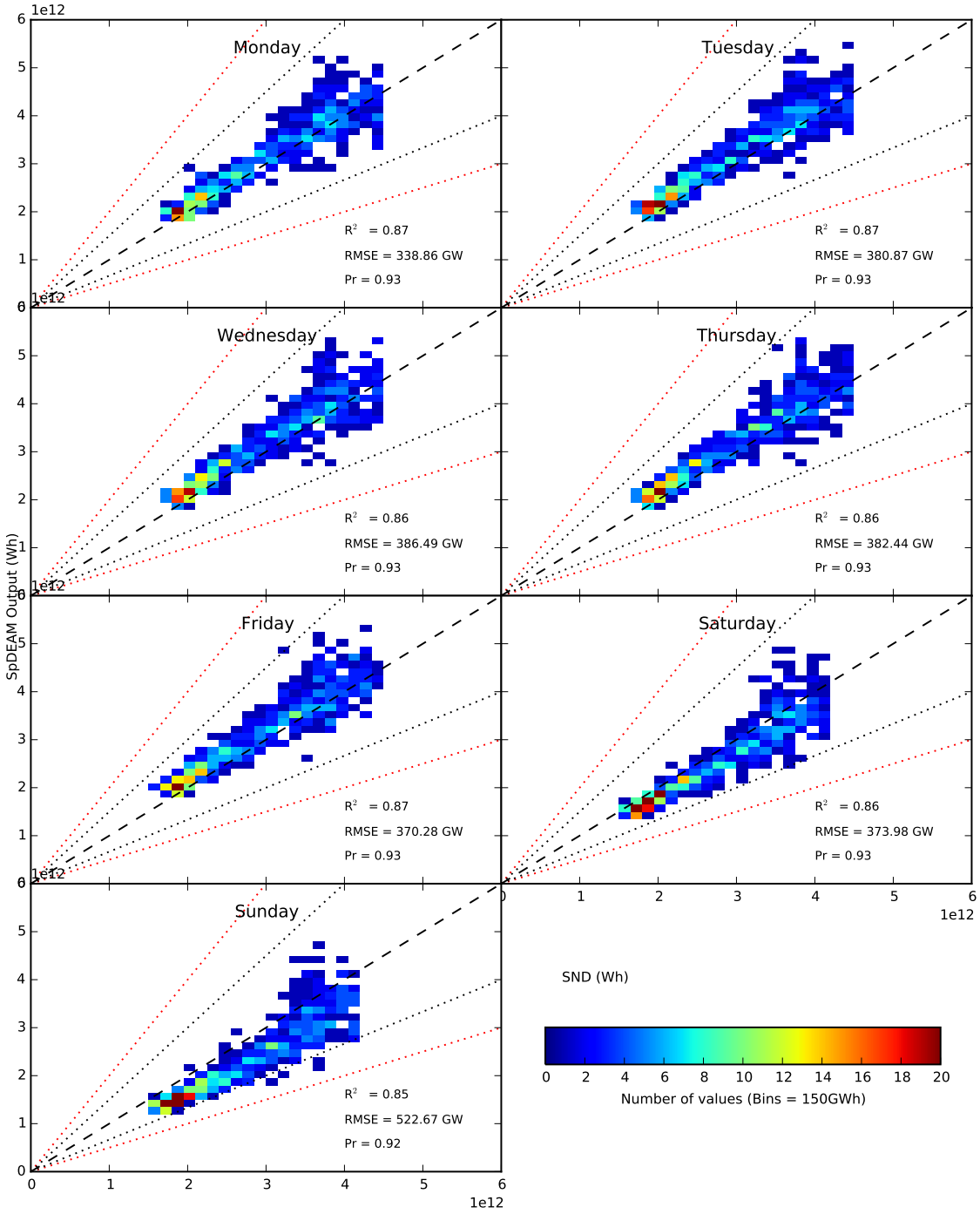

Figure 5.35.: Correlation between SpDEAM and LDZ daily gas, by days.

5.3.4.5. Calibration of electricity demand

Figure 5.36 shows how RMSE and correlation between SpDEAM total hourly electricity demand and National Grid measured data change before and after each calibration step. The blue time series in each of the plots describes the correlation between SpDEAM and the National Grid data before any calibration has been performed, the light brown time series shows the metrics after the calibration of the hourly activity profiles and the dark brown time series shows the metrics after the calibration of the monthly activity profiles. The plot demonstrates that, before calibration has been performed, the largest RMSE errors are experienced at an hourly resolution. There is also more variation in RMSE and correlation between hours than seen in the other time periods, where the error is more consistent. Therefore the first calibration performed was an alteration of hourly non domestic activity profiles.

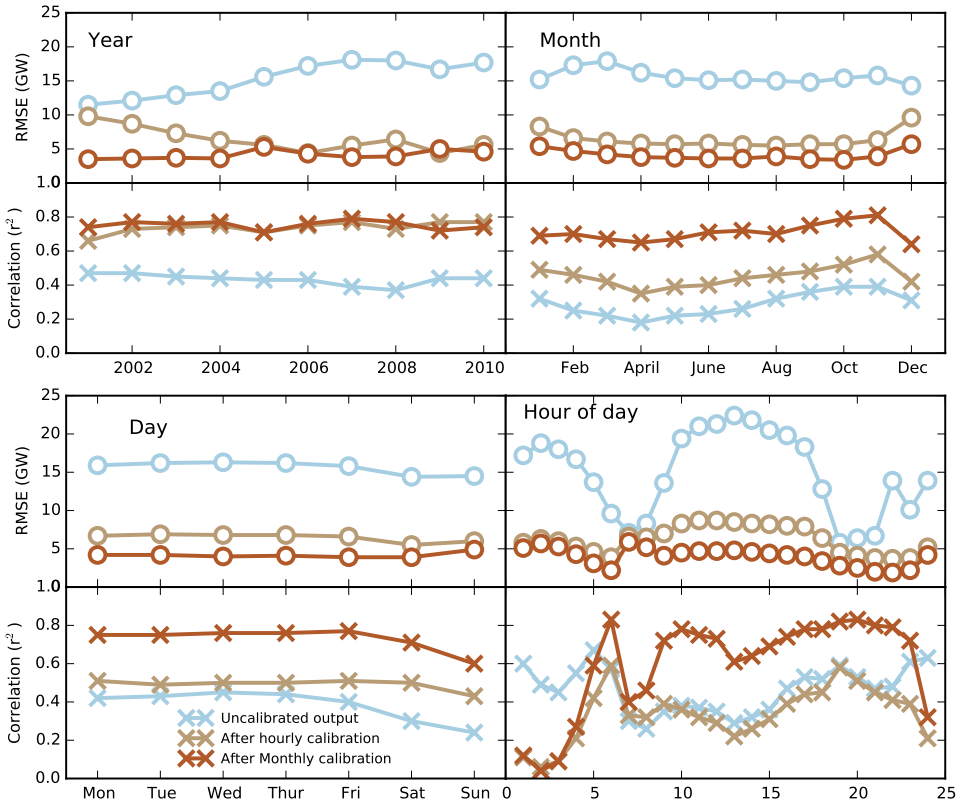

Figure 5.36.: Changing difference between total electricity demand from SpDEAM and measured data over different time steps.

Figure 5.36 shows that the calibration of the model significantly reduced the RMSE at all temporal resolutions from between 6 - 23 GW to between 4 - 10 GW. The correlation plot for hour of day shows that reducing the RMSE does not necessarily increase correlation, particularly between midnight and 5 AM where R^2 reduces from 0.6 to less than 0.2. This is a result of only applying the correction to the non domestic activity profile having determined the correction factor using total demand. Unfortunately this is unavoidable given the limited data available on sectorally disaggregated electricity demand. The correlation is significantly improved by this calibration step at all other temporal resolutions, when aggregated by year R^2 increases from between 0.4 -

0.5 to 0.6 - 0.8, when aggregated by month R^2 increases from between 0.2 - 0.4 to 0.4 - 0.6. The second and final step in the calibration of the electricity demand model altered the monthly activity profile. The monthly plots in the top right corner of Figure 5.36 show that this step reduces RMSE further to between 3 - 6 GW and increased R^2 to between 0.6 - 0.8. The results described by the dark brown, final, time series are described in more detail by Figure 5.37, Figure 5.38, Figure 5.39, Figure 5.40 and Figure 5.41.

Figure 5.37 demonstrates a high correlation coefficient between measured hourly electricity demand and SpDEAM outputs over the whole evaluation period ($R^2 = 0.75$). There is noise at all demand magnitudes, but hourly RMSE is low (4.2 GW). The plot exhibits a high density of points with ideal correlation, showing that the model performs extremely well at the majority of time steps. Lower demand periods exhibit greater variation, in contrast to gas demand. The highest level demand hours are of a lower frequency than gas. The plot is an effective representation of the demand on the grid with a very high frequency of hours experiencing demand between 30 GW and 45 GW and more hours spent at 20 to 30 GW than 50 to 60 GW.

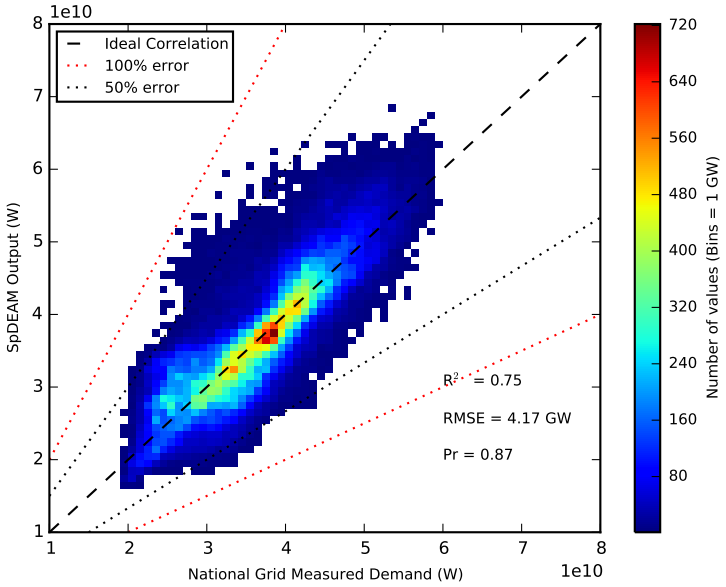

Figure 5.37.: Correlation between SpDEAM and National Grid electricity demand, all time steps.

Figure 5.38 demonstrates that the annual correction factor has been successful as the correlation is consistent between years (R^2 between 0.69 - 0.79). The plot exaggerates the greater variety in correlation at lower demand levels, particularly in latter years. RMSE is a similar magnitude to the error shown in the annual plot but exhibits and experiences the largest RMSE (5.4 GW) and lowest R^2 (0.69). However neither of these metrics are significantly worse than other years. Figure 5.39 demonstrates that the monthly correction factor has also been successful, as the correlation and RMSE are consistent between months and in the same range as annual metrics (R^2 between 0.63 - 0.8, RMSE between 3.4 - 5.6 GW). This is important as it shows seasonal variation is captured. No daily correction factor was applied, Figure 5.40 shows why this was not necessary. The DEAM method, when adapted using the correction factors for other time periods, estimates variation over days of the week well. The plots shows that the issue with low demand periods being overestimated by SpDEAM only occur during the week. Otherwise R^2 is very consistent between different days

and demonstrates a good correlation (0.59 - 0.77). RMSE is also consistent and a similar magnitude to that shown in the demand aggregated by year and month (RMSE between 3.9 - 4.9 GW). This shows that weekly demand is quite predictable based on the activity profile approach. Figure 5.41 shows that it is more difficult to estimate hourly demand than with aggregated time periods. Correlation coefficients vary across the day and those periods with low correlation coefficients vary in direction of error meaning the method of correction used before will not help (R^2 between 0.06 - 0.08). SpDEAM estimates demand well at all periods other than between 01:00 and 04:00 when SpDEAM can either over or underestimate demand (R^2 between 0.06 - 0.29). The model performs particularly well after midday (R^2 between 0.74 - 0.8). The hours with lower correlation coefficients experience a lower magnitude demand, which means that RMSE is consistent, between 1.9 - 5.6 GW.

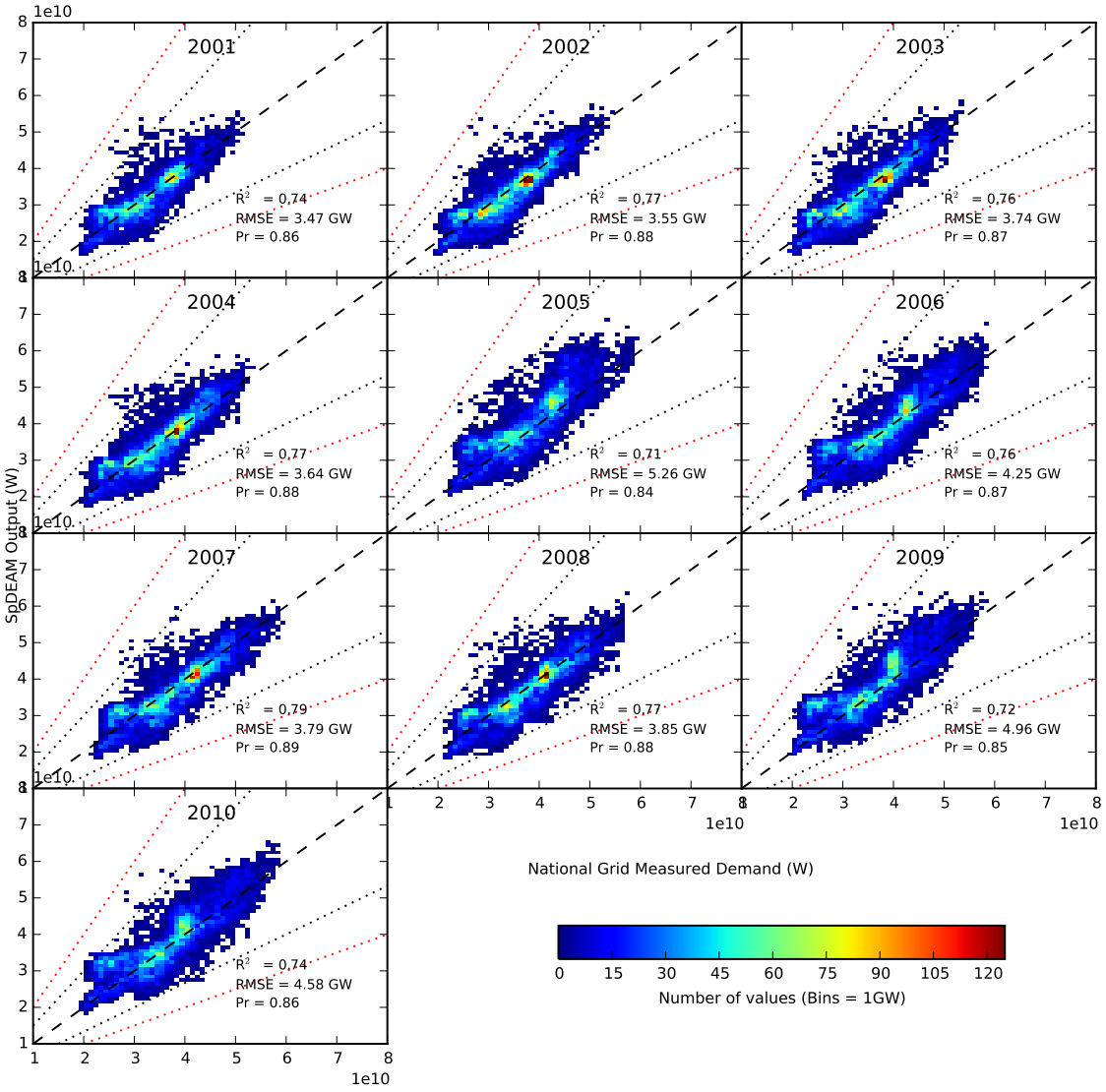

Figure 5.38.: Correlation between SpDEAM and National Grid electricity demand, by year.

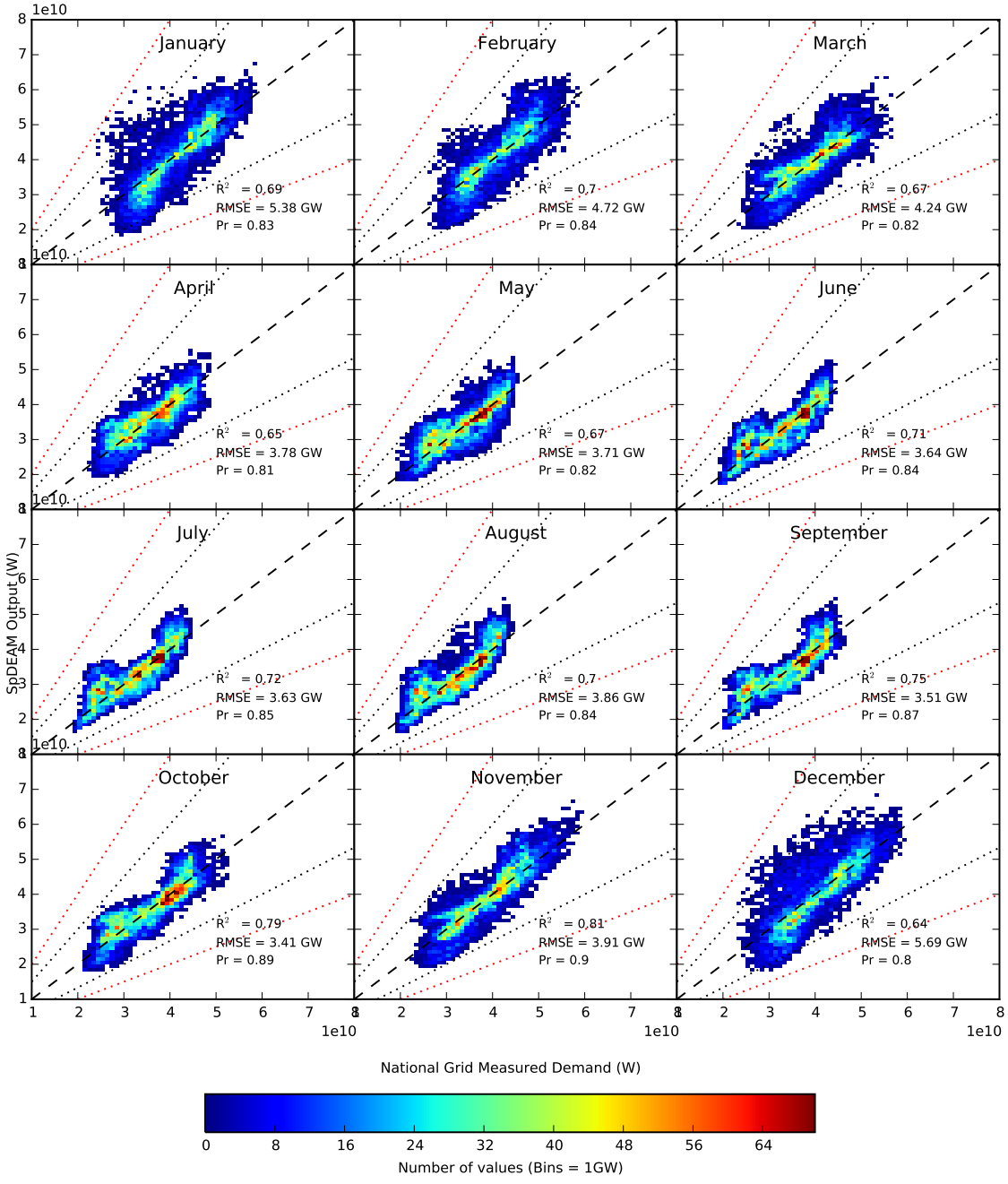

Figure 5.39.: Correlation between SpDEAM and National Grid electricity demand, by month.

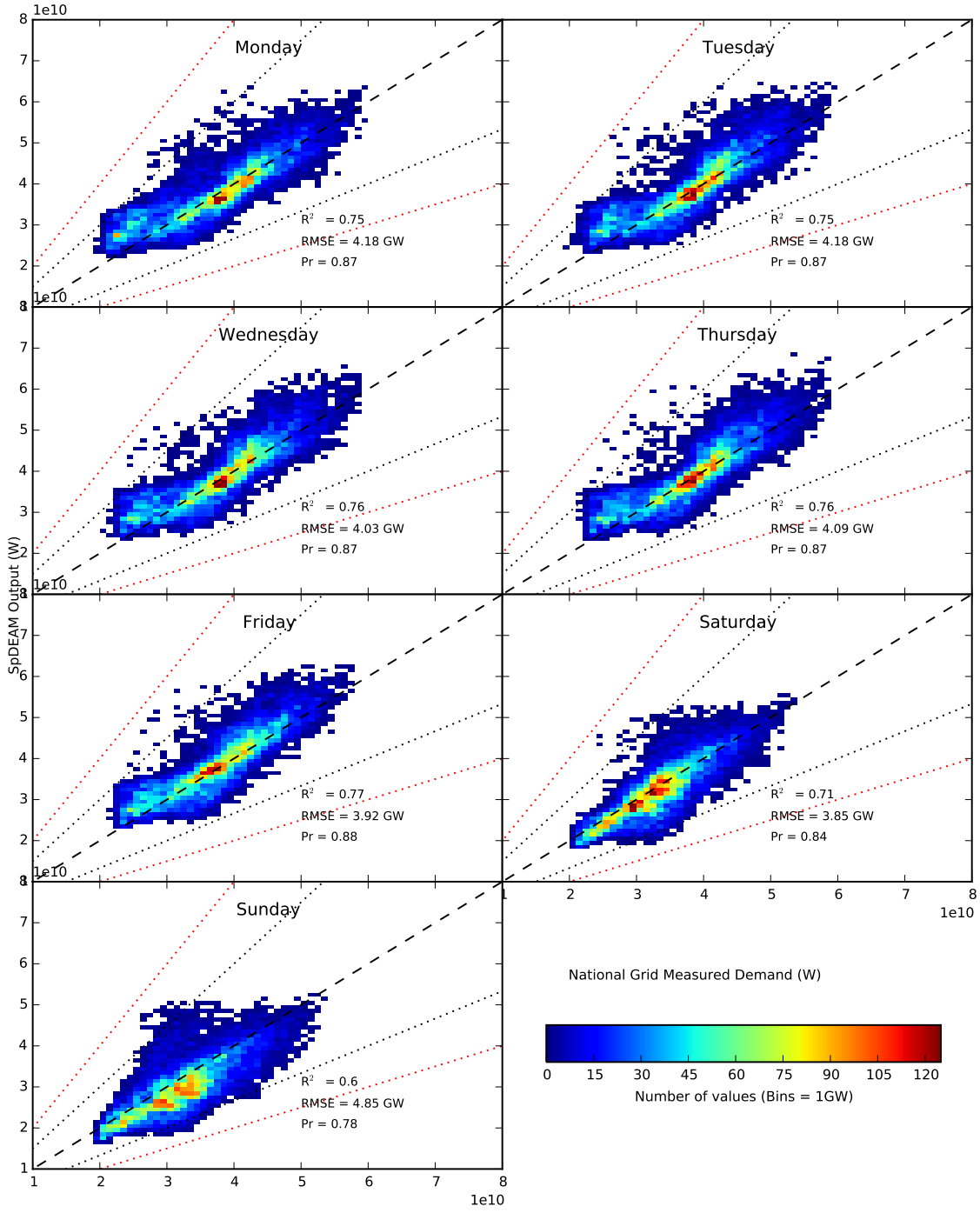

Figure 5.40.: Correlation between SpDEAM and National Grid electricity demand, by days.

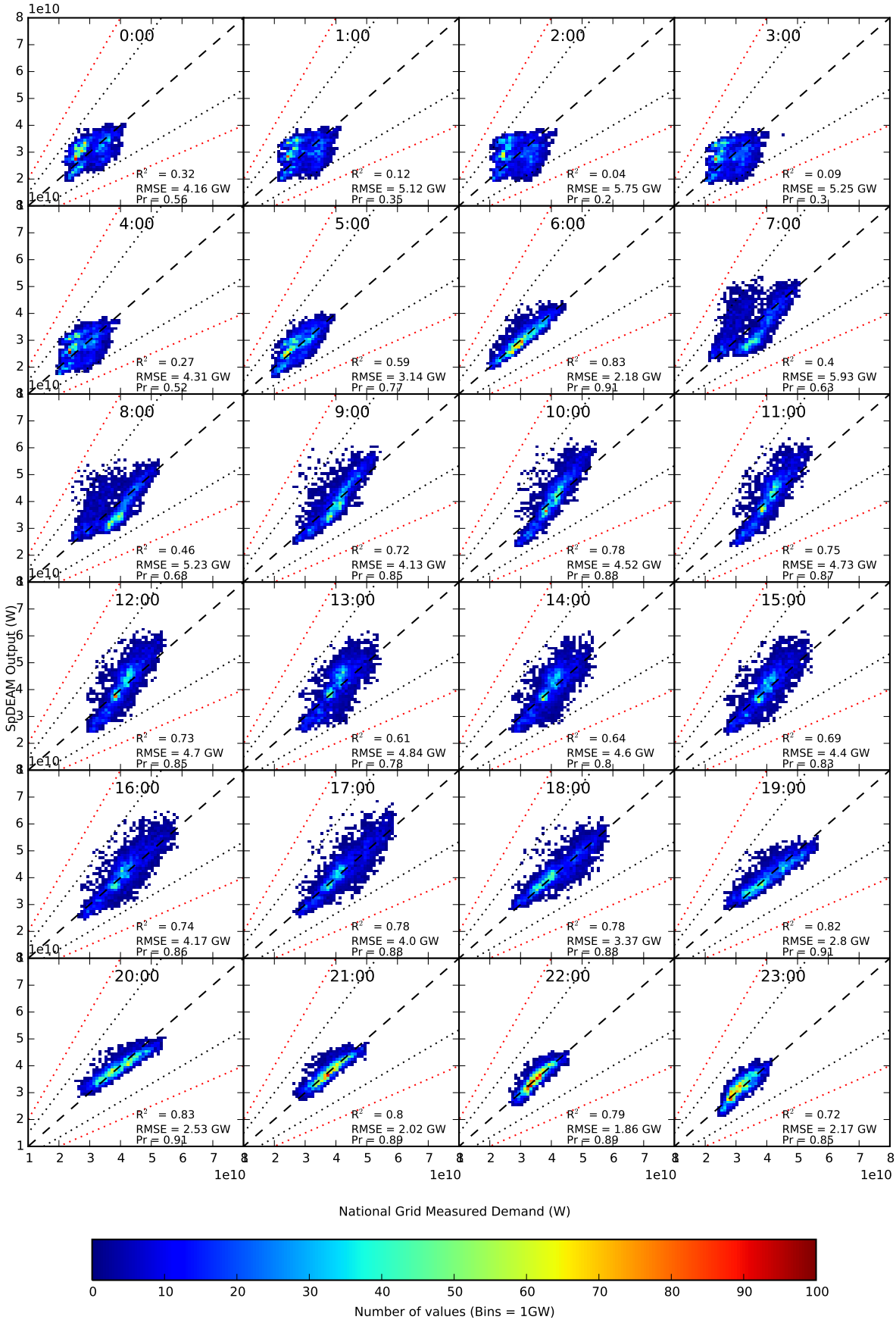

Figure 5.41.: Correlation between SpDEAM and National Grid electricity demand, by hour.

5.3.4.6. Total demand after calibration

Figure 5.42 shows the total annual demand from SpDEAM for gas and electricity after calibration in comparison with published data. The plot shows that bias in electricity demand has been reduced to between -6.3% and 2.4%. This is a significant improvement from the 29.6% to 44.4% shown in Figure 5.30. Bias in gas demand data is between -10.3% and 2.4%, compared to 28.8% to 38.4% shown in Figure 5.30. 2010 exhibits more error than the preceding years, as noted above, this was a particularly cold year, with associated high gas demand. The correlation between temperature and energy demand is explored in detail in chapter 7 and chapter 8.

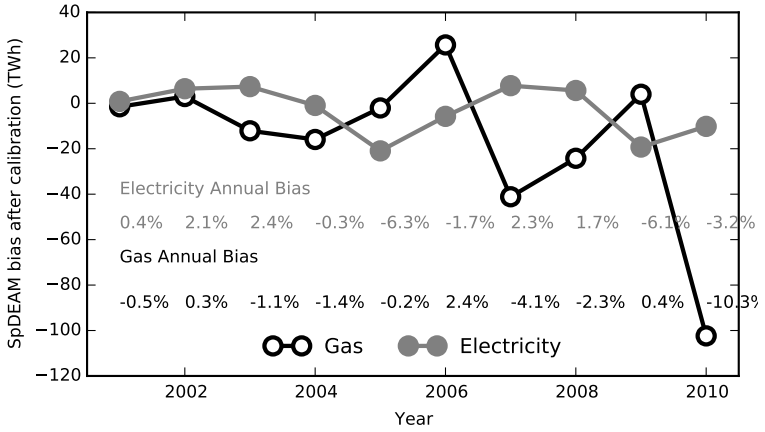

Figure 5.42.: SpDEAM bias after calibration.

5.3.4.7. Calibrated non domestic activity profiles

Figure 5.43, Figure 5.44 and Figure 5.45 show the difference between the original DEAM profiles and the SpDEAM profiles after calibration. The difference in the sectoral monthly electricity profiles described in the top sections of Figure 5.43 demonstrates that there is some summer electricity demand not incorporated into the ECUK data, this is likely to be from cooling and air conditioning demand which is larger in non domestic sectors than domestic. The plot also shows the changes made to individual end uses as a result of the correction factor in the bottom section. It must be noted that, although the end use profiles have been changed, this method does not necessarily accurately reflect how energy is demanded for each end use, as the correction factor is for all demands. The plot shows, however, that the monthly correction factor does not completely distort the profiles, as the shape remains similar. The changes are less than 10%, which is well within the error stated for some modelled demand data (~18%).

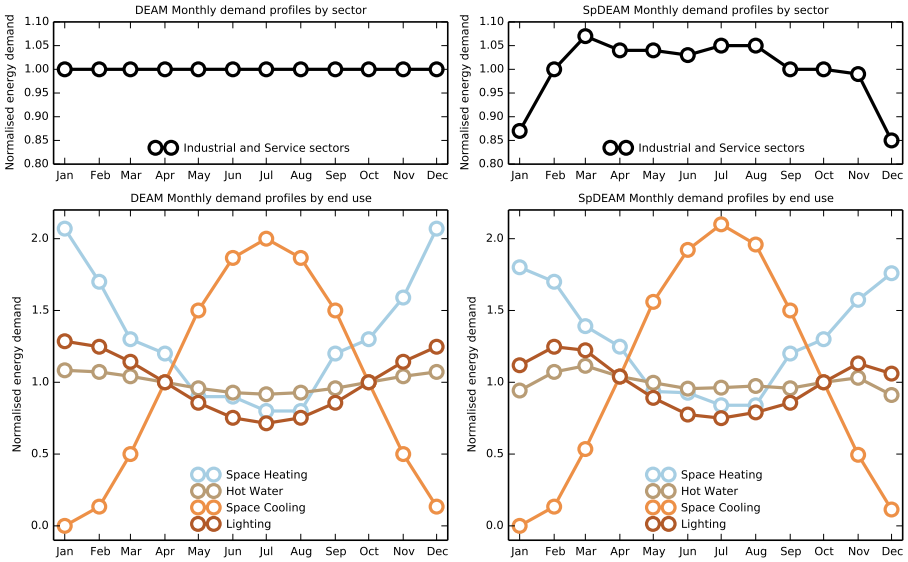

Figure 5.43.: Non domestic monthly adapted electricity SpDEAM profiles compared to DEAM profiles.

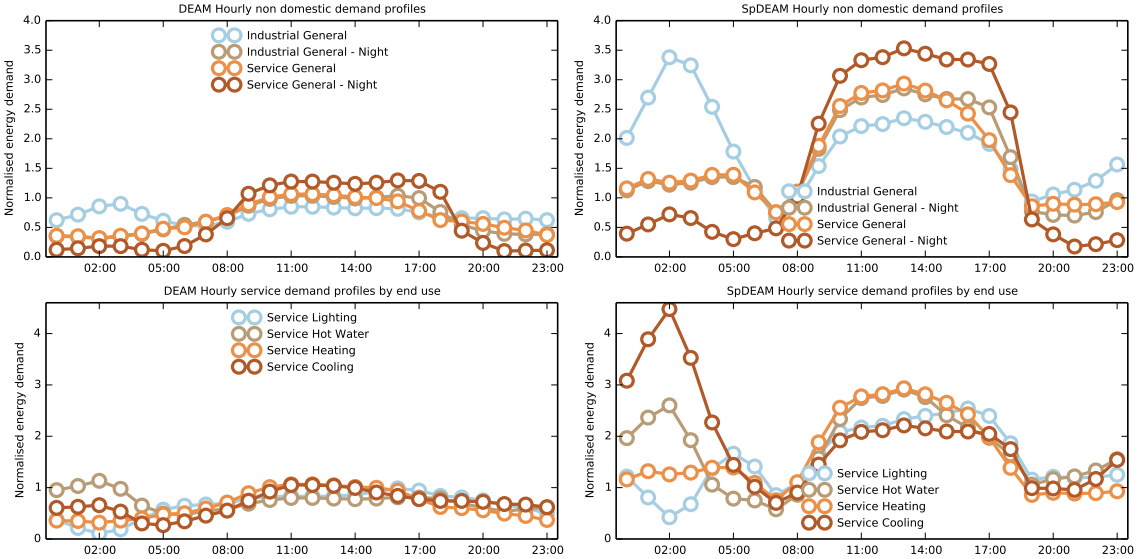

Figure 5.44.: Non domestic hourly adapted electricity SpDEAM profiles compared to DEAM profiles.

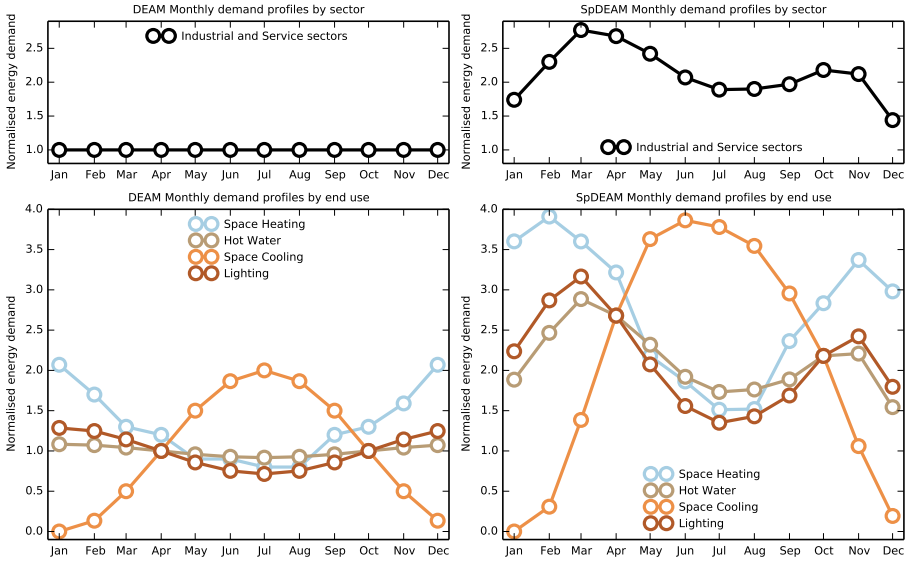

Figure 5.45.: Non domestic monthly adapted gas SpDEAM profiles compared to DEAM profiles.

5.4. Evaluation of SpDEAM

The analysis described above has shown that the calibration of SpDEAM has significantly improved its ability to estimate hourly electricity demand and daily gas demand. The results of the calibrated model have been compared against the same data that was used to calibrate it, therefore it would be expected that the error is small. Also there is a significant amount of longitudinal data available for the calibration period describing drivers of energy demand, that will not be available for the scenario modelling, meaning that it will be necessary to make a number of assumptions to model scenarios. Therefore it is necessary to evaluate SpDEAM against another set of published data using the same conditions as the scenario modelling, to ensure that the accuracy described in the calibration of the model applies to future depictions of the energy system. The evaluation of SpDEAM described in this section evaluates total gas and electricity demand between 2010 - 2014. This time period covers the first four years of the scenario modelling and bridges the gap between the calibration period and the most up to date data describing gas and electricity demand. Weather data from those years has been obtained from CFSR v2. The data was filtered in the same way as the previously used CFSR data. This is the only use of weather data from CFSR v2, the scenario modelling uses data from CFSR v1 (the previously used data has been retrospectively named CFSR v1, which is why it is referred to simply as CFSR in the rest of the thesis).

Input data and assumptions are summarised in Table 5.5, these follow the variables and data set out above, or those developed for scenario modelling. The variables and data developed for scenario modelling are described in detail in chapter 6, the table points to the relevant section for each variable which describes variable choice in detail. The scenarios described in the next chapter follow very similar paths for the first four years of the scenario period, but the Gone Green[1] scenario was selected for the evaluation.

Input parameter or dataset	Method used to set parameter or create dataset
National annual value of energy consumption	DUKES 2010 - 2014, ECUK 2010-2014
Weather data	CFSR v2
Desired internal temperature	As above
Technology efficiency	As above
Building floor area	As in scenario modelling, see subsection 6.3.3
Building Heat Loss	As in scenario modelling, see subsection 6.3.3
Dwelling spatial configuration	As in scenario modelling, see subsection 6.3.3
Dwelling numbers	As in scenario modelling, see subsection 6.3.3
Heating technologies	As in scenario modelling, see subsection 6.3.4
Population numbers	As in scenario modelling see subsection 6.3.2
Population distribution	As above
Gas evaluation data	As in the calibration for 2010-2014
Electricity evaluation data	As in the calibration for 2010-2014

Table 5.5.: Input data and assumptions used in the evaluation of SpDEAM.

Figure 5.46 shows that there was a close correlation found between SpDEAM daily gas demand and SND gas demand, $R^2 = 0.82$ and $Pr = 0.91$. There was a small positive RMSE of 537.46 GWh. This correlation and error is similar to that shown in the calibration of SpDEAM, where $R^2 = 0.8$, $Pr = 0.9$ and RMSE = 397.41 GWh.

[1] see chapter 6 for description of scenarios

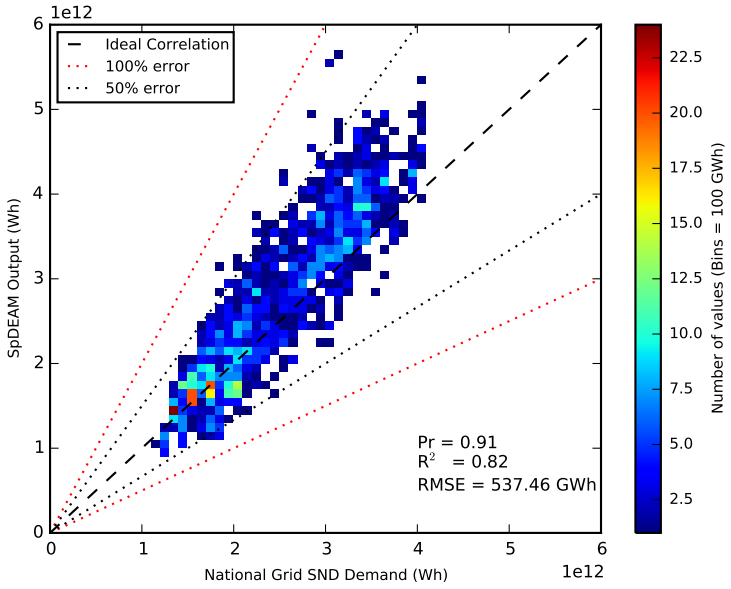

Figure 5.46.: Correlation between SpDEAM and LDZ daily gas under scenario conditions, all time steps.

Figure 5.47 shows that there was a close correlation found between SpDEAM and National Grid hourly electricity demand, $R^2 = 0.76$ and Pr = 0.87. There was a small positive RMSE of 4.57 GW. This correlation and error is similar to that shown in the calibration of SpDEAM, where $R^2 = 0.75$, Pr=0.87 and RMSE = 4.17 GW. The maximum overestimation of electricity demand is 30 GW and there are hours where error is nearly 100%. Overall, however, the model produces reasonable estimates of electricity demand at all time periods.

5.5. Discussion

DEAM was selected as the basis for SpDEAM because of its ability to disaggregate national energy demand values and aggregate heat demand from domestic dwellings to the same temporal resolution. To do this, DEAM uses a hybrid approach including top down and bottom up methods. These methods are positioned in the literature in chapter 2. Regular variation is taken into account by the top down method, which allows projection of energy demand into the future with very limited data. This method assumes that end uses remain the same and is therefore not suitable for modelling technological changes. Bottom up demand includes physical drivers which allows the introduction of technological change, demonstrating the advantage of the hybrid approach.

SpDEAM has built upon the ability of DEAM by adding spatial disaggregation of national electricity and gas demand. This spatial disaggregation has been performed using several key spatial datasets, which facilitate a more accurate spatial model and allow demand to be linked with weather (population and census buildings and heat technology data). Advantages and disadvantages of census based data have been described. Census data is indispensable in this work, however, issues with data collection and the answering of census questions must be understood if the data is to be used. Unfortunately not all data is spatially continuous over the desired geographical scope. Methods to fill spatial gaps have been described and applied. These have been shown

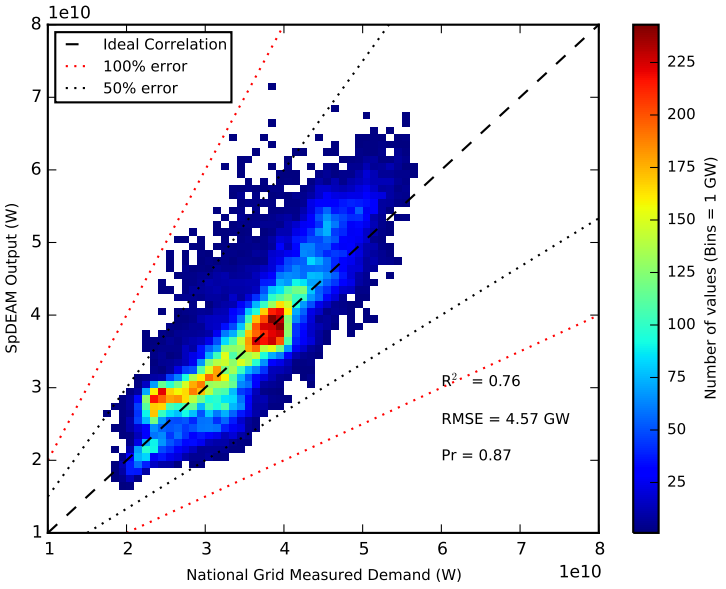

Figure 5.47.: Correlation between SpDEAM and National Grid Electricity demand under scenario conditions, all time steps.

to potentially introduce error due to the need to estimate distributions. For example the spatial heating technologies dataset was extrapolated to cover Scotland based on assumptions about the extension of English and Welsh data and divergence was shown in comparison with DECC sub national data. The census data represents the best available spatial data. The method developed for redistributing spatial data to the model grid was described in detail. This method is a key facilitator of the gridded approach, it facilitates simpler modelling of scenarios, offers scalability and means that the power of CFSR in terms of homogeneous data over a large scope at a fine spatial resolution can be harnessed. Maps have shown the difference between census geographies and the grid, demonstrating the effect of spatial aggregation and redistribution of census based data to the grid.

Gridded population data have been introduced and appropriate data selected. These data are a key element in the spatial allocation of demand, because fundamentally people use energy. A comprehensive list of datasets has been provided and analysis of divergence between them summarised. More detail is given on this analysis in Sharp [2012]. The availability of other data at a finer spatial resolution provides an example of the ability to model at a finer spatial resolution. As described previously, it is possible to interpolate or downscale reanalysis data to finer resolutions, which would facilitate modelling at a finer resolution. This however takes significant time and processing power. The resolution described is considered to be a sweet spot between fine detail and the ability to model over a large scope in both space and time.

SpDEAM introduces several novel elements to DEAM, applies the method to a scope and resolution not previously investigated and adds considerable spatial complexity. It was therefore necessary to compare the results from the initial model against measured data where possible. The model has therefore been set up to disaggregate and simulate demand from 2000 - 2010 so that activity profiles could be calibrated. Assumptions were necessary to set the model up, these have been described - with more time it would be possible to perform a sensitivity analysis on the impact of

the assumptions e.g. glazed area. Problems with input data are described; primary among these is the fact that it is very often necessary to use modelled data due to the limited amount of empirical data at the desired scope and resolution. As noted in chapter 2 these datasets are often based on samples then extrapolated to represent a larger population.

The comparison of modelled and published data between 2000 and 2010 has shown that between 28% - 39 % of total gas demand and 29% - 45% of total electricity demand has not been accounted for in SpDEAM. There are a number of potential sources of this demand. In particular there are a number of non domestic sub sectors not accounted for by the data used for the top down non-domestic model data, obtained from ECUK. For example there is no reference to demand from public lighting, transport, public buildings or the health and education sub sectors. Each of those sub sectors are particularly difficult to gather data from, it is therefore very difficult to assess how much they contribute to unmodelled demand. SpDEAM also does not account for transmission losses or theft which are included in the quantification of national demand, as both must be covered by supply. Because of the reasonable accuracy of the model after calibration, it was not considered necessary to explore unmodelled demand further, but future work could do so.

Unmodelled demand is accounted for through correction factors, developed by evaluating model output against measured data where possible and the best available modelled data otherwise. The correction factors are developed through comparison to total demand but applied to non domestic activity profiles. This method avoids corruption of the DEAM method for domestic simulation and therefore allows the alteration of this demand in future scenario modelling. The correction factors applied to the non domestic activity profiles account for unmodelled demand, drivers and losses. This can originate from a number of sources therefore the demand that is classified as non domestic may be distorted and could be labelled all other demand.

The simulation approach used for domestic energy demand is significantly more complex than that used for non domestic demand. This is necessary because of the need to introduce increased electrified heat demand in future scenario modelling, which requires bottom up modelling of heat demand and the ability to disaggregate top down demand by end use so that incidental heat demand can be calculated. It is also necessary to ensure that this approach is accurate so the insights gained into consequences of this increased demand can be made with confidence. The lack of change to the domestic method in the calibration of the model is based on the pre calibration evaluation of annual domestic gas demand, which demonstrated that the accuracy is reasonable, especially given the potentially large error in the modelled data used as inputs. Quarterly domestic demand output is very accurate. This should be expected as spatiotemporal aggregation smooths variation in temperature, therefore demand. However, since the modelling was performed at a disaggregated resolution then aggregated for comparison this indicates that the method for simulating gas demand is accurate.

The influence of weather in the model has been shown to be accurate where it is possible to measure this influence. For example in the sectorally disaggregated weather influenced demands, including daily domestic gas demand and demand for lighting. DECC sub national statistics were compared against SpDEAM outputs. Unfortunately data irregularities, including sectoral classification make direct comparison difficult.

Calibration of the model to total daily gas and total hourly electricity demand demonstrated promising results. Total annual bias after calibration was between -10% and 2.4% for gas and

between -6.1% and 2.4% for electricity, a significant reduction from the pre calibrated version of SpDEAM. RMSE for gas demand was reduced from 1140.73 GWh to 397.41 GWh, for electricity demand RMSE was reduced from 15.63 GW to 4.17 GW. Correlation also improved R^2 from 0.71 to 0.81 for gas and 0.38 to 0.75 for electricity. The reduced error demonstrates that the previously unmodelled demand has been accounted for and the improved correlation shows that this demand has been assigned to the correct time period. A key point to note is that this is comparison with seasonal normal demand from the LDZ, SpDEAM however represents a 'real' demand, which could be equivalent to either the high or low demand from the LDZ. Future work could include a comparison to the range of demand from the LDZ.

Following the calibration of the model it was necessary to evaluate model outputs against a separate set of data. As well as using a new set of evaluation data the model was run under scenario conditions so that insights could be gained into the accuracy of the model when depicting future changes to the energy system. The evaluation of the model has shown a good correlation between daily gas demand from SpDEAM and LDZ SND. RMSE between SpDEAM and SND has been shown to be small in comparison to total demand (536 GWh, 10% - 27% of demand). In some cases the difference between SpDEAM and SND exceeds 50%. Some divergence would be expected because SpDEAM gas demand is influenced by weather, whereas the SND represents gas demand on a seasonally normal day, therefore it is not particularly hot or cold. Total gas demand has been evaluated to demonstrate the overall accuracy of the model. Only a portion of this demand will be used in further analysis as it is the domestic heat demand which is of interest in the scenario analysis, this as discussed above has been shown to be accurate within the limitations of available data.

Total electricity demand has also been evaluated. The evaluation of the model has shown a good correlation between hourly total electricity demand from SpDEAM and National Grid. RMSE between SpDEAM and National Grid has been shown to be low (4.57 GW). In some cases the difference between SpDEAM and National Grid exceeds 50%. Importantly for analysing peak electricity demand the largest errors are seen when National Grid demand is not at its highest. Greater divergence would be expected between SpDEAM total electricity demand and measured data than the gas comparison due to the fact that the evaluation data is available at a finer temporal resolution (hourly vs. daily) and there is no associated smoothing. Also there are possibly a greater number of drivers of demand due to the complex use of electricity compared to gas which is limited to heating, cooking and hot water. The results described are therefore remarkably accurate. Overall SpDEAM has been demonstrated to be an effective adaptation of DEAM and a potentially excellent tool for augmenting and disaggregating national annual scenarios of demand in GB.

The results of the evaluation are very close to those from the calibration. This demonstrates that the calibration of the model was effective and that the analysis of the scenarios is as accurate as possible given the described limitations of SpDEAM. This is important as there are a number of assumptions made on the spatial configuration of people, buildings and heating technologies, all of which are described in the next chapter.

5.6. Summary

SpDEAM is based on the structure and algorithms of the existing DEAM. The modelling methods of DEAM have been described. SpDEAM therefore aggregates DEAM methods to an hourly resolution to match the temporal resolution of CFSR, the wind model described in the previous chapter and published data describing demand used in calibration and evaluation. Some DEAM end use profiles are aggregated in SpDEAM, due to the necessity of limiting complexity. The method, however, allows any number of demands to be modelled in SpDEAM in the future.

SpDEAM disaggregates DEAM to the spatial resolution of CFSR and the wind model through the use of spatially explicit data on heating technology type, building characteristics and population. This ensures, as far as possible that demand is realistically spatially weighted and is therefore influenced by realistic weather and reduces the risk that when comparing supply and demand difference in weather drives divergence. The data and methods for spatial disaggregation have been described. SpDEAM is unique in terms of modelling spatially explicit temporal demand from all sectors across GB. None of the models reviewed in chapter 2 have this ability.

SpDEAM has been set up to depict historic demand so that initially model outputs can be compared against published energy demand data, to ensure that there is not significant divergence between the two. This led to the identification of a significant amount of unmodelled demand being identified. This unmodelled demand has been accounted for through the alteration of non domestic activity profiles, after establishing that the method for simulating domestic electricity and gas demand was accurate. The calibration was shown to be effective through the evaluation of model outputs under both calibration and scenario based conditions

Demand for both electricity and gas have been shown to be remarkably accurate given the challenge of modelling the entire GB electricity system with limited data and necessary simplification and grouping of demands. In the long term errors have been shown to be small and correlation high between SpDEAM and evaluation data. The analysis has shown that DEAM can be adapted to accurately model electricity demand at the same spatiotemporal resolution as CFSR, therefore answering research question 2 (section 2.4).

6. Scenario Creation

6.1. Introduction

Scenarios, according to WEC [2013, p. 1], are "alternative views of the future, which can be used to explore the implications of different sets of assumptions and to determine the degree of robustness of possible future developments". The scenarios described in this chapter, and used in subsequent modelling, base future developments in the energy system on those depicted in National Grid's (NG) UK Future Energy Scenarios (UKFES) [National Grid, 2014]. The focus of the scenario modelling is electricity demand and wind generation, with particular attention paid to the domestic sector. It is important to understand the relationship between weather driven supply and electricity demand to ensure security of supply, due to the inherent variability of wind generation, the difficulty and expense of storing electricity and the likelihood of changes to the temporal pattern of demand from electrification of heat. The methods described in the previous chapters and applied here can be used to investigate other energy vectors such as district heating and electrification of transport. Through the use of the models described in previous chapters, the implications of these potential developments can be explored at a spatially and temporally disaggregated resolution, building on NG's analysis, which is carried out at a national annual resolution.

The UKFES have been chosen primarily because they depict different levels of wind capacity and electrified domestic heat demand, which matches the scope of this thesis. Also because comprehensive data describing a number of the input variable to both the wind model and SpDEAM are provided in supplementary spreadsheets. This is not the case for all scenarios, many of which do not provide data. It should be noted that NG scenarios explore a relatively narrow set of options for the decarbonisation of both demand and supply, however the disaggregation of the data means that it will be possible to gain insights into what other measures may be necessary in order to ensure security of supply.

The scenarios cover the period between 2013 and 2025 and describe four different versions of the UK energy system (Figure 6.1). Analysis performed here, based on these scenarios, covers the period from 2010 - 2035, so that modelling continues from the evaluated period described in previous chapters. NG provide data that covers this period for many variables, in other cases it was necessary to interpolate from the data used in the SpDEAM and wind model evaluations. Future modelling assumes that weather experienced in the past 25 years represents that which will be experienced in the next 25 years, this is sometimes referred to as hindcasting. The weather period chosen to represent 2010 - 2035 is 1985 - 2010. This was chosen as it represents the most recent data in this thesis and therefore should incorporate the best available measurements and modelling from CFSR. Hindcasting is an established method, which provides a pragmatic solution to the lack of measured data on some variables and need to model the effect of various changes

to the system. Assuming that future weather is the same as the past means that factors such as climate change and inevitable variation are not taken into account. This means that analysis in the next several chapters discusses the relationship between demand and supply under a set of described conditions, rather than attempting to predict the absolute amount in a particular place and time. Attempts to understand absolute demand or supply would be better performed using probabilistic methods where, for example, all weather conditions experienced at a particular time and place each year are used to model each scenario and therefore a range of possible demand and supply is calculated. This has not been performed here, but the method described could be adapted to carry out this type of analysis. This type of method is applied by some research described in Chapter 2, predominantly those studies which are examining only the wind resource.

Figure 6.1 describes the four scenarios used by NG, which occupy different positions on a matrix of affordability and sustainability. Economic environment, consumer behaviour, target setting and achievement, and political will have been considered in the development of the scenarios. Two different economic forecasts are used; in both Gone Green (GG) and Low Carbon Life (LCL) the economy quickly recovers to historic pre-recession levels, annual growth averages 2.5% per annum over the scenario period. In Slow Progression (SP) and No Progression (NP) the economy also recovers relatively quickly but remains on a lower economic growth trajectory. Annual growth averages 2% per annum over the scenario period. Scenarios take into account some of the policies described in Chapter 1; including the climate change act, carbon budgets, 202020 targets and the renewable energy directive. Future energy targets are formed around ongoing work on the 2030 Energy and Climate Change framework for European energy policy and GHG reduction.

The data necessary to model growth in wind supply and electrified domestic heat demand in detail have been adapted and integrated into the model as described below. Unless otherwise stated, the modelling follows the method described in Chapter 5. As described in Chapter 5, the top down section of SpDEAM requires national annual values for energy demand. The NG scenarios provide these, the values are based on exogenous econometric modelling performed by NG (the method is described in Chapter 2) which takes into account both economic growth and technological change, such as increased numbers of electric vehicles and electrification of heat demand (only in the non domestic sector as domestic electrified heat demand is removed, the major technological shift in these scenarios, as described below). This means that the ensuing analysis includes a large number of changes to energy demand, however no changes to the hourly dynamics of demand are made. Therefore analysis assumes that temporal dynamics do not significantly change in the future, apart from those associated with heat, which are modelled bottom up. This is unlikely to be the case, therefore the scenarios depicted may be different to what actually happens, however, altering specific elements of SpDEAM allows a more detailed analysis of the implications of the modelled changes, therefore fulfilling the purpose of scenarios as described above.

6.2. Wind Scenarios

6.2.1. Annual wind capacities

Figure 6.2 describes the NG wind capacity scenarios and compares them to those reviewed in Chapter 2. Onshore, the NG scenarios are within the quartiles of other estimates and appear to

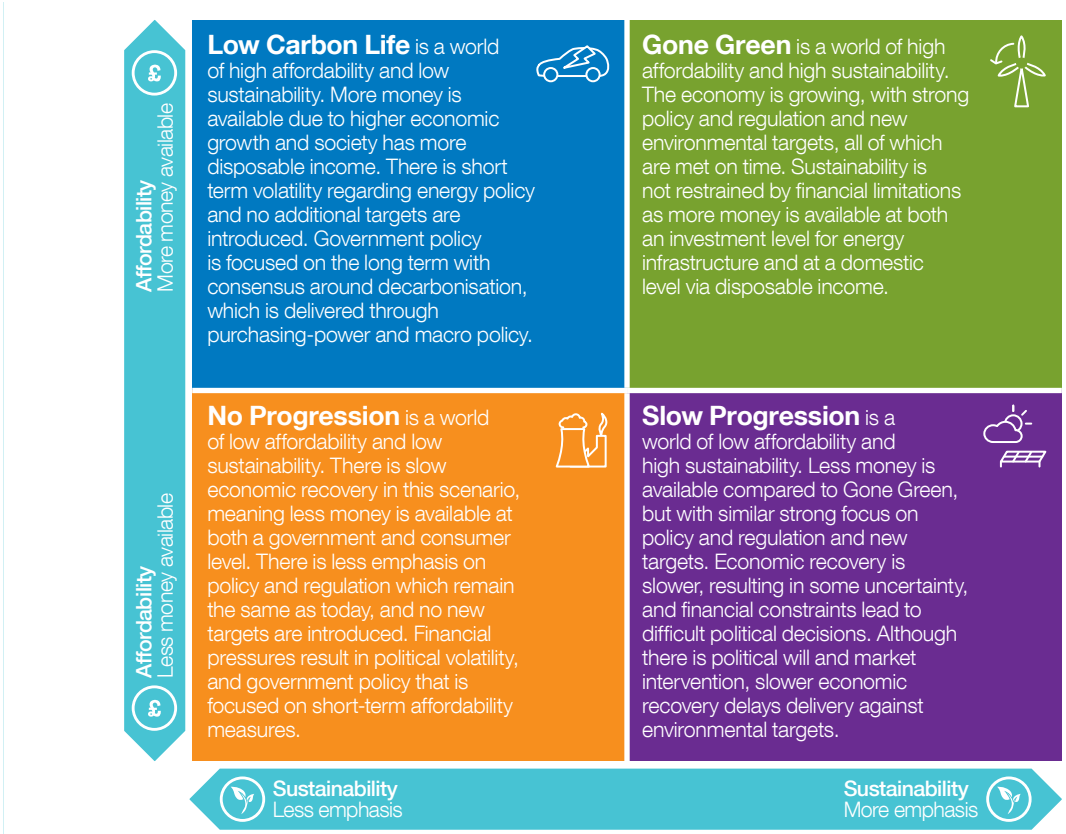

Figure 6.1.: National Grid's scenario matrix, source: National Grid [2014, p. 5].

be slightly more conservative than the highest predictions, though the NP scenario is not the most pessimistic of those reviewed. Growth rates are similar and the GG scenario exceeds the maximum capacity predicted, although this occurs several years later. There is a clear capacity ceiling in each of the scenarios, reached in approximately 2026.

Offshore, the scenarios appear conservative in the short term, as all of the scenarios remain below the upper quartiles of the previously reviewed predictions. NG use the same year as a ceiling for capacity in the NP and LCL scenarios (2026). However capacity in the GG and SP scenarios continue to grow beyond this point. In order to explore these scenarios using the previously described wind model they were spatially distributed using the methods described below.

6.2.2. Spatial wind capacities

Section 2.1.1 summarises the studies which have estimated the GB wind resource using different combinations of constraints on development. In this section the geographical restrictions and designations are explored in more detail, so that they can be applied to GB and a map of developable areas created using the same geographical reference as the wind model. Analysis is performed at the sub grid level, as spatial data is available at this level of disaggregation, results are then aggregated to the model grid, so that capacity described by each scenario can be placed by grid square. This method ensures that realistic onshore and offshore locations are chosen and generation that will arise from the simulation of the NG scenarios will be appropriately weighted to the

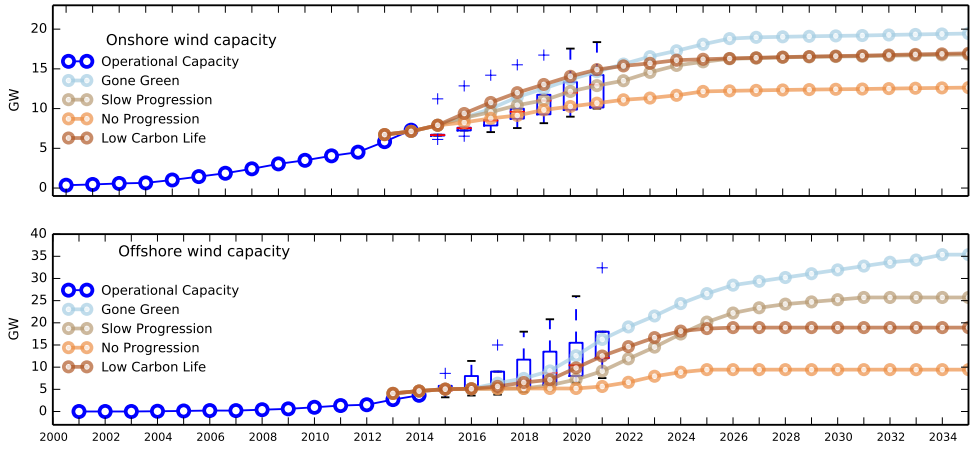

Figure 6.2.: GB wind capacities 2000 - 2035, data sources: National Grid [2014], the line plot describe NG scenarios, see Figure 1.1 for a description of the boxplots.

geographically diverse wind speeds experienced over GB.

6.2.2.1. Onshore restrictions

Table 6.1 shows those areas which have been excluded absolutely from development by Friends of the Earth [1995], Brocklehurst [1996] and Boehme et al. [2006]. Many of these designations are also noted by DECC [2014b] as being restricted. Some of the designations cover a wider geographical scope and are therefore also used in non GB studies, e.g. RAMSAR sites in Möller [2011]. The table also shows the results of a spatial analysis describing the size of each designation, demonstrating that the majority of these areas eliminate a very small amount of land from wind farm development in GB. There are, however, several designations which cover a significant amount of land (AONB, SSSI and SAC all cover more than 9% of GB). Many of the areas overlap, after they have been dissolved into a single polygon the combined area is equivalent to 31% of GB. Figure 6.3 shows that part of every country in GB is excluded from wind farm development using this method. Significant areas of exclusion include the Scottish Highlands, the Lake and Peak Districts, north western Wales and a large proportion of the south coast of England. The map also shows that, despite the consensus in the literature on the designation of excluded areas, there have been wind farms built within these zones between 1990 and 2014. There are 56 operational wind farms in areas with protected environmental status. These wind farms contain 671 turbines and total 980 MW of capacity. There are fewer farms in these areas that are under construction or awaiting construction (21), however, these farms are larger, with a combined capacity of 692 MW.

The fact that larger wind farms have been granted planning permission in protected areas suggests that planning rules may be have been relaxed at some point in the past, as larger wind farms are likely to make more of a visual impact, which is one of the arguments against placing them in these locations. However the increased capacity may be a result of the use of larger capacity turbines.

Despite the existence of approved wind farms in the environmentally protected areas and apparent continuation of the slightly relaxed policy of placement, these areas have been excluded from

further development in all scenarios. No model grid square is entirely excluded from development using this classification, therefore potential spatial diversity of wind capacity is not threatened.

Designation	Countries covered	Area (km^2)	PCT of GB
Area of Outstanding Natural Beauty (AONB)	England and Wales	20553	9%
Sites of Special Scientific Interest (SSSI)	GB	23582	10%
Biogenetic Reserves	Wales	5.92	>1%
Biosphere Reserves	England and Wales	983	>1%
Heritage Coast	England and Wales	57	>1%
Special Areas of Conservation (SAC)	GB	18161	8%
Special Protection Areas (SPA)	GB	7718	3%
RAMSAR (wetlands of international importance)	GB	33382	14%
National Parks	England and Wales	911	>1%
World Heritage Site	GB	2163	1%
Country Park	England	9	>1%
Scheduled Ancient Monuments	Scotland and England	1637	1%
Water Bodies	GB	4789	2%
Sum excluding overlap		70242	31%

Table 6.1.: Environmental restrictions on wind farm development, list gathered from Friends of the Earth [1995], Brocklehurst [1996], Boehme et al. [2006] and DECC [2014b].

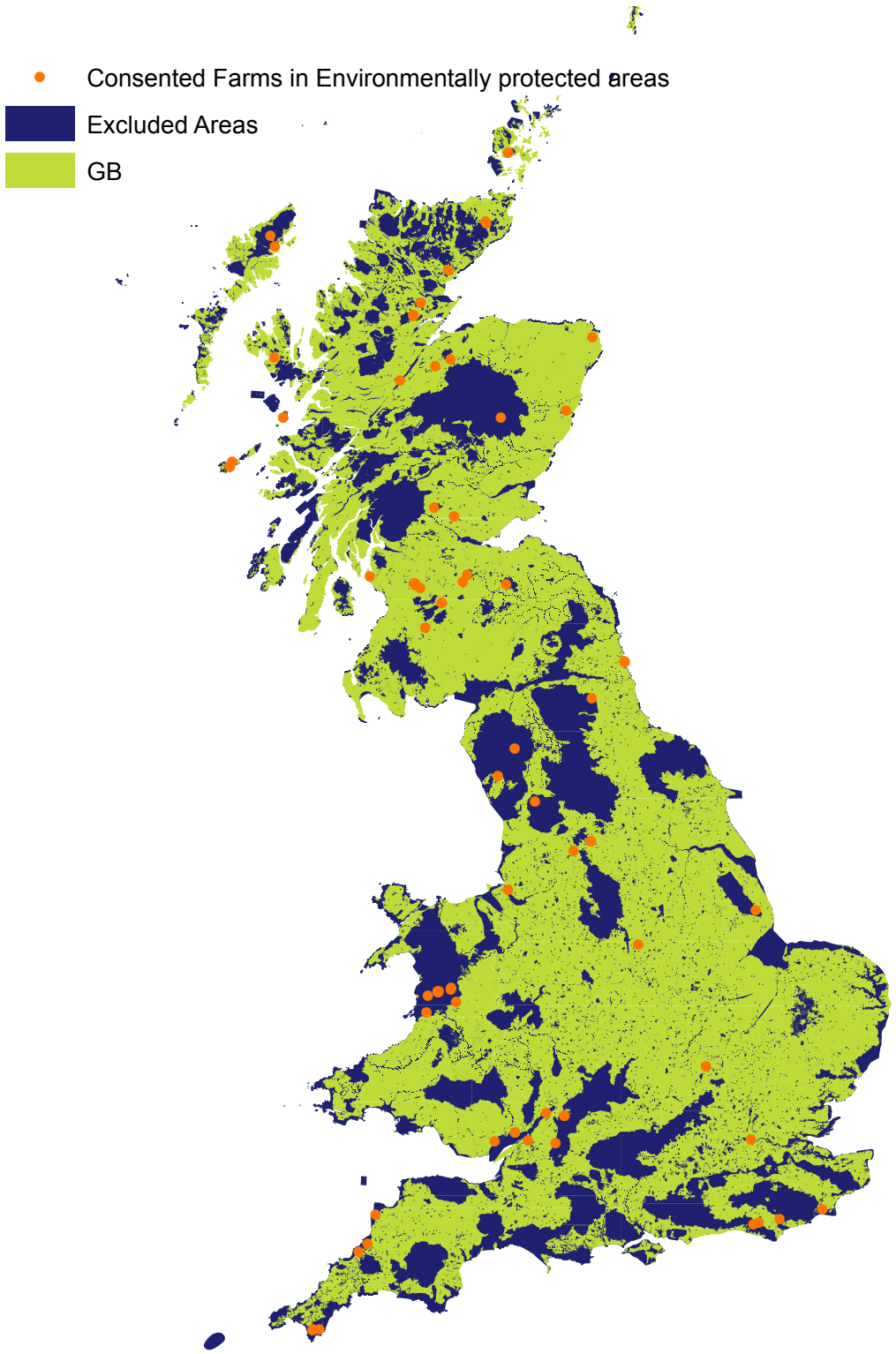

Figure 6.3.: Map of consented farms in environmentally protected areas, 2014.

Criteria based restrictions Table 6.2 describes the designation of areas that are excluded from development in the literature based on criteria. Where possible, the literature has been used as a guide for restrictions in this analysis, in some cases it was not possible to apply the restriction, predominantly due to lack of data. The review of geographical resource estimates in (Chapter 2) demonstrated that the selection of criteria for these restrictions can significantly alter the available resource. In order to ensure that appropriate criteria were selected, the land excluded by classifications which may not be absolute restrictions was compared to existing and approved wind farms. This comparison not only verifies that validity of the designation and criteria but also to some extent links the analysis to planning consent, which relies on other factors such as local opposition. The table also shows the amount of land that has been removed using this criteria (for reference GB covers 229,848 km^2).

Designation	Criteria and Notes	Source	Criteria applied in model	Area (km^2)
Slope	Less than 10%	Baban and Parry (2001)	Slopes greater than 30° excluded	1941
	Less than 15%	Boehme et al. (2006)		
	0 -7 excellent, 7 - 16 good, 16 - 30 fair, 30 - 40 poor, 40+ unsuitable (degrees)	Rodman and Meentemeyer (2006)		
	less than 10°	Brocklehurst (1996)		
Summit of hills	Cost	Baban and Parry (2001), Nguyen (2007)	Areas above 600m	5390
Airport Proximity	15 - 30 Km around airfields	Boehme et al. (2006)	5 Km	11000
	5 Km around airfields	Lejeune and Feltz (2008)		
	2.5 Km around airports	Nguyen (2007)		
	6 Km	Brocklehurst (1996)		
Low flying zones	Ranked on potential interruption	DECC, MOD	See Figure	10326
		Hassan (2001)		
		Boehme et al. (2006)		
Aviation Safeguarding		DECC (RESTATS), Boehme et al. (2006)	20 m tip height	64634
Met Office weather radar	Two classifications	DECC, UKMO	"Concerns will be difficult to overcome"	1244
Eskdalemuir seismological station	10 Km	DECC (RESTATS), Boehme et al. (2006)	10 Km	314
Distance to Grid	Beyond 10 Km is too expensive	Baban and Parry (2001)	No Data	N/A
Turbine density	150 KW/Km^2 is socially unacceptable	Boehme et al. (2006)	1.5, 2.5 MW turbines per Km ² (0.64 Km^2 per turbine)	N/A
	Socially acceptable limit	Hassan (2001)		
	10 rotor diameters limits array efficiency to 60%	Johansson and Burnham (1993)		
	3, 2.5 MW turbines in a 1 Km^2 grid sq	Boehme et al. (2006)		
	Five 2 MW per Km^2 grid sq onshore	EEA (2009)		
Already developed land			0.302 km^2 per existing turbine in exact location of operational wind farms pre 2014	1231
			Consented	824
Proximity to Woodland	500 m	Baban and Parry (2001) (large stand of trees)	N/A	
	150 m	ETSU (1994)		
	100 m	Brocklehurst (1996)		
Proximity to Dwellings	500 m	Baban and Parry (2001)	see land use section	
Proximity to protected areas	1 Km	Baban and Parry (2001)	1 Km	100
Urban / living areas	Noise and visual impact + 2000m	Nguyen (2007)	Excluded in later land use analysis	
	150 m	ETSU (1994)		
	400 m	Brocklehurst (1996)		
	500 m	Baban and Parry (2001)		
Proximity to Rail and Road	100 m buffer	Nguyen (2007)	N/A	
	150 m	ETSU (1994)		
	100 m	Brocklehurst (1996)		
	Within 10 Km	Baban and Parry (2001)		
Wind speed	Greater than 5 m/s	Baban and Parry (2001)		

Table 6.2.: Areas where development restrictions are applied in the literature and criteria applied in scenario capacity allocation.

Slope and Height There is some deviation in the literature on the maximum slope of land which can be developed, including in the units used. The scale developed by Rodman and Meentemeyer [2006] appears to be the most sophisticated, therefore it has been used as a guide here (Table 6.2).

Land above 600 m was also excluded from development, because previous analysis in Chapter 3 showed that wind speed data from CFSR does not represent the conditions in these areas well. Therefore using these sites may result in inaccurate simulations. Although wind speed is likely to be high at these sites, due to the previously described speed up, it is unlikely that they would be used for development as they are inaccessible and almost always designated as one of the restricted areas described above. Slope and height was calculated using data from the Shuttle Radar Topography Mission Digital Elevation Model (SRTM DEM) [USGS, 2006a].

Flight paths and radar There is disagreement in the literature on how much land to exclude from development around airports. A 15 km buffer, as applied by Boehme et al. [2006], was considered. However, this buffer contains approximately 10% of operational and consented GB wind farms, demonstrating that is it possible to build wind farms within these zones. A 5 km buffer contains only 1.5% of operational and consented GB wind farms, therefore a this was applied.

There are a number of other restricted areas due to flight paths applied by Boehme et al. [2006]. Data are provided by DECC and the Ministry of Defence (MOD) on these restrictions. The MOD rank areas depending on the potential interruption to low flying exercises. Figure 6.4 shows those areas where the MOD anticipates that the construction of wind turbines would result in "considerable and significant concerns, due to their likely effect on the UK low flying system" [MOD, 2014, p. 1]. The map shows that there has been significant development in one of these zones, suggesting that planning may be granted, despite these concerns. For this reason, only the northernmost zones, which include far fewer wind farms, were excluded from development. It is possible that this northernmost zone contains fewer wind farms because it coincides with land which is more remote and therefore less suitable for development, this is not a problem as it will be excluded through one of the measures described above.

DECC and the MOD also provide data on aviation safeguarding. Boundaries are provided to show areas where turbines with tip heights of varying sizes would be in the line of sight of at least one of the primary surveillance radar. The accompanying documentation does not state that development will be prohibited in these areas, but that consultation will be required in order to receive planning consent. Based on the archetypal turbines used for onshore simulation (hub height of 80 m, tip height of 120 m) the area highlighted by this data covers a very significant portion of GB and contains nearly 50% of consented wind farms, including all of the turbines in central England. It is possible that the turbines in these areas are smaller than the archetype turbines used in simulations, so may have received consent on the basis of not interfering with specific radar. The development of wind farms within these areas clearly shows, however, that this restriction is not absolute. Therefore the number of wind farms in zones with lower height restrictions were analysed. The 40 m restriction zone contains more than 25% of farms, and the 20 m zone contained almost 15% of consented farms. This analysis demonstrates that it is possible to develop wind farms in all of these zones, the 20 m area was therefore initially added to the list of restrictions.

DECC also provide data on the areas where wind farm development may interrupt weather radar under two classifications:

1. Areas likely to raise significant concerns, which will be difficult to overcome - if overcome mitigation will be necessary.
2. Areas likely to raise concerns and mitigation may be necessary.

Comparing these areas to installed wind farms showed that land in classification 1 contains only 13 consented wind farms, whereas land in classification 2 contains 135. Therefore the land in the second classification has been excluded from development. A buffer was also applied to the area surrounding the Eskdalemuir seismic station as turbines create seismic vibrations, the buffer is line with that applied by Boehme et al. [2006] (Table 6.2).

Distance to grid Eliminating areas which are too far from the grid is used in the literature as a way to incorporate cost restriction on development, as building new infrastructure to connect wind farms is expensive. There is an economic optimum between building more transmission and reaching good wind sites. A whole system optimum will consider the spatiotemporal nature of demand and wind supply, existing and possible transmission, other conventional renewable generation, storage and trade. Therefore the distance to grid metric may only represent a small part of the total cost of introducing wind capacity. This restriction is difficult to apply in GB, due to lack of data. Spatial data are available describing overhead 132 kv, 275 kv and 400 kv and underground cable in England and Wales. Unfortunately, Scottish data are owned by Scottish Power and Scottish and Southern Energy and are not publicly available. Also, many wind farms are connected to low voltage regional electricity networks and spatial data are not available for these networks. This explains why Boehme et al. [2006] use grid supply points to measure distance to grid, disregarding embedded generation. No restriction has been applied here as the most remote locations have been removed by other restrictions. The resource estimate is therefore an estimate of technical potential following the description of the estimates in Chapter 2. This estimate is more robust and detailed than the theoretical potential but is likely to be larger than the potential that applies a greater number of restrictions that may include economic restrictions.

Area used by wind farms The area that a wind farm occupies is of interest here as the land which is already used for turbines cannot be developed, and an appropriate amount of land must be found for new development. The area used by a wind farm can be defined as that which is impacted by everything associated with the project, sometimes referred to as the direct impact area, including access roads, substations and service buildings. Total wind plant area is more commonly used, this is the footprint of the project, which may just be the area defined by the outermost turbines. The former definition is more likely to be be applied to large wind farms with larger amounts of associated infrastructure. The latter definition is more suitable for small farms. The actual land use, or land that a turbine completely stops being used for another purpose is approximately 1% of the total area, the rest of the land can still be used for some purposes e.g. grazing. Typical farm shape is difficult to define because turbines can be placed in different configurations to make best use of space or wind conditions. An alternative method for allocating space for wind farms is to use standard turbine spacing. This is measured in rotor diameters between masts. Manufacturers provide minimum turbine spacing to counter wake effects. There have also been studies on the optimum spacing, e.g. 10 rotor diameters limits array efficiency to 60% [Johansson and Burnham, 1993], these losses are accounted for in the model through calibrating the output against measured generation data. This may mean that the model is calibrated against current spacing and the

resultant wake losses, however this is difficult to account for due to the influence of other factors such as terrain and shut downs. For simplicity and applicability a 10 rotor diameter restriction has been applied to new development. This is generous in relation to installed capacity. Using the parameters from the archetypal onshore turbine this results in the need for 0.64 km^2 per new turbine. The spacing is only used here for land allocation so does not influence model output, other than altering the spatial weighting of capacity and therefore the spatial variability in the harnessing of GB wind conditions.

It should be noted that although every measure possible has been taken to identify suitable land with the highest possibility of achieving permission, it is possible that it will not be granted due to opposition etc. Approval of wind farms has fallen from 84% of capacity approved in 2008/09, to 68% of capacity consented in 2011/12 and 62 % in 2012/13 [XiEC, 2014]. Recent reports suggest that this has fallen even further, onshore approval was approximately 33% in 2014 [Renewable-UK, 2014].

The same method was used to exclude land that already contained turbines from development. Using the data described in Figure 2.1, a mean hub height of installed capacity was calculated and used as a proxy for rotor diameter. Therefore the operational farms were allotted 10 x 55m rotor diameter area or 0.34 km^2 each. A buffer was applied based on a circle around a number of turbines. Development of turbines continues to include smaller turbines (Figure 2.1), therefore the same method was used for those under consent. Analysis of individual sites could use specific wind farm details available in the REPD, this also applies for restriction analysis. This approach is rarely applied in the literature (e.g. Staffell and Green [2014]) due to the time taken.

Final combination Figure 6.5 shows the result of combining the restrictions described above. The remaining designations in Table 6.2, those related to land use and wind speed, are analysed below. In the final combination the 20 m low flying zones were not included, because these zones create a large new area of exclusion when combined with other restrictions. Including these areas, 250 operational farms would be excluded (3159 MW, 1962 turbines) and 237 consented wind farms (3033 MW, 1276 turbines). Figure 6.5 shows that the final exclusion zones contain 86 operational farms (1195 MW, 827 turbines) and 45 consented farms (1610 MW, 545 turbines). The difference demonstrates that the no fly zone is widely used for development and that the zones finally selected for exclusion represent a more stringent set of restrictions than are currently applied to GB onshore wind farm development. This should ensure that capacity is placed in areas where development is more likely to be granted and therefore represent realistic wind conditions experienced by future wind fleets.

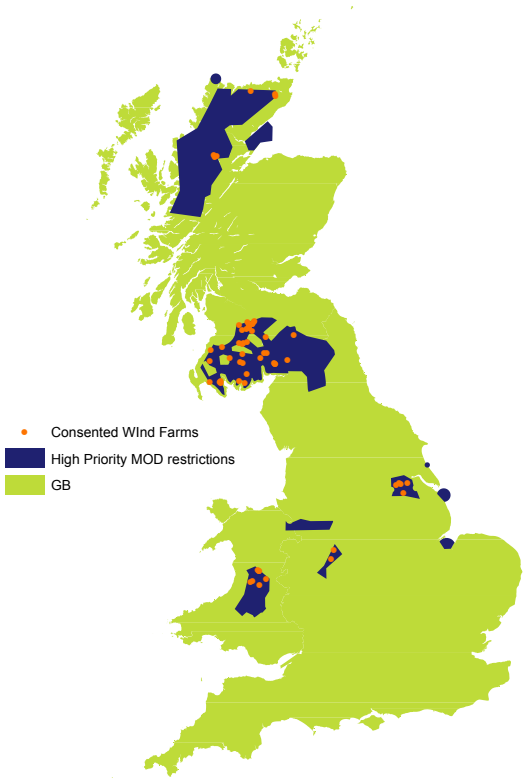

Figure 6.4.: Map of operational and consented farms in MOD low flying zones.

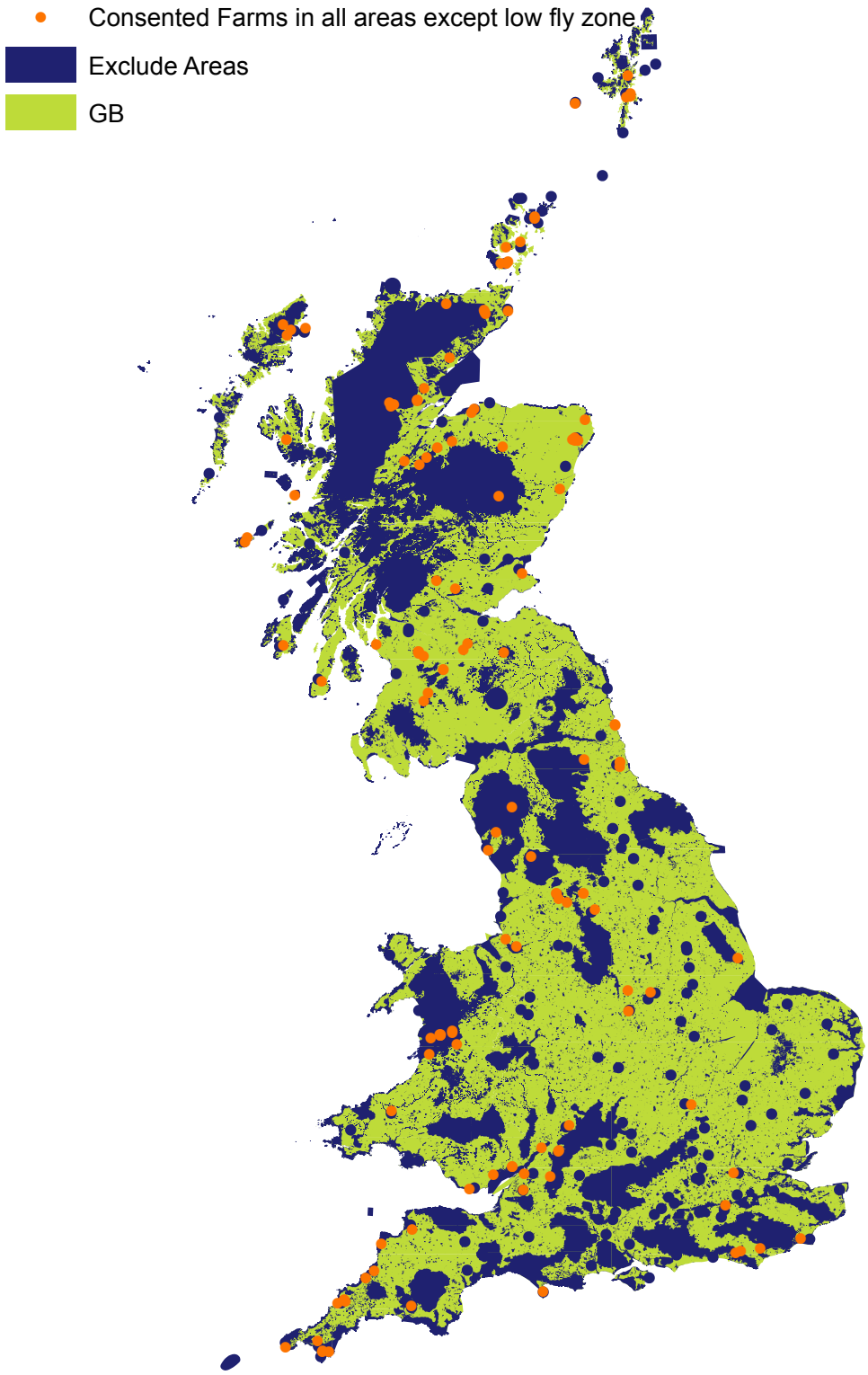

Figure 6.5.: Map of consented farms in all excluded areas except the 20 m height restricted radar zones.

6.2.2.2. Land use of existing turbines

The area available for development and the amount of that area needed per turbine has been established. There are, however, questions remaining on which land within the remaining areas to prioritise. There are several parameters in Table 6.2 related to land use that have not yet been used in the analysis of available land. There is also reference to preferential land use types for development within the literature. Baban and Parry [2001] suggest that Grade 1 and 2 Agricultural land should be avoided as it is better used for crops. Rodman and Meentemeyer [2006] state that barren farmland is excellent, grass is fair, shrubs poor and wetlands unsuitable.

These classifications are somewhat subjective, with little supporting evidence provided. Fortunately, the spatial data available for GB means that the land use at the site of existing wind farms can be defined and this can be used to guide rules for development. Figure 6.6 describes land use at the location of onshore GB wind farms that have achieved planning permission. Analysis is possible at a greater level of disaggregation in terms of land use classification. However, as described in Section 3.2.3 the CORINE database may be misaligned, therefore an aggregated classification was used. The allocation of turbines to forested areas shows that land use is generalised. Turbines are unlikely to be located in dense forest (although the size of turbines means that turbine blades would comfortably be above trees, there are issues with wind quality as well as installation and maintenance). The problem with inland waters seen in previous analysis is repeated, these areas are ignored in this analysis to ensure no turbines in lakes. Although this land use classification is not perfect it is adequate for the purpose of selecting appropriate land for development, as turbines are allocated to grid squares rather than specific positions within these grid squares. It is very unlikely that there will not be some spare space under some other classification, a point explored further below.

Figure 6.6 shows a clear division between land uses have that been used for wind farm development and those which have not. This division has been used as a guide for development so that land classified as Scrub, Herbaceous Vegetation, Forest, Pasture, Arable land and Inland Wetland is preferred for development. If this is not enough land to contain the capacities described above; Industrial, Commercial, Transport, Urban Fabric, heterogeneous agricultural and sparsely vegetated land can be used. Other land uses are discounted from development. The four preferred categories of land constitute over 80% of GB. The use of inland wetlands goes against the advice of Rodman and Meentemeyer [2006], however the generalised classification means that the turbines in this land class are likely to be in areas around the part of wetlands that these authors believe are unsuitable.

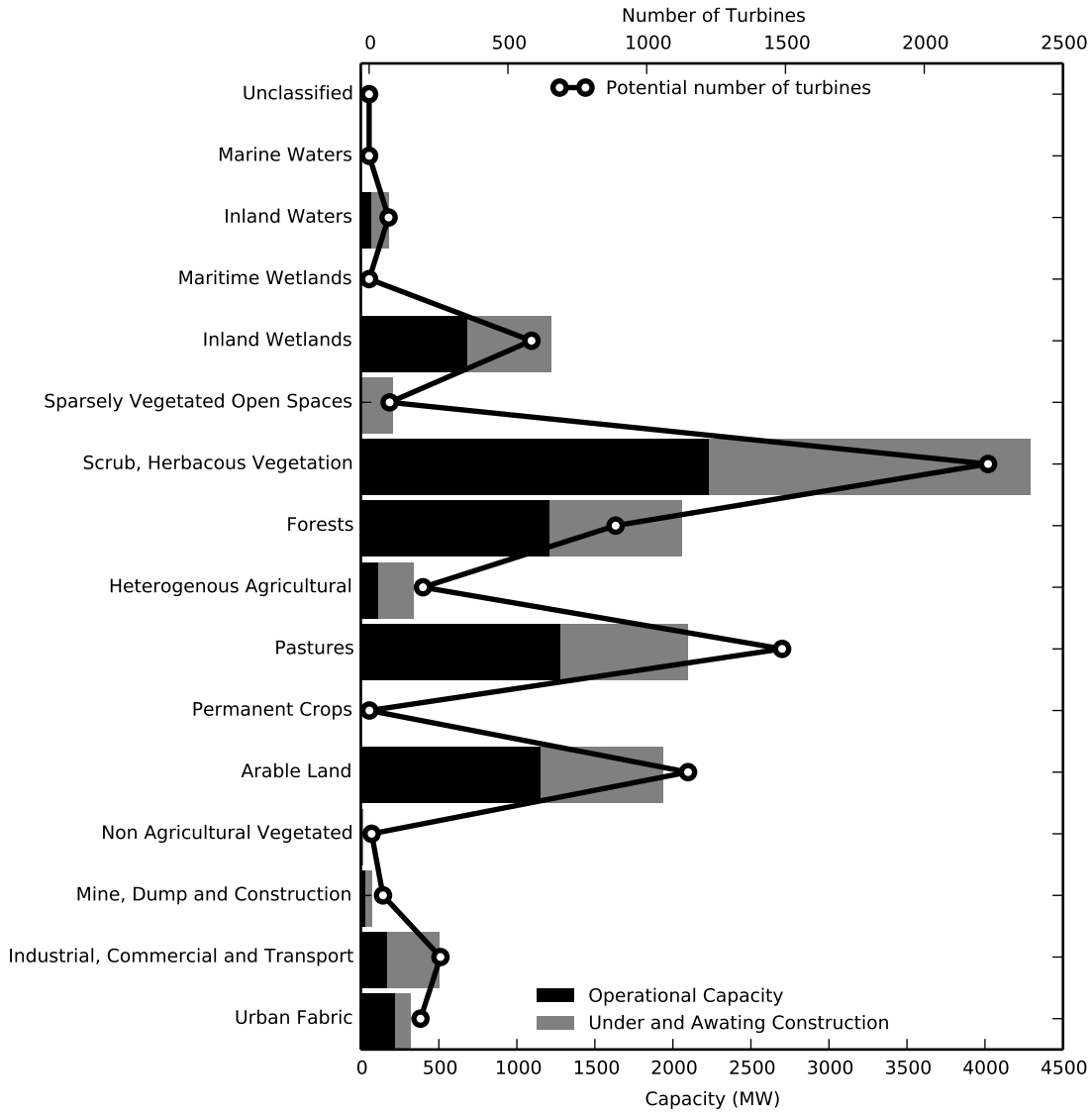

Figure 6.6.: Land use at the location of operational wind farms and those which are either under construction or awaiting construction, as of August 2014. Data sources: DECC [2014a] and EEA [2000].

6.2.2.3. Onshore wind speed

Section 2.1.1 has described how mean average wind speed has historically been the most dominant factor in the selection of suitable locations in resource estimates. Figure 6.7 shows a characterisation of onshore GB wind speeds at 60 m created using the CFSR data, extrapolated to 60 m elevation using the methods described in Chapter 5. The map uses three different methods for classifying wind speed. The first is the traditional mean annual wind speed using the most widely used threshold described in Section 2.1.1, 5 m/s, the second is the percentage of hours where the wind speed is within the power producing range of the archetypal onshore wind turbine curve (5 - 25 m/s), and the third is the percentage of hours where the wind speed should produce peak output from onshore turbines (14 -25 m/s). All of these were calculated using the entire CFSR time series (31 years). It is slightly misleading to directly compare the three methods, as the first uses different units to the latter two. However a natural breaks classification was used with the same number of divisions, so that they could be contrasted against each other.

All three methods show that the best wind speeds are experienced on the western coast of GB, especially in north western Scotland, similar levels are experienced in the Scottish isles. All coastal areas experience high wind speeds, although the eastern edge of England is on the lower end of this scale. Central and southern England experience the least suitable wind speed for power production, particularly when it comes to the peak production hours. However, the whole of GB is classified as having a mean annual wind speed of over 5 m/s, although variations within grid squares may reduce the extent of this classification. In terms of using a classification method in subsequent analysis, the first method has been disregarded as it is an over simplification of the GB conditions. The last does not appear to be any more nuanced and ignores some wind speeds that are of use for power production which are likely to be experienced for long periods (see Figure 4.14). Therefore the percentage of hours in the power producing range, the second method, is used as a driver in the location of onshore wind capacity. This method does, of course, rely on the fact that the height correction of the wind speed data is correct, as this effects the number of hours in the wind producing range. Previous analysis has shown that the method has resulted in underestimated wind speeds. It would be useful in future analysis to attempt to improve the height correction method and compare the results to those shown here. The use of this metric as a primary driver of turbine location alongside suitable land for development should ensure maximum output over a year. Ultimately other factors that influence system cost such as cost of transmission should influence turbine placement, these factors can be explored in further analysis.

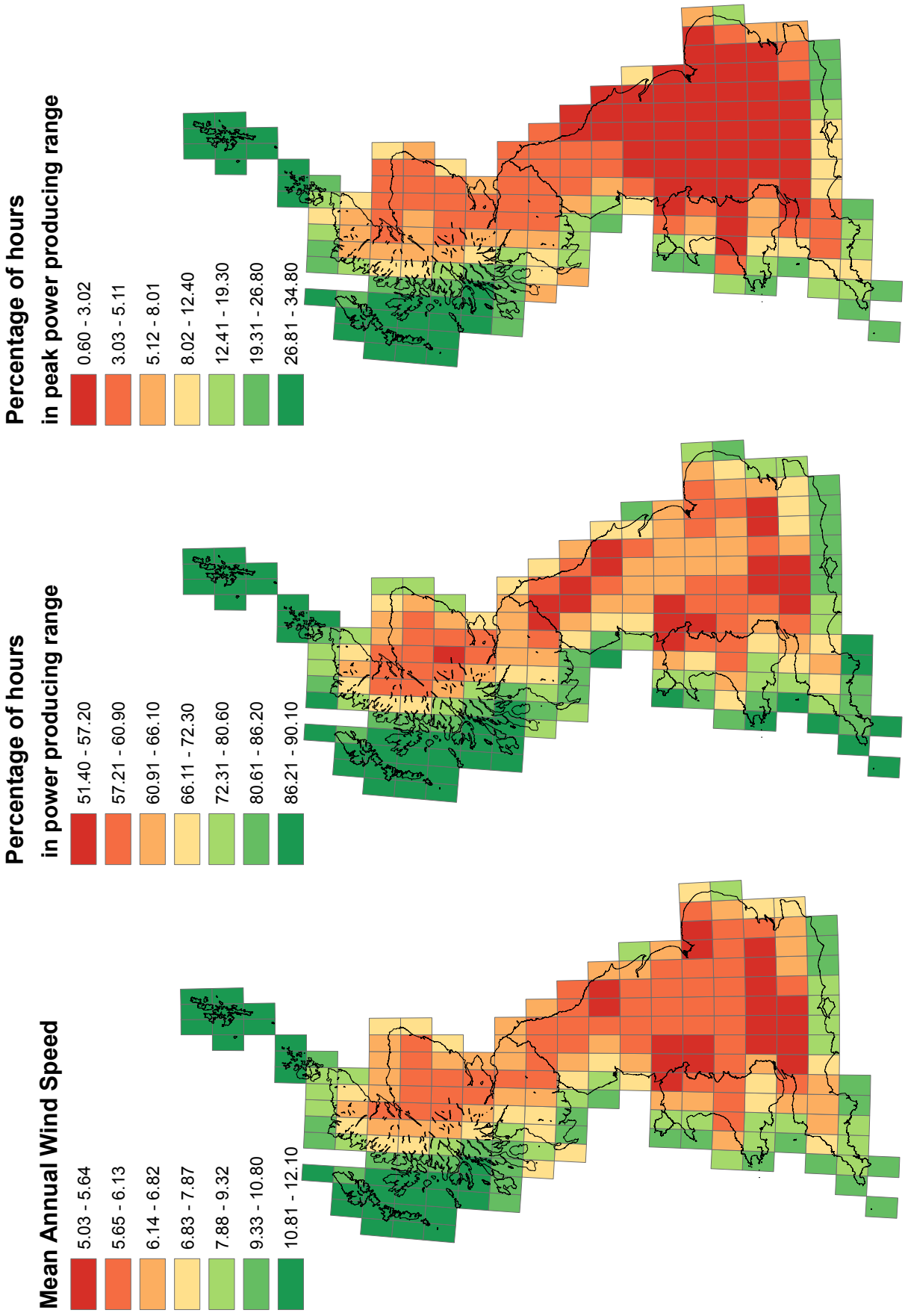

Figure 6.7.: Map showing the spatial variation in onshore wind speed over GB at 60 m elevation.

6.2.2.4. Allocation of onshore capacity

Criteria Figure 6.8 shows the results of the analysis of free land and wind speed side by side. The free land, is the land that is classified as any of the preferred land uses which is not excluded as a result of the restrictions described above (Figure 6.5). The analysis shows that, unfortunately, the grid squares that experience the most hours in the power producing range appear to be negatively correlated with the grid squares with the largest amount of available land. This relationship is heavily influenced by the smaller amount of land available in the coastal areas which experience the highest wind speeds.

In order to compare the results of the restriction analysis to the literature summarised in Table 2.1, the resource has been estimated. Because all grid squares exhibit a mean wind speed above 5m/s the technical potential covers the whole of GB and equates to 897 GW (based on 229,848 km^2 land and turbines using 0.64 km^2). Analysis above has shown that environmental restrictions remove 31% of land from development resulting in 158,595 km^2 free with room for 619 GW capacity. The final level of restrictions including the criteria based restrictions and the land use analysis results in a total onshore free area of 122,740 km^2 or 53% of GB, equivalent to 191,781 turbines or 481 GW.

Unfortunately, of the resource estimates reviewed in Chapter 2 only Gross and Chapman [2001] provide a capacity estimate, rather than a resource estimate (Table 2.1). The values found by Gross and Chapman, are considerably lower than those found here. The other studies giving resource estimates have values in line with Gross and Chapman suggesting that their capacity estimates would also be considerably lower than found here and the studies evaluating single countries in GB also give low estimates. No estimate of the electricity produced is performed here, as this will be simulated in a more sophisticated manner in subsequent chapters.

The large capacity estimate found here is slightly surprising, as analysis has shown that some of the land excluded has been developed, suggesting that the criteria are in fact quite strict. The large estimate may be due to the fact that large turbines are used or that there is a significant amount of land in the remaining area that would be excluded by unused restrictions, such as distance to grid. Although this amount of capacity would never be installed in GB, not only due to socially acceptable limits but also because it far exceeds peak demand and the costs would be prohibitive even if the electricity produced could be exported; the availability demonstrates the strength of the resource in GB. The issue of socially acceptable limits is interesting, previous studies have quantified it as a capacity per unit area, it may also be useful to consider this at different levels of aggregation so that a single region or country does not end up completely covered in turbines.

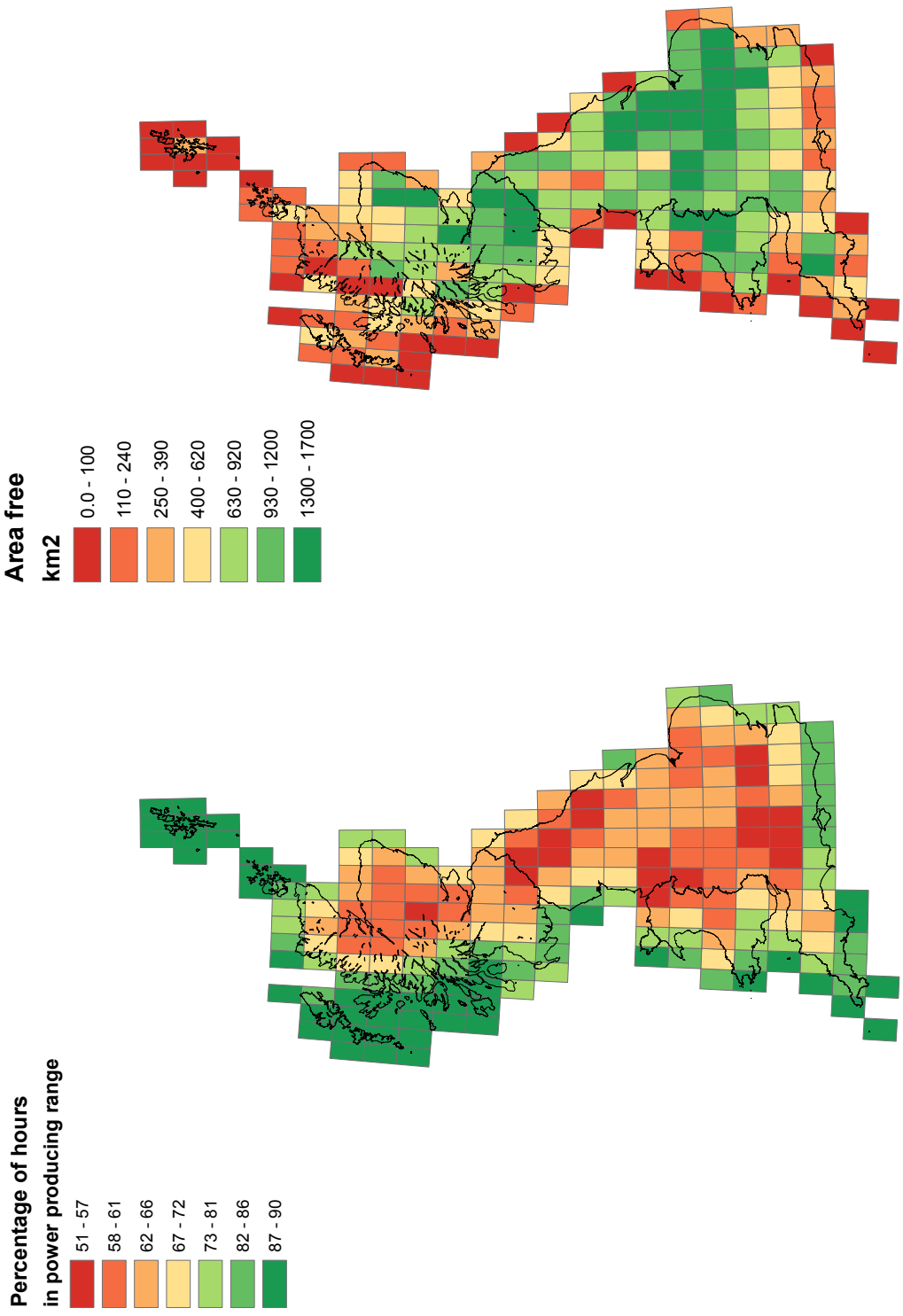

Figure 6.8.: Map showing spatial variation in wind speed over GB and land available for wind farm development after resource estimation.

Method As described above, scenario modelling is performed from 2010 - 2035. Since the location and magnitude of installed capacity to 2014 is known, this capacity was used for the first four years of each scenario where possible. Unfortunately, the capacity for the first few years of the NG scenarios does not exactly match that shown by the end of year REPD capacities. Therefore it was necessary to use the operational, under construction and awaiting construction capacity in instalments in that order, depending on the capacity projected by each scenario. Data is also available on future approved capacity, this was used next to fill the scenarios. Projects awaiting construction are not guaranteed to be completed, however their use ensures that the scenarios utilise realistic locations. The site order is the same as in the REPD, the same order is used for each scenario. Data from the REPD shows that there is a total of 13,232 MW of onshore capacity in GB combining operational, under construction and awaiting construction. Table 6.3 shows that all of the NG scenarios use the capacity that is currently under construction at a very similar rate. After this the capacity that is described as awaiting construction by the REPD is not built for another three years under the fastest scenario, which may not be unreasonable, especially as some wind projects will not be completed. However, under the NP scenario this level of capacity is never reached. This suggests that no new capacity is ever approved, demonstrating that the NP scenario describes a future with immediate restrictions on wind supply. When considered in conjunction with the large resource estimate in comparison to the final onshore capacities this also suggests that the NG onshore scenarios may be conservative in terms of what is possible. For this reason, a final onshore scenario has been added for the analysis of turbine output, this adds 1.4 GW of wind capacity each year to 2035, which still falls far short of the maximum possible capacity. This explores another GG scenario where more wind is integrated into the system than is currently assumed by NG scenarios. This scenario is likely to necessitate solutions to combat the variability of wind such as storage, demand side management, increased exports etc.

Additional capacity was added to those scenarios which require it by allocating turbines to grid squares in 25 MW, or ten turbine, blocks. Grid squares with less than 200 km^2 free were disregarded, as this indicates that the land may be inaccessible or too close to restricted areas. This removes almost all of the coastal areas where grid squares are predominantly sea, therefore also eliminates isolated areas and ensures that wind speeds are not too skewed by higher winds offshore. Those grid squares in the lowest level of classification according to Figure 6.8 (<58% of hours with wind speeds in the desired range) were also disregarded. The capacity was then allocated according to grid squares with the highest classification of wind speed moving to lower classification, until that years capacity was complete. The next year starts at the grid square with the next highest wind speed classification. Once all available land is used, the grid square was no longer used. This method ensures spatial diversity and represents gradual increase in capacity in those grid squares with suitable wind and large free areas. The method also uses the sites which give the best quality wind for power generation. At the end of the scenarios only the highest wind speed grid squares with available land were used as the capacity reached maximum. Hopefully this method represents what might happen in reality if a capacity plan is made and followed. The plan would mean that high wind quality sites are used first. Figure 6.9 describes the initial capacity and the final capacity for each of the scenarios following this method of spatial allocation. The map demonstrates that, in relation to 2010, onshore spatial diversity significantly increases for all of the scenarios. It also demonstrates that changes to the transmission system may be necessary given the preference of this method for capacity in Scotland. Analysis of wind speed and available areas shows that it may not be possible to avoid this unless sites with lower quality wind are chosen. The model

could be used in future work to demonstrate the need for power in one part of GB (e.g. south east England) in relation to supply in another (e.g. Scotland) and therefore inform development of network capacity.

Scenario	Year that under construction capacity is used	Year that awaiting construction capacity is used
GG	2016	2019
SP	2016	2021
NP	2017	Never
LCL	2016	2019

Table 6.3.: Currently approved capacity under NG scenarios.

6.2.2.5. Offshore

All of the studies reviewed in Section 2.1.1 produce an estimate of the offshore resource, some of these carry out a detailed restrictions analysis of GB offshore areas. Table 6.4 summarises the designation of these areas and the criteria used. Here, it is not necessary to carry out this type of analysis because a resource for realistic placement of offshore capacity exists, in the form of development zones. These development zones represent offshore areas earmarked for wind farm development, where licensing is controlled by the Crown Estate, who have authority outside of the traditional 12 nautical mile from shore limit. These sites are ideal as they have already been subject to the sort of analysis described in the literature and been identified as suitable for development, as well as being approved and therefore more likely to gain the infrastructure necessary for electricity transmission. These zones are described in Figure 6.10.

The first of these development zones, launched in 2001, encapsulates areas close to the shore, with a potential capacity of 1.5 GW, the sites shown in the map demonstrates that 1.17 GW of capacity has been added. The second round, launched in 2003, provided a larger area with room for another 7 GW capacity, 2.6 GW is currently operating there, 1.4 GW under construction and 2.3 GW awaiting construction, total 6.3 GW. The last round was released in 2010, currently 7 MW is operational and 3 GW is awaiting construction, applications have been submitted for another 8 GW. The Scottish government have also created a development program allowing 5 GW across 6 sites. None of which are currently operational according to the REPD, and only one of which is awaiting construction (0.6 GW). Further details of development zones and other offshore wind farms can be found in Higgins and Foley [2014].

Wind shear is lower offshore and conditions are less turbulent due to lack of obstruction and lower vertical temperature gradients [Boehme et al., 2006]. Therefore offshore wind farms require greater spacing so that wakes can regain energy. Boehme et al. [2006] only place 1, 5MW turbine, per 1 km^2 grid cell, EEA [2009] use 1.25 km^2 per 8 MW turbine. Here 15 rotor diameters have been used to allow a greater amount of area per turbine than onshore. The archetypal curve used for offshore simulation represents a turbine with a 120 m rotor diameter, therefore each turbine requires 3.24 km^2, this is significantly more than previous studies but should ensure that losses are minimal. This will result in capacity allocations quickly using up the development zones. If extra space is required beyond these scenarios this value could be revised and more turbine placed using the same amount of seabed. The use of a greater amount of area than is currently used may mean that the correction factor created in previous analysis will result in under estimated output, it also

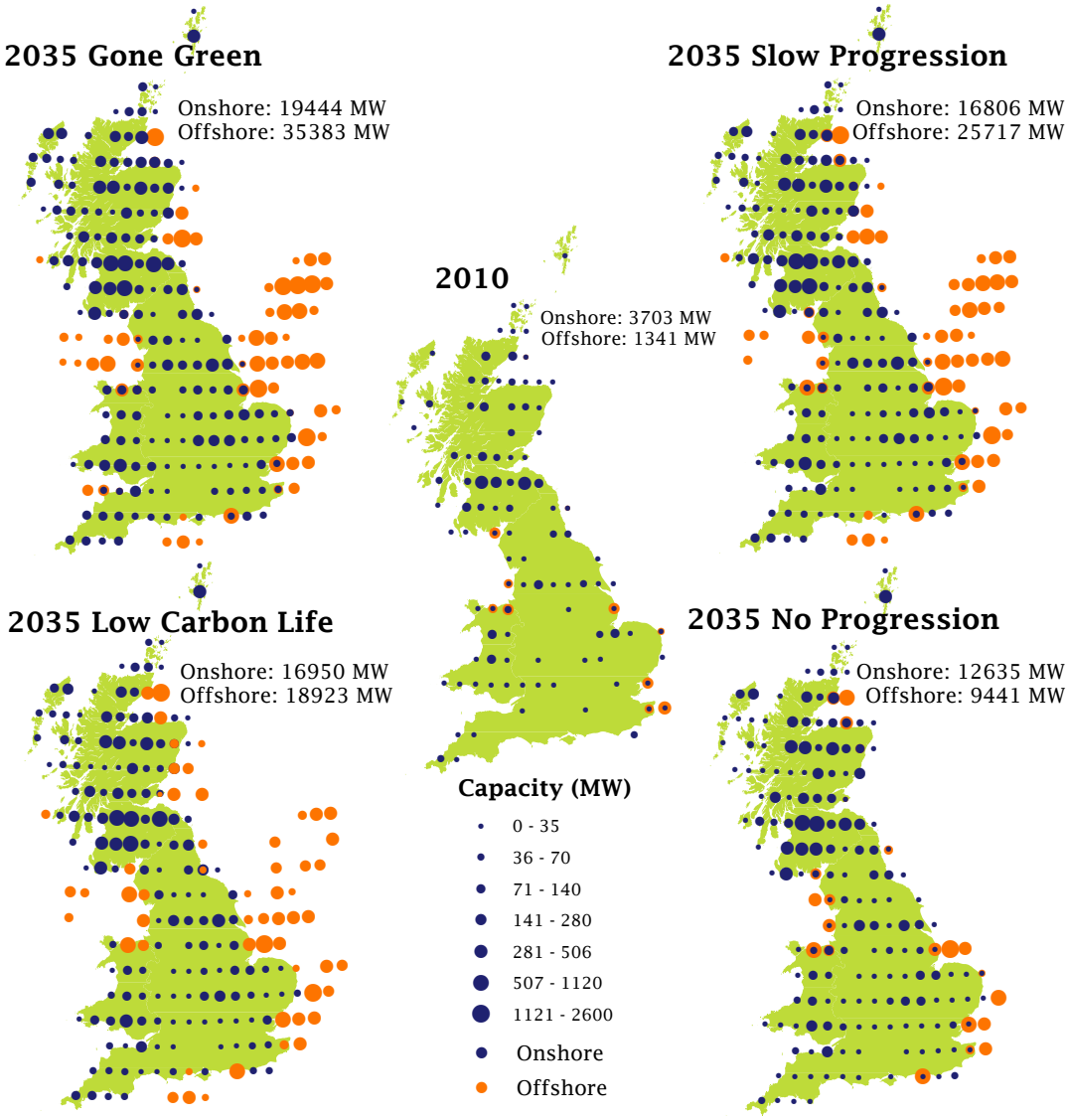

Figure 6.9.: Maps of wind capacity spatial scenarios, 2010 and 2035.

assumes that the gain from increased output outweighs the loss or expense of extra transmission. Figure 6.10 shows the number of turbines that this will allow in each of the currently approved offshore zone (orange polygons).

As with onshore capacity, the operational and consented capacity according to the REPD was used to fill the first years of the scenarios. In some cases it was necessary to assume that the larger wind farms would be built in stages, as smaller capacities were needed to match the NG scenarios. The NP scenario again did not use all of the approved REPD approved capacity, leaving 1765 MW of close to shore capacity, and therefore does not develop any of the proposed zones. The GG scenario requires new capacity after 2019, LCL after 2020 and SP after 2021.

New capacity was again added in blocks of 10 turbines, grid squares were ranked in order of available sea and those with the greater area filled first. Those scenarios that did not fill all the available land, preferred the zones closer to shore to ensure these were filled and spatial diversity was achieved. The GG scenario uses all of the available land allotted by the Crown Estate by 2032 with 2660

MW remaining to be allocated. In order to accommodate this capacity, the initial round three zone shapefile was consulted, this contained several areas which have since been removed, shown in Figure 6.10 in blue. Using the thresholds described above, these polygons have enough room for the remaining capacity and increase the spatial diversity of the wind fleet, therefore they were used for the remaining offshore capacity. Because the GG scenario uses all available development land, unlike onshore, no GG Plus scenario was developed. Offshore spatial configurations of capacity in 2010 and 2035 are shown alongside onshore in Figure 6.9. Although a detailed analysis of the available offshore resource has not been carried out this method gives an indication of the feasibly usable resource (up to 55 GW). Interestingly, this is considerably lower than the technical resource estimate made by Gross and Chapman [2001] (1489.8 GW). Given that 55 GW is at the very top of a scenario designed by the network operators this shows how capacity and resource estimates may not be an ideal way to evaluate the wind resource. Through using realistic scenarios, spatially redistributing them and simulating generation, a more nuanced and realistic evaluation of the resource can be performed. The estimate of capacity made by Garrad Hassan [2001] seems very high given the need to transport electricity to demand centres, the estimate made by [Boehme et al., 2006] seems more realistic (0 - 3 GW).

Designation	Excluded (E) or Restricted (R)
SAC with marine component	E
Marine	E
Offshore SAC	E
SPA with marine component	E
< 5km from land	E
Navigation Risk	E
Practice and Exercise Areas	E
Ammunition Dumps	E
Pipelines and Cables	E
Marine Consultation Areas	E
Protected Wreck Sites	E
Depth (30 - 40m)	R
Distance to grid	R
Territorial limits	R

Table 6.4.: Offshore development exclusion areas and restrictions as designated by studies reviewed in Chapter 2.

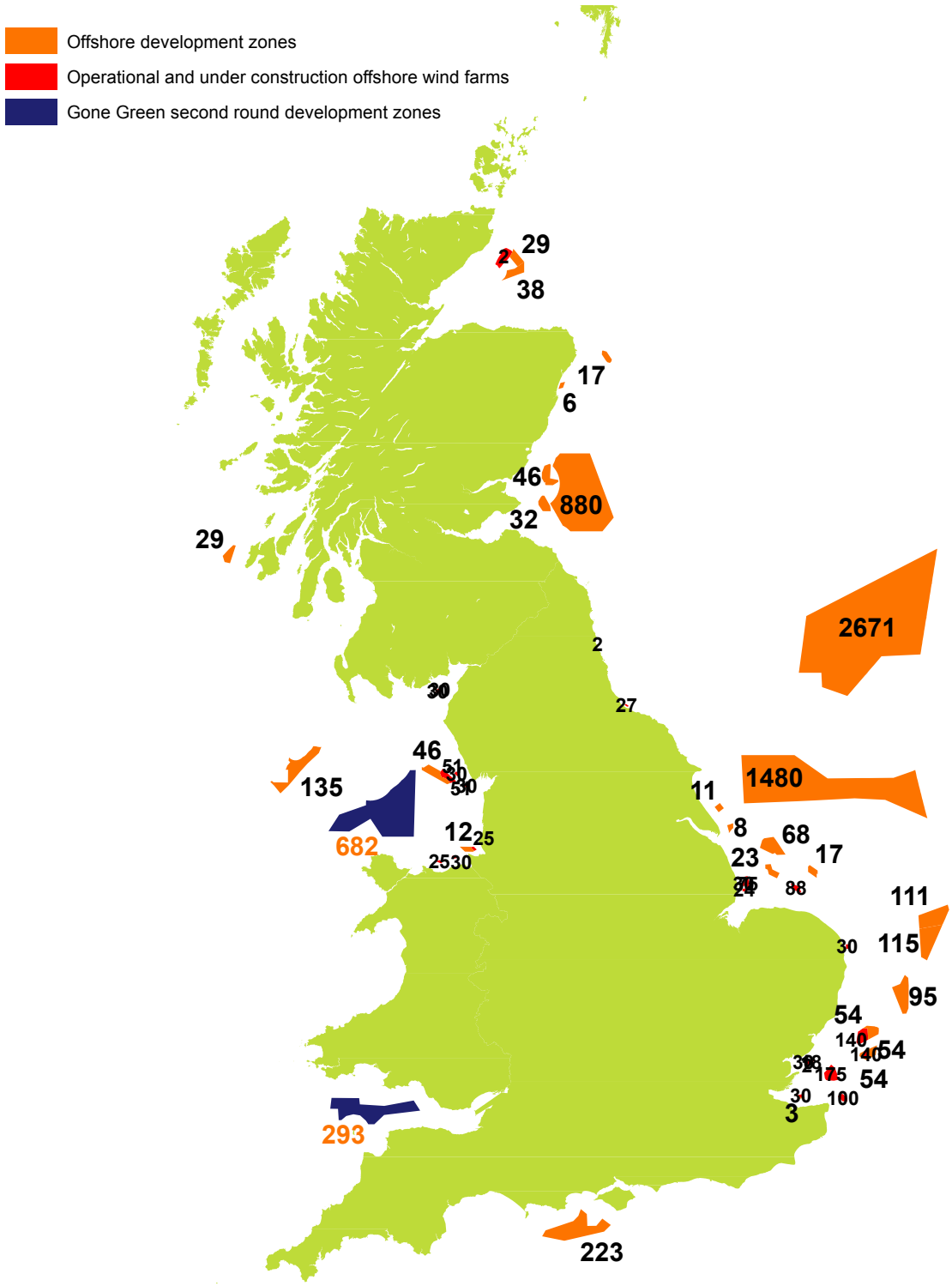

Figure 6.10.: Map of offshore development zones and existing generation within them, smaller font represents installed capacity, larger font represents potential capacity in MW.

6.3. Demand Scenarios

Scenario modelling of demand focusses on the domestic sector, in particular electrified heat demand. Other changing drivers including population and buildings are also modelled. The focus on domestic demand is a result of the potential that this sector has for altering the temporal profile of electricity demand and therefore the relationship between demand and supply. Heat demand is very large and somewhat rigid, as it is dictated by activity which is unlikely to change e.g. the working day. This means that if demand for other fuels is switched to electricity it is likely that peak electricity demand will increase, which will have to be reflected in capacity and has a potentially large impact on performance metrics of variable supply such as capacity credit. There are, of course, other potential drivers of demand that may have large implications of these issues, such as increased use of electric vehicles and demand side management. The resultant demand for electricity from these drivers is, however, less rigid. For example, electric vehicles can be charged at night when demand is lower. Also these drivers are less dependent on weather, which is the primary driver in the model and the use of CFSR data is one of the greatest model strengths. Similar methods to those described in this thesis could be used to model these drivers in the future.

NG scenario data provides the basis for the SpDEAM inputs in subsequent modelling, however it was necessary to make changes in order to align this data with the model structure. These changes and additional data are described in this section. Not all variables have been changed in the scenarios, this reduces complexity and allows meaningful analysis of the effects of the changes outlined above, some static variables are discussed below, variables not described in this chapter remain as described in the previous chapter.

6.3.1. National annual energy demand values

SpDEAM requires national annual energy demand values for the top down part of the model.

Domestic Figure 6.11 describes the national annual values provided by NG for total domestic electricity demand. To ensure that these values were consistent with the values used in the evaluation and therefore the calibrated model they were compared. Where these values overlap the difference does not exceed 5%. SpDEAM allocates a proportion of this demand to end uses, using the values described in Figure 5.15, heat demand is modelled separately in SpDEAM. The allocation method removes electricity demand which arises from electric resistive heating and will do the same for the NG values. However, the values from NG labelled as all demand in Figure 6.11 also include electricity demand from domestic heat pumps, which will be modelled separately here using the bottom up method to introduce weather as a driver and show realistic spatially weighted and spatiotemporally disaggregated demand. Fortunately, NG also provide disaggregated data on heat pump demand, which has therefore been removed from all the demand values to provide the values to be used in modelled scenarios. Both the values including electrified domestic heat demand and those which do not are illustrated in Figure 6.11.

Data describing gas demand in the NG scenarios is also similar to that used in the SpDEAM evaluation (less than 6% difference), therefore these values have been used as the input for national annual demand (Figure 6.12). The close matching of the data suggests that it has been gathered

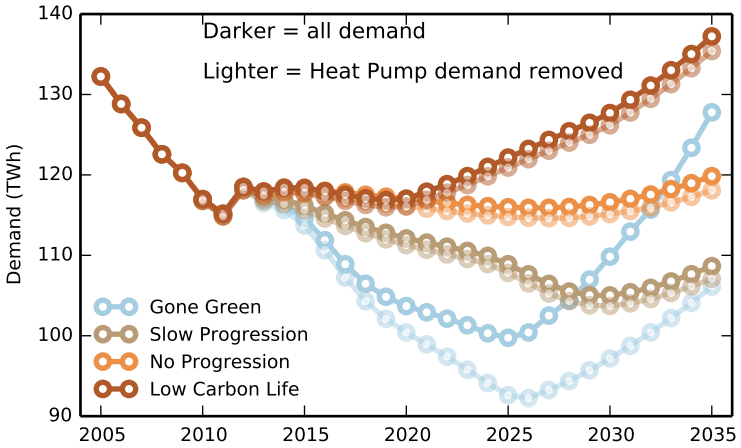

Figure 6.11.: Domestic power demand 2005 - 2035, according to National Grid scenarios.

from the same source for the years that have already passed. For both electricity and gas demand the scenarios modelled in SpDEAM assume that the allocation of demand to end uses remains static using data from 2010. It is likely that end use demand will change in the next 25 years, for example through increased use of gadgets in the home or installation of more efficient light bulbs. The proportion of electricity demand allotted to each end use can be changed in future use of this method to investigate the implications of these and other changes to the way in which energy is demanded in domestic buildings. Gas demand from heat in the NG values is removed using the proportional allocation to end uses and calculated using the SpDEAM methodology and the scenarios described below.

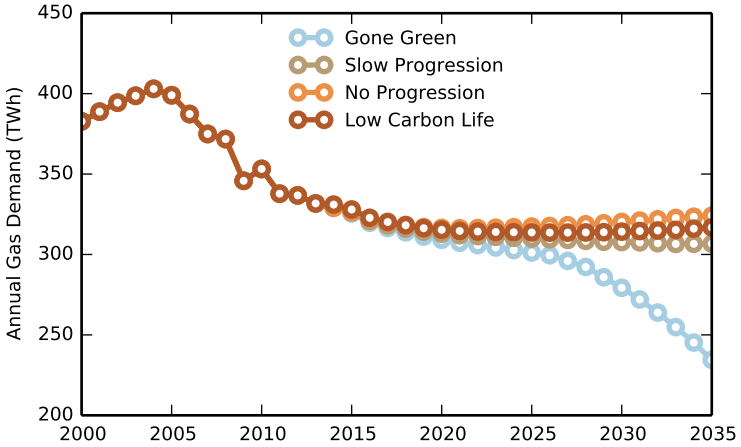

Figure 6.12.: Annual residential gas demand 2000 -2035, according to National Grid scenarios.

Non-Domestic As described in Chapter 5 non domestic demand is modelled using only the top down method, with fewer activity profiles than the domestic sector. The data used for this modelling previously may have been missing some sub sectors and is therefore submitted to significant correction, which take accounts of un-modelled demands and losses. The NG scenarios do not

disaggregate non domestic demand in their scenarios and these demands are enveloped in the econometric modelling, which is not described in detail in the accompanying documentation. It is, however, stated that the changes made to the domestic sector, including that increased electrification of heat demand are mirrored.

NG provide national annual values for "industrial" and commercial demand", which are suitable for input into the non domestic section of the model. Unfortunately these do not match SpDEAM inputs as closely as the domestic values described above. This may be due to the use of different sub sectoral classification. To ensure that the same correction factors can be used, data from NG was scaled to match the previously used data for 2010. The rest of the NG values were then scaled using the same factor so that the growth patterns described in Figure 6.13 and Figure 6.14 were followed. Non domestic demand is then calculated using the scaled national annual values and the method described in the previous chapter.

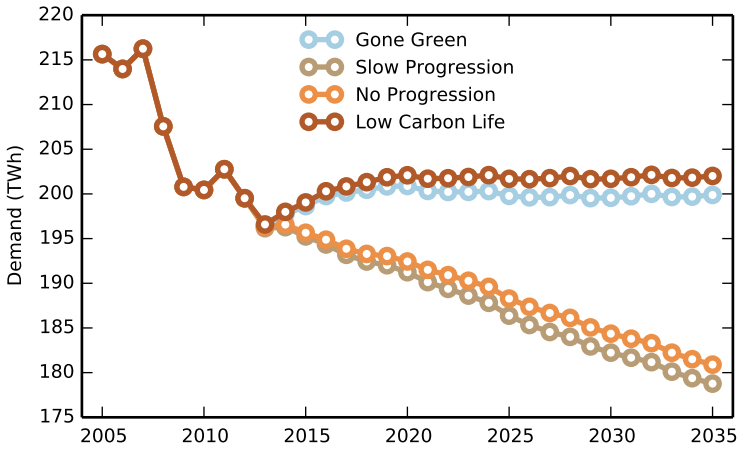

Figure 6.13.: Industrial and commercial power demand 2005 -2035, according to National Grid scenarios. .

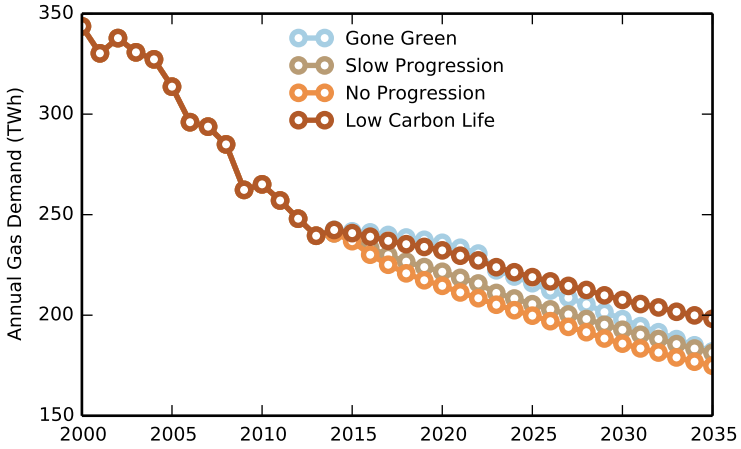

Figure 6.14.: Non Domestic gas demand 2000 -2035, according to National Grid scenarios.

6.3.2. Population change

Population projections from the ONS, as described in Figure 6.15, are used in the scenario modelling. These national level values are spatially redistributed to the grid using the population distribution described in Chapter 5 and integrated using the methods described in the same chapter. The distribution is assumed to remain static, therefore it is assumed that the growth is even in all locations. SpDEAM could be used in the future to investigate the implications of population increasing or decreasing as well as different regions growing or declining at different rates.

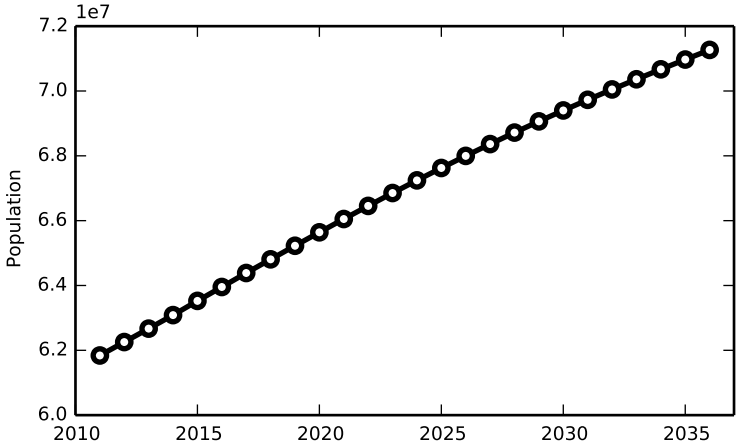

Figure 6.15.: GB population projection, 2011 - 2036, data source: ONS [2014b].

6.3.3. Building stock model

Projecting the building stock 25 years into the future at the resolution of the model grid is a complex task. The solution presented here has been developed so that the strength of SpDEAM, in this case the use of accurate census based data, is preserved. Figure 6.16 shows overall dwelling numbers projected into the future using an average number of people per dwelling and the population projection described in Figure 6.15. The average number of people per dwelling data is provided by the ONS through the Department of Communities and Local Government (DCLG) [DCLG, 2010]. To extend this data to 2035 the same average reduction in household size from the preceding years is used to extrapolate the data (-0.6 people per household, per year). These values only represent England and are an average of different household types. As discussed in Chapter 5, a possible improvement to the model would be to allocate people to building types using different numbers of people per household, DCLG [2010] provide data that makes this possible.

This temporal scenario was spatially disaggregated using the data described in Section 5.2.2.1. The total number of dwellings each year was divided among the archetypes, assuming the percentage of each type will remain the same as 2011 (using census data; detached = 22%, semi detached = 29%, terraced = 23%, purpose built flats = 17%, converted flats = 4%, flats in a commercial building = 4%, caravans = < 1% (percentages are rounded)). These values were then allocated to grid squares using the same distribution as 2011, e.g. grid square 201 contains 3% of 2011 detached dwellings.

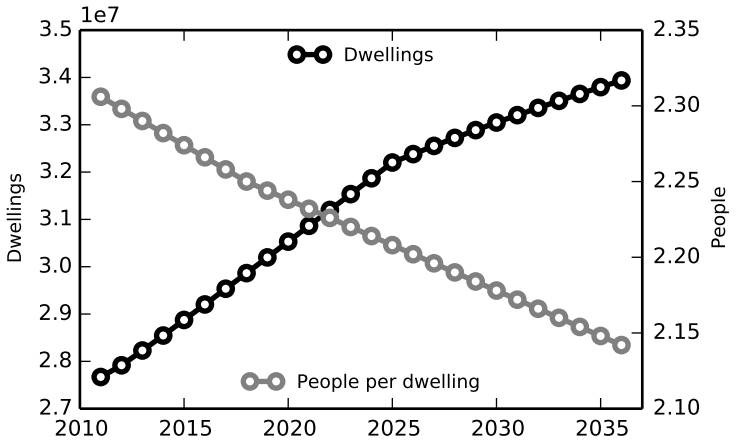

Figure 6.16.: Number of dwellings and average number of occupants in GB 2010 - 2035.

This method provided a total number of dwellings per archetype per grid square. In order to establish how many new buildings must be built to satisfy this demand for housing it was necessary to also establish how many dwellings will be demolished. According to Boardman et al. [2005] nearly 160,000 dwellings were demolished between 1996-2005 or approximately 20,000 per year, they use a value of 60,000 per year in future depictions of building stocks to achieve the changes necessary to reach climate goals. Here a much lower figure has been used of 25,000 dwellings demolished annually (in line with historical values), as the intention is to model realistic rather than ambitious change. These demolitions were redistributed using the same method as total buildings and added to the number of dwellings that must be built each year. The result of this process was an annual dataset depicting new build dwellings per grid square for each archetype and the same for existing buildings.

Heat Loss and floor area Old stock floor area remains the same as the final value used in SpDEAM evaluation (2010). New dwellings steadily reduce in size.

The creation of two separate building stock models, for new buildings and old stock respectively, allows the use of divergent heat loss characteristics between old and new dwellings as well as different criteria for the scenarios. Heat loss characteristics of old stock will change as result of improving glazing and fitting insulation, new buildings will incorporate these and other building fabric changes at varying rates. The aim of zero carbon houses by 2018 is used as a guide for the scenarios. In the GG scenario new build heat loss quickly reduces to meet zero carbon targets and remains static post 2018, the old stock improves more steadily to similar levels. SP new stock reaches the same level as GG, but takes another ten years, the old stock improves slightly less than GG. LCL improves at the same rate as SP but falters at 2018 for new stock, old stock continues to improve but does not reach the same level as GG. The heat loss characteristics for the NP scenario remain static with no change to 2010 heat loss coefficients for either old or new stock.

6.3.4. Heating technologies

Heat pumps are the only decarbonisation solution considered here, in part due to constraints including time and modelling complexity. It should be noted that there are barriers to their

successful uptake. One barrier is cost, as they are currently expensive to install. It has been suggested that they may only be cost effective in homes without access to the gas grid [Fawcett, 2011]. Another barrier is the fact that heat pumps require a low temperature heat distribution system which are not currently installed in many homes. Existing homes in GB are also unlikely to be efficient enough to retain the heat. Therefore significant retrofit would be necessary in old homes, which increases the expense. The barrier of a decarbonised supply system is covered in part in the scenarios through the introduction of wind capacity. This study goes some way to investigating the impacts of the introduction of the two technologies at a spatiotemporally disaggregated resolution, although, clearly, there are many questions that remain to be answered. For a complete review of domestic heat pumps in GB including potential research gaps see Fawcett [2011].

Heat pump uptake NG provide two different pathways for heat pump use, one describing the number of heat pumps installed each year for GG and the other for the remaining scenarios (Figure 6.17). The scenarios also specify whether the heat pumps should be placed in new buildings or replace a particular technology in existing dwellings. Figure 6.18 shows that the proportions of replacement are similar between the two sets of scenarios, but the absolute values, also described in Figure 6.17, are very different, there are more that ten times as many heat pumps in the GG scenario. These scenarios are based on Building Services Research and Information Association (BSRIA) sales data and analysis from NG including expert stakeholders. The large difference between the two scenarios is attributed to the need for both behaviour and policy changes for the GG scenario to come to fruition, as the technology is currently expensive, and would need to be supported by a policy such as the Renewable Heat Incentive (RHI). Replacement of gas boilers with heat pumps occurs later which is because it is assumed that by then the increase in thermal efficiency of dwellings and the decarbonisation of supply necessary to ensure operational and cost effectiveness have been achieved.

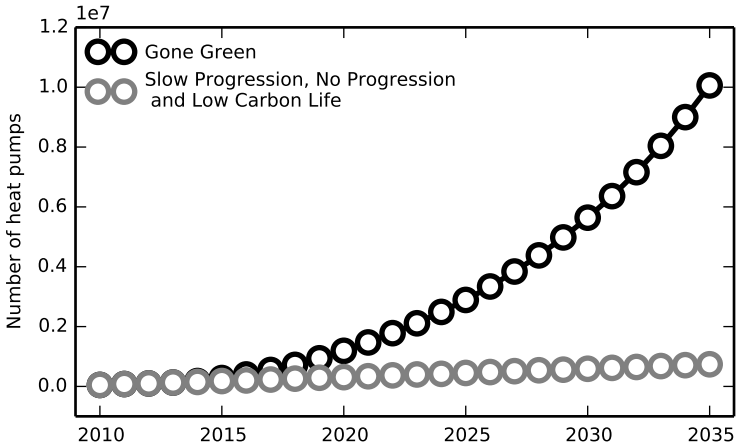

Figure 6.17.: Heat pump take up scenarios, data source: National Grid [2014].

Heating technology data used for the evaluation version of SpDEAM is in the form of percentages, e.g. 60% of heating in a grid square comes from gas boilers (Section 5.2.2.2). In order to adapt the absolute numbers of heat pumps provided by NG to this format it was necessary to first calculate how many dwellings would be heated by a technology in each grid square, using the heating type model developed from census data. Then subtract the number of heat pumps that

would replace this technology, assuming that they are evenly distributed over dwelling archetypes and spatially. The percentage of heating in each grid square was then recalculated. As with the evaluated version of SpDEAM, this assumes that all dwelling types are heated in the same way. This method preserves the spatial variation of traditional heating technologies but results in heat pumps being utilised evenly over space. This may not be realistic but cannot be more detailed due to lack of data.

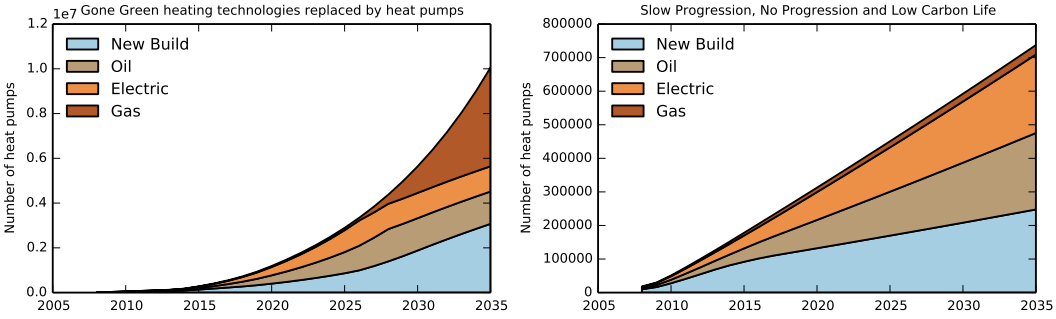

Figure 6.18.: Heat pump installations and heating technologies that will be replaced, data source: National Grid [2014].

Heat pump coefficient of performance [1] Heat pumps turn low temperature heat into higher temperature heat using electrical energy. A heat pump can be air-source or ground-source, which define where the device gathers the heat. Ground source heat pumps can provide better energy performance but are more expensive to install and require land or water for the installation of heat collectors.

The key parameter for the performance of a heat pump, particularly when studying the impact of replacing other technologies, is the Coefficient of Performance (COP). When the heat pump is being used to heat a space (they can also be used to cool - this is not modelled here due to the limited current use of domestic cooling or air conditioning but may have a significant impact on the demand from this technology) the COP is is the ratio of heat provided, to the electricity that is consumed by the compressor. COP = heat produced/equivalent electrical energy consumed.

The coefficient of performance of air source heat pumps is dependent on the external (source) temperature, but also depends on the desired temperature as it is easier to heat to a lower temperature. COPs vary second by second, therefore the Seasonal Performance Factors (SPF) which is the average over a year is often stated.

In order to use the existing methods in SpDEAM and directly replace demand for other fuels with heat pumps and electricity demand the method assumes a slightly simplified operation of heat pumps. The same equation is used for calculating heat demand as described in Chapter 5. This means that heat pumps essentially provide heat on demand and heat to the desired temperature. This heat demand is converted to electrical demand using the COP. In reality heat pumps provide heat at 20-35°C and traditional UK radiators provide heat at 60-75°C [Fawcett, 2011], therefore there would be a lag in heat delivery and electricity may be demanded earlier in the day. Future

[1] Content in this section has already been published as part of a blog post http://esenergyvis.wordpress.com/2014/04/04/animated-hourly-heat-pump-performance-factors-across-great-britain-during-2010/

iterations of the model could explore more complicated methods for calculating electricity demand from heat pumps. Future iterations could also investigate the use of heat stores so that heat pumps can be more efficiently operated and connection of heat pumps to hot water demand.

Current heat pump COPs are quite low, for example the Energy Savings Trust (EST) field trial (collecting data on UK heat pumps) found an average SPF of 1.9 for air source heat pumps [EST, 2013]. This is similar to countries where use is wide spread, for example the Finish heat pump association state that the COP of air source heat pumps in operation in 2008 was 1.9 [SULPU, 2010] .

Here it is assumed that heat pumps should be the best available, because the only scenario that uses them widely is the Gone Green scenario which assumes that barriers to sustainability are broken. This also reflects the fact that SPF's should be high if heat pumps are to be included as renewable energy sources that contribute towards EU policy goals. It has been estimated that SPFs should be greater than 2.875 [Fawcett, 2011].

The Energy Savings Trust collected data from installed heat pumps in Switzerland, here it is assumed that these field trials represent what can be expected from the next generation of heat pumps in this country. This data is used here to provide COPs which are related to ambient temperature. This provided a reasonably linearly increasing range of performance factors for a given external temperature, ranging between 2 at -5 degrees centigrade to over 4 above 10 degrees (Figure 6.19). Above and below theses temperatures the COP was assumed to be static, due to lack of information. These COPs very closely match those used by projects modelling the impact of new generations of heat pumps in Scandinavia [VTT TIEDOTTEITA, 2009] and the most efficient SPF for air source heat pumps in the Energy Savings Trust UK field trial was 3.0. A sensitivity analysis of the impact of differing COP's would be an interesting addition to the modelling in the future.

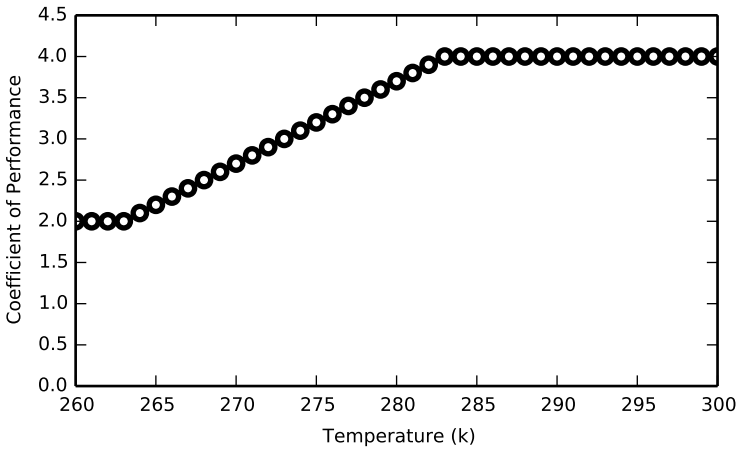

Figure 6.19.: Heat Pump coefficient of performance field trial data.

Boiler replacements NG model improvements in gas boiler efficiencies through the displacement of non condensing ageing boilers by assuming that 1.5 million boilers are purchased each year. Figure 6.20 shows the efficiency projections based on this level of replacement. These were calculated by assuming that current boiler efficiencies are normally distributed around 80% (the value

used in Chapter 5). It is possible that the distribution is not normal as it is likely that there are a number of boilers that are performing well below their rated efficiencies. However the extent of this under performance is unknown and the normal distribution provides a simple method where the highest efficiencies do not exceed 94%. Under the modelled scenarios, 1.5 million of the boilers with the lowest efficiency are replaced with the highest performing boilers each year (these are assumed to be normally distributed around 90% with a standard deviation of 1). This results in a steady increase of the mean boiler efficiency in GB which plateaus at 90%, this is deemed a reasonable limit, considering that when this plateau is reached, boilers will still be ageing and the efficiency will also be lower than that stated by manufacturers.

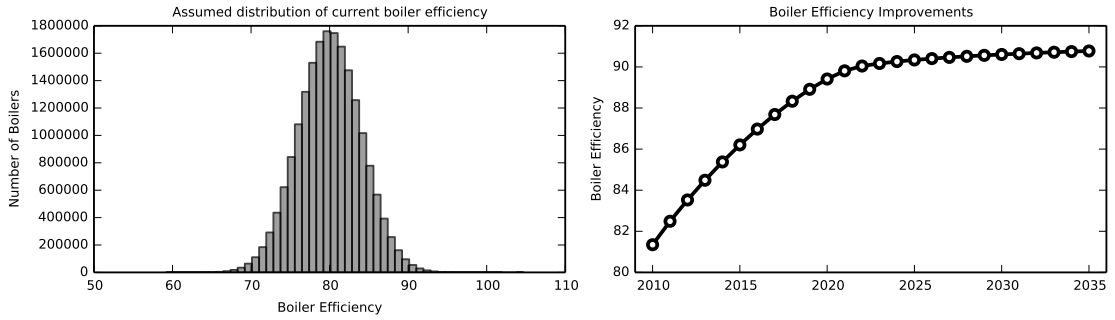

Figure 6.20.: Boiler efficiency projections.

6.4. Summary

NG scenarios are described, including the economic basis and technological changes. The econometric modelling which forms the basis of NG projections provides the core of energy demand and supply changes for SpDEAM to augment and disaggregate in ensuing analysis. NG supply scenarios provide detail on the national annual difference in capacity, but no spatial information or technological details.

Therefore in order to understand potential locations for onshore wind development a detailed spatial analysis of free land for offshore wind farm development has been performed. Criteria for restrictions, shown to be a decisive factor in the estimations described in Chapter 2, are evaluated against existing wind farms. Results show that theoretically there is plenty of suitable land for onshore development, more than will ever realistically be used. It is clear from this analysis that in some cases wind farms have been developed in areas that should be protected. The discussion of criteria for onshore restriction highlights the factors which may prevent the development of wind farms in a particular place. The final selection is used to show how much potential land is available in each grid square. The resultant resource estimate is an estimate of technical onshore potential. This estimate is more robust and detailed than theoretical potential, but is likely to be larger than a potential that applies a greater number of restrictions, for example economic restrictions. The land use of existing turbines have been analysed and the results used to reduce the estimate of available land and find the most appropriate locations for turbine placement in each scenario. This analysis is very interesting as it demonstrates a very clear division between those land uses that are used to place wind farms and those which are not.

Analysis of annual mean onshore wind speed has shown that the whole of GB experiences suitable wind conditions for wind turbine placement when using standard criteria. This is not the case of course at a finer level of spatial aggregation than the model grid, where factors such as topography will alter local wind conditions. Offshore turbine placement is simplified by the existence of development zones which encompass all of the NG projected capacity, even with generous spacing allowed. Therefore it was not necessary to examine suitable locations further. Spatial analysis shows the current state of these zones. A method for joining installed capacity to projected capacity both onshore and offshore has been developed, which uses only available land/sea and tries to harness high annual mean wind speed sites and ensure spatial diversity.

Demand scenarios follow NG's primary decarbonisation strategy of electrified domestic heat demand, other changes to the demand system are enveloped in NG econometric modelling. National annual values for input to the top down section of the domestic demand model are very close in magnitude to those used in the evaluation process, therefore are integrated without alteration. It was, however, necessary to scale national annual values representing non domestic demand to ensure that the correction value developed during the evaluation still applied.

Using NG projections and spatial redistribution methods, it was possible to build a rich spatiotemporally explicit building stock model. This model allows SpDEAM to model the impacts of changes to buildings and the people in them under the influence of varying weather conditions. This is a particular strength of the method and model and considerable addition to NG modelling. Stock models for new and old dwellings were created. The thermal efficiency and size of these homes change at different rates reflecting the need to improve efficiency alongside technological change in order to decarbonise the domestic sector. NG's heat pump scenario dictates uptake and technological replacement. These are redistributed to the grid assuming that this uptake is even across GB. A very efficient heat pump is assumed to be used, on the basis of the fact that NG scenarios state that the GG scenario (the only scenario which integrates significant numbers of heat pumps) overcomes barriers.

7. Scenario Analysis 1

Chapter 2 set out four research questions to be addressed by this thesis. The first of these research questions was addressed in Chapter 3 and Chapter 4 by the combined analysis of CFSR data and SpWind[1]. The second research question was addressed in Chapter 5 by the creation, calibration and evaluation of SpDEAM. Therefore, research questions 3 and 4 remain:

3. Is a gridded approach appropriate for the disaggregation of national scenarios of increased wind capacity and electrified heat?

4. What are the combined implications of electrifying heat and introducing more wind capacity?

This chapter presents the results of the scenario modelling in the context of the remaining research questions. The evaluations of SpWind and SpDEAM have gone some way to answering research question 3, by establishing that a gridded approach provides accurate estimates of wind generation, electricity demand and gas demand. SpDEAM has also been evaluated against measured electricity demand data and published gas demand data, using the first four years of the GG scenario, demonstrating high correlation and low RMSE with both datasets. All of the simulations used in these evaluations have been carried out using weather data describing the same year as the evaluation data. The approach taken for scenario modelling has been to hindcast weather using CFSR data from between 1985 - 2010 to represent 2010 - 2035. Therefore, in order to fully answer the first of the remaining research questions, it is necessary to examine scenario modelling outputs in more detail and compare them against data provided by NG. This chapter therefore considers wind generation from SpWind and electricity demand from SpDEAM. Outputs from both models are compared against NG data and the reasons for divergence discussed.

This chapter also begins to answer research question 4, by exploring the implications of increased wind capacity and the changes to dwellings and heating technologies. The impact of these changes are considered individually in this chapter, the next chapter goes onto answer research question 4 in full, by examining the combined implications of increased wind capacity and electrified heat demand in dwellings.

7.1. Wind generation

7.1.1. Capacity factors

NG estimate annual wind generation from the capacity depicted under each scenario by assuming an annual mean onshore capacity factor of 28% and an offshore capacity factor of 38%. Although

[1] In the following chapters scenario modelling outputs from both the wind model and SpDEAM are compared to various data. To ensure that the origins of the data are clear, the wind model developed for this thesis is henceforth referred to as the Spatiotemporal Wind model (SpWind).

the use of capacity factors to estimate wind generation is an established method, there is no consensus on the appropriate values to use in estimates of GB wind generation. Appropriate capacity factor values are widely discussed in the literature and are calculated in different ways; for example, Sinden [2007] used a mean capacity factor of 30% in his analysis of the UK wind resource, which was calculated from onshore wind measurements between 1970 and 2003. Cannon et al. [2015] find a slightly higher mean capacity factor of 32.5% using MERRA wind speed data. Values have also been calculated from operational data; for example, Staffell and Green [2014] demonstrate from onshore measured generation data that the mean capacity factor is 28.5% when turbines are new, declining to 21% when they are 19 years old. Feng et al. [2010] demonstrate a capacity factor of between 24% and 35% for operational GB offshore wind farms. Other studies have used far higher offshore capacity factors of up to 60% for offshore farms [e.g. Oswald et al., 2008].

There are several publicly available datasets that describe capacity factors. DUKES provide data on annual mean capacity factors calculated in two different ways, either assuming a static annual capacity or a capacity that changes over the year. Staffell and Green [2014] provide annual mean capacity factors by wind farm in their supplementary data, which can also be calculated from raw ROC data. Finally capacity factors can also be calculated from the Elexon data. Each of these datasets were discussed in more detail in Chapter 4. Figure 7.1 shows historic capacity factors based on the aforementioned datasets.

Comparing the capacity factors used by NG to those discussed in the literature and described by Figure 7.1 demonstrates that NG have selected values that are reasonably high. They assume that historic values represent those expected under scenarios depicting future capacity. Significantly higher values have been used in some research, particularly for offshore capacity, as described above.

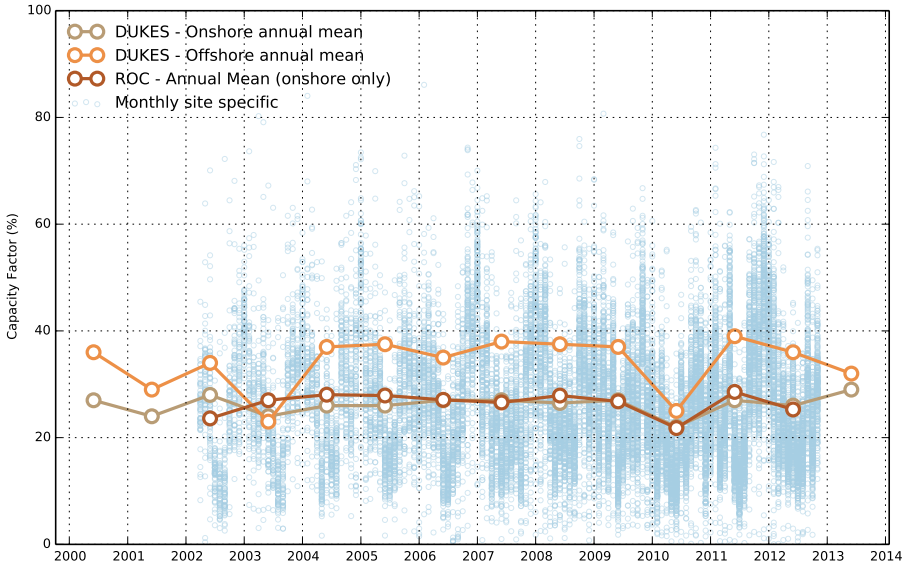

Figure 7.1.: Historic national average capacity factors, data source DUKES.

SpWind uses a different method to estimate wind generation from NG depictions of capacity. The key differences between SpWind and using a static capacity factor are that SpWind estimates wind generation using hourly wind speed data which is variable over both time and space and spatially

allocates wind capacity to realistic future locations. This results in spatial variability between scenarios. Mean annual capacity factors have been calculated from SpWind output. Table 7.1 shows the average onshore and offshore capacity factors over the whole scenario period. The table demonstrates that under all scenarios offshore capacity factors derived from SpWind are higher than those used by NG (between 12.4% and 19.2% higher). In contrast, onshore capacity factors derived from SpWind are lower than those used by NG (between 1.9% and 2.6% lower). The values shown in the table also demonstrate the magnitude of the difference between onshore and offshore capacity factors derived from SpWind. The difference between the smallest and largest capacity factors derived from SpWind is much smaller onshore (0.7%) than offshore (6.8%).

	GG	SP	LCL	NP	NG
Onshore	26.1	25.9	26.1	25.4	28
Offshore	57.2	55.4	54.8	50.4	38
Combined onshore and offshore	43.6	41.2	40.0	35.7	-

Table 7.1.: Mean SpWind capacity factors for each scenario and NG's assumed capacity factors.

Figure 7.2 shows how capacity factors from SpWind change over the course of the scenarios. As well as separate onshore and offshore capacity factors, the plot shows the capacity factor after the two have been combined. The dashed lined represent values used in NG estimations of wind generation. The plot demonstrates that offshore capacity factors increase over time under the scenarios which have large offshore capacity. The majority of this increase occurs between 2019 and 2023, after this offshore capacity factors stabilise. NG's use of a static offshore capacity factor means that the difference increases from 6% in 2010 to 28% under the GG scenario (the scenario with the largest offshore capacity). Onshore there is no apparent increase in SpWind capacity factors over the course of the scenarios, which means that the difference between SpWind and NG remains below 10% under all scenarios. Overall SpWind capacity factors in the GG, SP and LCL scenario clearly increase over time, due to the increasing influence of offshore capacity. Consequently, after 2022 SpWind weighted average capacity factors are larger than those used by NG for *offshore* capacity. The NP scenario has less offshore capacity which means that overall capacity factors do not increase as much as in the other scenarios.

Figure 7.2 shows that there is little difference in onshore capacity factors from SpWind between the scenarios (<1 %); offshore there is a larger difference (up to 6.8% between GG and SP). The relative differences demonstrate the limited diversity available onshore as installed capacity already reaches the extremities of the GB land mass (see 2010 in Figure 4.8) and new capacity is placed in similar locations (see 2035 in Figure 6.9). The magnitude of the onshore capacity does not affect the capacity factor, except when onshore and offshore output is combined. Offshore capacity factors diverge between scenarios to a greater extent, due to the different locations used and the differing amounts of capacity in those locations under each scenario. The difference in mean capacity factor between scenarios is therefore predominantly affected by offshore capacity. Although there is a large difference between GG and NP offshore there is a much smaller difference between the scenarios using the further from shore locations (GG, SP and LCL only differ by 2.2% in 2035). The difference between the GG, SP and LCL scenarios is driven by the amount of capacity that they have in those locations, indicated in Figure 6.9.

Onshore capacity factors derived from SpWind are in line with those described in the literature and the historic data summarised in Figure 7.1. SpWind offshore capacity factors are, however, much

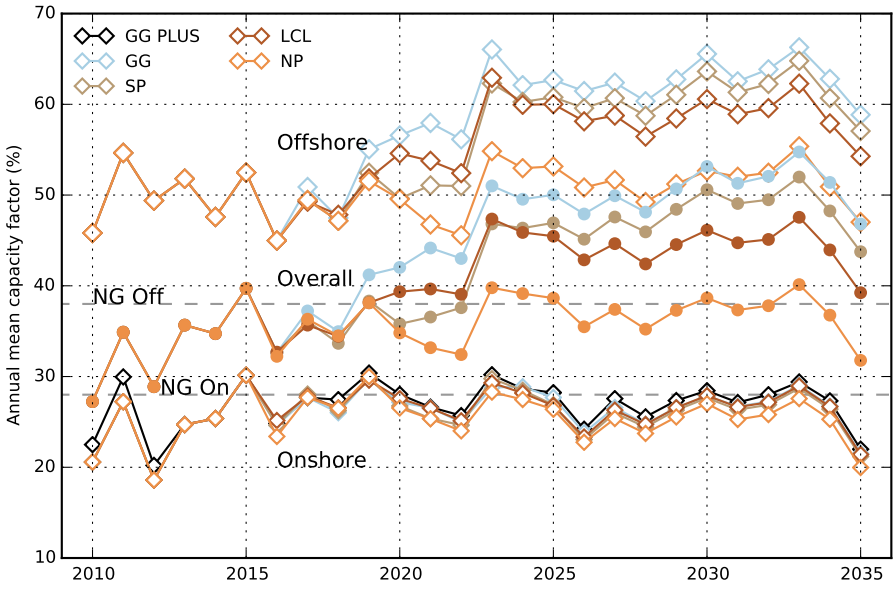

Figure 7.2.: Annual mean SpWind capacity factors, onshore vs. offshore.

greater than almost all of those discussed above, particularly in the GG, SP and LCL scenarios. These scenarios use locations that are further from shore than existing capacity, where wind speeds are higher, due to the smaller influence of the roughness of land surfaces. These locations are not used in the NP scenario which results in lower offshore capacity factors. The linear correction factor applied to SpWind has an effect on the capacity factor values described here. The correction factor of 1.55 when applied to hours of high generation after simulation means that in some cases generation exceeds 100% of the installed capacity. Where this was the case, generation has been capped at the maximum installed capacity. This may mean that there are a larger number of hours where the capacity factor is 100% than would be simulated without this correction factor. However high offshore capacity factors have been found elsewhere, for example in Denmark, where long term mean capacity factors of up to 50% have been experienced in locations closer to shore, such as the Anholt 1 wind farm, which is 21 km from shore [Energy Numbers, 2015]. This suggests that the impact of the correction factor may be small in this case. The effect of the correction factor on the number of hours where capacity factors are 100% is quantified in Section 7.1.4 and Section 8.4.

As well as demonstrating the difference between SpWind and NG data, Figure 7.2 describes variation in SpWind capacity factors from year to year, which is not seen when using an assumed average annual capacity factor to estimate generation. Some of the inter annual changes in capacity factors reflect those which have been experienced by historical wind capacity during the same wind years. For example Figure 7.1 shows that a significant reduction in measured capacity factors was experienced in 2001, 2003 and 2010. CFSR wind data from those years was used to simulate SpWind generation in 2026, 2028 and 2035. Figure 7.2 shows that the SpWind simulation resulted in the same reduction as seen in the historic data. This demonstrates that some of the inter annual change in capacity factors is driven by wind speed and that CFSR data represents annual changes in wind speed well. The rest of the inter annual change is driven by changes in capacity, both in terms of magnitude and location. Onshore inter annual variation in capacity factors, excluding

2035, is much smaller than that seen offshore. This suggests that wind speed changes becomes less volatile when exposed to land at aggregated spatial and temporal resolutions. Vincent et al. [2014] have found that this is also the case at smaller spatiotemporal resolutions using both mesoscale modelled wind data and in situ measurements. The smaller difference implies that onshore wind generation may be more predictable over long periods. Overall annual changes in capacity factors are mirrored in each of the scenarios, excluding a period between 2019 and 2022. Referring back to Figure 6.2 it is clear that this is a period where the rate of change in capacity differs between scenarios. The method used to allocate capacity to grid squares means that when the change in capacity differs between scenarios the capacity is likely to be placed in different locations. If the wind speed varies between these locations this can drive divergence in capacity factors between scenarios.

7.1.2. Annual wind generation

NG estimate annual generation from each of the scenarios based on the capacity factors described above. Figure 7.3 shows these values in comparison to those estimated using SpWind. The plot demonstrates that SpWind output is larger than that predicted by NG for all years. The underestimation of generation from NG in comparison with SpWind is a result of the underestimated offshore capacity factors described above. The difference between SpWind and NG is the same for all scenarios at the beginning of the scenario period. The magnitude of the underestimation increases over time owing to the introduction of greater levels of offshore capacity. Those scenarios which introduce more offshore capacity, further from shore, where the highest wind speeds and therefore capacity factors are experienced, show the greatest difference between SpWind and NG. The plot emphasises the difference between using a static capacity factor and variable wind speed data to estimate generation, as the SpWind method introduces inter annual variability.

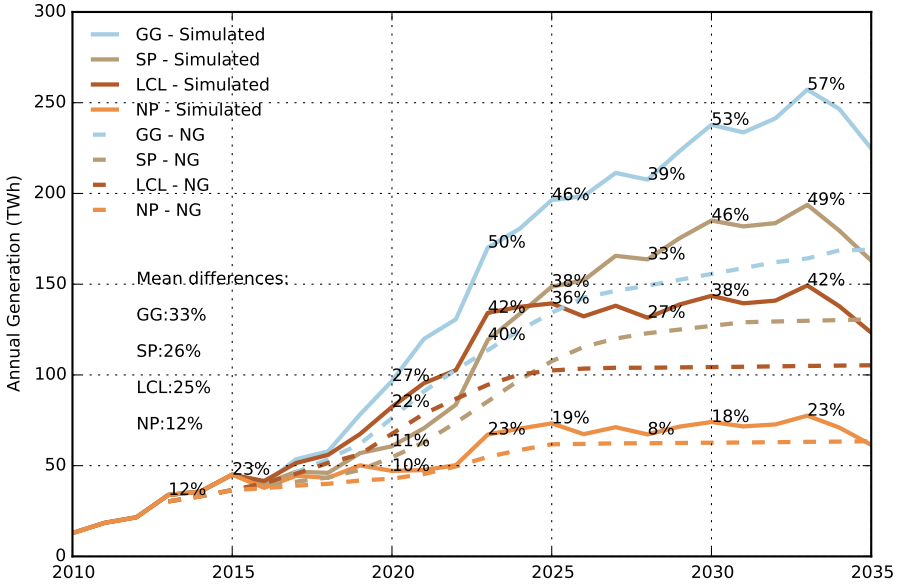

Figure 7.3.: Annual wind generation, comparison between SpWind and NG data.

Comparing aggregated onshore and offshore generation has shown the combined impact of NG using similar onshore capacity factors and lower offshore capacity factors than those derived from the

SpWind method. Figure 7.4 shows the onshore and offshore generation separately. This demonstrates the extent to which onshore and offshore generation contribute to the difference in generation between the two methods. As NG do not provide disaggregated output, onshore and offshore generation were derived using the data provided on capacity and capacity factors.

The plot shows that in most years SpWind onshore generation is lower than NG, and that SpWind onshore generation never significantly exceeds that depicted by NG. In the long term, SpWind onshore generation is 4% less than NG in the GG scenario, 9% less in SP, 7% less in NP and approximately the same in LCL. SpWind offshore generation is higher than NG for all years. For the NP scenario the difference does not increase significantly, starting at 37% and rising to 46%. The difference between SpWind and NG increases from 27% to 64% at its peak in the LCL scenario, 71% in the SP scenario and 75% in the GG scenario. Therefore the plot shows that the difference in combined generation between SpWind and NG described in Figure 7.3 is driven entirely by the difference in offshore wind speeds assumed by NG and modelled by SpWind. Comparing the percentage differences shown in Figure 7.3 and Figure 7.4 demonstrates that by combining onshore and offshore generation the difference between SpWind and NG is reduced by approximately 20%.

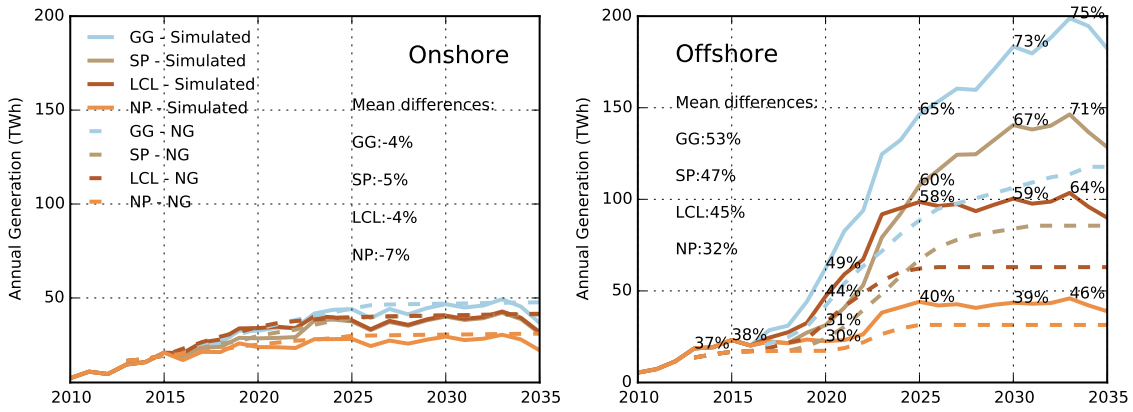

Figure 7.4.: Annual wind generation, comparison between SpWind and NG, onshore vs. offshore.

Comparing Figure 7.4 and Figure 6.2 shows that the growth in offshore generation follows the growth in offshore capacity. In the case of NG, generation and growth follow each other because of the linear relationship between generation and capacity, which is a result of the use of a single capacity factor. The increase in SpWind offshore generation is not as smooth as seen in the NG output, this is due to the use of historic, variable wind speeds used to simulate generation and the non linear curve used to estimate generation from those wind speeds (Figure 4.11). The percentage difference between SpWind and NG offshore generation is shown for each scenario for selected years in Figure 7.4. The plot shows that in each of those years the difference is largest in the GG scenario, then SP then LCL then NP. This is dictated by a combination of the magnitude of offshore capacity and the wind speeds harnessed by that capacity. The capacity factors described in Figure 7.2 remove the influence of capacity so the difference between scenarios each year demonstrates the effect of the spatial configuration of capacity in isolation. Figure 7.5 shows the percentage difference between SpWind and NG offshore output alongside SpWind offshore capacity factors. The plot shows that annual changes to capacity factors are mirrored in generation. The difference between scenarios increases at a similar rate and stabilises at the same time. This indicates that the difference between the scenarios is predominantly driven by levels of offshore capacity.

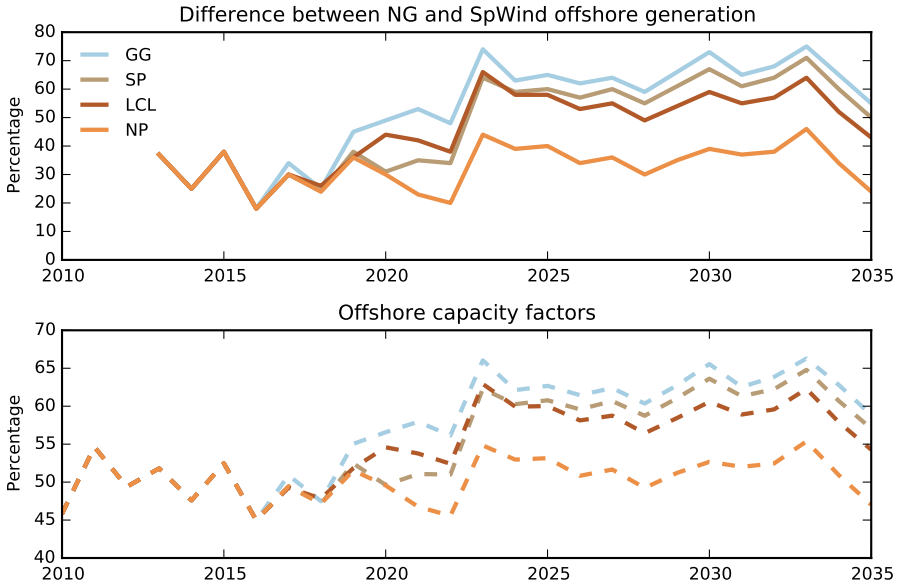

Figure 7.5.: Percentage difference between SpWind and NG, offshore generation and capacity factors.

An alternative way to remove the influence of capacity on the difference between the NG and SpWind methods is to explore how the percentage difference in generation between the two varies when capacity in a scenario remains static between years. Static capacity ensures that there is no change in the spatial layout, therefore variation in the percentage difference will demonstrate the extent to which the different wind conditions experienced each year affect the difference in generation between NG and SpWind. Figure 7.6 shows how the percentage difference between NG and SpWind offshore generation varies depending on the level of offshore capacity. In the NP scenario, offshore capacity remains at 9 GW for 14 years (between 2022 and 2035) and changes in wind speed each year mean that the difference with NG varies between 22% and 46%. In the LCL scenario, offshore capacity remains at 19 GW for 11 years (between 2025 and 2035) and the difference varies between 42% and 61%. In the SP scenario, offshore capacity remains at 26 GW for 6 years (between 2030 and 2035) and the difference varies between 50% and 70%. This demonstrates that by using a static capacity factor the NG method does not take into account potential changes in offshore generation of over 20%.

This section has demonstrated an advantage of the disaggregated, gridded, modelling approach employed in SpWind over an approach that assumes the same wind conditions will be harnessed by all capacity under different scenarios, in the ability to quantify the consequences of the location of diverging levels of onshore and offshore capacity between scenarios and over different meteorological years. This can improve the planning of wind farm siting and of how wind can be integrated into the system with transmission, storage and back-up generation.

7.1.3. GB wind speed

The analysis so far shows temporal variation in wind speed and generation at an annual resolution. This section explores how the data from CFSR on GB wind speed varies during each year, both

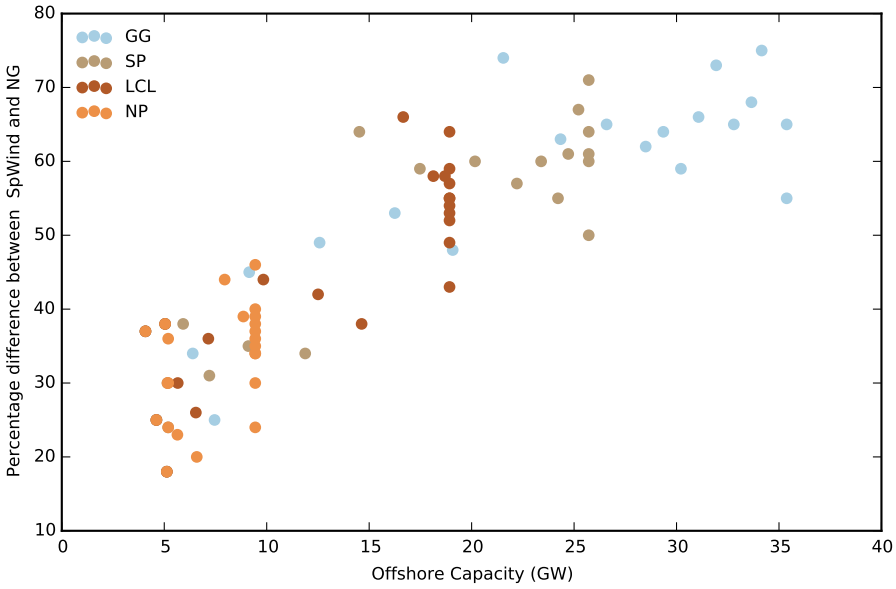

Figure 7.6.: The percentage difference between SpWind and NG at different capacities.

onshore and offshore, to highlight the driving force behind changes in wind generation in SpWind.

Figure 7.7 describes the difference between onshore and offshore wind conditions for each of the years in the CFSR v1 dataset. The grey histograms describe the distribution of onshore wind speeds at 60 m (the hub height used in SpWind onshore simulations) over the year. A national mean wind speed was calculated using each onshore grid square for each hour of the year (each bin = 0.5 m/s). Each grey histogram is followed by a red histogram which describes the offshore wind conditions for the same year. Mean offshore hourly wind speed at 80 m (the hub height used in SpWind offshore simulations) was calculated for all of the grid squares which contain offshore development zones; therefore the histogram represents those wind speeds which will be harnessed by offshore capacity. Not all of those grid squares may be used in that year, particularly in the case of the NP scenario which only uses those development zones close to shore.

The range of national hourly mean onshore wind speeds (2 m/s - 20m/s) is smaller than offshore (2 m/s - 25 m/s). Therefore there are more hours where the national hourly mean wind speed is on or closer to the median, onshore than offshore. The median national hourly mean onshore wind speed is between 6 m/s and 7 m/s. The offshore median hourly national hourly mean onshore wind speed is between 9 m/s and 10 m/s. Offshore, a greater proportion of hours experience a higher wind speed, demonstrated by the greater number of values on the right hand side of the distribution. The differences between national hourly mean wind speed onshore and offshore illustrate some of the reasons why capacity factors are larger offshore than onshore, which drives increased wind generation. Capacity factors are also affected by turbine size and consequently the way in which wind speeds are harnessed.

The analysis above has shown that there is clear difference in offshore capacity factors between SpWind and NG. This difference has been attributed to the fact that NG base their capacity factors on historical offshore generation that has used locations that are close to shore, whereas SpWind places capacity in locations further from shore, where wind speeds are higher. The higher wind speeds also drive the difference between scenarios in SpWind, as some scenarios place more

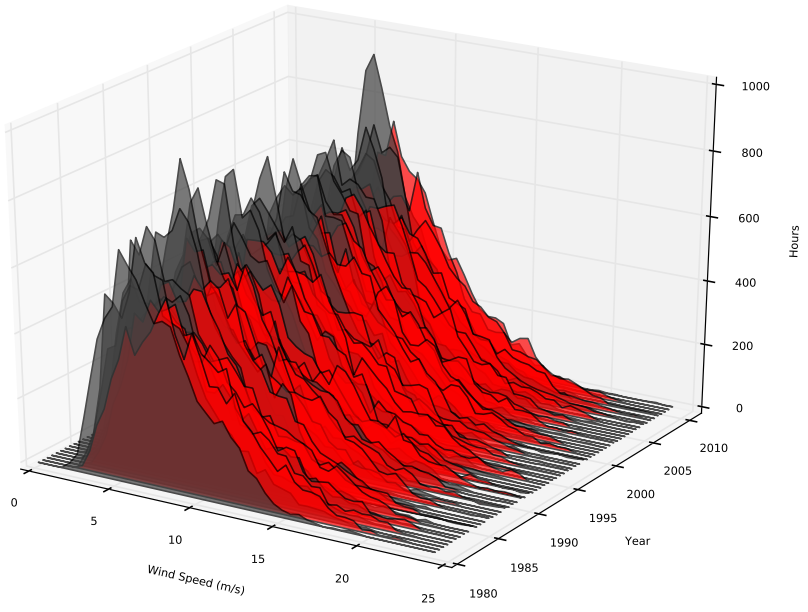

Figure 7.7.: Onshore and offshore wind speeds, 1980 - 2010. The grey histograms represent onshore wind speeds, the red histograms represent offshore wind speeds.

capacity in the further from shore locations than others. Figure 7.8 shows histograms of national hourly mean offshore wind speed. The grey histograms represent the wind speeds experienced in the offshore grid squares used for capacity in the NP scenario, which does not use the development zones further from shore. The red histograms represent the wind speeds experienced in the offshore grid squares used for capacity in the GG scenario, which does use development zones further from shore. The difference between the spatial configuration of capacity between the two scenarios is illustrated in Figure 6.9. Figure 7.8 shows that by using development zones further from shore the mean hourly wind speed that capacity is exposed to is increased. The maximum mean wind speed increases from less than 20 m/s to up to 25m/s. Furthermore, there are more hours where the mean wind speed is between 10 m/s and 15 m/s and the median wind speed increases from 6 m/s and 7 m/s to between 9 m/s and 10 m/s. In many respects the offshore wind speeds experienced by the NP scenario are more similar to the onshore wind speeds described by the grey histograms in Figure 7.7 than the offshore wind speeds experienced by the GG scenario. Figure 7.2 shows that there is a difference, as the offshore capacity factors in the NP scenario are significantly higher than onshore.

It should be noted that CFSR may underestimate onshore wind speed to a greater extent than offshore, as it averages over a 0.5° x 0.5° grid. Topology and surface roughness, which affect wind speed, vary significantly on land within the grid squares, unlike at sea. Previous analysis in this thesis has shown that high elevation sites onshore, where higher than average grid wind speeds would be expected, are not well represented, whereas offshore wind speed has been shown to be more homogeneous. This difference is unlikely to significantly alter the shape of the onshore histogram in GB, owing to the limited number of high elevation locations and limited number of grid squares where the majority of land is at a high elevation. In more mountainous locations this difference may be more pronounced. The effect that this potential underestimation of onshore

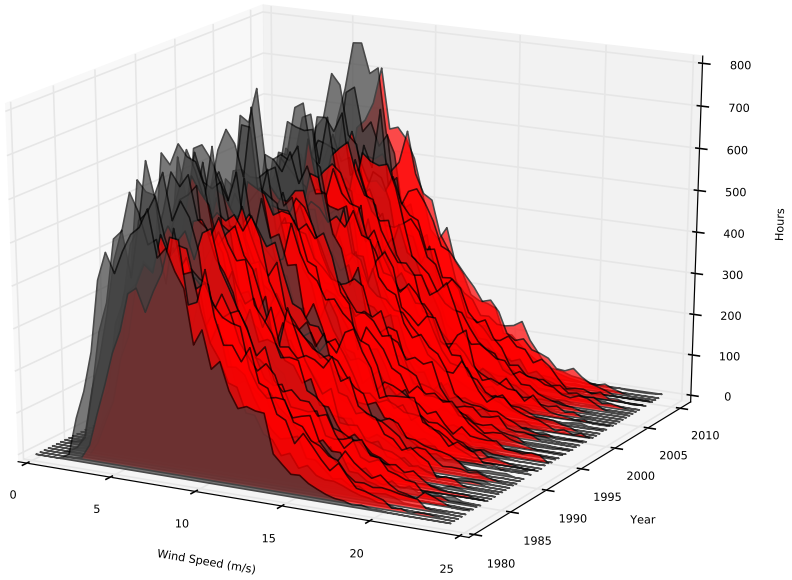

Figure 7.8.: Offshore wind speeds in wind farms development zones, 1980 - 2010. The grey histograms represent the zones used in the NP scenario, the red histograms the zones used in the GG scenario.

wind speed has on estimated generation in SpWind has been limited by removing high elevation sites from consideration for wind farm development.

As well as demonstrating that wind speeds are different onshore and offshore, the analysis of wind generation and capacity factors from SpWind has shown that wind speeds vary between years.Figure 7.2 shows that there are several periods where capacity factors increase or decrease significantly in comparison with the preceding years. Two periods have been selected to explore the changes in wind speed that drive the change in capacity factors: 2021 to 2023 and 2032 to 2035. These years are driven by wind data from 1997 to 1999 and 2007 to 2010 respectively.

Figure 7.9 demonstrates that the higher capacity factor described by SpWind in 2022 (driven by 1998 wind speed data) compared to the previous and subsequent years is a result of a greater number of hours when the national mean wind speed was slightly higher than the annual median (1-2 m/s higher), rather than more hours where the wind speed was very high ($>$ 20 m/s). Onshore there were more hours when wind speed was between 7-10 m/s and fewer hours where wind speed was between between 3-5 m/s. Offshore there were more hours between 7-12 m/s and fewer between 3-5 m/s.

Figure 7.10 shows that the lower capacity factors described by SpWind in 2034 and 2035 (driven by 2009 and 2010 wind speed data) compared to previous years are a result of fewer hours where onshore mean national wind speed is greater than 10 m/s and offshore mean national wind speed is greater than 15 m/s. The combination of Figure 7.9 and Figure 7.10 show that wind speed conditions are complex and differences in generation between years can be driven by changes to extreme wind speeds and changes to more moderate wind speeds.

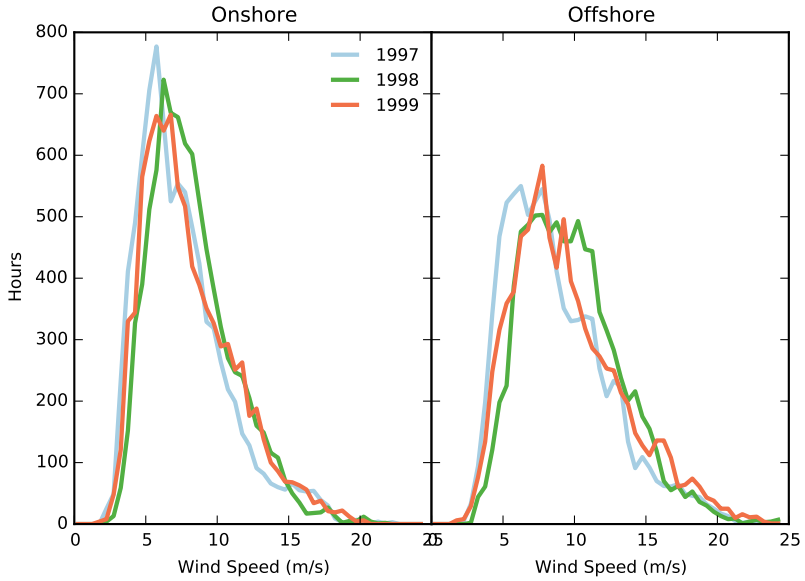

Figure 7.9.: Histograms of onshore and offshore mean national wind speeds, 1997 - 1999.

7.1.4. Load duration

Analysis of the wind speed data has shown the yearly distribution of wind speeds for each scenario. This section explores how that distribution is harnessed by each scenario, by examining how hourly capacity factors vary over the scenario period and across different years. Load duration curves are used to show how power varies over a given time period. In the literature these are used to show the likelihood of power output being above a certain threshold [e.g. SKM, 2008, Ofgem, 2012b, Oswald et al., 2008].

Figure 7.11 shows the load duration curves for each scenario. Onshore and offshore curves are shown separately, alongside total generation, for the whole length of the scenarios. For comparison, a historic load duration curve is shown, calculated using the Elexon data. The plot illustrates the extent of the different distributions of capacity factors between SpWind generation and historic measured generation. Overall the difference is that a higher capacity factor is experienced by SpWind capacity for a greater proportion of time than historic capacity. This increase is primarily driven by an increase in offshore capacity factors, as the onshore load curves are lower than the combined historical load curve, indicating that higher capacity factors are experienced for a smaller percentage of the time. For example SpWind scenarios experience onshore capacity factors above 50% for approximately 15% of the time compared to 20% of the time under historic Elexon capacity. Onshore SpWind capacities exhibit very small differences between scenarios of less than 2% of hours at any given capacity factor, equating to less than 500 hours over the scenario period. This reinforces the observation made above that onshore capacity factors vary very little between scenarios. The GG, SP and LCL capacities follow similar paths in terms of overall capacity factors with differences of less than 10% of hours at any capacity factor. The differences between LCL and SP are between 2% and 4%. Differences of a similar magnitude are experienced offshore. Owing to a lack of offshore capacity the NP scenario clearly diverges from other scenarios, showing differences in terms of hours of more than 10% in comparison to the GG scenario.

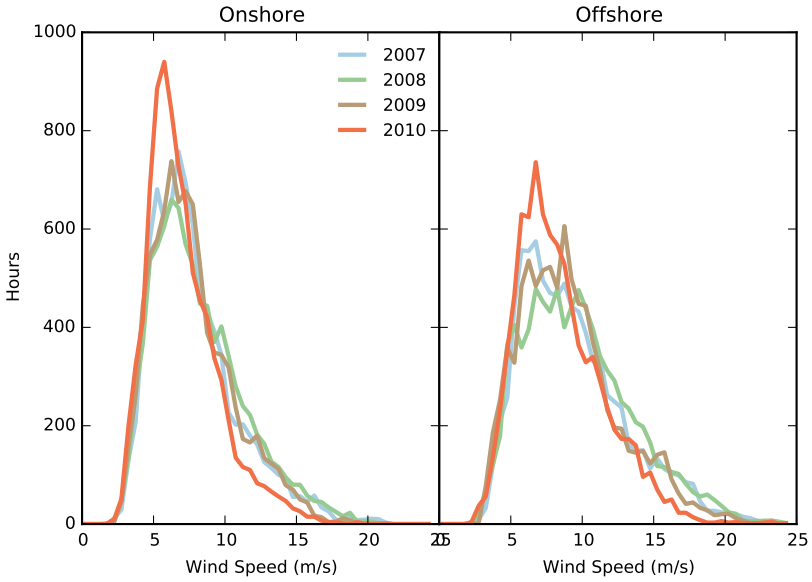

Figure 7.10.: Histograms of onshore and offshore mean national wind speeds, 2007 - 2010.

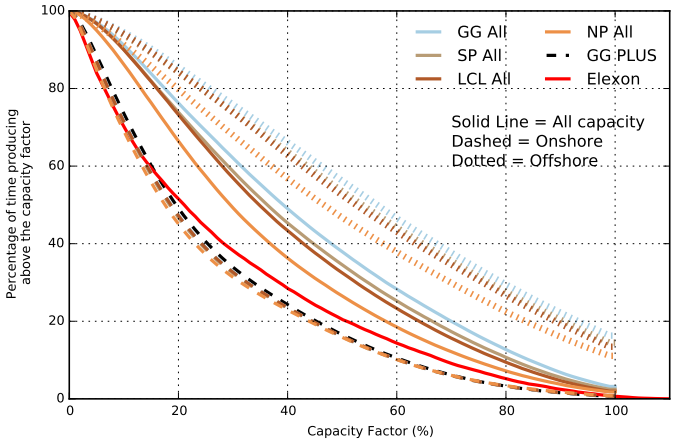

Figure 7.11.: Load duration curves for each scenario.

The plot shows that SpWind offshore hourly capacity factors are 100% for between 10% and 16% of the time over the whole scenario period (GG= 16%, SP = 14%, LCL= 13% and NP= 10%). Onshore capacity factors do not reach 100%. Figure 2.2 shows that for turbines to operate at 100% of rated output the wind speed must be between 15 m/s and 25 m/s, both onshore and offshore. Therefore in order for the capacity factor to be 100% the mean wind speed across the areas where capacity is installed must be in the same range. Figure 7.12 shows the percentage of time that wind speed is between 15 m/s and 25 m/s in the grid squares used for the GG and NP scenarios (the LCL and SP scenarios are not shown but are very similar to the GG scenario; the percentage of hours between 15 m/s and 25 m/s are 9.3% and 10.2%). Comparing the number of hours between 15 m/s and 25m/s to the percentage of time at 100% capacity shows that there is a difference of 5.7% in the GG scenario, 3.8% in SP, 3.7% in LCL and 5.9% in NP. This difference is a result of the correction factor applied to SpWind output to account for the underestimation of generation, where a number of hours increase to the equivalent of 15 - 25 m/s wind speed. The percentage

change is quite small and shows that the correction factor does not have a large impact in this respect.

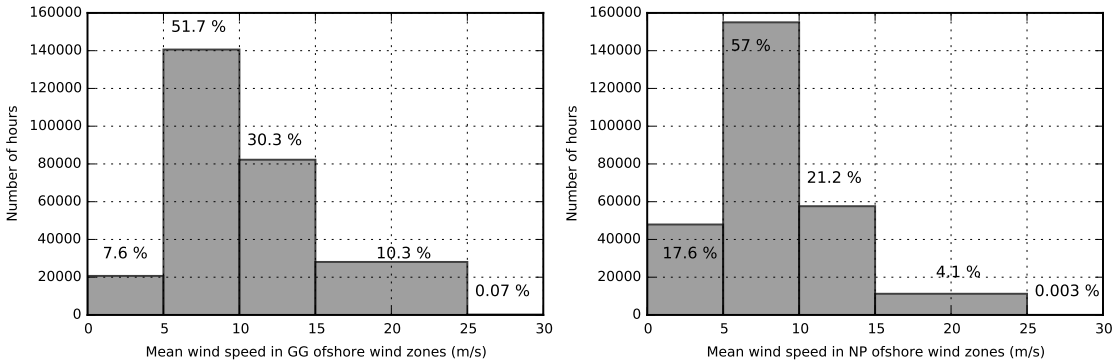

Figure 7.12.: Histograms of offshore wind speeds in grid squares used by the GG and NP scenarios.

Figure 7.13 shows how load duration curves change over time. The top left subplot, which describes combined onshore and offshore generation, demonstrates that, overall, there is an improvement in the way that the fleet harnesses the wind between 2010 and 2035 for all scenarios, as the load duration curves shift to the right, indicating an increase in capacity factors (2010 output is the same for all scenarios). In 2010 the mean capacity factor is above 50% 15% of the time. In 2035 this increases to 18% of the time in the NP scenario, 30% in LCL, 38 % in SP and 40% for GG.

The top right subplot of Figure 7.13, which describes onshore generation, shows that there is little, if any, difference in the way that onshore turbines harness the wind in GB between 2010 and 2035 for any of the scenarios, suggesting that the current onshore wind fleet may have reached the peak of geographical diversity that GB has to offer. The previous analysis of capacity factors and wind speeds has shown that the wind years used to simulate those capacities (1985 and 2010) are similar, meaning that the primary difference is the magnitude and spatial diversity of capacity.

The bottom left subplot of Figure 7.13, which describes offshore generation, demonstrates that the majority of the difference between 2010 and 2035 is driven by capacity being exposed to different offshore wind conditions. In 2010 the mean capacity factor is above 50% for 40% of the time. In 2035 this remains at 40% of the time in the NP scenario, but increases to 50% in LCL, 55% in SP and 57% for GG. These percentage changes are smaller than those seen in the combined capacity factors as a result of the increasing share of capacity that is offshore. The subplot also shows that the higher capacity factors experienced in 2010 are not experienced in 2035 by the NP capacity. This effect is driven by wind speed differences between the years, because no offshore capacity has been removed from any of the scenarios over the period of the scenarios.

The bottom right subplot of Figure 7.13 shows the annual change in load duration over the whole scenario period under the GG scenario. The GG scenario has been selected as an example because it experiences the biggest change in both magnitude of capacity and spatial diversity. The subplot demonstrates that 2035 is not the peak of the load duration curve, despite having the largest capacity, highlighting the dependence of generation on wind speed. As Figure 7.2 has shown, the wind speed data used to simulate 2035 (2010) does not have the highest number of hours in the power producing range. The subplot demonstrates that a smaller capacity can produce an improved load duration curve as the 2016 curve describes the highest capacity factors over time

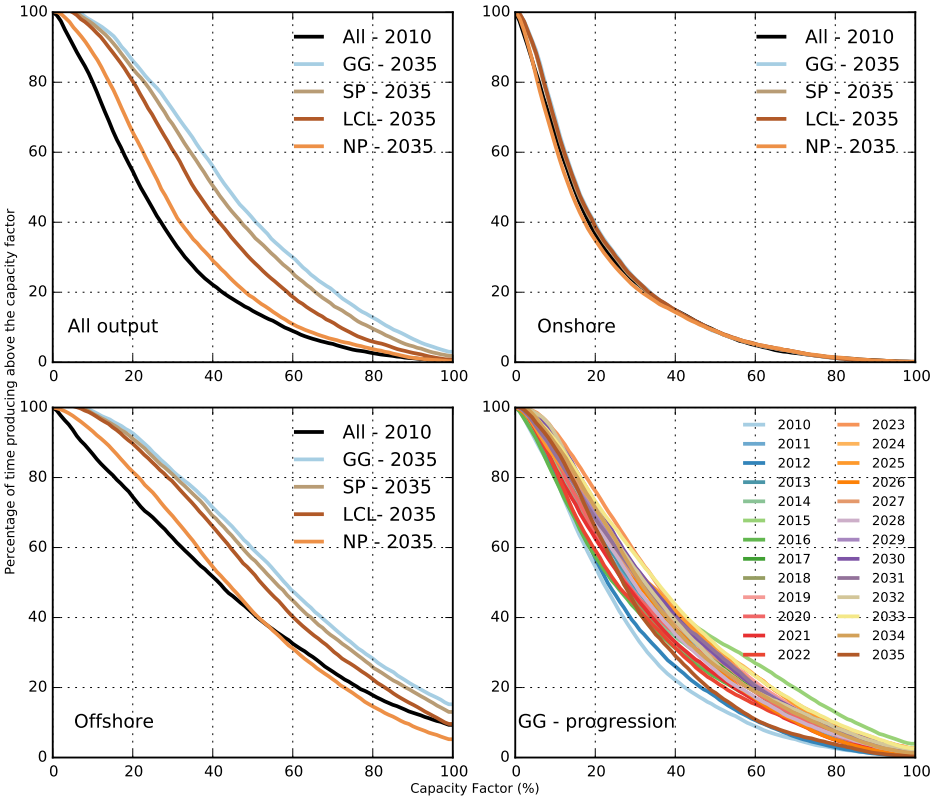

Figure 7.13.: Change in load duration 2010 - 2035.

(using wind speed data from 1991). However, the general trend is that increased capacity and greater harnessing of high offshore wind speeds in the scenarios, improves the load duration curve and therefore the effectiveness of a wind fleet. This improvement comes at the cost of increased investment in cabling, larger turbine foundations and towers, and offshore maintenance. The costs of installing wind capacity in expensive locations must be balanced against cost savings elsewhere in the energy system, such as a reduction in the need for storage or backup generation. Future work can include the introduction of cost per grid square so that the cost of improved capacity factors can be quantified. One example of how the work carried out in this study may be extended to economic and other analyses.

7.1.5. Geographical diversity

Temporally disaggregated analysis of wind generation has been performed. This section continues the disaggregation of the generation data by exploring the relationship between the wind producing grid squares, therefore introducing spatial disaggregation. The method used follows that developed by Sinden [2007], who carried out an analysis that neatly described the difference between onshore in situ measurements of wind speed, by comparing the distance between pairs of wind speed sites and the correlation between time series of simulated output at each of the sites (using Pearson's r). The evaluation of CFSR used the same set of onshore in situ measurements as Sinden's analysis who assumed that the sites represent the wind resource that would be harnessed by a "diversified" wind network. Figure 7.14 shows the results of that analysis, a plot of distance against correlation, which demonstrates that the further apart the sites, the lower the correlation between the output.

The maximum distance between sites approaches 1200 km as the study covered the whole of the UK. The plot describes a fairly narrow range of coefficients at each distance. Between 700 km and 1100 km the correlation between output is very low and there are several pairs of sites which exhibit no correlation (Pr = 0). The correlation between the closest sites (which are approximately 20-30 km apart) is very high (Pr = 0.9). The difference in wind speeds between locations, that increases with distance, is potentially important for the value of wind power if wind farms are built far enough apart so that wind power will be generated at different times, because the magnitude of matching mechanisms will reduce alongside the rate of change of wind generation.

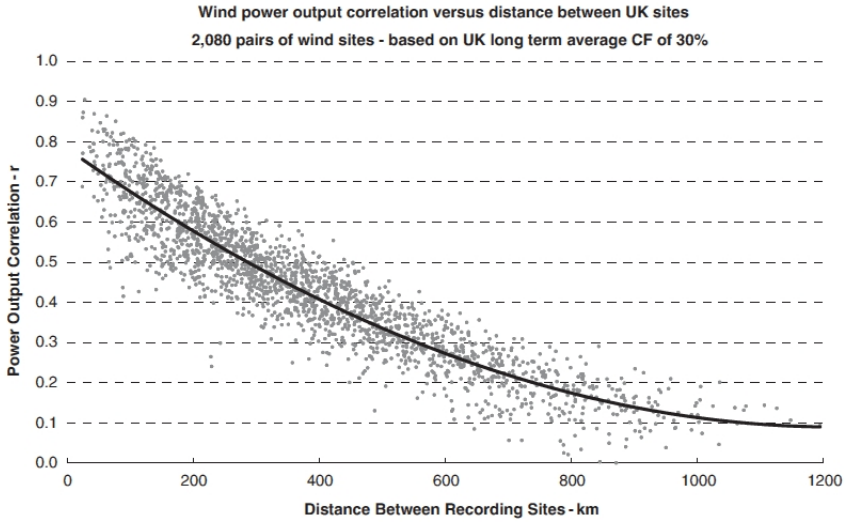

Figure 7.14.: UK wind power output correlation by distance between recording sites, figure source Sinden [2007, p.118].

Here Sinden's method is used to analyse whether the spatially allocated capacity from each of NG's scenarios follows the same pattern. This has the advantage of analysing wind speeds weighted to realistic locations, rather than assuming that site specific data represents distributed future capacity. The analysis performed here also adds offshore locations, which may alter the relationship between wind speed time series, because of the difference in wind conditions described in Figure 7.7. This difference could add extra distance to the equation. The analysis performed here is limited to GB and offshore development zones. There is significant overlap in wind speed data between the analysis performed here (1985 - 2010) and Sinden's analysis, which uses wind speed data from 1970 - 2003 (few of the in situ measurements extend to the earliest period of Sinden's analysis, as shown in the evaluation of the CFSR data, which uses the same data); therefore results can be compared.

Figure 7.15 shows the effect of distance on the correlation between time series of generation under each SpWind scenario. The longest time series possible for each grid square was used; these time series vary in length owing to different operational commencement years. Where one grid square time series was shorter than the other, only the shorter length of time is used for comparison. Unlike Sinden's analysis, capacity varies in *each* grid square over that time, particularly offshore. The likely effect of this will be a reduction in correlation coefficients. In contrast, the use of more generalised wind speed time series in this analysis from CFSR, as opposed to the site specific locations used in Sinden's analysis, may increase the correlation coefficients. The plots are divided

to show the difference between onshore and offshore correlation, so that the first column shows the correlation between onshore and offshore sites, the second onshore and onshore and the third offshore and offshore.

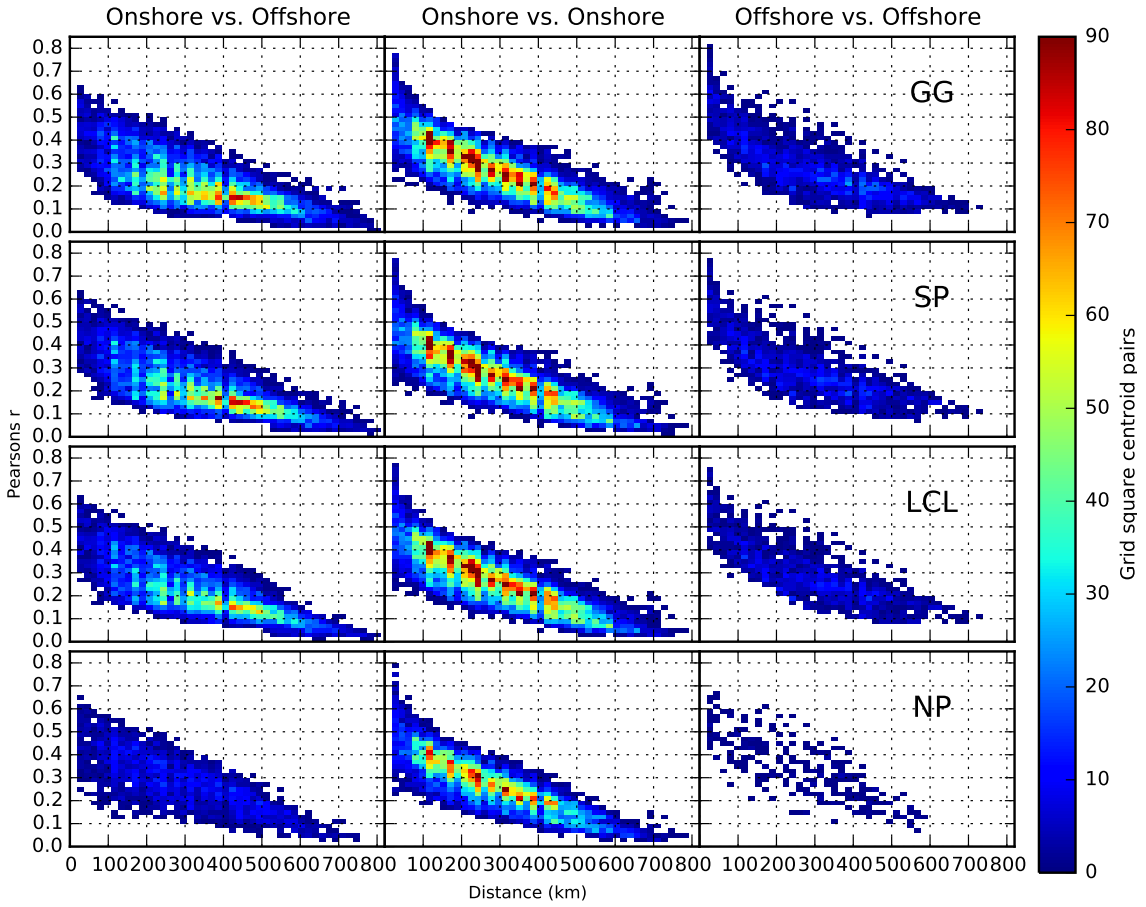

Figure 7.15.: Correlation between generating grid squares for each scenario, 2010 - 2035.

The onshore v.s onshore plots in the central column of Figure 7.15 show that the reduction in correlation as distance increases described by SpWind is similar to that found by Sinden. In contrast to the analysis performed by Sinden, the largest distance between grid squares is limited to less than 800 km by restricting analysis to GB rather than UK. The largest distance is also slightly reduced by the use of grid squares rather than points, as the minimum distance between grid square centroids (used to calculate distances) is 35 km. The removal of the sites that are more than 800 km away from each other results in a lack of sites with a correlation of 0. The use of grid squares also reduces the number of highly correlated sites, as a result of not having sites closer together than 35 km, whereas some of the sites used in Sinden's analysis are less than 30 km apart. Generally correlations are lower over the same distances as those shown by Sinden. This may be due to differences introduced by hub height correction methods, however it could also be due to differing changes in capacity between grid squares (capacity is static in Sinden's analysis). There is little discernible difference between scenarios in terms of onshore correlation, other than a few isolated locations which are approximately 700 km apart in all of the scenarios other than NP.

The left hand column of Figure 7.15 shows that adding offshore wind capacity increases the maximum distance achieved with solely onshore locations by approximately 50 km for the GG, SP and

LCL scenarios. The maximum distance in the NP scenario is lower in the onshore vs. offshore analysis than the solely onshore, also the NP plot contains fewer grid square pairs overall, as fewer offshore locations were used to place capacity (Figure 6.9). The lack of increase in maximum distance on the NP scenario demonstrates that it is necessary to use the development zones that are furthest from shore to increase the temporal diversity of GB wind generation. The small increase in the maximum distance and number of sites at this distance in the GG, SP and LCL scenarios show that it may be necessary to use locations outside of the development zones described in this thesis, to achieve a significant increase on the temporal diversity that is achievable with solely onshore locations. The use of offshore sites also has the effect of reducing correlation between sites over a similar distance in comparison with solely onshore locations. The plot shows that the majority of sites are a similar distance apart to the bulk of onshore sites (300 - 600 km), but exhibit slightly lower correlation coefficients (0.1-0.2 in onshore vs. offshore and 0.2-0.3 onshore vs. onshore). These lower correlations are due to the greater difference in onshore and offshore wind conditions. Correlations are also lower for sites that are close together, this is a result of the large changes in wind speed when transitioning from sea to land, which may represent the most significant alteration in surface roughness in GB between two grid squares. This demonstrates that temporal diversity can be achieved without the need to build wind turbines in locations that are far from shore, a solution which may be prohibitively expensive.

The correlations between the offshore sites (right hand column of Figure 7.15) exhibit an increase in correlation coefficients over all distances, in comparison to those analyses which include onshore winds. This demonstrates that wind speeds are more homogeneous offshore than onshore, owing to the lack of obstacles and consistent surface roughness. Also, different albedos on land can cause localised variation in solar heating and subsequent changes in wind speed. The maximum distance between offshore sites is less than seen in analyses which include onshore capacity. This is a result of the separation primarily being east to west across GB which is a shorter distance than the north to south separation in onshore capacity at maximum distances. This would change if further development occurred in offshore locations to the north or south of GB. The lack of development of the further offshore zones in the NP scenario is highlighted, with no sites more than 600 km from each other and fewer sites at shorter separation distances. The GG scenario demonstrates the highest correlation between grid squares (0.8). This is very likely to be the relationship between the extra sites located in the Bristol channel, which are not used in other scenarios. This shows that those sites experience highly related wind speeds, possibly due to the wind coming off the sea with little influence from land.

This analysis has shown that in terms of distance alone there is not a great deal of benefit from offshore wind farms in the current development zones. However it is clear that wind conditions offshore are different to those onshore. The analysis suggests that wind speeds at the greatest extent of these zones are similarly unrelated as onshore wind at the same distances. This points towards there being limited benefit in offshore wind, however, this is in terms of geographical diversity alone, as capacity factor analysis found offshore wind to be of a higher quality in terms of power generation. Geographical diversity is clearly limited by the use of the development zones for offshore capacity. Further analysis should investigate the correlation between these locations and grid squares further from shore or in different directions, for example the north west coast. In particular the impact of prevailing wind direction on the spatial correlation of different turbine sites, which may impact the effectiveness of spatial diversity reducing the magnitude of matching

mechanisms.

7.2. Electricity demand

The analysis of wind generation has demonstrated a clear divergence between SpWind outputs and NG data. This divergence can be easily attributed to the modelling method because NG use assumptions about constant capacity factors, whereas SpWind is driven by spatiotemporally disaggregated weather data. Comparison of demand from SpDEAM and NG data is considerably more complicated. In part this is due to electricity demand being driven by a greater number of factors. The comparison is complicated further by the lack of description of NG's methods in their scenario documentation. Nevertheless, demand from both methods must be compared, because SpDEAM has been developed as a tool to disaggregate the scenario modelling, therefore outputs should match closely. The NG method has also been augmented in SpDEAM with bottom up modelling of heat demand, which incorporates weather as a driver of demand. Therefore divergence between outputs from both methods can be assessed through comparison. The following comparison focusses on electricity demand as this is the element required to produce an analysis of residual demand, which is presented in the next chapter. Heat demand is considered in detail only in its electrified form.

The bottom up SpDEAM model outputs should closely match the NG data, however some difference is expected, particularly as the influence of annual change in weather is introduced. Total electricity demand in the NG scenarios includes domestic, industrial, commercial demand as well as losses and exports to Ireland. SpDEAM includes all of these demands, except exports to Ireland, because it was calibrated using data from NG on total national electricity demand. The data used for calibration also includes embedded generation, which is therefore included in SpDEAM non domestic demand (Chapter 5). The most recent iterations of that NG data include estimates of the amount of electricity being produced by embedded wind; however, this was not available when the calibration was performed. Embedded generation is seen as a negative demand in national grid data, consequently demand in SpDEAM may be lower than that estimated by NG. Embedded capacity is also simulated in SpWind, which means that generation may be slightly overestimated. The combination of these two simulations of embedded generation may result in an underestimation of residual demand. Figure 4.1 gives a reasonable indicator of the amount of generation that is embedded as it is not included in the ROC system (~ 1 GW at the peak). Although this is capacity rather than generation, assuming a 28% capacity factor this would result in 280 MW on average and 1 GW peaks. Embedded generation also includes industrial CHP and domestic solar which may increase the average value and peaks owing to larger capacity and capacity factors. It is not the intention to exactly match NG data but to ensure that the difference is not large so that disaggregated analysis represents the situation presented by the scenarios. Future iterations of SpDEAM and SpWind, which use newly available data, will be able to correct the possible bias introduced by embedded generation.

7.2.1. Annual total demand

Figure 7.16 shows the difference between all electricity demand as depicted by NG and that simulated using SpDEAM. The plot shows that SpDEAM consistently underestimates demand in

comparison with NG, but that the magnitude of this difference is small. The difference between SpDEAM and NG is very similar in percentage terms for the SP, LCL and NP scenarios (between 0% and -3%). The magnitude of the difference increases slightly in the GG scenario (up to -5%). If the average hourly embedded generation is 280 MW as described above this equates to between 0.65% and 0.75% of NG annual demand. This shows that other factors contribute to the lower values predicted by SpDEAM.

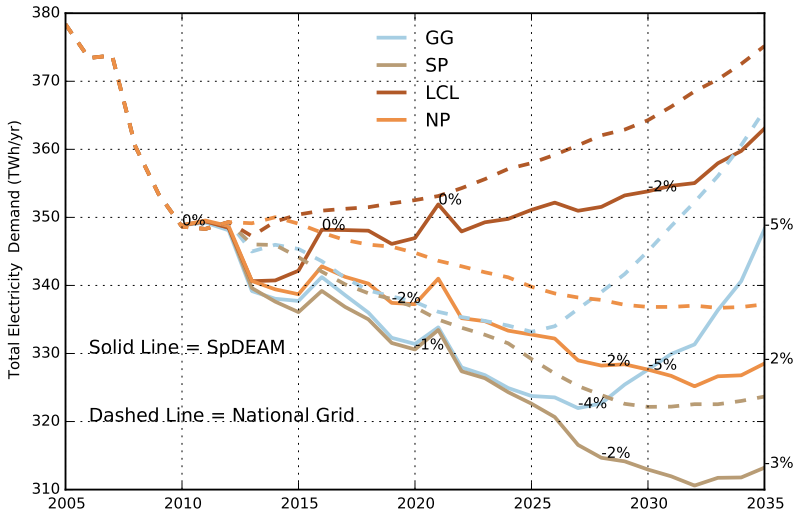

Figure 7.16.: Total annual electricity demand, NG vs. SpDEAM.

NG's demand outputs are weather corrected, as one aim is to show annual changes in demand. Variable weather conditions between years in SpDEAM drive the inter annual variability shown in Figure 7.16. Only three years demonstrate a noticeable divergence from the general trend of growth or decline (2013, 2016 and 2021). Demand is simulated in these years using historical weather data from 1988, 1991 and 1996. Figure 7.17 shows histograms of national mean hourly temperature during those years and the previous and subsequent years, calculated using values from all onshore grid squares. The plot shows that the decrease in electricity demand seen when using 1988 data in comparison to previous and subsequent years is a result of milder temperatures. There were more hours when the national mean temperature was between 5°C and 15°C and no hours where the temperature was below 0°C. This contrasts with 1987 which experienced a cold winter with many hours where the national mean temperature was below 0°C. This demonstrates that a winter that lacks very cold periods will result in lower mean electricity demand, at least according to the electric space heating assumptions used in SpDEAM. The increase in demand relative to the previous and subsequent years driven by the weather data from 1991 and 1996 is a result of a greater number of hours where the national mean temperature is close to 0°C. It is difficult to conclusively deduce from these three years that these are the temperatures that dictate high electricity demand, but it is clear that they contribute as the change in the distribution of mean temperatures coincides with changes to demand.

Figure 7.18 shows temperature histograms for all of the years from CFSR v1. The plot shows that there are multiple peaks in the occurrence of temperature. The peaks on the left hand side of each histogram represent median winter temperatures and the peaks on the right hand side represent the median summer temperatures. The temperatures between these peaks may occur during any of

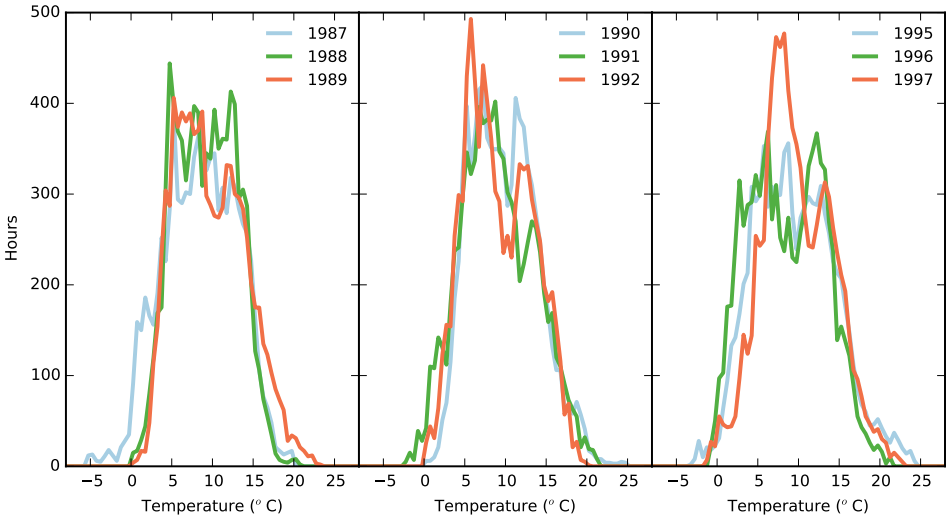

Figure 7.17.: Histograms of GB hourly mean temperature in exceptional years.

the seasons. The plot also demonstrates that there are several years where very cold winters have not resulted in exceptionally high demand from SpDEAM. For example 1986, 1987 and 2010 have very long tails, indicating very cold temperatures across GB; however, there is no noticeable change in demand compared to previous and subsequent years in the years where that data has been used for simulation (2010, 2011, 2035). This may be because the earlier years do not have any preceding baseline data and because 2035 is preceded by several years of increased demand. However it may also be caused by other demand drivers such as economic growth and recession. All changes are mirrored in each scenario, at similar magnitudes. This demonstrates the similarity between the scenarios where the same weather conditions are experienced. In this respect the demand side of these scenarios is simpler than the supply side as there is less difference to the spatial configuration of demand. The configuration of population and dwelling types is the same in all scenarios; while heating technologies vary as a result of the need to place more heat pumps in the GG scenario. Wind capacity development is geographically varying between scenarios, particularly offshore.

7.2.2. Annual domestic demand

Domestic and non domestic demand are estimated using different methods in SpDEAM; therefore, it is possible that one sector is responsible for more of the underestimation in total electricity demand than the other. Figure 7.19 shows annual domestic demand for electricity from SpDEAM alongside data from the NG scenarios. The plot demonstrates that, like total demand, SpDEAM underestimates domestic demand in comparison with NG. The percentage differences are slightly larger, between -1% and -9% for domestic demand compared to 0% to -5% for total demand. The GG and LCL scenarios result in larger magnitude differences than SP and NP. Inter annual changes, driven by temperature, broadly follow those described above in the context of total electricity demand. In some cases the magnitude of the inter annual change is larger with domestic demand than total demand (e.g. 2012, 2026 and 2032). This is due to domestic demand in SpDEAM being temperature dependent, whereas non domestic demand is weather independent; therefore when the two are combined the weather driven annual changes are diluted.

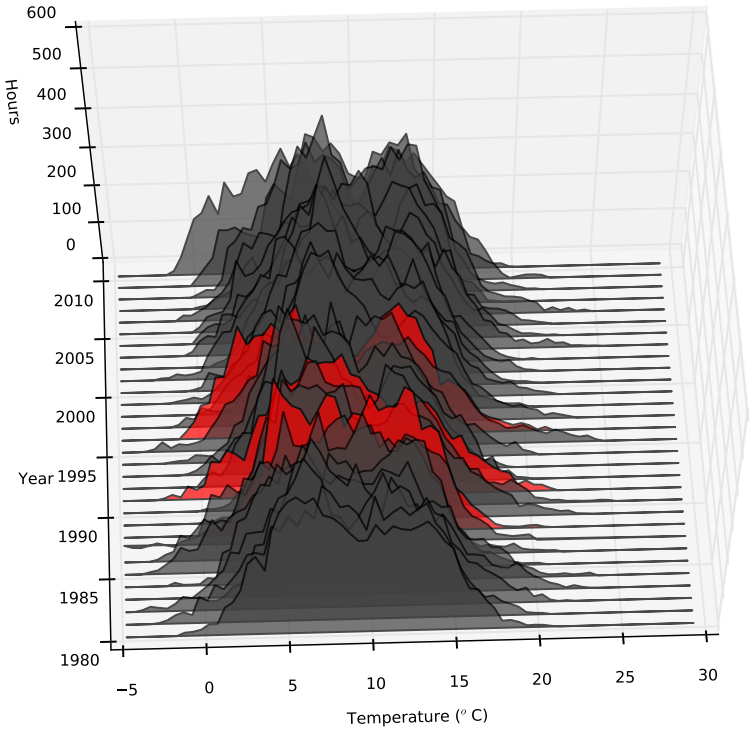

Figure 7.18.: Histograms of GB hourly mean temperature in all years.

7.2.3. Annual non domestic demand

Figure 7.20 shows annual non domestic demand for electricity from SpDEAM alongside data from NG. The plot shows that the difference is small, demonstrating that the difference in domestic demand contributes more significantly to the difference in total demand, despite being lower in magnitude. The difference is in the same direction as domestic demand, although some years exhibit a 0% difference and there are several years where SpDEAM output exceeds NG (2016 and 2017 under the GG scenarios and 2010, 2011, 2012 under all scenarios). There is a lot less variation; this is due to the lack of weather as a driver of demand. Space heat demand contributes less, proportionally, to energy demand in the non domestic sector than the domestic sector. However it is possible that electrified heat demand is more significant in the non domestic sector owing to the technology used to heat buildings, e.g. heating from an air conditioning unit. Lighting is also a significant demand in the non domestic sector. This may mean that there is significant inter annual variability in non domestic demand not captured by SpDEAM. Unfortunately, lack of data on these demands make it very difficult to model the non domestic sector using bottom up methods. SpDEAM growth and decline in non domestic electricity demand closely follows NG, owing to the use of the top down method. This, in combination with the close match of the outputs demonstrates that the top down method maintains the values, despite significant changes made to the normalised non domestic demand profiles described in Chapter 5.

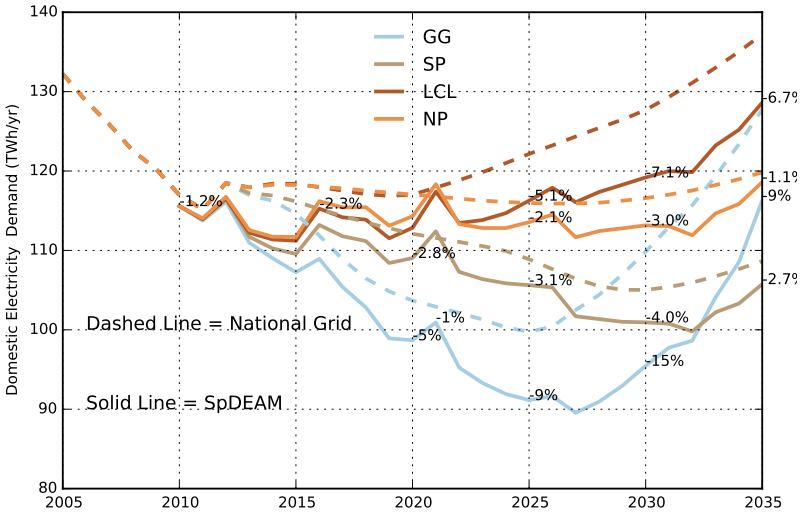

Figure 7.19.: Domestic electricity demand NG vs. SpDEAM.

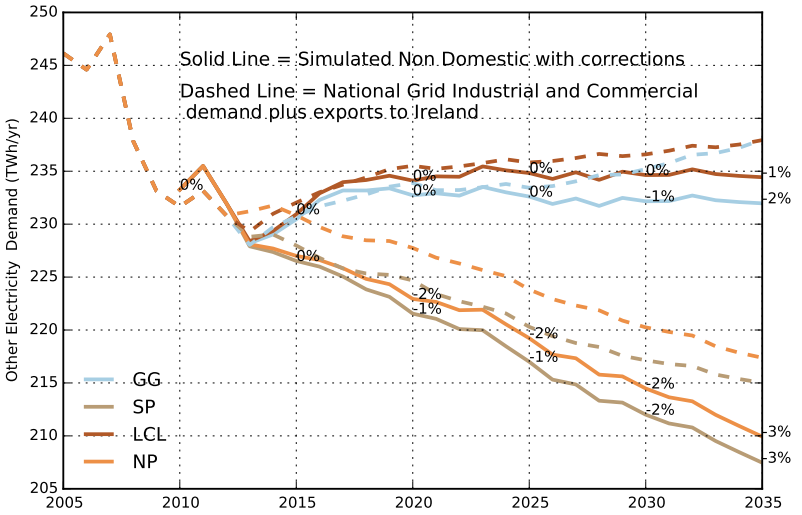

Figure 7.20.: Other electricity demand, NG vs. SpDEAM.

7.2.4. Domestic electrified heat demand

As previously discussed, the key difference between demand scenarios in SpDEAM is the spatial distribution of domestic heating technologies, particularly heat pumps. Therefore it is important to investigate the consequences of these differences. Figure 7.21 shows how electricity demand from heat varies under each scenario and demonstrates how the application of NG scenarios on heating technologies combine with the spatial heating technology data, derived from the 2011 census, to affect electricity demand at a national level.

The top left subplot of Figure 7.21 shows the difference between NG's depiction of electricity demand from electric resistive heating and non heat pump electrified heat demand from SpDEAM. The subplot demonstrates that under the NP, LCL and NP scenarios there is very little difference between SpDEAM and NG. This lack of difference is promising as the modelling methods are different and SpDEAM incorporates spatiotemporal complexities including allocation of heating

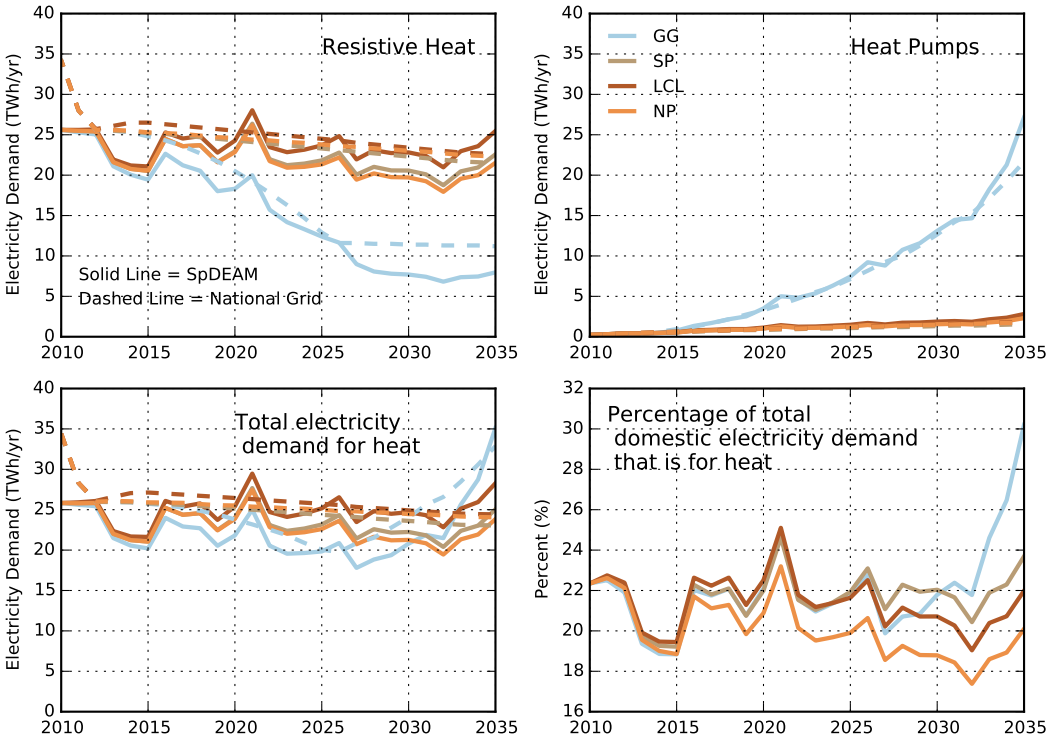

Figure 7.21.: Domestic electrified demand that is for heat under each scenario.

technologies, weather, allocation of people and buildings, allocation of incidental gains to buildings and heat loss in different building types. Weather introduces most of the variation between SpDEAM and NG. The larger changes in year to year demand occur in the same years as discussed above. The subplot also shows there is a larger difference between SpDEAM and NG under the GG scenario. Particularly after 2030 when a difference of more than 4 TWh/year is shown. As described in the previous chapter, the GG scenario has a different set of heating technology allocations than the other scenarios because of the introduction of a greater number of heat pumps. All of the other variables influencing heat demand remain the same. Therefore the difference between the two models is driven by SpDEAM emphasising the impact of replacing electric heaters with heat pumps.

The top right subplot of Figure 7.21 shows annual demand from heat pumps from SpDEAM and NG, demonstrating that there is very little difference between the two models. As discussed previously, heat pumps in SpDEAM operate at an efficiency that is higher than that of heat pumps currently used in GB. NG do not state the method for calculating heat demand in the documentation that accompanies their scenario data, their calculation of heat pump demand is also not subject to the disaggregated drivers applied in SpDEAM; therefore it is difficult to tell whether the same assumption is made on heat pump efficiency. However the plot does show that the use of this efficiency in SpDEAM does not cause bias between the two models.

Total electricity demand from heat is shown in the bottom left plot of Figure 7.21. This demonstrates that, despite a very large number of heat pumps being introduced in the GG scenario, the resultant demand for electricity from heat does not exceed electrified heat demand from other scenarios until after 2033 (when over 8 million domestic heat pumps are being used Figure 6.17).

This is only 3 years after the date depicted by NG. It should be noted that previous analysis has shown that the weather data used for the simulation of the final years of the scenarios describes very cold conditions, therefore depicting more or less the maximum demand possible from these heat pumps under the assumed conditions in SpDEAM. The subplot also shows that the reduction of non heat pump electricity demand from heat counteracts the increase in heat pump demand in the GG scenario, which results in similar total electrified heat demand in all of the scenarios, for the majority of the scenario period.

The bottom right subplot of Figure 7.21 shows the total electrified heat demand as a percentage of total domestic electricity demand for each of the scenarios. The subplot demonstrates that the effect of heat demand is exaggerated when considered as a percentage of total demand as the GG scenario diverts from the other scenarios to a greater extent than seen in the other subplots. However this is only the case after 2030, when the larger number of heat pumps is combined with cold weather and greater relative heat demand.

Overall Figure 7.21 demonstrates that the results from the heat demand calculations performed in SpDEAM using a disaggregated method generally agree with the estimates of demand from NG when they are aggregated. Although the two methods end up with reasonably similar depictions of aggregated electricity demand from heat, SpDEAM has the ability to alter the spatial distribution of heating technologies and buildings and the efficiency at which they operate. This means that more detail can be added in subsequent analysis of for example peak flows and residual demand, but also in future work which could for example investigate the impact of less efficient heat pumps used only in urban locations or larger extensions such as district heating with heat pumps. This demonstrates that SpDEAM is an effective complementary tool to NG's aggregated modelling.

7.2.5. Peak electricity demand

One way to investigate the impact of scenario changes at disaggregated resolution, and to judge the impact of these changes on the electricity system, is to compare the peak demands. Figure 7.22 shows how peak electricity demand from SpDEAM compares to that depicted by NG. The plot shows that SpDEAM predicts peak demands that are higher than NG every year for all scenarios. This is significant because capacity must be planned to meet this extra demand. The largest difference occurs at the very beginning of the scenarios (approximately 10 GW), which in theory should exhibit the least divergence from reality as SpDEAM has been calibrated to represent the previous ten years. The calibration of SpDEAM has shown that there are hours where demand can exceed or fall short of measured demand by up to 10GW at the peaks (Figure 5.37), these isolated hours of high demand could skew this analysis.

Figure 7.22 shows that the impact of heat pumps does not become evident until the very end of the scenarios, when peak demand in the GG scenarios exceeds other scenarios and historical demand. This occurs in 2032 in NG modelling and 2033 in SpDEAM. SpDEAM allows an investigation of when these peaks will occur during the year, as described in the following section.

7.2.6. Changing electricity demand profiles

The above analysis has demonstrated that under the scenario with the greatest number of heat pumps (GG), the electricity demand from those heat pumps is counteracted by reducing demand

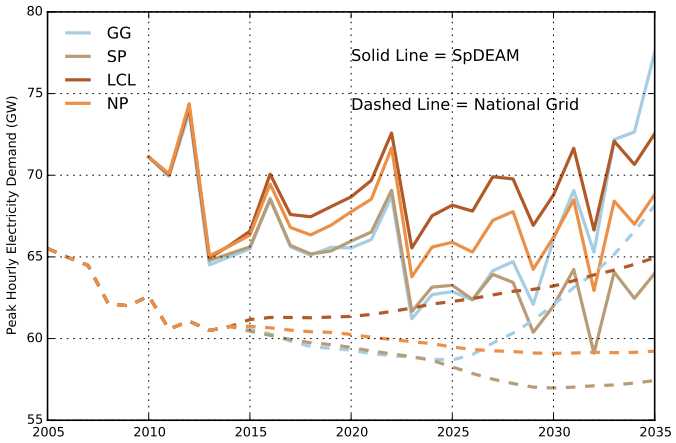

Figure 7.22.: Peak electricity demand under different National Grid scenarios.

from electric heaters. The effect of this is that total annual electricity demand from heat and peak electricity demand in the GG scenario does not exceed that experienced by other scenarios until 2033. This means that the impact of heat pumps on the demand profile may be hard to detect over the whole course of the scenarios. Despite this, the widespread introduction of this new technology still represents the major technological shift modelled by SpDEAM. Therefore the following section investigates how the demand profile from heat demand will alter the national electricity demand profile.

Figure 7.23 shows a 2D histogram of electricity demand profiles for every day of each year of the GG scenario. The maximum heat pump demand profile is also shown in black to demonstrate the extent to which it can contribute to total electricity demand during each hour of the day. The plot demonstrates that peak demand from heat pumps is very low to start with, with the magnitude gradually increasing over time. After 2033 a larger increase is demonstrated, as a result of low temperatures and more heat pumps. The plot shows that demand for heat from heat pumps is greater in the mornings than evenings. Figure 5.3 shows that this is in contrast to the heating profiles that dictate the temporal profile of demand, where demand for heat is higher in the evenings. This suggests that the other temporal drivers of demand, temperature and incidental gains, must be lower in the morning to create this pattern. During the later years of the scenarios the influence of heat pump demand becomes more significant and associated higher morning peaks are demonstrated.

Figure 7.23 shows that changes in the demand profile happen slowly and that overall changes are small. The green section in the middle of the plots demonstrates a large number of hours where demand is at that level over the year, which can contain both summer and winter demands, does not significantly change over time, staying at 30 - 40 GW at night, dipping below 30 GW in the early morning, rising to to between 40 and 50 GW during the day and dropping in the evening. There is less variability in this median demand during the day than at night. The lowest demand also changes very little over time, remaining between 20 GW and 30 GW depending on the time of day. The greatest change over the course of the scenarios shown in Figure 7.23 is seen in the peak demands. Peak demand is highest in the first few years (> 70 GW) and reduces slowly over time (to 60 GW) but increases at the end of the scenario period (back to > 70 GW) as the impact of heat pumps become more significant at an hourly resolution. The increase in peak demand is

likely to be driven by the low temperatures shown in Figure 7.17 and the lack of new building stock which has been modelled as more thermally efficient, old building stock also improves slightly over time in that respect, as well as the introduction of more heat pumps.

Figure 7.21 has shown the percentage of annual domestic electricity demand that is from heat. Figure 7.24 builds on this by showing the percentage of total electricity demand that is for domestic heat. This is important because the above analysis has demonstrated that for almost the entire period of the scenarios SpDEAM suggests that traditional forms of electrified heat are likely to be more significant in terms of the contribution to maximum demand than heat pumps. The plot shows that the GG scenario diverts from other scenarios in two ways. There are more hours where a lower percentage (0-10%), of total electricity demand is from heat. There are also a number of occasions when the percentage of demand that is from heat is greater than any occurrences in other scenarios, exceeding 50% on approximately 10 occasions. Figure 7.23 shows that it is likely that these will occur in winter mornings.

The analysis above has considered the electricity demand profile over the whole year. This masks the fact that electricity demand varies significantly over the course of the year. The following analysis considers demand during different seasons, so that the impact of electrified heat demand can be explored further. Seasons are defined here by their official northern hemisphere start dates:

- Winter is defined as 21st December - 19th March.
- Spring 20th March - 20th June.
- Summer 21st June - 21st September.
- Autumn 22nd September - 20th December.
- Winter periods are separated by year rather than a single winter.

Figure 7.25 shows 2035 winter electricity demand profiles, separated by weekdays and weekends. The plot shows that the key difference between the GG scenario, which contains the largest number of heat pumps, and the other scenarios, is the greater level of variability in total electricity demand, as well as a higher mean demand and greater maximum demand. For example at 8 am on winter weekdays, the minimum total demand is similar in all scenarios (approximately 40 GW). Mean demand varies between 40 GW and 50 GW depending on the scenario. The 75th and 25th percentiles in GG are much further from the median value than in other scenarios and the maximum value exceeds the median by almost 20 GW, or 40%. This pattern continues throughout the winter weekday, including at night. Very few outliers are shown in any scenario, demonstrating that variation is within the limit of 1.5 times the interquartile range at almost all times. The increased variability, denoted by the larger interquartile range and resultant extreme values, is repeated at the weekend. The other notable difference at the weekend is the increase in demand in the mornings. This is more marked than on weekdays, because during a weekday there is an increase in demand in the morning associated with the non domestic sector, when people start work, or travel to work. This may be very important, as it represents the clearest shift in demand patterns as a result of the introduction of increased numbers of heat pumps. The plot emphasises the relatively low demand from heat pumps in the scenarios that are not GG. The consequence of the high weekend demand in GG are that a new demand is experienced when demand is historically lower than other similar periods during the week. This represents a shift in electricity demand and shows the benefit of the bottom up approach as the magnitude of the change can be seen. The

effect is noticeable because the previous impact of heat pumps is low. It should be noted that if less efficient heat pumps were modelled then the impact would have been greater and experienced much earlier in the scenario period.

Figure 7.25 used winter demand as an example to illustrate the impact of heat pump demand on total national electricity demand. However, the use of official winter start times does not reflect that the heating season extends outside of winter, into autumn and in many cases spring. Therefore Figure 7.26 shows winter demand alongside demand during different seasons for 2035. The plot shows that like winter, demand is higher under the GG scenario during both weekdays and weekends in all seasons, but particularly in autumn and spring. The weekday demand in autumn in GG is slightly lower than winter, at least in terms of the peak, whereas peak weekend demand is the same in autumn as winter. This indicates that weekend demand may be affected to a greater extent than weekdays by heat pumps, where a certain level of demand is likely to be guaranteed by non domestic end uses, and that these changes will occur in the autumn and winter. Spring and summer demands look more similar between scenarios than autumn and winter, owing to the limited influence of heat demand, which removes the biggest difference in both the scenarios and the way in which SpDEAM models these scenarios.

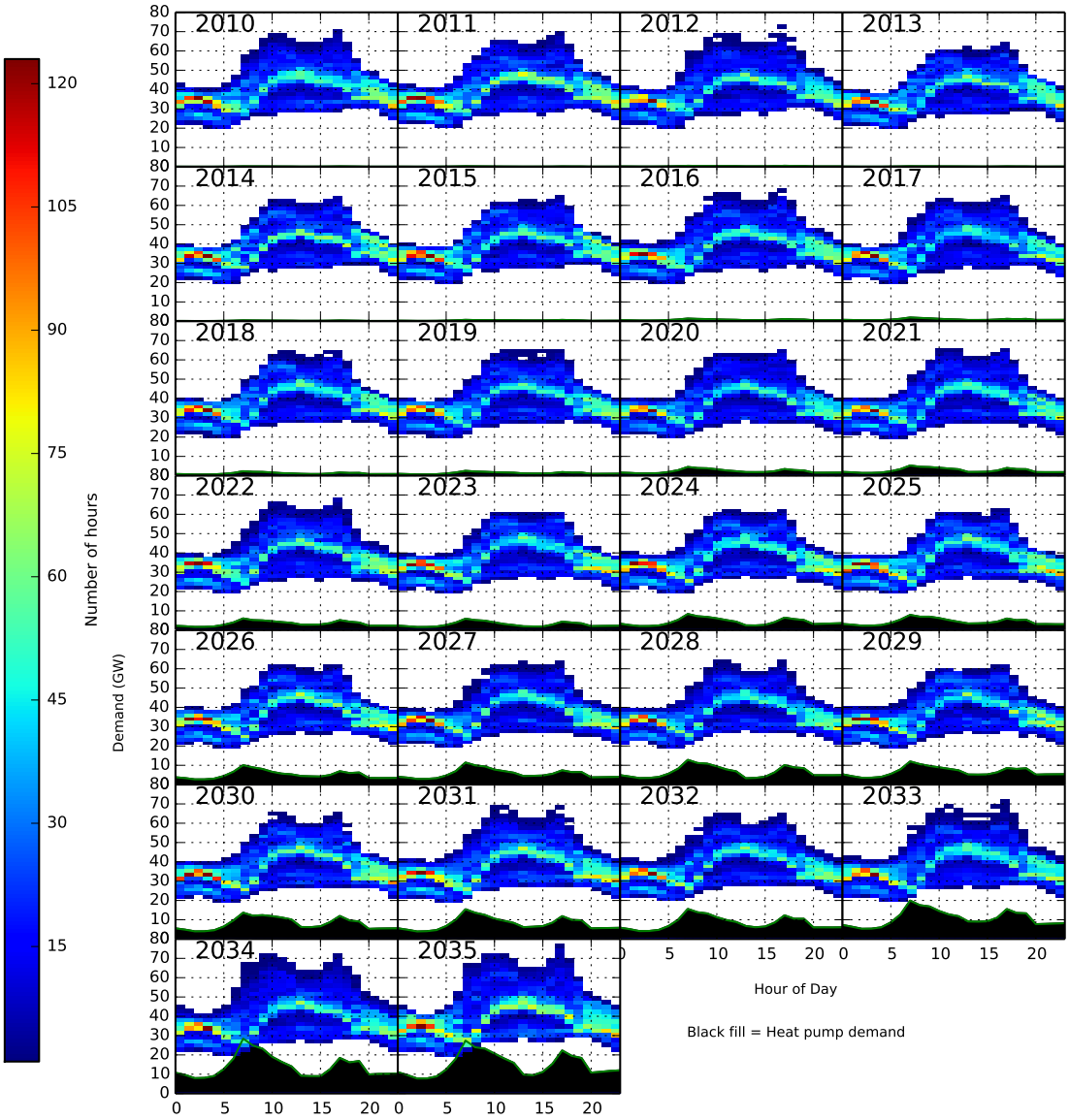

Figure 7.23.: Variation in electricity demand over time in the GG scenario, total demand and heat pump demand.

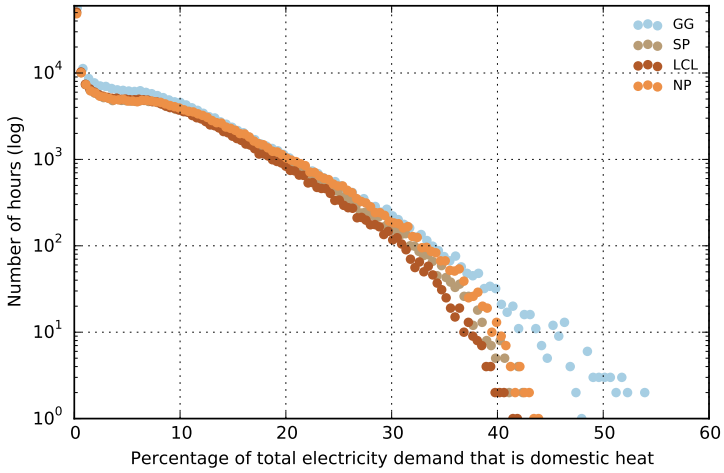

Figure 7.24.: Percentage of total electricity demand that is for domestic heat.

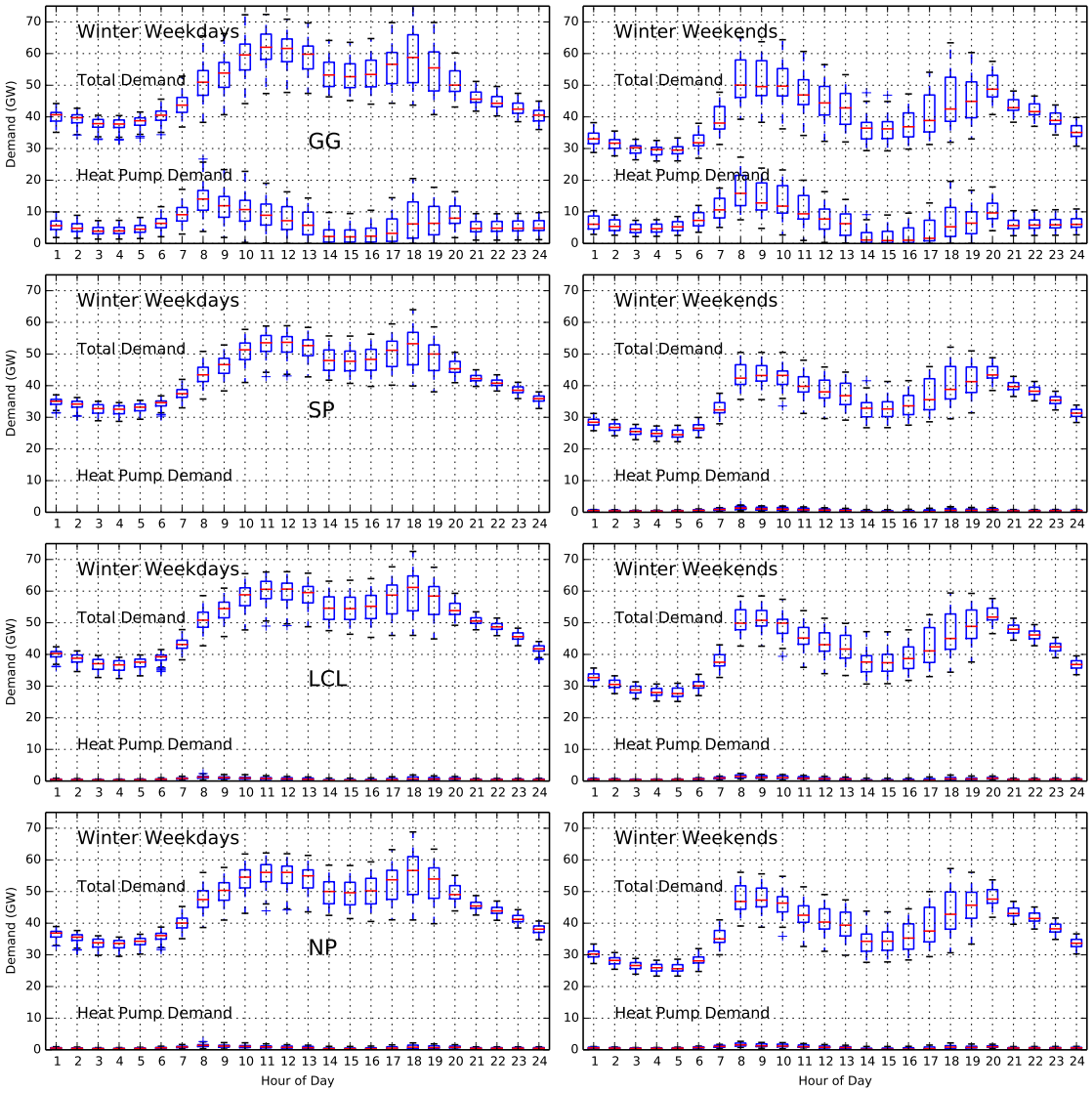

Figure 7.25.: Winter electricity demand profiles in 2035, total demand and heat pump demand, divided by weekend and weekday.

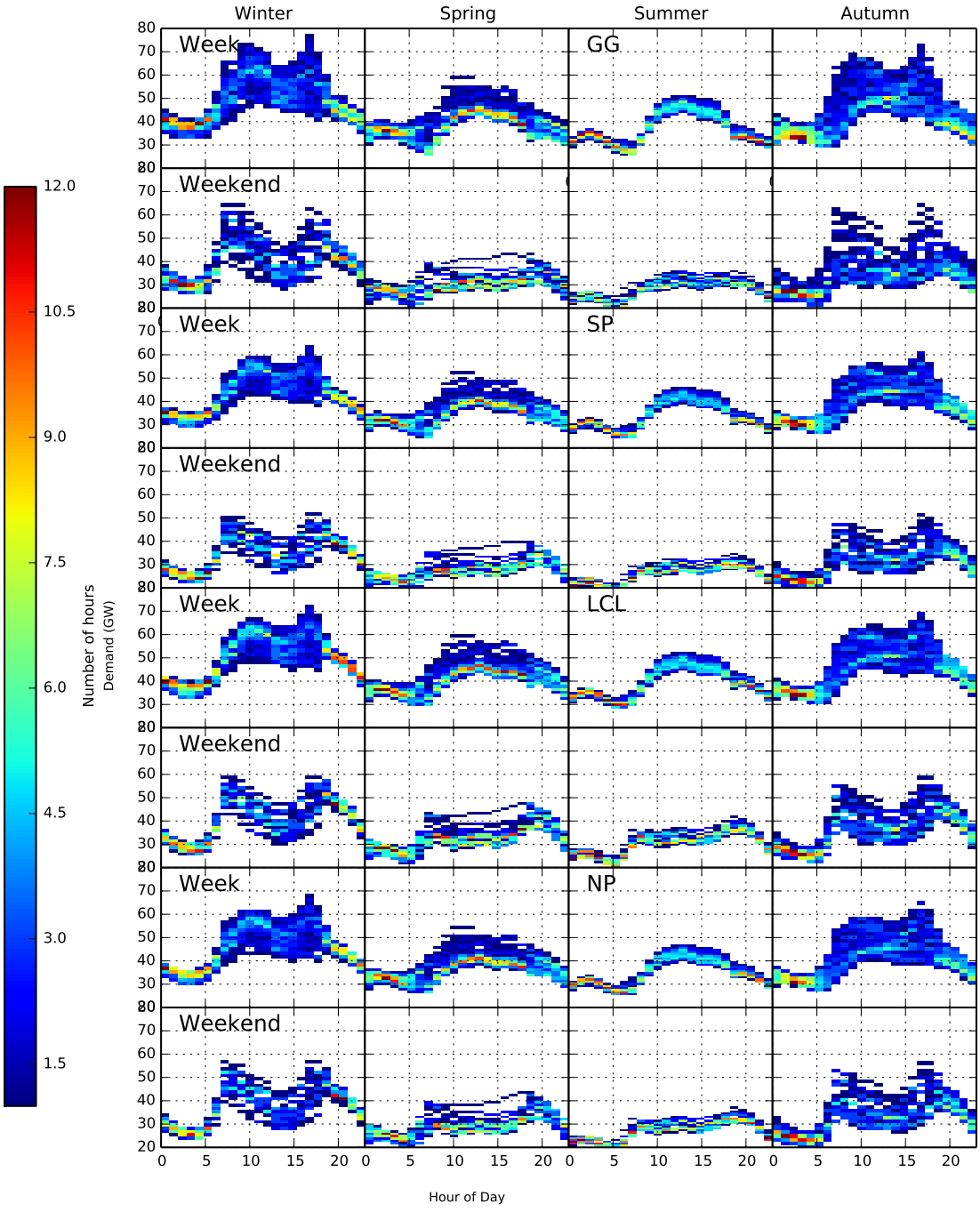

Figure 7.26.: Seasonal changes in electricity demand in 2035.

7.3. Summary

This chapter has analysed the wind generation and electricity demand from the modelled scenarios. Comparison of wind generation has demonstrated that SpWind estimates are larger than those made by NG. The offshore capacity factors assumed by NG are significantly lower than those calculated by SpWind using the CFSR data. This is largely because NG have used historic capacity factors as a guide, which do not take into account the fact that future wind farms may be further from shore, where wind speeds are higher. Onshore capacity factors are lower in SpWind that those used by NG, but the effect on generation is smaller in all but the NP scenario owing to smaller onshore capacities. This results in greater divergence between SpWind and NG data later in the scenarios as offshore capacities increase.

Exploring the difference in wind speed distributions over a year between onshore and offshore locations, demonstrates that wind speeds are higher offshore for longer periods. The analysis of wind speeds has shown that those years that experience a greater number of hours at the median wind speed will experience lower generation. This demonstrates the relationship between wind speed and power generation, which, as described in Chapter 2, follows a power law range with an exponent between 2 and 3 between 2 and 11 m/s. At lower wind speeds no electricity is produced and at higher wind speeds the relationship plateaus. The majority of wind generation divergence is driven by capacity being exposed to different offshore wind conditions. Once in 25 year wind conditions such as those experienced in 1991 can produce comparable load duration curves between fleets where onshore capacity dominates and those where offshore capacity dominates and lower wind speeds are experienced. In later years offshore capacity produces up to 80% of power.

The correction factor applied to SpWind outputs has been shown to account for between 3.7% and 5.7% of the difference between SpWind and NG at the highest capacity factor. This should not be considered erroneous because 100% capacity factors are likely in offshore locations with high wind speeds and the correction factor is a result of the calibration of SpWind to the best available data. This is, however, worth considering further in future iterations of SpWind where a more sophisticated post calibration correction could be carried out within the model by, for example, examining the impact of using a different method for altering the height of CFSR wind speeds or perhaps using MERRA wind speed data which provides data at multiple heights.

Geographical diversity was explored in more detail. In comparison to previous work by Sinden the impact of considering only GB, rather than UK, is that the maximum distance between sites is reduced and minimum correlation increased. Introducing offshore capacity further from shore does not increase the distance owing to the sites being separated in an east west direction as opposed to north south onshore which provides greater lengths. It is therefore necessary to use the development zones that are furthest from shore to introduce more sites where there is little relationship between sites in terms of wind speeds and power output.

Results indicate that there are offshore areas where wind speed is more homogeneous than others, such as the Bristol channel, but that these are no less related to wind conditions on the other side of GB than the wind speeds in the furthest apart onshore wind sites. Analysis is limited by the bounding box of the development zones. The same method could be used to explore the impact of using other areas for wind farm development which may reduce the correlation between wind generation sites and smooth the variability which complicates the resolution of issues with residual demand. The small difference in onshore capacity factors between scenarios indicates that there

is little to be gained by new capacity in terms of geographic diversity without the use of offshore development zones.

Comparison of modelled output with the scenario data shows that SpDEAM consistently underestimates electricity demand in comparison with NG, though the magnitude of this difference is small. There is more difference in the domestic demand and greater variability due to the use of weather data in SpDEAM and the adoption of a hybrid approach. SpDEAM non domestic demand is very close to NG data; this is to be expected owing to the use of the solely top down approach, but demonstrates that the corrections applied and the alterations to the input data are appropriate.

Demand for other fuels from heat is modelled by SpDEAM, however these demands do not directly contribute to the residual demand once wind generation has been taken into account. These demands can be used in future work, for example to analyse the impact of increased numbers of heat pumps on gas demand. However the analysis of demand for other fuels represents significant work as well as being outside of the remit of this thesis, and therefore has not been discussed here.

Modelled electrified heating has been shown to be very similar to that depicted by NG on a national annual basis. This is slightly surprising given the very efficient heat pumps used. The increase in demand associated with heat pumps in the GG scenario is counteracted by a concurrent reduction in other electrified heat demand. This reduction is of a slightly higher magnitude in the modelled output than NG. The result is that electrified heat demand from the GG scenario does not exceed the other scenarios until 2030. These scenarios have far fewer heat pumps but do not experience the same reduction in other electrified heat demand. This means that the impact of heat pumps on the national demand profile cannot really be detected until the end of the scenarios. Here the minimum and maximum electricity demand is higher under the GG scenario. This effect is accentuated at the weekends when there is less morning peak demand from the non domestic sector.

In general the difference between the both SpDEAM outputs and the NG data is small, meaning that future analysis of residual demand will be meaningful. Some divergence between SpWind and NG has been described, however the difference between the modelling approaches was identified by the disaggregated approach used in SpWind. The disaggregated approach has also facilitated further analysis of several important issues in the planning of the future energy system including the impact of increasing offshore capacity in previously unused locations and the impact of increasing the number of heat pumps. Therefore this chapter has achieved its aim of answering research question 3 by establishing that a gridded approach is appropriate for the disaggregation of national scenarios of increased wind capacity and electrified heat. The chapter has also begun to examine the implications of electrifying heat and introducing more wind capacity. The combined implications of the changes to the energy systems are explored in the next chapter.

8. Scenario Analysis 2

This chapter addresses the remaining research question; what are the combined implications of electrifying domestic heat and introducing more wind capacity? To answer this question, it is necessary to first establish how much electricity demand can be met by wind generation under each scenario. A benefit of the disaggregated approach described in this thesis is that this can be estimated at an hourly resolution, which allows a more detailed look at how much electricity demand can be satisfied with wind generation. The first section therefore also considers how hourly residual demands vary between scenarios and change over time. Wind generation at the level described by NG scenarios is unprecedented, which means that the mechanisms for integrating this capacity into the system are not yet established. These are referred to collectively as matching mechanisms in this chapter and can include any of the following:

Demand side measures:

- Fuel switching, where for example gas boilers are used to heat dwellings when electricity is too expensive/not available for heat pumps.
- Consumers may offer to curtail demand in exchange for compensation. This happens today.

Supply side measures:

- Electricity storage, which can be used to store excess electricity generated when wind generation exceeds electricity demand then released when the situation is reversed. Storage increases demand due to the losses associated with transmission and conversion.
- Heat storage, which can be used to store excess heat and shift the demand for electricity in those places which required electricity for heat.
- Other storage, e.g. making hydrogen with surplus electricity or scheduled water pumping in reservoirs.
- Dispatchable/flexible generation, which is required to meet demand when a combination of renewable electricity and storage is insufficient. This can only be used to meet a demand deficit.
- Transmission (Import/Export), where electricity is generated from other countries, bought by GB to meet demand and transmitted along HVDC lines. Increased demand due to the losses associated with transmission.
- Curtailment, where wind turbines are turned off to reduce generation when it is not needed or cannot be used/stored. In many cases this may be the most economically attractive option depending on the relative cost of matching mechanisms
- Inflexible large plant are not strictly a matching mechanism but the extent of their use may depict the extent to which other matching mechanisms must be used.

The intention is not to definitively calculate the need for each matching mechanism but rather show the amount of excess generation or deficit in supply to meet demand will occur on an hourly basis under each of NG's scenarios. These can of course be explored in more detail in future work.

The chapter discusses the implications of the different scenarios on matching mechanisms. Where possible the magnitude of the overall need for matching mechanism is quantified. This chapter does not attempt to recommend which of the described matching mechanisms should be used. This is a problem for future work and is one which the method described in this thesis could be effectively applied to.

Increased wind capacity and electrified heating are likely to lead to a greater number of higher magnitude extreme residual demand events than previously experienced. These events will dictate the need for matching mechanisms, therefore this chapter examines the magnitude, number and persistence of events with respect to capacity factors, wind generation and electricity demand. The implications of these events on matching mechanisms are discussed.

The changes depicted by NG scenarios, in particular increased wind capacity, will introduce increased variability to the electricity system, affecting the ability of current matching mechanisms to ensure demand is met by supply. Hourly variability of capacity factors, wind generation and electricity demand and the resultant residual demand are therefore quantified and the implications of this variability are discussed. Looking at whether the extremes from demand and wind generation occur at the same time, therefore increasing the maximum difference which must be handled by the electricity system.

Wind generation is variable because the wind speeds which drive output are variable across a range of spatial and temporal resolutions. The ability of the electricity system to absorb this variability will also be affected by the variability of electricity demand. Previous analysis has shown that the electricity demand from the heat pumps modelled in SpDEAM is counteracted to a certain extent by a concurrent reduction in electricity demand from resistive heat. Nevertheless, SpDEAM provides temporally disaggregated information on electricity demand from heat. This means that the relationship between this demand and wind generation can be investigated and the implication of strengthening the link between electricity demand and supply as a result of them being driven by weather examined.

8.1. Residual demand

Residual demand has been calculated for each hour of each scenario by subtracting wind generation from electricity demand. It has been assumed that there are no further losses than those which are in SpWind.

8.1.1. Mean hourly residual demand

The left hand subplot of Figure 8.1 demonstrates that mean annual residual demand reduces over time, under all of the scenarios. The right hand sub plot shows that, on an annual basis, the reduction in residual demand is approximately proportional to the increase in wind capacity (the plot describes total onshore and offshore wind capacity normalised to 2010). An increase in capacity equivalent to that operating in 2010 results in a 10% reduction in mean annual residual demand.

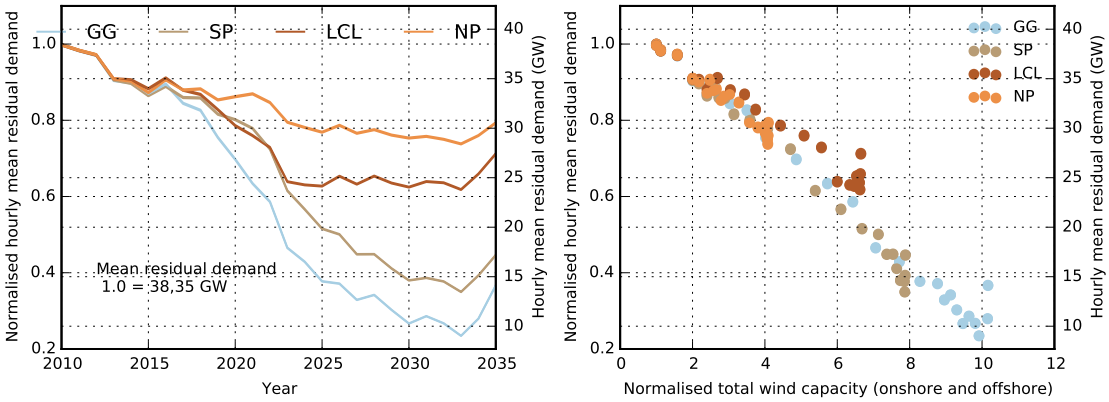

Figure 8.1.: Annual changes in residual demand.

Analysis in Chapter 7 has shown how the distribution of hourly mean wind speeds and temperatures across the year drives change in wind generation and electricity demand respectively. The inter annual changes in residual demand shown in the left hand sub plot of Figure 8.1 are a result of the combination of these distributions. There are years such as 2016 and the last three years of the scenario period, where demand increases and wind generation decreases as a result of decreased temperatures and wind speeds, which results in an increase in residual demand in all scenarios. In some years, such as 2021, decreased temperature and wind speed only result in an increase in residual demand in a single scenario, owing to significant increases in capacity in the other scenarios, which reduces the effect of wind speed on residual demand. There are also years where residual demand varies as a result of changes to only one weather variable. These are more evident later in the scenarios where larger wind capacities accentuate the effect of wind speed; for example, in 2026 and 2028 reduced wind speeds result in increased residual demand when there is not a notable change in temperature. These examples demonstrate that residual demand will vary with weather and that system planning will have to allow for this. Also changes in capacity and heating technologies can alter the relative influence of weather variables on annual mean residual demand.

The increased residual demand seen during the final years of the scenario period demonstrate that there may be lengthy periods of colder weather with reduced wind speeds, which will reduce the value of wind, as demand increases and generation decreases. These changes can be accentuated by shifts in the way in which electricity is consumed, as demonstrated by the steeper increase in residual demand under the GG scenario, where electricity demand from heat pumps exceeds electricity demand from resistive electric heat for the first time. The electricity system should be prepared for these periods, though they appear to be exceptional, they may occur earlier and more often if less efficient heat pumps are installed.

8.1.2. Distribution of hourly residual demand

The following analysis shows how residual demand is distributed on an hourly basis for each scenario. Figure 8.2 shows hourly residual demand over the entire scenario period. The plots demonstrate that long term median residual demand is very similar under each scenario (GG and SP 27.5 - 30 GW, LCL and NP 30 - 32.5 GW). The long tailed GG and SP histograms demonstrate a higher magnitude minimum residual demand. The GG and SP scenarios exhibit fewer hours

around the median than LCL and in particular NP as a result of this longer tail. This is due to more wind generation, but may also be due to stronger correlation between demand and supply. This correlation is explored in detail in Section 8.4. GG and SP show a significant number of hours where wind generation exceeds electricity demand and residual demand is negative. This excess wind generation will need to be addressed by one of, or a combination of, the matching mechanisms described above. All of the scenarios experience a similar number of hours above 40 GW, and the positive residual demand significantly exceeds the negative in the long term, demonstrating that all scenarios require significant alternative generation sources as part of the matching mechanisms. The overall difference between the scenarios is the lower residual demand in those scenarios with higher wind capacities.

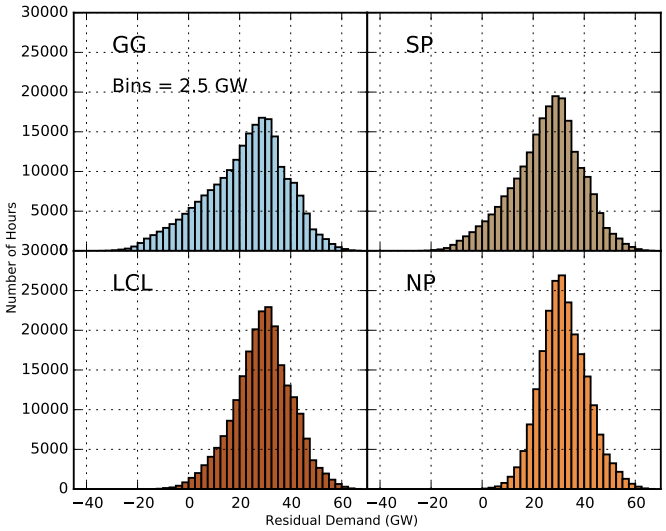

Figure 8.2.: Hourly residual demand over the whole scenario period.

Figure 8.3 describes the same information as Figure 8.2, but presents it in the form of residual demand duration curves. Hourly electricity demand from the GG scenario is also plotted alongside residual demand (demand curves are very similar between scenarios over the whole scenario period). The plot demonstrates that wind generation results in a non parallel shift in the residual demand duration curve with respect to the demand curve, as opposed to a parallel shift which would come from a non variable generator e.g. a nuclear power station. The curve shift is very similar between scenarios at higher levels of residual demand (40 - 60 GW), it is very likely that the majority of these hours occur at the beginning of the scenario periods when capacity is the same under each scenario. The difference between scenarios increases with the level of residual demand and the shift from the demand curve therefore becomes less parallel under those scenarios with larger wind capacity.

The load curves demonstrate the percentage of time that residual demand will be negative under each of the scenarios and therefore the percentage of hours where matching mechanisms will be needed to deal with either an excess or deficit in electricity generation. In the case of the GG scenario excess wind generation is experienced for approximately 10% of the scenario period, SP 5%, LCL 1% and NP 0%. The plot can also be used to show the impact of using inflexible large plant, such as nuclear power, by adding the level of generation to 0 GW on the y axis. For example 20 GW of nuclear generation results in the need to deal with excess wind 40% of the time under

the GG scenario, ~30% in the SP scenario, 20% in LCL and 10% in NP.

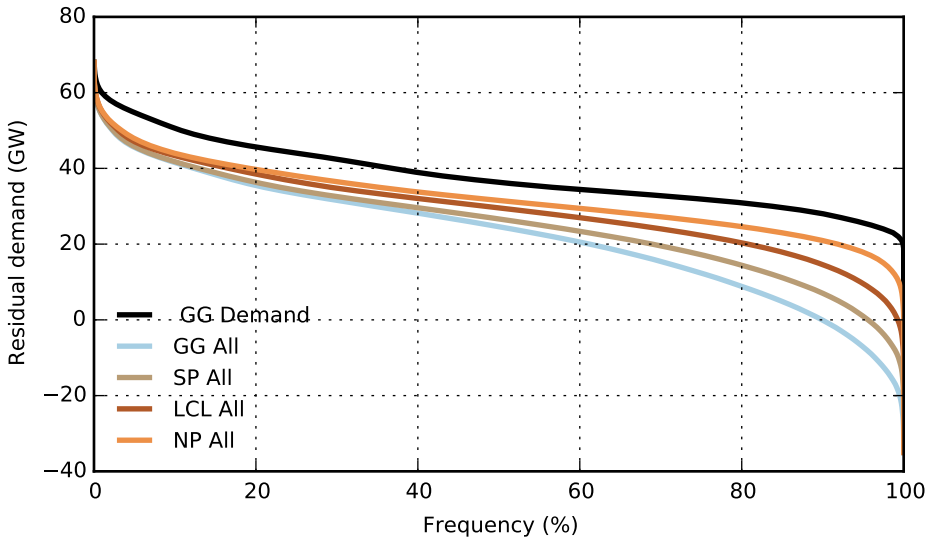

Figure 8.3.: Residual demand duration curves for each scenario.

8.1.3. Annual change in distribution of hourly residual demand

Figure 8.4 shows how hourly residual demand changes each year under the GG scenario, this allows an investigation of the changes over time both long term and between individual years. The histograms of residual demand clearly move towards the left over time, indicating an overall reduction in the amount of electricity required from other sources than wind. Fewer hours are experienced at the median residual demand and the range of maximum and minimum residual demand increases. Almost all of the hours with a residual demand over 40 GW occur at the beginning of the scenario. After 2022 residual demand above this magnitude occurs for less than 100 hours per year. Referring back to Figure 7.23 shows that this reduction is not due to a reduction in demand as there are still a significant number of hours where demand is between 40 GW and 60 GW for all years. This demonstrates that there is wind generation for a significant proportion of the time when demand is high. High residual demand periods do, however, continue to occur to the end of the scenario, demonstrating that the amount of required reserve capacity will not decrease. The small number of events above 40 GW later in the GG scenario mean that it will be viable to meet this deficit of supply with other matching mechanisms, e.g. imported electricity.

Figure 8.5 shows the annual maximum and minimum hourly residual demand under each scenario. The plot on the right shows that the *maximum* value in 2010 is nearly 70 GW, which, as described previously, may be an overestimation as peak demand was shown to be lower than this in measured data. Therefore normalised values are also provided so that the relative change over time can be examined. The plot demonstrates that the maximum hourly residual demand does decrease over time for all scenarios. The NP and LCL scenarios follow very similar trajectories in this respect, they experience up to a 20% reduction in maximum hourly residual demand, though this can vary up to 15% from year to year and in later years the reduction is as small as 5% of the 2010 peak. The GG and SP scenarios follow similar paths to each other, experiencing greater magnitude than

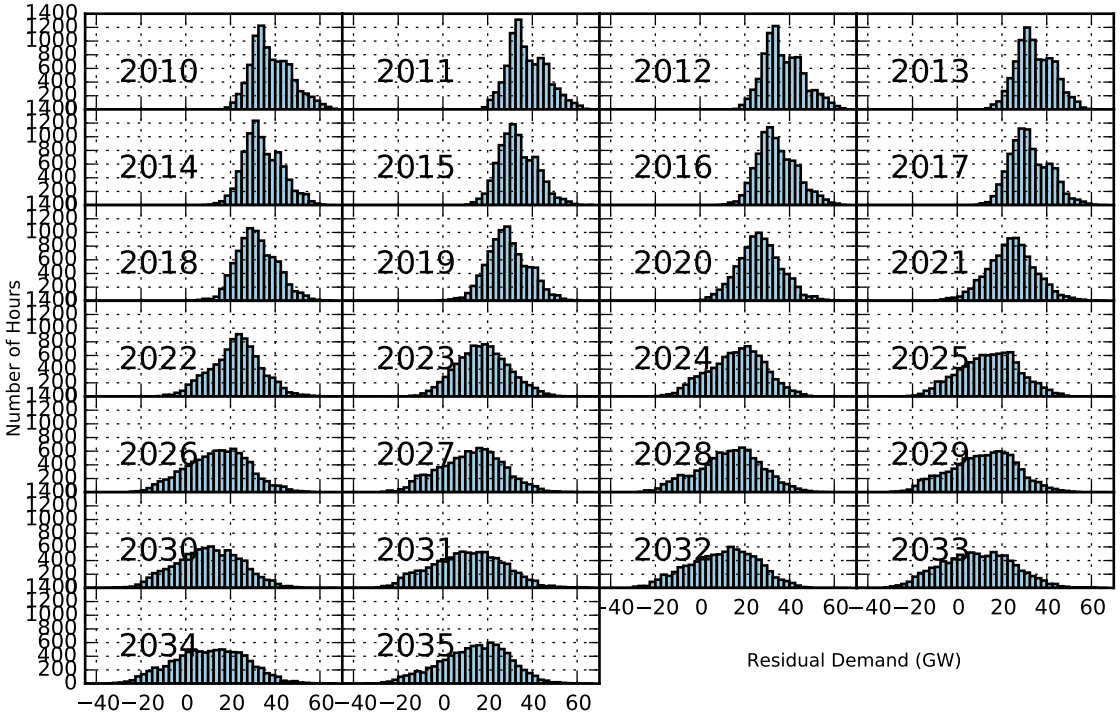

Figure 8.4.: Change in GG hourly residual demand, 2010 - 2035.

LCL and NP, with changes of up to 30%. After 2030 the two scenarios diverge; here, the number of heat pumps introduced to the GG scenarios results in maximum hourly residual demand values returning to 2010 levels.

Figure 8.5 also shows the extent to which *minimum* residual demand varies over time under each of the scenarios. Initially the scenarios follow similar paths, as the wind capacity does not differ, the paths diverge in 2017. The plot shows that under the GG scenario wind generation exceeds demand for the first time in 2020, SP and LCL in 2021 and NP much later, in 2034. The first three scenarios experience excess wind generation of increasing magnitude every year after the first instance. If wind generation is not curtailed, or demand shifted to times of peak generation, these minimum residual demands dictate the amount of electricity that must be dealt with by other matching mechanisms. For example if a combination of storage and transmission are used then the capacity must exist to move 34.2 GW of electricity under the GG scenario, 23 GW in SP, 14 GW in LCL and 0.8 GW in NP, at the peak of excess wind generation.

Figure 8.6 shows how the residual demand duration curves shown in Figure 8.3 change over time, by displaying a curve for each year of the scenarios. The plot demonstrates that the level of residual demand reduces for all scenarios over time. The steady annual reduction is a result of the influence of capacity change. The white space in the middle of the GG and SP curves, which is between 2022 and 2023 in both instances, is a result of rapidly increasing capacity factors due to the introduction of capacity in far from shore locations. Wind speeds also drive reduction, as illustrated by the overall lower residual demand in 2033 compared with 2035; 2033 does not have a larger capacity than 2035, but the wind speeds are higher.

Figure 8.6 shows that under the GG scenario excess wind generation is experienced for 1 % of the

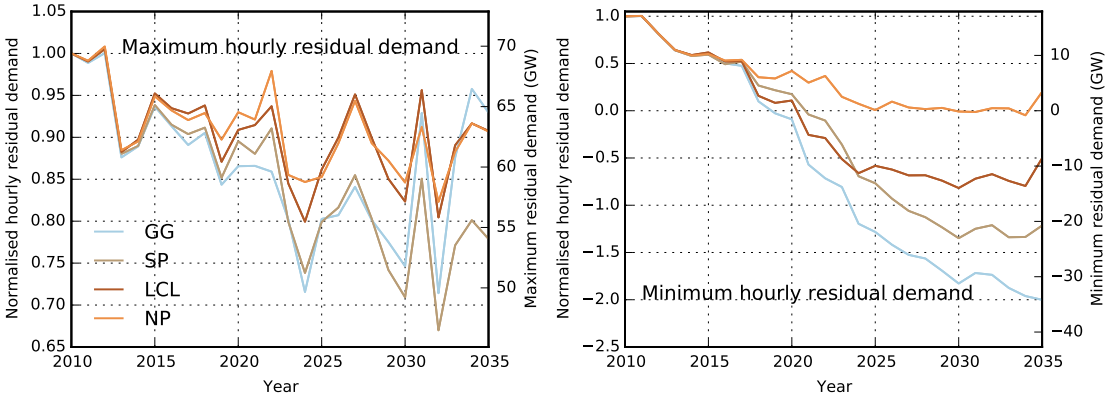

Figure 8.5.: Maximum and minimum hourly residual demand.

time in 2020; this increases to 30% of the time in the final years of the scenario period, in comparison to 10% of hours across all years. In the SP scenario excess wind generation is experienced for <20% of hours in the later years compared to 5% overall, and in the LCL scenario for < 5% in the later years compared to 1% overall. Using the 20 GW inflexible plant example described above would lead to excess wind generation for 75% of hours under the GG scenario at the peak, 70% in the SP scenario, 40% in the LCL scenario and 20% in the NP scenario. This demonstrates that the construction of inflexible plant will significantly increase the need for matching mechanisms under all of the scenarios presented by NG. These large excesses demonstrate that inflexible plant capacity is likely to be significantly lower than 20 GW under these scenarios.

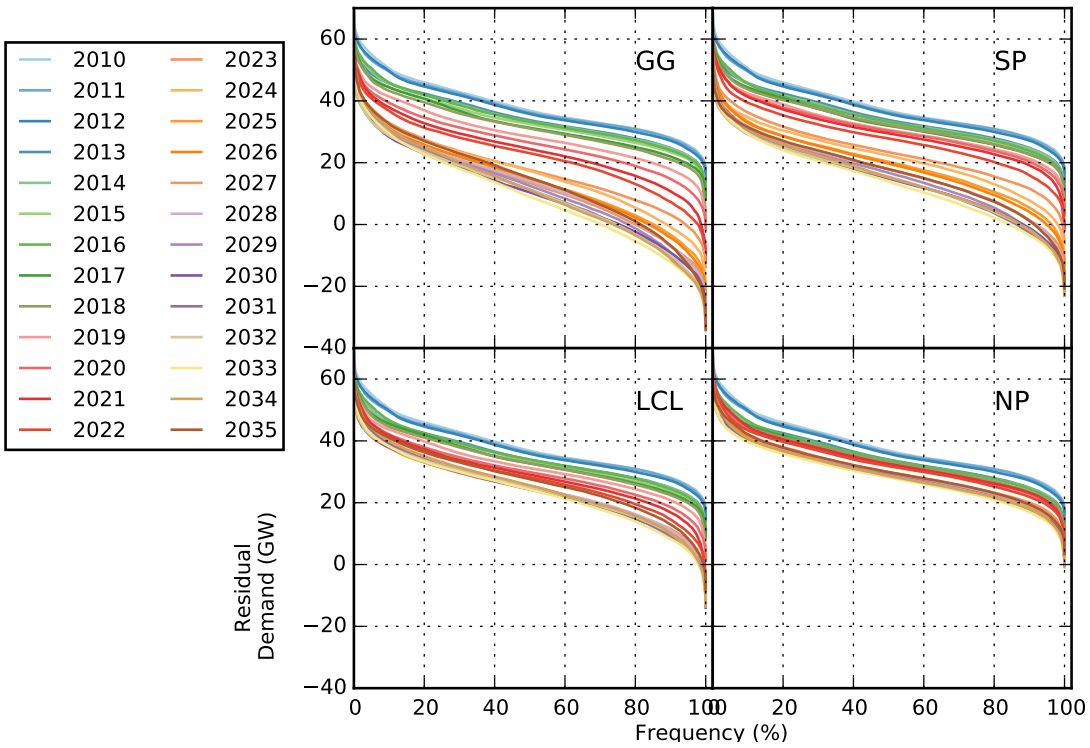

Figure 8.6.: Residual demand duration curves over time.

8.1.4. Cumulative excess wind generation

In the long term, the lack of hours where wind generation exceeds electricity demand means that there will be little accumulation of stored electricity, as it would quickly be required to meet shortfalls in generation. This situation will change if inflexible plant is used as part of the generation mix, as this would increase the level of excess generation that must be met by matching mechanisms. This section considers the contiguous hours of excess wind generation without any other other generation on the system. This analysis can be extended in future work to include the impact of other generation sources and any combination of matching mechanisms.

Figure 8.7 describes the maximum cumulative energy that results from the scenarios each year. The plot demonstrates that after 2020 the amount of energy that may need to be stored, curtailed or exported increases under each of the scenarios. Currently Dinorwig, the UK's largest pumped storage, can store 9 GWh. It is clear from the plot that this will only store a fraction of the excess wind generation, therefore more matching mechanisms will be needed. Those matching mechanisms will have to handle a cumulative excess of up to 91 GWh under the LCL scenario, 446 GWh under the SP scenario and 979 GWh under the GG scenario. There is significant inter annual variability, driven by weather. Interestingly this variation is different between scenarios, while in other annual analysis scenarios have closely followed each other. This demonstrates that the spatial weighting of capacity and heating technologies has an impact on contiguous hours of high generation and low demand.

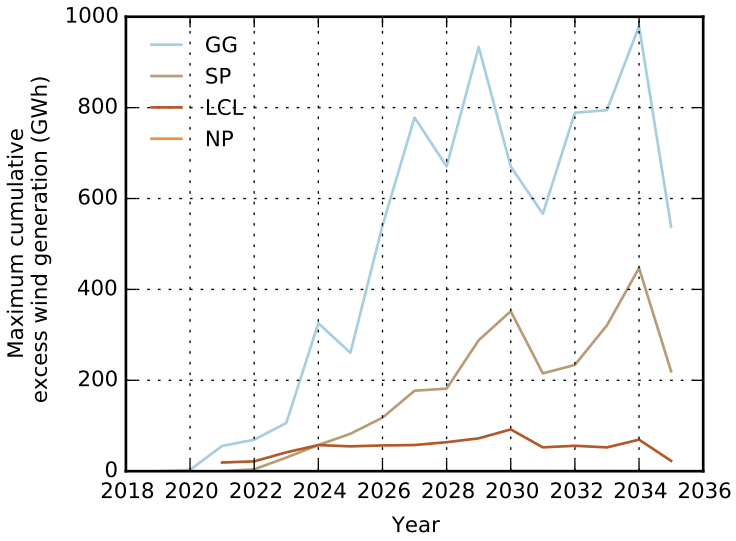

Figure 8.7.: Maximum cumulative excess wind generation per year.

Figure 8.8 shows the frequency of accumulation of excess wind generation each year post 2020 under the GG, SP and LCL scenarios. The plot shows only the peak accumulation values, not each hourly step, and describes the maximum amount of energy that needs to be stored etc. each time there is an accumulation of excess wind generation. The plot demonstrates that a very small percentage of the accumulation events occur at the magnitude described in Figure 8.7. 90% of the accumulation events are less than 200 GWh for all years of the GG scenario, 100 GWh for the SP scenario and 50 GWh for the LCL scenario. Under the GG scenario the remaining 10% of accumulation events lead to an increase in magnitude of less that double the lowest 90%. Under

the SP scenario the other 10% quadruple the magnitude and under the GG scenario the largest events are five times as big as those within the 90%. The plot shows the amount of energy that would have to be curtailed depending on the systems capacity for storage and export.

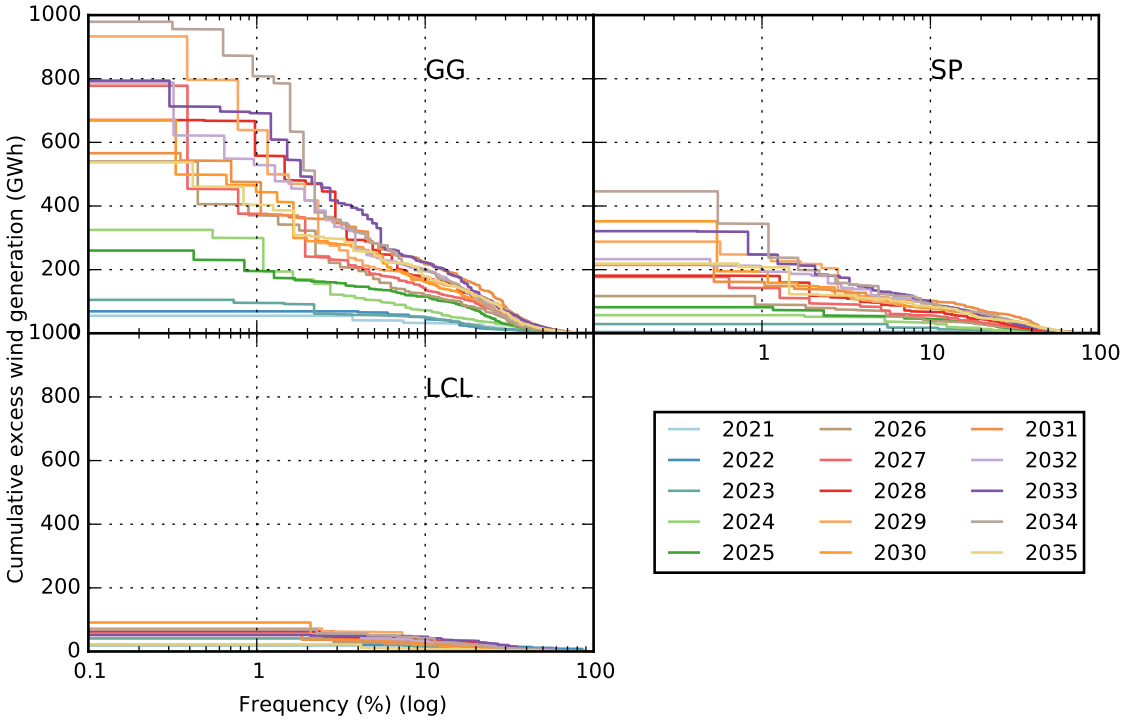

Figure 8.8.: Frequency of accumulation of excess wind generation.

8.2. Variability

8.2.1. Frequency of variability

Wind speed and therefore wind generation is variable. This variability must be resolved using a combination of the matching mechanisms described above, to ensure security of supply, and to limit the costs of integrating wind power into an energy system. Therefore, it is important to understand this variability and how it changes when different scenarios of wind capacity are adopted. Plots to show the frequency of changes over different time periods have been used by a number of studies previously reviewed in this thesis, including Coelingh [1999], Strbac and Ilex Consulting [2002], Boehme et al. [2006], and Østergaard [2008]. The plots are used here to demonstrate the variability of wind generation from SpWind, in terms of capacity factors in Figure 8.9 and hourly generation in Figure 8.10. Figure 8.10 also describes the variability of total hourly electricity demand and hourly residual demand under each of the scenarios. The y - axes are harmonised for all plots, which results in the paint drip effect in some cases, where the y - origin is below the minimum value for that plot.

8.2.1.1. Capacity factors

The left hand subplot of Figure 8.9 shows the relative distribution of hourly changes in onshore and offshore capacity factors over the whole scenario period. The plot shows that the offshore changes are larger than onshore. This may be because offshore capacity factors are generally higher, as described in Section 7.1. However, greater variability may also be a result of fewer locations being used offshore than onshore, because using more grid squares with different wind speed conditions during any particular hour smooths changes over time. Also, as previously discussed, wind speeds are more spatially homogeneous offshore, which may result in larger hourly changes if wind speed changes over large areas containing a large proportion of offshore capacity. There is little difference between the scenarios with respect to hourly change in capacity factor, either onshore or offshore. This would be expected with onshore capacity factors, as each scenario uses similar locations to place capacity, which results in similar onshore capacity factors between scenarios (see Section 7.1). The difference in capacity factors between scenarios is greater offshore, driven by the use of locations which are further from shore to place capacity in the GG, SP and LCL scenarios. Therefore it would be expected that the NP scenario would experience lower magnitude hourly changes in capacity factors, Figure 8.9 demonstrates that this is not the case.

The right hand side subplot of Figure 8.9 shows the distribution of changes in capacity factors when onshore and offshore generation are combined, both hourly and at a more aggregated temporal resolution (4 hours). The plot shows that combining onshore and offshore generation results in a reduction of hourly capacity factor changes, which is a result of the greater geographical diversity in wind speeds during any particular hour. The reduction in hourly change that results from the combination of onshore and offshore capacity is the same under each scenario. This demonstrates that the geographical diversity needed to reduce the hourly change can be achieved without using the far from shore locations. It also shows that there is no apparent penalty for the use of these far from shore locations in terms of increasing hourly capacity factor variability. This observation is supported by the lack of difference between scenarios in terms of offshore capacity factor change. This is important because greater variability would necessitate the use of larger

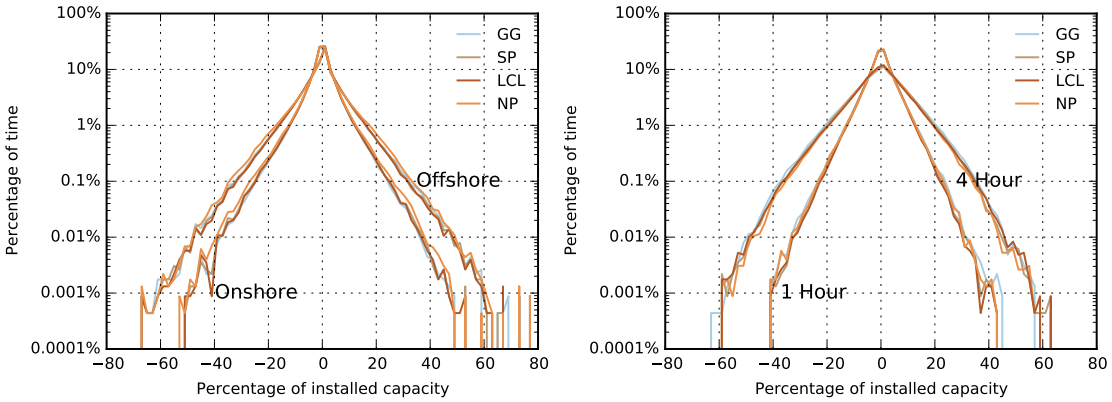

Figure 8.9.: Variability of capacity factors, the left plot separates onshore and offshore generation, the right plot shows hourly and four hourly generation changes.

magnitude matching mechanisms to ensure that demand is satisfied and therefore increase the cost of installing capacity further from shore. The plot of hourly changes is symmetrical, demonstrating that positive and negative changes are of very similar magnitudes; therefore matching mechanisms for meeting shortfalls in supply and handling excesses will also be of a similar magnitude. The most extreme changes over the course of over 26 years will be equivalent to approximately 40% of the installed capacity, which occur less than 3 times (the plots represent 227800 hours). Hourly changes equivalent to 30% of capacity occur approximately 10 times, 20% capacity changes occur 200 times and 10% changes occur 10,000 times.

8.2.1.2. Wind generation

Figure 8.10 shows the distribution of hourly changes in wind generation, electricity demand and residual demand. The plots in the left hand column describe changes under each scenario over the whole scenario period, while the right hand column shows the same changes in 2010 and 2033.

Figure 8.10 A describes changes in wind generation for the whole scenario period, demonstrating the extent of the divergence between scenarios. Analysis above has shown that the hourly changes in capacity factors are very similar between scenarios, the difference shown in Figure 8.10 A is a result of different amounts of capacity exposed to those changes in capacity factor. The GG scenario experiences maximum hourly wind generation increases and decreases of 15 GW, SP 10 GW, LCL 8 GW and NP 6 GW, which as Figure 8.9 has shown is equivalent to 40% of the installed capacity. This difference demonstrates the benefit of smaller capacities, particularly offshore, in terms of matching supply and demand, as these abrupt changes in generation must be met with matching mechanisms, which increase the cost of integrating renewables on to the grid.

The larger magnitude changes represent a small portion of the total scenario period. The plots show that a much greater percentage of hours experience smaller magnitude changes in capacity factor and wind generation and that there is no apparent difference between the scenarios in this respect. The nature of variability means that this does not necessarily make demand supply matching any easier, because variability is inherently unpredictable, though advances in wind speed forecasting may reduce this unpredictability in the future. Furthermore wind speed and therefore generation vary over smaller temporal resolutions, which have not been represented here because the finest

available temporal resolution wind speed data is hourly. Despite the variability of wind generation the plots show that maximum hourly changes are lower than shown in the demand plots and a greater percentage of hours experience very small changes (1-2 GW).

Figure 8.10 B describes changes in wind generation in 2010, where wind generation and electricity demand is the same for all scenarios, and 2033 where wind capacity is at its maximum level. It should be noted that 2033 represents a year of high mean wind speeds, whereas 2010 uses wind speed data from a low wind speed year. Previous analysis has shown that annual differences in wind speeds can account for up to 20% of changes in annual generation (see Section 7.1.2). However changes in capacity and the use of offshore locations cause far more significant increases in generation; therefore the difference between years predominantly reflects those changes. The figure shows that the maximum hourly change is very small in 2010 (2 GW) and increases significantly under all of the scenarios. This demonstrates that the matching mechanisms necessary for mitigating wind generation variability will have to increase in size in comparison to those currently in operation. In comparison with Figure 8.10 A, Figure 8.10 B also shows that the largest hourly changes in wind generation do not occur in 2033, despite the large capacity and overall high wind speeds.

8.2.1.3. Total electricity demand

Figure 8.10 C and Figure 8.10 D show hourly changes in total electricity demand from SpDEAM. Figure 8.10 C demonstrates that maximum hourly changes in electricity demand are a similar magnitude to maximum changes in wind generation. However, the curve is a different shape, demonstrating that demand changes are more often larger in magnitude. The only significant difference between the scenarios is the larger highest magnitude events experienced by the GG scenario. There are several hours where electricity demand increases or decreases by 15 GW or more in the GG scenario, whereas the largest change in the other scenarios is less than 15 GW. The larger events in the GG scenario occur because of the introduction of heat pumps and the resultant increased electricity demand. This is the clearest impact of heat pumps described by this thesis so far and shows that even with efficient heat pumps and a concurrent reduction in resistive electric heating their use will impact on the the magnitude of matching mechanisms necessary to facilitate their integration. It should be noted that heat pumps will often be connected to thermal storage - hot water tanks and that this will affect the impact of the technology on matching mechanisms by potentially increasing electricity demand and shifting the occurrence of demand in time and space.

Figure 8.10 D shows that the variability in electricity demand experienced in 2033 under the SP, LCL and NP scenarios is very similar to that experienced in 2010. This is to be expected given the small changes in electricity demand profiles discussed in the previous chapter. In contrast, the GG scenario clearly experiences more changes at a higher magnitude in 2033 compared to 2010 as a result of the introduction of a large number of heat pumps. The plot demonstrates that several of the largest changes in electricity demand that occur over the whole scenario period happen during 2033. These events are, however, in the minority, occurring between 1 and 10 times a year at magnitude of 11-15 GW. Though, for system design purposes, the worst conditions that might reasonably occur should be selected to ensure that demand is satisfied.

8.2.1.4. Residual electricity demand

As described above, the ultimate aim of this chapter is to establish the combined implications of increased wind capacity and electrified heat demand. In the context of variability the question to answer is whether the extremes from demand and wind generation occur at the same time, therefore increasing the maximum difference which must be handled by the electricity system. Figure 8.10 E hows that this is indeed the case; the extreme negative changes in residual demand reach 30 GW in GG, the sum of the greatest variability in demand and wind generation. The largest increase in GG residual demand is slightly less than the sum of the greatest increase in demand and wind generation. None of the other scenarios show an exact correlation between increase or reduction in demand and wind generation. This is important as it suggests that increasing the number of heat pumps will increase the correlation between peak total electricity demand and lowest wind generation and vice versa. Therefore the combined increase of wind capacity and heat pumps increases the magnitude of matching mechanisms and the cost of this decarbonisation option. The relationship between electricity demand for heat and wind generation is explored further in Section 8.4.

Figure 8.10 shows that residual demand variability is similar between 2010 and 2033 for the SP, LCL and NO scenarios, particularly in terms of increases. The magnitude of extreme decreases in residual demand is slightly higher in those scenarios in 2033 (1 - 5GW). The GG scenario experiences a much larger increase in residual demand variability in 2033 as a result of the combination of increased wind capacity and electricity demand for heat.

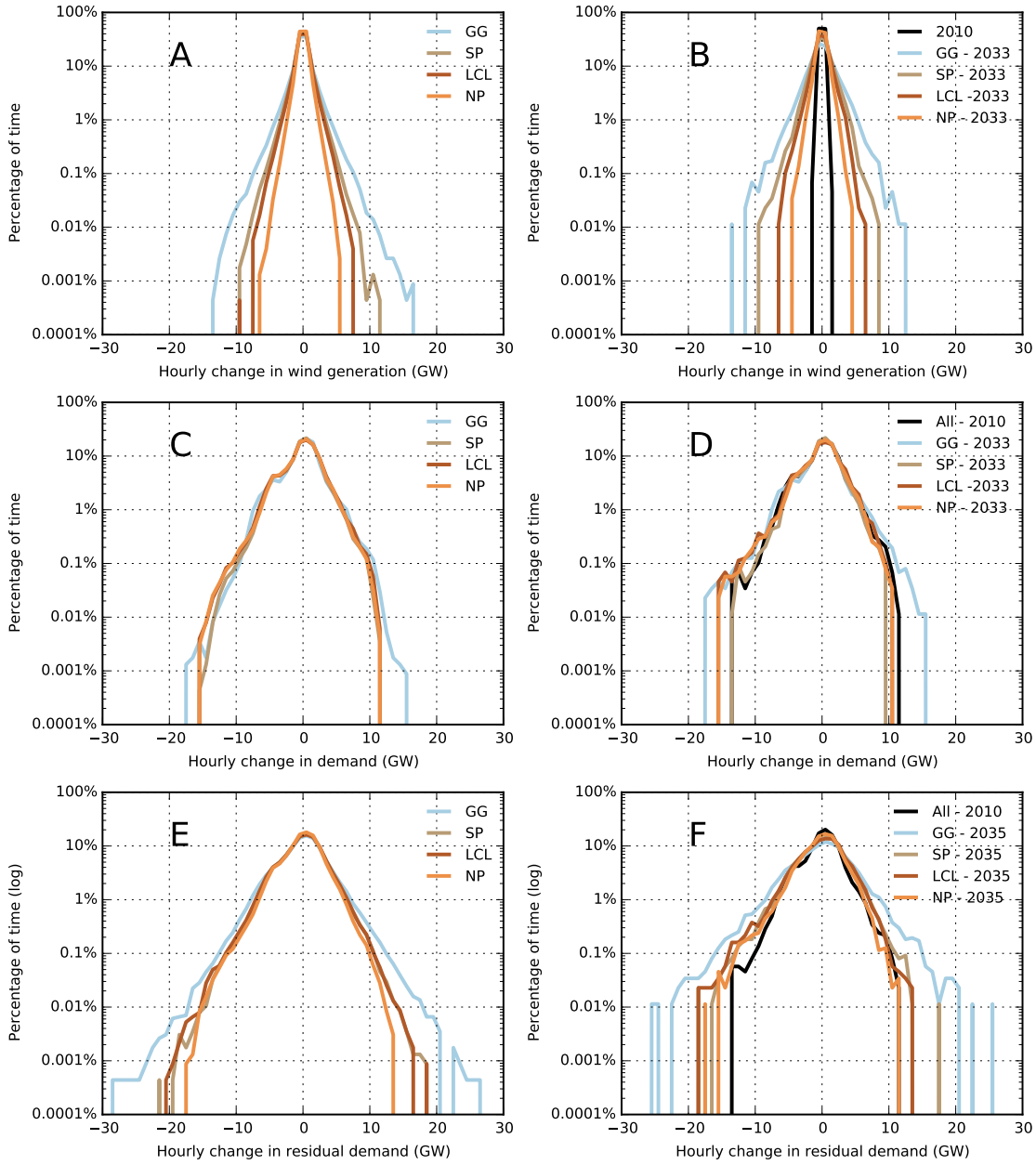

Figure 8.10.: Variability of wind generation, electricity demand and the resultant residual demand.

8.2.2. Seasonal and annual changes in variability

Figure 8.11 and Figure 8.12 show how variability in wind generation, electricity demand and residual electricity demand vary over the course of a year and as the scenarios progress for the GG and SP scenarios respectively. The top row of plots represents wind generation, the middle row electricity demand and the bottom row resultant residual electricity demand. Each column represents a different year; 2010, 2020, 2030 and 2035 have been selected to describe the evolution of each of the aspects through the scenario period. Each plot contains a row for each day of the year starting at the top and ending at the bottom; the row represents how generation, demand and residual demand varies during that day. The range is normalised to the year's maximum value for all the plots, so that each day can be compared to different days in that year, years can be compared against each other and generation, demand and residual demand can be compared.

The top row of plots in both Figure 8.11, and Figure 8.12 show that as capacity increases there are more hours where greater capacity factors are experienced. High capacity factors are experienced most often in the winter, but are increasingly experienced in the spring and autumn, particularly in the GG scenario. The SP scenario exhibits longer periods of low capacity factors in the summer than the GG scenario. The 2010 plot contains some of what has been referred to as the solar shadow [Coker, 2011], where wind speeds and generation increase in the daytime in the summer. This phenomenon is less evident in later years, it is likely that this is owing to the introduction of offshore wind capacity which is not exposed to the same solar driven speed up, caused by a warming land mass.

The middle row of plots shows that electricity demand variability is more regular than wind generation variability. The GG and SP scenario exhibit the same diurnal and seasonal patterns, dictated by changes in activity and weather. The GG scenario drives some difference in the variability of electricity demand over time. Demand in 2025 appears to be lower in the summer mornings and evenings relative to the winter than in the earlier years. There is also a more pronounced morning and evening peak in demand in the winter, as suggested by Figure 7.25. The typical pattern of demand still remains however. There is very little detectable change in demand in the SP scenario, the winter peaks are also evident, suggesting that they may not be a result of heat pumps, but rather the weather conditions, as 2035 is a low wind, low temperature year. The decrease in relative summer morning demand is less detectable than with the GG scenario.

The bottom row of plots shows the result of the combination of the electricity demand and wind generation illustrating the comparative strength of variability. The relatively small wind capacity in 2010 results in the variability of residual demand appearing very similar to electricity demand. This variability is far more regular than that of wind, therefore satisfying residual demand is a relatively simple prospect compared to later years when variability becomes gradually less predictable, as wind capacity reaches demand magnitudes.

In 2020 the pattern of daytime demand is still visible in the GG scenario, despite extended periods of low residual demand. Relative night time residual demand decreases significantly to between 0 - 20% of the annual peak. In 2030 and 2035 the periods of low residual demand increase significantly. The shape of demand can still be seen, but there are more periods where low residual demand extends over periods greater than 24 hours. The greater influence of wind means that peak residual demand can occur outside of winter. Figure 8.12 shows that under the SP scenario the plots representing residual demand remain similar in appearance to those representing demand,

demonstrating that the influence of the variability of wind on residual demand is a lot less severe than the GG scenario. There is a marked decrease in residual demand at night time; however this is much lower than the GG scenario. There are very few periods where this continues into the day and even fewer where the events persist. The result is a more predictable residual demand profile.

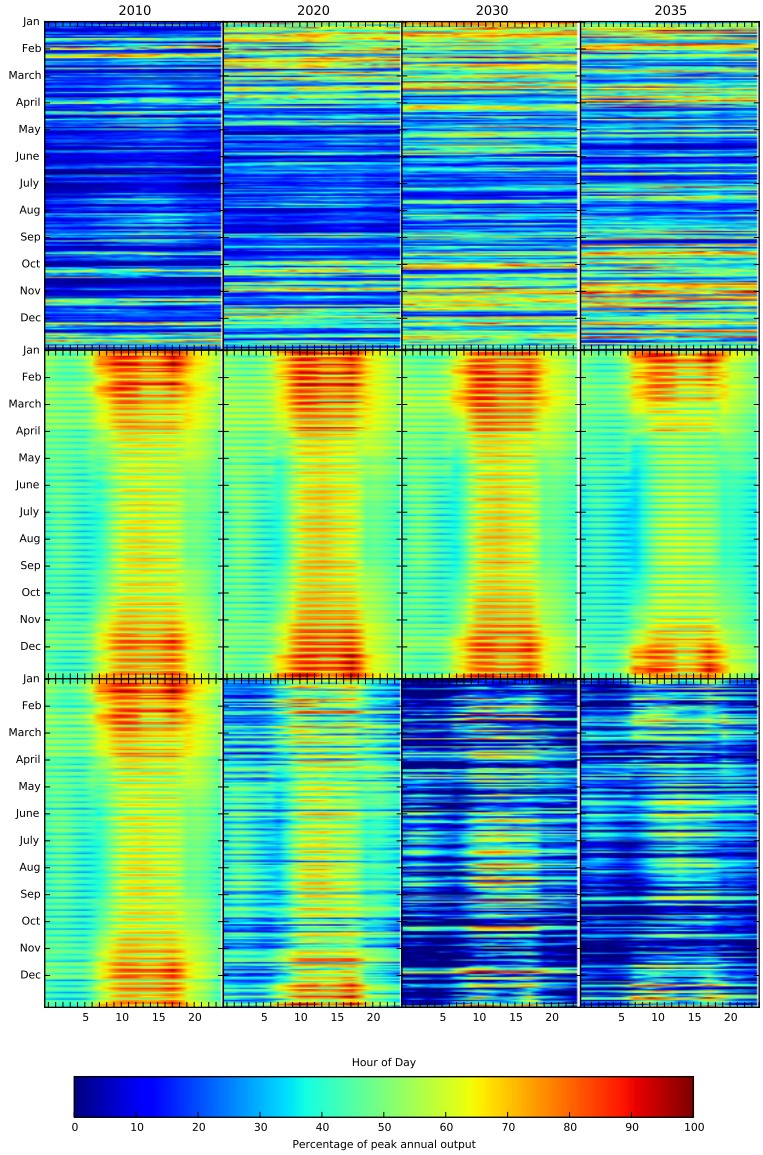

Figure 8.11.: Variability over each day in select scenario years in the GG scenario.

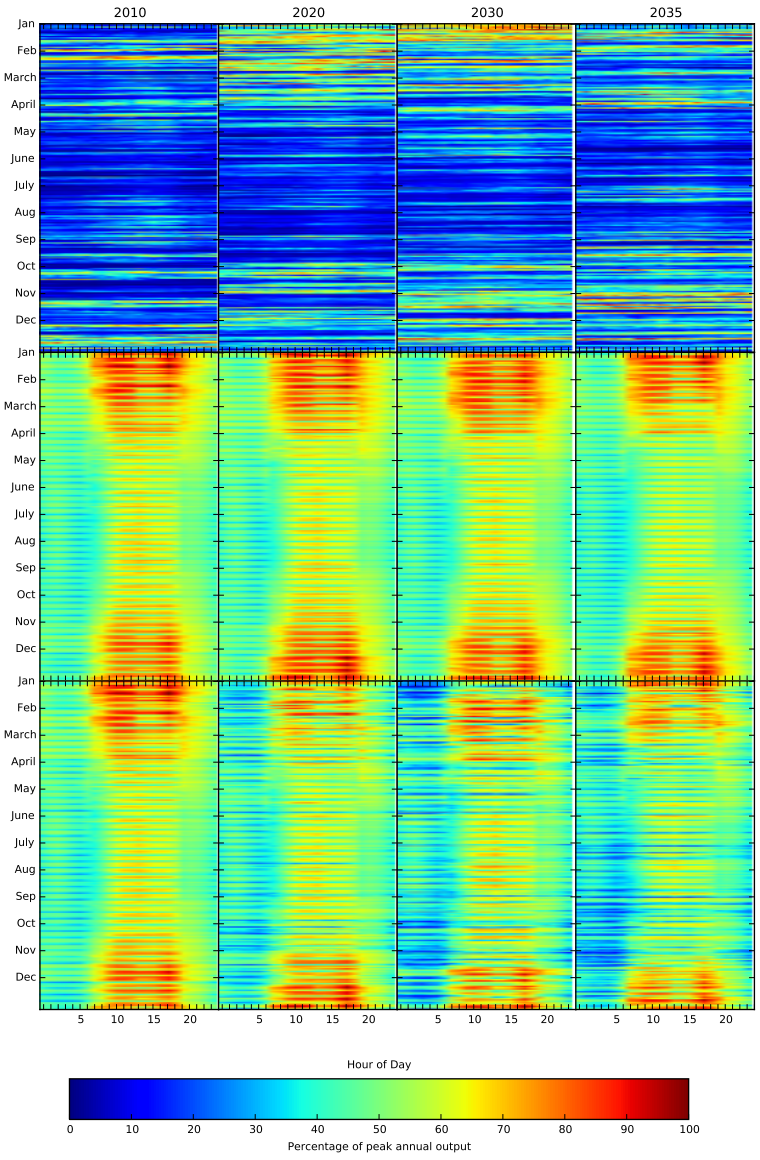

Figure 8.12.: Variability over each day in select scenario years in the NP scenario.

8.3. Extreme events

The following analysis uses a method established by Cannon et al. [2015], which was designed to examine the occurrence and persistence of extreme wind generation events. The authors simulate hourly wind generation using a manufacturer turbine curve approach and MERRA wind speed data over a 33 year period, as described in Chapter 2 and Chapter 4. They then define extreme events under percentiles of capacity factors, using the 1st, 10th, 20th brackets to represent very low wind events and the 80th, 90th and 99th brackets to represent very high wind events. The persistence of these events is plotted against a number of occurrences and the characteristics of GB's wind resource examined. Here, this method is used to show how variable wind resource is harnessed by each scenario, which is exposed to different wind conditions. Extreme wind events are examined in terms of the capacity factor that they create and the resultant generation. The method is then used to examine electricity demand and residual demand in the same way. The application of the method to different aspects of the future electricity system means that insights can be gained into the size of matching mechanisms and the contribution of wind generation and electricity demand to the magnitude of extreme events can be examined. Cannon et al's analysis of extreme events assumes a static capacity over all 33 years of their analysis. Their analysis considers all generation during those 33 years, providing insights into GB wind conditions. However, it doesn't consider how different capacities will harness these wind speeds and how this will evolve in the future. Here, their analysis is extended to show how extreme residual demand events change over the scenario period and during different seasons of each year.

Percentiles have been calculated separately for each scenario, and differ between scenarios. To allow direct comparison of the results, a mean value was also calculated for each percentile. All values are described in the tables below, while the plots use the mean values. Part of the analysis described in this section has been published in Sharp [2015a] and Sharp [2015b].

8.3.1. Over the entire scenario period

8.3.1.1. Wind generation - capacity factors

Table 8.1 shows the capacity factor percentile values for each of the scenarios demonstrating that there is some variation between scenarios with respect to extreme capacity factor events. The range of capacity factors is smallest in the 99th percentile where the value is the same for all scenarios, showing that all of the scenarios experience 100% capacity factor events a similar number of times over 26 years. This may be because these events occur at the beginning of the scenario period, when capacity and therefore generation is identical in all scenarios. However, this is unlikely because the highest capacity factors are associated with larger amounts of offshore capacity, which were not included in the earlier years of the scenario. Therefore this similarity between scenarios is likely to be driven by high wind conditions across all possible locations for capacity that occur later on in the scenario period. The 1st percentile also exhibits a small range of capacity factors between scenarios (2.8%), which are more likely to occur at the beginning of the scenario period when capacity factors are generally lower and there is less geographical diversity.

The difference between the scenarios increases to a range of 10% in the 90th percentile and 12% in the 80th percentile. This shows that there is greater variation between scenarios in terms of less

	High			Low		
Percentile	99	90	80	20	10	1
GG	100	84.3	70	17.5	10.8	2.6
SP	100	81.2	66.5	16.2	10	2.4
LCL	100	79	64.1	16	10	2.5
NP	100	74	58	13.1	8	1.9
Mean	100	79.6	64.65	15.6	9.7	2.35
Cannon et al. [2015]	87.1	69.6	55.3	10.3	6.3	2.2
Mean minus Cannon	12.9	10	9.3	5.3	3.4	0.1

Table 8.1.: Capacity factors under each scenario, in selected percentile brackets (%).

extreme high wind events. This is likely to be due to the extent of the capacity located in grid squares that experience high wind speeds; for example, as the GG scenario places more capacity in locations further from shore than the NP scenario, the high wind speeds in those locations have a stronger effect on extreme periods of generation. There is also greater variation between scenarios in terms of less extreme low wind events, illustrated by the fact that the largest range of values between scenarios is experienced in the 20th percentile (44%), while the range reduces to 10% in the 10th percentile. Previous analysis in Section 7.1.3 has shown that a much larger number of hours experience wind speeds between 5-10 m/s which are likely to drive generation in the 20th percentile; it is therefore likely that there is increased spatial variability in this wind speed band that drives the difference between the scenarios. Exploring the spatial variability of wind speed in different power producing bands, weighted by expected capacity locations, may be an interesting path for future work because this could dictate a more effective spatial configuration of capacity; however under the current spatial constraints it may be difficult to remove the likelihood of very low wind events.

In the low wind generation percentile brackets, approximately half of the range is caused by the difference between the GG, SP and LCL scenarios. The other half, to the the lowest value, is caused by the difference between those scenarios and the NP scenario. This demonstrates that the further from shore locations used by the these scenarios and the larger offshore capacities reduces the likelihood of low generation events. The same division is seen in the higher wind generation percentile brackets, which shows that the same scenarios result in an increased likelihood of extreme high generation events. Though more generation is desirable, these extreme events may result in the need for larger magnitude matching mechanisms.

The percentile values found by Cannon et al. [2015] are shown in Table 8.1. The table demonstrates that the values described by SpWind are higher in all brackets than those found by Cannon et al. Their method uses very similar wind years (starting slightly earlier), but wind generation is simulated for all of those years using a predominantly onshore static capacity, which is very similar to the capacity used in the first years of the scenario simulation. Section 7.1.1 has shown that capacity factors in SpWind increase significantly over time, owing to the introduction of offshore capacity. Therefore the larger percentile values found here would be expected to be higher than those found by Cannon et al. There may also be some difference driven by the use of different wind speed data and slightly different simulation methods.

Figure 8.13 shows how the persistence and occurrence of events in the mean percentile capacity factor brackets shown in Table 8.1 vary between scenarios. Overall the plot shows that there is not a lot of difference between scenarios in terms of the persistence or occurrence of events, but

variation increases as the events become less extreme.

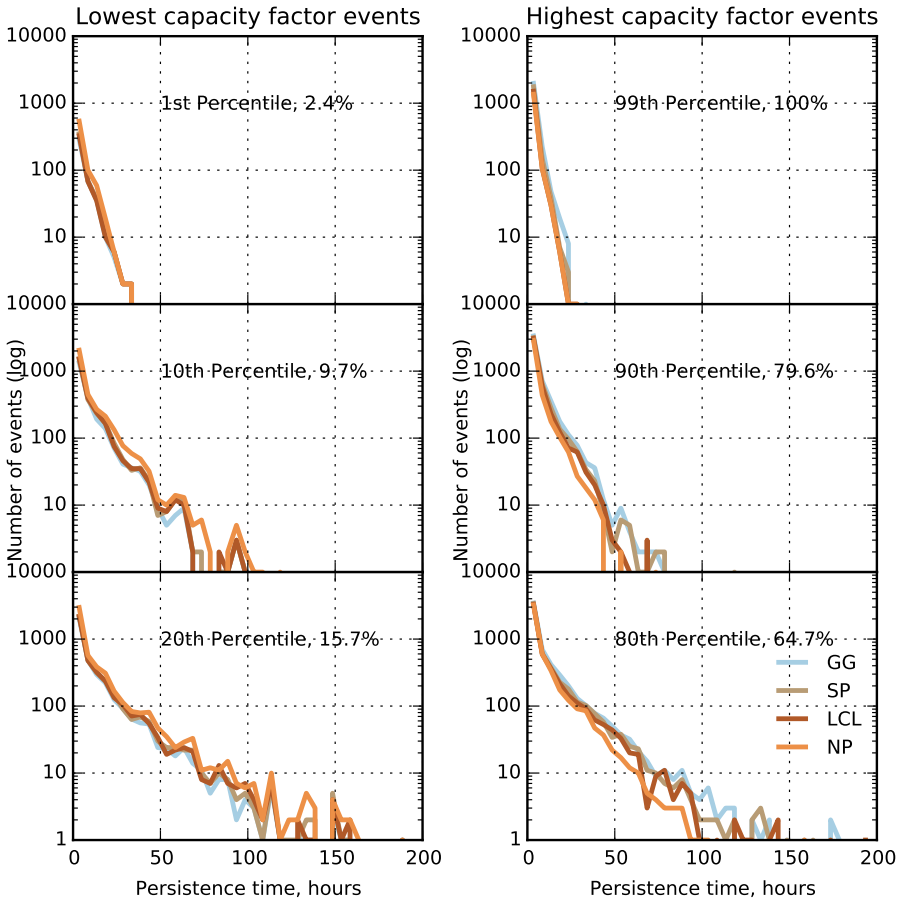

Figure 8.13.: Extreme events, supply capacity factors, bins = 5 hours.

The 1st percentile plot shows that all scenarios experience one event in 25 years where capacity drops below 2.35% for more than 35 hours. This shows there there can be extended periods of still conditions affecting large geographical areas. The shortest lasting events of this magnitude (1 hour) occur between 300 and 500 times over the course of the scenarios, or up to 20 times per year assuming consistent occurrence.

The persistence time increases in the 10th and 20th percentile plots, showing that the scenarios experience events where capacity factors remain below 9.7% for up to 100 hours and below 15.7% for up to 160 hours. The length of persistence of these events means it is impossible that they will only occur at times of low demand as they cover periods where the whole spectrum of electricity demand is experienced (20GW - 60 GW); therefore they will definitely result in a cumulation of positive residual demand, which must be met with matching mechanisms. The NP scenario experiences more low capacity factor events in the 10th and 20th percentile brackets than the other scenarios, which persist for longer. This shows that increased offshore capacity used in the other scenarios has a positive benefit in reducing the length of time that low wind speed events persist. Despite this divergence the longest lasting events in each of the scenario brackets are similar between scenarios.

The longest lasting 100% capacity factor events, in the 99th percentile, last more than 25 hours

under all scenarios. The difference between scenarios increases as the magnitude of the events decreases, so that events above 79.6% last between 40 and 75 hours and above 64.7% 90-175 hours. The shortest lasting extreme generation events of 1 hour occur more than 1000 times under all percentiles other than the 1st, demonstrating that high wind speed events are more common than low wind speed events.

The lack of divergence between scenarios shown in the high capacity factor plots (99th, 90th and 80th percentiles) demonstrates that, despite differing amounts of wind capacity, all scenarios experience similar levels of consistent high winds which cover all capacity. The NP scenario exhibits events that last less time than the other scenarios in the 80th and 90th percentile; this is due to the lack of capacity far from shore. This may be evidence of weather fronts moving from west to east where the NP capacity does not experience the high wind speeds for as long owing to the lack of capacity in the easternmost development zones.

8.3.1.2. Wind generation - absolute generation

Table 8.2 shows the percentile values for absolute wind generation. The difference between percentile brackets and scenarios follows a different pattern to that seen in the capacity factors. The range of values between scenarios reduces incrementally from 31 GW in the 99th percentile to 0 GW in the 1st. The gap between the NP scenario and the rest is increased in the high generation brackets and reduced in the low generation brackets with respect to capacity factors. In the case of the low events this is likely to be due to the NP scenario experiencing the lowest capacity factors with a slightly larger capacity. This is a result of the continued domination of onshore capacity in this scenario. In the case of high events the difference is driven by the larger offshore capacities in the other scenarios experiencing the high capacity factor events, which results in more generation. The result of NP experiencing significantly lower generation at the top end, means that the mean value is significantly larger than the NP value in the 99th, 90th and 80th percentile brackets. This will result in fewer values shown in the plots for the NP scenario.

	High			Low		
Percentile	99	90	80	20	10	1
GG	52.0	37.7	28.2	3.0	1.5	0.2
SP	41.2	28.8	21.0	2.6	1.4	0.2
LCL	34.8	24.6	18.4	2.7	1.4	0.2
NP	21.0	13.4	10.1	1.9	1.1	0.2
Mean	37.2	26.1	19.4	2.5	1.3	0.2

Table 8.2.: Wind generation under each scenario, in selected percentile brackets (GW).

Figure 8.14 shows extreme wind generation events, following the percentiles described in Table 8.2. Overall the plot shows that low generation events are very similar between scenarios, but high generation events exhibit much greater divergence.

The capacity factor plot (Figure 8.13) shows there is almost no difference between scenarios in the 1st percentile. The longest lasting low capacity factor events (2.4%) equate to generation of 0.2 GW. These events clearly occur at the beginning of the scenario, because later in the scenarios 2.4% of the larger capacities are greater than 0.2 GW.

Figure 8.14 exhibits a clearer difference in the persistence of events in the 10th and 20th percentile

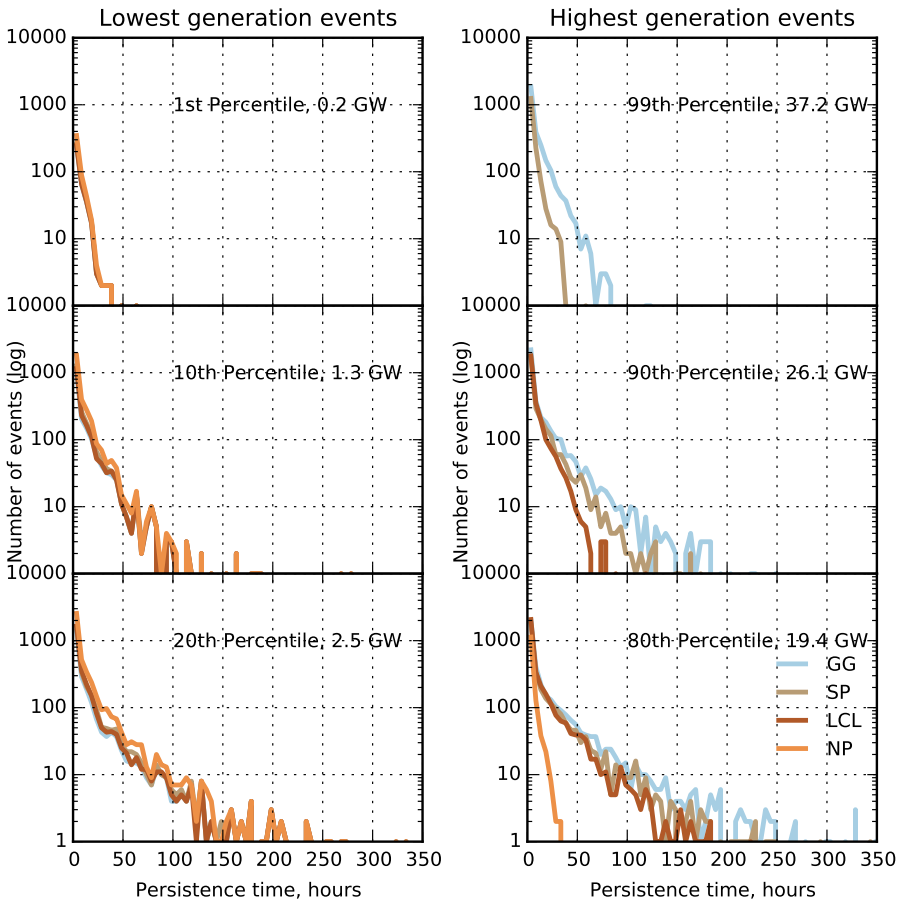

Figure 8.14.: Extreme events, wind generation, bins = 5 hours

than in the 1st percentile. NP events last 175 and 550 hours respectively (the extent of the persistence in the 20th percentile is not illustrated to ensure that the detail can be distinguished and that x - axes are harmonised to allow comparison between plots), whereas events in the other scenarios are limited to 100 and 150 hours. This divergence demonstrates that the events in those brackets occur later in the scenarios where capacity diverges and that the NP capacity does not reduce the risk of low wind events. This results in periods of up to 20 days of low generation.

The high generation event plots demonstrate the benefit of far from shore capacity as well as increased offshore capacity. The GG and SP scenarios clearly experience more events of larger persistence. The highest persistence events last between 40 - 80 hours in the 99th percentile; more than 37 GW is produced each hour during this time. Given that demand drops to approximately 20 GW during the night time of this period, this results in significant excess generation. 90th percentile events last over 150 hours in the GG and SP scenarios, compared to less than 75 hours in the LCL scenario.

8.3.1.3. Electricity demand

Table 8.3 shows the percentiles calculated for each of the demand scenarios. There is a much smaller difference between the scenarios in comparison to the percentiles of extreme wind generation events.

Ranges are 3 GW in the 99th percentile bracket, 3.3 GW in the 90th, 3 GW in the 80th, 2.3 GW in the 20th, 2.1 in the 10th and 1,71 GW in the 1st. GG percentiles are very close to the mean, despite the addition of heat pump demand. This is partly due to larger electricity demand in the LCL scenario than the GG scenario, which is driven by growth in other areas.

	High			Low		
Percentile	99	90	80	20	10	1
GG	60.0	50.6	45.6	30.9	28.0	22.6
SP	58.5	49.2	44.4	30.3	27.5	21.9
LCL	61.5	52.5	47.4	32.6	29.6	23.6
NP	59.6	50.5	45.3	31.1	28.2	22.4
Mean	59.9	50.7	45.7	31.2	28.3	22.6

Table 8.3.: Electricity demand under each scenario, in selected percentile brackets (GW).

Figure 8.15 describes extreme high and low demand events; the 1st, 10th and 20th plots represent very low demand events and the 80th, 90th and 99th percentile plots very high demand events. The 1st percentile plot shows that the extreme low demand events are relatively short, as there are no events below 22.6 GW for more than 10 hours. There is a slightly higher occurrence of these events under the SP scenario. There are more events that last longer for each scenario below the 10th percentile. SP contains slightly fewer events that last longer than the other three scenarios. In contrast to wind generation, there is more divergence between the scenarios in the low demand events.

There is a clear peak in high demand events lasting between 7 and 11 hours, which roughly matches the period over which demand is high during a typical day; this indicates that these periods will often last for much of, but not the whole, day. Here there are more occurrences in the LCL scenario, roughly four times as many as the other scenarios. The same pattern is seen in all scenarios, suggesting that whatever is driving the occurrences and persistence is relatively similar between scenario. Each scenario contains at least one event where demand will be over 59.9 GW for 11 hours. In the 90th percentile the persistence increases; the LCL scenario has more events at this higher persistence, but the scenarios converge at lower persistence. In all scenarios except LCL demand is over 50.7 GW for 14 hours at least once; these events increase to 16 hours for LCL and occur more regularly (8 times). There is little evidence of the impact of heat pumps.

8.3.1.4. Residual demand

Table 8.4 shows the percentile bracket values for residual demand. There is a much smaller difference between scenarios in high residual demand events than low residual demand events. Ranges are 1.2 GW in the 99th percentile, 2.5 GW in the 90th, 4.2 GW in the 80th, 15.8 GW in the 20th, 21.1 GW in the 10th and 28.8 GW in the 1st. Low events are affected most by supply where there is variability between scenarios, whereas high events are dictated by demand where there is less variation between scenarios. The mean percentile for residual demand is lower than the equivalent demand value, demonstrating the net effect of wind across all four scenarios. Some of the percentile values are negative, demonstrating that there will be large amount of excess wind generation under the GG and SP scenarios.

Figure 8.16 describes extreme high and low residual demand events; the 1st, 10th and 20th plots represent very low residual demand events and the 80th, 90th and 99th percentile plots represent

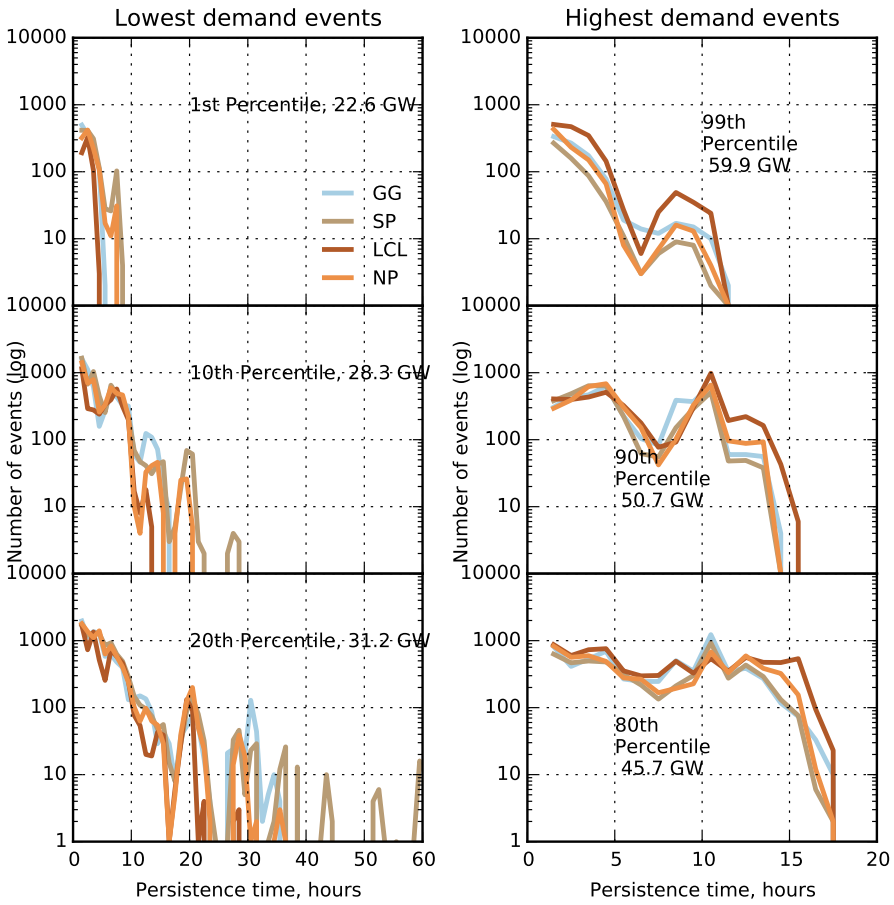

Figure 8.15.: Extreme events, electricity demand, bins=1 hour.

very high residual demand events. The discussion above has shown that wind generation exhibits greater variability between scenarios at the high end and demand shows greater variability between scenarios at the low end. The combined effect is greater variability between scenarios in terms of low residual demand.

The impact of larger wind capacities can clearly be seen in the low residual demand plots on the left hand side (Figure 8.16). The lowest events in the GG scenario persist longer than SP and LCL and there are no instances where residual demand is below -3.8 GW in the NP scenario. The 1st percentile plot demonstrates that under these conditions there will be periods of more than one day where GG can produce more electricity than is demanded in GB. There are over 100 times where this will last more than 10 hours. The 1st percentile plot also demonstrates a much clearer difference between the scenarios than the high demand events, demonstrating that negative residual demand events may be more of an issue in terms of wind integration than high demand. The SP scenario has a similar number of low residual demand events to GG in this percentile; however, they do not last as long. A similar pattern is shown for the 10th and 20th percentile to the 1st percentile. The events in the 10th and 20th percentile last much longer, but are less significant, as residual demand is not negative over this entire period. The NP scenario has some events in these brackets, indicating that they can be experienced with very little offshore capacity.

The pattern of high residual demand events is similar to that shown in Figure 8.15, demonstrating

	High			Low		
Percentile	99	90	80	20	10	1
GG	53.9	41.5	35.5	8.8	-0.3	-18.6
SP	54.0	41.8	36.3	14.4	6.9	-8.9
LCL	54.9	43.3	38.5	20.3	14.5	0.7
NP	55.1	44.0	39.7	24.6	20.9	11.4
Mean	54.5	42.6	37.5	17.0	10.5	-3.8

Table 8.4.: Residual demand under each scenario, in selected percentile brackets (GW).

that demand heavily influences these events. The slightly lower threshold, dictated by the mean percentile value, means that the events last slightly longer (7-14 hours in contrast to 7-11 hours). The same pattern is seen in the 90th and 80th percentile where the persistence of the events increases owing to lower thresholds, but the occurrences drop in some cases. This shows that these high events are dictated by demand, but that in some cases this may be reduced by wind in the lower persistence events. The 80th percentile plot shows some interesting patterns. There is no significant increase in the persistence of events at this magnitude from the 90th percentile, suggesting that that when cold snaps begin they have a finite period. It is possible that these events occur before large amounts of wind are modelled in the system so exhibit less influence of wind power than other parts of the plot. There is a significant increase in the occurrence of events that persist for 8-11 hours compared to events that last 11-16 hours or 6-8 hours. This could be due to the length of weather patterns or more likely the established pattern of national demand.

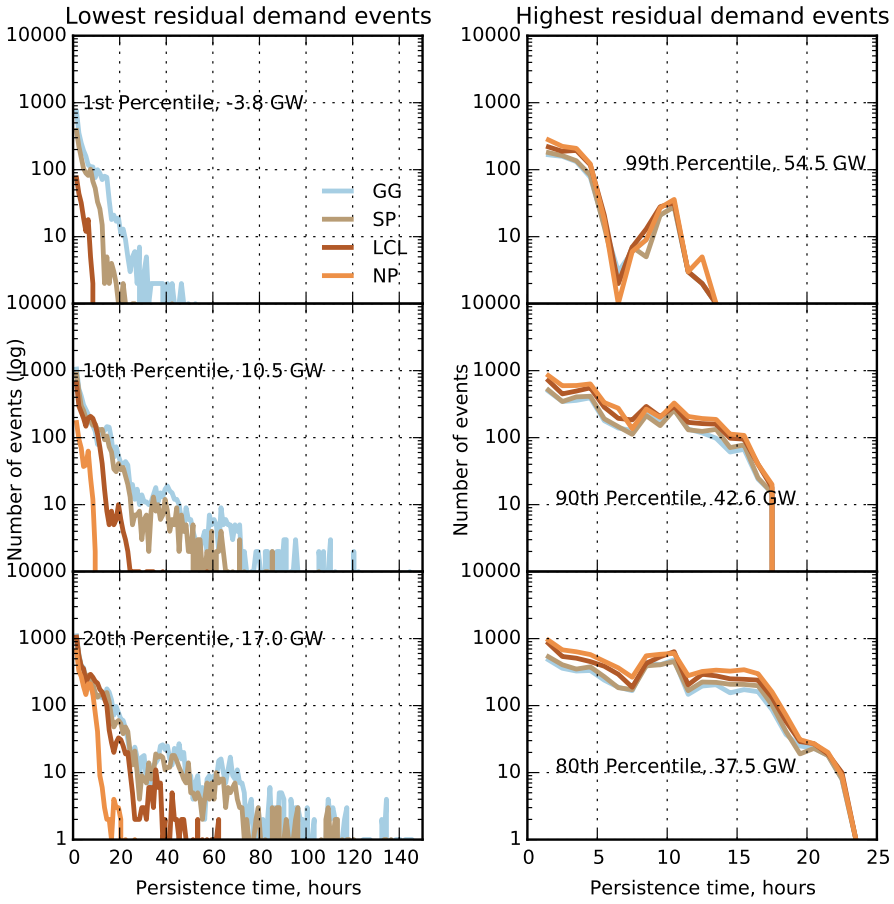

Figure 8.16.: Extreme residual demand events, low and high, organised by mean percentile, bins =1 hour

8.3.2. Seasonal and annual changes to extreme events

Figure 8.13 to Figure 8.16 showed the persistence and occurrence of extreme demand, wind generation and residual demand events over the course of 25 years for each of the scenarios. Comparing the plots provides insights into the causes of these events. The following plots show how these events vary over time (Figure 8.17 to Figure 8.20). Analysis of these plots shows what is causing the extreme events by comparing occurrence of extreme events with wind capacity and number of heat pumps (Figure 6.2 and Figure 6.17). Each plot is a 2d histogram of the extreme events. The number of occurrences at different levels of persistence are shown each year. The plots also show what season of the year that the events occur in. Four examples are given; Figure 8.17 shows the 99th percentile of residual demand for the GG scenario, Figure 8.18 contrasts this with the same percentile events for the NP scenario. These plots therefore represent two of the scenarios in the top right subplot of Figure 8.16 with different paths in terms of electricity demand. To compare, Figure 8.19 shows the 1st percentile for the GG scenario and Figure 8.20 shows the 1st percentile for the LCL scenario. The latter plots represent two scenarios from the top left subplot in Figure 8.16 with different paths in terms of wind capacity. The 1st percentile of the NP scenario could not be shown as it does not present any events where residual demand is below -3.8 GW.

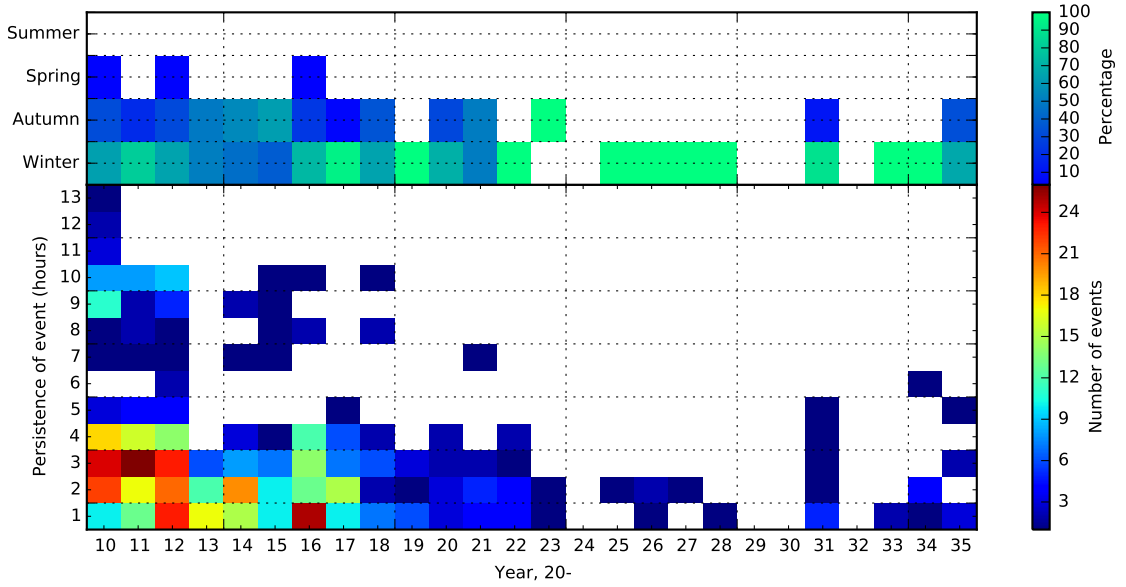

Figure 8.17.: Extreme residual demand events in the 99th percentile over time for the GG scenario.

In both Figure 8.17 and Figure 8.18 it is clear that the events of the highest persistence occur at the beginning of the scenarios; this demonstrates that as wind capacity increases, long lasting high residual demand events are reduced. The number of shorter lasting events also reduces significantly, particularly in the GG scenario, which sees significant amounts of wind introduced. Therefore, the majority of the high residual demand events shown in Figure 8.16 occur at the beginning of the scenarios, demonstrating that analysing the whole length of the scenarios at once can be misleading. Spring and summer events exist in both scenarios, but only at the beginning of the time period. In the GG scenario autumn events significantly reduce over time but remain consistent in the NP scenario.

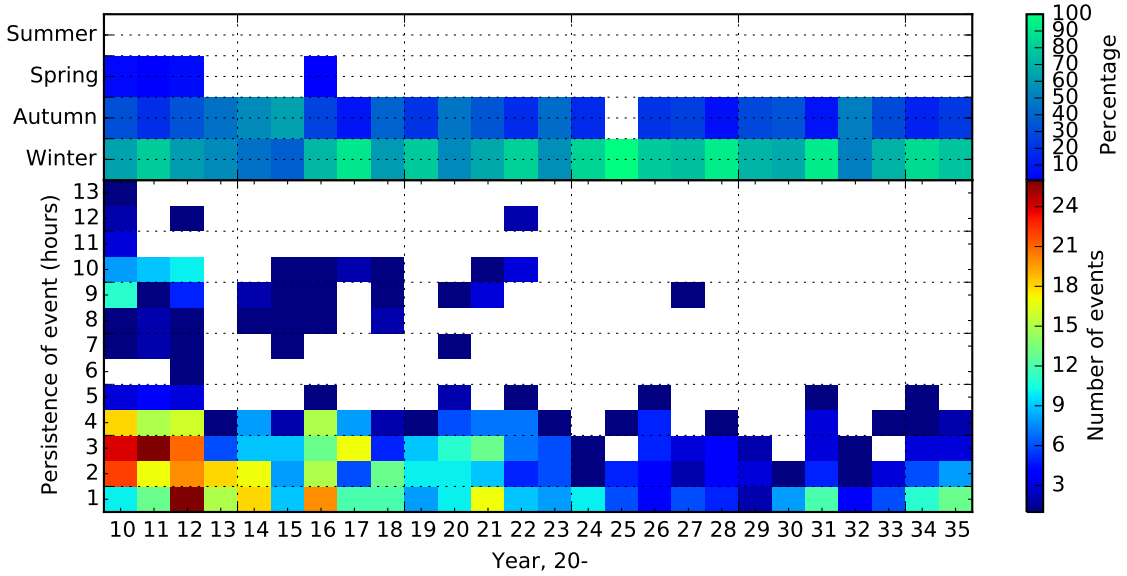

Figure 8.18.: Extreme residual demand events in the 99th percentile over time for the NP scenario.

The above analysis has shown that in terms of wind generation the scenarios experience very similar events in the low end percentiles. This could be due to a large number of these events being experienced at the beginning of the scenarios, where they share capacity. Alternatively, these events may continue to occur as new capacity is added. If the latter is the case it suggests that offshore wind is not harnessing the benefit of more diverse wind speeds, which is one of the situations that it should alleviate. This uncertainty can be addressed by looking at how these events occur over time. The 99th percentile array plots (Figure 8.17 and Figure 8.18) show that in both the GG and NP scenarios the number and persistence of high residual demand events is far greater at the beginning of the scenarios. Clearly, residual demand is also affected by demand; however, the fact that so many of these values are at the beginning of the scenario period indicates that the low generation events are reduced as wind capacity increases over time.

The analysis of the supply events has shown that all scenarios share the 2.4% events of the highest persistence; these plots show that they occur at the very beginning of the scenarios. They also show that the low wind speed conditions necessary to cause high residual demand events are counteracted by increased offshore capacity. Although the events still occur, but the persistence decreases to less than 5 hours.

The 1st percentile plots (Figure 8.19 and Figure 8.20) show an increase in number and persistence of events at the end of the scenario period, this contrasts with the 99th percentile plots (Figure 8.17 to Figure 8.20). From 2026 the Gone Green scenario experiences 1 event a year where residual demand is lower than -3.8 GW for 19-20 hours. During the same period Low Carbon Life only experiences 9-10 hour events. Short term events become more prevalent over time. Low residual demand events persist up to 58 hours, or over 2 days. A greater number of the events occur in the winter for both scenarios; however up to 50% of the events can occur in either summer or spring in certain years.

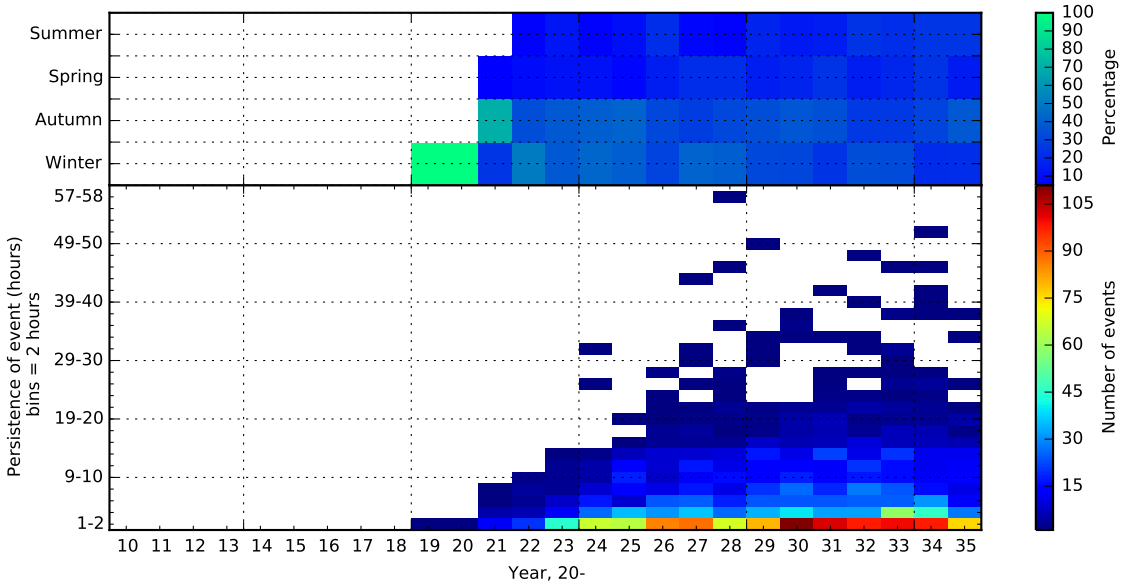

Figure 8.19.: Extreme residual demand events in the 1st percentile over time for the GG scenario.

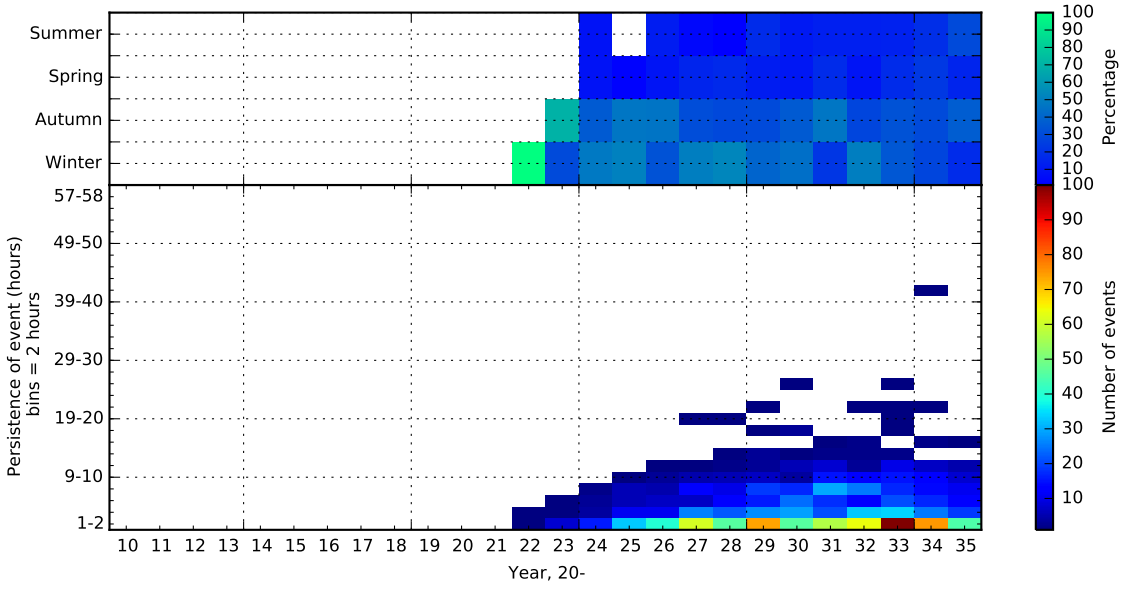

Figure 8.20.: Extreme residual demand events in the 1st percentile over time for the GG scenario, there is only one event in the NP scenario so it is not used here.

8.4. Coincidence

One of the potential implications of increasing wind capacity and electricity demand from heat concurrently is a stronger correlation between electricity demand and supply. If this correlation is positive, i.e. wind generation increases as demand for electricity increases, the value of this decarbonisation option increases and the need for matching mechanisms decreases[1]. If the correlation is negative, i.e. as electricity demand increases wind generation decreases (or vice versa), the need for matching mechanisms increases and with it the cost of integration. There has been limited evidence of increased correlation in the thesis to this point. The lack of evidence so far may be a result of the small impact of increased electrification of heat through introducing heat pumps, due to the concurrent decrease in other electrified heat demand. Analysis of variability has suggested that the maximum hourly changes in demand and supply occur at the same time in the scenario with the largest wind capacity and number of heat pumps, which results in increased maximum hourly changes in residual demand. There is a significant amount of spatially and temporally disaggregated data from both model inputs (weather data) and model outputs (specifically wind generation, total electricity demand and electrified heat demand) that allow an in depth examination of the relationship between the wind generation and electricity demand, including end use specific electricity demand for heat. Therefore this section uses this data to examine the relationship in more detail. The section is named coincidence as the analysis follows that performed by Boehme et al. [2006] who use similar plots to compare wind generation with electricity demand.

Wind speed and temperature are complicated variables over both space and time. Therefore, in order to analyse them and their impact, it is necessary to summarise them in some way. In this case that is done through the use of national mean hourly values. As in previous analysis of mean wind speeds, the onshore mean is calculated using all grid squares that contain land and the offshore mean using those grid squares containing development zones. Both of these represent a generalisation of the wind speeds experienced by GB. Not only because the mean wind speed spatially aggregates the data, but also because the grid squares used to calculate the mean do not necessarily contain capacity and because capacity varies over times. Mean temperature is calculated using the same method as onshore wind speed; these data are also generalised as this does not weight the temperature to population e.g. it is generally warmer in south England where there are more people than north Scotland where it is colder with fewer people. An interesting point for further work would be to analyse the impact of this weighting using spatial data on for example population or wind capacity. As well as weighted mean values, it would be possible to establish GB centroids.

Figure 8.21 and Figure 8.22 illustrate those elements of the electricity demand and supply equation which are most closely linked to weather, by showing the correlation between total hourly generation (both onshore and offshore) and mean wind speed (onshore and offshore respectively) for the whole scenario period. Figure 8.23 shows the correlation between total electrified heat demand and mean hourly temperature over the same period. Both wind generation and demand are normalised to the maximum annual value to mask annual growth in demand and wind capacity.

The wind speed plots (Figure 8.21 and Figure 8.22) demonstrate a very clear correlation between mean wind speed and power generation, both onshore and offshore. R^2 is between 0.7 and 0.88

[1] ventilation rate increases with wind speed, so therefore does space heat demand, this has not been accounted for in this analysis, but should be included in future SpDEAM iterations.

onshore and between 0.72 and 0.81 offshore; Pr is between 0.83 and 0.93 onshore and 0.85 and 0.9 offshore. These high correlation coefficients demonstrate that, despite variable conditions over space and different weighting of capacity, spatially aggregated GB wind generation is highly correlated to the mean wind speeds.

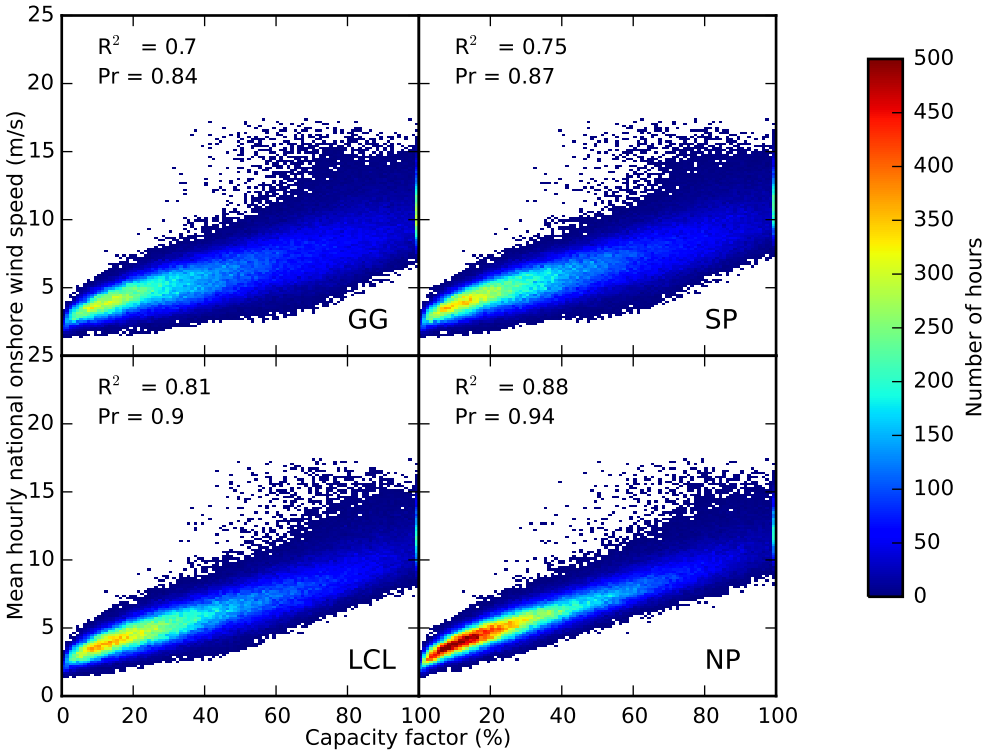

Figure 8.21.: Relationship between onshore mean wind speed and coincidence.

The largest divergence from the general trend is seen where high mean wind speeds result in slightly lower capacity factor. This divergence is seen in both onshore and offshore wind speeds. This may be due to high wind speeds occurring somewhere in the selected grid squares which are not being harnessed by the fleet, for example in the high elevation locations excluded from development, most likely at the beginning of the scenarios when there is less wind capacity. However, previous analysis has indicated that there is limited geographical diversity is introduced over time, particularly onshore where there is little to be gained.

Total generation in the NP scenario is more closely related to onshore wind speeds than the other scenarios (both Pr and R^2 are higher), owing to the lower levels of offshore capacity. Statistically the total output in NP is also more closely related to mean offshore wind speeds than other scenarios, despite not placing capacity in all of the grid squares used to calculate mean offshore wind speed. The correlation shows that this is because there are more hours at a low relative output, demonstrating the disproportionate influence of high values in statistical measurements and also the possibility that the NP scenario is experiencing wind speeds that are closer to the mean than the other scenarios. Otherwise the correlations are very similar between scenarios. The strength of these correlations suggests that it should be possible to approximately predict wind generation given limited information on wind speed. However, the use of far from shore locations may weaken the strength of this relationship. To fully establish this relationship future work should

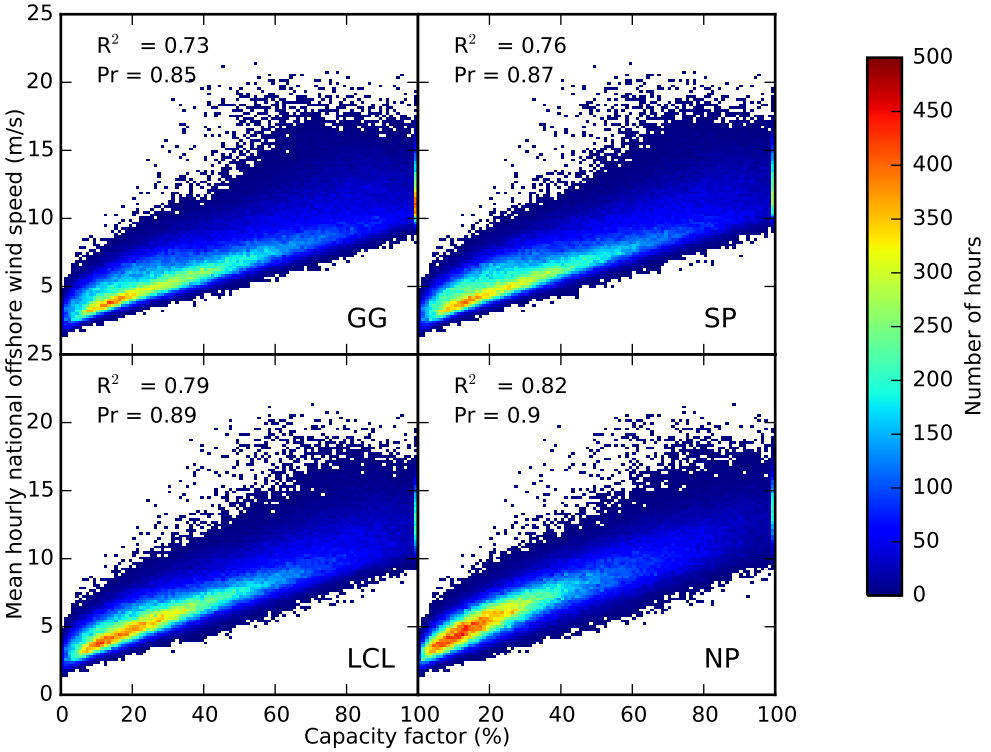

Figure 8.22.: Relationship between offshore mean wind speed and coincidence.

compare historical mean wind speed to historical measured generation data.

The relationship between national demand and temperature is more complicated than the relationship between wind speed and wind generation, as illustrated by Figure 8.23, which shows the correlation between annually normalised electricity demand for heat and mean national hourly temperature. The greater variability in the relationship between temperature and heat demand than between wind speed and wind generation is reflected in the lower magnitude correlation coefficients (Pr -0.73 compared to 0.9).

There is a clear negative correlation between heat demand and temperature, which is strongest when demand is between 0% and 20% of the annual maximum. However, there is a large amount of variation in the level of demand at lower temperatures. The variation in the relationship between national mean temperature and electricity demand for heat is caused by a number of factors that have been incorporated into the heat demand equation in SpDEAM. The largest divergence is likely to be caused by the spatial configuration of heat demand. For example there is a large amount of variation in heat demand when the national mean temperature is 2°C. This temperature could be caused by very cold temperatures in northern Scotland but slightly warmer conditions in southern England, which would result in relatively low heat demand as more people live in the south. If the mean national temperature were a result of cold temperatures in southern England, or the whole country, heat demand will be much higher. Solar radiation also varies spatially during cold periods which affects heat demand. Finally, dwelling efficiency improvements, which have been incorporated into the scenarios will mean that heat demands vary under the same weather conditions.

The relationship between mean temperature and electricity demand for heat is not significantly

different between the scenarios. This is interesting, as it this aspect of electricity demand where the most difference has been introduced between the scenarios (this difference is reflected in the number of heat pumps and associated divergence in heating technology spatial allocation described in Chapter 6). As previously discussed in Section 7.2.4, some resistive heating is replaced with higher efficiency heat pumps in the GG scenario. Consequently there is little difference in the annual electricity demand for heat between the GG scenario and the other scenarios until the end of the scenario period. Figure 8.23 shows that there is also apparently little divergence on an hourly basis, though looking at all hours may mask change at the end of the scenario period.

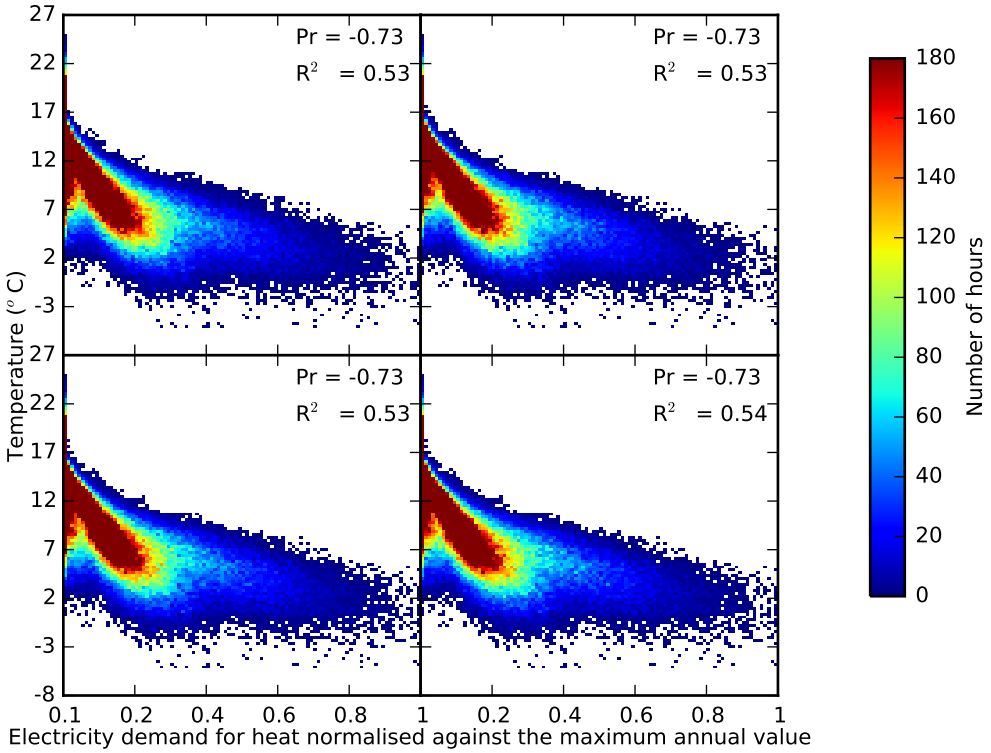

Figure 8.23.: Relationship between temperature and electrified heat demand.

Table 8.5 and Figure 8.24 show that there is little correlation between heat demand and wind generation. Interestingly, they also suggest that those scenarios with very few heat pumps have a very slightly more related demand and supply.

Scenario	R^2	Pr
GG	0.027	0.16
SP	0.036	0.19
LCL	0.04	0.20
NP	0.04	0.21

Table 8.5.: Correlation coefficients between electrified heat demand and wind generation.

So far, this section has discussed the relationships over the entire duration of the scenarios. Some of the annual variation has been removed through normalisation. However, as shown in Section 7.2.4, the effect of the increase in heat pumps in the GG scenario cannot really be discerned until the final few years of the scenarios. Therefore, to ensure that the relationship between heat pump demand

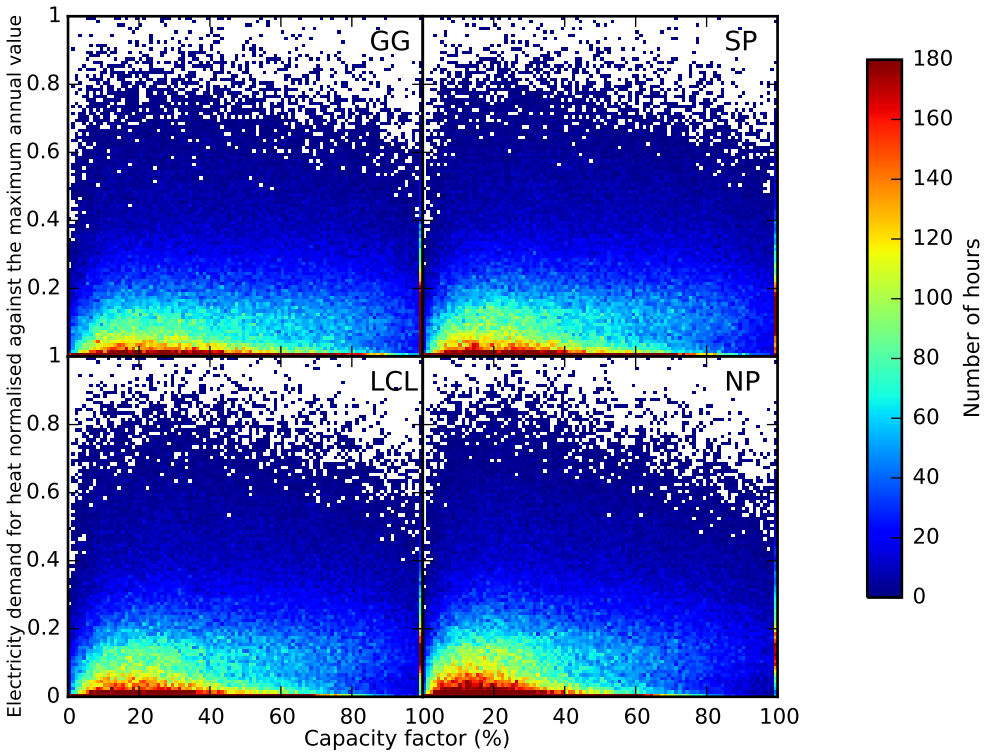

Figure 8.24.: Correlation between electrified heat demand and wind generation.

and wind generation is not masked by looking at all of the data at once, Figure 8.25 examines whether the correlation coefficient between electricity demand for heat and wind generation changes over the course of the scenarios (Pr is shown, but R^2 exhibits the same annual changes). The plot shows that the introduction of heat pumps reduces the strength of the correlation between this part of demand and supply. There is a change shown in 2035, but this is mirrored in the SP scenario, which does not contain significant numbers of heat pumps; therefore it is more likely to be due to offshore wind conditions, where the two scenarios contain similar capacities. This pattern again points to the limited impact of heat pumps when comparing demand and supply; however this is only part of the equation as it is not necessary for the two elements to be highly correlated for either to be of benefit in the decarbonisation of the electricity system.

Given the strength of the relationship between electrified heat demand and temperature, and wind generation and wind speed, the lack of correlation between heat demand and wind generation is likely to be predominantly due to a lack of correlation between temperature and wind speed. Figure 8.26 shows that there is little correlation between these over the course of the scenarios on an hourly basis. There is a small negative correlation showing that wind speed reduces as temperature increases (Pr -0.26). This is likely to be the impact of reducing wind speeds in the summer, when temperature increases. This phenomenon is illustrated by the contrasting seasonal changes in mean onshore wind speeds (Figure 8.27). This correlation is useful as it shows that wind generation will be greater in the winter months when demand is higher. However wind speed still needs to be higher during the right time of day in order to correlate with higher demand. The analysis presented in the previous chapter has suggested that temperature has a stronger seasonal correlation than wind speeds.

Figure 8.25.: Correlation between electrified heat demand and wind generation, annual changes.

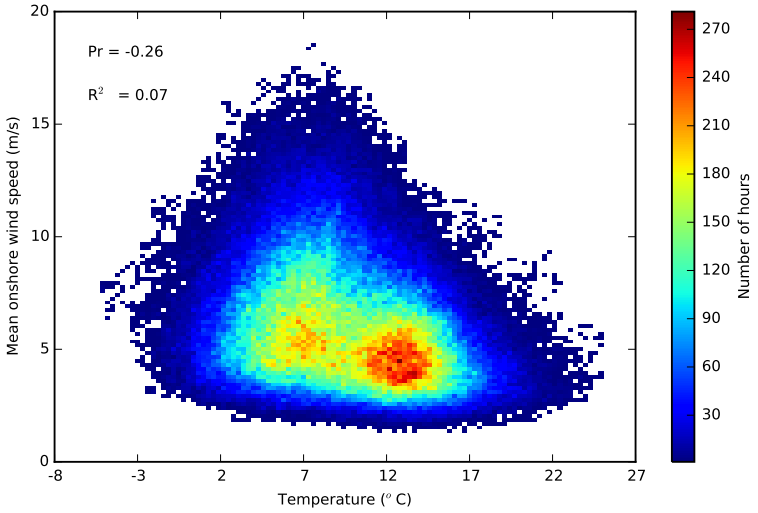

Figure 8.26.: Wind speed and temperature.

Factors other than temperature affect energy demand, particularly when non heat demand from SpDEAM is considered. The primary driver in SpDEAM, other than weather, is the time of day. It is possible that this will increase the value of wind, if for example wind speed increases during the day, when demand is greater, in comparison to night, when demand is lower. Figure 8.29 shows that over the course of the scenarios there is a high correlation between time of day and demand. The range of demands is a result of seasonal changes. GG is used as an example in this analysis, but other scenarios exhibit a very similar correlation. Figure 8.30 shows that this correlation is not mirrored by an increase in wind speed during the day, and as Figure 8.21 has shown, wind speed is highly correlated to wind generation. This demonstration of the lack of correlation between the primary drivers of demand and supply, other than seasonality, explains the lack of correlation between total electricity demand and wind generation.

Figure 8.31 shows the relationship between wind generation as a percentage of peak annual output and electricity demand as a percentage of the peak annual demand, for each scenario, over the entire scenario period. Table 8.6 describes the equivalent correlation coefficients. None of the

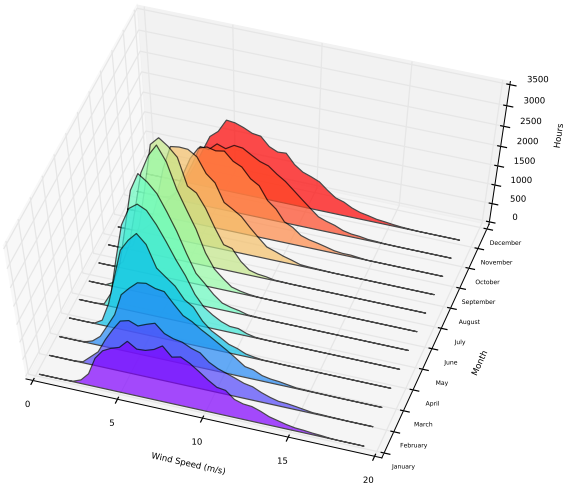

Figure 8.27.: Hourly GB mean onshore wind speed during different months of the year.

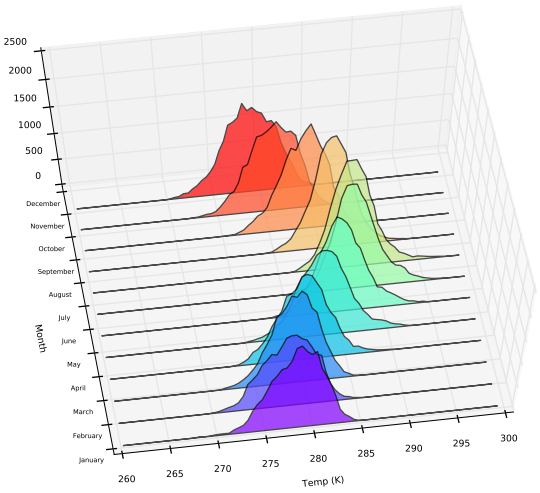

Figure 8.28.: Hourly mean GB temperature during different months of the year.

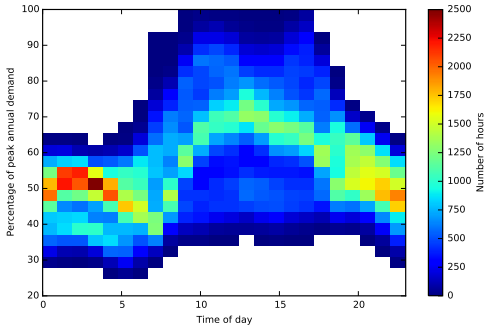

Figure 8.29.: Relationship between electricity demand and time of day, GG.

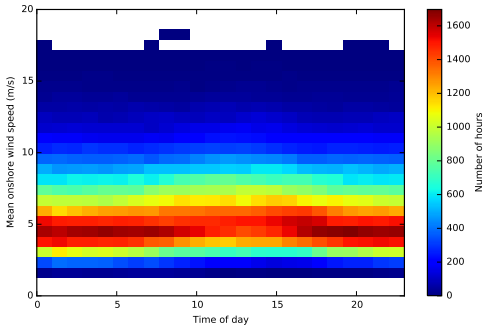

Figure 8.30.: Relationship between mean onshore wind speed and time of day.

scenarios display a difference in the way that generation relates to demand, this is due to a limited difference in the wind speeds experienced between the scenarios, particularly over a longer time period. This lack of difference is reflected in the very similar correlation statistics. NP shows slightly more hours at a low percentage output; as a result of the lower onshore capacity factors, this does not alter the correlation. The plot shows that demand is centred around 50% of the mean and wind generation is between 10% and 20% during this period, demonstrating that the median capacity factor may be lower than the mean, although this is distorted by the capped extreme values.

Scenario	R^2	Pr
GG	0.04	0.19
SP	0.05	0.22
LCL	0.05	0.23
NP	0.06	0.24

Table 8.6.: Correlation coefficients between wind generation and electricity demand.

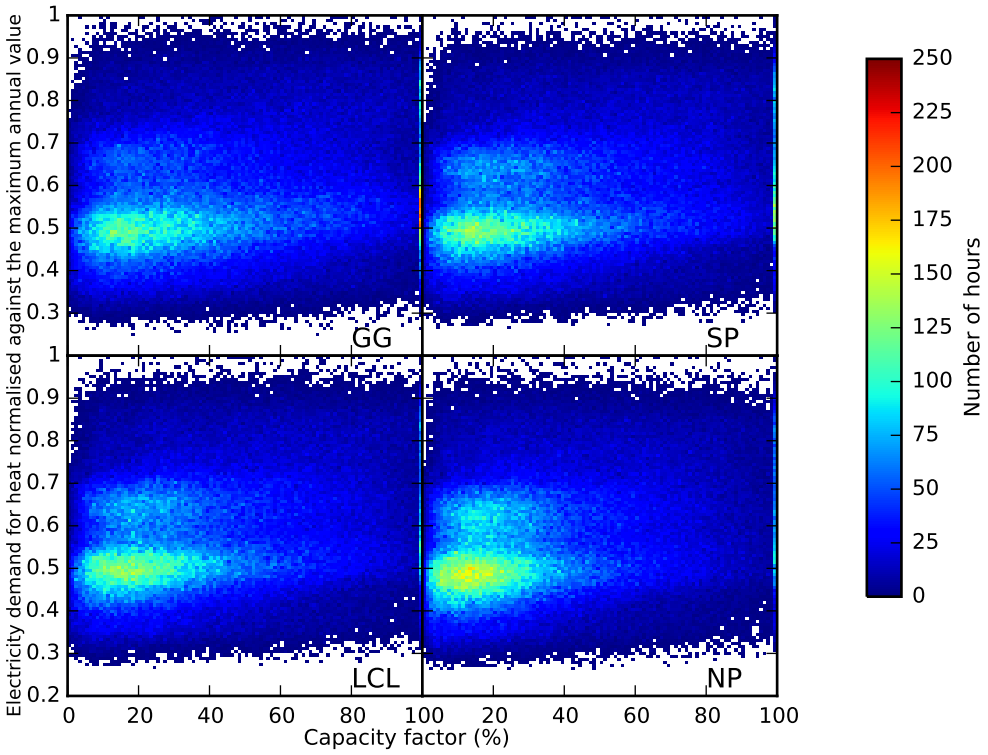

Figure 8.31.: Coincidence between wind generation and electricity demand for heat.

8.5. Summary

This chapter has addressed the final research question: What are the combined implications of electrifying domestic heat and introducing wind capacity? The question has been answered by looking at the distribution of hourly residual demands, cumulative excess wind generation, variability and extreme events in wind generation, electricity demand and residual demand, and the relationship between weather, electricity demand and wind generation. The extent to which matching mechanisms will be necessary under each scenario has been discussed. Analysis on the specific choice of matching mechanisms and therefore the implications of the scenarios on the electricity system as a whole will be explored in future work.

A reduction in residual demand at an annual temporal resolution has been shown to be primarily driven by capacity growth and the resultant wind generation. There is also variation in residual demand which is driven by weather. This inter annual weather driven variation in residual demand can be accentuated by increases in wind capacity or the use of heat pumps. In the long term, hourly residual demand is similar between scenarios but those scenarios with larger capacities do experience more hours with lower residual demand. The offshore capacity has been shown to accelerate scenarios to a point at which excess generation is created. This happens in 2020 - 2021 for the GG, SP and LCL scenarios but does not occur until the very end of the scenario period for NP. Overall negative residual demand is experienced between 1% and 10% of hours in those scenarios with larger wind capacities. This increases to between 5% and 30% of individual years at the end of the scenario period.

Maximum residual demand decreases over time under all scenarios, demonstrating that increasing the magnitude and geographical diversity of wind capacity results in some level of wind generation at all times of peak demand. The increased use of heat pumps and concurrent decreases in temperature and wind speed in the GG scenario means that maximum residual demand increases again at the end of the scenario period.

Despite the increasing occurrence of negative residual demand the majority of hours experience positive residual demand, which means that any stored electricity would be used in subsequent hours. Nevertheless there are an increasing number of hours where excess wind generation will accumulate under the GG, SP and LCL scenarios. Current storage capacity is significantly smaller than the excess wind generation accumulated during many hours of those scenarios. This demonstrates that future matching mechanisms will have to be of a greater magnitude than previously used, disregarding the impact of other changes to the system such as the use of inflexible plant or other renewables.

SpWind provides excellent data to investigate variability, as it applies the same weather conditions to all of the NG scenarios. A criticism of previous variability studies, set out in the literature review, was that by comparing simulated wind to measured electricity demand data it must be assumed that the weather data driving that demand was accurate. SpDEAM avoids this problem by using the same weather data as SpWind, therefore ensuring that both are driven by the same conditions. This means that the analysis of the variability of residual demand is as accurate as possible given the complexity of the models and the spatiotemporal scope and scale.

Greater variability would necessitate the use of larger magnitude matching mechanisms to ensure that demand is satisfied and to increase the cost of installing capacity further from shore. The

analysis above has shown that using locations that are further from shore does not increase variability. The larger demand change events in the GG scenario are a result of the introduction of heat pumps and the resultant increased electricity demand. This is the clearest impact of heat pumps described by this thesis so far and shows that even with efficient heat pumps and a concurrent reduction in resistive electric heating their use will impact on the the magnitude of matching mechanisms necessary to facilitate their integration.

Installing larger amounts of capacity increases the magnitude of variability. Overall, combining wind generation and electricity demand does increase variability in comparison to the individual elements. This is particularly the case in the GG scenario where the extreme changes in demand and supply appear to correlate. However there is no apparent correlation between electrified heat demand and wind generation in the analysis of coincidence. Seasonal and daily variability has been found to become significantly more unpredictable in those scenarios with larger wind capacities.

Analysis of extreme events of wind speeds, wind generation, electricity demand and residual demand has established that there is greater divergence between scenarios at high levels of wind generation and low levels of electricity demand than the opposite. These combine to create a more complex picture of low residual demand events. The lowest residual demand events of less than -3.8 GW can last up to 40 hours and there are nearly 100 occurrences of this level of residual demand under the highest wind scenarios, indicating that there will be significant periods where other sources of generation may not be needed.

High residual demand events are characterised by the same patterns as demand events as they are due to low levels of wind when demand is high, this shows clear evidence of the daily patterns of demand with peaks of events that last the same length as the daily increase in electricity demand. The highest residual demand events can occur at any point during the scenario period, but the persistence of the events reduces under all scenarios. These events occur in the winter and autumn when electricity demand is high. The lowest residual demand events only begin halfway through the scenario period and the persistence and occurrence of these events continues to increase to the end of the scenario period. These events can occur at any time of the year, but are more prevalent in the winter when wind speeds are higher.

Analysis of the correlation between electricity demand and wind generation has shown that, despite variable conditions over space and different weighting of capacity, the wind generation in GB is highly correlated to the mean wind speeds. The strength of the relationship between mean wind speed and wind generation suggest that it is possible to approximately predict wind generation given limited information on wind speed. There is a clear negative correlation between heat demand and temperature. However, there is a large amount of variation in the level of demand at lower temperatures. Unlike wind generation, there is no apparent statistical difference between the scenarios. There is very little evident correlation between wind speed and electrified heat demand, demonstrating that the value of wind is not increased by strengthening of the link between electricity demand and temperature, which would be the case is electricity demand were more strongly linked to temperature through the electrification of heat demand.

9. Discussion and Conclusion

9.1. Motivation for work

Scenarios depicting increased wind capacity and electrified heating are provided at a national annual resolution. Wind generation and electricity demand, and the drivers of both, are variable at significantly finer spatial and temporal resolutions. Consequently additional modelling and analysis is required to understand the implications of these scenarios.

The existing body of work on the variability of GB wind generation has used a number of weather data sources to accurately simulate wind generation interpolating to the site of farms or using downscaling, but has tended to use static capacities and explore the variability of the wind resource rather than future capacities and does not incorporate methods and knowledge from wind resource estimates.

Some variability studies have used historical demand data to consider the impacts of wind penetration on residual demand. There are two main issues with this data. Firstly, it is difficult to change its characteristics to represent the effect of changing demand behaviours and technologies, such as the uptake of heat pumps in domestic buildings. Secondly, the weather used to drive simulations of wind generation may not represent that experienced by consumers, which drives demand. A potential solution to these problems is to use the same weather data to simulate both electricity demand and wind generation.

Electricity demand is complex and there have been few attempts to model over a large scope at a spatiotemporal resolution as fine as CFSR and none by those studies examining variability. Models and methods do exist which could be combined, including the DEAM model and spatial redistribution methods.

The desire to augment scenarios of increased wind capacity and electrified heating with disaggregated modelling prompted the following research questions:

1. Is reanalysis wind speed data suitable for simulating turbine output?
2. Can DEAM be adapted to accurately model electricity demand at the same spatiotemporal resolution as CFSR?
3. Is a gridded approach appropriate for the disaggregation of national scenarios of increased wind capacity and electrified heat?
4. What are the combined implications of electrifying heat and introducing more wind capacity?

The following research aims were met:

1. Establish the validity of a climate reanalysis, NCEP CFSR, as a driver of energy models in GB.

2. Establish methods for the estimation of potential wind generation in GB driven by CFSR, which can estimate output from a range of scenarios without the need for significant changes to the model.
3. Determine where wind capacity can be developed across GB so that realistic locations and wind conditions can be used in analysis of the implications of variability.
4. Develop methods to spatially disaggregate an existing demand model (DEAM) to the same resolution as the wind model so that the demand model can be driven by the same weather conditions and the wind generation model.
5. Use the same meteorological dara as inputs for the wind supply and electricity demand models; this removes the assumption that the weather data matches reality and allow depiction of years where there is no measured demand data.
6. Adapt published national scenarios of increased wind capacity and electrified heat demand to the same scope and resolution of the developed models.
7. Integrate scenario modelling and the adapted demand model to so that all electricity demand can be simulated.
8. Use these methods to examine the disaggregated dynamics of wind supply and electricity demand under published scenarios.

9.2. Method and results

9.2.1. Evaluation CFSR data

Key Findings:

- Wind speeds at locations above 600 m above sea level are not represented well by CFSR.
  - Otherwise CFSR represents the range of conditions in GB well.
- Raw CFSR data is of a similar accuracy to interpolated and downscaled data in GB.

This thesis presented the most comprehensive evaluation of CSFR wind speed data performed to date, through comparison of the data to in situ measurement. Novel use of geographical information revealed an important weakness in the representation of wind speed across different terrains by CFSR. Wind speeds were found to be less accurate at high elevation locations, where mean wind speeds are higher than in the rest of GB. This use of these data in simulations could therefore lead to inaccurate simulations and analysis. This risk was subsequently corroborated in analysis of MERRA data by Cannon et al. [2015]. This observation is important for all users of reanalysis based wind speed data, particularly in regions which contain more high elevation locations than GB. Areas above 600 m were subsequently removed from consideration for wind farm development, ensuring that this inaccurate wind speed data was not used in wind generation simulations.

The impact of topographic conditions and land uses on the skill of the CFSR model were investigated for the first time. Other than at the high elevation locations, CFSR was shown to represent the range of conditions in GB well. Overall, CFSR wind speed data is as accurate as any other raw reanalysis dataset that has been evaluated to date and similarly accurate to interpolated and

downscaled data. This goes some way to answering research question number 1, though the question is not answered in full because there are a number of real world factors that introduce error when using modelled wind speed data to simulate wind fleets. Therefore, it was also necessary to evaluate the output of the simulation of wind generation. The other weather variables used in the modelling were not evaluated against in situ measurements. This is because they are less variable over space and time.

9.2.2. Wind generation simulation

Key findings:

- In GB there is a clear division between land uses that have been used for wind farm development and those which have not.
- There is a larger area of suitable land for onshore wind farm development than will ever realistically be used.
- SpWind offshore capacity factors are higher than those assumed in NG simulations, particularly in far from shore locations.
- NG use historical capacity factors as a guide for estimations of future wind generation, which are also used by a number of other studies. This means that those studies may be underestimating offshore generation.
- Median annual onshore wind speed is 2 m/s lower onshore than in offshore development zones.
- Offshore wind speeds are more spatially homogenous than onshore, but vary more year to year.
  - Inter annual changes in wind speed conditions can result in generation differences of up to 20% offshore.
- Years which experience the highest levels of generation benefit from higher national median wind speeds, but do not necessarily experience higher extreme wind speeds.
- Wind speed conditions close to shore, where current offshore wind farms are located, are more similar to onshore conditions than those in far from shore development zones (as depicted by CFSR).
- Simulated hourly total wind generation is highly correlated to national mean wind speed, onshore and offshore.
- The use of development zones to place offshore capacity does not add significantly more separation between the furthest apart and least correlated wind speeds than is available from solely onshore sites.
- Combining onshore and offshore capacity reduces the magnitude of hourly changes in capacity factor.
  - The reduction can be achieved without using far from shore locations.

Having established that CFSR data represents GB conditions adequately, the resolution of the reanalysis was adopted for subsequent modelling. SpWind was created to simulate hourly generation from any configuration of wind capacity within this framework. The model works by assigning a capacity to a grid square. Generation from that grid square is then estimated through the use of manufacturer wind turbine curves, which describe the relationship between turbine output and wind speed at the hub height. CFSR wind speed data is provided at 10 m above ground level; therefore it was necessary to interpolate wind speed. The increase in wind speed with height is dependent on surface roughness, atmospheric stability, temperature and topography. The method used for wind height correction assumes that these factors do not change over space or time. This assumption is a likely contributor to the underestimation of wind generation by SpWind.

Archetype onshore and offshore turbines were established using data on installed GB capacity. Some previous research has used specific turbine characteristics to simulate generation from each installed wind farm, which may have improved the accuracy of simulations. However, the archetype approach, which is also used in the literature, was adopted here because simulating potential future generation requires assumptions to be made on the characteristics of future wind fleets. 60 m was selected as a suitable height of simulation for past and future onshore capacity; 80 m was selected for the equivalent offshore capacity. Hub height may change in the future, for example if larger turbines are used offshore, which may result in more or less generation than described in this thesis.

Simulation using a manufacturer wind turbine curve does not take into account factors which may lead to an overestimation of generation. Such as the effects of the turbine operating within a farm, the ageing of turbines or the need for maintenance breaks. To assess the overall impact of the modelling assumptions and omissions it was necessary to evaluate SpWind. Evaluation of the wind speed data after height correction is not possible, owing to the lack of data at this elevation. Therefore the only way to evaluate SpWind was to compare results with historical data after simulating operational capacities. Wind farms that are part of the ROC scheme and those which report to the BMRS were simulated. Comparison against associated data demonstrated that SpWind systematically underestimates wind generation. The most likely cause of this underestimation is the method used for wind height correction, given that the other factors not incorporated into the model should mean that generation is overestimated, as has been seen in other similar studies.

Following the previous studies, a correction factor was used to reduce the RMSE of the results. The resultant accuracy is in line with other similar studies. This solution has been established in the literature and is based on a very large amount of data from two sources with different wind farms contributing. This reduces the likelihood of spatial bias being introduced, either from using a subset of farms or having imperfect information on wind farms. Therefore it was deemed appropriate, given the constraint on available time and the need to develop a demand model and apply both models to scenario analysis. Subsequent scenario analysis suggests that the correction factor applied to SpWind accounts for less than 6% difference between SpWind and NG at the highest capacity factor.

The reasonable accuracy of SpWind in combination with the evaluation of CFSR grid based data demonstrated that the reanalysis data is a suitable for simulating turbine output, answering research question 1. The limitations of SpWind are described in Section 9.3.4.

9.2.2.1. Scenario modelling

To use SpWind to simulate hourly generation from the capacity depicted by NG scenarios it was necessary to allocate this capacity to the model grid. A multi criteria analysis was used to calculate the amount of each grid square that is available for onshore development. Suitable constraints were established following a comprehensive review of the literature. This review demonstrated that resource estimates vary significantly, predominantly because of the choice of constraint boundaries. The constraints were evaluated, using installed capacity as a benchmark. Analysis showed that some wind farms have been developed in areas that should be protected. This analysis was used as a feedback to select appropriate constraints so that the land excluded from development followed previous planning restrictions where possible.

An analysis of the existing land uses around turbines in GB was carried out. This is a unique contribution of this thesis, as, to the author's knowledge, there are no previous examples of this analysis. The analysis demonstrated a clear division between suitable and unsuitable land uses for development. Those land use types that have been previously used for development were given priority in the allocation of capacity. Capacity was allocated to grid squares prioritising high mean annual wind speeds and geographical diversity. Generous turbine spacing was allowed, to eliminate the risk of excessive density, which has disadvantages from a wind farm operation perspective and is unlikely to be socially acceptable. This method can be applied to any scenarios depicting wind capacity growth, providing realistic locations for simulation, therefore achieving research aims 2 and 3. The method could be adpated and be applied to the location of solar generation or biogas/hydrogen production.

The primary aim of this analysis of land availability was to allow realistic placement of wind capacity in simulations of projected capacity. The methods were originally developed for resource assessments. To allow comparison with the literature, the land available for development was used to create an estimate of the onshore wind resource. Estimates of the potential capacity onshore show that, theoretically, there is plenty of suitable land for onshore development. More than will ever realistically be used. The resource estimate is larger than those reviewed; this is most likely due to the lack of economic constraints, distance to grid and socially acceptable limits.

Offshore, development zones have been identified by the Crown Estate as suitable on the basis of high wind speeds and suitable ocean depths. Therefore, it was not necessary to carry out an analysis of available areas. The development zones were filled with offshore capacity, prioritising close to shore locations initially and placing turbines in batches. Only the most ambitious offshore scenario required areas outside these zones, despite the allowance of 15 turbine diameters for turbine spacing under all scenarios. Those scenarios with larger offshore capacity use the far from shore locations.

Hourly wind generation from the redistributed scenarios was simulated using SpWind and wind speed data from CSFR. Weather data from 1985 – 2010 was used to represent the NG scenarios (2010 – 2035). This method is commonly referred to as hindcasting. Using a period of 25 years means that decade level changes in wind speed and temperature are captured. There may be longer term changes in climate which are not captured. Also, variability over finer temporal resolutions is not represented, for example sub hourly changes in wind speed. Another disadvantage of this method is the use of a single weather year to simulate a scenario year. Using more than one weather year for each scenario year would give a better idea of the range of generation and

demand that would be possible under each set of conditions. An example of the outputs from this approach can be seen in the range of generation from static capacities described in Figure 7.6. It is possible to downscale reanalysis data to finer resolutions, which would facilitate modelling at a finer resolution. However, this takes significant time and processing power. The resolution described here is considered an appropriate compromise between fine detail and the ability to model over a large scope in both space and time.

9.2.2.2. Results

Analysis of the wind generation scenario simulations revealed several interesting findings; these findings contribute to answering research question 3, because it is important to establish that using a gridded disaggregated approach provides complementary analysis to the aggregated scenario modelling. The results also contribute to answering research question 4, by showing some of the implications of wind capacity in isolation. Analysing electricity demand and residual demand covers question 4 more fully.

Analysis of the capacity factors under each scenario in SPWind has shown that onshore SpWind capacity factors are slightly lower than assumed by NG, which is reflected in the lower simulated generation (a mean difference of between 4% and 7% depending on the scenario). SpWind offshore capacity factors are much higher than assumed by NG, particularly in far from shore locations. Mean annual capacity factors exceed 60% in the last years of the scenarios, and mean values over the whole scenario period are between 50% and 57%. Depending on the scenario, NG assume a consistent offshore capacity factor of 38%, which means that offshore generation is significantly higher in SpWind. The mean annual difference in generation is between 32% and 53% in the long term with peaks of 46% and 75% when capacity is largest and wind speeds are highest.

The offshore capacity factors found by SpWind are much higher than previously experienced by GB wind capacity. This has consequences on systems planning, not only in GB, but also in Europe as it will affect the amount of electricity that GB would seek to export. Using historical data to optimise the electricity system may underestimate the matching mechanisms that will be necessary to deal with excess wind generation if offshore locations are used.

The difference between scenarios in terms of generation is driven by the amount of offshore capacity. This difference is accentuated by the placement of capacity in further from shore locations in the scenarios with more capacities. These locations experience the highest wind speeds and therefore generation and capacity factors. Analysis of wind speeds at hub height, both onshore and offshore, demonstrates that, over the course of each year, a greater range of wind speeds are experienced offshore; typically, this adds 5 m/s to the top wind speed, that may only be experienced for one hour each year. More hours experienced wind speeds closer to the median onshore which is typically between 6 m/s and 7 m/s and 2 m/s lower than offshore. Characterisation of GB wind speeds shows that offshore wind speeds are more spatially homogeneous than onshore, but vary more from year to year. Similar analysis has shown the difference between the close to shore and far from shore development zones; the close to shore zones experience conditions that are much more similar to the onshore locations than the offshore locations. This analysis only shows wind speeds as represented by CFSR. As previously noted, local conditions may differ significantly. This is particularly the case in coastal locations where topography varies greatly over small distances.

Changes in wind speed between years of consistent capacity result in annual changes in offshore generation of over 20%. Analysis of those years which result in the highest levels of generation has shown that they experience more hours at a slightly higher wind speed, resulting in a higher median, but do not necessarily experience more extreme wind speeds. Hourly total wind generation in GB is shown to be highly correlated with national mean wind speed. The strength of this relationship suggests that it is possible to approximately predict wind generation given limited information on wind speed.

The use of development zones to place offshore capacity does not add significantly more separation between the furthest apart and least correlated wind speeds than is available from solely onshore sites. It is therefore necessary to use the development zones that are furthest from shore to introduce more sites where there is little relationship between sites in terms of wind speeds. Results indicate that there are offshore areas where wind speed is more homogeneous than others, such as the Bristol channel, but that these are no less related to wind conditions on the other side of GB than the wind speeds in the furthest apart onshore wind sites.

9.2.2.3. Variability

SpWind and SpDEAM provide a coherent set of data with which to investigate variability. The analyses of variability and extremes were conducted under the assumption that model outputs represent conditions that will be experienced under each of the scenarios. The evaluations of the models have shown that during many hours there is significant bias compared to measured data and there are uncertainties in both measured and modelled data. Furthermore weather conditions may vary from those assumed under the hindcasting method. There are a number of findings that do not depend very heavily on the temporal accuracy of the model at an hourly resolution, such as the long term variability characteristics, the difference between scenarios, spatial variability and geographical diversity. These have been the focus of the analysis. Where appropriate, normalisation has been used to counteract the issue of accuracy.

In the long term there is little difference between scenarios in hourly capacity factor change, either onshore or offshore. Combining onshore and offshore generation results in a reduction of the hourly capacity factor changes. The geographical diversity needed to reduce the hourly change can be achieved without using the far from shore locations. This may mean that it is preferable to use closer to shore locations to avoid the need to install larger matching mechanisms to cope with changes, although analysis has also shown that there is no apparent penalty for the use of these far from shore locations in terms of increasing hourly capacity factor variability.

Capacity factor changes are very similar between scenarios, but hourly changes in generation become larger as capacity increases. The abrupt changes in generation must be met with matching mechanisms, which increases the cost of integrating renewables on to the grid. However, the largest changes occur for a small proportion of total scenario hours. Small changes still present challenges to wind integration and they occur more often. Changes will also occur at finer temporal resolutions, which cannot be represented by data at this temporal resolution.

Analysis of the temporal change in variability has shown that high capacity factors are experienced most often in the winter, but are increasingly experienced in the spring and autumn, particularly in the GG scenario. Solar shadow becomes less evident over time because of the introduction of

offshore capacity and the resultant reduction in the influence of solar heating of the land mass on the wind speeds experienced by a wind fleet.

9.2.2.4. Extreme events

The magnitude and occurrence of the highest capacity factors events are very similar across the scenarios. These are driven by high or low wind conditions across all possible locations for capacity. Low capacity factor events occur at the beginning of the scenario period when capacity is shared. High capacity factor events occur despite dissimilar capacities between scenarios because of the greater spatial homogeneity of offshore wind speeds. The further from shore the capacity, the lower the likelihood of low generation events.

The translation of extreme capacity factor events to generation events is highly influenced by the amount of far from shore capacity. Low generation events are very similar between scenarios, but high generation events exhibit much greater divergence.

9.2.3. Electricity demand simulation

Key findings:

- Hourly and annual changes to demand are less significant than supply. This is predominantly due to the NG scenarios, where heat pump demand (the major change depicted) is counteracted by a concurrent reduction in resistive electrical heat demand.
  - Therefore, there is little difference between scenarios until the final years in terms of annual demand.
  - Heat pumps do not introduce significantly more high residual demand events.
  - Heat pumps do increase variability, introducing a more pronounced morning and evening peak.
  - Other potential changes to energy consumption are not included in the bottom up modelling and therefore do not significantly impact the temporal profile of demand.

To fulfil research aim 4, SpDEAM, a hybrid energy demand simulation model, was developed to model all demand for electricity in GB at the same spatial and temporal resolution as SpWind and CFSR. The structure and algorithms of SpDEAM are based on the existing DEAM. DEAM has not been used to represent demand for the whole of GB before, nor applied on a gridded basis. Therefore it was necessary to adapt and disaggregate the DEAM algorithms. A domestic dwelling stock model, heating technology model and population dataset were created to fit the model grid. These datasets were used to adapt DEAM's bottom up methods to simulate domestic space heat demand. All other demand for electricity was simulated using top down methods from DEAM, though it was still necessary to assign this demand to the model grid so that incidental gain from end uses simulated using the top down approach could be incorporated into the heat demand equation.

The level of disaggregation applied to SpDEAM has not been performed before, either with DEAM, or other models. Therefore it was necessary to calibrate the model using measured data. It was

not always possible to use empirical data for calibration, evaluation and model inputs, because in many cases data is not collected over this scope, rather a subset is collected and the data is modelled and interpolated. Where this is the case it has been clearly stated. There is also a lack of spatially disaggregated data on energy demand. SpDEAM was calibrated using 10 years of historic demand data, hourly in the case of electricity demand, daily in the case of gas demand. Gas demand calibration was used as a proxy for heat demand, which is appropriate given the large proportion of heat demand that is currently satisfied using this fuel (>80% of domestic central heating, see Figure 5.8).

Evaluation revealed un modelled demand in the un-calibrated version of SpDEAM. The accuracy of simulated domestic electricity and gas demand was shown to be adequate. Therefore the calibration was carried out by altering the non domestic activity profiles one by one to reduce the bias between modelled and measured demand. The data used for calibration includes theft, losses and embedded generation - which is seen as a negative demand in the electricity demand dataset. Embedded generation is not used in the evaluation of SpWind, but is included in the REPD capacity that is used for placement in the scenarios. This is deducted from the total scenario growth so that it is not included twice. However, as it is possible to identify the locations of this embedded capacity and simulate the generation to a reasonable degree of accuracy this could be removed from SpDEAM.

The calibrated version of SpDEAM was evaluated under scenario conditions from 2010-2014. The results of the evaluation are very close to those from the calibration. This demonstrates that the calibration of the model was effective and that the analysis of the scenarios is as accurate as possible given the described limitations of SpDEAM. Demand for both electricity and gas are remarkably accurate given the challenge of modelling the entire GB electricity system with limited data and necessary simplification and grouping of demands. SpDEAM is unique in terms of modelling spatially explicit temporal demand from all sectors across GB. None of the models reviewed in chapter 2 have this ability. The development and subsequent evaluation of this novel method established that the DEAM model can be adapted to accurately model electricity demand at the same spatiotemporal resolution as CFSR and SpWind, therefore answering research question 2. The evaluation of SpWind and SpDEAM in combination fulfill research aim 1.

9.2.3.1. Scenario modelling

It was necessary to make a number of alterations to the dwelling model, heating technology model and in some cases input variables to simulate total hourly demand for electricity as depicted by NG scenarios using SpDEAM.

National annual input values to the top down section of the model were altered to align with those used in the model evaluation, so that the calibrated version of SpDEAM could be applied. New stock, including replacements for demolished dwellings, was introduced using the same spatial proportions as old stock. The thermal efficiency and size of these old and new homes change at different rates under each scenario reflecting the need to improve efficiency alongside technological change in order to decarbonise the domestic sector. The combination of the methods used to disaggregate NG's scenarios fulfilled research aim 6.

The version of SpDEAM used for calibration did not include changes to the consumption of energy. However, the use of bottom up methods allowed electricity demand from heat pumps to be

introduced in scenario modelling. This improved on the previously used method of statistically altering historical demand data. However, it does mean that this method is not included in the calibration or evaluation of SpDEAM. To ensure that the simulation of heat pump was accurate as possible, field trial results detailing the relationship between temperature and efficiency were used to estimate the demand for electricity from heat pumps. NG's econometric modelling also includes other demand changes; however, they do not provide information on these changes separately from the national annual demands. Therefore as it is difficult to separate these demands from their aggregated demand, they are not addressed in this thesis.

NG's heat pump scenario dictates rates of uptake and technological replacement. These rates were redistributed to the grid, assuming that the uptake is even across GB. Efficient heat pumps were assumed, which are an improvement on those currently used in GB, but are in operation elsewhere and are in line with the minimum standard required for decarbonisation, according to previous research. NG state that the GG scenario, which projects a large number of heat pumps, must overcome barriers to decarbonisation. Heat pump operation is intentionally simple in the model. At the resolution of the model more complicated operation would increase computational load. Also heat storage etc. are considered to be part of the larger scheme of matching mechanisms and therefore should be investigated individually in detail elsewhere.

9.2.3.2. Results

Hourly demand was simulated under each scenario using weather data from the same years as SpWind, fulfilling research aims 5 and 7. Analysis of the SpDEAM outputs in isolation has also gone some way to answering research question 4. SpDEAM has been shown to consistently underestimate electricity demand in comparison with NG, though the magnitude of this difference is small. There is more difference in the domestic demand and greater variability due to the use of weather data in SpDEAM and the use of the bottom up approach. SpDEAM non domestic demand is very close to NG data; this is to be expected, owing to the use of the solely top down approach, but demonstrates that the corrections applied and the alterations to the input data are appropriate. NG's scenarios depict a reduction in resistive heat demand alongside the increased number of heat pumps. This means that the impact of heat pumps on the national demand profile cannot really be detected until the end of the scenarios. The assumption of efficient heat pumps means that there is not a big difference between scenarios in either total annual electricity demand for heat, or hourly electricity demand.

There is a clear negative correlation between heat demand and temperature. However, there is a large amount of variation in the level of demand at lower temperatures. Unlike wind generation, there is no apparent statistical difference between the scenarios.

9.2.3.3. Variability

Maximum hourly changes in electricity demand are a similar magnitude to maximum changes in wind generation, though demand changes are more often larger in magnitude. Only the GG scenario shows a significant change in variability between 2010 and 2035. This is because of the limited changes made to the temporal profile of demand. Changes not incorporated into the scenarios may mean that the temporal profile changes e.g. electrification of transport, demand

side response or more significant increases in efficiency of appliances and buildings. The larger demand change events in the GG scenario in the later years are a result of the introduction of heat pumps and the resultant increased electricity demand.

Analysis of the temporal profile of demand over different days of the year has illustrated the lack of change under the majority of scenarios. Under the GG scenario the same analysis has shown that electricity demand becomes lower in the summer mornings and evenings relative to the winter and there is a more pronounced morning and evening peak in demand during winter.

9.2.3.4. Extreme events

Both low and high extreme demand events are driven by diurnal and seasonal demand profiles. The shorter lasting lowest demand events can occur at any point of the year and do not exceed the length of demand between the morning and evening peak. The longer lasting low demand events occur during the summer and can last a day or more. The highest demand events occur during the winter and the persistence is again limited by the diurnal profile of demand; therefore the persistence is very similar across different magnitudes.

9.2.4. Analysis of residual demand

Key findings:

- Mean annual residual demand reduces over time, under all scenarios.
- Change is driven by capacity increases but is also influenced by weather.
- Maximum hourly residual demand decreases but does not reduce below 75% of the baseline value (2010).
  - There are no periods of very low wind generation at times of peak demand.
  - Low generation events are not eradicated under any of the scenarios.
- Excess wind generation, excluding the influence of other forms of generation, begins from 2020 under the NG scenarios.
  - Matching mechanisms will need to be in place before then and could increase to 100 times the magnitude of Dinorwig.
- Variability of residual demand is increased by the correlation of heat demand and wind generation.
  - Extreme hourly changes correlate in the scenario which includes significant numbers of heat pumps.
- Diurnal variability of residual demand is reasonably predictable at times when the influence of demand exceeds that of wind generation.
- Extreme residual demand events have very different characteristics depending on whether they are high or low.
  - High residual demand events follow patterns of high demand events.

  - Low residual demand events are influenced by high levels of wind generation and low levels of electricity demand.
  - Offshore capacity increases the magnitude and persistence of low residual demand events.

- There is very little evident correlation between wind speed and electrified heat demand in the modelled output.
- Although changes to supply have been shown to have more significant impacts than changes to consumption there are cases where the two combine to increase the magnitude of changes to residual demand.
  - Heat pumps accentuate the effect of weather on residual demand, especially in cold years.

The analysis of residual demand completes the answer to research question 4 and research aim 8. The answer is provided within the boundaries of the thesis, which were set so that analysis concentrated on the impact of the combination of wind and electrified heat demand and the establishment of complimentary findings to the aggregated scenario modelling carried out by NG. This approach did not include significant analysis on other mechanisms that may become part of the energy system; this is considered to be a subject for future work.

Mean annual residual demand has been shown to reduce over time, under all of the scenarios. The reduction is approximately proportional to the increase in wind capacity. Inter annual change in mean residual demand is heavily influenced by weather, but changing wind capacities can reduce or increase the magnitude of this influence. The introduction of heat pumps accentuates the effect of weather on the demand side, in particular during cold years with lower wind speeds.

Maximum hourly residual demand decreases over time for all scenarios, but remains between 75% and 100% of the 2010 value. This demonstrates that increasing the magnitude and geographical diversity of wind capacity results in some level of wind generation at all times of peak demand. The increased use of heat pumps and concurrent decreases in temperature and wind speed in the GG scenario means that maximum residual demand increases again at the end of the scenario period.

Under all but the lowest wind capacity scenario (NP) there is significant excess production, which begins from approximately 2020. Solutions for coping with this excess will have to be in place before then. The maximum cumulative residual demand (GWh) is between 10 and 100 times the capacity of Dinorwig, depending on the scenario. However, events of this magnitude represent a very small percentage of the total, with the largest 10% doubling the previous 90% under the GG scenario, therefore it may not be worthwhile building storage capacity at this magnitude, particularly given the other matching mechanisms available. It should be noted that these calculations were performed assuming no inflexible generation such as nuclear, therefore the amount of excess generation may increase significantly. It is unlikely to decrease, other than in those hours where SpWind overestimates generation or SpDEAM underestimates demand, which the evaluations of the model show do occur.

9.2.4.1. Variability

Analysis of residual demand has shown that combining wind generation and electricity demand increases variability in comparison to the individual elements. This is particularly the case in the GG scenario where the extreme changes in demand and supply appear to correlate. However there is no apparent correlation between electrified heat demand and wind generation in the analysis of coincidence.

Seasonal and daily variability has been found to increase significantly in those scenarios with larger wind capacities. Early in the scenarios the pattern of residual demand is very similar to demand but variability becomes gradually less predictable, as wind capacity reaches demand magnitudes.

9.2.4.2. Extreme events

High residual demand events follow patterns of high demand events, which, as noted above are strongly influenced by the daily demand profile. The highest magnitude events do not exceed the length of demand between the morning and evening peak. As the magnitude decreases the persistence of the events increases to greater than a single day.

High residual demand events are very similar between scenarios, demonstrating that using offshore capacity does not eliminate periods of low generation. The events can occur at any point during the scenario period, but the persistence of the events reduces over time. The number of shorter lasting events also reduces significantly. Throughout the scenario period they occur almost exclusively in the autumn and winter. Despite the addition of significant numbers of heat pumps the Gone Green does not exhibit significantly more high residual demand events than other scenarios.

Low residual demand events are influenced by high levels of generation and low levels of electricity demand. These combine to create a more complex picture of low residual demand events. Offshore capacity increases the magnitude and persistence of these events, which increase in frequency and persistence of events at the end of the scenario period. A greater number of the events occur in the winter for both scenarios; however up to 50% of the events can occur in either summer or spring in certain years.

9.2.5. Coincidence

Analysis of coincidence has shown that simulated wind generation in SpWind is highly correlated to national mean wind speed. The strength of this relationship suggests that these wind speeds could be used to approximately predict hourly generation under different scenarios of capacity. However, there is divergence from this relationship, particularly when wind speed is high but the capacity factor varies. This relationship is observed using simulated rather than measured generation; previous analysis has demonstrated that the model does not perfectly match reality and this relationship may reflect the equations in the model rather than reality. Also calculating mean wind speed is a relatively simple task when using reanalysis data, but is significantly more complicated to predict. Future work could look at the correlation between mean CFSR wind speed and measured generation to explore the capacity of the dataset for wind generation prediction.

The link between weather and electricity demand is more complex than wind speed and wind generation, owing to the greater number of factors which influence demand. This is reflected

in the relationship between mean national temperature and electricity demand for heat, which shows a strong negative correlation under certain conditions but a considerable amount of noise, particularly at lower temperatures.

There is very little evident correlation between wind speed and electrified heat demand, demonstrating that the value of wind is not increased by the strengthening of the link between electricity demand and temperature.

9.3. Conclusion

9.3.1. Hypothesis

The work described in this thesis has shown that methods and data exist which facilitate spatiotemporally disaggregated modelling of wind generation and weather driven electricity demand. The adaptation of these methods and data to the framework of National Grid's Future Energy Scenarios and subsequent analysis of the modelled outputs has shown that they can be used to gain complementary insights to the aggregated modelling. Therefore the thesis provides evidence that the hypothesis stated in Section 1.3 is correct.

9.3.2. Contribution of research

The literature review identified two important gaps in research which examines the variability of wind generation. The first of these is the lack of demand modelling at the same resolution as wind generation. The second is the lack of modelling of scenarios of wind generation at a disaggregated resolution. To address these gaps, this thesis adapted existing methods from a range of sources to develop a novel method for disaggregating scenarios of wind generation and electricity demand to a coherent resolution in both space and time, so that they could be simulated using the same weather data.

As well as filling the research gaps the method provides the basis for disaggregating other national annual scenarios of demand and supply to a gridded framework so they too can be simulated using CFSR data. The gridded framework facilitates reasonably simple spatial disaggregation and the weather data and simulation method enable the estimation of demand and supply at a temporally disaggregated resolution.

The evaluation of CFSR has been published in Sharp et al. [2015] and the observations have relevance to other users of reanalysis data, particularly those who are looking at complex or high elevation locations or considering the use of raw reanalysis data against interpolated or downscaled data. The scenario analysis primarily provides complimentary insights to NG's modelling. There are several findings which apply to the GB, including the difference in wind speed between onshore and offshore locations, the effect of offshore development zones on geographical diversity, the relative influence of wind capacity and weather on annual generation and the relationship between capacity and excess generation. Key findings have been described above.

9.3.3. Strengths of approach

The gridded method developed for this thesis represents one of the major strengths of the work. The use of the grid has facilitated the modelling of electricity demand and wind generation with weather data from the same source. This alleviates some of the the issues with assuming that the weather data used for simulating one or the other matches reality.

The gridded approach has facilitated reasonably simple spatial allocation of capacity and the complementary use of methods developed for resource estimates means that realistic wind speeds have been used in simulations of generation. This includes offshore wind capacity, which other studies have found difficult to simulate because of lack of data. The use of spatial census data to attribute space heat demand assures as far as possible that the location of demand is correct. Another spatial strength of the approach is the considerable spatial analysis was performed to ensure accurate placement of wind capacity.

The spatial and temporal homogeneity of the grid, as well as the global coverage of CFSR, mean that the method is scalable, over space, as it can be applied to greater scopes, and over time, as the hindcasting method can be used for longer temporal scopes, and also to different scenarios (including those which depict different decarbonisation options). There are a number of potential avenues for future work, relating to the scalable nature of the modelling and the strength of the weather data; these are summarised in Section 9.4.

The hybrid modelling approach has facilitated the simulation of all electricity demand and some demand in detail. This allowed analysis of residual demand and complementary insights to aggregated scenario modelling, which achieved one of the primary aims of the thesis. Regular variation is well captured by the activity profile approach, and the introduction of the influence of weather in the bottom up modelling introduces some irregular variation.

As well as addressing the research questions and fulfilling the research aims the thesis has directly addressed some of the questions related to integrating variable generation in the context of the scenarios outlined by previous researchers (capacity factors and geographical diversity).

The evaluation of CFSR is the most comprehensive to date, the first performed for GB and the first to use extensive topographical and land use information. One of the most comprehensive reviews of past reanalysis wind speed evaluations has been performed as part of this work. The evaluations of both SpWind and SpDEAM are as comprehensive as possible given the lack of available data and have been performed over significant periods of time. The results of the evaluations demonstrate that the models are quite accurate, especially given the resolution and complexity of the processes.

9.3.4. Limitations of approach

Whilst there are a number of strengths to the gridded approach, there are also some limitations. Assuming that a grid point value represents the whole grid square means that it must also be assumed that the conditions within the grid square are homogenous, which they often aren't. There is inevitably spatial variability in wind speed and possibly temperature that is lost as a result of adopting an approach to facilitate the disaggregation of scenarios.

Modelling variability at the hourly resolution of CFSR, whilst in line with other studies, does not recognise the fact that wind speeds, and to a lesser extent temperature and solar radiation, vary

at smaller temporal resolutions. It is very likely that some temporal variability in wind generation and electricity demand, which must be handled by the system to ensure matching, has not been captured. As well as inter hourly changes to weather, the use of an hourly resolution may also smooth peaks and troughs in, for example, wind speed. There may also be long term extremes that are not captured during the 30 year historical period represented by CFSR.

The gridded approach represents a compromise between the desire to be able to place projected wind capacity and data describing drivers of demand without needing to specify exact locations and a spatial resolution that describes weather variability. There are, however, existing methods for performing simulations of wind generation at finer spatial resolutions that have not been utilised, which may have improved the accuracy of the method, including interpolation of wind speed data and dynamic downscaling.

CFSR was selected as the source of weather data for simulating wind generation and electricity demand on the basis of its spatial and temporal resolution and its novelty in GB variability research. The latest research published which uses MERRA data for simulations [e.g. Cannon et al., 2015] demonstrates that greater accuracy is achievable with that dataset, primarily owing to the availability of wind speed data at multiple heights, facilitating more accurate height correction. The wind height correction method is a likely source of error and assumes homogenous atmospheric and surface conditions; this is a clear area for improvement, described in more detail in the future work section below.

The need to apply a correction factor to SpWind, post simulation, demonstrates that there are factors affecting wind generation that have not been accounted for in the model (these are described above). Although the correction factor has been used in previous research it is possible that it could be improved upon as a method. The correction factor is based primarily on onshore wind generation as a result of the need to use historic time series for calibration, which means that offshore simulations may be skewed. As well as physical factors affecting wind generation, transmission losses have not been taken into account; this could significantly affect the amount of energy available from wind. Although this is a limitation of the approach, the method also presents an opportunity in this respect as the spatially explicit nature of the simulations mean that a network model could be included in future work.

Though the evaluations of the models have been highlighted as a strength of the approach, the accuracy of both models is only evaluated fully at a spatially aggregated resolution. This means that there may be error in the spatial variation of wind generation and electricity demand that has been masked by bias in the different direction in another location. Consequently, subsequent spatially disaggregated analysis, such as that describing the geographical diversity of wind generation and offshore capacity factors, could be incorrect. This could be examined further using newly available datasets on offshore generation.

NG scenarios have been disaggregated to demonstrate the ability of the gridded approach to complement aggregated modelling. These scenarios represent a single decarbonisation option, which may or may not be appropriate for GB. To understand the suitability of this option it is necessary to explore further options; this was not possible within the time limitations of this project. There are also a number of issues to do with the integration of wind that have not been fully addressed by the analysis performed in this thesis e.g. penetration, capacity credit, curtailment, as well as other challenges relating to matching mechanisms.

There is no consideration of the cost of wind integration in the modelling performed in this thesis. However, this is included in NG's econometric modelling so the results of the scenarios present the situation as prescribed by the conditions set out in each scenario.

Only domestic heat demand is modelled using bottom up methods. This means that the other changes incorporated into NG's scenarios have little effect on changing the temporal profile of demand. This may not reflect future changes, e.g. electric vehicles, which are include in NG's modelling but not modelled explicitly by SpDEAM are likely to increase night time demand. SpDEAM does not include all of the end uses included in DEAM. This was due to lack of data and the need to limit computational load, but may lead to lack of detail on the temporal profile of demand. The use of the top down method for the majority of demand means that irregular variation is not included. Also the activity profiles used in SpDEAM do not represent periods where activity varies from the norm e.g. bank holidays and Christmas.

The method used to model heat pump operation assumes that heat is provided on demand at a high efficiency. This may not represent reality either now or in the future, where less efficient heat pumps are used and heat is stored and energy is also used to provide hot water. This may affect the temporal profile of electricity demand and was not explored in detail.

The data used to calibrate and evaluate SpDEAM outputs includes some embedded generation, which is seen as a negative demand. Although this is counteracted by the capacity allocation method in SpWind it would be possible to simulate this generation and remove from the evaluation data given that the location of this capacity is known. SpDEAM was calibrated and evaluated using spatially aggregated data, more work could have been done in the use of DECC sub national statistics to evaluate the accuracy of simulating spatial variation in energy demand.

A number of assumptions on the spatial configuration of energy consumption were made, including even distribution of people in houses, even distribution of heating technology in different archetypes and even spatial growth in population, and new dwellings and technology take up. In reality some groups of people and buildings consume more energy than others and heating technologies vary by building archetype. This may affect the spatial configuration of demand. Other model assumptions were necessary; the impact changing these values could have been explored further, for example through a sensitivity analysis. Floor area and heat loss are quite generalised and derived from heavily modelled data, though this is the best available data for a model that covers the whole of GB. Unmodelled demand is accounted for through adaptation of activity profiles. More work could be done on identifying data describing this demand or where the data does include the demand.

9.4. Future work

The scope of the work presented here means that there are a very large number of avenues for future work. Here they have been grouped under four headings; 'Disaggregation', 'Model improvements' and 'New applications of the model'. Where possible these heading contain different sections for wind generation and electricity demand simulation. The final section described miscellaneous future work under the heading other.

9.4.1. Disaggregation

It is possible to represent variability at a finer spatial and temporal resolution than has been used in this thesis. Some of the key spatial drivers are available at a finer resolution; for example, population data can be obtained for 1 km grid squares, raw reanalysis is data available at 0.2 degrees for a limited number of years, and there are methods which could be used to make the resolution smaller e.g. downscaling for weather data. Other complementary datasets are available at a finer spatial resolution than used in this work; for example, dwelling data are available at the building level from openstreet map. Integrating these data and methods into temporally explicit models is difficult but they could be used to develop finer resolution models.

Temporally the resolution of the modelling is the same as other studies examining the variability of generation. Currently further temporal disaggregation is difficult due to the lack of weather data, though statistical alterations of the data could be applied to explore sub hourly variability.

9.4.2. Model improvements

There are a number of limitations to SpWind and SpDEAM described above which could be improved upon:

Wind generation

The method employed to alter wind speed data to hub height has been noted as a simplification of reality that does not take into account a number of factors. Information exists on a number of these which could be employed in the future to improve the method and reduce the error introduced to SpWind as a consequence. For example CFSR contains some information on atmospheric stability and surface roughness, humidity, air temperature, and surface temperature both of which have an effect on wind shear. Surface roughness information is also available from the CORINE database and elevation change can be determined from a digital elevation model which could be used to introduce the impact of onshore topology within a grid square. All of these data are spatial which facilitates a spatially explicit correction factor on a gridded or wind farm specific resolution. The CFSR data is also temporally disaggregated, facilitating the application of the correction on an hourly basis. Further evaluation would be necessary following improvements to this method and results could be compared to those found in this thesis. Rotor equivalent wind speed should also be explored in full as an alternative to the hub height approach

There are other physical factors not taken into account by SpWind which are more difficult to model using measured data, but could be incorporated into SpWind using statistical adjustments of SpWind outputs. These include: turbine spacing, wake effects, lag in turbine operation, decline in performance with age and maintenance breaks. Examples of adjustments have been given in the thesis, further potential improvements include the allowance for maintenance in the form of planned outage rates, which can be done through adequacy analysis, an assumption of 4% downtime or known strategies. Furthermore forced outage rates are unknown but can be modelled through security/monte carlo analysis.

The characteristics of all operational and planned wind farms are known; therefore these could be used to develop site specific turbine curves and hub heights. The effect of the use of these,

as opposed to the archetypal characteristics used in this thesis, could be measured by comparing simulated generation to the ROC and Elexon datasets. The size of future turbines is not known but it is possible that they will be larger than those assumed here; these could be changed and the impact of simulations analysed. Turbine curves can also be adapted to restart at 21 m/s after cutting out at 25 m/s following the method described by Cannon et al. [2015].

The multi turbine curve approach was shown to make no statistical difference to simulated generation in Chapter 3. However it was noted that the probability density function was appropriate for a smaller area, and that the turbulence density was assumed, therefore it may also be worthwhile revisiting this method and applying to smaller scopes.

The onshore multi criteria analysis could be improved by including socially acceptable limits on development and cost restrictions. This may eliminate certain areas from development and change wind generation simulations following allocation of capacity.

Electricity demand

The method used to simulate heat pump demand can be improved by including heat storage, hot water demand and the subsequent effect on performance factors. Heat pump efficiency can also be altered to more closely represent current efficiencies The effect of incrementally reducing the efficiency of heat pumps can also be examined.

There are additional factors which affect demand that can be incorporated into the bottom up section of SpDEAM. For example thermal mass can be included in buildings to examine the effect of delayed demand for heat. Wind driven cooling of buildings can also be integrated, given that the data is also available.

The division of demand among people, division of people among houses, placement of heating technology in buildings has been assumed to spatially homogenous and even amongst dwelling types etc. whereas in reality it will vary. These could be explored further.

Gas demand calibration was performed using seasonal normal demand, SpDEAM output could be compared against high and low demand. A sensitivity analysis of all input data and variables could also be carried out.

Currently SpDEAM only uses regular activity profiles. Analysis has shown that these do not represent irregular periods such as bank holidays and Christmas. Profiles could be calibrated against measured data to improve representation of these types of periods.

Domestic demand is simplified due to the resolution of the modelling. Future iterations could however introduce further disaggregation of end uses, e.g. include hot water demand. Non domestic demand could also be disaggregated further both in space and by end use.

9.4.3. New applications of the model

Wind generation

The offshore locations used to place capacity in the scenario modelling are restricted by the designated development zones. It is possible that using other offshore locations will result in better

correlation of wind generation and electricity demand, therefore reducing the need for matching mechanisms and mitigating some of the cost of offshore development. Applying a multi criteria analysis offshore can highlight suitable offshore areas outside of the existing development zones, within the model grid. Generation using capacity in these locations can then be simulated and the effect on residual demand explored.

The scenario modelling uses a single weather year for each future year. By applying all years of CSFR weather data to each year a better idea of the range of wind generation can be generated. One possible application of this method is to near future capacity, where the spatial configuration is more certain. This method could then be used for probabilistic forecasting. It may also be able to forecast sub hourly generation through statistical adjustments of CFSR data.

The gridded method developed for this thesis, including the analysis performed on available land, could also be applied to other renewables. For example for solar, identifying available rooftops and using CFSR data for simulation. Scenarios from other sources could be used to dictate growth of these renewables. If these include wind capacity residual demand etc. can be compared to that described here.

Electricity demand

Population growth is assumed to be spatially homogeneous in the current application of the model. It it possible that in the future population will grow more quickly in some places than others. SpDEAM can be used to investigate the implications of this on energy demand by exposing these populations to different weather conditions.

Other new forms of energy consumption than heat pumps can be modelled using the bottom up method; for example, electric vehicles and district heating.

SpDEAM and SpWind can be used in conjunction with a model of the electricity network to explore the implications of changes to the spatial configuration of wind capacity on network growth and operation.

Residual demand

The final analysis of the scenario modelling has begun to explore the role of matching mechanisms in the integration of wind under the NG scenarios. These have not been analysed in depth due to the complexity of their role given the influence of other demands and supplies in the electricity system. The same data and method could be used to examine these further.

Regional surpluses/shortfalls could be examined, both in GB and potentially larger spatial scopes, e.g. Europe.

A. Appendix

A.1. Extended dataset description

A.1.1. Gridded domestic heating technologies

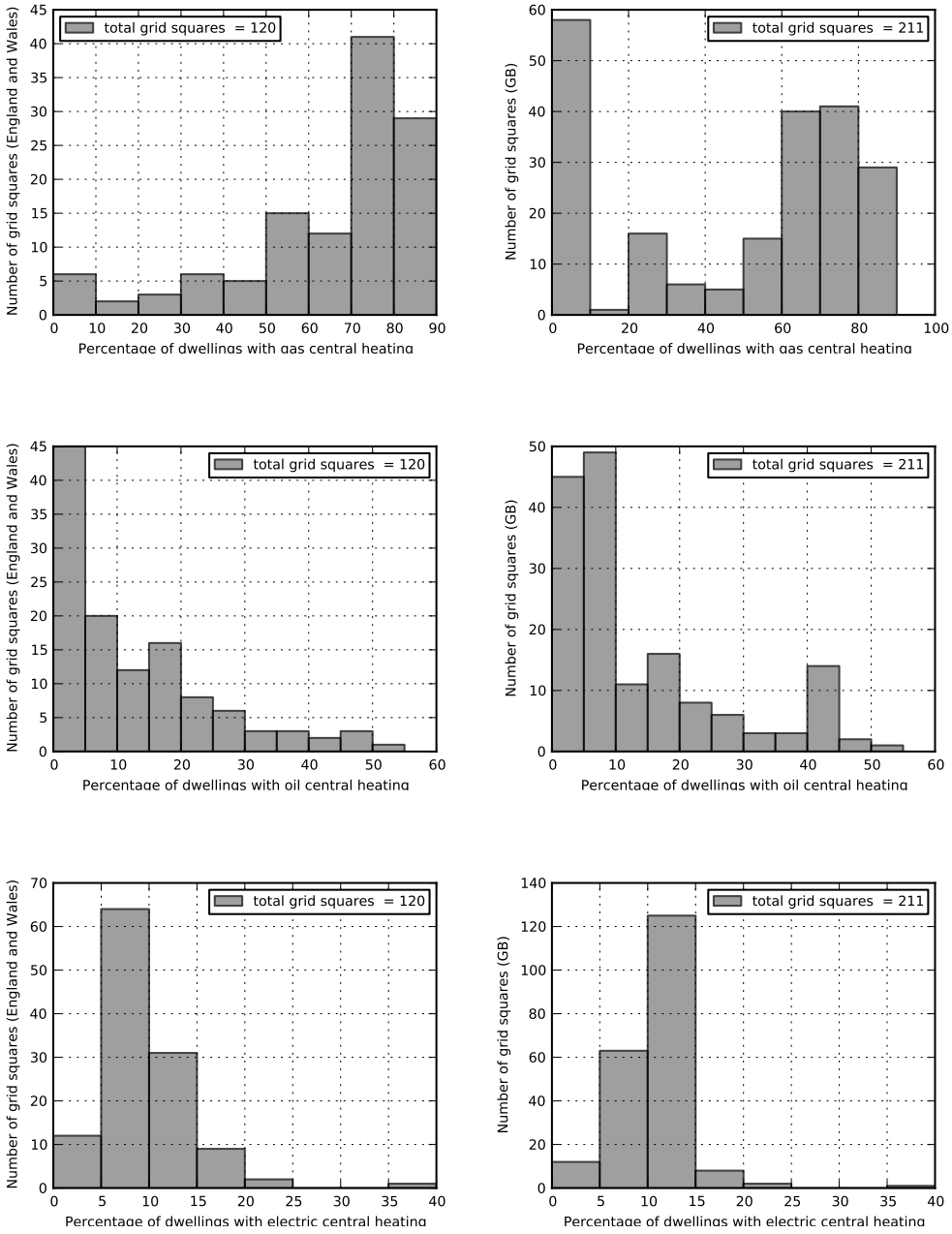

Figure A.1.: Heating type by grid square, comparison of England and Wales census data and GB data which includes assumptions on Scottish technologies, primary fuels. . Top left = England and Wales, gas, top right = GB gas. Middle left = England and Wales, oil, middle right = GB oil. Bottom left =England and Wales, electric, bottom right = GB electric.

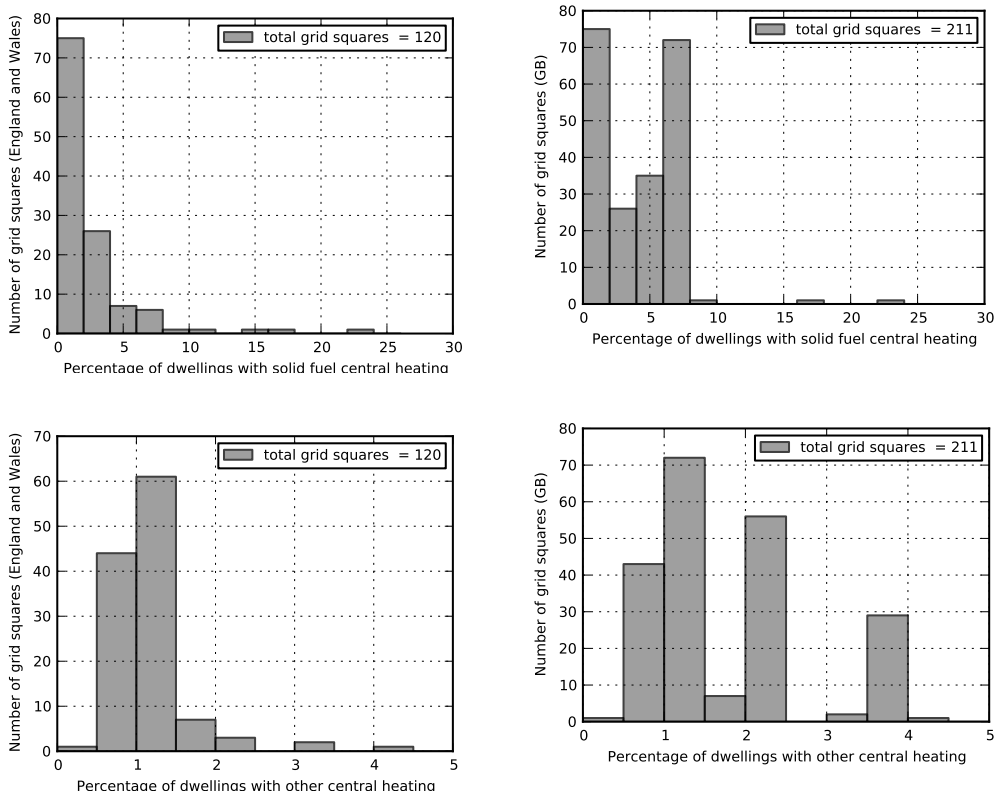

Figure A.2.: Heating type by grid square, comparison of England and Wales census data and GB data which includes assumptions on Scottish technologies, solid fuel and other fuel. Top left = England and Wales, solid fuel, top right = GB, solid fuel. Bottom left = England and Wales, other fuel, bottom right = GB other fuel.

A.1.2. Census based dwelling data

A.1.3. DECC Sub-National Statistics

A.1.3.1. Gas

Figure A.6 shows an example of the original census based gas DECC sub national statistics. This shows some grouping of gas demand with central and South Eastern England classified in the same band. South Western England exhibits less demand and Northern Scotland less still.

A.1.3.2. Electricity

Figure A.7 shows that there is less smoothing of the average consumption of electricity per meter than with gas (Figure A.6), demonstrating that electricity use is more consistent both over GB and locally. Cities contain the census areas with the least demand. In some cases this is smoothed when aggregated, e.g. the grid squares over London contain higher demand areas and are therefore moved into the next highest classification. Whereas cities in the North East and North West of England remain low demander's of electricity. This demonstrates that the effect of aggregation changes dependent on geography.

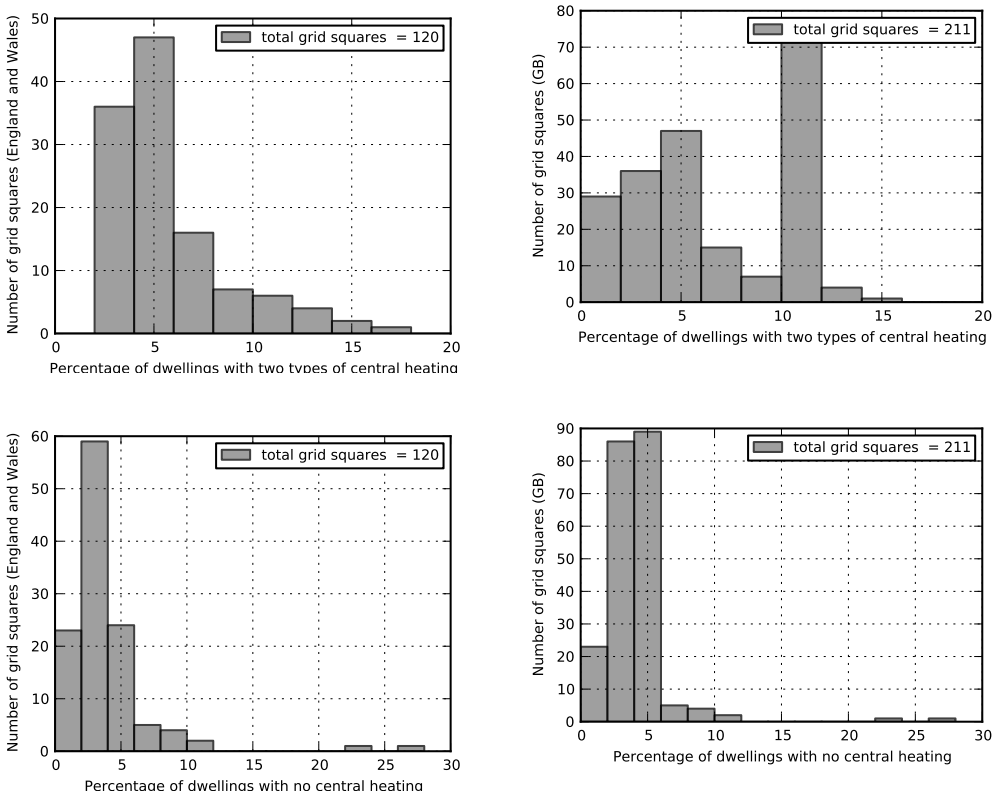

Figure A.3.: Heating type by grid square, comparison of England and Wales census data and GB data which includes assumptions on Scottish technologies, minor fuels. Top left = England and Wales, two types, top right = GB, two types. Bottom left = England and Wales, no central heating, bottom right = GB, no central heating.

A.2. Sample code

A.2.1. Downloading and adapting CFSR to the grid

Create UNIX wget code from http://rda.ucar.edu/datasets/ds093.1/ (CFSR selected hourly time series from 1979-2010, this is CFSR V1, CFSR V2 extends from this date to close to the present day but is not used in this study) this requires a free NCEP account. The website generates the code including filenames and username (appropriate filenames must be selected, which in this case are the U and V components of wind, downward shortwave radiation flux and temperature). There are options available which vary between these datasets, including height, grid and forecast (temporal) For continuity the T382 grid has been selected for all of the variables. A pre altered 0.5 degree grid is available for wind speed and temperature, however as this is not available for solar radiation the T382 grid is used and adapted using wgrib2, see below. The lowest height is chosen, 10m for wind, 2m for temperature and surface for solar radiation

Copy this wget code into a text editor, save as a .csh file. Make executable using chmod 755 (filename). Change shell from bash to cshell temporarirly using csh in the command line (this will end with the session and can be done by just closing the terminal). Run the code using ./filename

To interpolate to the new grid and extract the correct subset. Change back to a bash shell, run

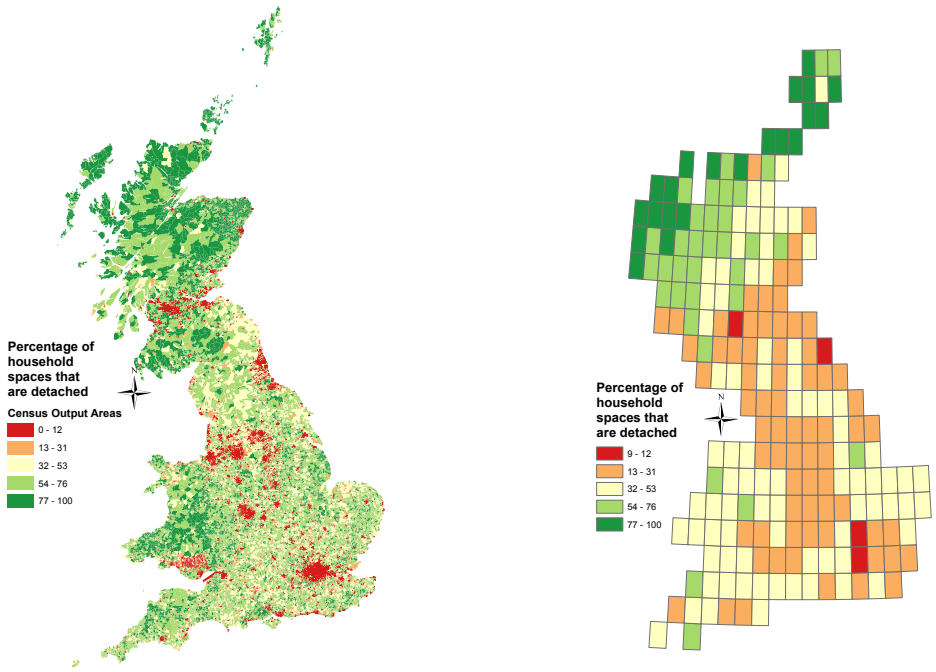

(a) Census base data on detached dwellings (2001).

(b) Redistributed to the grid

Figure A.4.: Example of spatial redistribution of census area statistics to the model grid, percentage of household space that are terraced 2001.

the ./interpolate code (must be executable): #!/bin/bash for f in *.grb2 do

wgrib2 "$f" -new_grid latlon 330:80:0.5 48:34:0.5 interpolated/"$f"

done

For the wind speed data only, convert u and v winds to speed using ./wind_speed.sh

#!/bin/bash for f in *.grb2 do

wgrib2 "$f" -wind_speed speed/"$f"

done

Convert to csvs using ./change_to_csv.sh

#!/bin/bash for f in *.grb2 do

wgrib2 “f$” -csv converted/”$f”.csv

done

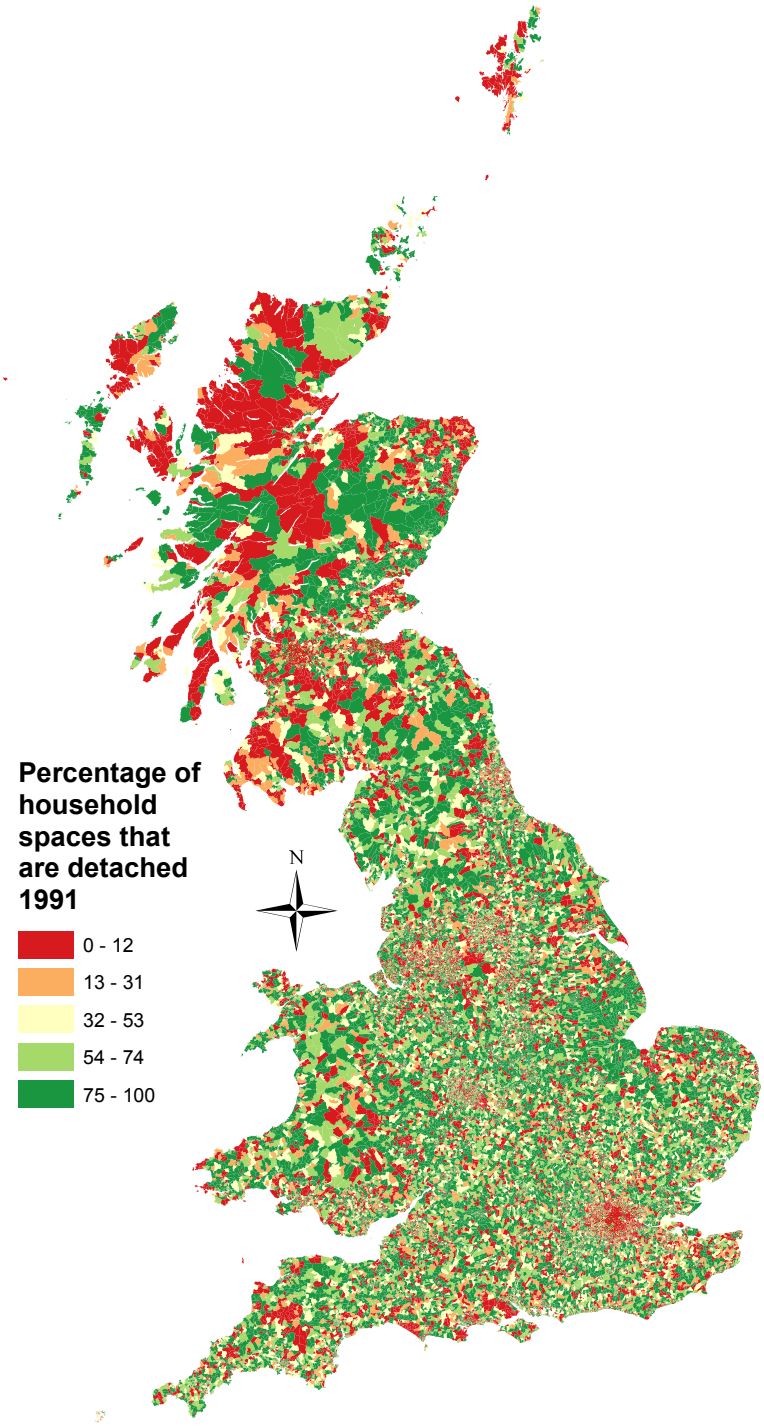

Figure A.5.: Map showing census data on detached houses 1991, this shows that there is a clear issue with the data as the distribution is wrong.

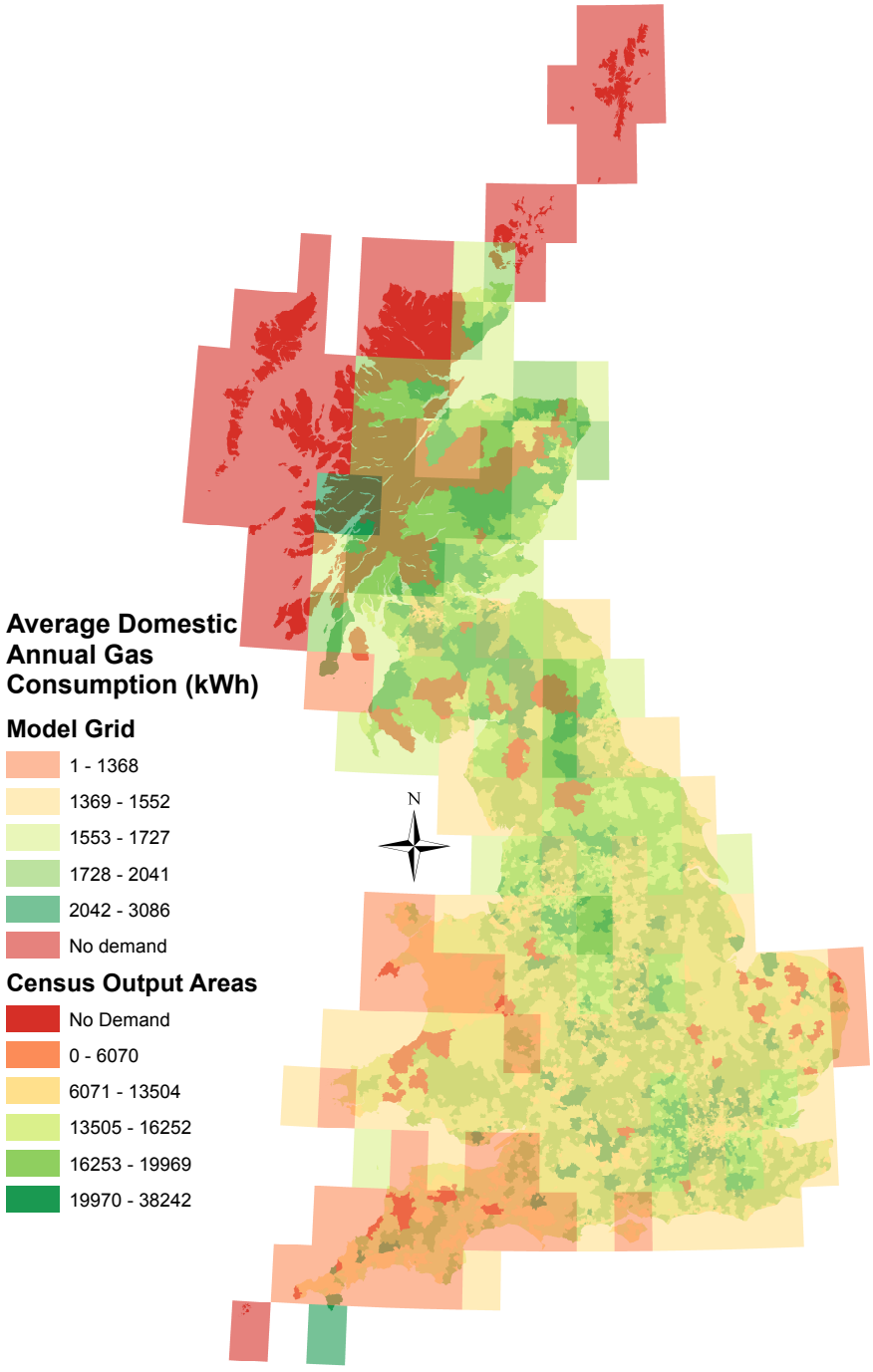

Figure A.6.: Average domestic annual gas consumption (kWh), LLSOAs and model grid, 2010, data source: DECC [2012b].

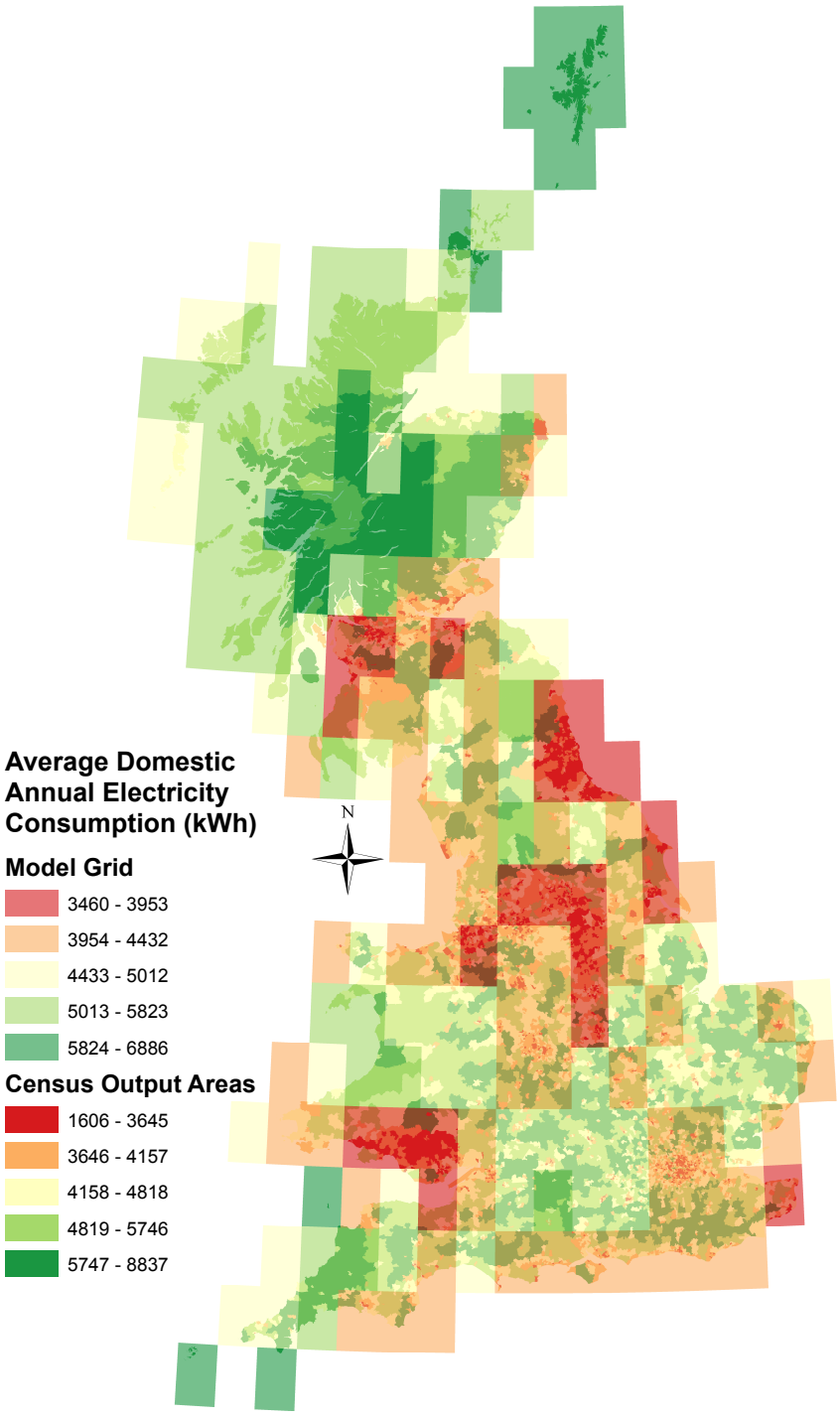

Figure A.7.: Average domestic annual electricity consumption (kWh), LLSOAs and model grid, data source: DECC [2012b].

Data Citations

Data Citations

Thank you to Iain Staffell and Richard Green for the supplementary data provided alongside Staffell and Green [2014]. This was a useful tool in the exploration of wind turbine simulation.

Population data: GPW: Center for International Earth Science Information Network (CIESIN), Columbia University; and Centro Internacional de Agricultura Tropical (CIAT). 2005. Gridded Population of the World, Version 3 (GPWv3): Population Count Grid. Palisades, NY: Socioeconomic Data and Applications Center (SEDAC), Columbia University. Available at http://sedac.ciesin.columbia.e [13/02/2012].

Borders: General Register Office for Scotland, 2001 Census: Digitised Boundary Data (Scotland) [computer file]. Census Geography Data Unit (UKBORDERS).

Office for National Statistics, 2001 Census: Digitised Boundary Data (England and Wales) [computer file]. Census Geography Data Unit (UKBORDERS).

Northern Ireland Statistics and Research Agency, 2001 Census: Digitised Boundary Data (Northern Ireland) [computer file]. Census Geography Data Unit (UKBORDERS).

Bibliography

T. Agami Reddy. Literature review on calibration of building energy simulation programs: uses, problems, procedures, uncertainty, and tools. *ASHRAE transactions*, pages 226–240, 2006.

T. Ahola, K. Virrantaus, J.M. Krisp, and G.J. Hunter. A spatio-temporal population model to support risk assessment and damage analysis for decision-making. *International Journal of Geographical Information Science*, 21(8):935–953, 2007. ISSN 1365-8816.

Dennis J. Aigner, Cyrus Sorooshian, and Pamela Kerwin. Conditional demand analysis for estimating residential end-use load profiles. *The Energy Journal*, pages 81–97, 1984.

Muhammad Ali, Julija Matevosyan, and J. V. Milanović. Probabilistic assessment of wind farm annual energy production. *Electric Power Systems Research*, 89:70–79, 2012.

B. Anderson and others. BREDEM-8 model description 2001 update—with corrections. *BRE, Watford, UK*, 2002.

B. R. Anderson, A. J. Clark, R. Baldwin, and N. O. Milbank. BREDEM-BRE domestic energy model: Background. *Philosophy and Description, Garston, Herts., Building Research Establishment*, 1985.

Brian Robert Anderson, P. F. Chapman, N. G. Cutland, C. M. Dickson, G. Henderson, J. H. Henderson, P. J. Iles, L. Kosmina, and L. D. Shorrock. *BREDEM-12: model description, 2001 update*. CRC, Construction Research Communications Limited, 2002.

Cristina L. Archer and Mark Z. Jacobson. Spatial and temporal distributions of US winds and wind power at 80 m derived from measurements. *Journal of Geophysical Research: Atmospheres (1984–2012)*, 108(D9), 2003.

Cristina L. Archer and Mark Z. Jacobson. Evaluation of global wind power. *Journal of Geophysical Research: Atmospheres (1984–2012)*, 110(D12), 2005.

Cristina L. Archer and Mark Z. Jacobson. Supplying baseload power and reducing transmission requirements by interconnecting wind farms. *Journal of Applied Meteorology and Climatology*, 46(11):1701–1717, 2007.

Cristina L. Archer and Mark Z. Jacobson. Geographical and seasonal variability of the global "practical" wind resources. *Applied Geography*, 45:119–130, 2013.

Sanjay R. Arwade, Matthew A. Lackner, and Mircea D. Grigoriu. Probabilistic models for wind turbine and wind farm performance. *Journal of Solar Energy Engineering*, 133(4):041006, 2011.

ASHRAE. Ashrae handbook - fundamentals, chapter 19 energy estimating and modelling. *American Society of Heating, Refrigerating and Air Conditioning Engineers, Atlanta*, 111, 2013. URL `http://shop.iccsafe.org/media/wysiwyg/material/8950P203-toc.pdf`.

European Wind Energy Association. *Pure Power-Wind energy targets for 2020 and 2030*. EWEA, 2011. URL http://books.google.co.uk/books?hl=en&lr=&id=cXuSk8jvHykC&oi=fnd&pg=PA8&dq=pure+power+wind+energy+targets&ots=HFC6dH43TR&sig=bDc49aW9Ms9ODUBQZKIW8ItZZEE.

Jonathan GB Atkinson, Tim Jackson, and Elizabeth Mullings-Smith. Market influence on the low carbon energy refurbishment of existing multi-residential buildings. *Energy Policy*, 37(7): 2582–2593, 2009.

S.M.J. Baban and T. Parry. Developing and applying a GIS-assisted approach to locating wind farms in the UK. *Renewable Energy*, 24(1):59–71, 2001. ISSN 0960-1481.

D. Balk and G. Yetman. The global distribution of population: evaluating the gains in resolution refinement. *New York: Center for International Earth Science Information Network (CIESIN), Columbia University*, 2004.

D. Balk, M. Brickman, B. Anderson, F. Pozzi, and G. Yetman. Estimates of future global population distribution to 2015. *Palisades, NY: CIESIN, Columbia University*, 2005.

DL Balk, U. Deichmann, G. Yetman, F. Pozzi, SI Hay, and A. Nelson. Determining global population distribution: methods, applications and data. *Advances in parasitology*, 62:119–156, 2006. ISSN 0065-308X.

Francisco Bañuelos-Ruedas, César Ángeles Camacho, and Sebastián Rios-Marcuello. Methodologies used in the extrapolation of wind speed data at different heights and its impact in the wind energy resource assessment in a region. *Wind Farm-Technical Regulations, Potential Estimation and Siting Assessment, InTech*, 2011.

Xinghua Bao and Fuqing Zhang. Evaluation of NCEP–CFSR, NCEP–NCAR, ERA-interim, and ERA-40 reanalysis datasets against independent sounding observations over the tibetan plateau. *Journal of Climate*, 26(1):206–214, 2013.

M. Barrett. A renewable electricity system for the UK. In *BOYLE, G. (ed.) Renewable Electricity and the Grid, The Challenge of Variability.* Earthscan, London.

Mark. Barrett and Catalina. Spataru. A dynamic energy agents-based model (DEAM) for demand supply, report to energy savings trust as part of the western power distribution FALCON (flexible approaches for low carbon optimised networks) project funded by low carbon networks. Technical report, Report to the Energy Savings Trust., 2012.

Mark Barrett and Catalina Spataru. DEAM - the dynamic energy agents model, UCL energy insitute models, 2014. URL http://www.ucl.ac.uk/energy-models/models/deam.

Barrett, Mark and Spataru, Catalina. DEAM - UCL energy institute models, 2014. URL http://www.ucl.ac.uk/energy-models/models/deam.

R.G. Barry and R.J. Chorley. *Atmosphere, weather and climate*. Taylor & Francis, 2009. ISBN 0415465702.

Rebecca Barthelmie, Gunner Larsen, Sara Pryor, Hans Jørgensen, Hans Bergström, Wolfgang Schlez, Kostas Rados, Bernhard Lange, Per Vølund, and Søren Neckelmann. ENDOW (efficient development of offshore wind farms): modelling wake and boundary layer interactions. *Wind Energy*, 7(3):225–245, 2004.

Rebecca Jane Barthelmie, Ole Rathmann, Sten Tron\a es Frandsen, K. S. Hansen, E. Politis, J. Prospathopoulos, K. Rados, D. Cabezon, W. Schlez, and J. Phillips. Modelling and measurements of wakes in large wind farms. In *Journal of Physics: Conference Series*, volume 75, page 012049. IOP Publishing, 2007.

Philippe Beaucage, Anna Glazer, Julien Choisnard, Wei Yu, Monique Bernier, Robert Benoit, and Gaëtan Lafrance. Wind assessment in a coastal environment using synthetic aperture radar satellite imagery and a numerical weather prediction model. *Canadian Journal of Remote Sensing*, 33(5):368–377, 2007.

Magnus Bengtsson, Yanjun Shen, and Taikan Oki. A SRES-based gridded global population dataset for 1990–2100. *Population and Environment*, 28(2):113–131, 2007. ISSN 0199-0039 1573-7810.

Hawthorne. Beyer. GME | SpatialEcology.com, 2014. URL `http://www.spatialecology.com/gme/`.

B. Bhaduri. Population distribution during the day. In S. Shekhar and H. Xiong, editors, *Encyclopedia of GIS*, pages 880 – 885. Springer, New York, 2008.

B. Bhaduri, E. Bright, P. Coleman, and J. Dobson. LandScan: Locating people is what matters. *Geoinformatics*, 5(2):34–37, 2002.

B. Bhaduri, E. Bright, P. Coleman, and M.L. Urban. LandScan USA: A high-resolution geospatial and temporal modeling approach for population distribution and dynamics. *GeoJournal*, 69(1): 103–117, 2007. ISSN 0343-2521.

Mahabir Bhandari, Som Shrestha, and Joshua New. Evaluation of weather datasets for building energy simulation. *Energy and Buildings*, 49:109–118, 2012.

M. Biberacher. *Modelling and Optimisation of Future Energy Systems: Using Spatial and Temporal Methods*. VDM Verlag Dr. Müller, 2004. ISBN 3836424355.

Brenda Boardman. Examining the carbon agenda via the 40% house scenario. *Building Research & Information*, 35(4):363–378, 2007.

Brenda Boardman, Sarah Darby, Gavin Killip, Mark Hinnels, Christian Jardine, Jane Palmer, and Graham Sinden. *40% House*. Environmental Change Institute, University of Oxford, 2005. URL `http://www.eci.ox.ac.uk/research/energy/downloads/40house/40house.pdf`.

Nicolas Boccard. Capacity factor of wind power realized values vs. estimates. *Energy Policy*, 37 (7):2679–2688, 2009.

T.H. Boehme, J. Taylor, R. Wallace, and J. Bialek. Matching renewable electricity generation with demand in scotland, 2006.

Thomas Boehme and A. Robin Wallace. Hindcasting hourly wind power across scotland based on met station data. *Wind Energy*, 11(3):233–244, 2008. ISSN 10954244 10991824.

M.G. Bosilovich. NASA's modern era retrospective-analysis for research and applications: Integrating earth observations. *Earthzine.[Online]. Retrieved on*, 26, 2008.

Mark A Bourassa, David M Legler, James J O'Brien, and Shawn R Smith. SeaWinds validation with research vessels. *Journal of Geophysical Research: Oceans (1978–2012)*, 108(C2), 2003. ISSN 2156-2202.

G. Boyle. *Renewable electricity and the grid: the challenge of variability.* Earthscan/James & James, 2008. ISBN 1844074188.

D. J. Brayshaw, C. Dent, and S. Zachary. Wind generation's contribution to supporting peak electricity demand–meteorological insights. *Proceedings of the Institution of Mechanical Engineers, Part O: Journal of Risk and Reliability*, pages 44–50S, 2011a.

David James Brayshaw, Alberto Troccoli, Rachael Fordham, and John Methven. The impact of large scale atmospheric circulation patterns on wind power generation and its potential predictability: A case study over the UK. *Renewable Energy*, 36(8):2087–2096, 2011b. ISSN 09601481.

BRE. The government's standard assessment procedure for energy rating of dwellings, 2011.

F. K. Brocklehurst. Wind resource in the UK. *Proceedings of the 1996 Eighteenth BWEA Wind Energy Conference*, pages 371 – 377, 1996.

SF Burch. *Computer modelling of the UK wind energy resource: phase II, application of the methodology.* Great Britain, Department of Trade and Industry, 1992.

Cambridge Architectural Research. Cambridge housing model and user guide - publications - GOV.UK, 2014. URL `https://www.gov.uk/government/statistics/cambridge-housing-model-and-user-guide`.

D. J. Cannon, D. J. Brayshaw, J. Methven, P. J. Coker, and D. Lenaghan. Using reanalysis data to quantify extreme wind power generation statistics: A 33 year case study in great britain. *Renewable Energy*, 75:767–778, 2015.

D. Carvalho, A. Rocha, M. Gómez-Gesteira, and C. Silva Santos. Comparison of reanalyzed, analyzed, satellite-retrieved and NWP modelled winds with buoy data along the iberian peninsula coast. *Remote Sensing of Environment*, 152:480–492, 2014a.

D. Carvalho, A. Rocha, M. Gómez-Gesteira, and C. Silva Santos. Offshore wind energy resource simulation forced by different reanalyses: Comparison with observed data in the iberian peninsula. *Applied Energy*, 134:57–64, 2014b.

D. Carvalho, A. Rocha, M. Gómez-Gesteira, and C. Silva Santos. WRF wind simulation and wind energy production estimates forced by different reanalyses: Comparison with observed data for portugal. *Applied Energy*, 117:116–126, 2014c.

Chris Chatfield. *The analysis of time series: an introduction.* CRC press, 2003. ISBN 0203491688.

Arun Chawla, Deanna M. Spindler, and Hendrik L. Tolman. Validation of a thirty year wave hindcast using the climate forecast system reanalysis winds. *Ocean Modelling*, 70:189–206, 2013. URL `http://www.sciencedirect.com/science/article/pii/S1463500312001047`.

Dudley B Chelton and Michael H Freilich. Scatterometer-based assessment of 10-m wind analyses from the operational ECMWF and NCEP numerical weather prediction models. *Monthly Weather Review*, 133(2):409–429, 2005. ISSN 1520-0493.

Vicky Cheng and Koen Steemers. Modelling domestic energy consumption at district scale: A tool to support national and local energy policies. *Environmental Modelling & Software*, 26(10): 1186–1198, 2011. ISSN 1364-8152.

Tanya Christidis and Jane Law. Review: The use of geographic information systems in wind turbine and wind energy research. *Journal of Renewable and Sustainable Energy*, 4(1):012701, 2012.

C Clack, A Alexander, A Choukulkar, and A MacDonald. Improvements in wind resource assessment incorporating wind shear and consideration of resource variability. *Wind Energy*, pages 1–16, 2014a.

C Clack, A Alexander, A Choukulkhar, and A MacDonald. Improvements in wind resource assessment incorporatingwind shear and consideration of resource variability. *Wind Energy*, pages 1–16, 2014b.

J. Peter Clinch, John D. Healy, and Ciarán King. Modelling improvements in domestic energy efficiency. *Environmental Modelling & Software*, 16(1):87–106, 2001.

S. Cockings, D. Martin, and S. Leung. Population 24/7: building space-time specific population surface models. *In, Hakley, M., Morley, J. and Rahemtulla, H. (eds.) Proceedings of the GIS Research UK 18th Annual Conference GISRUK 2010. London, University College London, 41-48.*, 2010.

JP Coelingh. Geographical dispersion of wind power output in ireland. *Irish Wind Energy Association, study conducted by Ecofys, available online at/http://www.iwea.com/contentFiles/documents/Ecofys2*, 1999.

P. Coker. *Assessing the variability of UK renewables.* PhD thesis, University of Reading, 2011.

Phil Coker, Janet Barlow, Tim Cockerill, and David Shipworth. Measuring significant variability characteristics: An assessment of three UK renewables. *Renewable Energy*, 53:111–120, 2013. ISSN 0960-1481.

G.P. Compo, J.S. Whitaker, and P.D. Sardeshmukh. Feasibility of a 100-year reanalysis using only surface pressure data. *Bulletin of the American Meteorological Society*, 87(2):175–190, 2006. ISSN 0003-0007.

G.P. Compo, J.S. Whitaker, P.D. Sardeshmukh, N. Matsui, RJ Allan, X. Yin, BE Gleason, RS Vose, G. Rutledge, and P. Bessemoulin. The twentieth century reanalysis project. *Quarterly Journal of the Royal Meteorological Society*, 137(654):1–28, 2011. ISSN 1477-870X.

H Cook, J Palutikoff, and T Davies. The effect if geographical dispersion on the variability of wind energy. London, UK, March 1988.

J. Counihan. Adiabatic atmospheric boundary layers: a review and analysis of data from the period 1880–1972. *Atmospheric Environment (1967)*, 9(10):871–905, 1975.

Lucy C. Cradden, Francesco Restuccia, Samuel L. Hawkins, and Gareth P. Harrison. Consideration of wind speed variability in creating a regional aggregate wind power time series. *Resources*, 3 (1):215–234, 2014.

G. Czisch and G. Giebel. A comparison of intra-and extraeuropean options for an energy supply with wind power. 2000.

Gregor Czisch and Bernhard Ernst. High wind power penetration by the systematic use of smoothing effects within huge catchment areas shown in a european example. *Windpower 2001*, 2001.

Lewis Dale, David Milborrow, Richard Slark, and Goran Strbac. Total cost estimates for large-scale wind scenarios in UK. *Energy Policy*, 32(17):1949–1956, 2004.

DCLG. Household projections (2008 to 2033)., 2010. URL `https://www.gov.uk/government/statistics/household-projections-2008-to-2033-in-england`.

DCLG. English house condition survey 2003 - 2005, December 2013a.

DCLG. English housing survey 2007 - 2011, 2013b.

J. P. Deane, Alessandro Chiodi, Maurizio Gargiulo, and Brian P. Ó Gallachóir. Soft-linking of a power systems model to an energy systems model. *Energy*, 42(1):303–312, 2012. 00016.

DECC. National renewable energy action pland for the united kingdom, article 4 of the renewable energy directive, 2010.

DECC. UK renewable energy roadmap. Technical report, London, UK, 2011.

DECC. Household electricity survey - publications - GOV.UK, 2011. URL https://www.gov.uk/government/publications/household-electricity-survey--2.

DECC. Housing energy FactFile, 2012. Technical report, London, UK., 2012a. URL https://www.gov.uk/government/publications/housing-energy-fact-file-2012-energy-use-in-homes.

DECC. Sub-national energy consumption statistics, 2012b. URL http://www.decc.gov.uk/en/content/cms/statistics/energy_stats/regional/regional.aspx.

DECC. Digest of UK energy statistics. Technical report, London, UK, 2012c.

DECC. Our electricity transmission network: a vision for 2020. Technical report, 2012d. URL http://www.decc.gov.uk/assets/decc/11/meeting-energy-demand/future-elec-network/4264-ensg-summary.pdf.

DECC. Digest of united kingdom energy statistics table 6.4, 2013a.

DECC. Energy trends, 2013b. URL https://www.gov.uk/government/collections/energy-trends.

DECC. UK renewable energy roadmap update 2013. Technical report, London, UK, 2013c. URL https://www.gov.uk/government/uploads/system/uploads/attachment_data/file/255182/UK_Renewable_Energy_Roadmap_-_5_November_-_FINAL_DOCUMENT_FOR_PUBLICATIO___.pdf.

DECC. 2013 UK Greenhouse Gas Emissions, Final Figures, 2013. URL https://www.gov.uk/government/uploads/system/uploads/attachment_data/file/407432/20150203_2013_Final_Emissions_statistics.pdf.

DECC. Digest of united kingdom energy statistics, 2013a.

DECC. Digest of UK energy statistics - energy consumption in the UK, domestic consumption, 2013b.

DECC. Energy trends, 2013c.

DECC. Renewable energy planning database, 2014a. URL https://restats.decc.gov.uk/cms/planning-database/.

DECC. *Renewable Energy Planning Database*. 2014b. URL https://restats.decc.gov.uk/cms/planning-database/.

DECC. Energy trends: June 2014, 2014a. URL https://www.gov.uk/government/uploads/system/uploads/attachment_data/file/326368/ET_June_2014.pdf.

DECC. Sub national methodology and guidance booklet, 2014b. URL https://www.gov.uk/government/uploads/system/uploads/attachment_data/file/324877/Sub-national_methodology_and_guidance_booklet.pdf.

DECC. Household electricity survey - publications - GOV.UK, 2014. URL https://www.gov.uk/government/publications/household-electricity-survey--2.

Mark Decker, Michael A. Brunke, Zhuo Wang, Koichi Sakaguchi, Xubin Zeng, and Michael G. Bosilovich. Evaluation of the reanalysis products from GSFC, NCEP, and ECMWF using flux tower observations. *Journal of Climate*, 25(6), 2012.

Dick. Dee, John. Fasullo, Dennis. Shea, and John. Walsh. The climate data guide: Atmospheric reanalysis: Overview & comparison tables., April 2014. URL https://climatedataguide.ucar.edu/climate-data/atmospheric-reanalysis-overview-comparison-tables.

Uwe Deichmann, Deborah Balk, and Greg Yetman. Transforming population data for interdisciplinary usages: from census to grid. *Washington (DC): Center for International Earth Science Information Network*, 2001. URL http://sedac.ciesin.org/gpw-v2/GPWdocumentation.pdf.

C. J. Dent, Andrew Keane, and Janusz W. Bialek. Simplified methods for renewable generation capacity credit calculation: A critical review. In *Power and Energy Society General Meeting, 2010 IEEE*, pages 1–8. IEEE, 2010.

Department for Education. EduBase2, 2014. URL http://www.education.gov.uk/edubase/home.xhtml;jsessionid=A6BCD53864CA37ED8E22BBC5437E24AB.

Conor Devitt, John Fitz Gerald, Hugh Hennessy, Marie Hyland, Seán Lyons, Laura Malaguzzi Valeri, Joanne McLaughlin, and Richard Tol. A strategic energy scenario planning model for northern ireland - final report for the strategic investment board northern ireland, November 2011. URL http://www.sibni.org/a_strategic_energy_scenario_planning_model_for_northern_ireland_-_final_report.pdf.

A. Dhanju, P. Whitaker, and W. Kempton. Assessing offshore wind resources: An accessible methodology. *Renewable Energy*, 33(1):55–64, 2008. ISSN 0960-1481.

C. M. Dickson, J. E. Dunster, S. Z. Lafferty, and L. D. Shorrock. BREDEM: Testing monthly and seasonal versions against measurements and against detailed simulation models. *Building Services Engineering Research and Technology*, 17(3):135–140, 1996.

H. Dobesch, P. Dumolard, and I. Dyras. Spatial interpolation for climate data. *ISTE Ltd., London*, 2007.

J.E. Dobson, E.A. Bright, P.R. Coleman, R.C. Durfee, and B.A. Worley. LandScan: a global population database for estimating populations at risk. *Photogrammetric engineering and remote sensing*, 66(7):849–857, 2000. ISSN 0099-1112.

Daniel R. Drew, Dirk J. Cannon, David J. Brayshaw, Janet F. Barlow, and Phil J. Coker. The Impact of Future Offshore Wind Farms on Wind Power Generation in Great Britain. *Resources*, 4(1):155–171, 2015.

DTI. Renewable energy in the UK. prospects for the 21st century, supporting analysis for the renewables obligation consultation, 1998.

DTI. Future offshore, a strategic framework for the offshore wind industry, 2002.

R. Dutra and A. Szklo. Assessing long-term incentive programs for implementing wind power in brazil using GIS rule-based methods. *Renewable Energy*, 33(12):2507–2515, 2008. ISSN 0960-1481.

Nick Earl, Steve Dorling, Richard Hewston, and Roland von Glasow. 1980–2010 variability in UK surface wind climate. *Journal of Climate*, 26(4):1172–1191, 2013.

W. Ebisuzaki and L. Zhang. A comparison of the climate forecast system reanalysis (CFSR) with the ERA-40, JRA-25, NCEP/NCAR, NCEP/DOE and MERRA reanalyses. volume 1, page 0298, 2010.

W. Ebisuzaki and L. Zhang. Assessing the performance of the CFSR by an ensemble of analyses. *Climate Dynamics*, pages 1–10, 2011. ISSN 0930-7575.

ECI. Background material a: United kingdom domestic carbon model (UKDCM), description, method and analysis. In *40% House Project*. Environmental Change Institute, University of Oxford, 2005. URL `http://www.eci.ox.ac.uk/research/energy/downloads/40house/background_doc_a.pdf`.

Ottmar Edenhofer, Ramón Pichs-Madruga, Youba Sokona, Kristin Seyboth, Susanne Kadner, Timm Zwickel, Patrick Eickemeier, Gerrit Hansen, Steffen Schlömer, Christoph von Stechow, and others. *Renewable energy sources and climate change mitigation: Special report of the intergovernmental panel on climate change*. Cambridge University Press, 2011.

EEA. CORINE land cover technical guide – addendum 2000 (technical report no. 40). Technical report, EEA, Copenhagen, 2000.

EEA. Europe's onshore and offshore wind energy potential, an assessment of environmental and economic constraints:, 2009. URL `http://www.energy.eu/publications/a07.pdf`.

M. B. Ek, K. E. Mitchell, Y. Lin, E. Rogers, P. Grunmann, V. Koren, G. Gayno, and J. D. Tarpley. Implementation of noah land surface model advances in the national centers for environmental prediction operational mesoscale eta model. *Journal of Geophysical Research: Atmospheres (1984–2012)*, 108(D22), 2003.

Paul Ekins, Ilkka Keppo, Jim Skea, Neil Strachan, Will Usher, and Gabrial Anandarajah. The UK energy system in 2050: Comparing Low-Carbon, Resilient Scenarios, 2013. URL `TheUKenergysystemin2050:ComparingLow-Carbon, ResilientScenarios-Seemoreat:http://www.ukerc.ac.uk/publications/the-uk-energy-system-in-2050-comparing-low-carbon-resilient-scenarios.html#sthash.HWXsfRHQ.dpuf`.

Elexon. BM units database, 2014a. URL `https://www.elexonportal.co.uk`.

Elexon. Half hourly generation by fuel type, 2014b. URL `https://www.elexonportal.co.uk`.

MR Elkinton, AL Rogers, and JG McGowan. An investigation of wind-shear models and experimental data trends for different terrains. *Wind Engineering*, 30(4):341–350, 2006. ISSN 0309-524X.

Energy Numbers. Capacity factors at Danish offshore wind farms, 2015. URL `http://energynumbers.info/capacity-factors-at-danish-offshore-wind-farms`.

L.A. Ensor and S.M. Robeson. Statistical characteristics of daily precipitation: comparisons of gridded and point datasets. *Journal of Applied Meteorology and Climatology*, 47(9):2468–2476, 2008. ISSN 1558-8432.

EST. Analysis from the energy saving trust's heat pump field trial - publications - GOV.UK, 2013. URL `https://www.gov.uk/government/publications/analysis-from-the-first-phase-of-the-energy-saving-trust-s-heat-pump-field-trial`.

ETSU. An assessment of renwable energy for the UK, 1994.

European Commission. The 2020 climate and energy package - European Commission, 2015. URL `http://ec.europa.eu/clima/policies/package/index_en.htm`.

Tina Fawcett. The future role of heat pumps in the domestic sector. *Proceedings of ECEEE 2011 Summer Study, Energy efficiency first: The Foundation of a Low-Carbon Society*, pages 1547–1557, 2011.

A Fellows. *The Potential of Wind Energy to Reduce Carbon dioxide Emissions*. Garrad Hassan and Partners Ltd, 2000.

Y. Feng, P. J. Tavner, H. Long, and J. W. Bialek. Review of early operation of UK round 1 offshore wind farms. In *Power and Energy Society General Meeting, 2010 IEEE*, pages 1–8. IEEE, 2010.

Steven Firth, K. Lomas, A. Wright, and R. Wall. Identifying trends in the use of domestic appliances from household electricity consumption measurements. *Energy and Buildings*, 40(5): 926–936, 2008.

Steven K. Firth, Kevin J. Lomas, and A. J. Wright. Targeting household energy-efficiency measures using sensitivity analysis. *Building Research & Information*, 38(1):25–41, 2010.

Aurélie Foucquier, Sylvain Robert, Frédéric Suard, Louis Stéphan, and Arnaud Jay. State of the art in building modelling and energy performances prediction: A review. *Renewable and Sustainable Energy Reviews*, 23:272–288, 2013.

Jennifer A. Francis. Validation of reanalysis upper-level winds in the arctic with independent rawinsonde data. *Geophysical research letters*, 29(9):29–1, 2002.

S. Frandsen and C.J. Christensen. Accuracy of estimation of energy production from wind power plants. *Wind Engineering*, 16(5):257–268, 1992. ISSN 0309-524X.

L.L. Freris and D.G. Infield. *Renewable energy in power systems*. Wiley, 2008. ISBN 047001749X.

Friends of the Earth. Planning for wind power: Guidelines for project developers and local planners, 1995.

Frontier Economics. National grid's gas demand forecasting methodology, a final report for OFGEM. Technical report, London, UK., 2006.

Wolf-Gerrit Früh. Long-term wind resource and uncertainty estimation using wind records from scotland as example. *Renewable Energy*, 50:1014–1026, 2013.

Nelson Fumo. A review on the basics of building energy estimation. *Renewable and Sustainable Energy Reviews*, 31:53–60, 2014.

S.R. Gaffin, C. Rosenzweig, X. Xing, and G. Yetman. Downscaling and geo-spatial gridding of socio-economic projections from the IPCC special report on emissions scenarios (SRES). *Global Environmental Change Part A*, 14(2):105–123, 2004. ISSN 0959-3780.

Francisco Javier Gallego. A population density grid of the european union. *Population and Environment*, 31(6):460–473, 2010. ISSN 0199-0039 1573-7810.

E. García-Bustamante, J. F. González-Rouco, P. A. Jiménez, J. Navarro, and J. P. Montávez. A comparison of methodologies for monthly wind energy estimation. *Wind Energy*, 12(7):640–659, 2009.

Garrad Hassan. Scotland's renewable resource 2001: Volume i - the analysis, 2001.

Madeleine Gibescu, Arno J. Brand, and Wil L. Kling. Estimation of variability and predictability of large-scale wind energy in the netherlands. *Wind Energy*, 12(3):241–260, 2009.

JK Gibson. *ECMWF re-analysis project report series: ERA description*, volume 1. European Centre for Medium-Range Weather Forecasts, 1997.

G. Giebel. *Equalizing effects of the wind energy production in Northern Europe determined from reanalysis data*, volume 1182. Risø National Laboratory, 2000. ISBN 8755026982.

Gregor Giebel. A variance analysis of the capacity displaced by wind energy in europe. *Wind energy*, 10(1):69–79, 2007.

R.N. Giere. *Explaining science: A cognitive approach*. University of Chicago Press, 1990. ISBN 0226292061.

Paul Gipe. Wind power for home and business renewable. *Wind Engineering*, 28(5):629–631, 2004. ISSN 0309-524X.

M.F. Goodchild and N.S. Lam. *Areal interpolation: a variant of the traditional spatial problem*. Dept. of Geography, University of Western Ontario, 1980. ISBN 0771402260.

M.F. Goodchild, L. Anselin, and U. Deichmann. A framework for the areal interpolation of socioeconomic data. *Environment and Planning A*, 25(3):383–397, 1993.

A. M. Gormally, J. D. Whyatt, R. J. Timmis, and C. G. Pooley. A regional-scale assessment of local renewable energy resources in cumbria, UK. *Energy Policy*, 50:283–293, 2012.

Bhupendra Nath Goswami and D. Sengupta. A note on the deficiency of NCEP/NCAR reanalysis surface winds over the equatorial indian ocean. *Journal of Geophysical Research: Oceans (1978–2012)*, 108(C4), 2003.

Arnaud Grandjean, Jérôme Adnot, and Guillaume Binet. A review and an analysis of the residential electric load curve models. *Renewable and Sustainable Energy Reviews*, 16(9):6539–6565, 2012.

Richard Green and Nicholas Vasilakos. Market behaviour with large amounts of intermittent generation. *Energy Policy*, 38(7):3211–3220, 2010. ISSN 0301-4215.

Richard Green, Helen Hu, and Nicholas Vasilakos. Turning the wind into hydrogen: The long-run impact on electricity prices and generating capacity. *Energy Policy*, 39(7):3992–3998, 2011.

Richard. Green, Iain. Staffell, and Nicholas. Vasilakos. Divide and conquer? k means clustering of demand data allows rapid and accurate simulations of the british electricity system. *IEEE TRANSACTIONS ON ENGINEERING MANAGEMENT*, In press, 2014.

S. M. Griffies and R. W. Hallberg. MJ harrison, RC pacanowski, and a. rosati, 2003: A technical guide to MOM4. GFDL ocean group tech. rep. 5, NOAA. *Geophysical Fluid Dynamics Laboratory, Princeton, NJ*.

Griffies, S. M., M. J. Harrison, R. C. Pacanowski, and A. Rosati. A technical guide to MOM4. GFDL ocean group tech. rep. 5, 2004. URL `http://www.gfdl.noaa.gov/bibliography/related_files/smg0301.pdf.]`.

R. Gross. Technologies and innovation for system change in the UK: status, prospects and system requirements of some leading renewable energy options. *Energy Policy*, 32:1905 – 1919, 2004.

R Gross and J Chapman. *Technical and economic potential of renewable energy generating technologies: Potentials and costs reductions to 2020. PIU Working Paper for the Energy Review.* The Cabinet Office, London, 2001.

R. Gross, P. Heptonstall, D. Anderson, T. Green, M. Leach, and J. Skea. *The Costs and Impacts of Intermittency: An assessment of the evidence on the costs and impacts of intermittent generation on the British electricity network.* UK Energy Research Centre, 2006. ISBN 1903144043.

M.J. Grubb. The integration of renewable electricity sources. *Energy Policy*, 19(7):670–688, 1991. ISSN 0301-4215.

M.J. Grubb and N.I. Meyer. Wind energy: resources, systems, and regional strategies. In *Renewable energy: sources for fuels and electricity.* Island Press, 1993.

Markus Haller, Sylvie Ludig, and Nico Bauer. Decarbonization scenarios for the EU and MENA power system: Considering spatial distribution and short term dynamics of renewable generation. *Energy Policy*, 47:282–290, 2012.

H.S. Hansen. GIS-based multi-criteria analysis of wind farm development. 2005. ISSN 9173231266.

Keir Harman, Ross Walker, and Michael Wilkinson. Availability trends observed at operational wind farms. In *European Wind Energy Conference*, 2008.

Bernhard Hasche. General statistics of geographically dispersed wind power. *Wind Energy*, 13(8): 773–784, 2010.

Erich Hau and Horst von Renouard. *The Wind Resource.* Springer, 2006.

S Hawkins, D Eager, and GP Harrison. Characterising the reliability of production from future british offshore wind fleets. 2011.

S. Heiple and D. Sailor. Using building energy simulation and geospatial modelling techniques to determine high resolution building sector energy consumption profiles. *Energy and Buildings*, 40 (8):1426–1436, 2008. ISSN 03787788.

Richard Hewston and Stephen R Dorling. An analysis of observed daily maximum wind gusts in the UK. *Journal of wind engineering and industrial aerodynamics*, 99(8):845–856, 2011. ISSN 0167-6105.

Paraic Higgins and Aoife Foley. The evolution of offshore wind power in the united kingdom. *Renewable and Sustainable Energy Reviews*, 37:599–612, 2014.

Mark Hinnells, Brenda Boardman, Russell Layberry, Sarah Darby, and Gavin Killip. The UK housing stock 2005 to 2050: Assumptions used in scenarios and sensitivity analysis in UKDCM2 report. *Environmental Change Institute/University of Oxford/IDAE*, 2007.

Sung H. Hong, Tadj Oreszczyn, and Ian Ridley. The impact of energy efficient refurbishment on the space heating fuel consumption in english dwellings. *Energy and Buildings*, 38(10):1171–1181, 2006.

Monique Hoogwijk, Bert de Vries, and Wim Turkenburg. Assessment of the global and regional geographical, technical and economic potential of onshore wind energy. *Energy Economics*, 26 (5):889–919, 2004.

Monique Maria Hoogwijk. *On the global and regional potential of renewable energy sources*. Universiteit Utrecht, Faculteit Scheikunde, 2004.

Tom Howard and Peter Clark. Correction and downscaling of NWP wind speed forecasts. *Meteorological Applications*, 14(2):105–116, 2007.

S. A. Hsu, Eric A. Meindl, and David B. Gilhousen. Determining the power-law wind-profile exponent under near-neutral stability conditions at sea. *Journal of Applied Meteorology*, 33(6): 757–765, 1994.

Gordon Hughes. The performance of wind farms in the united kingdom and denmark. *Renewable Energy Foundation: London, UK*, 2012.

G. Johannesson, J. Stewart, C. Barr, L.B. Sabeff, R. George, D. Heimiller, and A. Milbrandt. Adapting existing spatial data sets to new uses: An example from energy modeling. *Journal of Map & Geography Libraries*, 4(2):285–295, 2008. ISSN 1542-0353.

Thomas B. Johansson and Laurie Burnham. *Renewable energy: sources for fuels and electricity*. Island Press, 1993.

Clint Johnson, Andrew Tindal, Marc LeBlanc, A. Graves, and Keir Harman. Validation of GH north american energy predictions by comparison to actual production. In *2008 AWEA WINDPOWER Conference*, 2008.

D. Johnston, R. Lowe, and M. Bell. An exploration of the technical feasibility of achieving CO< sub> 2</sub> emission reductions in excess of 60% within the UK housing stock by the year 2050. *Energy Policy*, 33(13):1643–1659, 2005.

Eric. Jones, Travis. Oliphant, and Pearu. Peterson. SciPy: Open source scientific tools for python, 2001a. URL `http://www.scipy.org/`.

P. J. Jones, S. Lannon, and J. Williams. Modelling building energy use at urban scale. In *seventh international IBPSA conference, Rio de Janeiro, Brazil*, pages 175–180, 2001b.

Phil Jones, Joanne Patterson, and Simon Lannon. Modelling the built environment at an urban scale—energy and health impacts in relation to housing. *Landscape and Urban Planning*, 83(1): 39–49, 2007.

Hans E Jørgensen, Morten Nielsen, Rebecca J Barthelmie, and Niels G Mortensen. Modelling offshore wind resources and wind conditions. *Risø National Laboratory, Roskilde, Denmark*, 2005.

Jagadish Chandran Kaimal and John J. Finnigan. Atmospheric boundary layer flows: their structure and measurement. 1994. URL `http://www.citeulike.org/group/7763/article/3716071`.

E. Kalnay, M. Kanamitsu, R. Kistler, W. Collins, D. Deaven, L. Gandin, M. Iredell, S. Saha, G. White, and J. Woollen. The NCEP/NCAR 40-year reanalysis project. *Bulletin of the American Meteorological Society*, 77(3):437–471, 1996. ISSN 0003-0007.

Martin Kaltschmitt, Wolfgang Streicher, and Andreas Wiese. *Renewable energy: technology, economics and environment.* Springer, 2007. ISBN 3540709495.

M. Kanamitsu, W. Ebisuzaki, J. Woollen, S.K. Yang, JJ Hnilo, M. Fiorino, and GL Potter. Ncepdoe amip-ii reanalysis (r-2). *Bulletin of the American Meteorological Society*, 83(11):1631–1644, 2002. ISSN 0003-0007.

Tom Kane, Steven K. Firth, David Allinson, Katherine Irvine, and Kevin J. Lomas. Understanding occupant heating practices in UK dwellings. *World Renewable Energy Congress 2011 Sweden*, page 412–425, 2011.

R. Kannan and H Turton. Long-term electricity dispatch model with the TIMES framework. *Environ Model Assess*, 18:325–343, 2013.

M. Kavgic, A. Mavrogianni, D. Mumovic, A. Summerfield, Z. Stevanovic, and M. Djurovic-Petrovic. A review of bottom-up building stock models for energy consumption in the residential sector. *Building and environment*, 45(7):1683–1697, 2010. ISSN 0360-1323.

Scott Kennedy. Wind power planning: assessing long-term costs and benefits. *Energy Policy*, 33 (13):1661–1675, 2005.

Sabena Khan and Emily Wilkes. Energy consumption in the UK, user guide 2014, 2014. URL `https://www.gov.uk/government/uploads/system/uploads/attachment_data/file/337462/ecuk_user_guide_2014.pdf`.

D. B. Kidner. Optimal site selection for wind farms - the role of geographical information systems. *Proceedings of the 1996 Eighteenth BWEA Wind Energy Conference*, pages 185 – 1990, 1996.

Péter Kiss and Imre M. Jánosi. Comprehensive empirical analysis of ERA-40 surface wind speed distribution over europe. *Energy Conversion and Management*, 49(8):2142–2151, 2008.

Péter Kiss, László Varga, and Imre M Jánosi. Comparison of wind power estimates from the ECMWF reanalyses with direct turbine measurements. *Journal of Renewable and Sustainable Energy*, 1(3):033105, 2009. ISSN 1941-7012.

R. Kistler, E. Kalnay, W. Collins, S. Saha, G. White, J. Woollen, M. Chelliah, W. Ebisuzaki, M. Kanamitsu, and V. Kousky. The NCEP-NCAR 50-year reanalysis: Monthly means CD-ROM and documentation. *Bulletin-American Meteorological Society*, 82(2):247–268, 2001. ISSN 0003-0007.

ML Kubik, PJ Coker, and C Hunt. Using meteorological wind data to estimate turbine generation output: a sensitivity analysis. *Volume 15 Wind Energy Applications*, page 4074, 2011.

ML Kubik, David J Brayshaw, Phil J Coker, and Janet F Barlow. Exploring the role of reanalysis data in simulating regional wind generation variability over northern ireland. *Renewable Energy*, 57:558–561, 2013a. ISSN 0960-1481.

ML Kubik, PJ Coker, JF Barlow, and C Hunt. A study into the accuracy of using meteorological wind data to estimate turbine generation output. *Renewable Energy*, 51:153–158, 2013b. ISSN 0960-1481.

A. Kusiak and Z. Song. Design of wind farm layout for maximum wind energy capture. *Renewable Energy*, 35(3):685–694, 2010. ISSN 0960-1481.

Lars Landberg, Lisbeth Myllerup, Ole Rathmann, Erik Lundtang Petersen, Bo Hoffmann Jørgensen, Jake Badger, and Niels Gylling Mortensen. Wind resource estimation—an overview. *Wind Energy*, 6(3):261–271, 2003.

M. Langford and D.J. Unwin. Generating and mapping population density surfaces within a geographical information system. *Cartographic Journal, The*, 31(1):21–26, 1994. ISSN 0008-7041.

G.C. Larsen and K.S. Hansen. Database on wind characteristics-contents of database bank. *Report No. Risø*, 2001.

Steven M. Lazarus and Jennifer Bewley. Evaluation of a wind power parameterization using tower observations. *Journal of Geophysical Research: Atmospheres (1984–2012)*, 110(D7), 2005.

PG Leahy and AM Foley. Wind generation output during cold weather-driven electricity demand peaks in ireland. *Energy*, 2011. ISSN 0360-5442.

P. Lejeune and C. Feltz. Development of a decision support system for setting up a wind energy policy across the walloon region (southern belgium). *Renewable Energy*, 33(11):2416–2422, 2008. ISSN 0960-1481.

S. Liléo and O. Petrik. Investigation on the use of NCEP/NCAR, MERRA and NCEP/CFSR reanalysis data in wind resource analysis. *sigma*, 1(2), 2010.

Sónia Liléo, Erik Berge, Ove Undheim, Rickard Klinkert, and Rolv E. Bredesen. Long-term correction of wind measurements state-of-the-art, guidelines and future work. *complexity*, 1:2–3, 2013.

Craig Lindberg and Anthony J. Broccoli. Representation of topography in spectral climate models and its effect on simulated precipitation. *Journal of climate*, 9(11):2641–2659, 1996.

Tadeusz Liszka. An interpolation method for an irregular net of nodes. *International Journal for Numerical Methods in Engineering*, 20(9):1599–1612, 1984.

Llorenç Lledó, Team Lead, and Jason Dubois. A STUDY OF WIND SPEED VARIABILITY USING GLOBAL REANALYSIS DATA. 2013.

Robert Lowe. Technical options and strategies for decarbonizing UK housing. *Building Research & Information*, 35(4):412–425, 2007.

Sylvie Ludig, Markus Haller, Eva Schmid, and Nico Bauer. Fluctuating renewables in a long-term climate change mitigation strategy. *Energy*, 36(11):6674–6685, 2011.

David JC MacKay. Could energy-intensive industries be powered by carbon-free electricity? *Philosophical Transactions of the Royal Society A: Mathematical, Physical and Engineering Sciences*, 371(1986):20110560, 2013.

Iman Mansouri, Marcus Newborough, and Douglas Probert. Energy consumption in UK households: impact of domestic electrical appliances. *Applied Energy*, 54(3):211–285, 1996.

James F. Manwell, Jon G. McGowan, and Anthony L. Rogers. *Wind Energy Explained: Theory, Design and Application*. John Wiley & Sons, 2010.

D. Martin. Directions in population GIS. *Geography Compass*, 5(9):655–665, 2011. ISSN 1749-8198.

David Martin. *Gridded population data for the UK–redistribution models and applications.* 2006. URL http://www.dpi.inpe.br/sil/CST310/Referencias/I_POSDEM_Oficinia_NEPO_ABEP_2010/Material_AndreGavlak/Bibliografias/Martin_S.A..pdf.

T.N. McPherson, J. Rush, H. Khalsa, A. Ivey, and M.J. Brown. A day-night population exchange model for better exposure and consequence management assessments. pages 1–6, 2006.

CA Mears, Deborah K Smith, and Frank J Wentz. Comparison of special sensor microwave imager and buoy-measured wind speeds from 1987 to 1997. *Journal of Geophysical Research*, 106(C6): 11719–11,729, 2001. ISSN 0148-0227.

Melisa Menendez, A Tomás, P Camus, M Garcia-Diez, L Fita, J Fernandez, FJ Méndez, and IJ Losada. A methodology to evaluate regional-scale offshore wind energy resources. pages 1–8. IEEE, 2011. ISBN 1457700867.

H.-T. Mengelkamp. Wind climate simulation over complex terrain and wind turbine energy output estimation. *Theoretical and applied climatology*, 63(3-4):129–139, 1999.

J. Mennis. Generating surface models of population using dasymetric mapping*. *The Professional Geographer*, 55(1):31–42, 2003. ISSN 0033-0124.

D. Milborrow. Wind power on the grid. In *Boyle, G. (ed.) Renewable electricity and the grid: The challenge of variability*, pages 31–45. Earthscan, London, 2007.

MOD. Caveat – MOD air traffic control and air defence radar coverage maps, 2014. URL https://restats.decc.gov.uk/cms/assets/SiteFiles/datasets/ModMapCaveats.pdf.

Bernd Möller. Changing wind-power landscapes: regional assessment of visual impact on land use and population in northern jutland, denmark. *Applied energy*, 83(5):477–494, 2006.

Bernd Möller. Continuous spatial modelling to analyse planning and economic consequences of offshore wind energy. *Energy Policy*, 39(2):511–517, 2011.

Sukumar Natarajan and Geoffrey J. Levermore. Predicting future UK housing stock and carbon emissions. *Energy Policy*, 35(11):5719–5727, 2007.

Sukumar Natarajan, Julian Padget, and Liam Elliott. Modelling UK domestic energy and carbon emissions: an agent-based approach. *Energy and Buildings*, 43(10):2602–2612, 2011. ISSN 0378-7788.

National Grid. UK future energy scenarios 2011. Technical report, National Grid plc, UK, 2011.

National Grid. Metered half-hourly electricity demands, 2012. URL http://www.nationalgrid.com/uk/Electricity/Data/Demand+Data/.

National Grid. Seasonal normal gas demand, LDZ model, 2013. URL http://www.nationalgrid.com/uk/Gas/Data/misc/index.htm.

National Grid. UK future energy scenarios: UK gas and electricity transmission, 2014. URL http://www2.nationalgrid.com/uk/industry-information/future-of-energy/future-energy-scenarios/.

NCAR. The climate data guide: FLUXNET., September 2013. URL https://climatedataguide.ucar.edu/climate-data/fluxnet.

NCAR. Atmospheric reanalysis: Overview & comparison tables | NCAR - climate data guide, May 2014. URL https://climatedataguide.ucar.edu/climate-data/atmospheric-reanalysis-overview-comparison-tables.

K Newton and S Burch. Estimation of the UK wind energy resource using computer modelling techniques report on phase i : Optimisation of the methodology, 1992.

K. Newton and SF Burch. *Estimation of the UK wind energy resource using computer modelling techniques and map data: a pilot study.* Department of Energy Energy Technology Support Unit, 1983.

H. Nfaoui, J. Buret, and AAM Sayigh. Wind characteristics and wind energy potential in morocco. *Solar Energy*, 63(1):51–60, 1998. ISSN 0038-092X.

Khanh Q. Nguyen. Wind energy in vietnam: Resource assessment, development status and future implications. *Energy Policy*, 35(2):1405–1413, 2007.

Per Norgaard and Hannele Holttinen. A multi-turbine power curve approach. In *Nordic Wind Power Conference*, volume 1, page 1–2, 2004.

OFGEM. Renewables obligation (RO). URL https://www.ofgem.gov.uk/environmental-programmes/renewables-obligation-ro.

Ofgem. Electricity capacity a ssessment, 2012a. URL https://www.ofgem.gov.uk/ofgem-publications/40203/electricity-capacity-assessment-2012.pdf.

Ofgem. Electricity capacity assessment, 2012b. URL https://www.ofgem.gov.uk/ofgem-publications/40203/electricity-capacity-assessment-2012.pdf.

Ofgem. *Electricity Capacity A ssessment.* 2012c. URL https://www.ofgem.gov.uk/ofgem-publications/40203/electricity-capacity-assessment-2012.pdf.

Ofgem. Renewables obligation (RO), 2014. URL https://www.ofgem.gov.uk/environmental-programmes/renewables-obligation-ro.

K. Onogi, J. TSUTSUI, H. KOIDE, M. SAKAMOTO, S. KOBAYASHI, H. HATSUSHIKA, T. MATSUMOTO, N. YAMAZAKI, H. KAMAHORI, and K. TAKAHASHI. The JRA-25 reanalysis. *????*, 85(3):369–432, 2007. ISSN 0026-1165.

ONS. Population: UK national statistics publication hub, 2014a. URL http://www.statistics.gov.uk/hub/population.

ONS. National population projections, 2012-based projections, 2014b. URL http://www.ons.gov.uk/ons/publications/re-reference-tables.html?edition=tcm%3A77-318453.

Poul A. Østergaard. Geographic aggregation and wind power output variance in denmark. *Energy*, 33(9):1453–1460, 2008.

J. Oswald, M. Raine, and H. Ashraf-Ball. Will british weather provide reliable electricity? *Energy Policy*, 36(8):3212–3225, 2008. ISSN 0301-4215.

Jane Palmer, Brenda Boardman, Catherine Bottrill, Sarah Darby, Mark Hinnells, Gavin Killip, Russell Layberry, and Heather Lovell. Reducing the environmental impact of housing: Final report. *Consultancy Study in Support of the Royal Commission on Environmental Pollution's*, 26, 2006.

DA Paolino, Q. Yang, B. Doty, JL Kinter III, J. Shukla, and D.M. Straus. A pilot reanalysis project at COLA. *Bulletin of the American Meteorological Society*, 76(5):697–710, 1995. ISSN 0003-0007.

L. Patterson, M. Urban, A. Myers, B. Bhaduri, E. Bright, and P. Coleman. Assessing spatial and attribute errors in large national datasets for population distribution models: a case study of philadelphia county schools. *GeoJournal*, 69(1):93–102, 2007. ISSN 0343-2521.

Linda Pedersen. Use of different methodologies for thermal load and energy estimations in buildings including meteorological and sociological input parameters. *Renewable and Sustainable Energy Reviews*, 11(5):998–1007, 2007.

Erik L. Petersen, Niels G. Mortensen, Lars Landberg, J. Højstrup, and Helmut P. Frank. Wind power meteorology. part i: climate and turbulence. *Wind Energy, pilot issue*, 1998a.

Erik L. Petersen, Niels G. Mortensen, Lars Landberg, Jørgen Højstrup, and Helmut P. Frank. Wind power meteorology. part II: siting and models. *Wind Energy*, 1(2):55–72, 1998b.

Ernest W. Peterson and Joseph P. Hennessey Jr. On the use of power laws for estimates of wind power potential. *Journal of Applied Meteorology*, 17(3):390–394, 1978.

Stefan Pfenninger, Adam Hawkes, and James Keirstead. Energy systems modeling for twenty-first century energy challenges. *Renewable and Sustainable Energy Reviews*, 33:74–86, 2014. 00001.

J. L. Phillips, S. D. Cox, A. R. Henderson, and J. P. Gill. Wake effects within and between large wind projects: the challenge of scale, density and neighbours–onshore and offshore. In *Proceedings of the European Wind Energy Association Conference*, 2010.

André Pina, Carlos A. Silva, and Paulo Ferrão. High-resolution modeling framework for planning electricity systems with high penetration of renewables. *Applied Energy*, 112:215–223, 2013.

AEA Technology plc. RESTATS - renewable energy statistics database for the united kingdom. URL `https://restats.decc.gov.uk/cms/planning-database/`.

Pöyry. Impact of intermittency: How wind variability could change the shape of the british and irish electricity markets. *Pöyry Energy Consulting report*, 2009a.

Pöyry. Impact of intermittency: How wind variability could change the shape of the british and irish electricity markets: Methodology document, 2009b. URL `http://www.poyry.co.uk/sites/www.poyry.uk/files/IntermittencyMethodologyv1_0.pdf`.

S. C. Pryor and R. J. Barthelmie. Climate change impacts on wind energy: A review. *Renewable and sustainable energy reviews*, 14(1):430–437, 2010.

S. C. Pryor, Justin T. Schoof, and R. J. Barthelmie. Empirical downscaling of wind speed probability distributions. *Journal of Geophysical Research: Atmospheres (1984–2012)*, 110(D19), 2005.

S. C. Pryor, Rebecca Jane Barthelmie, and J. T. Schoof. Inter-annual variability of wind indices across europe. *Wind Energy*, 9(1-2):27–38, 2006.

BE Psiloglou, C. Giannakopoulos, S. Majithia, and M. Petrakis. Factors affecting electricity demand in athens, greece and london, UK: A comparative assessment. *Energy*, 34(11):1855–1863, 2009. ISSN 0360-5442.

T. V. Ramachandra and B. V. Shruthi. Wind energy potential mapping in karnataka, india, using GIS. *Energy Conversion and Management*, 46(9):1561–1578, 2005.

T. V. Ramachandra and B. V. Shruthi. Spatial mapping of renewable energy potential. *Renewable and Sustainable Energy Reviews*, 11(7):1460–1480, 2007.

L. Reason and A. Clarke. *PROJECTING ENERGY USE AND CO2 EMISSIONS FROM LOW ENERGY BUILDINGS; A COMPARISON OF THE PASSIVHAUS PLANNING PACKAGE (PHPP) AND SAP*. AECB, 2008.

Renewable-UK. Wind energy in the UK, state of the industry report 2013. Technical report, London, UK, 2013.

Renewable-UK. RenewableUK | the voice of wind & marine energy, 2014. URL `http://www.renewableuk.com/`.

Ian Richardson, Murray Thomson, and David Infield. A high-resolution domestic building occupancy model for energy demand simulations. *Energy and Buildings*, 40(8):1560–1566, 2008.

Michele M Rienecker, Max J Suarez, Ronald Gelaro, Ricardo Todling, Julio Bacmeister, Emily Liu, Michael G Bosilovich, Siegfried D Schubert, Lawrence Takacs, and Gi-Kong Kim. MERRA: NASA's modern-era retrospective analysis for research and applications. *Journal of climate*, 24 (14):3624–3648, 2011a. ISSN 0894-8755.

M.M. Rienecker, M.J. Suarez, R. Gelaro, R. Todling, J. Bacmeister, E. Liu, M.G. Bosilovich, S.D. Schubert, L. Takacs, and G.K. Kim. MERRA-NASA's modern-era retrospective analysis for research and applications. *Bulletin of the American Meteorological Society*, 2011b. ISSN 1520-0442.

L.C. Rodman and R.K. Meentemeyer. A geographic analysis of wind turbine placement in northern california. *Energy Policy*, 34(15):2137–2149, 2006. ISSN 0301-4215.

Paolo M Ruti, Salvatore Marullo, Fabrizio D'Ortenzio, and Michel Tremant. Comparison of analyzed and measured wind speeds in the perspective of oceanic simulations over the mediterranean basin: Analyses, QuikSCAT and buoy data. *Journal of Marine Systems*, 70(1):33–48, 2008. ISSN 0924-7963.

A. Sabesan, K. Abercrombie, A.R. Ganguly, B. Bhaduri, E.A. Bright, and P.R. Coleman. Metrics for the comparative analysis of geospatial datasets with applications to high-resolution grid-based population data. *GeoJournal*, 69(1):81–91, 2007. ISSN 0343-2521.

S. Saha, S. Moorthi, H.L. Pan, X. Wu, J. Wang, S. Nadiga, P. Tripp, R. Kistler, J. Woollen, and D. Behringer. The NCEP climate forecast system reanalysis. *Bulletin of the American Meteorological Society*, 91(8):1015–1057, 2010. ISSN 0003-0007.

D.J. Sailor and L. Lu. A top–down methodology for developing diurnal and seasonal anthropogenic heating profiles for urban areas. *Atmospheric Environment*, 38(17):2737–2748, 2004. ISSN 1352-2310.

M. Salvatore, F. Pozzi, E. Ataman, B. Huddleston, M. Bloise, D. Balk, M. Brickman, B. Anderson, and G. Yetman. Mapping global urban and rural population distributions. *Rome: FAO*, 2005.

Julieta Schallenberg-Rodriguez. A methodological review to estimate techno-economical wind energy production. *Renewable and Sustainable Energy Reviews*, 21:272–287, 2013. ISSN 1364-0321.

SD Schubert, W. Min, L. Takacs, and J. Joiner. Reanalysis of historical observations and its role in the development of the goddard EOS climate data assimilation system. *Advances in Space Research*, 19(3):491–501, 1997. ISSN 0273-1177.

M.N. Schwartz. Wind resource estimation and mapping at the national renewable energy laboratory. pages 249–254. AMERICAN SOLAR ENERGY SOCIETY; AMERICAN INSTITUTE OF ARCHITECTS, 1999.

Scottish-Enterprise. Energy industry market forecasts, renwable energy, 2009-2014. Technical report, Aberdeen, Scotland, 2009.

Anna Maria Sempreviva, Rebecca Jane Barthelmie, and SC Pryor. Review of methodologies for offshore wind resource assessment in european seas. *Surveys in Geophysics*, 29(6):471–497, 2008. ISSN 0169-3298.

Javier Serrano González, Manuel Burgos Payán, Jesús Manuel Riquelme Santos, and Francisco González-Longatt. A review and recent developments in the optimal wind-turbine micro-siting problem. *Renewable and Sustainable Energy Reviews*, 30:133–144, 2014.

John Seryak and Kelly Kissock. Occupancy and behavioral affects on residential energy use. In *Proceedings of the Solar conference*, pages 717–722. AMERICAN SOLAR ENERGY SOCIETY; AMERICAN INSTITUTE OF ARCHITECTS, 2003.

Ed. Sharp. Life, death and gridded population datasets. *Royal Geographical Society Annual Conference*, 2012.

Ed Sharp. Spatial and temporal disaggregation of GB energy scenarios depicting increasing wind capacity and electrified heating to 2035. Karlsruhe, Germany, 2015a.

Ed Sharp. Spatiotemporal Disaggregation of GB Scenarios Depicting Increased Wind Capacity and Electrified Heat Demand in Dwellings. Antalya, Turkey, 2015b.

Ed Sharp, Catalina. Spataru, Mark Barrett, and Paul Dodds. Incorporating building specific heat loss and associated energy demand into electricity demand models for great britain. Building Simulation and Optimisation UCL, London, 2014.

Ed Sharp, Paul Dodds, Catalina. Spataru, and Mark Barrett. Evaluating the accuracy of CFSR reanalysis hourly wind speed forecasts for the uk, using in situ measurements and geographical information. *Renewable Energy*, 77:527–538, 2015.

Michelle Shipworth, Steven K. Firth, Michael I. Gentry, Andrew J. Wright, David T. Shipworth, and Kevin J. Lomas. Central heating thermostat settings and timing: building demographics. *Building Research & Information*, 38(1):50–69, 2010.

L. D. Shorrock and B.R. Anderson. Guide to the devel- opment of BREDEM. information paper no. IP 4/95, 1995.

L. D. Shorrock and J. E. Dunster. The physically-based model BREHOMES and its use in deriving scenarios for the energy use and carbon dioxide emissions of the UK housing stock. *Energy Policy*, 25(12):1027–1037, 1997.

L. D. Shorrock and J. I. Utley. *Domestic energy fact file 2003.* BRE Bookshop, 2003.

M. Shravan Kumar and V. K. Anandan. Comparision of the NCEP/NCAR reanalysis II winds with those observed over a complex terrain in lower atmospheric boundary layer. *Geophysical Research Letters*, 36(1), 2009.

A. Simmons, S. Uppala, D. Dee, and S. Kobayashi. ERA-interim: New ECMWF reanalysis products from 1989 onwards. *ECMWF newsletter*, 110:25–35, 2007.

S Simoes, T. Huld, D Mayr, J Schmidt, and M Zeyringer. The impact of location on competitiveness of wind and PV power plants – case study for austria. *10th International Conference on the European Energy Market EEM13,*, 2013.

G. Sinden. Characteristics of the UK wind resource: Long-term patterns and relationship to electricity demand. *Energy Policy*, 35(1):112–127, 2007. ISSN 0301-4215. doi: 10.1016/j.enpol.2005.10.003.

WC Skamarock, JB Klemp, J Dudhia, DO Gill, and DM Barker. A description of the advanced research WRF version 3. NCAR tech. Technical report, Note NCAR/TN-4751STR, 2005.

J Skea, P Ekins, and M Winskel. *Energy 2050 Mking the transition to a secure low carbon energy system*. Earthscan, London, 2011.

SKM. Growth scenarios for UK renewables generation and implications for future developments and operation of electricity networks. *BERR Publication URN*, 8:121, 2008.

B. Sorensen. GIS management of solar resource data. *Solar energy materials and solar cells*, 67 (1-4):503–509, 2001. ISSN 0927-0248.

B Sorenson and P Meibom. GIS tools for renewable energy modelling. *Renewable Energy*, 16:1262 – 1267, 1999.

Iain Staffell and Richard Green. How does wind farm performance decline with age? *Renewable Energy*, 66(0):775–786, 2014. ISSN 0960-1481.

Iain Staffell, Dan Brett, Nigel Brandon, and Adam Hawkes. A review of domestic heat pumps. *Energy & Environmental Science*, 5(11):9291–9306, 2012.

Koen Steemers and Geun Young Yun. Household energy consumption: a study of the role of occupants. *Building Research & Information*, 37(5-6):625–637, 2009.

Justin E. Stopa and Kwok Fai Cheung. Intercomparison of wind and wave data from the ECMWF reanalysis interim and the NCEP climate forecast system reanalysis. *Ocean Modelling*, 75:65–83, 2014.

Eric D. Stoutenburg, Nicholas Jenkins, and Mark Z. Jacobson. Power output variations of co-located offshore wind turbines and wave energy converters in california. *Renewable Energy*, 35 (12):2781–2791, 2010.

G. Strbac and Ilex Consulting. Quantifying the system costs of additional renewables in 2020. *Report to UK Department of Trade and Industry*, 2002.

Goran Strbac, Anser Shakoor, Mary Black, Danny Pudjianto, and Thomas Bopp. Impact of wind generation on the operation and development of the UK electricity systems. *Electric Power Systems Research*, 77(9):1214–1227, 2007.

Roland B. Stull. *An introduction to boundary layer meteorology*, volume 13. Springer, 1988.

A Sturt and G Strbac. A times series model for the aggregate GB wind output circa 2030. pages 1–6. IET, 2011.

L. Suganthi and Anand A. Samuel. Energy models for demand forecasting—a review. *Renewable and Sustainable Energy Reviews*, 16(2):1223–1240, 2012.

SULPU. SULPU - suomen lämpöpumppuyhdistys - tervetuloa, 2010. URL `http://www.sulpu.fi/`.

A. J. Summerfield, R. J. Lowe, and T. Oreszczyn. Two models for benchmarking UK domestic delivered energy. *Building Research & Information*, 38(1):12–24, 2010.

Lukas G Swan and V Ismet Ugursal. Modeling of end-use energy consumption in the residential sector: A review of modeling techniques. *Renewable and Sustainable Energy Reviews*, 13(8): 1819–1835, 2009. ISSN 1364-0321.

N.J. Tate. Surfaces for GIScience. *Transactions in GIS*, 4(4):301–303, 2000. ISSN 1467-9671.

J.W. Taylor and R. Buizza. Using weather ensemble predictions in electricity demand forecasting. *International Journal of Forecasting*, 19(1), 2003. ISSN 0169-2070.

W.R. Tobler. Smooth pycnophylactic interpolation for geographical regions. *Journal of the American Statistical Association*, pages 519–530, 1979. ISSN 0162-1459.

Jonas Tornberg and Liane Thuvander. A GIS energy model for the building stock of goteborg. In *ESRI International User Conference Proceedings*, 2005.

A.C. Torres Sibille, V.A. Cloquell-Ballester, and R. Darton. Development and validation of a multicriteria indicator for the assessment of objective aesthetic impact of wind farms. *Renewable and Sustainable Energy Reviews*, 13(1):40–66, 2009. ISSN 1364-0321.

IELP Troen and Erik Lundtang Petersen. *European wind atlas*. Risø National Laboratory, 1989a.

IELP Troen and Erik Lundtang Petersen. *European wind atlas*. Risø National Laboratory, 1989b.

UKERC. Electricity user load profiles by profile class, 2012. URL `http://data.ukedc.rl.ac.uk/cgi-bin/dataset_catalogue/view.cgi.py?id=6`.

UKGOV. Green Deal: energy saving for your home - GOV.UK, 2015. URL `https://www.gov.uk/green-deal-energy-saving-measures/overview`.

UKMO. Met office integrated data archive system (MIDAS) land and marine surface stations data (1853-current), 2012.

S.M. Uppala, PW Kållberg, AJ Simmons, U. Andrae, V. Bechtold, M. Fiorino, JK Gibson, J. Haseler, A. Hernandez, and GA Kelly. The ERA-40 re-analysis. *Quarterly Journal of the Royal Meteorological Society*, 131(612):2961–3012, 2005. ISSN 1477-870X.

US DOE. Building energy software tools directory: Tools by subjects, 2014. URL `http://apps1.eere.energy.gov/buildings/tools_directory/subjects_sub.cfm`.

USGS. Shuttle radar topography mission, digital elevation model, 2006a.

USGS. Shuttle radar topography mission, digital elevation model, 2006b.

Rob Van Haaren and Vasilis Fthenakis. GIS-based wind farm site selection using spatial multi-criteria analysis (SMCA): Evaluating the case for new york state. *Renewable and Sustainable Energy Reviews*, 15(7):3332–3340, 2011.

Claire Vincent, Andrea Hahmann, and jake Badger. Maps of mesoscale wind variability over the North Sea region. Barcelona, Spain, 2014.

K.R. Voorspools and W.D. D'haeseleer. An analytical formula for the capacity credit of wind power. *Renewable Energy*, 31(1):45–54, 2006. ISSN 0960-1481.

VTT TIEDOTTEITA. Future development trends in electricity demand, 2009. URL `http://www2.vtt.fi/inf/pdf/tiedotteet/2009/T2470`.

Rozenn Wagner, Ioannis Antoniou, Søren M. Pedersen, Michael S. Courtney, and Hans E. Jørgensen. The influence of the wind speed profile on wind turbine performance measurements. *Wind Energy*, 12(4):348–362, 2009.

L. Wang, M. Goldberg, X. Liu, and L. Zhou. Assessment of reanalysis datasets using AIRS and IASI hyperspectral radiances. pages 2936–2939. IEEE, 2010. ISBN 1424495652.

WEC. *1989 Survey of Energy Resources*. Holywell Press Ltd., Oxford, United Kingdom, 1989.

WEC. *New Renewable Energy Resources—A Guide to the Future*, volume 387. Kogan Page, London, 1994.

WEC. World energy scenarios: Composing energy futures to 2050, 2013. URL `http://www.worldenergy.org/wp-content/uploads/2013/10/World-Energy-Scenarios_Composing-energy-futures-to-2050_Executive-summary.pdf`.

J.R. Weeks. *Population: an introduction to concepts and issues*. Wadsworth Pub Co, 2008. ISBN 0495096377.

Manuel Welsch, Mark Howells, M. Bazilian, J. F. DeCarolis, Sebastian Hermann, and H. H. Rogner. Modelling elements of smart grids–enhancing the OSeMOSYS (open source energy modelling system) code. *Energy*, 46(1):337–350, 2012.

Jörg Winterfeldt, Axel Andersson, Christian Klepp, Stephan Bakan, and Ralf Weisse. Comparison of HOAPS, QuikSCAT, and buoy wind speed in the eastern north atlantic and the north sea. *Geoscience and Remote Sensing, IEEE Transactions on*, 48(1):338–348, 2010. ISSN 0196-2892.

J.K. Wright. A method of mapping densities of population: With cape cod as an example. *Geographical Review*, 26(1):103–110, 1936. ISSN 0016-7428.

XiEC. Seismic vibration produced by wind turbines in the eskdalemuir region, 2014. URL `http://www.scotland.gov.uk/Resource/0045/00454076.pdf`.

R. Yao and K. Steemers. A method of formulating energy load profile for domestic buildings in the UK. *Energy and Buildings*, 37(6):663–671, 2005. ISSN 0378-7788.

S. Zachary, CJ Dent, and DJ Brayshaw. Challenges in quantifying wind generation's contribution to securing peak demand. pages 1–8. IEEE, 2011. ISBN 1457710005.

Zero-Carbon-Hub. FABRIC ENERGY EFFICIENCY FOR PART l 2013 - WORKED EXAMPLES AND FABRIC SPECIFICATIONS, 2012. URL `http://www.zerocarbonhub.org/sites/default/files/resources/reports/Fabric_Standards_for_2013-Worked_Examples_and_Fabric_Specification.pdf`.

Hai-xiang Zhao and Frédéric Magoulès. A review on the prediction of building energy consumption. *Renewable and Sustainable Energy Reviews*, 16(6):3586–3592, 2012.

Yuyu Zhou and Steven J. Smith. Spatial and temporal patterns of global onshore wind speed distribution. *Environmental Research Letters*, 8(3):034029, 2013.

Dan Zhu, Shu Tao, Rong Wang, Huizhong Shen, Ye Huang, Guofeng Shen, Bin Wang, Wei Li, Yanyan Zhang, Han Chen, and others. Temporal and spatial trends of residential energy consumption and air pollutant emissions in china. *Applied Energy*, 106:17–24, 2013.